frontiers | Research Topics

Cannabinoids as potential treatment for neurological diseases

Edited by
María Gómez-Cañas, Onintza Sagredo, Valentina Satta,
Concepcion Garcia, Paula Morales and Carmen Rodriguez Cueto

Published in
Frontiers in Pharmacology
Frontiers in Neuroanatomy

ISSN 1664-8714
ISBN 978-2-83251-269-2
DOI 10.3389/978-2-83251-269-2

About Frontiers

Frontiers is more than just an open access publisher of scholarly articles: it is a pioneering approach to the world of academia, radically improving the way scholarly research is managed. The grand vision of Frontiers is a world where all people have an equal opportunity to seek, share and generate knowledge. Frontiers provides immediate and permanent online open access to all its publications, but this alone is not enough to realize our grand goals.

Frontiers journal series

The Frontiers journal series is a multi-tier and interdisciplinary set of open-access, online journals, promising a paradigm shift from the current review, selection and dissemination processes in academic publishing. All Frontiers journals are driven by researchers for researchers; therefore, they constitute a service to the scholarly community. At the same time, the *Frontiers journal series* operates on a revolutionary invention, the tiered publishing system, initially addressing specific communities of scholars, and gradually climbing up to broader public understanding, thus serving the interests of the lay society, too.

Dedication to quality

Each Frontiers article is a landmark of the highest quality, thanks to genuinely collaborative interactions between authors and review editors, who include some of the world's best academicians. Research must be certified by peers before entering a stream of knowledge that may eventually reach the public - and shape society; therefore, Frontiers only applies the most rigorous and unbiased reviews. Frontiers revolutionizes research publishing by freely delivering the most outstanding research, evaluated with no bias from both the academic and social point of view. By applying the most advanced information technologies, Frontiers is catapulting scholarly publishing into a new generation.

What are Frontiers Research Topics?

Frontiers Research Topics are very popular trademarks of the *Frontiers journals series*: they are collections of at least ten articles, all centered on a particular subject. With their unique mix of varied contributions from Original Research to Review Articles, Frontiers Research Topics unify the most influential researchers, the latest key findings and historical advances in a hot research area.

Find out more on how to host your own Frontiers Research Topic or contribute to one as an author by contacting the Frontiers editorial office: frontiersin.org/about/contact

Cannabinoids as potential treatment for neurological diseases

Topic editors

María Gómez-Cañas — Complutense University of Madrid, Spain
Onintza Sagredo — Universidad Complutense de Madrid, Spain
Valentina Satta — Complutense University of Madrid, Spain
Concepcion Garcia — Complutense University of Madrid, Spain
Paula Morales — Institute of Medical Chemistry, Spanish National Research Council (CSIC), Spain
Carmen Rodriguez Cueto — Center for Biomedical Research on Neurodegenerative Diseases (CIBERNED), Spain

Citation

Gómez-Cañas, M., Sagredo, O., Satta, V., Garcia, C., Morales, P., Cueto, C. R., eds. (2023). *Cannabinoids as potential treatment for neurological diseases*. Lausanne: Frontiers Media SA. doi: 10.3389/978-2-83251-269-2

Table of contents

frontiers | Frontiers in Neuroscience

TYPE Editorial
PUBLISHED 20 December 2022
DOI 10.3389/fnins.2022.1108101

OPEN ACCESS

EDITED AND REVIEWED BY
Nicholas M. Barnes,
University of Birmingham,
United Kingdom

*CORRESPONDENCE
María Gómez-Cañas
✉ mgc@med.ucm.es

SPECIALTY SECTION
This article was submitted to Neuropharmacology, a section of the journal Frontiers in Neuroscience

RECEIVED 25 November 2022
ACCEPTED 30 November 2022
PUBLISHED 20 December 2022

CITATION
Gómez-Cañas M, Morales P, Satta V, Rodríguez-Cueto C, García C and Sagredo O (2022) Editorial: Cannabinoids as potential treatment for neurological diseases. *Front. Neurosci.* 16:1108101. doi: 10.3389/fnins.2022.1108101

Editorial: Cannabinoids as potential treatment for neurological diseases

María Gómez-Cañas[1,2,3]*, Paula Morales[4], Valentina Satta[1,2,3], Carmen Rodríguez-Cueto[1,2,3], Concepción García[1,2,3] and Onintza Sagredo[1,2,3]

[1]Instituto Universitario de Investigación en Neuroquímica, Departamento de Bioquímica y Biología Molecular, Facultad de Medicina, Universidad Complutense, Madrid, Spain, [2]Centro de Investigación Biomédica en Red de Enfermedades Neurodegenerativas (CIBERNED), Instituto de Salud Carlos III, Madrid, Spain, [3]Instituto Ramón y Cajal de Investigación Sanitaria (IRYCIS), Madrid, Spain, [4]Instituto de Química Médica, Consejo Superior de Investigaciones Científicas (CSIC), Madrid, Spain

KEYWORDS

neurological diseases, cannabinoid, endocannabinoid system, neuroprotection, drug discovery

Editorial on the Research Topic
Cannabinoids as potential treatment for neurological diseases

Due to the wide distribution of the endocannabinoid system (ECS) throughout the organism and its role on the maintenance of the homeostatic balance in the body, the modulation of this system has been proposed as a therapeutic strategy for the treatment of several diseases (Lowe et al., 2021). The relevant role of the ECS in the central nervous system (Croxford, 2003) and the neuroprotective potential of cannabinoids (Aymerich et al., 2018) has focused the interest of numerous researchers. Indeed, an increasing number of studies are validating the role of this system in different neurological and neurodegenerative diseases, as well as the therapeutic effects that cannabinoids-based drugs have over these pathologies (Kaur et al., 2016; Fraguas-Sánchez and Torres-Suárez, 2018).

Although much progress has already been made in this field, its complex pharmacology evidences that many aspects still remain to be unraveled. The synergistic effects of cannabinoids with other systems, their interactions with diverse receptors or further understanding of its signaling pathways need to be further addressed (Kilaru and Chapman, 2020).

This Research Topic provides insights into new pathways of action of the cannabinoid system, promising new molecules for the treatment of neurological diseases, and proposals of the ECS as a tool for the detection of these diseases.

In this regard, Liu L. et al. presents an interesting study which reveals the hot spots and frontiers of cannabidiol (CBD) research using bibliometric and data visualization methods. They attached a great importance of CBD, especially in the treatment of neuropsychiatric disorders, such as epilepsy, anxiety, and schizophrenia. Besides, they explain its interest on a variety of receptors including CB1 and CB2 receptors 5-HT1A, and GPR55 which are involved in the pharmacology of CBD.

Continuing with this promising molecule in the treatment of neurological diseases, Shen et al. propose CBD as a neuroprotective agent against the neurotoxicity caused by drugs of abuse such as methamphetamine. These authors show that CBD have anti-apoptotic effects by reducing the neurotoxicity caused by methamphetamine which is mediated by dopamine D1 receptor-mediated phosphorylation of the Methyl-CpG-binding protein.

This Research Topic also includes several articles reflecting on the role of ECS in different neurological diseases on the different processes involved in these pathologies. This is the case of an interesting article that provides a comprehensive review of the potential for pharmacological manipulation of the endocannabinoid system in glial cells, including microglia, astrocytes, and oligodendrocytes, in ischemic stroke. In this review Vicente-Acosta et al. highlight the interest in modulating the ECS to slow down the damage associated with this pathology.

Li et al. reflect on their study about how sleep deprivation is a common feature of modern society and, when chronic, can negatively impact on brain function, resulting in significant decreases in cognitive function. Moreover, the authors demonstrate that tanshinone IIA (an important lipid-soluble component of Salvia miltiorrhiza), could exert neuroprotective effects by regulating the CNR1/PI3K/AKT signaling pathway and improve sleep deprivation-induced spatial recognition and learning memory dysfunction.

Hu et al. introduce new strategies to treat anxiety and pain through the activation of the ECS. Authors focused their study on the possible electroacupuncture's (EA) ability to attenuate inflammatory bowel disease (IBD) induced visceral pain and anxiety *via* the ventral hippocampus (vHPC). They demonstrated that EA may exert anxiolytic effect *via* downregulating CB1R in GABAergic neurons and activating CB1R in glutamatergic neurons in the vHPC, thus reducing the release of glutamate and inhibiting the anxiogenic neuronal circuits related to vHPC. This technique does not only activate CB1R, Zhang, He, et al. suggest that EA reduces visceral pain *via* CB2R in a mouse model of inflammatory bowel disease. They explain that EA attenuates mechanical allodynia and visceral hypersensitivity associated with IBD by activating CB2 receptors and subsequent inhibition of macrophage activation and expression of IL-1β and iNOS.

In fact, on numerous occasions, the benefits found in the symptomatology of some pathologies in which patients are treated with cannabinoids are attributed to the activation of both receptors and/or to the interaction of both. The study of Liu Y. et al., demonstrated CB1R in primary sensory neurons functions as an endogenous analgesic mediator, but also that suppression of the CB1R in peripheral sensory neurons produces changes in downstream transcriptome expression. In this sense, the authors expose that CB2 is the downstream gene of CB1R in peripheral sensory neurons and CB2R mediates the development of neuropathic pain. Therefore, by antagonizing CB2R the excessive activation of astrocytes could be inhibited and neuroinflammation improving neuropathic pain. This complexity derived from the activation of cannabinoid receptors can also be observed in the findings obtained by Kim et al. In this case it is not an interaction between the cannabinoid receptors themselves, but between cannabinoid and orexin receptors. In this study, the authors demonstrate that physical or molecular interactions between cannabinoid and orexin systems (that are not only expressed in the same brain regions modulating these functions, but physically interact as heterodimers) may provide valuable insight into drug-drug interactions between cannabinoid and orexin drugs for the treatment of insomnia, pain, and other disorders. However, the complexity of the ECS is not limited to cannabinoid receptors and their interactions with each other or with other receptors, but to the whole enzymatic machinery involved in the regulation of endocannabinoid levels or ligand-receptor interaction, among others. Therefore, Zhang, Li, et al. have contributed to this Research Topic, providing an interesting overview about the α/β-Hydrolase domain-containing 6 (ABHD6), a transmembrane serine hydrolase that hydrolyzes monoacylglycerol (MAG) lipids such as endocannabinoid 2-arachidonoyl glycerol (2-AG). This study recapitulates the molecular machinery of ABHD6, particularly its involvement in the pathogenesis of neurological diseases, contributing to establish supplemental basis for new pharmacological interventions *via* targeting of ABHD6.

In line with the complexity of ECS signaling, currently, one of the most promising areas of study is the development of new modulators with potential for the treatment of neurological diseases. The identification of these novel molecules along with their pharmacological profile and interaction with receptors is of great interest in the cannabinoid community. In this sense, two research articles by Lapraire and colleages are included in this Research Topic. They present the pharmacological evaluation of phytogenic, cannabis by-products and non-cannabis phytomolecules (Zagzoog et al.) and new synthetic compounds (Brandt et al.). Zagzoog et al. demonstrated that minor phytocannabinoids such as $\Delta^{6a,10a}$-THC, 11-OH-Δ^{9}-THC or CBN partially activate CB1R, whereas the non-cannabis molecules tested were inactive. Brandt et al. exhaustively studied the molecular pharmacology of the enantiomerically separated CB1 PAMs, GAT591, and GAT593. *In vitro* and *in vivo* assays showed that the R-enantiomers displayed mixed allosteric agonist-PAM activity at CB1R while the S-enantiomers showed moderate activity. Molecular modeling studies provided structural insights into their distinct binding sites.

The importance of the ECS in the regulation of different processes involved in neurological diseases is clear, but unfortunately human neurodegenerative disease diagnosis may only be possible when the first symptoms are present. At this point, irreversible damage to the central nervous system has already occurred and will spread over time. The findings obtained by

Vidal-Palencia et al. indicated that the ECS is already altered in APP/PS1 mice at the pre-symptomatic stage, suggesting that it could be an early event contributing to the pathophysiology of AD or being a potential predictive biomarker.

The preclinical potential of the ECS as a therapeutic strategy for the treatment of neurological diseases was already more than demonstrated before this Research Topic (Lowe et al., 2021), however, the contribution of the articles included in this special issue, provide new findings that strengthen this hypothesis. Although the ultimate aim of this research field is to translate the results achieved to the clinical level, unfortunately in most cases it has not yet been possible. So far, most clinical trials that have been developed with cannabinoid molecules have tested their potential for the treatment of symptoms of some neurodegenerative diseases but did not show the effects observed in animal models or present inconsistencies among them (Ball et al., 2015; Herrmann et al., 2019; Timler et al., 2020). On the one hand, the psychoactivity related to CB1 activation, is delaying the development of cannabinoids as medicines, on the other hand, the clinical trials are still in early stages in order to ensure the safety of the potential drug. In this regard, many researchers are focusing their efforts on developing therapeutic strategies with CB2R ligands, which lack these harmful effects. However, the clinical results using CB2R ligands have been ineffective (Morales et al., 2016; An et al., 2020). Also in this sense, the use of CBD is having a lot of success. A drug based on this cannabinoid called Epidiolex has been developed and has recently been approved by the Food and Drug Administration (FDA) and several clinical trials have developed with it. But again, the results between clinical trials are inconsistent (Pauli et al., 2020). In this aspect, it is worth thinking that perhaps the doses should be readjusted or the pharmacokinetic properties in humans should be determined. However, it is also true that the complexity of this system has become apparent and it is necessary to work to clarify the increasingly complicated signaling of the ECS, the interactions with other receptors or systems, as well as the mechanisms of action that ligands exert on this system. But it is also of vital importance to develop future drugs with selectivity and suitable pharmacokinetic properties to obtain the desired effects in the treatments, as well as to know the state of the target (ECS) for treatment in pre- and post-symptomatic stages of the pathologies, or the auto-regulation of the ECS after its modulation.

In summary, ECS modulation is a great therapeutic strategy for the treatment of neurological and neurodegenerative diseases, and although every day we are one step closer, there is still a long way to go to achieve optimal results in the development of new drugs for the treatment of patients suffering from these pathologies.

Author contributions

All authors listed have made a substantial, direct, and intellectual contribution to the work and approved it for publication.

Conflict of interest

The authors declare that the research was conducted in the absence of any commercial or financial relationships that could be construed as a potential conflict of interest.

Publisher's note

All claims expressed in this article are solely those of the authors and do not necessarily represent those of their affiliated organizations, or those of the publisher, the editors and the reviewers. Any product that may be evaluated in this article, or claim that may be made by its manufacturer, is not guaranteed or endorsed by the publisher.

References

An, D., Peigneur, S., Hendrickx, L. A., and Tytgat, J. (2020). Targeting cannabinoid receptors: current status and prospects of natural products. *Int. J. Mol. Sci.* 21, 5064. doi: 10.3390/ijms21145064

Aymerich, M. S., Aso, E., Abellanas, M. A., Tolon, R. M., Ramos, J. A., Ferrer, I., et al. (2018). Cannabinoid pharmacology/therapeutics in chronic degenerative disorders affecting the central nervous system. *Biochem. Pharmacol.* 157, 67–84. doi: 10.1016/j.bcp.2018.08.016

Ball, S., Vickery, J., Hobart, J., Wright, D., Green, C., Shearer, J., et al. (2015). The cannabinoid use in progressive inflammatory brain disease (CUPID) trial: a randomised double-blind placebo-controlled parallel-group multicentre trial and economic evaluation of cannabinoids to slow progression in multiple sclerosis. *Health Technol. Assess.* 19, 1–188. doi: 10.3310/hta19120

Croxford, J. L. (2003). Therapeutic potential of cannabinoids in CNS disease. *CNS Drugs* 17, 179–202. doi: 10.2165/00023210-200317030-00004

Fraguas-Sánchez, A. I., and Torres-Suárez, A. I. (2018). Medical use of cannabinoids. *Drugs* 78, 1665–1703. doi: 10.1007/s40265-018-0996-1

Herrmann, N., Ruthirakuhan, M., Gallagher, D., Verhoeff, N. P. L. G., Kiss, A., Black, S. E., et al. (2019). Randomized placebo-controlled trial of nabilone for agitation in Alzheimer's disease. *Am. J. Geriatr. Psychiatry* 27, 1161–1173. doi: 10.1016/j.jagp.2019.05.002

Kaur, R. R., Ambwani, S., and Singh, S. (2016). Endocannabinoid system: a multi-facet therapeutic target. *Curr. Clin. Pharmacol.* 11, 110–117. doi: 10.2174/1574884711666160418105339

Kilaru, A., and Chapman, K. D. (2020). The endocannabinoid system. *Essays Biochem.* 64, 485–499. doi: 10.1042/EBC20190086

Lowe, H., Toyang, N., Steele, B., Bryant, J., and Ngwa, W. (2021). The endocannabinoid system: a potential target for the treatment of various diseases. *Int. J. Mol. Sci.* 22, 9472. doi: 10.3390/ijms22179472

Morales, P., Hernandez-Folgado, L., Goya, P., and Jagerovic, N. (2016). Cannabinoid receptor 2 (CB_2) agonists and antagonists: a patent update. *Exp. Opin. Ther. Pat.* 26, 843–856. doi: 10.1080/13543776.2016.1193157

Pauli, C. S., Conroy, M., vanden Heuvel, B. D., and Park, S.-H. (2020). Cannabidiol drugs clinical trial outcomes and adverse effects. *Front. Pharmacol.* 11, 63. doi: 10.3389/fphar.2020.00063

Timler, A., Bulsara, C., Bulsara, M., Vickery, A., Smith, J., and Codde, J. (2020). Use of cannabinoid-based medicine among older residential care recipients diagnosed with dementia: study protocol for a double-blind randomised crossover trial. *Trials* 21, 188. doi: 10.1186/s13063-020-4085-x

frontiers in Pharmacology

REVIEW
published: 02 December 2021
doi: 10.3389/fphar.2021.784202

Alpha/Beta-Hydrolase Domain-Containing 6: Signaling and Function in the Central Nervous System

Haofuzi Zhang[1†], *Xin Li*[2†], *Dan Liao*[1†], *Peng Luo*[1*] *and Xiaofan Jiang*[1*]

[1]Department of Neurosurgery, Xijing Hospital, Fourth Military Medical University, Xi'an, China, [2]Department of Anesthesiology, Xijing Hospital, Fourth Military Medical University, Xi'an, China

OPEN ACCESS

Edited by:
Valentina Satta,
Complutense University of Madrid, Spain

Reviewed by:
Igor Ivanov,
Moscow Technological University, Russia
Robert B. Laprairie,
University of Saskatchewan, Canada
Simar Singh,
University of Washington, United States

***Correspondence:**
Peng Luo
lpmail_19@126.com
Xiaofan Jiang
jiangxf@fmmu.edu.cn

†These authors have contributed equally to this work

Specialty section:
This article was submitted to Neuropharmacology, a section of the journal Frontiers in Pharmacology

Received: 27 September 2021
Accepted: 18 November 2021
Published: 02 December 2021

Citation:
Zhang H, Li X, Liao D, Luo P and Jiang X (2021) Alpha/Beta-Hydrolase Domain-Containing 6: Signaling and Function in the Central Nervous System. Front. Pharmacol. 12:784202. doi: 10.3389/fphar.2021.784202

Endocannabinoid (eCB) signaling plays an important role in the central nervous system (CNS). α/β-Hydrolase domain-containing 6 (ABHD6) is a transmembrane serine hydrolase that hydrolyzes monoacylglycerol (MAG) lipids such as endocannabinoid 2-arachidonoyl glycerol (2-AG). ABHD6 participates in neurotransmission, inflammation, brain energy metabolism, tumorigenesis and other biological processes and is a potential therapeutic target for various neurological diseases, such as traumatic brain injury (TBI), multiple sclerosis (MS), epilepsy, mental illness, and pain. This review summarizes the molecular mechanisms of action and biological functions of ABHD6, particularly its mechanism of action in the pathogenesis of neurological diseases, and provides a theoretical basis for new pharmacological interventions *via* targeting of ABHD6.

Keywords: ABHD6, endocannabinoid system, CPT1C, AMPA receptor, neurological diseases

INTRODUCTION

The endocannabinoid system (ECS) is a lipid signal transduction system that includes endogenous cannabinoids (eCBs), cannabinoid receptors and enzymes responsible for the synthesis and hydrolyzation of eCBs, with an important role in the regulation of central nervous system (CNS) function (Jung et al., 2021; Lu and Mackie, 2021). α/β-Hydrolase domain-containing 6 (ABHD6) is an integral membrane protein with recently discovered serine hydrolase activity that is, mainly expressed in immune cell-enriched tissues and the CNS(Poursharifi et al., 2017). The hydrolytic substrates of ABHD6 are mainly monoacylglycerols (MAGs) (Poursharifi et al., 2020), such as endogenous cannabinoid 2-arachidonoylglycerol (2-AG) and arachidonic acid (Noguchi et al., 2021), which are precursors of prostaglandins and other inflammatory mediators (Ghosh et al., 2020; Larsson et al., 2021; Trostchansky et al., 2021). As the main hydrolase of postsynaptic eCBs, ABHD6 is involved in regulating neuronal ECS function (Cao et al., 2019). In addition, ABHD6 is an important component of the α-amino-3-hydroxy-5-methyl-4-isoxazole-propionic acid receptor (AMPAR) complex (Schwenk et al., 2019), which inhibits translocation of AMPAR to the postsynaptic membrane and the excitability of AMPAR (Wei et al., 2017). ABHD6 plays a potential regulatory role in the neuroinflammatory pathway (Tanaka et al., 2017; Wen et al., 2018) and autoimmunity (Manterola et al., 2018b; Rahaman et al., 2019) and is expected to become a new target for intervention in nervous system diseases (Kind and Kursula, 2019). Inhibitors of ABHD6 have been explored within analgesia, anti-anxiety, anti-inflammatory contexts, as well as other areas, and are therefore promising in the treatment of inflammatory and degenerative diseases of the CNS (Deng and Li, 2020b). In this review, the latest research progress on ABHD6 for the

treatment of nervous system diseases is reviewed in terms of its molecular structure, expression, and mechanism of action in the CNS.

THE ENDOCANNABINOID SYSTEM AND IDENTIFICATION OF ABHD6

The Endocannabinoid System

The canonical endogenous cannabinoid system consists of cannabinoid receptors, signaling lipids called eCBs, and enzymes that produce and inactivate eCBs. Some atypical receptors, including several transient receptor potential (TRP) channels, G protein-coupled receptor 55 (GPR55), and glycine receptors, have also been discovered. The concept of this signaling system originated from study of the biological activity of Δ-9-tetrahydrocannabinol (THC) (Cao et al., 2019). Three decades ago, researchers discovered the ECS when seeking to identify a cannabinoid receptor that interacts with the psychoactive compounds in cannabis. Since then, research on eCBs has exploded, and more receptors, their lipid mediators and signaling pathways have been revealed (Kilaru and Chapman, 2020). Evidence-based studies have shown that eCBs regulate various aspects of human physiological and pathophysiological functions in the CNS and immune system, which has become a hot research topic (Joshi and Onaivi, 2019). The biological effects of eCBs are mediated mainly by two members of the G protein-coupled receptor family: CB_1R and CB_2R. CB_1R is widely considered a potential therapeutic target in neuropsychological and neurodegenerative diseases; CB_2R selectively regulates the function of immune cells. In addition, cannabinoids regulate signal transduction pathways and have profound roles in peripheral regions. Although cannabinoids possess therapeutic potential, their psychoactive effect limits their clinical application to a great extent (Zou and Kumar, 2018). In particular, activation of CB_1R may cause CNS effects. Nevertheless, the discovery of CB_2R and endogenous cannabinoid receptor ligands (namely, eCBs) provides new possibilities for safely targeting the ECS (Cristino et al., 2020). Notably, 2-AG is one of the ligands that can be metabolized by several hydrolytic enzymes. In this review, we focus particular attention to the hydrolase ABHD6.

Identification of ABHD6

A vital component of the ECS, ABHD6 is an enzyme that regulates hydrolysis of 2-AG, which is an endogenous signaling lipid that activates CB_1R and CB_2R and is an important lipid precursor of the eicosanoic acid signaling pathway (Sugiura et al., 1995). 2-AG is generally believed to be metabolized to arachidonic acid (AA) and glycerol by monoacylglycerol lipase (MAGL); recent evidence suggests that other lipases, such as ABHD6 and ABHD12, are also involved in 2-AG degradation in many tissues. Among these lipases, MAGL is responsible for approximately 85% of the 2-AG degradation occurring in the CNS, whereas ABHD6 and ABHD12 account for approximately 4 and 9% of 2-AG hydrolysis, respectively (Savinainen et al., 2012). As MAGL, ABHD6, and ABHD12 are distributed is different manners and have different subcellular localizations, they regulate 2-AG hydrolysis at different times and sites. ABHD6 is an important cell signaling regulator not only in the CNS but also in peripheral tissues, with an important role in the pathogenesis of many diseases, such as metabolic syndrome (Thomas et al., 2013), obesity (Zhao et al., 2016), and autoimmune diseases and cancer (Yu et al., 2016). Genetic and pharmacological studies have revealed the therapeutic potential of ABHD6, making it an attractive target for the treatment of various diseases (Naydenov et al., 2014).

BIOCHEMICAL CHARACTERIZATION AND EXPRESSION PROFILE OF ABHD6

Biochemical Characterization of ABHD6

The ABHD6 gene is located on chromosome 3 p14.3 and consists of 10 exons. Its open reading frame encodes a protein with 337 amino acids and a molecular weight of 38 kDa (Poursharifi et al., 2017). Based on amino acid sequence, ABHD6 is a cytoplasmic type II integrated membrane protein belonging to the serine hydrolase family (Long and Cravatt, 2011). ABHD6 includes an eight-stranded parallel α/β-structure with a second antiparallel structure. The hydrolytic activity of ABHD6 derives from the catalytic triad Ser148-Asp278-His306 (Lord et al., 2013) located on the cytoplasmic side of the cell membrane (**Figure 1**) (Kind and Kursula, 2019). To confirm the accuracy of the predicted structure, researchers have assessed the activity of the enzyme and invoked a multidimensional protein identification platform known as activity-based protein profiling (ABPP). Site-directed mutation of the catalytic residues leads to loss of hydrolytic activity (**Figure 1**) (Thomas et al., 2013). Although the crystal structure of ABHD6 remains unclear, the primary structure is well conserved among species, with 94% sequence homology between human and mouse orthologs (Long and Cravatt, 2011).

The order of hydrolytic activity of ABHD6 is 1-arachidonoylglycerol (1-AG) > 2-AG > 2-LG, as measured *in vitro* using homogenate from an overexpression system (Navia-Paldanius et al., 2012). 1-AG is a similarly bioactive isomer of 2-AG that may have a role in stabilizing the strength of the cannabinoid signal (Docs et al., 2017). In primary neuronal cell culture, chemical inhibition of ABHD6 reduces 2-AG degradation by 50% and leads to 2-AG accumulation. In addition to its established MAG lipase activity, ABDH6 exhibits significant diacylglycerol lipase (DGL) activity in Neuro2A cells (van Esbroeck et al., 2019). DGLs mainly catalyze "on-demand" biosynthesis of bioactive MAGs, including 2-AG,2-linoleoylglycerol (2-LG) (Yuan et al., 2016). Because hydrolysis of 2-AG leads to release of AA, the precursor of prostaglandins, ABHD6 may be related to the inflammatory process and autoimmune diseases. Indeed, blocking ABHD6 in macrophages has anti-inflammatory effects, such as increasing the anti-inflammatory agent prostaglandin-d2-glycerol ester (PGD2-GE) (Alhouayek et al., 2013). Furthermore, ABHD6 regulates glucose-stimulated insulin secretion (GSIS), which is essential for glucose homeostasis in different tissues. A variety of different ABHD6 inhibitors have

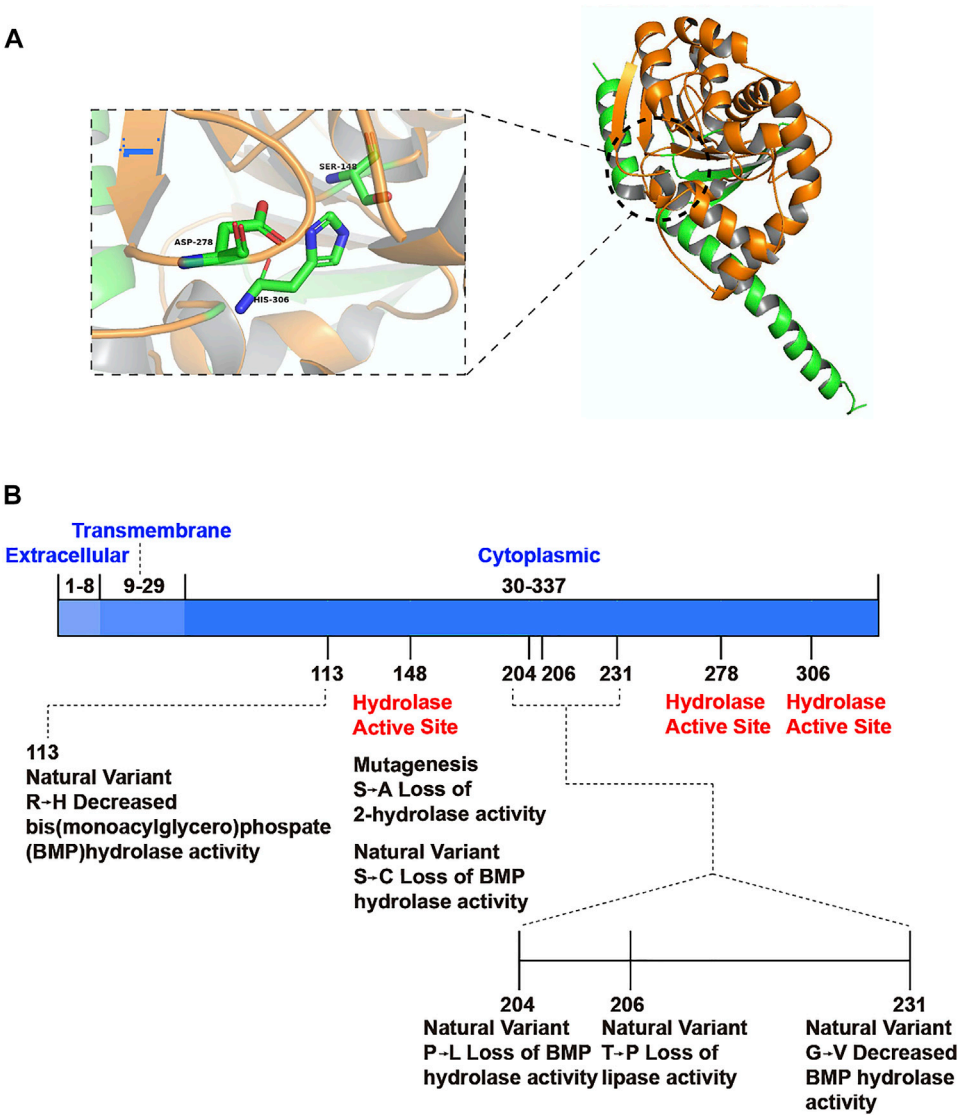

FIGURE 1 | Spatial structure model of ABHD6 and its functional sites. **(A)** ABHD6 consists of an eight chain β-sheet with surrounding α-helices. The catalytic triad is composed of a nucleophilic residue (Ser148), an acidic residue (Asp278) and a histidine (His306). **(B)** Mutation or natural variation may occur at some sites of ABHD6, resulting in the decrease or loss of partial hydrolytic function of the enzyme. There is no document report that ABHD6 has modification sites on protein structures.

been developed through clinical disease treatment research. However, mutation of the gene encoding ABHD6 is not related to human diseases (Lord et al., 2013).

Expression Profile of ABHD6

ABHD6 is widely expressed, especially in the CNS; enzymatic activity measured using ABPP in the mouse brain showed particular expression in the cerebral cortex (Moreno-Luna et al., 2021), pituitary (Cao et al., 2019), and hippocampus (Longaretti et al., 2020a), as well as in the spleen and small intestine and the liver, kidney, and ovary (Drehmer et al., 2019; Deng and Li, 2020b). In the CNS, ABHD6 has been identified as the key regulatory point of the ECS (Gokce et al., 2016; Cao et al., 2019). Expression of ABHD6 is regulated by estrogen and other hormones, suggesting sex differences (Drehmer et al., 2019). The distribution of ABHD6 differs in various brain regions and neural cell subtypes. Studies have shown the highest enzyme activity of ABHD6 in the frontal cortex, hippocampus, striatum, and cerebellum (Baggelaar et al., 2017). ABHD6 activity in these regions is much higher than that of ABHD12 and even that of MAGL. Although MAGL is the main enzyme related to 2-AG degradation in the brain, the role of ABHD6 is independent of MAGL and controls accumulation of 2-AG in intact neurons (Marrs et al., 2010; Owens et al., 2017). Moreover, results of single-cell sequencing showed that ABHD6 is mainly distributed in progenitor cells and astrocytes in young mice; in adult mice, it is mainly

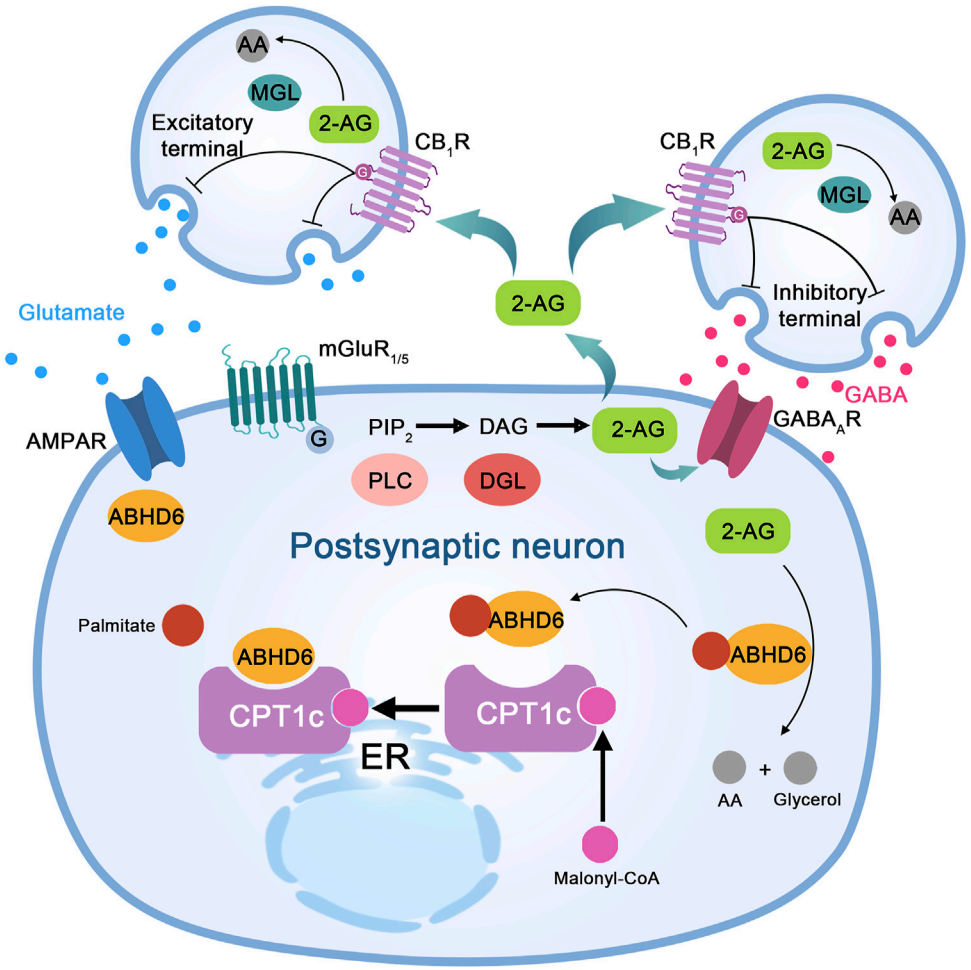

FIGURE 2 | The proposed molecular mechanism of ABHD6 in neurons and neurological diseases. Stimulation of excitatory neurons to release glutamate activates metabotropic glutamate receptor 1/5 (mGluR1/5) on postsynaptic neurons, which couples to a G protein, activates phospholipase C (PLC), and leads to diacylglycerol (DAG) production from inositol diphosphate (PIP2). DAG is cleaved by DAG lipase (DGL) to produce 2-arachidonic acid glycerol (2-AG). Its functions are as follows: (I) acting as a paracrine agonist of the CB1 receptor (CB_1R) expressed at the excitatory end, releasing glutamate to activate mGluR1/5 and α-amino-3-hydroxy-5-methyl-4-isoxazolpropionic acid (AMPA) receptors; (II) CB_1R paracrine agonists release GABA and activate GABAA receptor (GABAAR) on postsynaptic neurons through inhibitory terminal expression; and (III) autocrine positive allosteric regulators of GABAA receptors in postsynaptic neurons. Monoacylglycerol lipase (MGL) in presynaptic neurons or α/β-hydrolase domain-containing 6 (ABHD6) in postsynaptic neurons hydrolyzes excess 2-AG to arachidonic acid (AA) and glycerol (not shown). ABHD6 interacts with the AMPA receptor and controls its transport to the postsynaptic compartment membrane. Bioinformatic analysis indicates the presence of amino acid sites of palmitoylation/depalmitoylation modification in ABHD6. Protein interaction between CPT1c and ABHD6 depends on the presence of malonyl-COA; when malonyl-COA is absent, the inhibitory effect of CPT1c on ABHD6 enzyme activity is lost.

expressed in specific types of neurons (such as GABAergic neurons) and astrocytes (Marrs et al., 2010; Gokce et al., 2016). At the subcellular level, ABHD6 is mainly expressed in the cytoplasm of glutamatergic neuron dendrites and colocalizes with microtubule-associated protein 2 (MAP2), suggesting that ABHD6 plays an important role in the regulation of postsynaptic nerve function (Marrs et al., 2010). In addition, ABHD6 is significantly expressed in dendrites and postsynapses, which complements the presynaptic expression of MAGL (Straiker and Mackie, 2007), and the observed localization of ABHD6 and MAGL suggests that each enzyme controls a subcellular pool of 2-AG.

MOLECULAR MECHANISM OF ABHD6-SPECIFIC SIGNALING

ABHD6 and ECS

As an important hydrolase of 2-AG, ABHD6 is directly involved in regulating the ECS. In turn, ECS regulation by ABHD6 can affect the synaptic plasticity of neurons and play a role in CNS-injuring diseases such as epilepsy and brain injury (Deng and Li, 2020b). Muccioli et al. found that BV-2 cells do not express MAGL but can effectively hydrolyze 2-AG (Muccioli et al., 2007), proving for the first time that an enzyme other than MAGL can hydrolyze 2-AG. Further studies revealed that ABHD6 acts as a 2-

AG hydrolase in BV-2 cells and is a novel type of 2-AG hydrolase (Marrs et al., 2010). In addition to its expression in the BV-2 cell line, ABHD6 is expressed in neurons and astrocytes (**Figure 2**). Inhibition of its expression or activity enhances activation of CB_1R and CB_2R upon 2-AG accumulation (Marrs et al., 2010). Marrs, W.R. and others first proposed that ABHD6 participates in long-term synaptic depression (Ltd.). Their study revealed that WWL-70, an ABHD6 inhibitor, reduces the Ltd. threshold of glutamate synapses, lasting for at least 40 min after induction (Marrs et al., 2010; Marrs et al., 2011). In contrast, WWL-70 has no effect on short-term synaptic plasticity, such as depolarization-induced suppression of inhibition (DSI) or depolarization-induced suppression of excitation (DSE) (Straiker et al., 2009; Colmers and Bains, 2018). *In vitro* recordings of neurons have shown that MAGL and cyclooxygenase-2 (COX-2), but not ABHD6, mediate this process (Straiker et al., 2009; Colmers and Bains, 2018; Lopez and Ballaz, 2020). These studies distinguish the biological roles of ABHD6, MAGL, and COX-2 by emphasizing their involvement in short-term and long-term synaptic plasticity.

ABHD6 and AMPAR

AMPAR is the major postsynaptic glutamate receptor that mediates synaptic transmission. ABHD6 specifically reduces surface expression of postsynaptic AMPARs through a hydrolase-independent mechanism (**Figure 2**). By using high-resolution proteomics, one study revealed that ABHD6 is a component of the AMPAR macromolecular complex (Wei et al., 2016; Chen and Gouaux, 2019). Decreased surface expression of AMPAR is due to a reduction in surface expression of GluA1, a subunit of AMPAR. Binding of ABHD6 to AMPAR subunits (GluA1, GluA2, and GluA3) is mediated by the C-terminus of subunit GluA1 (Wei et al., 2017). However evidence shows that mutation of the Ser148 site, which is crucial for the serine hydrolytic activity of ABHD6, does not affect the ability of ABHD6 to regulate postsynaptic membrane expression of AMPAR in either neurons or transfected HEK293T cells, indicating that the ABHD6-AMPAR association is endocannabinoid independent (Wei et al., 2016). ABHD6 downregulates glutamate signaling by regulating functional expression of AMPAR, which differs from its eCB-dependent effect of enhancing sensitivity to Ltd. (Wei et al., 2016). Therefore, the effects of ABHD6 on the long-term plasticity of excitatory synapses might be mediated by two distinct mechanisms: an eCB-dependent and an eCB-independent mechanism (Cao et al., 2019).

ABHD6 and CPT1C

Carnitine palmitoyl transferase 1c (CPT1c) is a member of the carnitine palmitoyl transferase 1 family (which includes CPT1a and CPT1b), participating in the regulation of physiological functions such as energy metabolism and feeding (Obici et al., 2003). Proteomic studies have revealed that CPT1c and ABHD6 may interact (Brechet et al., 2017; Schwenk et al., 2019), and Miralpeix et al. confirmed this through coimmunoprecipitation (co-IP) and fluorescence resonance energy transfer (FRET) analyses (Miralpeix et al., 2021). Furthermore, the content of eCB in CPT1c-knockout (KO) mice is decreased (Lee and Wolfgang, 2012), indicating that interaction between CPT1c and ABHD6 may be involved in eCB hydrolysis. Further studies have confirmed that CPT1c has a significant effect on the enzymatic activity of ABHD6. Upon CPT1c overexpression, ABHD6 enzyme activity is decreased by approximately 60%, whereas activity increases significantly in CPT1c-KO mice (Miralpeix et al., 2021). Protein interaction between CPT1c and ABHD6 depends on malonyl-CoA (**Figure 2**). When the malonyl-CoA level is deficient, inhibition of ABHD6 enzyme activity by CPT1c disappears, indicating that cell energy metabolism can affect ABHD6 enzyme activity through the malonyl-CoA/CPT1c axis (Miralpeix et al., 2021). Overall, expression of CPT1c in tumor cells increases significantly. Moreover, the tolerance of tumor cells with high expression of CPT1c to ischemia and hypoxia is significantly enhanced (Zaugg et al., 2011; Reilly and Mak, 2012), and inhibiting expression of CPT1c has the opposite effect (Sanchez-Macedo et al., 2013). High CPT1c expression is related to enhanced cell viability under energy-deficient conditions.

BIOLOGICAL FUNCTION OF ABHD6

ABHD6 and Neurotransmission

As a bona fide member of the ECS, ABHD6 regulates neuronal function through different mechanisms. DSI and DSE are mainly regulated by 2-AG degradation. Therefore, blocking hydrolysis of 2-AG may help to prolong the time course of DSI and DSE (Chevaleyre et al., 2006). Regardless, it is noteworthy that inactivation of MAGL induces DSE prolongation at Purkinje cell synapses in granule cells and olivary nuclei (Zhong et al., 2011) but that inhibition of ABHD6 has no effect on DSI or DSE in autapse preparations (Straiker et al., 2009; Straiker and Mackie, 2009). In addition, overexpression of ABHD6 or ABHD12 does not affect DSEs (Straiker and Mackie, 2009). Conversely, pharmacological inhibition of ABHD6 reduces the threshold of CB1-dependent Ltd. at glutamatergic synapses in murine cortical slices (Marrs et al., 2011). ABHD6 negatively regulates the surface transmission and synaptic function of AMPAR in neurons (Wei et al., 2016), and the physiological function of ABHD6 binding to AMPAR is considered to be independent of eCBs. These findings provide a deeper understanding of the molecular mechanism by which ABHD6 regulates synaptic AMPAR trafficking.

ABHD6 and Neuroinflammation

Neuroinflammation is related to many neurological diseases, such as epilepsy and neurodegenerative diseases (including multiple sclerosis, Alzheimer's disease and Parkinson's disease), and is also linked to traumatic brain injury and ischemia-induced nerve injury. The ECS is thought to be associated with the inflammatory process and the immune system, as CB_2R overexpression has been detected in immune cells (Hubler and Kennedy, 2016). In fact, in mouse models of experimental autoimmune encephalomyelitis and traumatic brain injury, ABHD6 inhibition reduces microglial reactivity and COX-2 expression (Martinez-Torres et al., 2019).

Pharmacological blockade of ABHD6 raises the level of 2-AG, especially in microglia and macrophages (Wen et al., 2018); 2-AG inhibits infiltration of immune cells into the CNS, resulting in long-term beneficial effects in the chronic phase of autoimmune encephalomyelitis (Mecha et al., 2018). Arachidonic acid (AA), the product of 2-AG hydrolysis, is the main precursor in proinflammatory prostaglandin synthesis (Ricciotti and FitzGerald, 2011). Compared with inhibition of MAGL, also a potential target for inflammatory disease (Deng and Li, 2020a), ABHD6 inhibition has fewer side effects (detailed in subsection 5, *ABHD6 and Neurological Diseases*). Therefore, ABHD6 regulates hydrolysis of 2-AG, rendering ABHD6 a promising anti-inflammatory therapeutic target in the CNS.

ABHD6 and Energy Homeostasis

Energy homeostasis is achieved through complex brain circuits that strictly maintain energy levels by affecting food intake and energy consumption. In general, interactions between the brain and different adipose depots play a key role in maintaining energy balance, facilitating survival, and coping with metabolic challenges such as cold exposure and starvation. The brain regulates the metabolism of brown adipose tissue (BAT), white adipose tissue (WAT), and beige adipose tissue (BeAT) through efferent pathways, and in turn, these tissues transmit information about energy storage status to the brain through sensory innervation and hormone secretion (Caron et al., 2018). It is well known that eCBs are endogenous agonists of cannabinoid receptors that regulate various physiological processes, including metabolism and food intake (Nicholson et al., 2015). The ECS is expected to regulate feed and energy consumption through ventromedial hypothalamic neurons (Busquets-Garcia et al., 2015). For example, Fisette et al. reported that mice lacking ABHD6 in neurons of the ventromedial hypothalamus (VMH) with higher VMH 2-AG levels under conditions of eCB recruitment were physiologically unable to adapt to critical metabolic challenges, suggesting that ABHD6 in the VMH is very important for flexible regulation of energy metabolism (Fisette et al., 2016). Additionally, some studies have shown that ABHD6 is a negative regulator of WAT thermogenesis (Poursharifi et al., 2020). These studies implicate the important role of ABHD6 in the regulation of energy homeostasis by modulating brain circuits.

ABHD6 and Tumors

It has been reported that expression of ABHD6 is related to the pathogenesis of Epstein-Barr virus (EBV)-associated malignant tumors, such as Hodgkin's lymphoma, endemic Burkitt's lymphoma, and posttransplant lymphoma (Maier et al., 2006). Moreover, increased expression of ABHD6 is found in U2OS (bone), Jurkat (leukocyte), PC-3 (prostate) and other tumor cell lines (Li et al., 2009). Abnormally high expression of ABHD6 is also observed in Ewing family tumors (EFTs) but not in other sarcomas, suggesting that it may be a new diagnostic target for these tumors (Max et al., 2009). Recently, Tang et al. found that ABHD6 plays a major role as an MAG lipase and oncogene in nonsmall-cell lung cancer (NSCLC) (Tang et al., 2020). ABHD6 correlates significantly with the tumor lymph node metastasis stage, which indicates a poor overall survival in NSCLC patients. Notably, ABHD6 silencing reduces the migration and invasion of NSCLC cells *in vitro* as well as metastasis and tumor growth *in vivo*. In contrast, ectopic overexpression of ABHD6 stimulates its pathogenic potential (Tang et al., 2020). ABHD6 is highly expressed in human and murine pancreatic ductal adenocarcinoma (PDAC) tissues and cells. PDAC is one of the most lethal cancers with a high metastasis rate (Gruner et al., 2016), and pharmacological and genetic inhibition of ABHD6 confirms reduced PADC cell proliferation *in vitro* and tumor metastasis *in vivo* (Gruner et al., 2016). Hepatocellular carcinoma (HCC) is one of the most common malignant tumors, and Yu et al. conducted a systematic transcriptome study on HCC, determining that the methylation level of zinc finger and SCAN domain-containing 18 (ZSCAN18) can be used as an indicator for HCC prognosis and that ABHD6 is a potential tumor suppressor (Yu et al., 2016). These results indicate expression of ABHD6 in malignant tumors. Overall, it is very important to confirm whether ABHD6 acts as a diagnostic marker and therapeutic target for malignant tumors.

ABHD6 AND NEUROLOGICAL DISEASES

ABHD6 regulates eCB signaling by degrading the key lipid messenger 2-AG, which controls appetite, pain and learning and is associated with Alzheimer's disease and Parkinson's disease (Bleffert et al., 2019). Various studies have shown the therapeutic potential of targeting ABHD6 in the treatment of CNS diseases. Chronic pharmacological inhibition of MAGL is known to cause 2-AG overload, partial desensitization of CB_1R, and loss of cannabinoid-mediated effects in specific brain regions, leading to adverse side effects such as low activity and hyperreflexia (Schlosburg et al., 2010). In contrast to MAGL targeting, genetic or pharmacological blockade of ABHD6 results in moderate accumulation of 2-AG without CB1-related side effects (Alhouayek et al., 2013; Deng and Li, 2020b). Therefore, inhibition of ABHD6 may help in preventing CB_1R desensitization, making ABHD6 a promising new pharmacological target for the treatment of neurological diseases (**Table 1**).

ABHD6 and TBI

ABHD6 inhibitors are beneficial to patients with traumatic brain injury (TBI). In TBI, secondary injury mediated by excitotoxicity, neuroinflammation, and oxidative stress is partially a result of an insufficient increase in 2-AG that fails to counteract these pathological processes (Schurman and Lichtman, 2017). WWL-70, an ABHD6 inhibitor, improves motor coordination and working memory performance in mice with TBI but does not affect spatial learning or memory impairment. Although WWL-70 has been used to explore the role of ABHD6 inhibition in TBI, genetic tools and more selective ABHD6 inhibitors need to be applied for verification (Tchantchou and Zhang, 2013).

TABLE 1 | Overview of reported neurological disease treatments targeting ABHD6.

Disease	Therapeutic methods	Therapeutic effect
Traumatic Brain Injury (TBI)	ABHD6 Inhibitor (WWL-70)	improved motor coordination and working memory performance (mouse model)
Multiple Sclerosis (MS)	ABHD6 Inhibitor (WWL-70, KT-182)	reduced production of iNOS, COX-2, TNF-a and IL-1b, as well as phosphorylation of NF-kB (mouse model)
Epilepsy	ABHD6 Inhibitor (WWL-123)	significantly decreased seizure frequency (mouse model)
Psychiatric Disorders	Transcriptional Inhibition of ABHD6	terminating the stress response and inhibiting excitation after anxiety (mouse model)
Neuropathic Pain	ABHD6 Inhibitor (WWL-70)	significantly reduced thermal hyperalgesia and mechanical allodynia (mouse model)

ABHD6 and Multiple Sclerosis

Multiple sclerosis (MS) is a chronic inflammatory disease that involves demyelination and axonal degeneration (Faissner et al., 2019). The histopathological manifestations of MS involve immune-dependent attack of oligodendrocytes and primary oligodendrocyte death (Jakel et al., 2019). The ECS plays a key role in the control of autoimmune demyelination. Cannabinoid drugs have therapeutic potential for MS patients (Goncalves and Dutra, 2019), but they also have limitations. Within this context, there is increasing evidence that hydrolysis of 2-AG, a major eCB, may tip the benefit-risk balance in favor of the use of 2-AG over the use of existing cannabinoid drugs for MS treatment (Manterola et al., 2018a). Based on the observation that WWL-70 plays a protective anti-inflammatory role in experimental autoimmune encephalomyelitis (EAE), blocking ABHD6 is considered to be a new strategy for the treatment of MS. Furthermore, Wen et al. found that inhibition of ABHD6 in an MS mouse model can improve the clinical symptoms of cerebral hemorrhage, indicating the therapeutic effect of targeting ABHD6 on MS (Wen et al., 2015). Nevertheless, recent data indicate that ABHD6 blockade exerts only modest therapeutic effects against autoimmune demyelination, which calls into question its utility as a novel therapeutic target in MS (Manterola et al., 2018b).

ABHD6 and Epilepsy

Pharmacological inhibition of ABHD6 has an antiepileptic role in pentylenetetrazol-induced epilepsy and spontaneous epilepsy mouse models (Naydenov et al., 2014). Studies have shown that ABHD6 blockers regulate activity-dependent 2-AG production and subsequent CB_1R activation, which is characteristic of some forms of epilepsy (Marrs et al., 2010). Inhibition of ABHD6 by WWL-123 significantly reduces the frequency of chemically and genetically induced seizures in mice (Naydenov et al., 2014), though this inhibitory effect that reduces seizure frequency is likely due to increased GABAA receptor activity and not CB_1R or CB_2R activation. This suggests that ABHD6 inhibitors inhibit excessive excitatory transmission in epileptic seizures through two mechanisms, providing a new entry point for clinical treatment. For example, ABHD6 elevates the level of endogenous ligand 2-AG, not that of the GABAA receptor, or it can allosterically increase GABAA receptor signal transduction, and not directly target receptor-binding sites. In either case, the mechanism reduces treatment tolerance.

ABHD6 and Psychiatric Disorders

Over the past decade, much evidence has consistently strengthened the link between life stress and the prevalence of mood and anxiety disorders (Pizzagalli, 2014). Although acute environmental stress rarely causes long-term neurophysiological or behavioral changes (Rusconi and Battaglioli, 2018), chronic stress has a strong toxic effect on glutamatergic synapses (Yang et al., 2020). Physiological changes caused by chronic stress are considered to be the core characteristics of neuropsychiatric disorders (Zhang et al., 2019), and the ECS plays a key role in the homeostasis of acute stress. In particular, stress induces an increase in 2-AG synthesis (Morena et al., 2016). 2-AG stimulates presynaptic CB_1R and inhibits glutamate release, terminating the stress response and inhibiting excitation after anxiety. Longaretti et al. revealed that ECS-mediated synaptic regulation is mediated by transcriptional inhibition of ABHD6 and MAGL in response to acute psychosocial stress in the mouse hippocampus (Longaretti et al., 2020a). This process is coordinated by the epigenetic corepressor lysine-specific demethylase 1A (LSD1, also named KDM1A), which directly interacts with the promoter regulatory regions of the ABHD6 and MAGL genes (Longaretti et al., 2020b).

ABHD6 and Pain

Wen et al. have shown that WWL-70 can significantly reduce thermal hyperalgesia and mechanical allodynia induced by chronic constriction injury (CCI) (Wen et al., 2018). Notably, no cannabinoid receptor antagonist to date is able to reverse the anti-injury and anti-inflammatory effects of WWL-70, suggesting that a novel mechanism is involved in the antinociceptive effect of the 2-AG catabolic enzyme ABHD6 inhibitor WWL-70. Indeed, WWL-70 treatment does not alter phosphorylation levels of 2-AG, AA or phospholipase A2 (cPLA2) in injured sciatic nerves but significantly inhibits production of prostaglandin E2 (PGE2) and expression of COX-2 and prostaglandin E synthase 2 (PGES2) (Wen et al., 2018). Because AA production and cPLA2 phosphorylation are not affected by WWL-70, it has been speculated that this inhibitor may interfere with the eicosanoid signaling cascade downstream of AA production by inhibiting prostaglandin synthase and prostanoid E (EP) receptor-mediated signal transduction. Hence, compared with COX inhibitors, such as nonsteroidal anti-inflammatory drugs (NSAIDs), which cause significant gastrointestinal and cardiovascular side effects, the use of WWL-70 may be a better treatment option for neuropathic pain.

CONCLUSION AND PERSPECTIVES

In the past decade, research on ABHD6 has enabled us to initially understand its molecular mechanism and biological function in the CNS. Furthermore, by employing ABHD6 inhibitors, we have been able to explore the potential effect of ABHD6 in the treatment of CNS diseases.

The number of signaling lipids and interacting proteins regulated by ABHD6 suggests that it has multiple functions and is positioned as a key molecular hub for regulating multiple signaling systems. Previous studies have provided a solid foundation for the establishment of this enzyme as a bona fide member of the ECS; however, ABHD6 regulates additional signaling systems through different mechanisms independent of eCBs, including GABAA and AMPAR.

Recent studies have reported that targeting ABHD6 may have many therapeutic benefits in the treatment of CNS diseases. First, ABHD6 can control the availability of 2-AG and subsequent activation of CB_1R, suggesting the therapeutic potential of targeting ABHD6 in epilepsy. Nevertheless, further solid experiments are still needed to thoroughly explore the exact mechanism before ABHD6 inhibitors are applied in the treatment of epilepsy. In addition, selective ABHD6 inhibitors have been found to have the potential to ameliorate TBI and other neurological and neurodegenerative diseases. Although ABHD6 inhibitors can improve the clinical symptoms of MS in animal models, only a moderate therapeutic effect in humans has been shown. Therefore, using ABHD6 as a drug target for MS remains controversial.

Concerning the physiological function of ABHD6 outside the CNS, ABHD6 inhibitors may have therapeutic effects on metabolic disorders. For example, the role of ABHD6 in lipid metabolism suggests that some peripheral diseases may be attenuated by targeting ABHD6. Additionally, ABHD6 inhibition may have potential in anticancer therapy; studies have shown that this enzyme is highly expressed in several tumors, though the exact role of ABHD6 in cancer remains unclear. In the future, it will be imperative to comprehensively and systematically study the role of ABHD6 in cancer.

Because ABHD6 is widely expressed, its physiological and pathophysiological roles in different tissues need to be thoroughly elucidated in cell, animal and clinical studies. Overall, ABHD6 expression and function in different cells of the CNS have not been fully elucidated, especially in astrocytes and microglia. Furthermore, although ABHD6 is highly expressed in the brain, experiments on its activity in brain homogenates have indicated that it is responsible for only a small portion of the 2-AG that is, hydrolyzed. What are the main functional lipids of ABHD6 metabolism? With high mortality and morbidity, ischemic stroke has become a major health challenge. Activation of the ECS can alleviate cerebral ischemia injury, for which the initiating factor is energy deficiency, and it needs to be determined whether energy deficiency after cerebral ischemia changes CPT1 regulation of ABHD6 enzyme activity. In summary, in-depth exploration of the ABHD6 mechanism of action in the CNS will provide not only a new theoretical basis for the occurrence and development of CNS diseases but also a new target for their treatment.

AUTHOR CONTRIBUTIONS

All authors listed have made a substantial, direct, and intellectual contribution to the work and approved it for publication.

FUNDING

This work was supported by the National Natural Science Foundation of China (nos. 81871023, 82171458, 81771322, 82171363, 82171321) and the Youth Nova Program of Shaanxi (no. 2021KJXX-19).

REFERENCES

Alhouayek, M., Masquelier, J., Cani, P. D., Lambert, D. M., and Muccioli, G. G. (2013). Implication of the Anti-inflammatory Bioactive Lipid Prostaglandin D2-Glycerol Ester in the Control of Macrophage Activation and Inflammation by ABHD6. *Proc. Natl. Acad. Sci. U S A.* 110 (43), 17558–17563. doi:10.1073/pnas.1314017110

Baggelaar, M. P., van Esbroeck, A. C., van Rooden, E. J., Florea, B. I., Overkleeft, H. S., Marsicano, G., et al. (2017). Chemical Proteomics Maps Brain Region Specific Activity of Endocannabinoid Hydrolases. *ACS Chem. Biol.* 12 (3), 852–861. doi:10.1021/acschembio.6b01052

Bleffert, F., Granzin, J., Gohlke, H., Batra-Safferling, R., Jaeger, K. E., and Kovacic, F. (2019). Pseudomonas aeruginosa Esterase PA2949, a Bacterial Homolog of the Human Membrane Esterase ABHD6: Expression, Purification and Crystallization. *Acta Crystallogr. F Struct. Biol. Commun.* 75 (Pt 4), 270–277. doi:10.1107/S2053230X19002152

Brechet, A., Buchert, R., Schwenk, J., Boudkkazi, S., Zolles, G., Siquier-Pernet, K., et al. (2017). AMPA-receptor Specific Biogenesis Complexes Control Synaptic Transmission and Intellectual Ability. *Nat. Commun.* 8, 15910. doi:10.1038/ncomms15910

Busquets-Garcia, A., Desprez, T., Metna-Laurent, M., Bellocchio, L., Marsicano, G., and Soria-Gomez, E. (2015). Dissecting the Cannabinergic Control of Behavior: The where Matters. *Bioessays* 37 (11), 1215–1225. doi:10.1002/bies.201500046

Cao, J. K., Kaplan, J., and Stella, N. (2019). ABHD6: Its Place in Endocannabinoid Signaling and beyond. *Trends Pharmacol. Sci.* 40 (4), 267–277. doi:10.1016/j.tips.2019.02.002

Caron, A., Lee, S., Elmquist, J. K., and Gautron, L. (2018). Leptin and Brain-Adipose Crosstalks. *Nat. Rev. Neurosci.* 19 (3), 153–165. doi:10.1038/nrn.2018.7

Chen, S., and Gouaux, E. (2019). Structure and Mechanism of AMPA Receptor - Auxiliary Protein Complexes. *Curr. Opin. Struct. Biol.* 54, 104–111. doi:10.1016/j.sbi.2019.01.011

Chevaleyre, V., Takahashi, K. A., and Castillo, P. E. (2006). Endocannabinoid-mediated Synaptic Plasticity in the CNS. *Annu. Rev. Neurosci.* 29, 37–76. doi:10.1146/annurev.neuro.29.051605.112834

Colmers, P. L. W., and Bains, J. S. (2018). Presynaptic mGluRs Control the Duration of Endocannabinoid-Mediated DSI. *J. Neurosci.* 38 (49), 10444–10453. doi:10.1523/JNEUROSCI.1097-18.2018

Cristino, L., Bisogno, T., and Di Marzo, V. (2020). Cannabinoids and the Expanded Endocannabinoid System in Neurological Disorders. *Nat. Rev. Neurol.* 16 (1), 9–29. doi:10.1038/s41582-019-0284-z

Deng, H., and Li, W. (2020a). Monoacylglycerol Lipase Inhibitors: Modulators for Lipid Metabolism in Cancer Malignancy, Neurological and Metabolic Disorders. *Acta Pharm. Sin B* 10 (4), 582–602. doi:10.1016/j.apsb.2019.10.006

Deng, H., and Li, W. (2020b). Therapeutic Potential of Targeting α/β-Hydrolase Domain-Containing 6 (ABHD6). *Eur. J. Med. Chem.* 198, 112353. doi:10.1016/j.ejmech.2020.112353

Dócs, K., Mészár, Z., Gonda, S., Kiss-Szikszai, A., Holló, K., Antal, M., et al. (2017). The Ratio of 2-AG to its Isomer 1-AG as an Intrinsic Fine Tuning Mechanism of CB1 Receptor Activation. *Front Cel Neurosci* 11, 39. doi:10.3389/fncel.2017.00039

Drehmer, M. N., Muniz, Y. C. N., Marrero, A. R., and Löfgren, S. E. (2019). Gene Expression of ABHD6, a Key Factor in the Endocannabinoid System, Can Be Modulated by Female Hormones in Human Immune Cells. *Biochem. Genet.* 57 (1), 35–45. doi:10.1007/s10528-018-9871-8

Faissner, S., Plemel, J. R., Gold, R., and Yong, V. W. (2019). Progressive Multiple Sclerosis: from Pathophysiology to Therapeutic Strategies. *Nat. Rev. Drug Discov.* 18 (12), 905–922. doi:10.1038/s41573-019-0035-2

Fisette, A., Tobin, S., Décarie-Spain, L., Bouyakdan, K., Peyot, M. L., Madiraju, S. R. M., et al. (2016). α/β-Hydrolase Domain 6 in the Ventromedial Hypothalamus Controls Energy Metabolism Flexibility. *Cell Rep* 17 (5), 1217–1226. doi:10.1016/j.celrep.2016.10.004

Ghosh, A., Comerota, M. M., Wan, D., Chen, F., Propson, N. E., Hwang, S. H., et al. (2020). An Epoxide Hydrolase Inhibitor Reduces Neuroinflammation in a Mouse Model of Alzheimer's Disease. *Sci. Transl Med.* 12 (573). eabb1206. doi:10.1126/scitranslmed.abb1206

Gokce, O., Stanley, G. M., Treutlein, B., Neff, N. F., Camp, J. G., Malenka, R. C., et al. (2016). Cellular Taxonomy of the Mouse Striatum as Revealed by Single-Cell RNA-Seq. *Cel Rep* 16 (4), 1126–1137. doi:10.1016/j.celrep.2016.06.059

Gonçalves, E. D., and Dutra, R. C. (2019). Cannabinoid Receptors as Therapeutic Targets for Autoimmune Diseases: where Do We Stand. *Drug Discov. Today* 24 (9), 1845–1853. doi:10.1016/j.drudis.2019.05.023

Grüner, B. M., Schulze, C. J., Yang, D., Ogasawara, D., Dix, M. M., Rogers, Z. N., et al. (2016). An *In Vivo* Multiplexed Small-Molecule Screening Platform. *Nat. Methods* 13 (10), 883–889. doi:10.1038/nmeth.3992

Hubler, M. J., and Kennedy, A. J. (2016). Role of Lipids in the Metabolism and Activation of Immune Cells. *J. Nutr. Biochem.* 34, 1–7. doi:10.1016/j.jnutbio.2015.11.002

Jäkel, S., Agirre, E., Mendanha Falcão, A., van Bruggen, D., Lee, K. W., Knuesel, I., et al. (2019). Altered Human Oligodendrocyte Heterogeneity in Multiple Sclerosis. *Nature* 566 (7745), 543–547. doi:10.1038/s41586-019-0903-2

Joshi, N., and Onaivi, E. S. (2019). Endocannabinoid System Components: Overview and Tissue Distribution. *Adv. Exp. Med. Biol.* 1162, 1–12. doi:10.1007/978-3-030-21737-2_1

Jung, K.-M., Lin, L., and Piomelli, D. (2021). The Endocannabinoid System in the Adipose Organ. *Rev. Endocr. Metab. Disord.*. doi:10.1007/s11154-020-09623-z

Kilaru, A., and Chapman, K. D. (2020). The Endocannabinoid System. *Essays Biochem.* 64 (3), 485–499. doi:10.1042/EBC20190086

Kind, L., and Kursula, P. (2019). Structural Properties and Role of the Endocannabinoid Lipases ABHD6 and ABHD12 in Lipid Signalling and Disease. *Amino Acids* 51 (2), 151–174. doi:10.1007/s00726-018-2682-8

Larsson, S. C., Carter, P., Vithayathil, M., Mason, A. M., Michaëlsson, K., Baron, J. A., et al. (2021). Genetically Predicted Plasma Phospholipid Arachidonic Acid Concentrations and 10 Site-specific Cancers in UK Biobank and Genetic Consortia Participants: A Mendelian Randomization Study. *Clin. Nutr.* 40 (5), 3332–3337. doi:10.1016/j.clnu.2020.11.004

Lee, J., and Wolfgang, M. J. (2012). Metabolomic Profiling Reveals a Role for CPT1c in Neuronal Oxidative Metabolism. *BMC Biochem.* 13, 23. doi:10.1186/1471-2091-13-23

Li, F., Fei, X., Xu, J., and Ji, C. (2009). An Unannotated Alpha/beta Hydrolase Superfamily Member, ABHD6 Differentially Expressed Among Cancer Cell Lines. *Mol. Biol. Rep.* 36 (4), 691–696. doi:10.1007/s11033-008-9230-7

Long, J. Z., and Cravatt, B. F. (2011). The Metabolic Serine Hydrolases and Their Functions in Mammalian Physiology and Disease. *Chem. Rev.* 111 (10), 6022–6063. doi:10.1021/cr200075y

Longaretti, A., Forastieri, C., Gabaglio, M., Rubino, T., Battaglioli, E., and Rusconi, F. (2020a). Termination of Acute Stress Response by the Endocannabinoid System Is Regulated through Lysine-specific Demethylase 1-mediated Transcriptional Repression of 2-AG Hydrolases ABHD6 and MAGL. *J. Neurochem.* 155 (1), 98–110. doi:10.1111/jnc.15000

Longaretti, A., Forastieri, C., Toffolo, E., Caffino, L., Locarno, A., Misevičiūtė, I., et al. (2020b). LSD1 Is an Environmental Stress-Sensitive Negative Modulator of the Glutamatergic Synapse. *Neurobiol. Stress* 13, 100280. doi:10.1016/j.ynstr.2020.100280

López, D. E., and Ballaz, S. J. (2020). The Role of Brain Cyclooxygenase-2 (Cox-2) beyond Neuroinflammation: Neuronal Homeostasis in Memory and Anxiety. *Mol. Neurobiol.* 57 (12), 5167–5176. doi:10.1007/s12035-020-02087-x

Lord, C. C., Thomas, G., and Brown, J. M. (2013). Mammalian Alpha Beta Hydrolase Domain (ABHD) Proteins: Lipid Metabolizing Enzymes at the Interface of Cell Signaling and Energy Metabolism. *Biochim. Biophys. Acta* 1831 (4), 792–802. doi:10.1016/j.bbalip.2013.01.002

Lu, H. C., and Mackie, K. (2021). Review of the Endocannabinoid System. *Biol. Psychiatry Cogn. Neurosci. Neuroimaging* 6 (6), 607–615. doi:10.1016/j.bpsc.2020.07.016

Maier, S., Staffler, G., Hartmann, A., Höck, J., Henning, K., Grabusic, K., et al. (2006). Cellular Target Genes of Epstein-Barr Virus Nuclear Antigen 2. *J. Virol.* 80 (19), 9761–9771. doi:10.1128/JVI.00665-06

Manterola, A., Bernal-Chico, A., Cipriani, R., Canedo-Antelo, M., Moreno-García, Á., Martín-Fontecha, M., et al. (2018a). Deregulation of the Endocannabinoid System and Therapeutic Potential of ABHD6 Blockade in the Cuprizone Model of Demyelination. *Biochem. Pharmacol.* 157, 189–201. doi:10.1016/j.bcp.2018.07.042

Manterola, A., Bernal-Chico, A., Cipriani, R., Ruiz, A., Pérez-Samartín, A., Moreno-Rodríguez, M., et al. (2018b). Re-examining the Potential of Targeting ABHD6 in Multiple Sclerosis: Efficacy of Systemic and Peripherally Restricted Inhibitors in Experimental Autoimmune Encephalomyelitis. *Neuropharmacology* 141, 181–191. doi:10.1016/j.neuropharm.2018.08.038

Marrs, W. R., Blankman, J. L., Horne, E. A., Thomazeau, A., Lin, Y. H., Coy, J., et al. (2010). The Serine Hydrolase ABHD6 Controls the Accumulation and Efficacy of 2-AG at Cannabinoid Receptors. *Nat. Neurosci.* 13 (8), 951–957. doi:10.1038/nn.2601

Marrs, W. R., Horne, E. A., Ortega-Gutierrez, S., Cisneros, J. A., Xu, C., Lin, Y. H., et al. (2011). Dual Inhibition of Alpha/beta-Hydrolase Domain 6 and Fatty Acid Amide Hydrolase Increases Endocannabinoid Levels in Neurons. *J. Biol. Chem.* 286 (33), 28723–28728. doi:10.1074/jbc.M110.202853

Martínez-Torres, S., Cutando, L., Pastor, A., Kato, A., Sakimura, K., de la Torre, R., et al. (2019). Monoacylglycerol Lipase Blockade Impairs fine Motor Coordination and Triggers Cerebellar Neuroinflammation through Cyclooxygenase-2. *Brain Behav. Immun.* 81, 399–409. doi:10.1016/j.bbi.2019.06.036

Max, D., Hesse, M., Volkmer, I., and Staege, M. S. (2009). High Expression of the Evolutionarily Conserved Alpha/beta Hydrolase Domain Containing 6 (ABHD6) in Ewing Tumors. *Cancer Sci.* 100 (12), 2383–2389. doi:10.1111/j.1349-7006.2009.01347.x

Mecha, M., Feliú, A., Machín, I., Cordero, C., Carrillo-Salinas, F., Mestre, L., et al. (2018). 2-AG Limits Theiler's Virus Induced Acute Neuroinflammation by Modulating Microglia and Promoting MDSCs. *Glia* 66 (7), 1447–1463. doi:10.1002/glia.23317

Miralpeix, C., Reguera, A. C., Fosch, A., Casas, M., Lillo, J., Navarro, G., et al. (2021). Carnitine Palmitoyltransferase 1C Negatively Regulates the Endocannabinoid Hydrolase ABHD6 in Mice, Depending on Nutritional Status. *Br. J. Pharmacol.* 178 (7), 1507–1523. doi:10.1111/bph.15377

Morena, M., Patel, S., Bains, J. S., and Hill, M. N. (2016). Neurobiological Interactions between Stress and the Endocannabinoid System. *Neuropsychopharmacology* 41 (1), 80–102. doi:10.1038/npp.2015.166

Moreno-Luna, R., Esteban, P. F., Paniagua-Torija, B., Arevalo-Martin, A., Garcia-Ovejero, D., and Molina-Holgado, E. (2021). Heterogeneity of the Endocannabinoid System between Cerebral Cortex and Spinal Cord Oligodendrocytes. *Mol. Neurobiol.* 58 (2), 689–702. doi:10.1007/s12035-020-02148-1

Muccioli, G. G., Xu, C., Odah, E., Cudaback, E., Cisneros, J. A., Lambert, D. M., et al. (2007). Identification of a Novel Endocannabinoid-Hydrolyzing Enzyme Expressed by Microglial Cells. *J. Neurosci.* 27 (11), 2883–2889. doi:10.1523/JNEUROSCI.4830-06.2007

Navia-Paldanius, D., Savinainen, J. R., and Laitinen, J. T. (2012). Biochemical and Pharmacological Characterization of Human α/β-hydrolase Domain Containing 6 (ABHD6) and 12 (ABHD12). *J. Lipid Res.* 53 (11), 2413–2424. doi:10.1194/jlr.M030411

Naydenov, A. V., Horne, E. A., Cheah, C. S., Swinney, K., Hsu, K. L., Cao, J. K., et al. (2014). ABHD6 Blockade Exerts Antiepileptic Activity in PTZ-Induced Seizures and in Spontaneous Seizures in R6/2 Mice. *Neuron* 83 (2), 361–371. doi:10.1016/j.neuron.2014.06.030

Nicholson, J., Azim, S., Rebecchi, M. J., Galbavy, W., Feng, T., Reinsel, R., et al. (2015). Leptin Levels Are Negatively Correlated with 2-arachidonoylglycerol in the Cerebrospinal Fluid of Patients with Osteoarthritis. *PLoS One* 10 (4), e0123132. doi:10.1371/journal.pone.0123132

Noguchi, K., Kadekawa, K., Nishijima, S., Sakanashi, M., Okitsu-Sakurayama, S., Higa-Nakamine, S., et al. (2021). Phenotypic Characterization of the Endocannabinoid-Degrading Enzyme Alpha/Beta-Hydrolase Domain 6 Knockout Rat. *Cannabis Cannabinoid Res.* [Epub ahead of Print]. doi:10.1089/can.2021.0011

Obici, S., Feng, Z., Arduini, A., Conti, R., and Rossetti, L. (2003). Inhibition of Hypothalamic Carnitine Palmitoyltransferase-1 Decreases Food Intake and Glucose Production. *Nat. Med.* 9 (6), 756–761. doi:10.1038/nm873

Owens, R. A., Mustafa, M. A., Ignatowska-Jankowska, B. M., Damaj, M. I., Beardsley, P. M., Wiley, J. L., et al. (2017). Inhibition of the Endocannabinoid-Regulating Enzyme Monoacylglycerol Lipase Elicits a CB1 Receptor-Mediated Discriminative Stimulus in Mice. *Neuropharmacology* 125, 80–86. doi:10.1016/j.neuropharm.2017.06.032

Pizzagalli, D. A. (2014). Depression, Stress, and Anhedonia: toward a Synthesis and Integrated Model. *Annu. Rev. Clin. Psychol.* 10, 393–423. doi:10.1146/annurev-clinpsy-050212-185606

Poursharifi, P., Attané, C., Mugabo, Y., Al-Mass, A., Ghosh, A., Schmitt, C., et al. (2020). Adipose ABHD6 Regulates Tolerance to Cold and Thermogenic Programs. *JCI Insight* 5 (24), 140294. doi:10.1172/jci.insight.140294

Poursharifi, P., Madiraju, S. R. M., and Prentki, M. (2017). Monoacylglycerol Signalling and ABHD6 in Health and Disease. *Diabetes Obes. Metab.* 19 (Suppl. 1), 76–89. doi:10.1111/dom.13008

Rahaman, O., Bhattacharya, R., Liu, C. S. C., Raychaudhuri, D., Ghosh, A. R., Bandopadhyay, P., et al. (2019). Cutting Edge: Dysregulated Endocannabinoid-Rheostat for Plasmacytoid Dendritic Cell Activation in a Systemic Lupus Endophenotype. *J. Immunol.* 202 (6), 1674–1679. doi:10.4049/jimmunol.1801521

Reilly, P. T., and Mak, T. W. (2012). Molecular Pathways: Tumor Cells Co-opt the Brain-specific Metabolism Gene CPT1C to Promote Survival. *Clin. Cancer Res.* 18 (21), 5850–5855. doi:10.1158/1078-0432.CCR-11-3281

Ricciotti, E., and FitzGerald, G. A. (2011). Prostaglandins and Inflammation. *Arterioscler Thromb. Vasc. Biol.* 31 (5), 986–1000. doi:10.1161/ATVBAHA.110.207449

Rusconi, F., and Battaglioli, E. (2018). Acute Stress-Induced Epigenetic Modulations and Their Potential Protective Role toward Depression. *Front. Mol. Neurosci.* 11, 184. doi:10.3389/fnmol.2018.00184

Sanchez-Macedo, N., Feng, J., Faubert, B., Chang, N., Elia, A., Rushing, E. J., et al. (2013). Depletion of the Novel P53-Target Gene Carnitine Palmitoyltransferase 1C Delays Tumor Growth in the Neurofibromatosis Type I Tumor Model. *Cell Death Differ* 20 (4), 659–668. doi:10.1038/cdd.2012.168

Savinainen, J. R., Saario, S. M., and Laitinen, J. T. (2012). The Serine Hydrolases MAGL, ABHD6 and ABHD12 as Guardians of 2-arachidonoylglycerol Signalling through Cannabinoid Receptors. *Acta Physiol. (Oxf)* 204 (2), 267–276. doi:10.1111/j.1748-1716.2011.02280.x

Schlosburg, J. E., Blankman, J. L., Long, J. Z., Nomura, D. K., Pan, B., Kinsey, S. G., et al. (2010). Chronic Monoacylglycerol Lipase Blockade Causes Functional Antagonism of the Endocannabinoid System. *Nat. Neurosci.* 13 (9), 1113–1119. doi:10.1038/nn.2616

Schurman, L. D., and Lichtman, A. H. (2017). Endocannabinoids: A Promising Impact for Traumatic Brain Injury. *Front. Pharmacol.* 8, 69. doi:10.3389/fphar.2017.00069

Schwenk, J., Boudkkazi, S., Kocylowski, M. K., Brechet, A., Zolles, G., Bus, T., et al. (2019). An ER Assembly Line of AMPA-Receptors Controls Excitatory Neurotransmission and its Plasticity. *Neuron* 104 (4), 680–e9. doi:10.1016/j.neuron.2019.08.033

Straiker, A., Hu, S. S., Long, J. Z., Arnold, A., Wager-Miller, J., Cravatt, B. F., et al. (2009). Monoacylglycerol Lipase Limits the Duration of Endocannabinoid-Mediated Depolarization-Induced Suppression of Excitation in Autaptic Hippocampal Neurons. *Mol. Pharmacol.* 76 (6), 1220–1227. doi:10.1124/mol.109.059030

Straiker, A., and Mackie, K. (2009). Cannabinoid Signaling in Inhibitory Autaptic Hippocampal Neurons. *Neuroscience* 163 (1), 190–201. doi:10.1016/j.neuroscience.2009.06.004

Straiker, A., and Mackie, K. (2007). Metabotropic Suppression of Excitation in Murine Autaptic Hippocampal Neurons. *J. Physiol.* 578 (Pt 3), 773–785. doi:10.1113/jphysiol.2006.117499

Sugiura, T., Kondo, S., Sukagawa, A., Nakane, S., Shinoda, A., Itoh, K., et al. (1995). 2-Arachidonoylglycerol: a Possible Endogenous Cannabinoid Receptor Ligand in Brain. *Biochem. Biophys. Res. Commun.* 215 (1), 89–97. doi:10.1006/bbrc.1995.2437

Tanaka, M., Moran, S., Wen, J., Affram, K., Chen, T., Symes, A. J., et al. (2017). WWL70 Attenuates PGE2 Production Derived from 2-arachidonoylglycerol in Microglia by ABHD6-independent Mechanism. *J. Neuroinflammation* 14 (1), 7. doi:10.1186/s12974-016-0783-4

Tang, Z., Xie, H., Heier, C., Huang, J., Zheng, Q., Eichmann, T. O., et al. (2020). Enhanced Monoacylglycerol Lipolysis by ABHD6 Promotes NSCLC Pathogenesis. *EBioMedicine* 53, 102696. doi:10.1016/j.ebiom.2020.102696

Tchantchou, F., and Zhang, Y. (2013). Selective Inhibition of Alpha/beta-Hydrolase Domain 6 Attenuates Neurodegeneration, Alleviates Blood Brain Barrier Breakdown, and Improves Functional Recovery in a Mouse Model of Traumatic Brain Injury. *J. Neurotrauma* 30 (7), 565–579. doi:10.1089/neu.2012.2647

Thomas, G., Betters, J. L., Lord, C. C., Brown, A. L., Marshall, S., Ferguson, D., et al. (2013). The Serine Hydrolase ABHD6 Is a Critical Regulator of the Metabolic Syndrome. *Cel Rep* 5 (2), 508–520. doi:10.1016/j.celrep.2013.08.047

Trostchansky, A., Wood, I., and Rubbo, H. (2021). Regulation of Arachidonic Acid Oxidation and Metabolism by Lipid Electrophiles. *Prostaglandins Other Lipid Mediat* 152, 106482. doi:10.1016/j.prostaglandins.2020.106482

van Esbroeck, A. C. M., Kantae, V., Di, X., van der Wel, T., den Dulk, H., Stevens, A. F., et al. (2019). Identification of α,β-Hydrolase Domain Containing Protein 6 as a Diacylglycerol Lipase in Neuro-2a Cells. *Front. Mol. Neurosci.* 12, 286. doi:10.3389/fnmol.2019.00286

Wei, M., Jia, M., Zhang, J., Yu, L., Zhao, Y., Chen, Y., et al. (2017). The Inhibitory Effect of α/β-Hydrolase Domain-Containing 6 (ABHD6) on the Surface Targeting of GluA2- and GluA3-Containing AMPA Receptors. *Front. Mol. Neurosci.* 10, 55. doi:10.3389/fnmol.2017.00055

Wei, M., Zhang, J., Jia, M., Yang, C., Pan, Y., Li, S., et al. (2016). α/β-Hydrolase Domain-Containing 6 (ABHD6) Negatively Regulates the Surface Delivery and Synaptic Function of AMPA Receptors. *Proc. Natl. Acad. Sci. U S A.* 113 (19), E2695–E2704. doi:10.1073/pnas.1524589113

Wen, J., Jones, M., Tanaka, M., Selvaraj, P., Symes, A. J., Cox, B., et al. (2018). WWL70 Protects against Chronic Constriction Injury-Induced Neuropathic Pain in Mice by Cannabinoid Receptor-independent Mechanisms. *J. Neuroinflammation* 15 (1), 9. doi:10.1186/s12974-017-1045-9

Wen, J., Ribeiro, R., Tanaka, M., and Zhang, Y. (2015). Activation of CB2 Receptor Is Required for the Therapeutic Effect of ABHD6 Inhibition in Experimental Autoimmune Encephalomyelitis. *Neuropharmacology* 99, 196–209. doi:10.1016/j.neuropharm.2015.07.010

Yang, F., Liu, Y., Chen, S., Dai, Z., Yang, D., Gao, D., et al. (2020). A GABAergic Neural Circuit in the Ventromedial Hypothalamus Mediates Chronic Stress-Induced Bone Loss. *J. Clin. Invest.* 130 (12), 6539–6554. doi:10.1172/JCI136105

Yu, C. B., Zhu, L. Y., Wang, Y. G., Li, F., Zhang, X. Y., and Dai, W. J. (2016). Systemic Transcriptome Analysis of Hepatocellular Carcinoma. *Tumour Biol.* 37 (10), 13323–13331. doi:10.1007/s13277-016-5286-5

Yuan, D., Wu, Z., and Wang, Y. (2016). Evolution of the Diacylglycerol Lipases. *Prog. Lipid Res.* 64, 85–97. doi:10.1016/j.plipres.2016.08.004

Zaugg, K., Yao, Y., Reilly, P. T., Kannan, K., Kiarash, R., Mason, J., et al. (2011). Carnitine Palmitoyltransferase 1C Promotes Cell Survival and Tumor Growth under Conditions of Metabolic Stress. *Genes Dev.* 25 (10), 1041–1051. doi:10.1101/gad.1987211

Zhang, J. Y., Liu, T. H., He, Y., Pan, H. Q., Zhang, W. H., Yin, X. P., et al. (2019). Chronic Stress Remodels Synapses in an Amygdala Circuit-specific Manner. *Biol. Psychiatry* 85 (3), 189–201. doi:10.1016/j.biopsych.2018.06.019

Zhao, S., Mugabo, Y., Ballentine, G., Attane, C., Iglesias, J., Poursharifi, P., et al. (2016). α/β-Hydrolase Domain 6 Deletion Induces Adipose Browning and

Prevents Obesity and Type 2 Diabetes. *Cel Rep* 14 (12), 2872–2888. doi:10.1016/j.celrep.2016.02.076

Zhong, P., Pan, B., Gao, X. P., Blankman, J. L., Cravatt, B. F., and Liu, Q. S. (2011). Genetic Deletion of Monoacylglycerol Lipase Alters Endocannabinoid-Mediated Retrograde Synaptic Depression in the Cerebellum. *J. Physiol.* 589 (Pt 20), 4847–4855. doi:10.1113/jphysiol.2011.215509

Zou, S., and Kumar, U. (2018). Cannabinoid Receptors and the Endocannabinoid System: Signaling and Function in the Central Nervous System. *Int. J. Mol. Sci.* 19 (3). doi:10.3390/ijms19030833

Conflict of Interest: The authors declare that the research was conducted in the absence of any commercial or financial relationships that could be construed as a potential conflict of interest.

Publisher's Note: All claims expressed in this article are solely those of the authors and do not necessarily represent those of their affiliated organizations, or those of the publisher, the editors and the reviewers. Any product that may be evaluated in this article, or claim that may be made by its manufacturer, is not guaranteed or endorsed by the publisher.

frontiers in Neuroscience

ORIGINAL RESEARCH
published: 21 December 2021
doi: 10.3389/fnins.2021.790546

In vivo Evidence for Brain Region-Specific Molecular Interactions Between Cannabinoid and Orexin Receptors

*Hye Ji J. Kim[1], Ayat Zagzoog[1], Anna Maria Smolyakova[1], Udoka C. Ezeaka[1], Michael J. Benko[1], Teagan Holt[1] and Robert B. Laprairie[1,2]**

[1] College of Pharmacy and Nutrition, University of Saskatchewan, Saskatoon, SK, Canada, [2] Department of Pharmacology, College of Medicine, Dalhousie University, Halifax, NS, Canada

OPEN ACCESS

Edited by:
Paula Morales, Institute of Medical Chemistry, Spanish National Research Council (CSIC), Spain

Reviewed by:
Fabrizio Sanna, University of Cagliari, Italy
Luigi Bellocchio, INSERM U1215 Neurocentre Magendie, France

***Correspondence:**
Robert B. Laprairie
robert.laprairie@usask.ca

Specialty section:
This article was submitted to Neuropharmacology, a section of the journal Frontiers in Neuroscience

Received: *06 October 2021*
Accepted: *02 December 2021*
Published: *21 December 2021*

Citation:
Kim HJJ, Zagzoog A, Smolyakova AM, Ezeaka UC, Benko MJ, Holt T and Laprairie RB (2021) In vivo Evidence for Brain Region-Specific Molecular Interactions Between Cannabinoid and Orexin Receptors. Front. Neurosci. 15:790546. doi: 10.3389/fnins.2021.790546

The endocannabinoid and orexin neuromodulatory systems serve key roles in many of the same biological functions such as sleep, appetite, pain processing, and emotional behaviors related to reward. The type 1 cannabinoid receptor (CB1R) and both subtypes of the orexin receptor, orexin receptor type 1 (OX1R) and orexin receptor type 2 (OX2R) are not only expressed in the same brain regions modulating these functions, but physically interact as heterodimers in recombinant and neuronal cell cultures. In the current study, male and female C57BL/6 mice were co-treated with the cannabinoid receptor agonist CP55,940 and either the OX2R antagonist TCS-OX2-29 or the dual orexin receptor antagonist (DORA) TCS-1102. Mice were then evaluated for catalepsy, body temperature, thermal anti-nociception, and locomotion, after which their brains were collected for receptor colocalization analysis. Combined treatment with the DORA TCS-1102 and CP55,940 potentiated catalepsy more than CP55,940 alone, but this effect was not observed for changes in body temperature, nociception, locomotion, or *via* selective OX2R antagonism. Co-treatment with CP55,940 and TCS-1102 also led to increased CB1R-OX1R colocalization in the ventral striatum. This was not seen following co-treatment with TCS-OX2-29, nor in CB1R-OX2R colocalization. The magnitude of effects following co-treatment with CP55,940 and either the DORA or OX2R-selective antagonist was greater in males than females. These data show that CB1R-OX1R colocalization in the ventral striatum underlies cataleptic additivity between CP55,940 and the DORA TCS-1102. Moreover, cannabinoid-orexin receptor interactions are sex-specific with regards to brain region and functionality. Physical or molecular interactions between these two systems may provide valuable insight into drug-drug interactions between cannabinoid and orexin drugs for the treatment of insomnia, pain, and other disorders.

Keywords: cannabinoid, cannabinoid receptor, receptor antagonist, orexin receptor, heterodimerization, colocalization, tetrad analysis, ventral striatum

INTRODUCTION

Endocannabinoid and orexin interdependence has been a topic of growing interest in the last two decades. Within the endocannabinoid system (ECS), lipid-based agonists, anandamide (AEA) and 2-arachidonoylglycerol (2-AG) primarily bind to 2 subtypes of the cannabinoid G protein-coupled receptors (GPCR), cannabinoid receptor type 1 (CB1R) and cannabinoid receptor type 2 (CB2R). The orexin system shares many physical and functional similarities with the ECS (Berrendero et al., 2018). It consists of the neuropeptides orexin A (OXA) and orexin B (OXB), which activate GPCRs, orexin receptor type 1 (OX1R) and type 2 (OX2R). Cannabinoid and orexin receptors are found in many of the same brain regions underlying complex behaviors such as sleep, appetite, and reward processing. In mice and humans, cannabinoid receptor (CBR) activation leads to sedative effects such as catalepsy, hypothermia, analgesia, and anti-locomotion (Metna-Laurent et al., 2017; Zagzoog et al., 2020, 2021). Orexin receptor activation increases arousal, body temperature, and modulates anti-nociception at the spinal and supraspinal levels (Yamanaka et al., 2003; Monda et al., 2005; Chiou et al., 2010). Dual orexin receptor antagonists (DORA) are emerging as safe and effective treatments for insomnia (Herring et al., 2019), while phytocannabinoids such as cannabidiol and Δ^9-tetrahydrocannabinol (Δ^9-THC), are used as off-label sleep aids as they affect the same sleep-wake neuropathways (Babson et al., 2017). Molecular and cellular interactions between these neuromodulatory systems have physiological implications in homeostasis, neurological and psychiatric disorders, as well as in drug-drug interactions between cannabinoid and orexin drugs.

Evidence for physical interactions between the endocannabinoid and orexin systems lies in the colocalization and potential heterodimerization of these two system's receptors (Jäntti et al., 2014; Berrendero et al., 2018). CB1R co-localizes with both OX1R and OX2R in the neocortex, hippocampus, thalamus, hypothalamus, amygdala, ventral tegmental area, periaqueductal gray, dorsal raphe nucleus, and deep cerebellar nuclei (Marcus et al., 2001; Mackie, 2005; Flores et al., 2014). Bioluminescence resonance energy transfer studies have found that OX1R and OX2R are capable of forming homo- and heterodimeric complexes with one another and with CB1R (Jäntti et al., 2014). Moreover, fluorescence resonance energy transfer imaging demonstrates that CB1R-OX1R heterodimers reside in intracellular vesicles following CB1R agonist-mediated receptor internalization (Ellis et al., 2006; Ward et al., 2011). In recombinant cells co-expressing these receptor subtypes, OX1R activity not only induces 2-AG synthesis, but it also potentiates extracellular-signal-regulated kinase (ERK) activity of these recombinant cells (Jäntti et al., 2014). The reverse has been shown, as CB1R activation increases OXA's potency to activate ERK in cells where CB1R and OX1R are co-localized and potentially heterodimerized (Hilairet et al., 2003). In addition to recombinant cells, CB1R-OX1R complexes have also been observed in embryonic mouse hypothalamic neurons, supporting the workings of these heterodimers *in vivo* (Imperatore et al., 2016).

Although CB1R-OX1R heterodimers have not previously been directly observed in animals, rodent studies in which cannabinoid and orexin compounds are co-administered have described unique physiological and behavioral outcomes based on (1) the receptor subtype targeted, and (2) separate versus combined compound treatments. Activating CBRs while blocking orexin receptors causes sedation or sleep-like effects (Flores et al., 2016; Petrunich-Rutherford and Calik, 2021). In contrast, acutely activating both cannabinoid and orexin receptors increases appetite (Mechoulam and Fride, 2001; Merroun et al., 2015) and reward sensitivity (Plaza-Zabala et al., 2012; Flores et al., 2014; Yazdi et al., 2015). Thus, cannabinoid and orexin receptors may potentiate one another in brain regions modulating appetite and reward, while having antagonistic interactions in regions underlying arousal and sleep. Dual control of these biological functions is receptor-subtype specific. Physiological and behavioral regulation of body temperature, nociception processing, locomotion, appetite, and cognition are thought to be primarily CB1R-dependent based on the higher abundance of CB1R compared to CB2R (Zanettini et al., 2011). Between the orexin receptor subtypes, persistent OX2R activity is believed to be more critical for maintaining arousal (Willie et al., 2003; Mieda et al., 2011) and caloric homeostasis (Funato et al., 2009). The combined observations of heterodimerization *in vitro*, existence in the same brain regions *in vivo*, and overlapping physiological effects of the ECS and orexin system support the hypothesis that co-manipulation of both systems will produce a fundamentally different outcome than targeting either system alone.

MATERIALS AND METHODS

Compounds

CP55,940 (Cat # 90084) and TCS-1102 (Cat # 18495) were purchased from Cayman Chemical Company (Ann Arbor, MI). TCS-OX2-29 was purchased from Abcam (Waltham, MA, Cat # 141316). All compounds were stored at −20°C until use. CP55,940 was first dissolved in 100% methanol, then added to a vehicle solution consisting of: 1 part ethanol, 1 part Kolliphor EL (MilliporeSigma, Oakville), and 18 parts 1 M phosphate-buffered saline (PBS) (Fisher, Waltham, MA). The concentration of stock solution used for CP55,940 varied based on animal weight and treatment dose. TCS-OX2-29 and TCS-1102 were first dissolved in a 10% DMSO solution in PBS, then added to a vehicle solution consisting of 1 part ethanol, 1 part Kolliphor EL, and 18 parts PBS. TCS-OX2-29 was prepared as a 5 mg/mL stock solution. TCS-1102 was prepared as a 1.5 mg/mL stock solution. All compounds were prepared at room temperature, after which they were stored at 4°C overnight before use the next morning.

Animals and Tetrad Testing

Adult male and female C57BL/6 mice aged 6–12 weeks (mean weight of males: 22 ± 0.3 g; mean weight of females: 20 ± 0.3 g) were purchased from Charles River Labs (Senneville, QC). Mice were group housed (males: 3 per cage; females: 5 per cage) with *ad libitum* access to food, water, and environmental enrichment. All mice were maintained on a 12 h light:dark cycle

(07:00-19:00/19:00-07:00). Mice were randomly designated to receive 2 intraperitoneal (i.p.) injections (1 on each side) of the following treatment combinations: vehicle and CP55,940 at 5 doses (0.1, 0.3, 1, and 3 mg/kg), vehicle and TCS-OX2-29 at 4 doses (1, 10, 18, and 30 mg/kg), vehicle and TCS-1102 at 4 doses (0.1, 0.3, 1, and 10 mg/kg), 1 mg/kg CP55,940 and TCS-OX2-29 (1, 10, 18, and 30 mg/kg) at 4 doses, or 1 mg/kg CP55,940 and TCS-1102 (0.1, 0.3, 1, and 10 mg/kg) at 4 doses, totaling 22 treatment groups (n = 6 per group). CP55,940 doses were based on previously published studies from our group in the same battery of *in vivo* assays (Zagzoog et al., 2020, 2021). TCS-OX2-29 doses were chosen to build on the work of Flores et al. (2016), who had tested 10 mg/kg of TCS-OX2-29 in mice. Because TCS-1102 has not previously been assessed in the tetrad, doses of TCS-1102 were also chosen based on Flores et al. (2016). For combination treatments, 1 mg/kg CP55,940 was chosen as an approximation of the ED_{80} for this compound. These doses were piloted by our group for safety and effect prior to data collection for the current study. These 22 treatment groups were tested in both males and females, totaling 264 mice used throughout the study. All protocols were in accordance with the guidelines detailed by the Canadian Council on Animal Care (CCAC; Ottawa ON: Vol. 1, second Ed., 1993; Vol. 2, 1984) and approved by the Animal Research Ethics Board and the Scientific Merit Review Committee for Animal Behavior at the University of Saskatchewan. In keeping with the Animal Research: Reporting of *In Vivo* Experiments (ARRIVE) guidelines, power analyses were conducted to determine the minimum number of mice required for the study, and mice were purchased, rather than bred, to limit animal waste (Kilkenny et al., 2010).

Tetrad testing commenced 10 min after i.p. injections with the ring holding assay to measure catalepsy. For this assay, mice were placed on the ring apparatus such that their forepaws clasped the 5 mm ring positioned 5 cm above the surface of the testing platform. The length of time that the ring was clasped was recorded (s). The trial was completed when the mouse turned its head or body, made 3 consecutive escape attempts, or at 60 s of immobility [i.e., maximum possible effect (MPE) = 60 s]. Internal body temperature was recorded 15 min after the injections *via* a rectal thermometer (°C). Thermal antinociception was assessed by the tail flick latency test 20 min following the injections. Mice were restrained with their tails placed $\sim$ 1 cm into 52 $\pm$ 2°C water. The time until the tail was removed from the water was recorded as the tail flick latency (s). Tails were removed after 20 s if they had not been removed already (i.e., MPE = 20 s). Locomotion was measured in the open field test 25 min following the injections. Mice were placed in the 55 cm $\times$ 55 cm square-shaped open field for 10 min, during which they were free to roam. Distance traveled (m) and average velocity (cm/s) were measured with EthoVision XT (Noldus Information Technology Inc., Leesburg, VA). Distance and velocity scores were then normalized and expressed as a percentage of vehicle means (%Vehicle). For statistical processing, tetrad scores were averaged between mice in the same drug treatment group (Zagzoog et al., 2020, 2021).

Tissue Perfusion and Immunohistochemistry

A separate set of mice were euthanized, and their brains were collected 30 min after i.p. injections. This tissue collection time was based on the tetrad timeline, as treated mice finished the tetrad test 30–35 min post-injection. Mice were placed in a rodent vapor chamber, which delivered a mixture of oxygen and isoflurane for approximately 2 min before the animal was fully anesthetized. Mice were then transcardially perfused with 5 mL of ice cold 0.9% saline solution, followed by 5 mL of ice cold 4% paraformaldehyde solution. Brains were rapidly dissected from the skull then submerged in 4% paraformaldehyde solution on ice. The perfused mouse brains were then stored at 4°C for 1 day before being submerged in 30% sucrose solution and stored at 4°C for another 1–1.5 days. Once the brains sunk to the bottom of the sucrose solution, the sucrose solution was drained, and the brains underwent flash-freezing using liquid nitrogen. Frozen brains were stored at −80°C prior to slicing. For slicing, frozen brains were embedded in Tissue-Plus™. C.T. Compound (Fisher, Waltham, MA), then sliced at a thickness of 20 μm using a cryostat held at −20°C. Slices were mounted on Superfrost™ Plus microscope slides (Fisher, Waltham, MA) then stored at −20°C until they were used for immunohistochemistry.

The immunohistochemistry procedure consisted of the following steps: (1) blocking endogenous peroxidase by incubating with 0.3% H_2O_2 at room temperature for 10 min, (2) rinsing in 1 M PBS 3 times for 5 min each time, (3) blocking non-specific binding at room temperature by incubating in 10% fetal bovine serum at room temperature for 2 h, (4) incubating with primary antibodies at 4°C for 24 h, (5) rinsing in 1 M PBS 3 times for 5 min each, (6) incubating in secondary antibodies at room temperature for 1 h, at which point all steps proceeded in the dark due to the secondary antibodies' light sensitivity, (7) rinsing in 1 M PBS 3 times for 5 min each, and (8) mounting the immuno-stained slices using ProLong™ Gold Antifade Mountant with DAPI (ThermoFisher Scientific, Waltham, Massachusetts). All immune-stained slices were stored at 4°C before imaging. The following primary antibodies were used: cannabinoid receptor CB1R monoclonal antibody (mouse, Synaptic Systems, Göttingen, Germany, Lot 1–3, Cat # 258011) diluted at 1:500, orexin receptor 1 polyclonal antibody (rabbit, Enzo Life Sciences, Farmingdale, NY, Lot 10122020, Cat # BML-KI508) diluted at 1:50, orexin receptor 2 polyclonal antibody (rabbit, Enzo Life Sciences, Farmingdale, NY, Lot 10122020, Cat # BML-KI507) diluted at 1:200. The following secondary antibodies were used: Goat Anti-Mouse IgG H&L (Alexa Fluor® 594) (Invitrogen, Eugene, Oregon, Lot 2179228, Cat # A11005) diluted at 1:500 was used for the mouse anti-CB1R primary antibody, while Goat Anti-Rabbit IgG H&L (Alexa Fluor® 488) (Invitrogen, Eugene, Oregon, Lot 2179202, Cat # A11008) diluted at 1:500 was used for the rabbit-anti-OX1R and -OX2R antibodies. Each brain region was triple-labeled with (1) DAPI-CB1R-OX1R or (2) DAPI-CB1R-OX2R.

Confocal Microscopy and Colocalization Analysis

A Zeiss LSM700 confocal microscope (Carl Zeiss, Oberkochen, Germany) equipped with Zeiss ZEN Black (version 2.3 SP1) software (Carl Zeiss, Oberkochen, Germany) was used to obtain fluorescent 3D images of the immuno-stained brain slices. 10–12 Z-stacks encompassing an average tissue depth of 15 μm were collected at 63X oil immersion from each ventral striatum and primary motor cortex. ImageJ (version 2.1.0) (NIH, Bethesda, MD, United States) was used to merge the Z-stacks to form 3D images for analysis. Within each image, DAPI-immunolabeled cells were randomly chosen for colocalization analysis on ImageJ and its Fiji package (NIH, Bethesda, MD, United States). Pearson's correlation coefficients were calculated for (1) CB1R-OX1R, and (2) CB1R-OX2R (Zinchuk and Zinchuk, 2008). For statistical processing, CB1R-OX1R and CB1R-OX2R colocalization coefficients were averaged between $n = 6$ cells in the same sex and drug treatment group.

Statistical Analysis

Tetrad data are presented as mean ± SEM where "n" represents the number of animals per treatment group. Data from the ring holding assay and tail flick assay are reported as percent maximum possible effect (%MPE) for catalepsy and %MPE for anti-nociception, respectively. Results from the open field test are stated as a percentage of vehicle scores (%Vehicle). Dose-response curves were fit using a three parameter non-linear regression to yield the ED_{50} and E_{max} values (GraphPad, Prism, v. 9.0.1, San Diego, CA). For data without a clear dose-response (i.e., non-converged/"n.c."), E_{max} was reported as the maximum response observed. All E_{max} data are reported as mean ± SEM. ED_{50} data are reported as the mean with 95% confidence interval (CI). Isobolographic analyses for body temperature were conducted using ED_{50} data with 95% CI only because ED_{50} could not be estimated in other data sets. Homogeneity of variance was confirmed using Bartlett's test. Statistical analyses for tetrad data were conducted by two-way analysis of variance (ANOVA) to account for both sex and drug treatment. Immunohistochemistry colocalization data are presented as a mean ± SEM where "n" represents individual cells counted within the brain region of a single mouse. Colocalization means are denoted as Pearson's correlation coefficients. Statistical analyses for the colocalization data were conducted by two-way ANOVA to account for both sex and drug treatment. *Post hoc* analyses were performed using Tukey's (two-way ANOVA) test. Significance was set as $p < 0.05$.

RESULTS

Catalepsy

Male and female C57BL/6 mice were treated with CP55,940 (0.1–10 mg/kg), TCS-OX2-29 (1–30 mg/kg), TCS-1102 (0.1–10 mg/kg), and co-treatments of 1 mg/kg CP55,940 and either TCS-OX2-29 (1–30 mg/kg) or TCS-1102 (0.1–10 mg/kg). Treatment with CP55,940 alone or 1 mg/kg CP55,940 + TCS-1102 produced a dose-dependent increase in catalepsy in both sexes (**Figures 1A,B**). Co-treatment with 1 mg/kg

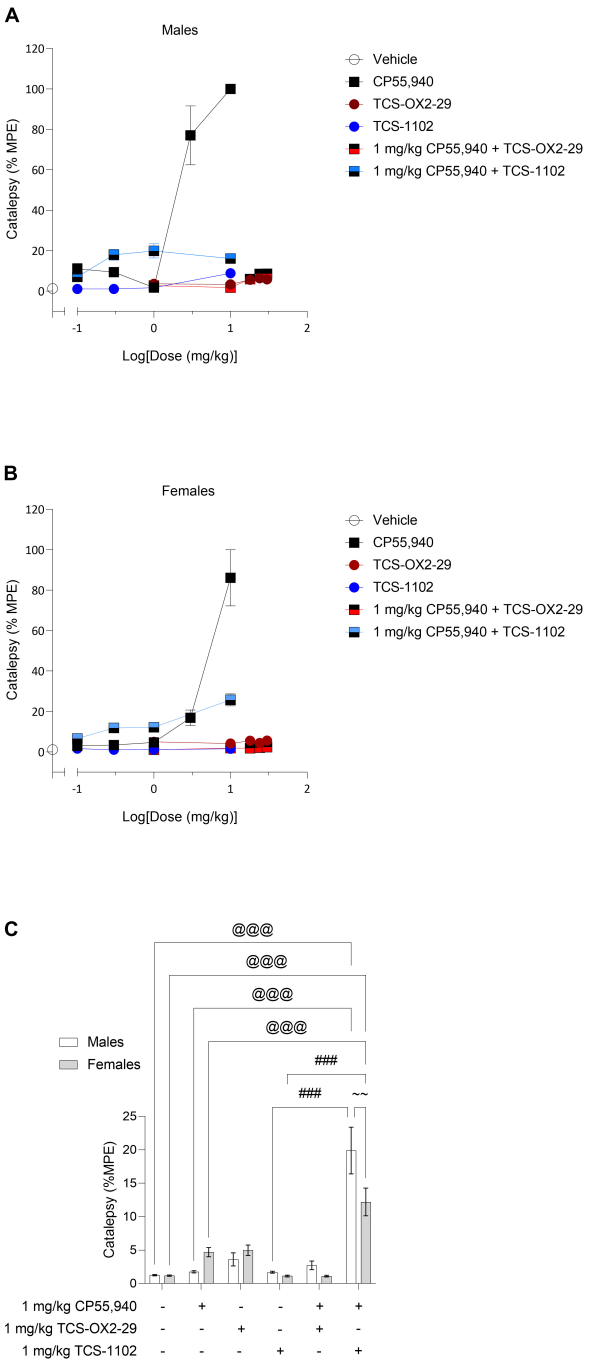

FIGURE 1 | Acute catalepsy effects following cannabinoid and orexin drug treatments. Male **(A)** and female **(B)** C57BL/6 mice aged 6–12 weeks were i.p. administered one of the following dose ranges: CP55,940 (0.1–10 mg/kg), TCS-OX2-29 (1–30 mg/kg), TCS-1102 (0.1–10 mg/kg), 1 mg/kg CP55,940 + TCS-OX2-29 (1–30 mg/kg), or 1 mg/kg CP55,940 + TCS-1102 (0.1–10 mg/kg). 10 min post-injections, mice were assessed for catalepsy in the ring holding assay. **(C)** Cataleptic responses were compared within (sex) and between (drugs) the following experimental groups: 1 mg/kg CP55,940, 1 mg/kg TCS-OX2-29, 1 mg/kg TCS-1102, 1 mg/kg CP55,940 + 1 mg/kg TCS-OX2-29, or 1 mg/kg CP55,940 + 1 mg/kg TCS-1102. All catalepsy data are expressed as %MPE (MPE = 60 s), and as means ± SEM. $n = 6$ for all treatment groups. Significance was calculated using a two-way ANOVA

(Continued)

FIGURE 1 | followed by Tukey's *post hoc* analyses. @@@ $p < 0.001$ compared to Vehicle within sexes. ###$p < 0.001$ compared between 1 mg/kg TCS-1102 and 1 mg/kg CP55,940 + 1 mg/kg TCS-1102. ∼∼$p < 0.01$ compared between sexes, within treatment groups.

CP55,940 + TCS-1102 was less potent in producing catalepsy compared to CP55,940 alone in both sexes (**Table 1**). There were no sex differences within drug treatments. Potency differences could not be calculated between or within these other experimental groups because no clear dose-response was observed for all treatments (**Table 1**). Co-treatments of 1 mg/kg CP55,940 + TCS-OX2-29 or 1 mg/kg CP55,940 + TCS-1102 were less efficacious than 1 mg/kg CP55,940 alone ($p < 0.001$) (**Table 1**). Looking at the TCS-1102 treatments in females, co-treatment with 1 mg/kg CP55,940 + TCS-1102 was more efficacious than TCS-1102 alone ($p = 0.0159$) (**Table 1**). There were no efficacy differences between any of the other drug treatments, nor between sexes.

Co-treatment with 1 mg/kg CP55,940 + 1 mg/kg TCS-1102 produced a larger cataleptic response compared to either 1 mg/kg CP55,940 alone or 1 mg/kg TCS-1102 alone in both sexes ($p < 0.001$) (**Figure 1C**). Thus, the combination of 1 mg/kg of CP55,940 + 1 mg/kg of TCS-1102 potentiated catalepsy, suggesting additivity between these two drugs. Considering that only co-treatment with the DORA TCS-1102 potentiated catalepsy, these results imply that compared to OX2R antagonism, OX1R antagonism is more critical in potentiating CP55,940-induced catalepsy. In terms of sex differences, males had a larger cataleptic response to the co-treatment with CP55,940 + TCS-1102 compared to females, demonstrating that males are more sensitive to the cataleptic effects of co-administered cannabinoid and DORA ($p = 0.0032$) (**Figure 1C**).

TABLE 1 | ED_{50} and E_{max} values reflecting catalepsy responses to cannabinoid and orexin drug treatments.

Treatment	ED_{50} (mg/kg) (95% CI)	E_{max} (%MPE) ± SEM
	Males	
CP55,940	2.4 (1.3–4.3)	100
TCS-OX2-29	n.c.	5.8 ± 0.83
TCS-1102	n.c.	8.8 ± 1.2
1 mg/kg CP55,940 + TCS-OX2-29	n.c.	8.6 ± 0.52*
1 mg/kg CP55,940 + TCS-1102	41 (19–87)*	19 ± 1.5*
	Females	
CP55,940	5.7 (3.6–9.3)	86 ± 14
TCS-OX2-29	n.c.	5.7 ± 1.2
TCS-1102	n.c.	1.6 ± 0.29
1 mg/kg CP55,940 + TCS-OX2-29	n.c.	2.8 ± 1.5*
1 mg/kg CP55,940 + TCS-1102	26 (18–38)*	26 ± 3.0*#

Data were fit to a three parameter non-linear regression with a system minimum and maximum constrained to 0 and 100, respectively (GraphPad, Prism, v. 8.0). n.c., not converged.

For data without a clear dose–response (i.e., "n.c."), E_{max} is reported as the maximum response observed.

Data are expressed as mg/kg with 95% CI or %MPE ± SEM.

$p < 0.05$ compared to CP55,940 within sexes, and #$p < 0.05$ compared between 1 mg/kg TCS-1102 and 1 mg/kg CP55,940 + 1 mg/kg TCS-1102, as determined by non-overlapping 95% CI or two-way ANOVA followed by Tukey's post hoc test. Corresponding graph is presented in **Figure 1.*

Body Temperature

With the exception of TCS-1102 treatment in males, all compounds tested produced a dose-dependent decrease in body temperature (**Figures 2A,B**). Co-treatment with 1 mg/kg CP55,940 + TCS-OX2-29 was a less potent mediator of hypothermia than CP55,940 alone in both sexes (**Table 2**). Co-treatment with 1 mg/kg CP55,940 + TCS-OX2-29 was more efficacious in producing hypothermia than TCS-OX2-29 alone in both sexes ($p < 0.001$). Co-treatment with 1 mg/kg CP55,940 + TCS-1102 was also more efficacious in producing hypothermia compared to TCS-1102 alone in males ($p < 0.001$) and females ($p = 0.0049$) (**Table 2**). There were no potency or efficacy differences between any of the other drug treatments, nor between sexes.

Co-treatment with 1 mg/kg CP55,940 + 1 mg/kg TCS-1102 produced more hypothermia than 1 mg/kg TCS-1102 alone in both males ($p < 0.001$) and females ($p = 0.0049$) (**Figure 2C**). Co-treatment with 1 mg/kg CP55,940 + 1 mg/kg TCS-OX2-29 produced a greater decrease in body temperature than 1 mg/kg TCS-OX2-29 alone in both sexes ($p < 0.001$) (**Figure 2C**). Because these co-treatment effects are not greater than that of CP55,940 alone, hypothermia was likely CP55,940-driven. There were no sex differences in temperature between any of the other 1 mg/kg treatment groups. CP55,940-dependent hypothermia in mice appears to be CBR-dependent and not co-regulated by either OX1R or OX2R, nor sex-dependent.

Isobolograms comparing compound ED_{50} values from **Table 2** were constructed for body temperature data (**Figure 3**). Based on these isobolograms, co-treatments with CP55,940 + TCS-OX2-29 or CP55,940 + TCS-1102 were mapped to the non-significant antagonistic range in both sexes. This is in accordance with the conclusion drawn from **Figure 2**.

Anti-nociception

Dose-response relationships were observed for all groups excluding TCS-OX2-29 in females (**Figures 4A,B**). For experimental groups without clear dose-response plateaus, ED_{50} was estimated to be greater than the maximum dose evaluated (**Table 3**). Based on this, the co-treatment with 1 mg/kg CP55,940 + TCS-1102 was more potent than 1 mg/kg CP55,940 alone in producing anti-nociception in males (**Table 3**). The co-treatment with 1 mg/kg CP55,940 + TCS-1102 was more than TCS-1102 alone in females (**Table 3**). The co-treatment with 1 mg/kg CP55,940 + TCS-OX2-29 was more potent compared to TCS-OX2-29 alone, but less potent compared to CP55,940 alone in females (**Table 3**). Lastly, the co-treatments with 1 mg/kg CP55,940 + TCS-OX2-29, and 1 mg/kg CP55,940 + TCS/1102, were more efficacious than TCS-OX2-29 alone ($p < 0.001$), and TCS-1102 alone (males: $p < 0.001$, females: $p = 0.093$),

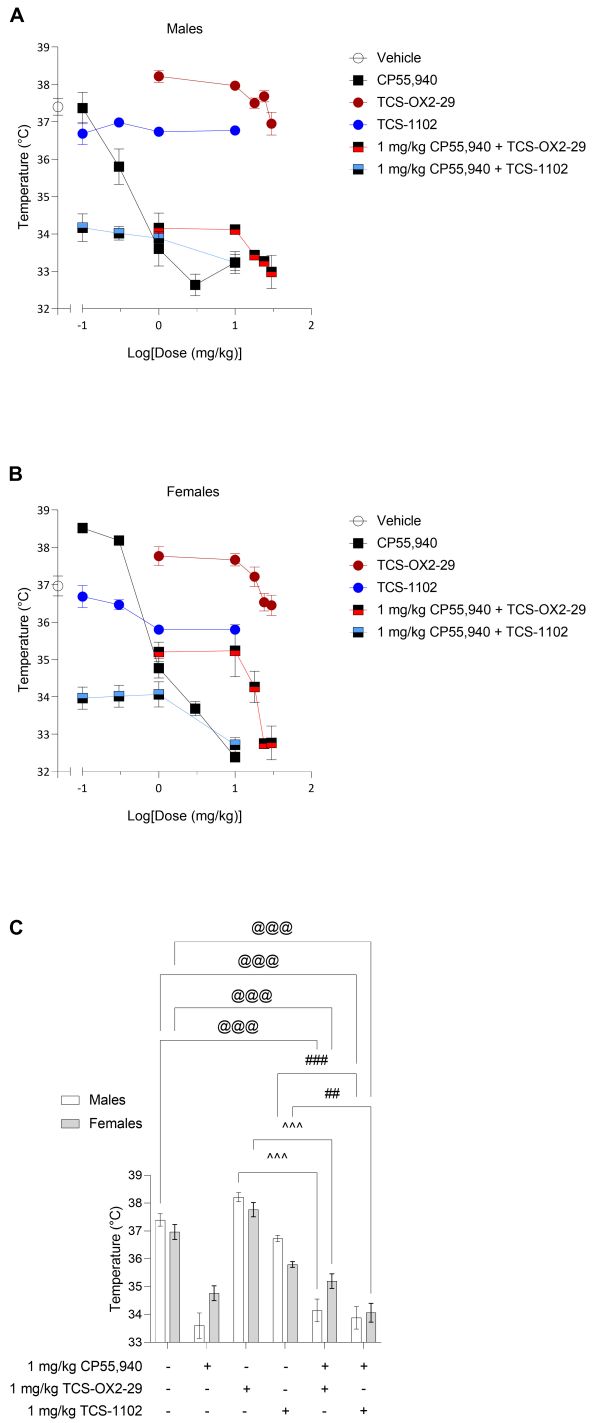

FIGURE 2 | Acute body temperature effects from cannabinoid and orexin drug treatments. Male **(A)** and female **(B)** C57BL/6 mice aged 6–12 weeks were i.p. administered one of the following dose ranges: CP55,940 (0.1–10 mg/kg), TCS-OX2-29 (1–30 mg/kg), TCS-1102 (0.1–10 mg/kg), 1 mg/kg CP55,940 + TCS-OX2-29 (1–30 mg/kg), or 1 mg/kg CP55,940 + TCS-1102 (0.1–10 mg/kg). 15 min post-injections, a rectal thermometer was used to measure internal body temperature. **(C)** Temperature responses were compared within (sex) and between (drugs) the following experimental groups: 1 mg/kg CP55,940, 1 mg/kg TCS-OX2-29, 1 mg/kg TCS-1102,

(Continued)

FIGURE 2 | 1 mg/kg CP55,940 + 1 mg/kg TCS-OX2-29, or 1 mg/kg CP55,940 + 1 mg/kg TCS-1102. All catalepsy data are expressed as °C, and as means ± SEM. $n = 6$ for all treatment groups. Significance was calculated using a two-way ANOVA followed by Tukey's *post hoc* analyses. @@@$p < 0.001$ compared to Vehicle within sexes. ^^^$p < 0.001$ compared between 1 mg/kg TCS-OX2-29 and 1 mg/kg CP55,940 + 1 mg/kg TCS-OX2-29. ##/###$p < 0.01/0.001$ compared between 1 mg/kg TCS-1102 and 1 mg/kg CP55,940 + 1 mg/kg TCS-1102.

respectively (**Table 3**). No potency or efficacy differences were detected between any other groups, nor between sexes.

Co-treatment with 1 mg/kg CP55,940 + 1 mg/kg TCS-OX2-29 was associated with a greater anti-nociceptive response than 1 mg/kg TCS-OX2-29 alone in males ($p < 0.001$) (**Figure 4C**). Moreover, in males, co-treatment with 1 mg/kg CP55,940 + 1 mg/kg TCS-1102 produced a greater anti-nociceptive response than 1 mg/kg TCS-1102 alone ($p < 0.001$) (**Figure 4C**). There were no differences between compound treatments in females (**Figure 4C**). Given that neither of the co-treatments in males were more anti-nociceptive than CP55,940 alone, it was concluded that the anti-nociceptive effects of the co-treatments are CP55,940-driven (**Figure 4C**). With respect to sex differences, CP55,940 alone ($p = 0.0293$) and both co-treatments of CP55,940 + TCS-OX2-29 ($p < 0.001$), and CP55,940 + TCS-1102 ($p < 0.001$), had higher analgesic effects in males compared

TABLE 2 | ED_{50} and E_{max} values reflecting body temperature responses to cannabinoid and orexin drug treatments.

Treatment	ED_{50} (mg/kg) (95% CI)	E_{max} (°C) ± SEM
	Males	
CP55,940	8.8 (4.5–17)	32 ± 0.36
TCS-OX2-29	>30	37 ± 0.36
TCS-1102	n.c.	37 ± 0.090
1 mg/kg CP55,940 + TCS-OX2-29	>30	33 ± 0.45^
1 mg/kg CP55,940 + TCS-1102	12 (5–31)	33 ± 0.87#
	Females	
CP55,940	8.6 (4.2–17)	32 ± 0.31
TCS-OX2-29	>30	36 ± 0.27
TCS-1102	10 (4.0–26)	36 ± 0.20
1 mg/kg CP55,940 + TCS-OX2-29	>30	33 ± 0.45^
1 mg/kg CP55,940 + TCS-1102	13 (5.1–32)	33 ± 0.20#

Data were fit to a three parameter non-linear regression with a system minimum and maximum constrained to 0 and 100, respectively (GraphPad, Prism, v. 8.0). n.c., not converged.
For data without a clear dose-response (i.e., "n.c."), E_{max} is reported as the maximum response observed.
Data are expressed as mg/kg with 95% CI or °C ± SEM.
^$p < 0.05$ compared between 1 mg/kg TCS-OX2-29 and 1 mg/kg CP55,940 + 1 mg/kg TCS-OX2-29, and #$p < 0.05$ compared between 1 mg/kg TCS-1102 and 1 mg/kg CP55,940 + 1 mg/kg TCS-1102, as determined by non-overlapping 95% CI or two-way ANOVA followed by Tukey's post hoc test.
*Corresponding graph is presented in **Figure 2**.*

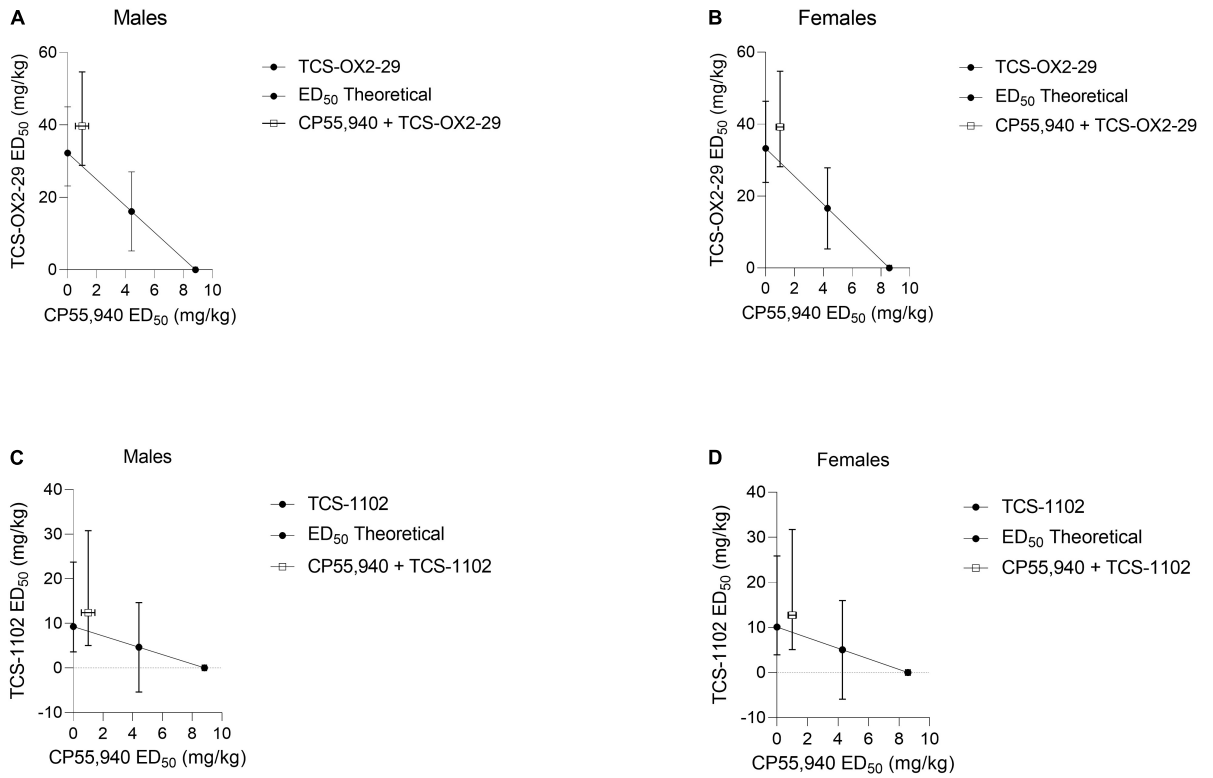

FIGURE 3 | Isobolograms determining drug-drug interactions between cannabinoid and orexin drugs with regards to body temperature. CP55,940 co-treatments with both TCS-OX2-29 **(A,B)** and TCS-1102 **(C,D)** caused non-significant antagonistic body temperature effects in both male **(A,C)** and female **(B,D)** C57BL/6 mice. Data were fit to a three parameter non-linear regression with a system minimum and a system maximum constrained to 0 and 100, respectively. Data are expressed as mg/kg with 95% CI.

to females (**Figure 4C**). Sex differences in nociception were not detected in the orexin receptor antagonist treatments. Therefore, CP55,940-dependent anti-nociception in mice is likely CB1R-dependent and not co-regulated by either OX1R or OX2R, nor sex-dependent.

Locomotion

CP55,940, TCS-OX2-29, and TCS-1102 produced dose-dependent decreases in locomotion and velocity in both sexes; however, ED_{50} values could not be estimated for 1 mg/kg CP55,940 + TCS-1102 as no plateau was observed (**Figure 5** and **Table 4**). No differences were seen between treatment groups, nor between sexes with regards to the potency in decreasing distance and velocity (**Table 4**). In both sexes, CP55,940 was more efficacious than TCS-OX2-29 alone and TCS-1102 alone in decreasing distance and velocity (distance in males: $p = 0.0399$; all other groups: $p < 0.0001$) (**Table 4**). Also in both sexes, co-treatment with 1 mg/kg CP55,940 + TCS-OX2-29 was more efficacious than TCS-OX2-29 alone in decreasing both distance and velocity in both sexes (velocity in females: $p = 0.0106$; all other groups: $p < 0.0001$) (**Table 4**). In females, co-treatment with 1 mg/kg CP55,940 + TCS-1102 was more efficacious than TCS-110 alone in decreasing distance ($p = 0.0005$) (**Table 4**). Co-treatment with 1 mg/kg CP55,940 + TCS-1102 was also more efficacious than TCS-1102 alone in decreasing velocity in both sexes ($p < 0.0001$) (**Table 4**). No other treatment or sex differences were observed in the distance and velocity E_{max} values.

Co-treatment with 1 mg/kg CP55,940 + 1 mg/kg TCS-OX2-29 had greater anti-locomotive effects (decreased distance and velocity) compared to TCS-OX2-29 alone in both sexes ($p < 0.001$) (**Figures 5E,F**). Similarly, co-treatment with 1 mg/kg CP55,940 + 1 mg/kg TCS-1102 had greater anti-locomotive effects (decreased distance and velocity) compared to TCS-1102 alone in both sexes ($p < 0.001$) (**Figures 5E,F**). Locomotion in the open field test is visualized in representative heat maps (**Figures 5G,H**). Because no co-treatment exacerbated the anti-locomotive effects of CP55,940 alone, the anti-locomotive effects are likely CP55,940-driven. Lastly, there were no sex differences within any of the drug treatments. Therefore, CP55,940-dependent locomotor effects in mice appear to be CB1R-dependent and not co-regulated by either OX1R or OX2R, nor sex-dependent.

CB1R and OX1R/OX2R Colocalization

Thirty min post-injection, brain tissue was collected from the following drug treatment groups: 1 mg/kg CP55,940, 1 mg/kg TCS-OX2-29, 1 mg/kg TCS-1102, 1 mg/kg CP55,940 + 1 mg/kg

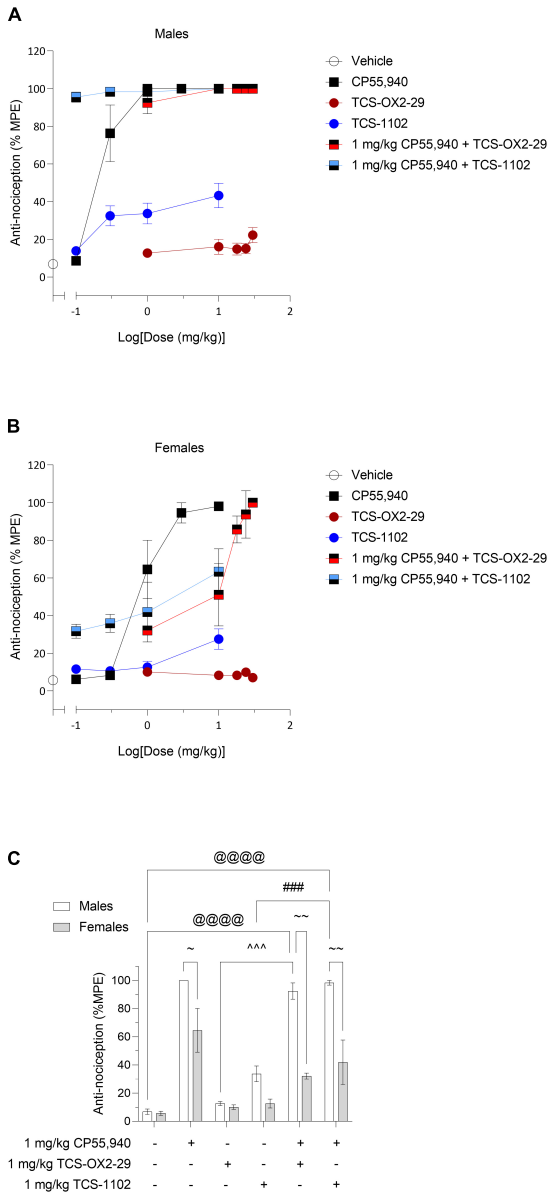

FIGURE 4 | Acute nociceptive effects as a result of cannabinoid and orexin drug treatments. Male **(A)** and female **(B)** C57BL/6 mice aged 6–12 weeks were i.p. administered one of the following dose ranges: CP55,940 (0.1–10 mg/kg), TCS-OX2-29 (1–30 mg/kg), TCS-1102 (0.1–10 mg/kg), 1 mg/kg CP55,940 + TCS-OX2-29 (1–30 mg/kg), or 1 mg/kg CP55,940 + TCS-1102 (0.1–10 mg/kg). 20 min post-injections, all mice underwent the tail flick test to assess anti-thermal nociception. **(C)** Anti–nociceptive responses were compared within (sex) and between (drugs) the following experimental groups: 1 mg/kg CP55,940, 1 mg/kg TCS-OX2-29, 1 mg/kg TCS-1102, 1 mg/kg CP55,940 + 1 mg/kg TCS-OX2-29, or 1 mg/kg CP55,940 + 1 mg/kg TCS-1102. All anti-nociceptive data are expressed as %MPE (MPE = 20 s), and as means ± SEM. $n = 6$ for all treatment groups. Significance was calculated using a two-way ANOVA followed by Tukey's *post hoc* analyses. @@@$p < 0.001$ compared to Vehicle within sexes. ~~~$p < 0.001$ compared between 1 mg/kg TCS-OX2-29 and 1 mg/kg CP55,940 + 1 mg/kg TCS-OX2-29. ###$p < 0.001$ compared between 1 mg/kg TCS-1102 and 1 mg/kg CP55,940 + 1 mg/kg TCS-1102. ~~$p < 0.01$ compared between sexes, within treatment groups.

TABLE 3 | ED_{50} and E_{max} values representing anti-nociception responses to cannabinoid and orexin drug treatments.

Treatment	ED_{50} (mg/kg) (95% CI)	E_{max} (%MPE) ± SEM
	Males	
CP55,940	0.19 (0.11–0.31)	100
TCS-OX2-29	>30	22 ± 4.0
TCS-1102	7.3 (3.4–15)	41 ± 4.7
1 mg/kg CP55,940 + TCS-OX2-29	n.c.	100^
1 mg/kg CP55,940 + TCS-1102	n.c.	100 ± 1.6#
	Females	
CP55,940	0.76 (0.48–1.2)	98 ± 1.9
TCS-OX2-29	n.c.	8.3 ± 1.8
TCS-1102	>10	28 ± 5.5
1 mg/kg CP55,940 + TCS-OX2-29	3.8 (2.0–7.2)*^	100^
1 mg/kg CP55,940 + TCS-1102	1.0 (0.46–2.3)#	72 ± 25#

Data were fit to a three parameter non-linear regression with a system minimum and maximum constrained to 0 and 100, respectively (GraphPad, Prism, v. 8.0). n.c., not converged.
For data without a clear dose-response (i.e., "n.c."), E_{max} is reported as the maximum response observed.
Data are expressed as mg/kg with 95% CI or %MPE ± SEM.
**$p < 0.05$ compared to 1 mg/kg CP55,940 within sexes, ^$p < 0.05$ compared between 1 mg/kg TCS-OX2-29 and 1 mg/kg CP55,940 + 1 mg/kg TCS-OX2-29, and #$p < 0.05$ compared between 1 mg/kg TCS-1102 and 1 mg/kg CP55,940 + 1 mg/kg TCS-1102, as determined by non-overlapping 95% CI or two-way ANOVA followed by Tukey's post hoc test.*
*Corresponding graph is presented in **Figure 4**.*

TCS-OX2-29, and 1 mg/kg CP55,940 + 1 mg/kg TCS-1102. Immunohistochemical experiments focused on two brain regions: (1) ventral striatum, a brain region thought to facilitate cataleptic effects (Turski et al., 1984; Ossowska et al., 1990; Anderson et al., 1996) and (2) primary motor cortex, a region that largely initiates and modulates locomotion (Sahni et al., 2020). In the ventral striatum, more whole-cell CB1R-OX1R colocalization was observed in males treated with 1 mg/kg TCS-OX2-29 compared to males treated with the combination of 1 mg/kg CP55,940 + 1 mg/kg TCS-OX2-29; this difference was not seen in treatment-matched females (**Figure 6A**). Between males and females treated with 1 mg/kg TCS-OX2-29, ventral striatum tissue from males had higher CB1R-OX1R colocalization (**Figure 6A**). In both sexes, CB1R-OX1R colocalization in the ventral striatum was greater following 1 mg/kg CP55,940 + 1 mg/kg TCS-1102 compared to both 1 mg/kg CP55,940 alone and 1 mg/kg TCS-1102 alone (**Figure 6B**); this is further illustrated by representative images (**Figure 6E**). No sex differences were observed within the TCS-1102-treated groups with regards to CB1R-OX1R colocalization in the ventral striatum (**Figure 6B**). In the primary motor cortex, there were no significant differences in CB1R-OX1R colocalization between any of the experimental groups (**Figures 7A,B,E**).

In both sexes, CB1R-OX2R colocalization in the ventral striatum was higher in 1 mg/kg TCS-OX2-29-treated mice

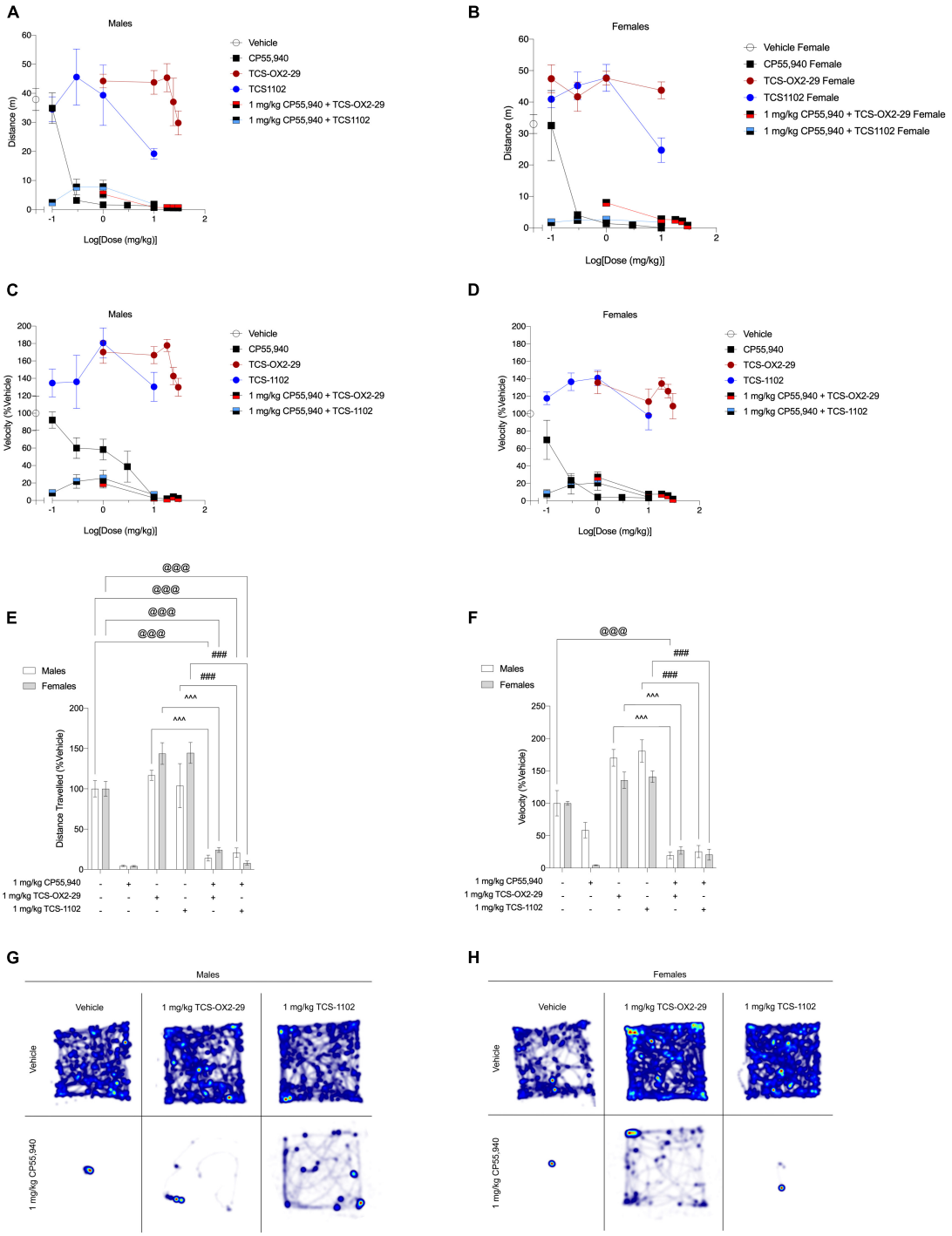

FIGURE 5 | Acute anti-locomotive effects from cannabinoid and orexin drug treatments. **(A–D)** Male and female C57BL/6 mice aged 6–12 weeks were i.p. administered one of the following dose ranges: CP55,940 (0.1–10 mg/kg), TCS-OX2-29 (1–30 mg/kg), TCS-1102 (0.1–10 mg/kg), 1 mg/kg CP55,940 + TCS-OX2-29 (1–30 mg/kg), or 1 mg/kg CP55,940 + TCS-1102 (0.1–10 mg/kg). 25 min post-injections, all mice underwent the open field test to assess locomotion. Distance traveled **(E)** and average velocity **(F)** were compared within (sex) and between (drugs) the following experimental groups: 1 mg/kg CP55,940, 1 mg/kg TCS-OX2-29, 1 mg/kg TCS-1102, 1 mg/kg CP55,940 + 1 mg/kg TCS-OX2-29, or 1 mg/kg CP55,940 + 1 mg/kg TCS-1102. All anti-locomotive data are expressed as m or cm/s, and as means ± SEM. $n = 6$ for all treatment groups. Significance was calculated using a two-way ANOVA followed by Tukey's *post hoc* analyses. @@@$p < 0.001$ compared to Vehicle within sexes. ^^^$p < 0.001$ compared between 1 mg/kg TCS-OX2-29 and 1 mg/kg CP55,940 + 1 mg/kg TCS-OX2-29. ###$p < 0.001$ compared between 1 mg/kg TCS-1102 and 1 mg/kg CP55,940 + 1 mg/kg TCS-1102. **(G,H)** Representative heat maps illustrating the locomotion of male **(G)** and female **(H)** C57BL/6 mice treated with either 1 mg/kg CP55,940, 1 mg/kg TCS-OX2-29, 1 mg/kg TCS-1102, 1 mg/kg CP55,940 + 1 mg/kg TCS-OX2-29, or 1 mg/kg CP55,940 + 1 mg/kg TCS-1102.

TABLE 4 | ED_{50} and E_{max} values summarizing cannabinoid- and orexin-induced locomotion responses.

Treatment	Distance traveled	Average velocity	Distance traveled (%Vehicle)	Average velocity (%Vehicle)
	ED_{50} (mg/kg) (95% CI)		E_{max} ± SEM	
			Males	
CP55,940	<0.10	0.51 (0.10–3.0)	3.3 ± 0.41	3.8 ± 1.1
TCS-OX2-29	>30	>30	77 ± 11*	130 ± 10*
TCS-1102	19 (0.10–3.0)	n.c.	51 ± 4.8*	130 ± 17*
1 mg/kg CP55,940 + TCS-OX2-29	n.c.	n.c.	1.0 ± 2.1^	1.7 ± 3.2^
1 mg/kg CP55,940 + TCS-1102	n.c.	n.c.	15 ± 5.3	17 ± 6.6#
			Females	
CP55,940	<0.10	<0.10	0	0.68 ± 7.4
TCS-OX2-29	n.c.	n.c.	122 ± 25*	109 ± 15*
TCS-1102	6.1 (0.10–3.0)	n.c.	75 ± 12*	98 ± 16*
1 mg/kg CP55,940 + TCS-OX2-29	n.c.	n.c.	0.63 ± 5.2^	1.2 ± 5.7^
1 mg/kg CP55,940 + TCS-1102	n.c.	n.c.	7.0 ± 1.6#	14 ± 7.0#

*Distance traveled **(a)** and average velocity **(b)** in the open field test were the measures of anti–locomotion.*
Data were fit to a three parameter non-linear regression with a system minimum and maximum constrained to 0 and 100, respectively (GraphPad, Prism, v. 8.0).
For data without a clear dose-response (i.e., "n.c."), E_{max} is reported as the maximum response observed.
Data are expressed as mg/kg with 95% CI or%Vehicle ± SEM.
p < 0.05 compared to 1 mg/kg CP55,940 within sexes, ^p < 0.05 compared between 1 mg/kg TCS-OX2-29 and 1 mg/kg CP55,940 + 1 mg/kg TCS-OX2-29, and #p < 0.05 compared between 1 mg/kg TCS-1102 and 1 mg/kg CP55,940 + 1 mg/kg TCS-1102, as determined by non-overlapping 95% CI or two-way ANOVA followed by Tukey's post hoc test. Corresponding graphs are presented in **Figure 5.*

compared to mice co-treated with 1 mg/kg CP55,940 + 1 mg/kg TCS-OX2-29 (**Figure 6C**). Compared to females, ventral striatum tissue from males treated with 1 mg/kg TCS-OX2-29 had larger CB1R-OX2R colocalization (**Figure 6C**); this is demonstrated in the representative images (**Figure 6F**). There were no differences in ventral striatum CB1R-OX2R colocalization within or between any of the groups treated with TCS-1102 (**Figure 6D**). Moreover, the primary motor cortex did not display differences in CB1R-OX2R colocalization between any of the experimental groups (**Figures 7C,D,F**). To summarize, 1 mg/kg CP55,940 + 1 mg/kg TCS-1102 was the only combination treatment that displayed higher CB1R-OX1R colocalization in the ventral striatum compared to its constituent drugs alone (**Figure 6B**). This supports the tetrad data, in which this combination treatment produced more catalepsy than each of its constituent drugs (**Figure 1C**). As for CB1R-OX2R colocalization in the ventral striatum, 1 mg/kg TCS-OX2-29 co-treatment was associated with more colocalization than the co-treatment with CP55,940 and TCS-OX2-29 (**Figure 6C**). Compared to OX2R antagonism, OX1R antagonism and subsequent changes in CB1R-OX1R colocalization following co-treatment with the CB1R agonist CP55,940 and the DORA TCS-1102 are likely to be the potentiators of catalepsy. None of the drug treatments produced significant CB1R-OX1R nor CB1R-OX2R colocalization changes in the primary motor cortex, which supports the lack of the CP55,940 and TCS-1102 additivity with regards to reduced movement in the open field test.

DISCUSSION

To date, the majority of endocannabinoid and orexin interaction studies have either characterized their molecular or physical interactions *in vitro*, or investigated their physiological interdependence in complex disease models related to sleep, appetite, and reward. One other study has assessed their dual modulation of body temperature, pain, locomotion, anxiety, and memory in healthy and transgenic male mice (Flores et al., 2016). The current study aimed to not only measure catalepsy alongside other measures of the tetrad, but utilize a full CB1R agonist and a clinically relevant DORA in both male and female mice. Compared to the CB1R partial agonist Δ^9-THC, which was used by Flores et al. (2016), CP55,940 is a full agonist of CB1R (Howlett and Abood, 2017) that is well-documented to produce more potent and efficacious responses *in vitro* and *in vivo* (Patel et al., 2020; Zagzoog et al., 2020; Henderson-Redmond et al., 2021). In the current study, CP55,940 (0.1–10 mg/kg) produced similar dose-dependent sedative effects in both males and females.

The OX2R antagonist TCS-OX2-29 and the DORA TCS-1102 were the orexin receptor compounds used in the current study. Treatment with either orexin receptor antagonist alone was associated with hypothermic, anti-nociceptive, and anti-locomotive effects of smaller magnitude than that of CP55,940. TCS-1102 was generally more efficacious compared to TCS-OX2-29, suggesting either a greater role for OX1R or both orexin receptor subtypes in controlling body temperature, nociception, and locomotion. In a previous study, OX1R antagonism *via* SB-334867 was found to potentiate Δ^9-THC-induced hypothermia, anti-nociception, and anxiolytic-like effects, while OX2R antagonism by TCS-OX2-29 was not (Flores et al., 2016). The current study was more focused on evaluating a clinically relevant DORA in conjunction with a cannabinoid. DORAs such as Suvorexant and Lemborexant are used for insomnia as they cause sedation by blocking the arousing effects of endogenous orexins (Yoshimichi et al., 2001; Patel et al., 2015;

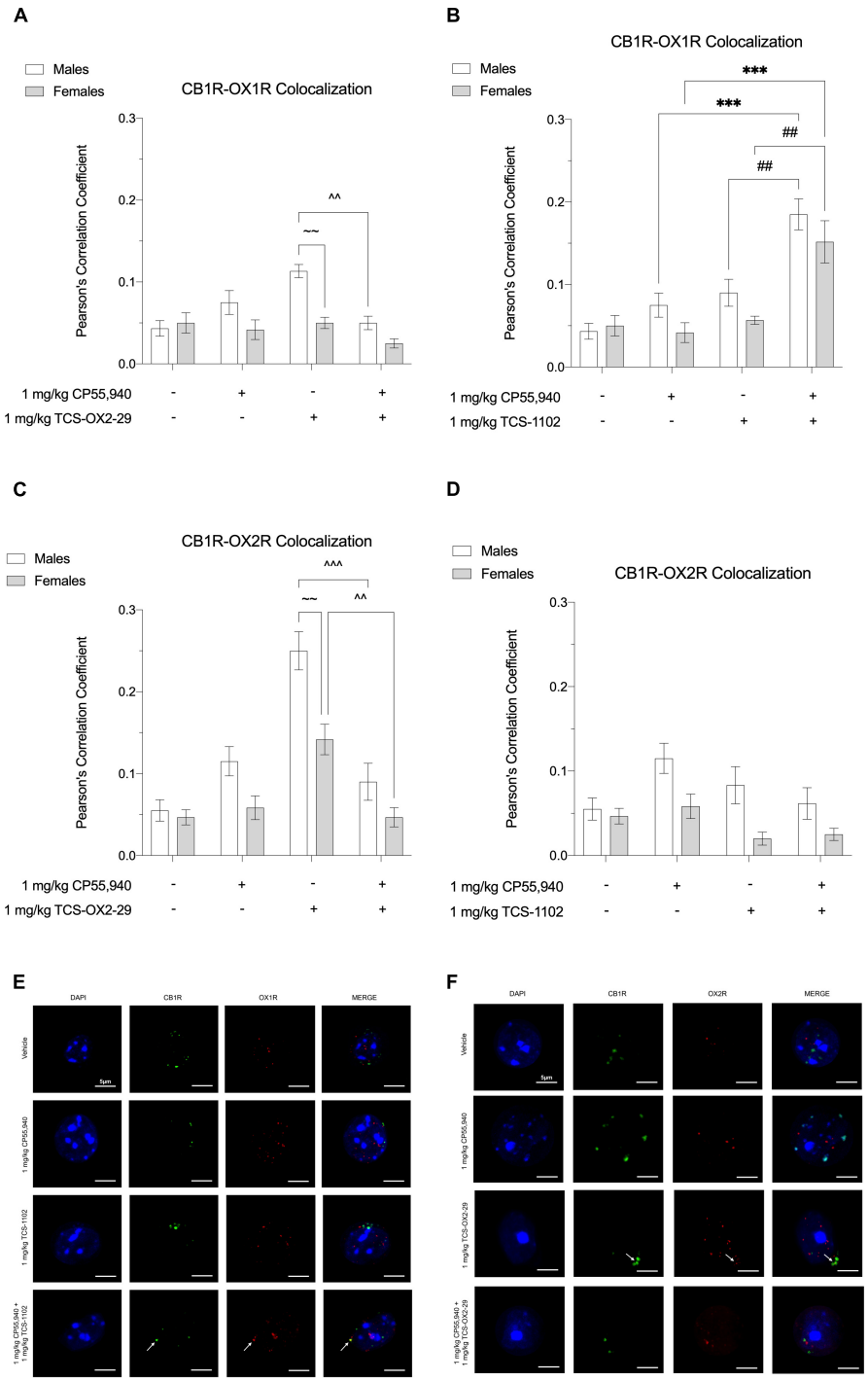

FIGURE 6 | CB1R-OX1R and CB1R-OX2R colocalization in the ventral striatum following cannabinoid and orexin drug treatments. Male and female C57BL/6 mice aged 6–12 weeks were i.p. administered one of the following dose ranges: CP55,940 (0.1–10 mg/kg), TCS-OX2-29 (1–30 mg/kg), TCS-1102 (0.1–10 mg/kg), 1 mg/kg CP55,940 + TCS-OX2-29 (1–30 mg/kg), or 1 mg/kg CP55,940 + TCS-1102 (0.1–10 mg/kg). 30 min post-injections, mice were euthanized, perfused, and their brains collected for immunohistochemistry. Colocalization between CB1R and OX1R **(A,B)** and CB1R and OX2R **(C,D)** was compared within (sex) and between (drugs) the following experimental groups: 1 mg/kg CP55,940, 1 mg/kg TCS-OX2-29, 1 mg/kg TCS-1102, 1 mg/kg CP55,940 + 1 mg/kg TCS-OX2-29, or 1 mg/kg CP55,940 + 1 mg/kg TCS-1102. All colocalization data are expressed as Pearson's Correlation Coefficients, and as means ± SEM. $n = 6$ (cells) for all treatment groups. Significance was calculated using a two-way ANOVA followed by Tukey's *post hoc* analyses. ***$p < 0.001$ compared to 1 mg/kg CP55,940 within sexes. ˜/˜˜$p < 0.01$/0.001 compared between 1 mg/kg TCS-OX2-29 and 1 mg/kg CP55,940 + 1 mg/kg TCS-OX2-29. ##$p < 0.01$ compared between 1 mg/kg TCS-1102 and 1 mg/kg CP55,940 + 1 mg/kg TCS-1102. ∼∼$p < 0.01$ compared between sexes, within treatment groups. **(E)** Representative images corresponding to panels **(A,B)** for CB1R-OX1R colocalization. **(F)** Representative images corresponding to panels **(C,D)** for CB1R-OX2R colocalization.

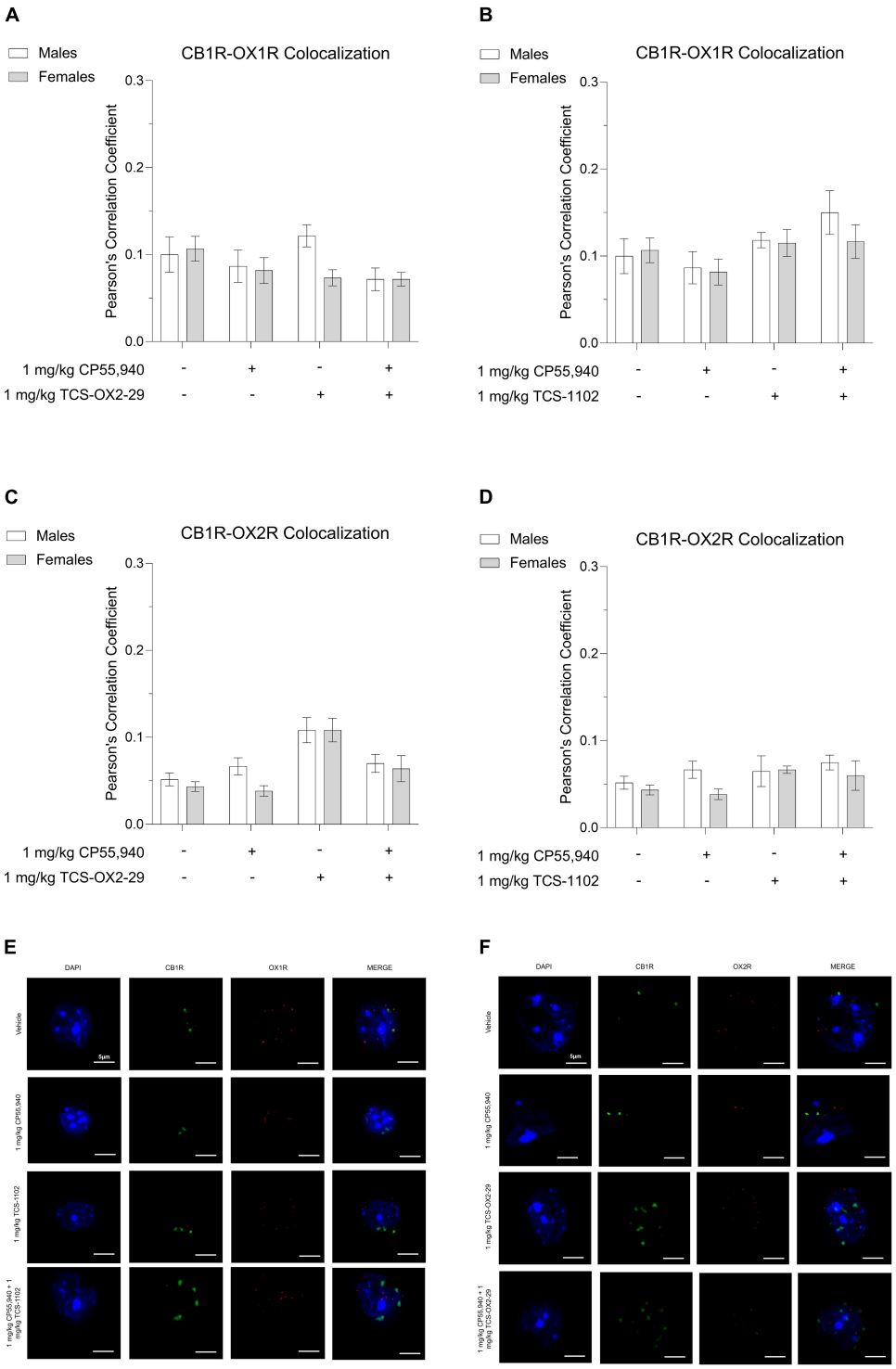

FIGURE 7 | CB1R-OX1R and CB1R-OX2R colocalization in the primary motor cortex following cannabinoid and orexin drug treatments. Male and female C57BL/6 mice aged 6–12 weeks were i.p. administered one of the following dose ranges: CP55,940 (0.1–10 mg/kg), TCS-OX2-29 (1–30 mg/kg), TCS-1102 (0.1–10 mg/kg), 1 mg/kg CP55,940 + TCS-OX2-29 (1–30 mg/kg), or 1 mg/kg CP55,940 + TCS-1102 (0.1–10 mg/kg). 30 min post-injections, mice were euthanized, perfused, and their brains collected for immunohistochemistry. Colocalization between CB1R and OX1R **(A,B)** and CB1R and OX2R **(C,D)** was compared within (sex) and between (drugs) the following experimental groups: 1 mg/kg CP55,940, 1 mg/kg TCS-OX2-29, 1 mg/kg TCS-1102, 1 mg/kg CP55,940 + 1 mg/kg TCS-OX2-29, or 1 mg/kg CP55,940 + 1 mg/kg TCS-1102. All colocalization data are expressed as Pearson's Correlation Coefficients, and as means ± SEM. $n = 6$ (cells) for all treatment groups. Significance was calculated using a two-way ANOVA followed by Tukey's *post hoc* analyses. **(E)** Representative images corresponding to panels **(A,B)** for CB1R-OX1R colocalization. **(F)** Representative images corresponding to panels **(C,D)** for CB1R-OX2R colocalization.

Herring et al., 2019). Comparisons between the orexin receptor subtypes in the context of the sleep-wake cycle have determined that although OX2R is more critical in inducing arousal, OX1R plays additional roles in promoting and maintaining wakefulness (Mieda et al., 2011; Mang et al., 2012).

Aside from catalepsy, co-manipulation of both cannabinoid and orexin receptors did not alter responses in the tetrad battery of assays compared to cannabinoid agonism alone. Thus, CP55,940-induced hypothermia, anti-nociception, and anti-locomotion are not regulated by OX1R- nor OX2R. Based on the dose-response curves for the co-treatments of CP55,940 and each of the orexin receptor antagonists, it can be confirmed that additivity between these two drug types with regards to hypothermia, anti-nociception, and anti-locomotion, does not exist at any dose. In terms of non-heterodimerized, non-interacting cannabinoid and orexin receptors, these results suggest that CBRs have a greater physiological role than orexin receptors in (1) the preoptic anterior hypothalamus and control of body temperature (Rawls et al., 2002), (2) spine and periaqueductal gray area underlying nociception (Freund et al., 2003; Walker and Hohmann, 2005), and (3) cortical regions in modulating locomotion (Polissidis et al., 2013). CB1R remains one of the most abundant GPCRs in the CNS (Mackie, 2005; Kano et al., 2009). Orexin receptor mRNA is also found in these regions (Trivedi et al., 1998; Marcus et al., 2001), however, there are no studies comparing the relative abundance of cannabinoid and orexin receptors in the same samples.

Unlike body temperature, nociception, and locomotion, co-treatment with CP55,940 and TCS-1102 produced longer-lasting catalepsy than CP55,940 or TCS-1102 alone, demonstrating additivity where each drug had an equal role in producing catalepsy. This was not observed for the combination of CP55,940 and TCS-OX2-29, suggesting that OX1R antagonism is more critical in potentiating CP55,940-induced catalepsy. Additivity between these two drugs may be better explained by regional differences in CB1R-OX1R and CB1R-OX2R interactions or heterodimerization in the ventral striatum, a sub-cortical region that expresses all three receptor subtypes to modulate catalepsy (Turski et al., 1984; Ossowska et al., 1990; Flores et al., 2013). Beyond the ventral striatum, orexin receptors are sparse in the dorsal striatum and more densely expressed in the ventral striatum (Hervieu et al., 2001; Marcus et al., 2001; Mackie, 2005; Flores et al., 2013). Our current study used colocalization as a proof-of-concept for the main behavioral data; thus aimed to efficiently gather data from brain regions that are well-documented co-expressed both receptor types. Moreover, the nucleus accumbens and the olfactory tubercle (which composes the ventral striatum) expresses both CB1R and OX2R (Flores et al., 2013). Although the nucleus accumbens is known to process emotions and reward, it also integrates emotional or motivational stimuli as it relates to sedation (Valencia Garcia and Fort, 2018). Anti-locomotion is a focal point in our current study because both cannabinoids and orexin drugs cause sedation. The olfactory tubercle processes incoming sensory information which may include rewarding stimuli (Wesson and Wilson, 2011; Murata, 2020). When CBRs and OX1R were co-manipulated in the current study, there was more CB1R-OX1R colocalization in the ventral striatum. Similar observations have been made in recombinant cell cultures, where the OX1R antagonist SB-674042 and CB1R antagonist SR141716A alone caused relocalization of OX1R and CB1R together (Ellis et al., 2006). Neither of these antagonists had significant affinities for the other receptor type, suggesting that inhibiting one receptor type caused relocalization of the other by physical proxy (Ellis et al., 2006).

Sex differences were observed in two scenarios. First, male C57BL/6 mice were more sensitive to the cataleptic effects of 1 mg/kg C55,940 + 1 mg/kg TCS-1102 compared to treatment-matched females. Sex differences in catalepsy were not detected in the TCS-OX2-29-administered groups, indicating that males are more sensitive than females to simultaneous CBR and OX1R- but not OX2R-manipulation. Closer examination of the receptor colocalization results revealed that in the absence of cannabinoid and orexin drug administration, males and females had similar levels of CB1R-OX1R and CB1R-OX2R expression in the ventral striatum. Following treatment with TCS-OX2-29 alone, cells from the ventral striatum of males had higher levels of CB1R-OX1R/OX2R colocalization compared to females. In all other drug treatments, no significant difference in cannabinoid and orexin receptor colocalization was observed between sexes. Male rodents have lower hypothalamic mRNA levels of OXA and OXB precursor, prepro-orexin (Jöhren et al., 2002), as well as less basal activation of OXA containing lateral hypothalamic neurons (Grafe et al., 2017). Although female rodents are reported to have higher orexigenic functioning (Grafe and Bhatnagar, 2020), males may have greater expression and function of orexin receptors that interact, or are heterodimerized with CB1R. This may result in males being more sensitive to dual cannabinoid and orexin drug effects compared to females.

The second sex difference observed was within the tail flick test. Males were more sensitive to the analgesic effects of CP55,940 alone, as well as both combination drug treatments. Most behavioral studies have reported that females are more sensitive to the cataleptic and anti-nociceptive effects of phyto- and synthetic cannabinoid agonists (Tseng and Craft, 2001; Wiley et al., 2017). With regards to brain region-specific cannabinoid receptor expression and function, CB1R density is greater in the prefrontal cortex of male versus female rats (Castelli et al., 2014). Males also display higher CB1R binding in limbic regions such as the striatum (Rodríguez de Fonseca et al., 1994). It remains unclear how these molecular data translate to sex-dependent behavioral outcomes, as these types of experiments have never been conducted nor correlated in the same sample or study. Preclinical cannabinoid research is seeing more inclusion of female animals; however, endocannabinoid-sex hormone interactions are more complex than simply comparing testosterone-dominant males and estrogen-dominant females (Struik et al., 2018). The latter undergo hypothalamic-pituitary-gonadal-driven ovulation cycles that cause significant fluctuations in circulating estrogens and progestins. The mouse estrus cycle spans 4 days, throughout which these hormone levels influence endocannabinoid activity and physiological response to cannabinoids (Rodríguez de Fonseca et al., 1994; Wakley and Craft, 2011). For example, female rats in estrus are significantly

less sensitive to the sedative and analgesic effects of systemic Δ^9-THC compared to female rats in late proestrus (Wakley and Craft, 2011). Estrus cycle-dependent differences in cannabinoid and orexin drug responses are being investigated in a forthcoming proof-of-concept study.

Cannabis is one of the most highly consumed psychoactive drugs in the world (World Health Organization [WHO], 2016). Many people self-medicate with cannabis to induce relaxation; a subset of these individuals may co-administer cannabis with prescribed DORAs for insomnia. Sleep is a complicated behavior based on multiple physiological factors. Although both cannabinoid receptor agonists and orexin receptor antagonists individually promote sleep, they may differentially affect the conditions for sleep when combined. The current study found that catalepsy was the only tetrad measure equally potentiated by both drugs. Moreover, OX1R antagonism, rather than OX2R antagonism, resulted in increased CB1R-OX1R colocalization in the ventral striatum underlying this cataleptic additivity. The growing use of cannabinoids warrants more research in the area of cannabinoid-drug interactions. Knowledge of cannabinoid receptor heterodimerization with other GPCRs is key in understanding these pharmacodynamic interactions.

DATA AVAILABILITY STATEMENT

The raw data supporting the conclusions of this article will be made available by the authors, without undue reservation.

ETHICS STATEMENT

The animal study was reviewed and approved by Animal Research Ethics Board and the Scientific Merit Review Committee for Animal Behaviour at the University of Saskatchewan.

AUTHOR CONTRIBUTIONS

HJK designed and executed the experiments, analyzed the data, as well as wrote and edited the manuscript. AZ, AMS, UCE, MJB, and TH assisted with *in vivo* experiments and edited the manuscript. RBL aided in the design of the experiments, analyzed the data, and edited the manuscript.

FUNDING

This work was supported by the National Sciences and Engineering Research Council (NSERC) Discovery Grant (DGECR-2019-00207) held by RBL. AZ and UCE were supported by graduate scholarships from the College of Pharmacy and Nutrition, University of Saskatchewan. AMS was supported by an interdisciplinary undergraduate research award from the College of Medicine and College of Pharmacy and Nutrition, University of Saskatchewan.

ACKNOWLEDGMENTS

We thank Aditya Manek from the University of Saskatchewan Histology Core Facility for his guidance in developing the cryosectioning and immunohistochemistry protocols. We also thank Narsimha Pujari in the Western College of Veterinary Medicine at the University of Saskatchewan, for his assistance in confocal microscopy and colocalization analysis.

REFERENCES

Anderson, J. J., Kask, A. M., and Chase, T. N. (1996). Effects of cannabinoid receptor stimulation and blockade on catalepsy produced by dopamine receptor antagonists. *Eur. J.* 295, 163–168. doi: 10.1016/0014-2999(95)00661-3

Babson, K. A., Sottile, J., and Morabito, D. (2017). Cannabis, cannabinoids, and sleep: a review of the literature. *Curr. Psychiatry Rep.* 19:23. doi: 10.1007/s11920-017-0775-9

Berrendero, F., Flores, Á., and Robledo, P. (2018). When orexins meet cannabinoids: bidirectional functional interactions. *Biochem. Pharmacol.* 157, 43–50. doi: 10.1016/j.bcp.2018.08.040

Castelli, M. P., Fadda, P., Casu, A., Spano, M. S., Casti, A., Fratta, W., et al. (2014). Male and female rats differ in brain cannabinoid CB1 receptor density and function and in behavioural traits predisposing to drug addiction: effect of ovarian hormones. *Curr. Pharm. Des.* 20, 2100–2113. doi: 10.2174/13816128113199990430

Chiou, L. C., Lee, H. J., Ho, Y. C., Chen, S., Liao, Y. Y., Ma, C. H., et al. (2010). Orexins/hypocretins: pain regulation and cellular actions. *Curr. Pharm. Des.* 16, 3089–3100. doi: 10.2174/138161210793292483

Ellis, J., Pediani, J. D., Canals, M., Milasta, S., and Milligan, G. (2006). Orexin-1 receptor-cannabinoid CB1 receptor heterodimerization results in both ligand-dependent and -independent coordinated alterations of receptor localization and function. *J. Biol. Chem.* 281, 38812–38824. doi: 10.1074/jbc.M602494200

Flores, A., Maldonado, R., and Berrendero, F. (2013). Cannabinoid-hypocretin cross-talk in the central nervous system: what we know so far. *Front. Neurosci.* 7:256. doi: 10.3389/fnins.2013.00256

Flores, Á., Maldonado, R., and Berrendero, F. (2014). The hypocretin/orexin receptor-1 as a novel target to modulate cannabinoid reward. *Biol. Psychiatry* 75, 499–507. doi: 10.1016/j.biopsych.2013.06.012

Flores, Á, Julià-Hernández, M., Maldonado, R., and Berrendero, F. (2016). Involvement of the orexin/hypocretin system in the pharmacological effects induced by Δ9-tetrahydrocannabinol. *Br. J. Pharmacol.* 173, 1381–1392. doi: 10.1111/bph.13440

Freund, T. F., Katona, I., and Piomelli, D. (2003). Role of endogenous cannabinoids in synaptic signaling. *Physiol. Rev.* 83, 1017–1066. doi: 10.1152/physrev.00004.2003

Funato, H., Tsai, A. L., Willie, J. T., Kisanuki, Y., Williams, S. C., Sakurai, T., et al. (2009). Enhanced orexin receptor-2 signaling prevents diet-induced obesity and improves leptin sensitivity. *Cell Metab.* 9, 64–76. doi: 10.1016/j.cmet.2008.10.010

Grafe, L. S., and Bhatnagar, S. (2020). The contribution of orexins to sex differences in the stress response. *Brain Res.* 1731:145893. doi: 10.1016/j.brainres.2018.07.026

Grafe, L. A., Eacret, D., Luz, S., Gotter, A. L., Renger, J. J., Winrow, C. J., et al. (2017). Orexin 2 receptor regulation of the hypothalamic-pituitary-adrenal (HPA) response to acute and repeated stress. *Neuroscience* 348, 313–323. doi: 10.1016/j.neuroscience.2017.02.038

Henderson-Redmond, A. N., Sepulveda, D. E., Ferguson, E. L., Kline, A. M., Piscura, M. K., and Morgan, D. J. (2021). Sex-specific mechanisms of tolerance for the cannabinoid agonists CP55,940 and delta-9-tetrahydrocannabinol (Δ^9-THC). *Psychopharmacology* doi: 10.1007/s00213-021-05886-9 [Epub Online ahead of print].

Herring, W. J., Roth, T., Krystal, A. D., and Michelson, D. (2019). Orexin receptor antagonists for the treatment of insomnia and potential treatment of other neuropsychiatric indications. *J. Sleep Res.* 28:e12782. doi: 10.1111/jsr.12782

Hervieu, G. J., Cluderay, J. E., Harrison, D. C., Roberts, J. C., and Leslie, R. A. (2001). Gene expression and protein distribution of the orexin-1 receptor in the rat brain and spinal cord. *Neuroscience* 103, 777–797. doi: 10.1016/s0306-4522(01)00033-1

Hilairet, S., Bouaboula, M., Carrière, D., Le Fur, G., and Casellas, P. (2003). Hypersensitization of the orexin 1 receptor by the CB1 receptor: evidence for cross-talk blocked by the specific CB1 antagonist, SR141716. *J. Biol. Chem.* 278, 23731–23737. doi: 10.1074/jbc.M212369200

Howlett, A. C., and Abood, M. E. (2017). CB1 & CB2 receptor pharmacology. *Adv. Pharmacol.* 80, 169–206. doi: 10.1016/bs.apha.2017.03.007

Imperatore, R., Palomba, L., Morello, G., Spiezio, A. D., Piscitelli, F., Marzo, V. D., et al. (2016). Formation of OX-1R/CB1R heteromeric complexes in embryonic mouse hypothalamic cells: effect on intracellular calcium, 2-arachidonoylglycerol biosynthesis and ERK phosphorylation. *Pharmacol. Res.* 111, 600–609. doi: 10.1016/j.phrs.2016.07.009

Jäntti, M. H., Mandrika, I., and Kukkonen, J. P. (2014). Human orexin/hypocretin receptors form constitutive homo- and heteromeric complexes with each other and with human CB1 cannabinoid receptors. *Biochem. Biophys. Res. Commun.* 445, 486–490. doi: 10.1016/j.bbrc.2014.02.026

Jöhren, O., Neidert, S. J., Kummer, M., and Dominiak, P. (2002). Sexually dimorphic expression of prepro-orexin mRNA in the rat hypothalamus. *Peptides* 23, 1177–1180. doi: 10.1016/S0196-9781(02)00052-9

Kano, M., Ohno-Shosaku, T., Hashimotodani, Y., Uchigashima, M., and Watanabe, M. (2009). Endocannabinoid-mediated control of synaptic transmission. *Physiol. Rev.* 89, 309–380. doi: 10.1152/physrev.00019.2008

Kilkenny, C., Browne, W. J., Cuthill, I. C., Emerson, M., and Altman, D. G. (2010). Improving bioscience research reporting: the arrive guidelines for reporting animal research. *PLoS Biol.* 8:e1000412. doi: 10.1371/journal.pbio.1000412

Mackie, K. (2005). "Distribution of cannabinoid receptors in the central and peripheral nervous system," in *Cannabinoids*, ed. R. G. Pertwee (Heidelberg: Springer), 299–325.

Mang, G. M., Dürst, T., Bürki, H., Imobersteg, S., Abramowski, D., Schuepbach, E., et al. (2012). The dual orexin receptor antagonist almorexant induces sleep and decreases orexin-induced locomotion by blocking orexin 2 receptors. *Sleep* 35, 1625–1635. doi: 10.5665/sleep.2232

Marcus, J. N., Aschkenasi, C. J., Lee, C. E., Chemelli, R. M., Saper, C. B., Yanagisawa, M., et al. (2001). Differential expression of Orexin receptors 1 and 2 in the rat brain. *J. Comp. Neurol.* 435, 6–25. doi: 10.1002/cne.1190

Mechoulam, R., and Fride, E. (2001). Physiology: a hunger for cannabinoids. *Nature* 410, 763–765. doi: 10.1038/35071214

Merroun, I., El Mlili, N., Martinez, R., Porres, J. M., Llopis, J., Ahabrach, H., et al. (2015). Interaction between orexin A and cannabinoid system in the lateral hypothalamus of rats and effects of subchronic intraperitoneal administration of cannabinoid receptor inverse agonist on food intake and the nutritive utilization of protein. *J. Physiol. Pharmacol.* 66, 181–190.

Metna-Laurent, M., Mondésir, M., Grel, A., Vallée, M., and Piazza, P. V. (2017). Cannabinoid-induced tetrad in mice. *Curr. Protoc. Neurosci.* 80, 9.59.1–9.59.10. doi: 10.1002/cpns.31

Mieda, M., Hasegawa, E., Kisanuki, Y. Y., Sinton, C. M., Yanagisawa, M., and Sakurai, T. (2011). Differential roles of orexin receptor-1 and -2 in the regulation of Non-REM and REM sleep. *J. Neurosci.* 31, 6518–6526. doi: 10.1523/JNEUROSCI.6506-10.2011

Monda, M., Viggiano, A., Viggiano, A., Viggiano, E., Lanza, A., and De Luca, V. (2005). Hyperthermic reactions induced by orexin A: role of the ventromedial hypothalamus. *Eur. J. Neurosci.* 22, 1169–1175. doi: 10.1111/j.1460-9568.2005.04309.x

Murata, K. (2020). Hypothetical Roles of the Olfactory Tubercle in Odor-Guided Eating Behavior. *Front. Neural Circ.* 14:577880. doi: 10.3389/fncir.2020.577880

Ossowska, K., Karcz, M., Wardas, J., and Wolfarth, S. (1990). Striatal and nucleus accumbens D1/D2 dopamine receptors in neuroleptic catalepsy. *Eur. J. Pharmacol.* 182, 327–334. doi: 10.1016/0014-2999(90)90291-D

Patel, K. V., Aspesi, A. V., and Evoy, K. E. (2015). Suvorexant: a dual orexin receptor antagonist for the treatment of sleep onset and sleep maintenance insomnia. *Ann. Pharmacother.* 49, 477–483. doi: 10.1177/1060028015570467

Patel, M., Manning, J. J., Finlay, D. B., Javitch, J. A., Banister, S. D., Grimsey, N. L., et al. (2020). Signalling profiles of a structurally diverse panel of synthetic cannabinoid receptor agonists. *Biochem. Pharmacol.* 175:113871. doi: 10.1016/j.bcp.2020.113871

Petrunich-Rutherford, M. L., and Calik, M. W. (2021). Effects of cannabinoid agonists and antagonists on sleep in laboratory animals. *Adv. Exp. Med. Biol.* 1297, 97–109. doi: 10.1007/978-3-030-61663-2_7

Plaza-Zabala, A., Maldonado, R., and Berrendero, F. (2012). The hypocretin/orexin system: implications for drug reward and relapse. *Mol. Neurobiol.* 45, 424–439. doi: 10.1007/s12035-012-8255-z

Polissidis, A., Galanopoulos, A., Naxakis, G., Papahatjis, D., Papadopoulou-Daifoti, Z., and Antoniou, K. (2013). The cannabinoid CB1 receptor biphasically modulates motor activity and regulates dopamine and glutamate release region dependently. *Int. J. Neuropsychopharmacol.* 16, 393–403. doi: 10.1017/S1461145712000156

Rawls, S. M., Cabassa, J., Geller, E. B., and Adler, M. W. (2002). CB 1 Receptors in the Preoptic Anterior Hypothalamus Regulate WIN 55212-2 [(4,5-dihydro-2-methtyl-4(4-morpholinylmethyl0-1-(1-naphthalenyl-carbonyl)-6H-pyrrolo[3,2,1ij]quinolin-6-one]-induced Hypothermia. *J. Pharmacol. Exp. Ther.* 301, 963–968. doi: 10.1124/jpet.301.3.963

Rodríguez de Fonseca, F., Cebeira, M., Ramos, J. A., Martín, M., and Fernández-Ruiz, J. J. (1994). Cannabinoid receptors in rat brain areas: sexual differences, fluctuations during estrous cycle and changes after gonadectomy and sex steroid replacement. *Life Sci.* 54, 159–170. doi: 10.1016/0024-3205(94)00585-0

Sahni, V., Engmann, A., Ozkan, A., and Macklis, J. D. (2020). "Chapter 8 – Motor cortex connections," in *Neural Circuit and Cognitive Development*, eds J. Rubenstein, P. Rakic, B. Chen, and K. Y. Kwan (Cambridge: Academic Press), 167–199. doi: 10.1016/B978-0-12-814411-4.00008-1

Struik, D., Sanna, F., and Fattore, L. (2018). The modulating role of sex and anabolic-androgenic steroid hormones in cannabinoid sensitivity. *Front. Behav. Neurosci.* 12:249. doi: 10.3389/fnbeh.2018.00249

Trivedi, P., Yu, H., MacNeil, D. J., Van Der Ploeg, L. H. T., and Guan, X. M. (1998). Distribution of orexin receptor mRNA in the rat brain. *FEBS Lett.* 438, 71–75. doi: 10.1016/S0014-5793(98)01266-6

Tseng, A. H., and Craft, R. M. (2001). Sex differences in antinociceptive and motoric effects of cannabinoids. *Eur. J. Pharmacol.* 430, 41–47. doi: 10.1016/S0014-2999(01)01267-5

Turski, L., Havemann, U., and Kuschinsky, K. (1984). GABAergic mechanisms in mediating muscular rigidity, catalepsy and postural asymmetry in rats: differences between dorsal and ventral striatum. *Brain Res.* 322, 49–57. doi: 10.1016/0006-8993(84)91179-x

Valencia Garcia, S., and Fort, P. (2018). Nucleus Accumbens, a new sleep-regulating area through the integration of motivational stimuli. *Acta Pharmacol. Sin.* 39, 165–166. doi: 10.1038/aps.2017.168

Wakley, A. A., and Craft, R. M. (2011). Antinociception and sedation following intracerebroventricular administration of Δ9-tetrahydrocannabinol in female vs. male rats. *Behav. Brain Res.* 216, 200–206. doi: 10.1016/j.bbr.2010.07.037

Walker, J. M., and Hohmann, A. G. (2005). "Cannabinoid mechanisms of pain suppression," in *Cannabinoids*, ed. R. G. Pertwee (Heidelberg: Springer), 509–554.

Ward, R. J., Pediani, J. D., and Milligan, G. (2011). Heteromultimerization of cannabinoid CB 1 receptor and orexin OX 1 receptor generates a unique complex in which both protomers are regulated by orexin A. *Int. J. Biol. Chem.* 286, 37414–37428. doi: 10.1074/jbc.M111.287649

Wesson, D. W., and Wilson, D. A. (2011). Sniffing out the contributions of the olfactory tubercle to the sense of smell: hedonics, sensory integration, and more? *Neurosci. Biobehav. Rev.* 35, 655–668. doi: 10.1016/j.neubiorev.2010.08.004

Willie, J. T., Chemelli, R. M., Sinton, C. M., Tokita, S., Williams, S. C., Kisanuki, Y. Y., et al. (2003). Distinct narcolepsy syndromes in orexin receptor-2 and orexin null mice: molecular genetic dissection of non-REM and REM sleep

regulatory processes. *Neuron* 38, 715–730. doi: 10.1016/S0896-6273(03)00330-1

Wiley, J. L., Lefever, T. W., Marusich, J. A., and Craft, R. M. (2017). Comparison of the discriminative stimulus and response rate effects of Δ9-tetrahydrocannabinol and synthetic cannabinoids in female and male rats. *Drug Alcohol Depend.* 172, 51–59. doi: 10.1016/j.drugalcdep.2016.11.035

World Health Organization [WHO] (2016). *Cannabis*. Available Online at: https://www.who.int/teams/mental-health-and-substance-use/alcohol-drugs-and-addictive-behaviours/drugs-psychoactive/cannabis [Accessed Oct 1, 2021].

Yamanaka, A., Beuckmann, C. T., Willie, J. T., Hara, J., Tsujino, N., Mieda, M., et al. (2003). Hypothalamic orexin neurons regulate arousal according to energy balance in mice. *Neuron* 38, 701–713. doi: 10.1016/S0896-6273(03)00331-3

Yazdi, F., Jahangirvand, M., Pirasteh, A. H., Moradi, M., and Haghparast, A. (2015). Functional interaction between OX2 and CB1 receptors in the ventral tegmental area and the nucleus accumbens in response to place preference induced by chemical stimulation of the lateral hypothalamus. *Pharmacol. Biochem. Behav.* 139, 39–46. doi: 10.1016/j.pbb.2015.10.012

Yoshimichi, G., Yoshimatu, H., Masaki, T., and Sakata, T. (2001). Orexin-A regulates body temperature in coordination with arousal status. *Exp. Biol. Med.* 226, 468–476. doi: 10.1177/153537020122600513

Zagzoog, A., Brandt, A. L., Black, T., Kim, E. D., Burkart, R., Patel, M., et al. (2021). Assessment of select synthetic cannabinoid receptor agonist bias and selectivity between the type 1 and type 2 cannabinoid receptor. *Sci. Rep.* 11:10611. doi: 10.1038/s41598-021-90167-w

Zagzoog, A., Mohamed, K. A., Kim, H. J. J., Kim, E. D., Frank, C. S., Black, T., et al. (2020). *In vitro* and *in vivo* pharmacological activity of minor cannabinoids isolated from *Cannabis sativa*. *Sci. Rep.* 10:20405. doi: 10.1038/s41598-020-77175-y

Zanettini, C., Panlilio, L. V., Alicki, M., Goldberg, S. R., Haller, J., and Yasar, S. (2011). Effects of endocannabinoid system modulation on cognitive and emotional behavior. *Front. Behav. Neurosci.* 5:57. doi: 10.3389/fnbeh.2011.00057

Zinchuk, V., and Zinchuk, O. (2008). Quantitative colocalization analysis of confocal fluorescence microscopy images. *Curr. Protoc. Cell Biol.* 39, 1–4. doi: 10.1002/0471143030.cb0419s39

Conflict of Interest: The authors declare that the research was conducted in the absence of any commercial or financial relationships that could be construed as a potential conflict of interest.

Publisher's Note: All claims expressed in this article are solely those of the authors and do not necessarily represent those of their affiliated organizations, or those of the publisher, the editors and the reviewers. Any product that may be evaluated in this article, or claim that may be made by its manufacturer, is not guaranteed or endorsed by the publisher.

frontiers in Pharmacology

ORIGINAL RESEARCH
published: 03 January 2022
doi: 10.3389/fphar.2021.781237

Transcriptomic Profiling in Mice With CB1 receptor Deletion in Primary Sensory Neurons Suggests New Analgesic Targets for Neuropathic Pain

Yongmin Liu[1,2], Min Jia[3], Caihua Wu[4], Hong Zhang[1], Chao Chen[1], Wenqiang Ge[1], Kexing Wan[1], Yuye Lan[1], Shiya Liu[1], Yuanheng Li[1], Mengyue Fang[1], Jiexi He[1], Hui-Lin Pan[5], Jun-Qiang Si[6] and Man Li[1]**

[1]Department of Neurobiology, School of Basic Medicine, Tongji Medical College, Huazhong University of Science and Technology, Wuhan, China, [2]Department of Pathophysiology, Medical College of Shihezi University, Shihezi, China, [3]Clinical Laboratories, Wuhan First Hospital, Wuhan, China, [4]Department of Acupuncture, Wuhan First Hospital, Wuhan, China, [5]Department of Anesthesiology and Perioperative Medicine, The University of Texas MD Anderson Cancer Center, Houston, TX, United States, [6]Department of Physiology, Medical College of Shihezi University, Shihezi, China

Type 1 and type 2 cannabinoid receptors (CB1 and CB2, respectively) mediate cannabinoid-induced analgesia. Loss of endogenous CB1 is associated with hyperalgesia. However, the downstream targets affected by ablation of CB1 in primary sensory neurons remain unknown. In the present study, we hypothesized that conditional knockout of CB1 in primary sensory neurons (CB1cKO) alters downstream gene expression in the dorsal root ganglion (DRG) and that targeting these pathways alleviates neuropathic pain. We found that CB1cKO in primary sensory neurons induced by tamoxifen in adult Advillin-Cre:CB1-floxed mice showed persistent hyperalgesia. Transcriptome/RNA sequencing analysis of the DRG indicated that differentially expressed genes were enriched in energy regulation and complement and coagulation cascades at the early phase of CB1cKO, whereas pain regulation and nerve conduction pathways were affected at the late phase of CB1cKO. Chronic constriction injury in mice induced neuropathic pain and changed transcriptome expression in the DRG of CB1cKO mice, and differentially expressed genes were mainly associated with inflammatory and immune-related pathways. Nerve injury caused a much larger increase in CB2 expression in the DRG in CB1cKO than in wildtype mice. Interfering with downstream target genes of CB1, such as antagonizing CB2, inhibited activation of astrocytes, reduced neuroinflammation, and alleviated neuropathic pain. Our results demonstrate that CB1 in primary sensory neurons functions as an endogenous analgesic mediator. CB2 expression is regulated by CB1 and may be targeted for the treatment of neuropathic pain.

Keywords: cannabinoid receptor, transcriptome sequencing, neuropathic pain, dorsal root ganglia, downstream gene, neuroinflammation

OPEN ACCESS

Edited by:
Carmen Rodriguez Cueto, Center for Biomedical Research on Neurodegenerative Diseases (CIBERNED), Spain

Reviewed by:
Erin E. Young, University of Kansas Medical Center, United States
Shangdong Liang, Nanchang University, China

***Correspondence:**
Jun-Qiang Si
sijunqiang11@hotmail.com
Man Li
liman73@mails.tjmu.edu.cn

Specialty section:
This article was submitted to Neuropharmacology, a section of the journal Frontiers in Pharmacology

Received: *22 September 2021*
Accepted: *12 November 2021*
Published: *03 January 2022*

Citation:
Liu Y, Jia M, Wu C, Zhang H, Chen C, Ge W, Wan K, Lan Y, Liu S, Li Y, Fang M, He J, Pan H-L, Si J-Q and Li M (2022) Transcriptomic Profiling in Mice With CB1 receptor Deletion in Primary Sensory Neurons Suggests New Analgesic Targets for Neuropathic Pain. Front. Pharmacol. 12:781237. doi: 10.3389/fphar.2021.781237

INTRODUCTION

Neuropathic pain, caused by a lesion or disease affecting the somatosensory system, is a major clinical problem and has a considerable impact on the life quality of patients (Burke et al., 2017). The antinociceptive efficacy of cannabinoids has been unequivocally demonstrated in several models of neuropathic pain in animal studies (Walker and Hohmann, 2005). However, clinical application of cannabinoids is severely hindered by adverse reactions resulting from its central actions, such as cognitive deficits, memory impairment, motor disturbances, addiction, and cognitive impairment (Hossain et al., 2020).

Analgesic properties of cannabinoids are achieved mainly by activating G protein-coupled receptors, i.e., type 2 cannabinoid receptor (CB2) and type 1 cannabinoid receptor (CB1) (Matsuda et al., 1990; Munro et al., 1993). CB1 is mainly at the presynapse, where the activation of CB1 can suppress presynaptic neurotransmitter release through a short-term decrease in Ca2+ influx (Katona and Freund, 2012; Lutz et al., 2015; Lutz, 2020). Nerve injury induces long-lasting CB1 downregulation in dorsal root ganglion (DRG) neurons and diminishes the analgesic effect of the CB1 agonist on neuropathic pain (Luo et al., 2020), which is thought to be attributed to the reversed inhibition by endogenous cannabinoids. CB2 expressed on immune cells and the nervous system has also been implicated in cannabinoid analgesia (Walker and Hohmann, 2005; Ibrahim et al., 2006). CB2 was strongly upregulated in response to various insults, stroke, neuroinflammation, and chronic pain (e.g., Leung, 2004; Solas et al., 2013). Some previous studies reported that CB2 was mainly involved in analgesia through limiting neuroinflammation (Nackley et al., 2003; Elmes et al., 2005; Shang and Tang, 2017). Studies of global-knockout mice have confirmed that CB1 and CB2 were involved in cannabinoid-mediated analgesia (Ibrahim et al., 2006; Sain et al., 2009; Sideris et al., 2016). Moreover, after the selective deletion of CB1 in nociceptive (Nav1.8-expressing) sensory neurons, physiological and basal pain sensitivity was exaggerated, showing the significantly reduced reaction latencies to noxious heat and response thresholds to mechanical stimuli (Agarwal et al., 2007).

Peripheral nerve injury is accompanied by alterations in transcription reprogramming in the peripheral nervous system, which subsequently causes altered behaviors in animals. The variation of DRG gene expression is related to pain phenotypes (Bosma et al., 2020; Sun et al., 2020), which can be screened by RNA sequencing for identification of differentially expressed genes (DEGs) and their functional pathways related to neuropathic pain development. Moreover, single-cell sequencing technology revealed the gene expression patterns in subtypes of DRG neurons after peripheral nerve injury (Wang et al., 2021). Although CB1 knockout may exaggerate pain, it remains unknown how transcriptomic profiling changes in mice with CB1 deletion in peripheral sensory neurons and whether the downstream genes of CB1 may provide new analgesic targets in neuropathic pain.

Therefore, in this study, we investigated whether CB1 conditional knockout from peripheral sensory neurons (CB1cKO) in mice may present mechanical allodynia, thermal hyperalgesia, and a change in transcriptome expression in DRG. Then, we determined the effect of chronic constriction injury (CCI) model of CB1cKO mice on pain behavior and transcriptome expression of DRG. Moreover, we screened and analyzed the DEGs and their functional pathways after CCI and revealed the downstream of CB1. Finally, we observed whether intervention of the downstream target of CB1 may alleviate neuropathic pain. Our findings provided new evidence of the role of CB1 in the development of neuropathic pain and the downstream genes of CB1 may serve as therapeutic targets for neuropathic pain.

MATERIALS AND METHODS

Animals

Ethical guidelines of the International Association for the Study of Pain were strictly followed, and the protocol was approved by the local ACUC. All animals were housed at 22°C–24°C based on a 12-h light/dark cycle and were allowed free access to food and water.

C57BL/6J mice were used in the experiments. Adult male C57BL/6J mice (20–25 g; 8-week-old) were provided by Beijing Vital River Laboratory Animal Technology Co. Ltd.

AvCreERT2 (Advillin-CreERT2) mice (Jax Stock No. 026516) expressed a tamoxifen (TMX)-inducible iCre recombinase directed by mouse Avil (advillin) promoter elements. iCre recombinase activity was found in DRG neurons when induced by TMX.

$Cnr^{1tm1.2Ltz}$/J mice (Jax Stock No.036107) and CB1f/f mice have loxP sites flanking the entire coding region of the Cnr1 gene. After crossing Advillin-CreerT2 (AvCreerT2) mice and CNR1TM1.2LTZ/J mice for two generations, tissue/cell-specific knockout homozygous mice were obtained in the F3 generation after TMX induction (treatment details are shown in *Drug Treatment*), which are referred to as CB1cKO mice.

Identification of Transgenic Mice

Seven CB1cKO mice and seven wild-type littermates male mice (WT mice) were used for genotyping. Before TMX induction, the genomic DNA was extracted from the toes or tails of the genetic mice using chloroform/phenol and precipitated by isopropanol. It was then washed by ethanol (75%) and dissolved in deionized water. The primers for PCR are shown in **Supplementary Table S1**. The products of PCR reactions are shown in **Supplementary Table S2**. The products were dissolved on agarose gel (1.5%), stained with ethidium bromide, and photographed.

CB1 in DRG was verified by immunofluorescence and real-time polymerase chain reaction (RT-qPCR) on the 14th day after the final TMX induction (detailed method is shown in *Real-Time Polymerase Chain Reaction* and *Immunofluorescence*).

Drug Treatment

TMX (Sigma T5648) was dissolved into corn oil and was injected intraperitoneally (i.p.) once every other day, a total of five times, 2 mg/day (10 mg total dose) (Feil et al., 2009; Anastassiadis et al., 2010). Subsequent verification and CCI modeling were performed 14 days after the final injection.

AM1241 (Sigma A6478) is a CB2 agonist, and AM630 (Sigma SML0327) is a highly specific CB2 antagonist. The drug was dissolved in dimethyl sulfoxide (DMSO), Tween 80, and normal saline (the ratio is 1:2:7). To determine the relationship between neuropathic pain and CB2, 36 WT mice were randomly divided into WT CCI + vehicle (DMSO:Tween 80:normal saline = 1:2:7), WT CCI + 0.1, 1, 3 mg/kg AM1241 (Sigma A6478; Wu et al., 2021; Lozano-Ondoua et al., 2010; Ma et al., 2021) groups, and WT CCI + 1, 3 mg/kg AM630 (Sigma SML0327; Malan et al., 2001; Buffon et al., 2020; Sultana et al., 2021) groups ($n = 6$ at each group). Fifteen CB1cKO mice were randomly divided into CB1cKO CCI + vehicle and CB1cKO CCI + 3, 5 mg/kg AM630 ($n = 5$ at each group). AM1241/AM630 or its vehicle (0.1 ml) was injected i.p. daily from 12th to 17th day after CCI surgery.

Behavioral Testing

Ten CB1cKO mice and 10 WT mice were used to test tactile withdrawal threshold and thermal latency by von Frey and Hargreaves plantar tests before and every 3 days after TMX induction. To rule out the effect of TMX on the nociceptive threshold, WT mice were also i.p. injected with TMX at the same time and dose as CB1cKO mice.

The "up and down" method was used to determine the threshold of tactile withdrawal in mice (Chaplan et al., 1994). After adapting for half an hour, the plantar surface of the left hind paw was stimulated vertically by von Frey filaments (Stoelting, Wood Dale, IL, USA), and the stiffness was increased logarithmically. Positive response was defined as paw flinching or brisk withdrawal after stimulation for 5 s. Thresholds of tactile withdrawal were detected twice, and the average was taken. A hot plate with surface temperature controlled at 53°C was used to determine thermal latency. The withdrawal latency was defined as the interval between the moment mice were placed on the plate and the time point of flick of the paw or a quick withdrawal. In order to prevent tissue damage, 20 s were set as the cutoff time (Hargreaves et al., 1988). The thermal test was repeated three times, with an interval of 10 min, and the average was taken.

Chronic Constriction Injury Model Establishment

Fourteen WT mice were randomly divided into WT sham and WT CCI ($n = 7$ at each group), and 14 CB1cKO mice (eight male mice and six female mice) were randomly divided into CB1cKO sham and CB1cKO CCI ($n = 7$ at each group). All mice have received TMX induction. After the 14th day of the final TMX injection, the CCI model of neuropathic pain was chosen based on a previous description (Bennett and Xie, 1988). Then, 0.5% pentobarbital sodium was injected i.p. at a dose of 0.2 ml/10 g body weight. Corneal reflex, muscular tension, and respiratory and pain indicators were examined after intraperitoneal injection to ensure the anesthetic effect and the safety of animals. Experiments were conducted after the injection, and the body temperature was maintained by a heating pad during anesthesia. The left sciatic nerve was exposed at the midthigh level. Proximal to the sciatic trifurcation, two ligature knots (4–0 chromic gut) were loosely tied with a spacing of approximately 1 mm. However, in the sham-CCI group, muscles were separated and the sciatic nerve was exposed but not ligated with the chromic gut. The mechanical withdrawal threshold (MWT) and thermal withdrawal latency (TWL) of every mouse were measured as an assessment of nociception on days 0, 3, 5, 7, 10, and 13 after the CCI operation.

Real-Time Polymerase Chain Reaction

L4–L6 DRGs were harvested and immediately frozen on dry ice and stored at −80°C. TRIzol reagent (Invitrogen) was used to separate the total RNA that was extracted from DRG tissues (rapidly frozen). RT-qPCR was performed to determine the level of target gene and reference gene (gapdh), with Vazyme SYBR Premix Ex Taq II (Perfect Real Time). The total volume of the reaction system was 10 μl, which was composed of SYBR Premix Ex Taq TM(2×) (5 μl), cDNA (1 μl), ddH_2O (3.6 μl), and specific primer (0.2 μl; 10 μM). Reaction conditions: 95°C for 3 min; 95°C for 8 s, 60°C for 20 s, 40 cycles; melting. Data were normalized based on GAPDH, and the $2^{-\Delta\Delta}$Ct method was used. The primers for PCR are shown in **Supplementary Table S3**.

mRNA Library Constructs and Sequencing

Twelve CB1cKO mice and their six WT mice were randomly divided into six groups, including WT14, WT28, CB1cKO14, CB1cKO28, CB1cKO sham28, and CB1cKO CCI28 ($n = 3$ in each group). All mice have received TMX induction. On the 14th day and 28th day after the final injection of TMX, L4–L6 DRG of CB1cKO mice and WT mice was extracted for RNA sequencing, respectively. On the 13th day after CCI, L4–L6 DRG of CB1cKO mice was extracted for RNA sequencing.

mRNA was purified by magnetic beads with oligo (dT) and then fragmented into small pieces at a proper temperature using fragment buffer. The first-strand cDNA was produced by random reverse transcription (hexamer-primed), and the second-strand cDNA was then synthesized. RNA Index Adapters and A-Tailing Mix were added and incubated to terminate repair. PCR was performed for amplification of cDNA fragments harvested in the previous step, and the amplified products were further purified using Ampure XP Beads. The products were dissolved in EB solution and validated on the Agilent Technologies 2100 bioanalyzer for quality control. The double-stranded PCR products harvested were subjected to heating, denaturing, and circularization by the splint oligo sequence, and the library was constructed, with single-strand circle DNA (ssCir DNA) formatted. Amplification of the final library was performed using phi29 for a DNB (DNA nanoball), which had over 300 copies of one molecule. The DNB was loaded into the nanoarray, and single end reads with 50 bases were produced on the BGIseq500 platform (provided by BGI-Shenzhen, China).

Data Management and Gene Ontology and Kyoto Encyclopedia of Genes and Genomes Pathway Analysis

SOAPnuke (v1.5.2) was used to filter the sequencing data (Li et al., 2008): 1) reads that contained sequencing adapters were

removed; 2) reads with a quality base ratio (base quality ≤5) over 20% were removed; and 3) reads with an unknown base ("N" base) ratio over 5% were removed, and the harvested clean reads were stored in FASTQ format. Using HISAT2 (v2.0.4), the reads were mapped to the reference genome (Kim et al., 2015). Then, rMATS (V3.2.5) (Shen et al., 2014) and Ericscript (v0.5.5) (Benelli et al., 2012) were utilized to determine differential splicing genes (DSGs) and fusion genes, respectively. Using Bowtie2 (v2.2.5) (Langmead and Salzberg, 2012), the reads were aligned to the gene set, a database constructed by BGI (Beijing Genomic Institute in Shenzhen), which covered novel, known, noncoding, and coding transcripts. The RSEM (v1.2.12) (Li and Dewey, 2011) was used to calculate the gene expression level. The pheatmap (v1.0.8) was utilized to draw the heatmap based on gene expressions in a variety of samples. The DESeq2 (v1.4.5) (Love et al., 2014) was used for differential expression analysis, with Q value ≤0.05.

Kyoto Encyclopedia of Genes and Genomes (KEGG) pathway and Gene Ontology (GO) analyses were performed to explore the roles of all DE mRNAs. Briefly, GO analysis was carried out to elucidate genetic regulatory networks of interest by forming hierarchical categories based on the biological process (BP), cellular component (CC), and molecular function (MF) of DEGs. In order to determine the phenotypes, KEGG (https://www.kegg.jp/) enrichment and GO (http://www.geneontology.org/) analyses of annotated DEGs were carried out using Phyper (https://en.wikipedia.org/wiki/Hypergeometric distribution) and Hypergeometric test. The significant levels of pathways and terms were corrected by Bonferroni based on Q value ≤0.05.

Immunofluorescence

Anesthesia of the mice was performed using chloral hydrate (4%; 10 ml/kg, i.p.). The DRGs were fixed in paraformaldehyde (PFA; 4%) and phosphate buffered saline (PBS; 0.1 M, pH 7.4) for 4–8 h, followed by dehydration in PBS (0.1 M) with 20% and 30% sucrose. After embedding in OCT (provided by Miles Inc., Elkhart, IN, USA), the fixed DRG was vertically sectioned (15 μM in thickness). The sections were harvested and mounted on a slide coated by chrome-alum-gelatin. After PBS (0.1 M) rinsing, the section was blocked by triton X-100 (1.2%) and donkey serum (5%) for 2 h at room temperature. Then, the sections were incubated with primary antibodies of rabbit anti-CB1 (Abcam, #ab137410, 1:200 dilution) and glial fibrillary acidic protein (GFAP; Abcam, #ab4674, 1:5,000 dilution) overnight at 4°C. The primary antibodies were incubated with AffiniPure donkey anti-rabbit IgG (Alexa Fluor 488-conjugated, 1:350 dilution, Jackson) and donkey anti-Chicken IgG (Alexa Fluor 488-conjugated, 1:450 dilution, Jackson) and then observed. Images were acquired using a fluorescence microscope (BX51, Olympus, Japan), and NIH ImageJ software (provided by NIH, Bethesda, MD, USA) was used for their analysis.

Statistical Analysis

The data were expressed as mean ± SEM. Multiple groups were compared by two-way ANOVA with Bonferroni's *post-hoc* test, and two groups were compared by Student's *t*-test. $p < 0.05$ indicated a significant difference.

RESULTS

Generation and Verification of CB1cKO Mice

Before TMX induction, agarose gel electrophoresis images of tail DNA of transgenic mice were shown in **Supplementary Figure S1**. The knockout efficiency of CB1 in DRG was verified by immunofluorescence and RT-qPCR on the 14th day after the final TMX induction. Immunofluorescence labeling showed that CB1 was expressed in DRG neurons of WT mice and was present on the cell membrane and in the cytoplasm (**Figure 1A**, indicated by the thin white arrow). More than 90% of CB1 were knocked out on DRG neurons in CB1cKOmice (**Figure 1A**, thick white arrow). qPCR assay showed that compared with WT mice, CB1 mRNA was significantly reduced in the DRG of CB1cKO mice (**Figure 1B**, $p < 0.001$). However, the mRNA level of CB1 in the dorsal spinal horn did not differ significantly between the two groups of mice (**Figure 1B**, $p > 0.05$). These results indicated that the expression of CB1 was only reduced in DRG neurons of CB1cKO mice.

CB1cKO Mice Presented Tactile Allodynia

Next, we examined nociceptive withdrawal thresholds of CB1cKO mice after TMX induction. An experimental design time line is presented in **Figure 2A**. CB1cKO mice had a normal mechanical withdrawal threshold (MWT) and thermal latency before TMX induction (**Figures 3A, B**). After TMX induction, the MWT of CB1cKO mice was significantly reduced from the eighth day to the 28th day after the final TMX injection and reached the lowest level on the 14th day after the final TMX injection (day-14) and remained stable, lasting until day-28 (*$p < 0.05$, **Figure 3A**). Compared with WT mice, CB1cKO mice had significantly reduced MWT from day-11 to day-28, showing that physiological, basal pain sensitivity was exaggerated in CB1cKO mice (#$p < 0.05$, **Figure 3A**). We also found that the MWT of WT mice has decreased temporarily on day-8 after the same dose of TMX induction and then returned to normal. Notably, TMX induced long-lasting thermal hyperalgesia in both WT mice and CB1cKO mice (*$p < 0.05$, **Figure 3B**). So, we only observed a significant difference in the thermal latency between CB1cKO mice and WT mice on day-28 (#$p < 0.05$, **Figure 3B**). Together, these results showed that knocking down CB1 in DRG induced tactile allodynia and thermal hyperalgesia. In addition, TMX also caused tactile allodynia and thermal hyperalgesia, but the MWT could return to normal on day-14 in WT mice.

Differentially Expressed Gene Profile and Functional Enrichment Analysis After CB1 Knockdown

To gain molecular insights into persistent tactile allodynia that are mediated by CB1 of DRG, we conducted mRNA sequencing (mRNA-Seq) analysis. Detailed grouping information and experimental processing are presented in **Figures 2A and B**. In this project, 18 samples were measured using the DNBSEQ platform, and each sample produced an average of 6.59G data.

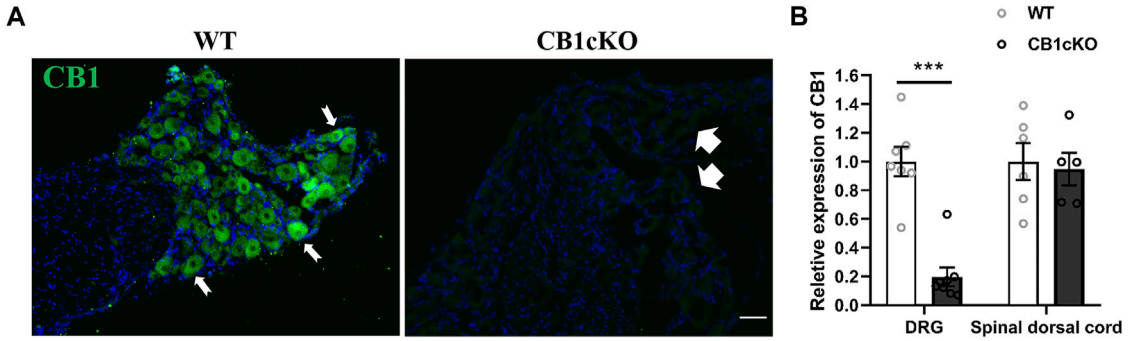

FIGURE 1 | Demonstration of conditional deletion of CB1 in peripheral sensory neuron-specific knockout CB1 mice (CB1cKO). **(A)** Immunofluorescence results of dorsal root ganglion (DRG) sections display the CB1-positive neuron (green) in CB1cKO and wild-type (WT) mice. **(B)** The mRNA relative expression of CB1 in the DRG and dorsal spinal cord on 14 days after the final injection of tamoxifen (TMX). Data are expressed as means ± SEM ($n = 7$ mice/group). The endogenous reference gene is Gapdh, and the mean value in the WT group was set to 1. ***$p < 0.001$ compared with the WT group at the same time point, two-tailed t test. Scale bar, 100 μm.

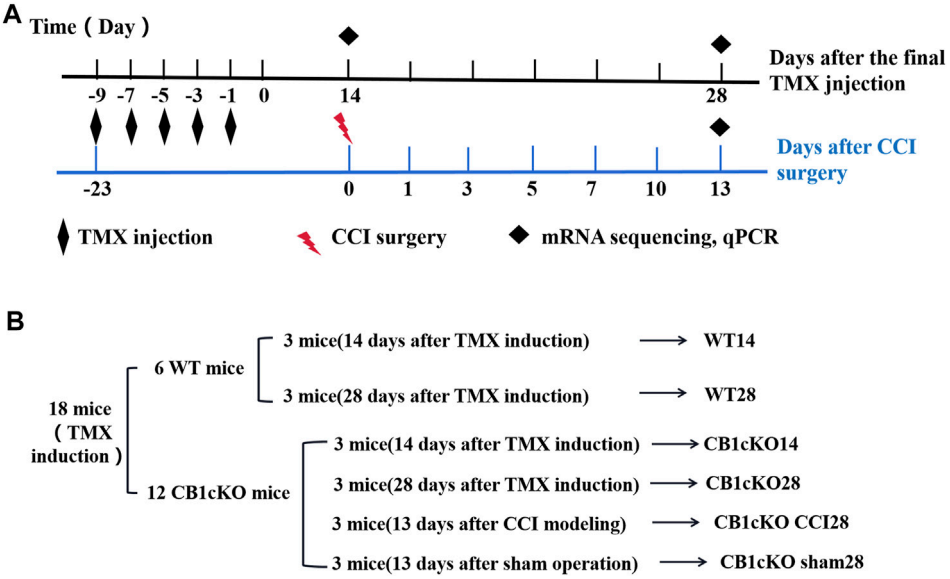

FIGURE 2 | Experimental flowchart and grouping of RNA sequencing (RNA-Seq).

The average sample ratio for the genome was 87.69% and 74.54% for the gene set. A total of 18,901 genes were detected. The raw data in this study are available in the NCBI SRA database.

In the early phase of CB1cKO (14 days after the final injection of TMX), compared with WT mice (WT14), 95 mRNAs were upregulated and 20 mRNAs were downregulated in CB1cKO mice (CB1KO 14, **Figure 4A**); the upregulated DEGs were mainly major urinary protein family (*mup7*, *10*, *11*, *19*, *22*), peptidase inhibitor (*Serpina1a*, *1b*, *1c*, *1d*), and enzymes required for material metabolism. **Figure 4B** lists the top 20 upregulated and top 10 downregulated DEGs (detailed information on DEGs is shown in **Supplementary Table S4**). Interestingly, most of them returned to normal after 2 weeks, such as major urinary protein family and peptidase inhibitor.

To better understand the associated functions of the DEGs in DRG after CB1 knockdown, KEGG and GO enrichment analyses of 115 DEGs were performed to identify the most relevant KEGG pathway, biological processes (GO-Process), and molecular functions (GO-Function). Specifically, the DEGs were mostly enriched related to complement and coagulation cascades in the KEGG pathway ($p < 0.05$, **Figure 4C**). The biological process of DEGs was mainly involved in heat generation; locomotor rhythm; synthesis and metabolism of glucose, fat, and energy; and negative regulation of endopeptidase or peptidase action ($p < 0.01$, **Figure 4D**). The molecular function of DEGs mainly associated with identical protein binding, calcium ion binding, and endopeptidase inhibitor activity ($p < 0.01$, **Figure 4E**). These results suggested that imbalances of

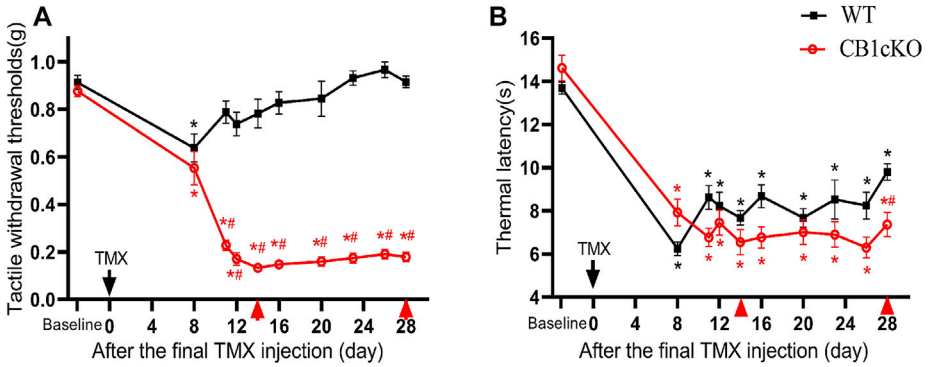

FIGURE 3 | Genetic deletion of CB1 in dorsal root ganglion (DRG) neurons induced tactile allodynia and thermal hyperalgesia. **(A, B)** Time course of the effect of tamoxifen (TMX) induction on the tactile withdrawal thresholds **(A)** and thermal latency **(B)** in CB1cKO and wild-type (WT) mice (n = 10 mice/group). Data are expressed as mean ± SEM, *p < 0.05, compared with the baseline of the respective group; #p < 0.05, compared with the WT group at the same time point (two-way ANOVA with Bonferroni's *post-hoc* test). The red arrows indicated two time points on day-14 (the early phase of CB1 knockout) and day-28 (the late phase of CB1 knockout) after TMX induction.

material metabolism and energy regulation were the stress responses in the early phase of CB1 knockdown.

Next, we screened for 266 DEGs in the late phase of CB1cKO (WT28 vs. CB1cKO28); 161 mRNAs were upregulated, and 105 mRNAs were downregulated (**Figure 5A**), 209 of which did not change in the early phase of CB1cKO. Many of them were closely related to pain, such as *npy*, *sprr1a*, *gpr151*, *nts*, and so on. **Figure 5B** lists the top 20 upregulated and downregulated DEGs (detailed information of DEGs is shown in **Supplementary Table S5**).

Furthermore, we analyzed and predicted the functional pathways of these DEGs of the late phase of CB1cKO. The most significantly enriched KEGG pathways were neuroactive ligand–receptor interaction, retrograde endocannabinoid signaling, morphine addiction, and circadian rhythm ($p < 0.05$, **Figure 5C**), and the specific genes in the pathway are listed in **Supplementary Table S6**. GO-processes analysis suggested that most of the altered genes were involved in axon guidance, regulation of sensory perception of pain, neuropeptide signaling pathway, ion transport, sensory perception of pain, and innate immune response ($p < 0.05$, **Figure 5D**), and the specific genes of biological processes are listed in **Supplementary Table S8**. GO-function analysis suggested that most of the altered genes were associated with protein binding, potassium channel activity, neuropeptide hormone activity, and structural constituent of myelin sheath ($p < 0.05$, **Figure 5E**). These results suggest that nerve conduction and sensory perception of pain are mainly a response to the late phase of CB1 knockdown.

Chronic Constriction Injury Induced More Severe Neuropathic Pain and Alteration of Transcriptomic Profiling in CB1cKO Mice

According to the above results, lack of CB1 in DRG neurons can lead to mechanical allodynia and thermal sensitivity. How does CB1cKO affect the development of neuropathic pain? Therefore, we detected the responses to nociceptive stimuli in both CB1cKO mice and WT mice after CCI. Fourteen CB1cKO mice and their 14 WT littermates were randomly divided into sham and CCI groups, respectively. All mice received CCI surgery or sham treatment on day-14 (14 days after the final TMX injection). The experimental process is shown in **Figure 2A**. Both CB1cKO and WT mice showed reduced latency to mechanical stimuli and thermal stimuli applied with von Frey and Hargreaves plantar tests in comparison with sham-treated littermates of the same genotype (**Figures 6A, B**; *p < 0.05). Compared with WT CCI mice, CB1cKO had lower MWT and thermal latency after 5 days of CCI (0.24 g in WT CCI group and 0.04 g in CB1cKO CCI group; **Figures 6A, B**; #p < 0.05). Moreover, the area under the response-vs.-time curve (AUC) revealed an exaggerated mechanical hypersensitivity and thermal hyperalgesia in CB1cKO mice as compared with WT mice after CCI (**Figures 6C, D**; #p < 0.05). Thus, our results suggested that peripheral nerve damage could cause more severe neuropathic pain in CB1cKO mice.

Fourteen days after CCI modeling, we collected the DRG tissue and sent it for mRNA sequencing, and the results showed that compared with CB1cKO mice of sham operation (CB1KOsham28), 373 genes were upregulated and 50 genes were downregulated in CB1cKO mice of CCI (CB1cKO CCI28) (**Figure 7A**). The upregulated genes were almost always associated with inflammation and immunity, such as chemokine (C-C motif) and chemokine receptor family, complement component, cytochrome, and interleukin family and receptors, and the difference multiples of the top 20 genes were all more than six times, while some of the downregulated genes were associated with potassium channels. **Figure 7B** lists the top 20 upregulated and downregulated DEGs (detailed information of DEGs is shown in **Supplementary Table S6**). Interestingly, we found that compared with CB1cKO mice of sham operation, the expression of DRG CB2 increased significantly by 5.7 times after CCI (**Figure 7B**, its gene name is *cnr2*). We also found that many glial markers were significantly increased after CCI in CB1cKO mice, such as *cd68*, *gfap*, *csf1*, and *csf1r*. It suggested that the overactivation of CB2 and glial cells may mediate neuropathic pain after CB1 knockout.

Furthermore, we analyzed the functional pathway of 433 DEGs of CB1cKO DRG under neuropathic pain conditions. KEGG analysis revealed that the DEGs were significantly enriched in bacterial or

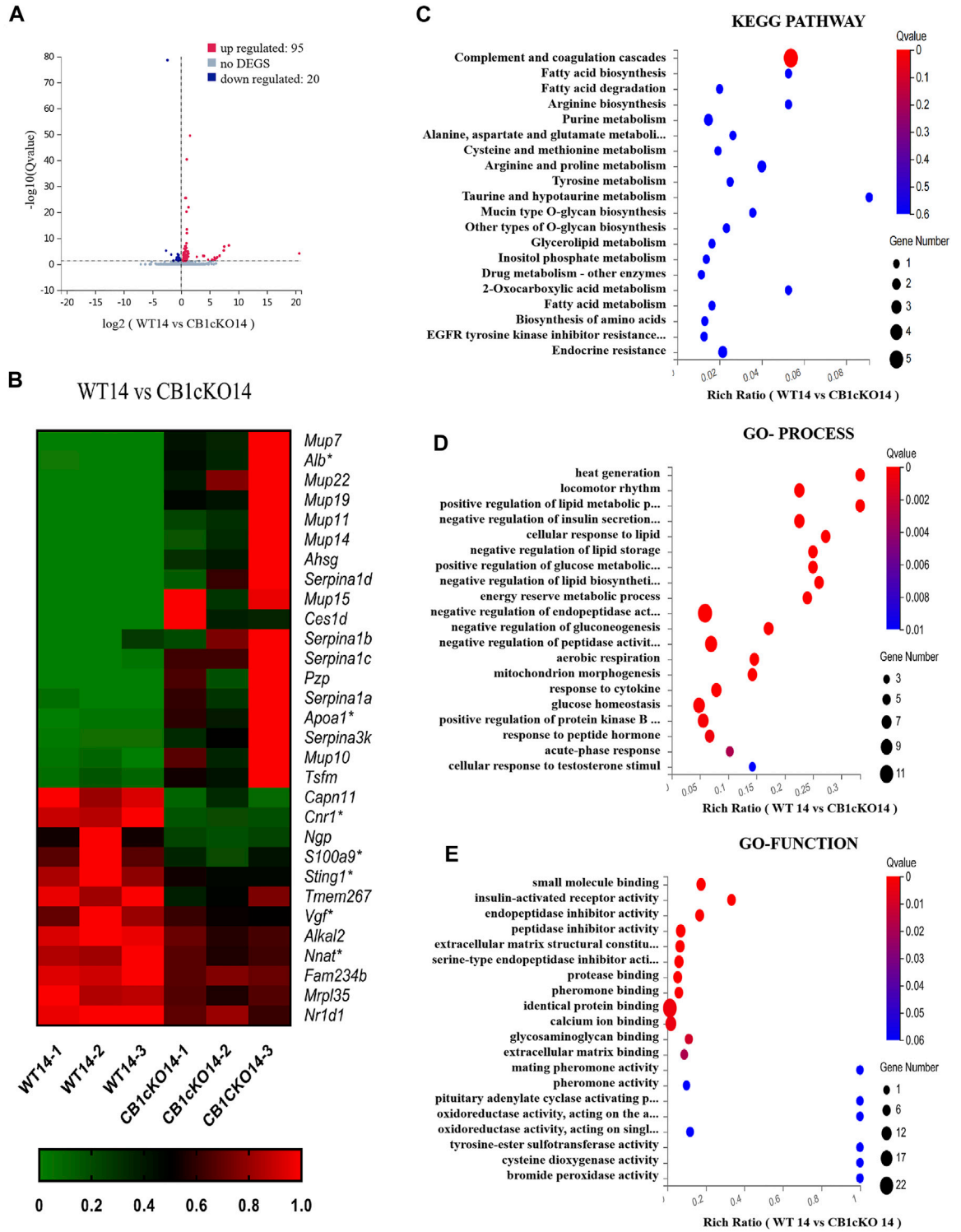

FIGURE 4 | Transcriptomic changes and functional analysis of dorsal root ganglion (DRG) in early CB1 knockdown of peripheral sensory neurons (WT14 vs. CB1cKO14). **(A)** Volcano plot indicated the upregulated and downregulated differentially expressed genes (DEGs) in the early phase of CB1 knockdown. **(B)** Heatmap of the top 20 upregulated and downregulated DEGs in the early phase of CB1 knockout. *This gene is related to pain. #This gene is related to inflammation. **(C–E)** Kyoto Encyclopedia of Genes and Genomes (KEGG) **(C)**, Gene Ontology (GO)-biological processes **(D)**, and GO-molecular function **(E)** enrichment analysis of the DEGs in the early phase of CB1 knockout.

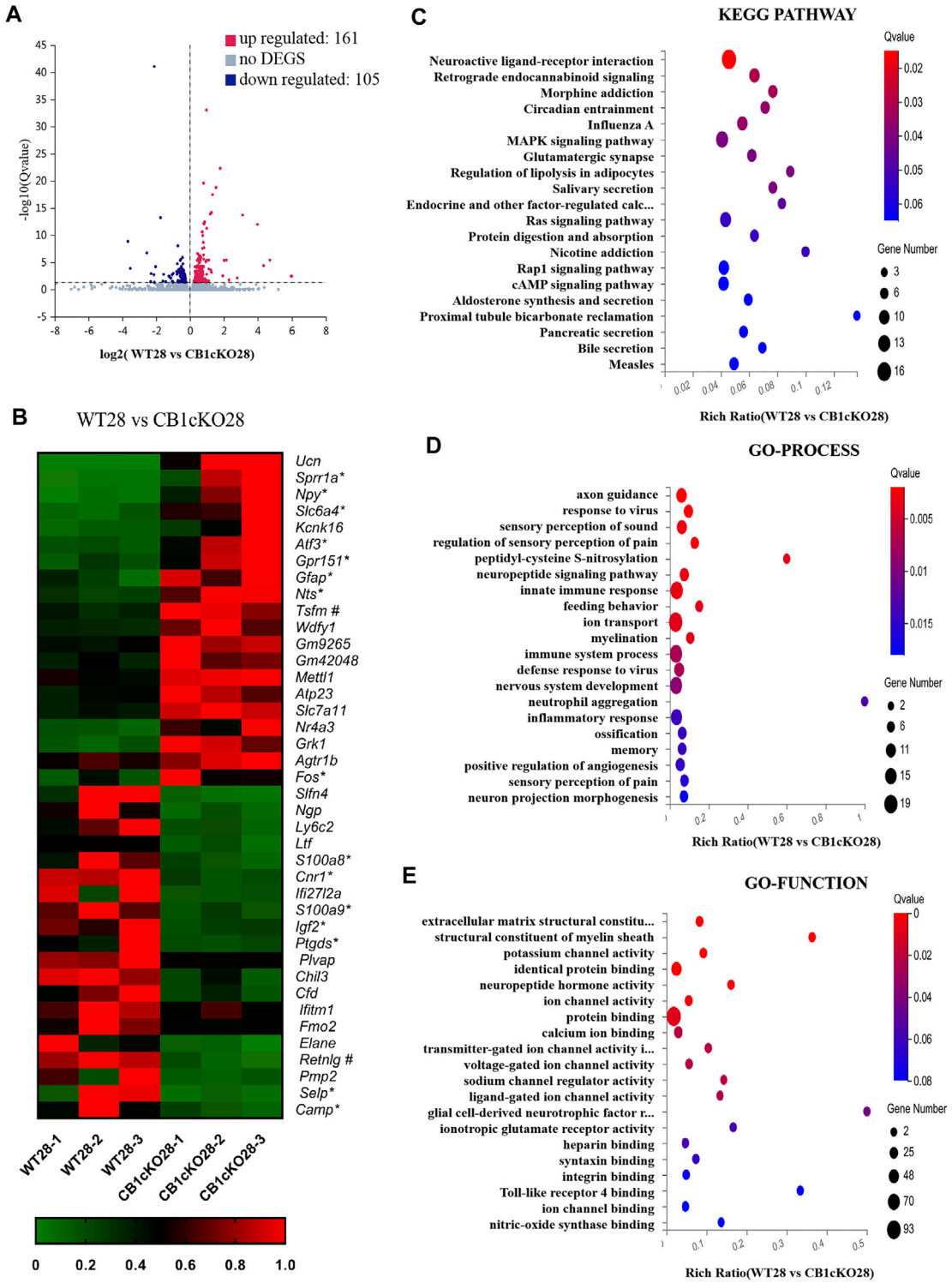

FIGURE 5 | Transcriptomic changes and functional analysis of dorsal root ganglion (DRG) in late CB1 knockdown of peripheral sensory neurons (WT28 vs. CB1cKO28). **(A)** Volcano plot indicated the upregulated and downregulated differentially expressed genes (DEGs) in the late phase of CB1 knockdown. **(B)** Heatmap of the top 20 upregulated and downregulated DEGs in the late phase of CB1 knockout. *This gene is related to pain. #This gene is related to inflammation. **(C–E)** Kyoto Encyclopedia of Genes and Genomes (KEGG) **(C)**, Gene Ontology (GO)-biological processes **(D)**, and GO-molecular function **(E)** enrichment analysis of the DEGs in the late phase of CB1 knockdown.

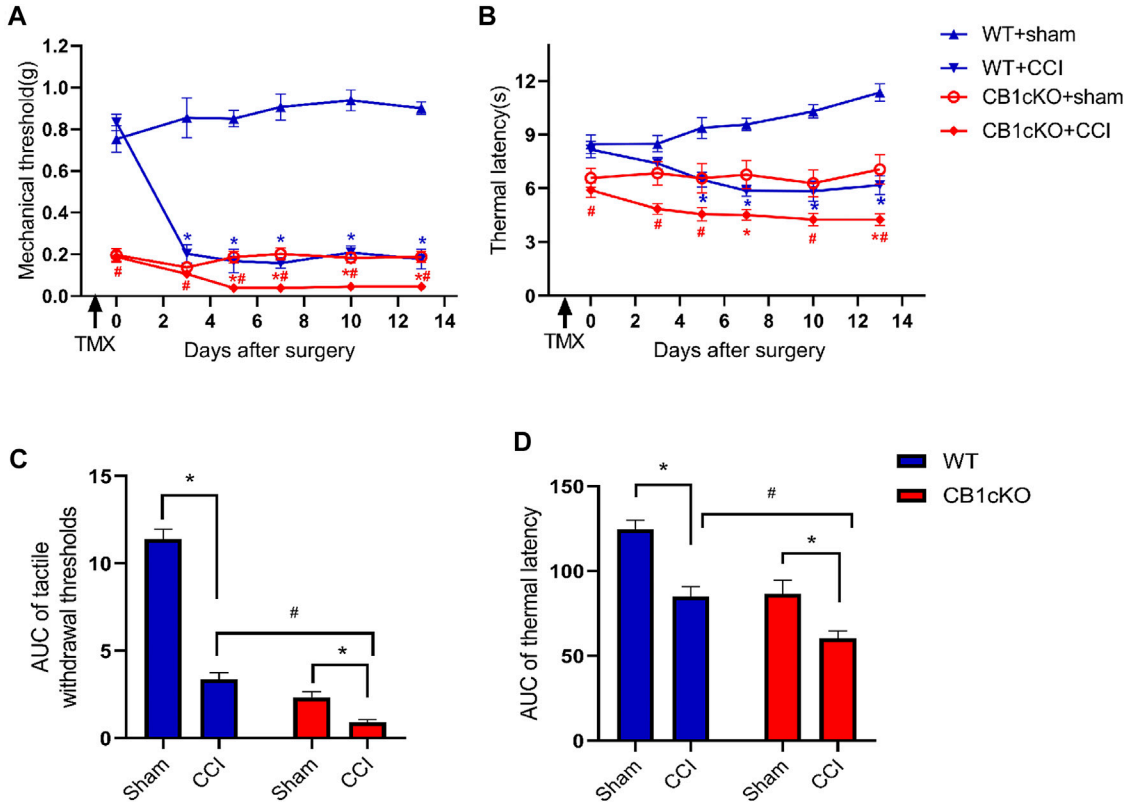

FIGURE 6 | Ablation of CB1 in dorsal root ganglion (DRG) neurons exaggerated tactile allodynia and thermal hyperalgesia induced by nerve injury. **(A, C)** Time course of the tactile withdrawal thresholds in response to von Frey filaments [represented as integrated area under the curve (AUC) in panel **C**] in wild-type (WT) and CB1cKO mice after sham or chronic constriction injury (CCI) surgery. **(B, D)** Time course of the thermal latency to hot plate (represented as integrated AUC in panel **D**) in WT and CB1cKO mice after sham or CCI surgery ($n = 7$ mice/group). Data are represented as mean ± SEM, *$p < 0.05$, compared with the baseline of the respective group; #$p < 0.05$, compared with WT CCI group at the same time point (two-way ANOVA followed by Bonferroni's *post-hoc* test).

viral infections and immune response, including B-cell receptor signaling pathway, Fc gamma R-mediated phagocytosis, complement and coagulation cascades (**Figure 7C**, $p < 0.001$), and the specific genes in the pathway are listed in **Supplementary Table S9**. Significantly different biological processes of these DEGs also focused on immune response (*csf1*, *csf1r*, *npy*, *cfd*, and *c3*), inflammatory response (*s100a8/s100a9*, *ccr1*, *ccr2*, *pld4*, *adam8*, and *agtr1b*), and defense response to bacteria (*mnda*, *ly6a*, *cfd*, and *fabp4*) (**Figure 7D**, $p < 0.001$), and the specific genes of biological processes are listed in **Supplementary Table S10**. The most significantly enriched molecular functions were concentrated in protein binding, integrin binding, and the binding of various receptors ($p < 0.01$, **Figure 7E**). Since GO and KEGG pathway analyses pointed to immune response and inflammatory responses, it suggested that the neuropathic pain of CB1cKO mice with CCI was mediated by a complex and severe neuroinflammatory immune response.

Targeting Downstream Genes of CB1, Such as CB2, Alleviates Neuropathic Pain

From the sequencing results, we found that the expression of CB2 in DRG was 5.7 times higher in CB1cKO mice after CCI (**Figure 8B**, $p < 0.001$). qPCR results were consistent with unbiased RNA-Seq data ($p < 0.001$, **Figure 8C**). In contrast, in WT mice, there was only a slight increase (1.45 times) of CB2 in DRG after CCI modeling (**Figure 8D**, $p < 0.05$). It indicated that CB2 was a potential downstream molecule of CB1, and upregulation of expression of CB2 in DRG may play an important role in neuropathic pain after CB1 deletion.

We next determined whether intervention with CB2 may improve neuropathic pain. We treated WT CCI mice (12 days after CCI surgery) with daily intraperitoneal injection of AM630 (a highly specific CB2 antagonist) and AM1241 (a CB2 agonist) for 6 days. An experimental design time line with the day and time of all manipulations is presented in **Figure 8A**. In WT mice subjected to CCI, 1 and 3 mg/kg of AM630 significantly increased the MWT and thermal latency (**Figures 8E, F**; *$p < 0.05$, $n = 5$ mice). The analgesic effect was better when the dosage of AM630 was 3 mg/kg, and MWT can return to normal after the third day (**Figure 8E**, #$p < 0.05$, $n = 5$ mice). In contrast, 0.1, 1, and 3 mg/kg AM1241 had no significant effect on the tactile allodynia and thermal hyperalgesia (**Figures 8E, F**; $p > 0.05$, $n = 5$ mice). Thus, our results suggested that CB2 activation promotes the development of neuropathic pain; antagonizing CB2 can play an analgesic effect.

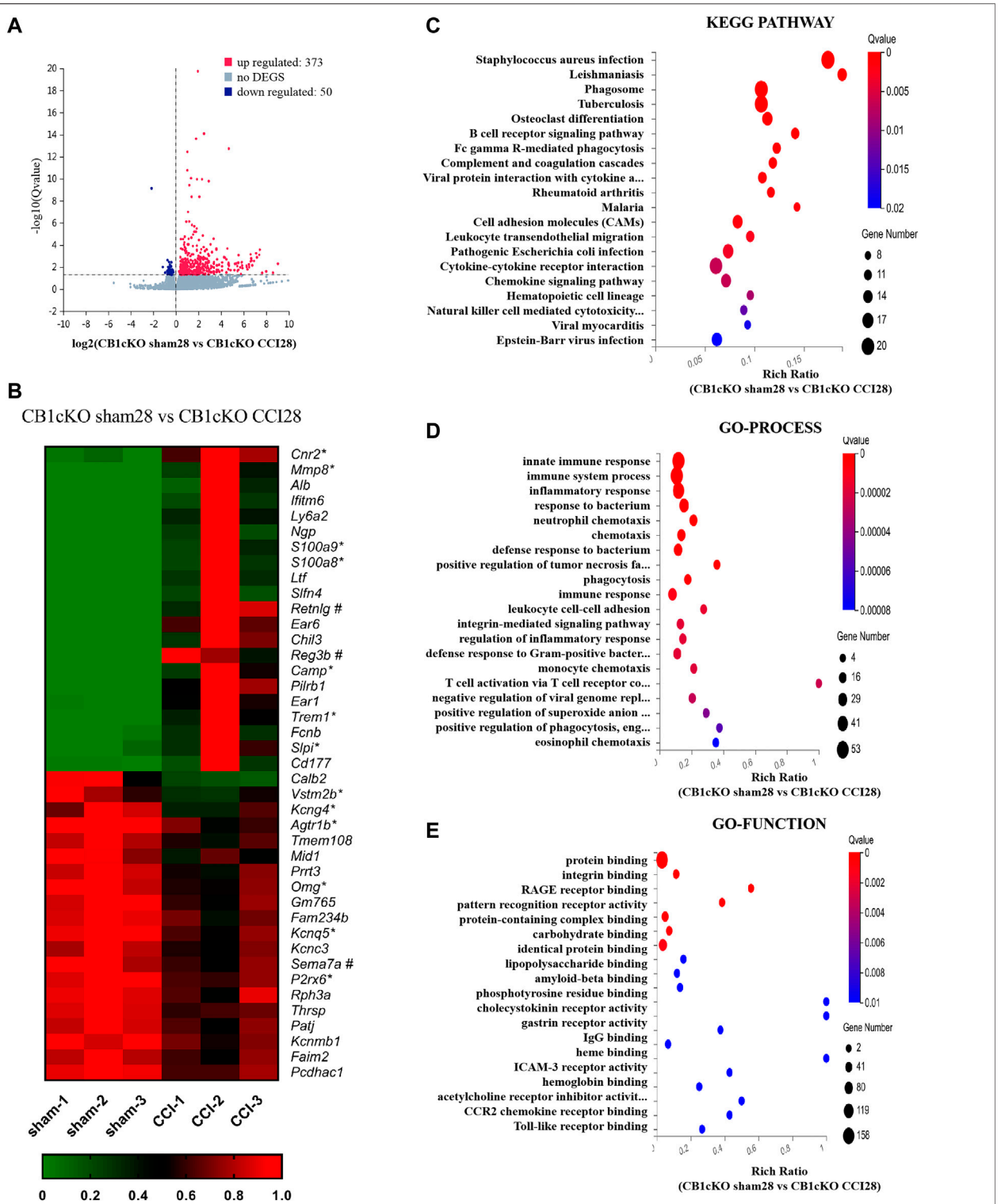

FIGURE 7 | Transcriptomic changes and functional analysis of dorsal root ganglion (DRG) in CB1cKO mice subjected to chronic constriction injury (CCI) (CB1cKO sham28 vs. CB1cKO CCI28). **(A)** Volcano plot indicated the upregulated and downregulated differentially expressed genes (DEGs) in CB1cKO mice after CCI modeling. **(B)** Heatmap of the top 20 upregulated and downregulated DEGs in CB1cKO mice after CCI modeling. *This gene is related to pain. #This gene is related to inflammation. **(C–E)** Kyoto Encyclopedia of Genes and Genomes (KEGG) **(C)**, Gene Ontology (GO)-biological processes **(D)**, and GO-molecular function **(E)** enrichment analysis of the DEGs in CB1cKO mice subjected to CCI.

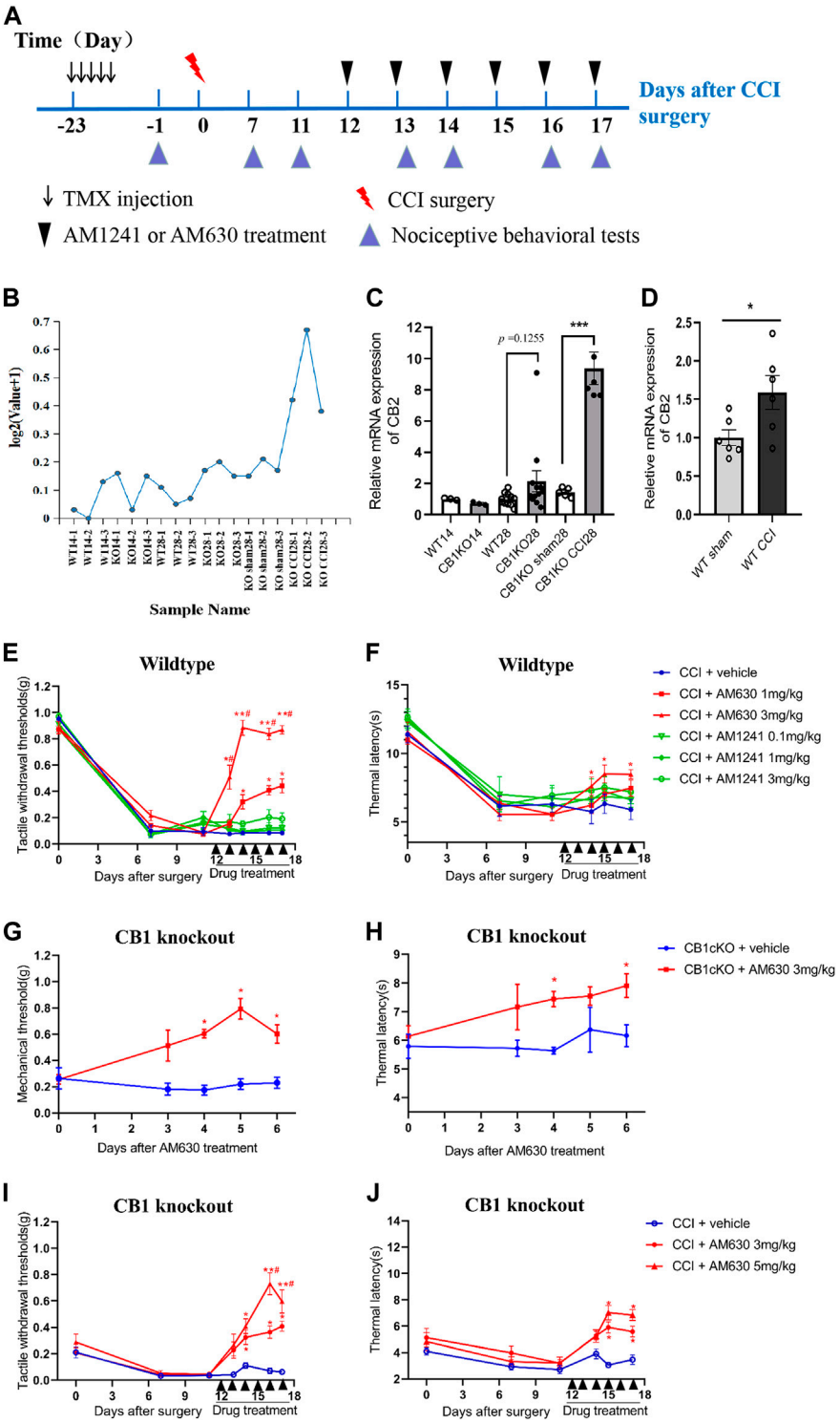

FIGURE 8 | CB2 mediated neuropathic pain in CB1cKO mice subjected to chronic constriction injury (CCI). **(A)** Experimental flowchart. **(B)** RNA-seq shows a broken line graph of the expression levels of CB2 in the dorsal root ganglion (DRG) in different phases of CB1 knockout and after CCI surgery. **(C)** Real-time PCR data showing the mRNA level of CB2 in the DRG in different phases of CB1 knockout and after CCI surgery (n = 3–5 samples/group). Gapdh was used as an endogenous control, and the mean value in the WT14 group was set to 1. ***p < 0.001, one-way ANOVA, Fisher's test. **(D)** Real-time PCR data showing the mRNA level of CB2 in the DRG of wild-type (WT) mice at 14 days after sham or CCI surgery (n = 6 each for CCI and 5 each for sham). Gapdh was used as an endogenous control gene, and the mean value of WT sham group was set to 1. *p < 0.05, two-tailed t test. **(E, F)** Time course of the tactile withdrawal thresholds **(E)** and thermal latency **(F)** in WT CCI mice treated with vehicle, AM630 (1, 3 mg/kg/day for 6 consecutive days), or AM1241 (0.1, 1, 3 mg/kg/day for 6 consecutive days) 11 days after CCI surgery (n = 6 each

(*Continued*)

FIGURE 8 | group). *p < 0.05, **p < 0.01, compared with WT CCI plus vehicle group; #p < 0.05, compared with WT CCI plus 1 mg/kg AM630 (two-way ANOVA with Bonferroni's *post-hoc* test). **(G, H)** Time course of the tactile withdrawal thresholds **(G)** and thermal latency **(H)** in WT CCI and CB1cKO mice treated with vehicle, AM630 (3, 5 mg/kg/day for 6 consecutive days) 11 days after CCI surgery (n = 5 each group), *p < 0.05, **p < 0.01, compared with the respective CCI plus vehicle; #p < 0.05, compared with CB1cKO CCI plus 3 mg/kg AM630 (two-way ANOVA followed by Bonferroni's *post-hoc* test). All data represent mean ± SEM.

Although both RNA sequencing and qPCR results showed that DRG CB2 expression was not significantly increased compared with WT mice in the late phase of CB1 knockout (**Figure 8C**, p = 0.1255, n = 10–12), we measured the effect of AM630 in CB1cKO mice (28 days after TMX induction without CCI modeling). Behavioral results showed that 3 mg/kg AM630 (once a day for 6 days) significantly increased the MWT and thermal latency in CB1cKO mice (**Figures 8G, H**; n = 5, *p < 0.05). It indicated that antagonizing CB2 by AM630 plays a good analgesic effect in CB1cKO mice without CCI modeling.

Furthermore, we measured the effect of AM630 in CB1cKO mice 12 days after surgery with daily intraperitoneal injection for 6 days. Likewise, AM630 at both 3 and 5 mg/kg significantly increased the MWT and thermal latency in CB1cKO mice 2 weeks after CCI, and compared with 3 mg/kg of AM630, the dose of 5 mg/kg had better analgesic effect (**Figures 8I, J**; #p < 0.05, n = 5 mice). From these data, we can confirm that CB2 was a downstream gene of CB1, and CB2 mediated the development of neuropathic pain. These data provided new evidence that CB2 in DRG was indispensable for nerve injury–induced neuropathic pain; antagonizing CB2 can play an analgesic effect on neuropathic pain.

AM630 Ameliorates Neuropathic Pain by Inhibiting Overactivation of Astrocytes and Neuroinflammation

Since antagonizing CB2 by AM630 alleviated CCI-induced neuropathic pain, we wondered whether AM630 can inhibit glial overactivation or neuroinflammation in DRG induced by CCI. The mRNA expression of GFAP (an astrocyte marker), s100a8/s100a9 in DRG of CB1cKO CCI group was significantly higher than that of CB1cKO sham group (**Figures 9A–C**, *p < 0.01, n = 5). Compared with CB1cKO CCI group, AM630 significantly reduced the mRNA expression of GFAP, s100a8/s100a9 in DRG (**Figures 9A–C**, #p < 0.05, n = 5). Immunofluorescence staining of DRG also demonstrated that CCI significantly enlarged the cell body of astrocyte and upregulated GFAP expression in CB1cKO mice, which was significantly decreased by AM630 (**Figure 9D**). These results confirmed that in the condition of CB1 deletion in peripheral sensory neurons, after peripheral nerve injury, CB2 led to overactivation of glial cells and severe neuroinflammation, while antagonizing CB2 inhibited excessive activation of astrocytes and neuroinflammation, thus relieving neuropathic pain.

DISCUSSION

The development of neuropathic pain involves complicated processes, e.g., activation of certain pathways and aberrant gene expression. In this study, our data showed that CB1cKO mice presented persistent hyperalgesia and changed transcriptome expression in DRG in early and late phases of CB1cKO. CCI aggravated pain behavior and changed transcriptome expression (such as CB2) in DRG of CB1cKO mice. Finally, we found that interfering with downstream genes of CB1, such as antagonizing CB2, ameliorated neuropathic pain by inhibiting overactivation of astrocytes and neuroinflammation. Herein, our current data are the first to identify the transcriptome expression of CB1cKO in DRG before and after CCI modeling and provided new evidence that intervention with downstream genes of CB1 would be a potential treatment for neuropathic pain.

In neuropathic pain, cannabinoids produce analgesic effects primarily through activation of CB1 (Bridges et al., 2001). The mice that lacked CB1 in nociceptive (Nav1.8 promoter) sensory neurons presented tactile allodynia and thermal hyperalgesia (Agarwal et al., 2007). Consistently, in our study, CB1cKO mice also showed the above pain behavior in physiological conditions. Moreover, we found that CB1cKO mice after CCI modeling had exaggerated neuropathic pain compared to the WT CCI mice. In contrast, there was no significant difference between CB1cKO (in nociceptive sensory neurons) mice and WT littermates in pain behavior after spared nerve injury (SNI) (Agarwal et al., 2007), which probably results from a ceiling effect after SNI. Therefore, CCI had less damage to peripheral nerves and may be more sensitive to evaluate pain behavior. The present study showed that CB1 on peripheral sensory neurons mainly played a direct analgesic role.

Recent studies indicated that TMX not only activated Cre recombinase in transgenic mice but also resulted in various side effects and potentially confounding the phenotypic findings of the model itself (Carboneau et al., 2016; Falke et al., 2017; Hammad et al., 2018). In the present study, we also observed that TMX caused temporarily mechanical allodynia, thermal hyperalgesia, weight loss, and diarrhea in WT mice at the beginning of TMX induction. These symptoms gradually disappeared after the TMX withdrawal (from day-8 to day-14) except for thermal hyperalgesia. We speculated that these symptoms could be side effects induced by TMX, which disappeared as a result of the drug degradation, while thermal latency was more sensitive to TMX and may take longer to recover. Considering the experimental period, we suggested that a 2-week waiting period after TMX treatment may reduce confounding factors in subsequent experiments.

A great number of studies have investigated the functions of the endocannabinoid system in the regulation of metabolic homeostasis (He and Shi, 2017). Notably, in the early phase of CB1cKO, the functional pathways of DEGs are mainly enriched in material metabolism, energy balance, and complement and coagulation cascades. Besides these pathways, we also found the following genes changed, such as *Alb* (Vincenzetti et al., 2019), *Apoa1* (Bellei et al., 2017; Oehler et al., 2020a; Oehler et al., 2020b), *Nnat* (Chen et al., 2010), *Vgf* (Rizzi et al., 2008; Fairbanks et al., 2014), and *Sting1* (Donnelly et al., 2021), which may be associated with hyperalgesia in the early phase of CB1 knockdown. Interestingly,

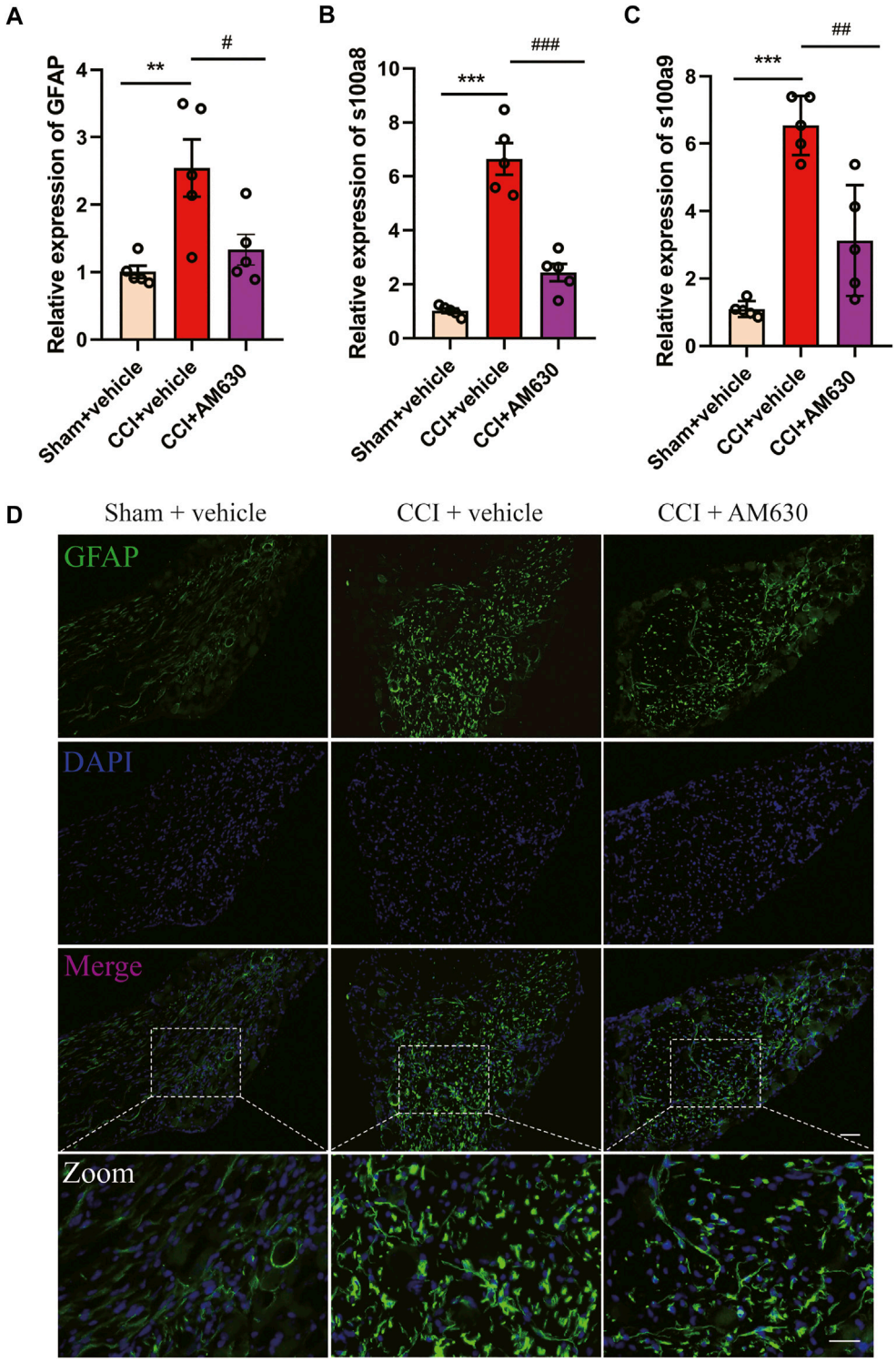

FIGURE 9 | AM630 ameliorates neuropathic pain by inhibiting overactivation of astrocytes and neuroinflammation. **(A–C)** Real-time PCR data showing the mRNA level of glial fibrillary acidic protein (GFAP), s100a8, s100a9 (n = 5 samples/group); the endogenous reference control was gapdh, and the mean value of CB1cKO sham group was set to 1. *p < 0.05, **p < 0.01, ***p < 0.001, compared with CB1cKO sham + vehicle group; #p < 0.05, ##p < 0.01, ###p < 0.001, compared with CB1cKO chronic constriction injury (CCI) + vehicle group, one-way ANOVA with Bonferroni test. **(D)** Representative immunofluorescence images of GFAP (green) in dorsal root ganglion (DRG) display activation of astrocytes. ×20, scale bar, 100 μm; zoom, scale bar, 50 μm.

most DEGs involved in material metabolism and energy balance in the early phase of CB1cKO returned to normal after 2 weeks (the late phase of CB1cKO), including major urinary protein family and serine (or cysteine) peptidase inhibitor family. Since the above genes determine the survival of peripheral sensory neurons, they returned to normal after a short-term imbalance to maintain the basic physiological functions of DRG.

In the late phase of CB1 knockout, we observed a lot of DEGs, many of them have been reported in several sequencing articles of DRG of neuropathic pain models (Wu et al., 2016; Sun et al., 2020; Tang et al., 2020), including npy, atf3, Sprr1a, and Slc6a4. Furthermore, DEGs observed in the present profiling specifically targeted neuropeptide signaling (npy, npy1r, nts, Sprr1a, and Slc6a4), retrograde endocannabinoid signaling, ion transport, and pain regulation pathways. Due to the deletion of CB1 on DRG neurons, its inhibitory effect on presynaptic neurotransmitter release is weakened (Balezina et al., 2021), so the synthesis and release of presynaptic neurotransmitters increase, such as upregulation of npy, npy1r, and nts, which in turn causes the excitement of postsynaptic neurons and finally causes pain. Collectively, our results proved that the DEGs in the late phase of CB1 knockout correlated closely with neuropathic pain, which may provide new analgesic targets for neuropathic pain.

Neuroinflammation is a crucial mechanism in many neurological disorders. Injury to the peripheral sensory nerves leads to a neuroinflammatory response in the somatosensory pathway, especially from DRG to spinal cord, which results in neuropathic pain (Hu et al., 2020). Our results showed that CB1 was absent on peripheral sensory neurons; the immune response and neuroinflammation caused by peripheral nerve injury were more serious. Due to the lack of presynaptic inhibition of CB1 (Balezina et al., 2021; Patzke et al., 2021), peripheral nerve injury leads to glial overactivation and the release of a large amount of pain-causing substances and inflammatory mediators, which eventually causes exaggerated neuropathic pain, and the specific deep-level mechanism needs to be further studied.

Nerve injury profoundly reduced the mRNA level of CB1 at 5 days after spinal nerve ligation (SNL) but increased the mRNA expression of CB2 on 10 and 21 days but not 5 days after SNL in the rat DRG (Luo et al., 2020). Consistently, our study showed that the mRNA levels of CB2 of WT mice only slightly increased (1.45 times) on the 14th day after CCI, while the expression of CB2 of CB1cKO mice increased up to 6.5 times on the 14th day after CCI. It suggested that without the inhibitory effect of CB1, nerve injury can cause a large increase in the expression of CB2, which may contribute to the development of neuropathic pain.

Behavioral results suggested that AM630 has good analgesic effect on CB1cKO mice (28 days after TMX induction and no CCI modeling), which indicated that even if the expression of CB2 is not significantly increased after CB1 knockout, its function is activated, and antagonizing CB2 can relieve pain. Furthermore, AM630 also alleviated neuropathic pain induced by CCI in both WT mice and CB1KO mice. From this, we can confirm that CB2 is the downstream gene of CB1, and CB2 mediates the development of neuropathic pain. Since CB1 agonists had no analgesic effect on the maintenance of neuropathic pain (Luo et al., 2020), CB2 antagonists should be used to treat it without the central side effects of CB1 agonists. Besides CB2, other downstream genes of CB1 may also be used as an effective target for neuropathic pain.

CB2 is particularly attractive as a target due to the lack of the side effects such as psychotropic activity caused by CB1 agonists (Lutz, 2020). Activation of peripheral CB2 receptors is sufficient to produce antinociception to an acute thermal stimulus (Malan et al., 2001). Four days after L5 nerve transection, intrathecal administration of JWH015 (a CB2 agonist) has an analgesic effect (Landry et al., 2012). In contrast, our data suggested that in 12–17 days after CCI modeling, antagonizing the function of CB2 had a significant analgesic effect in both WT mice and CB1KO mice, while CB2 agonists leads to no analgesic effect. This discrepancy might result from different models and different administration times of CB2 agonists after nerve injury. Consistently, at the early stage before the onset of CNS injury-induced immunodeficiency syndrome (CIDS), CB2 activation has the potential to alleviate CNS injury by limiting neuroinflammation and preventing the development of CIDS, while at the later stage with already established CIDS, CB2 inhibition with AM630 also restored the peripheral leukocyte response to endotoxin to improve the patient's outcome (Sultana et al., 2021). Our research found that in the maintenance phase of neuropathic pain, antagonizing CB2 can inhibit excessive activation of astrocytes and neuroinflammation that improves neuropathic pain induced by CCI.

In summary, our findings revealed that CB1 in peripheral sensory neurons mainly functioned as an endogenous analgesic factor. The action mechanisms of CB1cKO at early and late onsets of pain were different, as evidenced by our transcriptome sequencing results. CCI aggravated neuropathic pain and led to significant transcriptome profiling changes in DRG of CB1cKO mice. As a downstream target of CB1, CB2 worsened the neuropathic pain, and further use of CB2 antagonists reversed pain manifestations by inhibiting overactivation of astrocytes and neuroinflammation. These transcriptome profiling changes in DRG induced by CB1cKO and peripheral nerve injury could provide new directions and inspirations for developing novel drugs for neuropathic pain in the future.

DATA AVAILABILITY STATEMENT

The data presented in the study are deposited in the NCBI repository, accession number PRJNA780970 (https://dataview.ncbi.nlm.nih.gov/object/PRJNA780970?reviewer=8b9hq4nt4j721tik2lbib4557u).

ETHICS STATEMENT

Ethical guidelines of the International Association for the Study of Pain were strictly followed, and the protocol was approved by the local ACUC.

AUTHOR CONTRIBUTIONS

ML and JQS provided the conception and design of the research and drafted and revised the article. YML, MJ, and CW performed the experiments. HZ and CC helped analyze the data and interpreted the

results of the experiments. KW prepared the figures. WG, YYL, and SL provided some guidance in experimental designing. HLP, JH, YHL, and MF provided some help in the experiments. All authors approved the final edited version.

FUNDING

This work was supported by a grant from the National Natural Science Foundation of China (No. 81804187).

ACKNOWLEDGMENTS

The authors would like to express gratitude to their colleague (H-LP) from the Department of Anesthesiology and Perioperative Medicine, The University of Texas MD Anderson Cancer Center, for his careful revision of the article and valuable suggestions on experimental design.

SUPPLEMENTARY MATERIAL

The Supplementary Material for this article can be found online at: https://www.frontiersin.org/articles/10.3389/fphar.2021.781237/full#supplementary-material

Supplementary Figure S1 | Agarose gel electrophoresis images of tail DNA of transgenic mice. CB1cKO mice are homozygous model of tissue/cell specific knockdown of CB1R, which required both LOXP element and advilin cre gene insertion. **(A)** To detect the presence of LOXP components in CB1-FLOX. The 344 bp band means the presence of LOXP elements. The mice are CB1-FLOX positive. The 244 bp band means that the loxp element is absent and means CB1-FLOX negative. This data showed that the transgenic mice numbered 822 to 837 are all CB1-FLOX positive. **(B)** To detect whether the advilin cre gene has been inserted. The 152 bp band indicates positive advilin Cre, and no band means advilin cre negative. Figure B shows that only 9 transgenic mice (numbered 825–827, 830–833, and 835–836) were advilin cre positive. **(C)** To test whether there is gene leakage in the mice's tail (Whether CB1R is knocked out in the mice's tail). If the transgenic mice had a gene leak, 350 bp bands (null) would appear, and no band means that there is no gene leak in the tail of the mouse. Figure C shows that no gene leakage occurred in the tail of transgenic mice numbered 822–837. With all these results mentioned above, there is a conclusion that 9 double-positive mice (numbered 825–827, 830–833, and 835–836) were successfully identified without gene leakage.

REFERENCES

Agarwal, N., Pacher, P., Tegeder, I., Amaya, F., Constantin, C. E., Brenner, G. J., et al. (2007). Cannabinoids Mediate Analgesia Largely via Peripheral Type 1 Cannabinoid Receptors in Nociceptors. *Nat. Neurosci.* 10, 870–879. doi:10.1038/nn1916

Anastassiadis, K., Glaser, S., Kranz, A., Berhardt, K., and Stewart, A. F. (2010). A Practical Summary of Site-specific Recombination, Conditional Mutagenesis, and Tamoxifen Induction of CreERT2. *Methods Enzymol.* 477, 109–123. doi:10.1016/S0076-6879(10)77007-5

Balezina, O. P., Tarasova, E. O., and Gaydukov, A. E. (2021). Noncanonical Activity of Endocannabinoids and Their Receptors in Central and Peripheral Synapses. *Biochemistry (Mosc)* 86, 818–832. doi:10.1134/S0006297921070038

Bellei, E., Vilella, A., Monari, E., Bergamini, S., Tomasi, A., Cuoghi, A., et al. (2017). Serum Protein Changes in a Rat Model of Chronic Pain Show a Correlation between Animal and Humans. *Sci. Rep.* 7, 41723. doi:10.1038/srep41723

Benelli, M., Pescucci, C., Marseglia, G., Severgnini, M., Torricelli, F., and Magi, A. (2012). Discovering Chimeric Transcripts in Paired-End RNA-Seq Data by Using EricScript. *Bioinformatics* 28, 3232–3239. doi:10.1093/bioinformatics/bts617

Bennett, G. J., and Xie, Y. K. (1988). A Peripheral Mononeuropathy in Rat that Produces Disorders of Pain Sensation like Those Seen in Man. *Pain* 33, 87–107. doi:10.1016/0304-3959(88)90209-6

Bosma, S. C. J., Hoogstraat, M., Van Der Leij, F., De Maaker, M., Wesseling, J., Lips, E., et al. (2020). Response to Preoperative Radiation Therapy in Relation to Gene Expression Patterns in Breast Cancer Patients. *Int. J. Radiat. Oncol. Biol. Phys.* 106, 174–181. doi:10.1016/j.ijrobp.2019.09.002

Bridges, D., Ahmad, K., and Rice, A. S. (2001). The Synthetic Cannabinoid WIN55,212-2 Attenuates Hyperalgesia and Allodynia in a Rat Model of Neuropathic Pain. *Br. J. Pharmacol.* 133, 586–594. doi:10.1038/sj.bjp.0704110

Buffon, A. C., Javornik, M. A., Heymanns, A. C., Salm, D. C., Horewicz, V. V., Martins, D. F., et al. (2020). Role of the Endocannabinoid System on the Antihyperalgesic Action of Gabapentin in Animal Model of Neuropathic Pain Induced by Partial Sciatic Nerve Ligation. *Acad. Bras Cienc* 92, e20191155. doi:10.1590/0001-3765202020191155

Burke, D., Fullen, B. M., Stokes, D., and Lennon, O. (2017). Neuropathic Pain Prevalence Following Spinal Cord Injury: A Systematic Review and Meta-Analysis. *Eur. J. Pain* 21, 29–44. doi:10.1002/ejp.905

Carboneau, B. A., Le, T. D., Dunn, J. C., and Gannon, M. (2016). Unexpected Effects of the MIP-CreER Transgene and Tamoxifen on β-cell Growth in C57Bl6/J Male Mice. *Physiol. Rep.* 4, e12863. doi:10.14814/phy2.12863

Chaplan, S. R., Bach, F. W., Pogrel, J. W., Chung, J. M., and Yaksh, T. L. (1994). Quantitative Assessment of Tactile Allodynia in the Rat Paw. *J. Neurosci. Methods* 53, 55–63. doi:10.1016/0165-0270(94)90144-9

Chen, K. H., Yang, C. H., Cheng, J. T., Wu, C. H., Sy, W. D., and Lin, C. R. (2010). Altered Neuronatin Expression in the Rat Dorsal Root Ganglion after Sciatic Nerve Transection. *J. Biomed. Sci.* 17, 41. doi:10.1186/1423-0127-17-41

Donnelly, C. R., Jiang, C., Andriessen, A. S., Wang, K., Wang, Z., Ding, H., et al. (2021). STING Controls Nociception via Type I Interferon Signalling in Sensory Neurons. *Nature* 591, 275–280. doi:10.1038/s41586-020-03151-1

Elmes, S. J., Winyard, L. A., Medhurst, S. J., Clayton, N. M., Wilson, A. W., Kendall, D. A., et al. (2005). Activation of CB1 and CB2 Receptors Attenuates the Induction and Maintenance of Inflammatory Pain in the Rat. *Pain* 118, 327–335. doi:10.1016/j.pain.2005.09.005

Fairbanks, C. A., Peterson, C. D., Speltz, R. H., Riedl, M. S., Kitto, K. F., Dykstra, J. A., et al. (2014). The VGF-Derived Peptide TLQP-21 Contributes to Inflammatory and Nerve Injury-Induced Hypersensitivity. *Pain* 155, 1229–1237. doi:10.1016/j.pain.2014.03.012

Falke, L. L., Broekhuizen, R., Huitema, A., Maarseveen, E., Nguyen, T. Q., and Goldschmeding, R. (2017). Tamoxifen for Induction of Cre-Recombination May Confound Fibrosis Studies in Female Mice. *J. Cel Commun Signal* 11, 205–211. doi:10.1007/s12079-017-0390-x

Feil, S., Valtcheva, N., and Feil, R. (2009). Inducible Cre Mice. *Methods Mol. Biol.* 530, 343–363. doi:10.1007/978-1-59745-471-1_18

Hammad, S., Othman, A., Meyer, C., Telfah, A., Lambert, J., Dewidar, B., et al. (2018). Confounding Influence of Tamoxifen in Mouse Models of Cre Recombinase-Induced Gene Activity or Modulation. *Arch. Toxicol.* 92, 2549–2561. doi:10.1007/s00204-018-2254-4

Hargreaves, K., Dubner, R., Brown, F., Flores, C., and Joris, J. (1988). A New and Sensitive Method for Measuring thermal Nociception in Cutaneous Hyperalgesia. *Pain* 32, 77–88. doi:10.1016/0304-3959(88)90026-7

He, M., and Shi, B. (2017). Gut Microbiota as a Potential Target of Metabolic Syndrome: the Role of Probiotics and Prebiotics. *Cell Biosci* 7, 54. doi:10.1186/s13578-017-0183-1

Hossain, M. Z., Ando, H., Unno, S., and Kitagawa, J. (2020). Targeting Peripherally Restricted Cannabinoid Receptor 1, Cannabinoid Receptor 2, and Endocannabinoid-Degrading Enzymes for the Treatment of Neuropathic Pain Including Neuropathic Orofacial Pain. *Int. J. Mol. Sci.* 21, 1423. doi:10.3390/ijms21041423

Hu, Z., Deng, N., Liu, K., Zhou, N., Sun, Y., and Zeng, W. (2020). CNTF-STAT3-IL-6 Axis Mediates Neuroinflammatory Cascade across Schwann Cell-Neuron-Microglia. *Cell Rep* 31, 107657. doi:10.1016/j.celrep.2020.107657

Ibrahim, M. M., Rude, M. L., Stagg, N. J., Mata, H. P., Lai, J., Vanderah, T. W., et al. (2006). CB2 Cannabinoid Receptor Mediation of Antinociception. *Pain* 122, 36–42. doi:10.1016/j.pain.2005.12.018

Katona, I., and Freund, T. F. (2012). Multiple Functions of Endocannabinoid Signaling in the Brain. *Annu. Rev. Neurosci.* 35, 529–558. doi:10.1146/annurev-neuro-062111-150420

Kim, D., Langmead, B., and Salzberg, S. L. (2015). HISAT: a Fast Spliced Aligner with Low Memory Requirements. *Nat. Methods* 12, 357–360. doi:10.1038/nmeth.3317

Landry, R. P., Martinez, E., Deleo, J. A., and Romero-Sandoval, E. A. (2012). Spinal Cannabinoid Receptor Type 2 Agonist Reduces Mechanical Allodynia and Induces Mitogen-Activated Protein Kinase Phosphatases in a Rat Model of Neuropathic Pain. *J. Pain* 13, 836–848. doi:10.1016/j.jpain.2012.05.013

Langmead, B., and Salzberg, S. L. (2012). Fast Gapped-Read Alignment with Bowtie 2. *Nat. Methods* 9, 357–359. doi:10.1038/nmeth.1923

Leung, K. (2004). "Gadolinium-HU-308-incorporated Micelles," in *Molecular Imaging and Contrast Agent Database (MICAD)* (Bethesda (MD): National Center for Biotechnology Information).

Li, B., and Dewey, C. N. (2011). RSEM: Accurate Transcript Quantification from RNA-Seq Data with or without a Reference Genome. *BMC Bioinformatics* 12, 323. doi:10.1186/1471-2105-12-323

Li, R., Li, Y., Kristiansen, K., and Wang, J. (2008). SOAP: Short Oligonucleotide Alignment Program. *Bioinformatics* 24, 713–714. doi:10.1093/bioinformatics/btn025

Love, M. I., Huber, W., and Anders, S. (2014). Moderated Estimation of Fold Change and Dispersion for RNA-Seq Data with DESeq2. *Genome Biol.* 15, 550. doi:10.1186/s13059-014-0550-8

Lozano-Ondoua, A. N., Wright, C., Vardanyan, A., King, T., Largent-Milnes, T. M., Nelson, M., et al. (2010). A Cannabinoid 2 Receptor Agonist Attenuates Bone Cancer-Induced Pain and Bone Loss. *Life Sci.* 86, 646–653. doi:10.1016/j.lfs.2010.02.014

Luo, Y., Zhang, J., Chen, L., Chen, S. R., Chen, H., Zhang, G., et al. (2020). Histone Methyltransferase G9a Diminishes Expression of Cannabinoid CB1 Receptors in Primary Sensory Neurons in Neuropathic Pain. *J. Biol. Chem.* 295, 3553–3562. doi:10.1074/jbc.RA119.011053

Lutz, B., Marsicano, G., Maldonado, R., and Hillard, C. J. (2015). The Endocannabinoid System in Guarding against Fear, Anxiety and Stress. *Nat. Rev. Neurosci.* 16, 705–718. doi:10.1038/nrn4036

Lutz, B. (2020). Neurobiology of cannabinoid receptor signaling. *Dialogues Clin. Neurosci.* 22, 207–222. doi:10.31887/DCNS.2020.22.3/blutz

Ma, C., Zhang, M., Liu, L., Zhang, P., Liu, D., Zheng, X., et al. (2021). Low-dose Cannabinoid Receptor 2 Agonist Induces Microglial Activation in a Cancer Pain-Morphine Tolerance Rat Model. *Life Sci.* 264, 118635. doi:10.1016/j.lfs.2020.118635

Malan, T. P., Jr., Ibrahim, M. M., Deng, H., Liu, Q., Mata, H. P., Vanderah, T., et al. (2001). CB2 Cannabinoid Receptor-Mediated Peripheral Antinociception. *Pain* 93, 239–245. doi:10.1016/s0304-3959(01)00321-9

Matsuda, L. A., Lolait, S. J., Brownstein, M. J., Young, A. C., and Bonner, T. I. (1990). Structure of a Cannabinoid Receptor and Functional Expression of the Cloned cDNA. *Nature* 346, 561–564. doi:10.1038/346561a0

Munro, S., Thomas, K. L., and Abu-Shaar, M. (1993). Molecular Characterization of a Peripheral Receptor for Cannabinoids. *Nature* 365, 61–65. doi:10.1038/365061a0

Nackley, A. G., Makriyannis, A., and Hohmann, A. G. (2003). Selective Activation of Cannabinoid CB(2) Receptors Suppresses Spinal Fos Protein Expression and Pain Behavior in a Rat Model of Inflammation. *Neuroscience* 119, 747–757. doi:10.1016/s0306-4522(03)00126-x

Oehler, B., Brack, A., Blum, R., and Rittner, H. L. (2020a). Pain Control by Targeting Oxidized Phospholipids: Functions, Mechanisms, Perspectives. *Front. Endocrinol. (Lausanne)* 11, 613868. doi:10.3389/fendo.2020.613868

Oehler, B., Kloka, J., Mohammadi, M., Ben-Kraiem, A., and Rittner, H. L. (2020b). D-4F, an ApoA-I Mimetic Peptide Ameliorating TRPA1-Mediated Nocifensive Behaviour in a Model of Neurogenic Inflammation. *Mol. Pain* 16, 1744806920903848. doi:10.1177/1744806920903848

Patzke, C., Dai, J., Brockmann, M. M., Sun, Z., Fenske, P., Rosenmund, C., et al. (2021). Cannabinoid Receptor Activation Acutely Increases Synaptic Vesicle Numbers by Activating Synapsins in Human Synapses. *Mol. Psychiatry* 30. doi:10.1038/s41380-021-01095-0

Rizzi, R., Bartolomucci, A., Moles, A., D'amato, F., Sacerdote, P., Levi, A., et al. (2008). The VGF-Derived Peptide TLQP-21: a New Modulatory Peptide for Inflammatory Pain. *Neurosci. Lett.* 441, 129–133. doi:10.1016/j.neulet.2008.06.018

Sain, N. M., Liang, A., Kane, S. A., and Urban, M. O. (2009). Antinociceptive Effects of the Non-selective Cannabinoid Receptor Agonist CP 55,940 Are Absent in CB1(-/-) and Not CB2(-/-) Mice in Models of Acute and Persistent Pain. *Neuropharmacology* 57, 235–241. doi:10.1016/j.neuropharm.2009.06.004

Shang, Y., and Tang, Y. (2017). The central Cannabinoid Receptor Type-2 (CB2) and Chronic Pain. *Int. J. Neurosci.* 127, 812–823. doi:10.1080/00207454.2016.1257992

Shen, S., Park, J. W., Lu, Z. X., Lin, L., Henry, M. D., Wu, Y. N., et al. (2014). rMATS: Robust and Flexible Detection of Differential Alternative Splicing from Replicate RNA-Seq Data. *Proc. Natl. Acad. Sci. U S A.* 111, E5593–E5601. doi:10.1073/pnas.1419161111

Sideris, A., Piskoun, B., Russo, L., Norcini, M., Blanck, T., and Recio-Pinto, E. (2016). Cannabinoid 1 Receptor Knockout Mice Display Cold Allodynia, but Enhanced Recovery from Spared-Nerve Injury-Induced Mechanical Hypersensitivity. *Mol. Pain* 12, 1744806916649191. doi:10.1177/1744806916649191

Solas, M., Francis, P. T., Franco, R., and Ramirez, M. J. (2013). CB2 Receptor and Amyloid Pathology in Frontal Cortex of Alzheimer's Disease Patients. *Neurobiol. Aging* 34, 805–808. doi:10.1016/j.neurobiolaging.2012.06.005

Sultana, S., Burkovskiy, I., Zhou, J., Kelly, M. M., and Lehmann, C. (2021). Effect of Cannabinoid 2 Receptor Modulation on the Peripheral Immune Response in Central Nervous System Injury-Induced Immunodeficiency Syndrome. *Cannabis Cannabinoid Res.* 6, 327–339. doi:10.1089/can.2020.0130

Sun, W., Kou, D., Yu, Z., Yang, S., Jiang, C., Xiong, D., et al. (2020). A Transcriptomic Analysis of Neuropathic Pain in Rat Dorsal Root Ganglia Following Peripheral Nerve Injury. *Neuromolecular Med.* 22, 250–263. doi:10.1007/s12017-019-08581-3

Tang, S., Jing, H., Huang, Z., Huang, T., Lin, S., Liao, M., et al. (2020). Identification of Key Candidate Genes in Neuropathic Pain by Integrated Bioinformatic Analysis. *J. Cel Biochem* 121, 1635–1648. doi:10.1002/jcb.29398

Vincenzetti, S., Pucciarelli, S., Huang, Y., Ricciutelli, M., Lambertucci, C., Volpini, R., et al. (2019). Biomarkers Mapping of Neuropathic Pain in a Nerve Chronic Constriction Injury Mice Model. *Biochimie* 158, 172–179. doi:10.1016/j.biochi.2019.01.005

Walker, J. M., and Hohmann, A. G. (2005). Cannabinoid Mechanisms of Pain Suppression. *Handb Exp. Pharmacol.*, 509–554. doi:10.1007/3-540-26573-2_17

Wang, K., Wang, S., Chen, Y., Wu, D., Hu, X., Lu, Y., et al. (2021). Single-cell Transcriptomic Analysis of Somatosensory Neurons Uncovers Temporal Development of Neuropathic Pain. *Cell Res* 31 (8), 904–918. doi:10.1038/s41422-021-00479-9

Wu, S., Marie Lutz, B., Miao, X., Liang, L., Mo, K., Chang, Y. J., et al. (2016). Dorsal Root Ganglion Transcriptome Analysis Following Peripheral Nerve Injury in Mice. *Mol. Pain* 12, 1744806916629048. doi:10.1177/1744806916629048

Wu, Y., Ma, R., Long, C., Shu, Y., He, P., Zhou, Y., et al. (2021). The Protective Effect of Cannabinoid Type II Receptor Agonist AM1241 on ConA-Induced Liver Injury in Mice via Mitogen-Activated Protein Kinase Signalling Pathway. *Int. J. Immunopathol Pharmacol.* 35, 20587384211035251. doi:10.1177/20587384211035251

Conflict of Interest: The authors declare that the research was conducted in the absence of any commercial or financial relationships that could be construed as a potential conflict of interest.

Publisher's Note: All claims expressed in this article are solely those of the authors and do not necessarily represent those of their affiliated organizations or those of the publisher, the editors, and the reviewers. Any product that may be evaluated in this article, or claim that may be made by its manufacturer, is not guaranteed or endorsed by the publisher.

frontiers in Pharmacology

ORIGINAL RESEARCH
published: 28 February 2022
doi: 10.3389/fphar.2022.823732

Activation of CNR1/PI3K/AKT Pathway by Tanshinone IIA Protects Hippocampal Neurons and Ameliorates Sleep Deprivation-Induced Cognitive Dysfunction in Rats

Zi-Heng Li, Li Cheng, Chun Wen, Li Ding, Qiu-Yun You and Shun-Bo Zhang**

Faculty of Pharmacy, Hubei University of Chinese Medicine, Wuhan, China

OPEN ACCESS

Edited by:
Onintza Sagredo, Universidad Complutense de Madrid, Spain

Reviewed by:
Ning Liu, Tulane University, United States
Wenda Xue, Nanjing University of Chinese Medicine, China

***Correspondence:**
Qiu-Yun You
youqiuyun@126.com
Shun-Bo Zhang
zshunbo163@163.com

Specialty section:
This article was submitted to Neuropharmacology, a section of the journal Frontiers in Pharmacology

Received: 28 November 2021
Accepted: 26 January 2022
Published: 28 February 2022

Citation:
Li Z-H, Cheng L, Wen C, Ding L, You Q-Y and Zhang S-B (2022) Activation of CNR1/PI3K/AKT Pathway by Tanshinone IIA Protects Hippocampal Neurons and Ameliorates Sleep Deprivation-Induced Cognitive Dysfunction in Rats. Front. Pharmacol. 13:823732. doi: 10.3389/fphar.2022.823732

Sleep deprivation is commonplace in modern society, Short periods of continuous sleep deprivation (SD) may negatively affect brain and behavioral function and may lead to vehicle accidents and medical errors. Tanshinone IIA (Tan IIA) is an important lipid-soluble component of *Salvia miltiorrhiza*, which could exert neuroprotective effects. The aim of this study was to investigate the mechanism of neuroprotective effect of Tan IIA on acute sleep deprivation-induced cognitive dysfunction in rats. Tan IIA ameliorated behavioral abnormalities in sleep deprived rats, enhanced behavioral performance in WMW and NOR experiments, increased hippocampal dendritic spine density, and attenuated atrophic loss of hippocampal neurons. Tan IIA enhanced the expression of CB1, PI3K, AKT, STAT3 in rat hippocampus and down-regulated the expression ratio of Bax to Bcl-2. These effects were inhibited by cannabinoid receptor 1 antagonist (AM251). In conclusion, Tan IIA can play a neuroprotective role by activating the CNR1/PI3K/AKT signaling pathway to antagonize apoptosis in the hippocampus and improve sleep deprivation-induced spatial recognition and learning memory dysfunction in rats. Our study suggests that Tan IIA may be a candidate for the prevention of sleep deprivation-induced dysfunction in spatial recognition and learning memory.

Keywords: tanshinone IIA, sleep deprivation, cognitive dysfunction, cannabinoid receptor 1, hippocampal neurons

INTRODUCTION

Long enough undisturbed sleep is a pillar of human health, but sleep deprivation is commonplace in modern society, and chronic sleep deprivation can damage human health, increasing the risk of cardiovascular disease, obesity (Leslie, 2012; Wang et al., 2019), and is also associated with reduced cognitive function (Killgore, 2010; Javaheripour et al., 2019; Ma et al., 2020). Notably, short periods of sleep deprivation can also disrupt circadian physiology and have a negative impact on brain and behavioral function, resulting in significant decreases in cognitive function (Jewett et al., 1999; Choshen-Hillel et al., 2021), which in turn can contribute to increased risk of occupational and traffic accidents (Wu et al., 2013a; Hillman et al., 2018; Whelehan et al., 2021).

Salvia is the dried root and rhizome of *Salvia miltiorrhiza*, family Labiatae, which is considered by Traditional Chinese Medicine to have the effects of activating blood stasis, relieving pain, regulating heat and calming the mind (Jia et al., 2019) The pharmacological research of Salvia is very extensive, mainly with anti-tumor, anti-atherosclerosis and anti-neuroinflammatory effects (Zhou et al., 2016; Fu et al., 2020; Xu et al., 2021). Tanshinone IIA is an important lipid-soluble component of Salvia (Jiang et al., 2019), which has anticancer, neuroprotective, and cardioprotective pharmacological effects (Munagala et al., 2015; Xie et al., 2015; Zhu et al., 2017a; Zhao et al., 2019). Current studies have shown that Tan IIA's effects on disease exhibit obvious multi-target regulatory mechanisms, such as anti-inflammatory, antioxidant, and anti-apoptotic effects (Sung et al., 1999; Wu et al., 2013b; Cai et al., 2016; Guo et al., 2020; Liu et al., 2020). Its inhibition of apoptosis and enhancement of neuronal regeneration may be a potential mechanism for its protection of the nervous system (Shen et al., 2011; Qian et al., 2012). Similarly, a previous study found that Tan IIA improved the performance of streptozotocin-induced APP/PS1 transgenic mice in NOR tests demonstrating beneficial effects on cognitive memory function (He et al., 2020). Another study found that Tan IIA also alleviated cognitive dysfunction caused by other factors, such as diabetes-related, chemokine CC motif ligand 2 (CCL2)-induced, vascular dementia in rats, in experiments that relied on MWM assessment (Chen et al., 2018; Liao et al., 2020; Kong et al., 2021). However, the effect of Tan IIA on behavioral function in sleep deprivation model animals has not been elucidated, and whether Tan IIA has an effect on sleep deprivation-induced cognitive dysfunction has not been reported.

The hippocampus is one of the brain regions responsible for higher neural activities such as emotional integration, cognition and memory, and has an important role in spatial navigation and the integration of information from short-term to long-term memory (Zhong et al., 2020). Prolonged sleep deprivation may inhibit hippocampal cell proliferation and reduce neurogenesis and cell survival, which in turn leads to deterioration and impaired function of neurobehavior such as cognition and memory (Kim et al., 2005; Meerlo et al., 2009; McCoy and Strecker, 2011). Sleep deprivation has long been known to damage nerves (Bishir et al., 2020), but it is worth mentioning that sleep deprivation is particularly damaging to the hippocampal region of the brain, not only affecting the immune and redox systems, leading to neuroinflammation and oxidative stress (Nabaee et al., 2018), but also causing damage to hippocampal ultrastructure, inducing loss of pyramidal neurons and impairing cognitive function (Xie et al., 2021). Tan IIA has been reported to have a role in rescuing memory deficits in rodents, and although these memory deficits are not exclusively caused by sleep deprivation, they are associated with hippocampal neuronal damage (Zhu et al., 2017b; Kong et al., 2017; Chen et al., 2018).

Our preliminary bioinformatics exploration revealed that the key gene for Tan IIA in treating patients with cognitive dysfunction syndrome may be CNR1. This gene encodes Cannabinoid Receptor 1 (CB1), which is located mainly in the brain, spinal cord and peripheral nervous system. Activation of CB1 can reduce the release of some neurotransmitters, such as dopamine and GABA, to participate in the regulation of memory, cognition, and motor control (Szabó et al., 2014). It has been reported that PI3K and AKT are stimulated and phosphorylated when CNR1 is overexpressed and play a neuroprotective role in the pathogenesis of Alzheimer's disease (Li et al., 2020). The phosphatidylinositol 3-kinase (PI3K)/protein kinase B (AKT) signaling pathway is a classical signal transduction pathway that regulates cell survival, differentiation and apoptosis. Numerous studies have found that activation of the PI3K/AKT pathway contributes to neuroprotection and is involved in the survival, differentiation, and apoptosis of glial cells and neurons (Husain et al., 2012; Dou et al., 2016; Lai et al., 2016). These studies suggest that we have an upstream and downstream relationship between CNR1 and PI3K/AKT. Therefore, it can be predicted that Tan IIA may alleviate cognitive dysfunction by regulating the CNR1/PI3K/AKT signaling pathway.

In summary, the aim of this study was to investigate the ameliorative effects of Tanshinone IIA on sleep deprivation-induced cognitive dysfunction and whether these neuroprotective effects are regulated by the CNR1/PI3K/AKT pathway in the brain.

MATERIALS AND METHODS

Reagents and Apparatus

Tanshinone IIA (purity ≥95%) was purchased from Shanghai Yuanye Bio-Technology Co., Ltd. (Shanghai, China).AM251 (purity >98%) was purchased from Shanghai Hongye Biotechnology Co., Ltd. (Shanghai, China), the Chinese agent of GLPBIO. The animal trajectory tracking system was developed by Noldus Information Technology Co., Ltd. The Morris water maze (MWM) experimental instrument (DMS-2) was developed by the Institute of Materia Medica, Chinese Academy of Medical Sciences. The sleep deprivation device was made by the Institute of Gerontology, Hubei University of Traditional Chinese Medicine.

Screening Key Pathways and Targets by Bioinformatics

GEO (https://www.ncbi.nlm.nih.gov/geo) is a public repository of genomics data that helps users query and download gene expression profiles needed for experiments and planning. We downloaded data from GEO for 121 patients with cognitive impairment syndrome and 232 normal subjects. PubChem (https://pubchem.ncbi.nlm.nih.gov/) is a database of chemical modules which contains typical SMILES and two-dimensional structures of Tan IIA. The target genes associated with Tan IIA were retrieved from the SwissTargetPrediction (http://www.swisstargetprediction.ch/) database, which helps us to predict target genes associated with target small molecule compounds with assumed biological activity. The study was exempt from approval by the local ethics committee because the GEO data was publicly available.

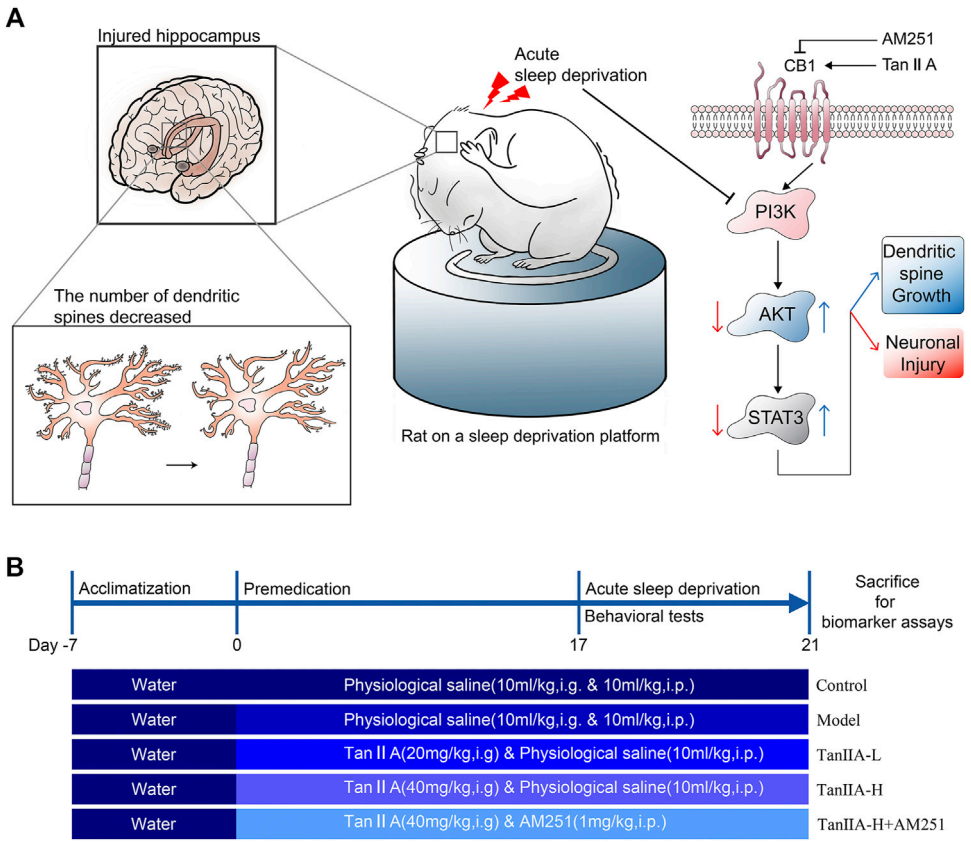

FIGURE 1 | Signaling pathway prediction and experimental flow. **(A)** Sleep deprivation inhibited PI3K/AKT/STAT3 signaling pathway, caused hippocampal damage and reduced neuronal dendritic spine density in rats; Tanshinone IIA may activate PI3K/AKT/STAT3 signaling pathway through cannabinoid receptor 1, protect rat hippocampal neurons and inhibit the damage caused by sleep deprivation. **(B)** Experimental procedure and drug administration method.

Differential gene expression was assessed by the software EdgeR (Empirical analysis of Digital Gene Expression in R). In the combined analysis, genes with adjusted $p < 0.05$ and |log2 fold change (FC)| >1.0 were considered as differentially expressed genes. Then, the cross-section of differentially expressed genes and Tan IIA -related genes were screened using Venny 2.1.0 software, and these genes were used as target genes of Tan IIA for cognitive impairment syndrome treatment.

Tan IIA as a core target for the treatment of cognitive dysfunction syndrome using Discovery Studio 2016 software. Structure of related proteins downloaded from the RSCB PDB database (https://www.rcsb.org/) Tan IIA compound structures were downloaded from the PubChem database (https://pubchem.ncbi.nlm.nih.gov/). It is generally considered that LiDockscore ≥90 represents a strong binding ability when docked to the target protein (Ge et al., 2018).

Animals and Treatments

All experimental procedures were approved by the Hubei University of Traditional Chinese Medicine experimental ethics committee. Male Wistar rats weighing 200–220 g were purchased from Liaoning Changsheng Biotechnology Co. Ltd. and kept in a controlled environment (room temperature 25 °C) with a 12-h light-dark cycle, and received standard chow and drinking water ad libitum. Animals were randomly allocated to five experiment groups ($n = 12$ per group) using random number table by investigators: the control group, SD group, Tan IIA-L (20 mg/kg, i. g.) group, Tan IIA-H (40 mg/kg, i. g.) group, and Tan IIA-L + AM251 group (1 mg/kg, i. p.). After 7 days of adaptive feeding, the rats were administered Tan IIA and AM251 preventively, once a day, for 21 days, and the control and SD groups received physiological saline (0.9% NaCl, 10 ml/kg, i. g.&i.p.) at the same time. From the 17th day, all groups except the control group were subjected to SD for 96 h (From 10 a.m. on day 17 to 10 a.m. on day 21). Conduct behavioral tests 24 h after sleep deprivation (Morris water maze hidden platform phase started on day 17). After all behavioral tests, the rats were sacrificed for biomarker analysis (As shown in **Figure 1B**).

Induction of the Acute SD Model

The acute sleep deprivation model was established by a modified multi-platform water environment method. Six interconnected stainless steel cylinders (Φ = 10 cm) are placed in the water tank (1 cm above the water surface). The distance between the 2 cylinders was 15 cm and a narrow passage was connected so

that the rat in a water-filled tank could move freely on each platform. Therefore, when the animal entered a sleep state, the its nasal tip would touch the water or fell into the water and woke up. The rats were continuously deprived of sleep for 96 h. During this 96-h sleep deprivation period, rats had free access to feed and water. The control group rats were kept only in tanks without water.

Novel Object Recognition Test

The NOR is a behavioral method that uses the rodent's natural tendency to approach and explore novel objects to assess the recognition and memory ability. The experiment consists of 3 main phases: habituation, training and testing phase. We used a cubic black acrylic box (40 cm × 40 cm × 50 cm) as the experimental device. Rats were spent 5 min to explore the experimental device for 3 days. Their trajectory and the time spent exploring different objects were recorded. On the first day, the rats were placed sequentially in the experimental device without any objects and allowed to explore freely to habituate the environment. On the second day, two identical cylinders A1 and A2 (Φ= 6 cm, height 15 cm) were placed in the experimental device. The rats were placed into the experimental set-up with their backs to the objects. On the third day, replace cylinder A2 with square column B (side length 6 cm, height 15 cm) and repeat the experiment of the second day. It is worth noting that, alcohol needs to be sprayed on the experimental device at every two experimental intervals to eliminate the odor. Interaction parameters were specified as contact with the object (nose-point, distance < 3 cm). The experimental index was expressed as "discrimination index". Discrimination index was calculated as the time to explore novel object (object B)/total time to explore (explore object A1 + explore object B).(As shown in **Figure 1A**).

Morris Water Maze Test

MWM is a classic experiment applied to assess the spatial memory ability of rodents. A black tank (Φ = 150 cm) was filled with a sufficient amount of fresh water (22–25°C) as the body of the experiment. Four different shapes of cardboard were hung from the curtain as visual cues. MWM test consists of 3 main phases: visible platform (1 day), hidden platform (4 days) and probe test (1 day). In the visible platform phase, a black cylinder (Φ = 5 cm) was put into the water as a platform and made 1 cm above the water surface. Each rat was allowed to search for the platform for 90 s. If it failed to find the platform, the experimenter guided the rat to climb the platform and familiarize itself with the environment for 15 s. In the hidden platform phase, water was injected to submerge the platform for 1 cm to make it invisible, and other operations were performed as in the visible platform period experiment. In the probe test phase, the black cylinder was withdrawn from the tank and each rat was allowed to swim for 90 s. The swimming trajectory and other parameters were recorded by the device. The experiment was repeated three times a day, and rats were placed from different quadrants with the same platform position.

Nissl Staining

We detected changes in rat hippocampal neuronal cell expression by Nissl staining. The selected 16 μm coronal sections of rat brain paraffin were placed on gelatin-coated glass slides in phosphate-buffered saline and placed in a dust-proof environment for 24 h to dry. Brain slices were placed horizontally for 10–20 min with drops of Nissl staining solution (1% toluidine blue). After rinsing quickly in distilled water, the sections were differentiated in 95% ethyl alcohol. After dehydration, the sections were scanned and the brain slices were observed by CaseViewer software. Four visual fields of the hippocampus (CA1, CA3, and CA4) and dentate gyrus (DG) were taken from each photograph. Cells containing Nissl vesicles were considered to be neurons and were counted manually.

Hematoxylin and Eosin (H & E) Staining

We processed rat brain sections with Hematoxylin and eosin (H & E) staining and evaluated morphological changes in the hippocampus under microscopic observation. First, put sections into the hematoxylin dyeing solution for 8–10 min, then washed with running water. Differentiated with differentiation liquid, then washed with running water. Use blue returning liquid to return blue. Then, the sections were dehydrated with 85 and 95% ethanol absolute for 5 min respectively, and dyed in eosin solution for 8–10 min. After completing the above steps, put sections into three cylinders of ethanol absolute for 5 min and two cylinders of xylene for 5 min. Finally, sealed the sections with neutral balsam. The sections were scanned and the brain slices were observed by CaseViewer software. Four visual fields of the hippocampus (CA1, CA3 and CA4) and dentate gyrus (DG) were taken from each photograph.

Golgi-Cox Staining and Spine Density Analysis

Treatment of experimental samples with Golgi-cox stain allows us to clearly see the dendritic spines on neurons. The whole brains of the rats were removed and immediately placed into paraformaldehyde (4%) fixative for more than 48 h. The rat brain tissue was cut into 2 mm thick tissue pieces, rinsed 3–4 times with saline, placed in 45 ml round bottom EP tubes and submerged in Golgi-Cox solution. The staining solution was changed every 48 h and placed in a cool place for 14 days to avoid light treatment. After staining, the tissues were washed three times with distilled water, poured into 80% glacial acetic acid to submerge the tissues overnight, washed in distilled water when the tissues became soft, and placed in 30% sucrose. The tissue was cut into 100 μm with an oscillating sectioner, attached to gelatin slides, and left overnight to dry away. Finally, the dried tissue slides were treated with concentrated ammonia for 15 mins, washed with distilled water for 1 min, treated with acidic firm film fixing solution for 15 mins, washed with distilled water again for 3 mins, dried, and sealed with glycerin gelatin. We acquired images the Pannoramic 250 (3D Histech) digital section scanner and processed the images with ImageJ software for subsequent analysis.

Western-Blot Analysis

Rat hippocampal tissues were washed 2–3 times with pre-chilled PBS, cut into small pieces and homogenized by adding ten times the volume of tissue in RIPA lysis buffer (Beyotime Institute of

Biotechnology, China). Then the supernatant was collected by centrifugation and homogenization (12,000 rpm, 4°C, 10 min), which is the total protein of rat hippocampal tissue. The BCA protein assay kit (AS1086, ASPEN, Wuhan, China) was used for the quantification of total proteins. Samples were separated by SDS PAGE and electro-transferred onto PVDF (0.45 um) membranes (Servicebio,G6015-0.45, Wuhan, China) after activation with methanol. The membranes were then incubated overnight at 4°C with specific primary antibodies: CB1 (Servicebio,GB111214), PI3K(BIOSS,BSM-33219M), P-PI3K (BIOSS,bs5570R), AKT (Servicebio,GB11689), P-AKT (Affinity,AF0908), STAT3 (Servicebio,GB11176), P-STAT3 (RuiyingBiological, RLP0250), Bcl2 (Servicebio, GB113375), BAX (Servicebio, GB11690),ACTIN(Servicebio, GB12001). The membranes were washed three times with TBST for 10 min each. After washing, the membranes were incubated with HRP anti-conjugated secondary antibody (Servicebio, GB23303) for 1 h. The membranes were washed in the same manner as described above. Membranes were scanned using the Fluor Chem FC3 system (Protein Simple, United States).

Immunohistochemical Detection

Formalin-fixed paraffin-embedded tissue sections were first baked and deparaffinized. The tissue sections were then placed in citric acid antigen repair buffer (pH 6.0) in a microwave oven for antigen repair. The tissue was placed in 3% hydrogen peroxide solution for 25 min to block endogenous peroxidase and then closed at room temperature for 30 min by adding 3% BSA dropwise to cover the tissue uniformly. primary antibodies (BAX, Servicebio, 50599-2-Ig, 1:300; Bcl-2, Servicebio B13439, 1:200) were added and stored overnight at 4°C and secondary antibodies [HRP IgG (H + L), Servicebio GB23302, 1:200] and incubated at room temperature for 50 min. Then freshly prepared DAB color development solution was added dropwise and the color development time was controlled under the microscope. The nuclei were re-stained with hematoxylin and then sealed by dehydration. The average optical density value was calculated for the relevant area of each section using Image-Pro-PLUS software, and the magnitude of the value was the degree of expression of the relevant subunit protein.

Statistical Analysis

Because the subjects were repeatedly measured at different time stages during the conduct of the MWM experiment, a two-way ANOVA was performed using repeated measures ANOVA to analyze the differences between groups. The analysis was performed using the open source software R (R version 4.1.2, URL https://www.R-project.org). The different experimental medication treatments (Group) and training time (Time) were treated as independent variables and the experimental subject number was used as a random variable to construct a linear mixed model using the lme4 package library lmer function (Bates et al., 2015) to test the effect of the two factors on the results. To further check the variability between the different groups, the Tukey post hoc paired test was performed on the results of the constructed models using the multcomp package library glht function (Hothorn et al., 2008).

All other data were statistically processed by SPSS 22.0 statistical software, and data results were expressed as means ± standard deviation (X ± S). Statistical differences were analyzed by one-way ANOVA and *t*-test by LSD method. $p < 0.05$ was considered statistically different, $p < 0.01$ was considered significantly different.

RESULTS

The Key Target of Tan IIA for the Treatment of Patients With Cognitive Dysfunction Syndrome May Be CNR1

We used bioinformatics-related methods to find that the key target of Tan IIA for the treatment of patients with cognitive dysfunction syndrome may be CNR1. In total, we identified 461 differentially expressed genes and displayed them in the volcano plot (**Figure 2B**), including 133 up-regulated genes and 328 down-regulated genes (**Figure 2A**). The expression of these 461 genes in the TCGA dataset (sample includes 121 patients with cognitive dysfunction syndrome and 232 normal individuals) is shown in the heat map (**Figure 2C**). Among these 461 differentially expressed genes, 2 intersected with Tan IIA-related targets (**Figure 2D**), and these 2 differentially expressed genes were regarded as the target genes of Tan IIA for the treatment of mild cognitive impairment syndrome, and they were CNR1 and C5AR1, respectively.

To further validate the potential of these 2 targets as important targets for Tan IIA in the treatment of mild cognitive impairment syndromes, we performed virtual molecular docking of Tan IIA and these 2 genes using AutoDockTools-1.5.6 software. The results showed that both CNR1 and C5AR1 had strong binding ability to Tan IIA (The 3D images of these two targets and the binding point are shown in **Figure 3**), but the docking score of CNR1 (130.672, **Figure 3B**) was higher than that of C5AR1 (110.642, **Figure 3A**). According to the literature analysis, we selected CNR1 as a key target protein for Tan II A in the treatment of mild cognitive impairment syndrome. This provided some basis for our biological experiments.

Tan IIA Suppresses Spatial Recognition and Learning Memory Dysfunction in Sleep Deprivation Model Rats

We deprived the rats of sleep for 96 consecutive hours and started the NOR experiment at the 24th hour. There was no significant difference in the total distance travelled by the rats in each group ($p > 0.05$, **Figure 4D**) Therefore, the interference of exercise on the experimental results could be excluded. The desire to explore new objects was significantly lower in the Model and Tan IIA-L + AM251 groups compared to the Control group ($\#\#p < 0.01$, $\#\#p < 0.01$, **Figure 4C**). Compared with the Model group, the Tan IIA treatment groups showed a significantly higher exploration index for new objects, with the high-dose group showing a significant difference ($^{**}p < 0.01$). The Tan IIA-L + AM251 group showed similar trajectory of action and exploration time to the Model group compared to the Tan IIA-H group ($\&p < 0.05$).

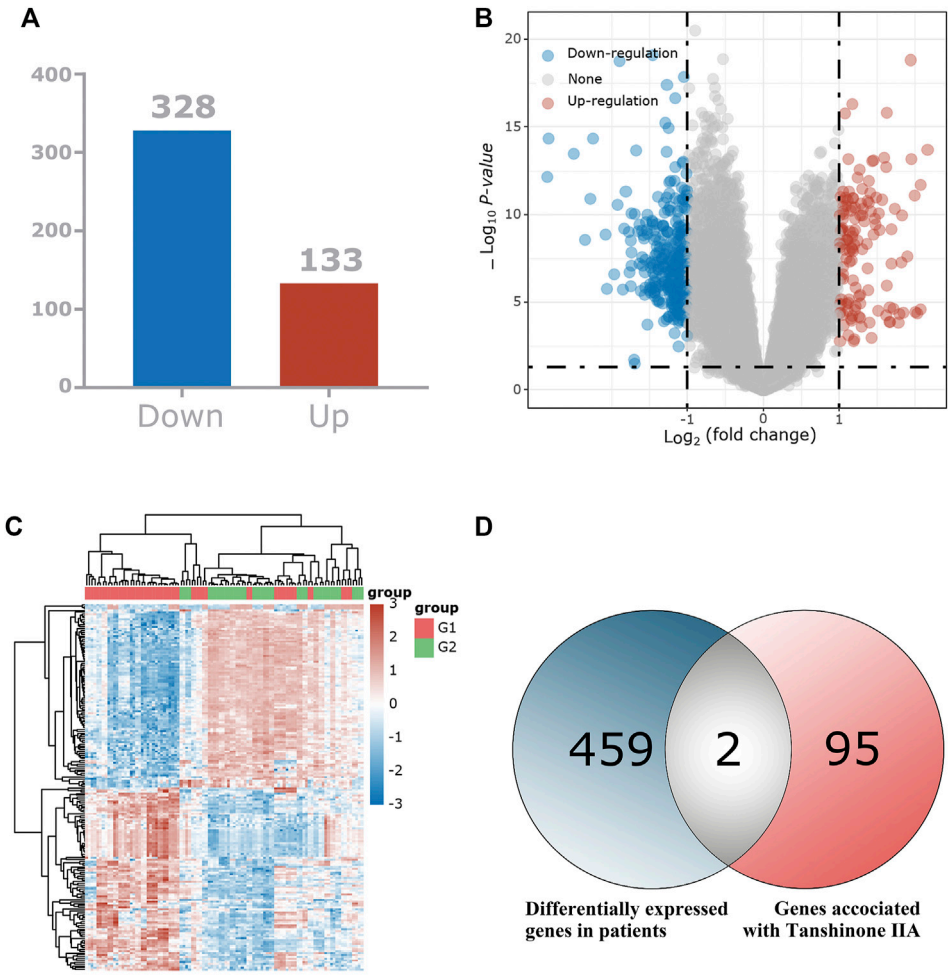

FIGURE 2 | Identification of the differentially expressed genes (DEGs) of patients with mild cognitive impairment syndrome in the GEO cohort. **(A)** The DEGs between Patients with mild cognitive impairment syndrome and normal tissues. **(B)** Volcano plots, to Visualize the DEGs. **(C)** The expression trend of 461 DEGs shown as heatmap. **(D)** Venn diagram to identify Tan IIA -related DEGs between Mild cognitive impairment syndrome patients and normal individuals.

The effect of both time and dose on the experimental results in the Morris water maze experiment was significant ($p < 0.05$, $p < 0.05$), and the time × dose interaction was not significant ($p > 0.05$). The latency (**Figure 5B**) to ascend the platform and the total distance swum decreased from the second day in all groups, but the decrease was flat in the Model and Tan IIA-L + AM251 groups. From the third day onwards, a significant difference in latency between the Model group and the Control group was observed ($\#p < 0.05$). The latency was significantly lower in the Tan IIA-L group compared with the Model group ($*p < 0.05$). On the fourth day of platform hiding period, both Model and Tan IIA-L + AM251 groups needed about 50 s to find the platform, and most of the rats in the Model group still maintained the marginal strategy to search the platform (**Figure 5A**). Meanwhile, the Control rats had been able to easily ascend the platform with an average elapsed time of less than 30 s ($\#\#p < 0.01$). Compared with the Model group, the incubation period of Tan IIA -treated rats were substantially shorter ($*p < 0.05$, $**p < 0.01$). The Tan IIA-L + AM251 group had a significantly longer latency than the Tan IIA -H group ($\&\&p < 0.01$). The swimming speed curves of the rats in each group tended to level off, with no significant differences ($p > 0.05$, **Figure 5C**). After removal of the platform, each rat was allowed to freely explore the tank for 90 s (**Figure 5D**). Rats in the Control group traversed the platform approximately 4 times, whereas the number of traversals in the Model group was less than 1time ($\#\#p < 0.01$). The number of platform crossing was significantly increased after Tan IIA treatment compared with the model group ($**p < 0.01$, $**p < 0.01$). Compared with Tan IIA-H, the Tan IIA-L + AM251 group crossed the platform significantly less times ($\&\&p < 0.01$).

Tan IIA Ameliorates Neural Damage in the Hippocampus of Sleep Deprivation Model Rats

The results of Nissl staining (**Figure 6A**) and HE staining (**Figure 6D**) showed that the neurons in all regions of the hippocampus of the Control rats were clearly hierarchical,

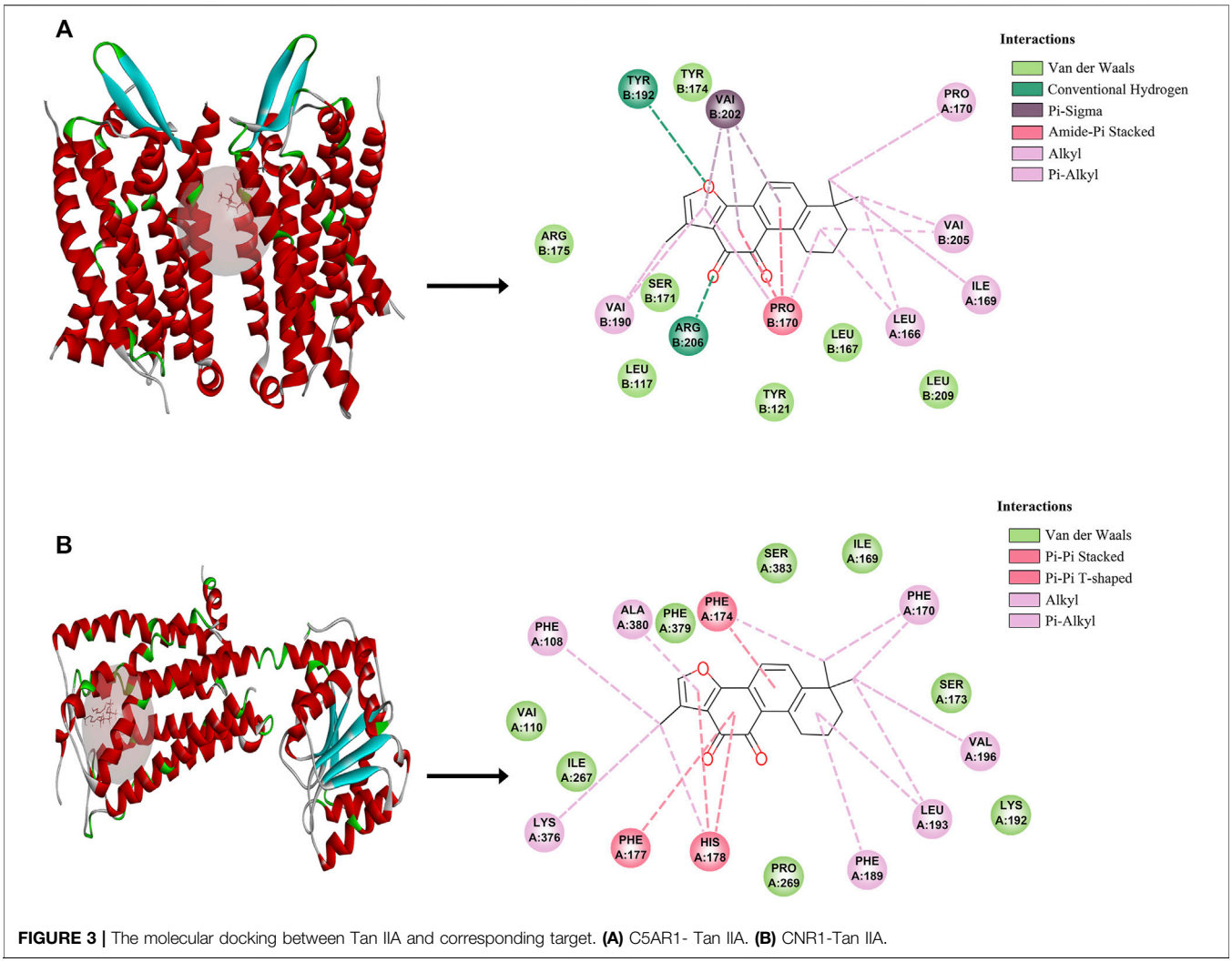

FIGURE 3 | The molecular docking between Tan IIA and corresponding target. **(A)** C5AR1- Tan IIA. **(B)** CNR1-Tan IIA.

closely and neatly arranged, without pathological abnormalities, and the Nissl vesicles in the neuronal cells were clearly stained and more numerous. The neurons in the hippocampal region of the Model group were reduced in level, loosely arranged, and the Nissl vesicles were reduced or disappeared, and showed obvious pathological abnormalities in the HE staining results, such as the disappearance of nuclear consolidation and deepening of cell staining, indicating that the hippocampal neurons in the model group began to degenerate. Tan IIA can prevent these histopathological damages. Statistically, acute sleep deprivation reduced the number of hippocampal neurons in all groups of rats, but no significant differences were seen in most regions, and only the loss of cells in CA1 area was significant in the model group rats (*##p < 0.01*, **Figure 6B**), which may be due to the insufficient duration of sleep deprivation.

Dendritic spines are the basic structural unit for learning and memory formation. We selected pyramidal neurons in the CA1 region and analyzed the density of dendritic spines by Golgi-Cox staining (**Figure 7C**). Consistent with the envisioned results, acute sleep deprivation significantly reduced the density of neuronal dendritic spines in the CA1 region compared with the Control group (*##p < 0.01*). Compared with the Model group, Tan IIA significantly increased dendritic spine density in acute sleep deprived rats (***p < 0.01, **p < 0.01*), while AM251 inhibited the effect of Tan IIA, the difference was not significant.

Tan IIA Activates the CNR1/PI3K/AKT Pathway to Exert Neuroprotective Effects

To evaluate whether CNR1 effectively mediated Tan IIA -induced neuroprotection, we examined the expression and activation of CB1, PI3K, AKT, and STAT3 in the hippocampus by Western-blot (**Figure 8**). Compared with the Control group, the expression of hippocampal CB1, P-PI3K, P-AKT, and P-STAT3 was decreased in the Model and Tan IIA-L + AM251 groups (*##p < 0.01, #p < 0.05*). Compared with the Model group, the expression of CB1, P-PI3K, P-AKT, and P-STAT3 was increased in the hippocampus of rats in the Tan IIA groups (**p < 0.05, **p < 0.01*).

To further explore the neuroprotective effects of Tan IIA, we also used immunohistochemistry to observe the changes of the

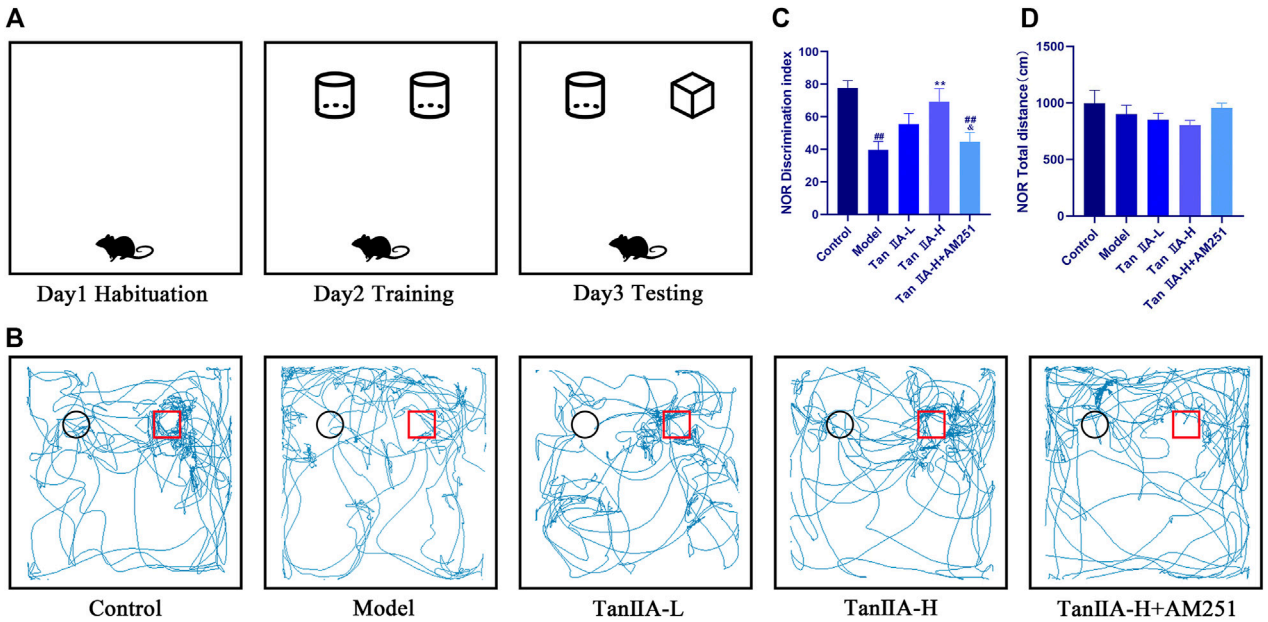

FIGURE 4 | New object recognition experiment. **(A)** Schematic diagram of three test phases. **(B)** Exploration trajectory of each group of rats: The rats in the control group had a strong desire to explore new objects; the rats in the model group preferred to walk against the wall and their trajectories had no obvious pattern; the rats in the Tan IIA administration restored their desire to explore new objects; the rats in the Tan IIA-L + AM251 group had confused trajectories. **(C)** Identification indices: model (*##p < 0.01*) vs control; Tan IIA-L + AM251 groups (*##p < 0.01*) vs. control; Tan IIA-H (***p < 0.01*) vs. model; Tan IIA-L + AM251 groups (*&p < 0.05*) vs. Tan IIA-L groups **(D)**No significant difference in the total distance travelled by the rats in each group.

pro-apoptotic factor bcl-2 Associated X Protein (Bax) and the inhibitory factor B cell lymphoma 2 (Bcl-2) in the rat hippocampus (**Figure 9**). The ratio of the average optical density of the two proteins was used as an object of analysis, and it was found that the ratio of Bax to Bcl-2 expression increased in the Model group (*##p < 0.01*), and the Bax/Bcl-2 ratio decreased significantly in both Tan IIA -treated groups compared to the Model group (***p < 0.01, **p < 0.01*). In contrast, the Bax/Bcl-2 ratio in the Tan IIA-L + AM251 group rebounded compared to the Tan IIA-L group (*&&p < 0.01*). Quantification of protein expression using immunohistochemical methods lacks accuracy. Therefore, we also used the Western-blot method to quantify the expression of BCL-2 and BAX proteins. BAX/BCL-2 values were increased in the model and Tan IIA-L + AM251 groups compared to the control group (*##p < 0.01, #p < 0.05*). Compared with the model group, the BAX/BCL-2 ratio decreased in the Tan IIA groups (**p < 0.05, *p < 0.05*) and the values rebounded in the Tan IIA-L + AM251 compared with the Tan IIA-H (*&p < 0.05*).

DISCUSSION

Our study showed that Tan ⅡA has a neuroprotective effect on acute sleep deprivation-induced cognitive impairment in rats, and its mechanism of action may be activating the CNR1/PI3K/AKT pathway in the hippocampal region, ameliorating hippocampal neuronal cell injury and inhibiting hippocampal cell apoptosis.

In the present study, several different behavioral tests (NOR and MWM) were used to evaluate the effects of acute sleep deprivation on cognitive function in rats and to evaluate the protective effect of Tan ⅡA. The NOR test is a behavioral method for detecting recognition memory in rodents on the basis of their natural instinct to approach and explore novel objects, and can be used to measure short-term spatial and short-term recognition memory in rodents (Grayson et al., 2015; Rajizadeh et al., 2018). Consistent with our expectation, the experimental results showed that acute sleep deprivation led to neurocognitive deficits in the NOR test and that the administration of Tan IIA could prevent these impairments in some extent, with higher doses of Tan IIA showing a stronger effect, suggesting a neuroprotective effect of Tan IIA on recognition memory capacity.

The Morris water maze experiment requires rodents to escape their aversive water environment by collecting and processing visual cues related to spatial orientation, an activity that involves long-term memory and spatial learning abilities (Vorhees and Williams, 2006). Same as previous reports (Wang et al., 2020a; Tai et al., 2020), different factors leading to different durations of sleep deprivation all affected the behavior of experimental animals in the WMW experiment, as evidenced by the prolonged latency of the platform concealment period and the reduced number of platform crossing during the platform-free period. MWM experiments are subject to a bivariate effect of time and dose and should therefore be assessed with matched subjects using a two-way (treatment × time) repeated measures ANOVA (with trial/time point as a repeated measures factor) followed by a Tukey post hoc multiple comparison test. Based on two-way

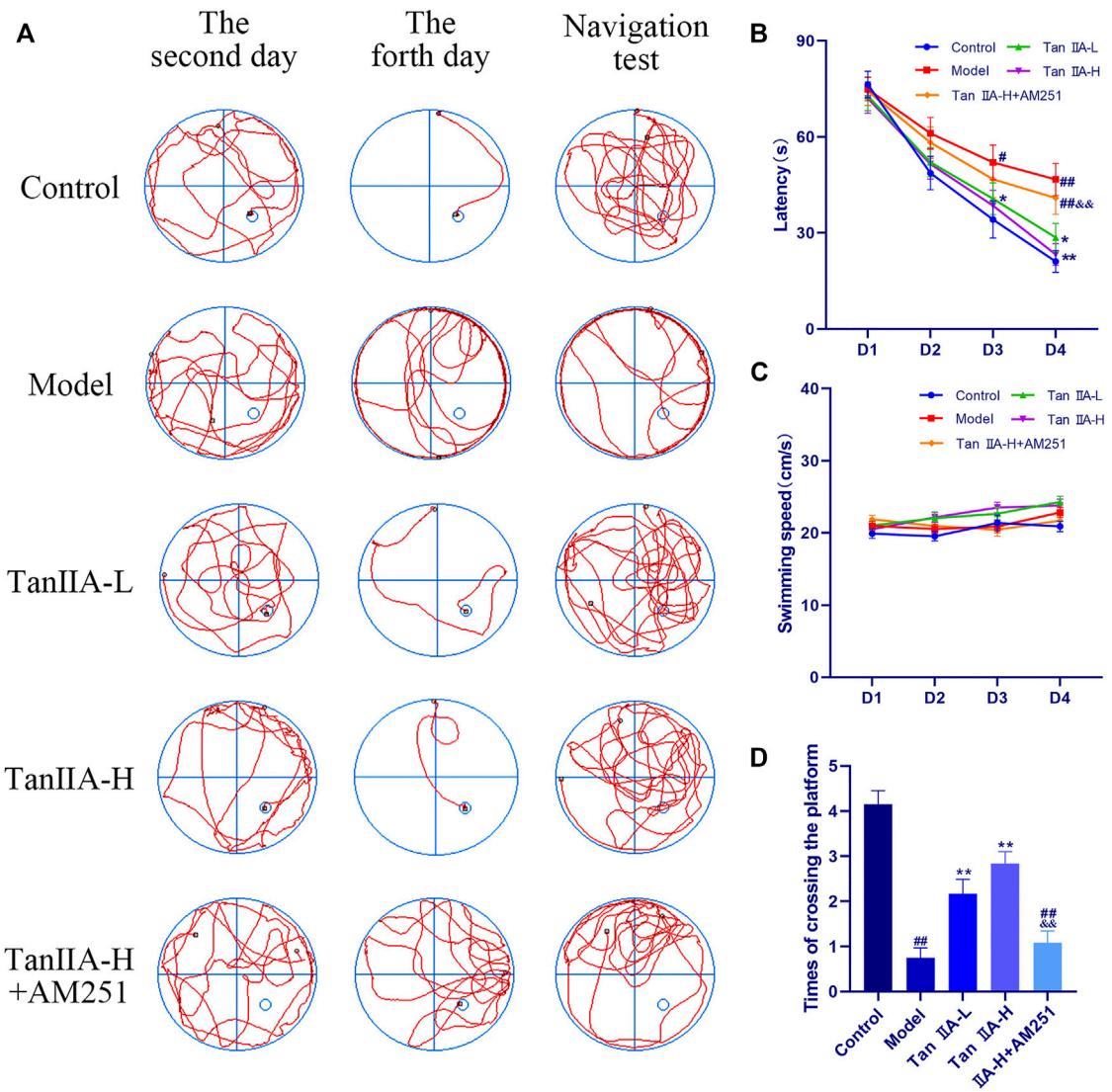

FIGURE 5 | Morris water maze experiment. **(A)** Swimming trajectory of rats on the second day, fourth day and navigation test. **(B)** Latency on Day4: model (##$p < 0.01$) vs. control; Tan IIA-L + AM251 groups (##$p < 0.01$) vs. control; Tan IIA-L (*$p < 0.05$) vs. model; Tan IIA-H (**$p < 0.01$) vs. model. Tan IIA-L + AM251 groups (&&$p < 0.01$) vs. Tan IIA-L groups. **(C)** Swimming speed of rats: no significant difference ($p > 0.05$). **(D)** Times of crossing the platform: model (##$p < 0.01$) vs. control; Tan IIA-L + AM251 groups (##$p < 0.01$) vs. control; Tan IIA-L (**$p < 0.01$) vs. model; Tan IIA-H (**$p < 0.01$) vs. model; Tan IIA-L + AM251 groups (&&$p < 0.01$) vs. Tan IIA-L groups.

repeated measures multivariate analysis of variance, we found that the administration of different doses of Tan IIA showed a significant effect on the reduction of escape latency during the training period in rats and showed a dose-dependent effect, mainly in the reduction of escape latency and the increase in the number of crossing platforms, indicating that it prevented sleep deprivation-induced spatial learning and long-term memory impairment. In the negative control group and Tan IIA -L group, it was observed that some rats would look around or stay in place after entering the water for a while and then swim directly to the stage after confirming the direction. This phenomenon indicates that these rats perform a better memory capacity. This behavior affects the swimming speed to some extent, but because the sample size was sufficient, there was no significant difference in the swimming locomotor ability of the rats from the groups as a whole. Thus, Tan IIA not only improves long-term and short-term memory impairment from sleep deprivation, but also plays a beneficial role at the level of spatial learning functions.

In the present study, 96 h of sleep deprivation caused significant impairment of spatial memory function in rats while atrophy of hippocampal neurons, nuclear fixation, and Nissl staining concentration were also observed in rats. All of the above pathological injuries recovered after Tan IIA administration and showed a dose dependence. Unfortunately, there was little change in the total number

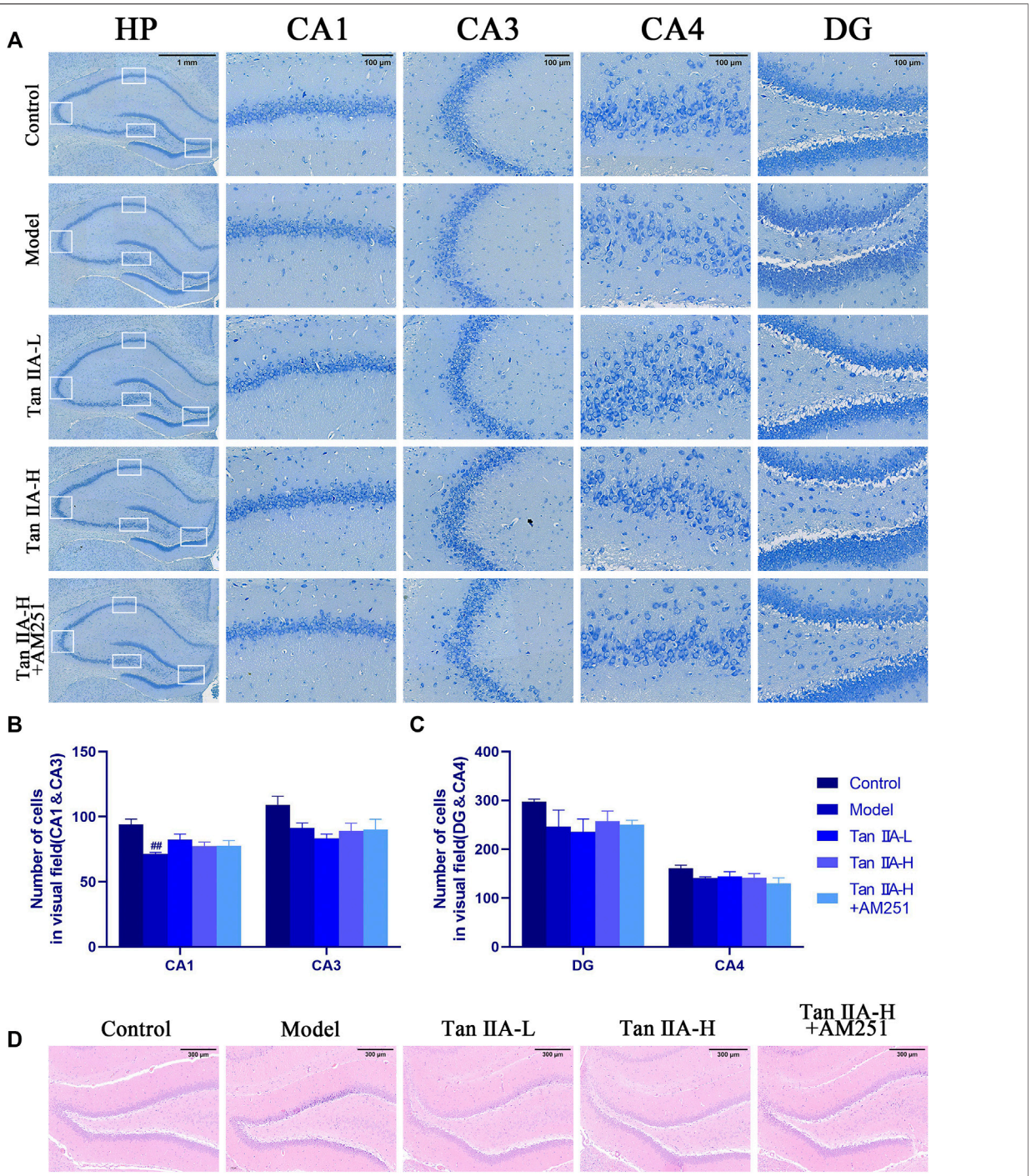

FIGURE 6 | Pathological damage in the hippocampus of rats. **(A)** Pathological sections of CA1, CA3, CA4 and DG areas of rat hippocampus with Nissl staining. **(B)** Number of cells in visual field (CA1&CA3) **(C)** Number of cells in visual field (CA4&DG) **(D)** HE staining in the DG area of rat hippocampus: The normal neurons in the hippocampal region of the control group were tightly arranged and neatly aligned, and the nuclei were clearly visible. The model group showed obvious pathological abnormalities, with sparse neuronal arrangement and nuclear consolidation in the hippocampal region. The pathological damage was reduced or disappeared after Tan IIA treatment.

of cells in all regions of the hippocampus, and only a greater decrease in cells was found in the model group of rats. We speculate that this is due to the insufficient length of sleep deprivation.

However, it has been shown that the ratio of the anti-apoptotic protein Bcl-2 to the pro-apoptotic protein Bax determines, to some extent, whether apoptosis occurs, and that cells with high Bax/Bcl-2 are more prone to apoptosis than those with low Bax/

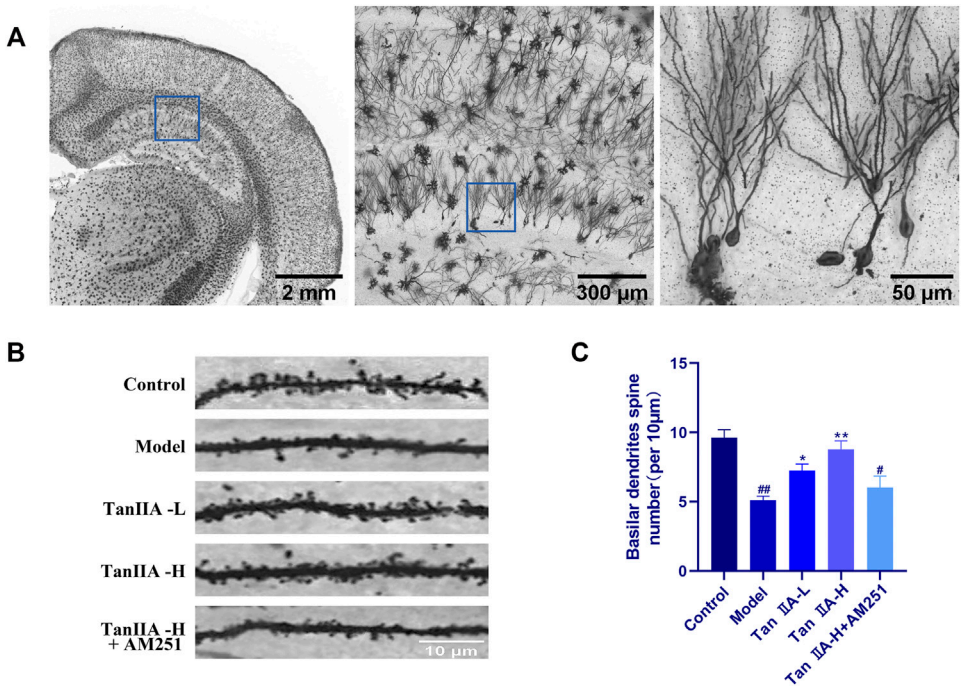

FIGURE 7 | Golgi-Cox staining. **(A)** Golgi-Cox staining pattern diagram: Dendritic spines on neurons are made visible. **(B)** Changes in dendritic spine density of neurons in each group: Higher number of dendritic spines in the control group; reduced in the model group; number rebounded after Tan IIA treatment in a dose-dependent manner; lower number of dendritic spines in AM251 **(C)** Neuronal dendritic spine density: model (##$p < 0.01$) vs. control; Tan IIA-L + AM251 groups (#$p < 0.05$) vs. control; Tan IIA-L (*$p < 0.05$) vs. model; Tan IIA-H (**$p < 0.01$) vs. model.

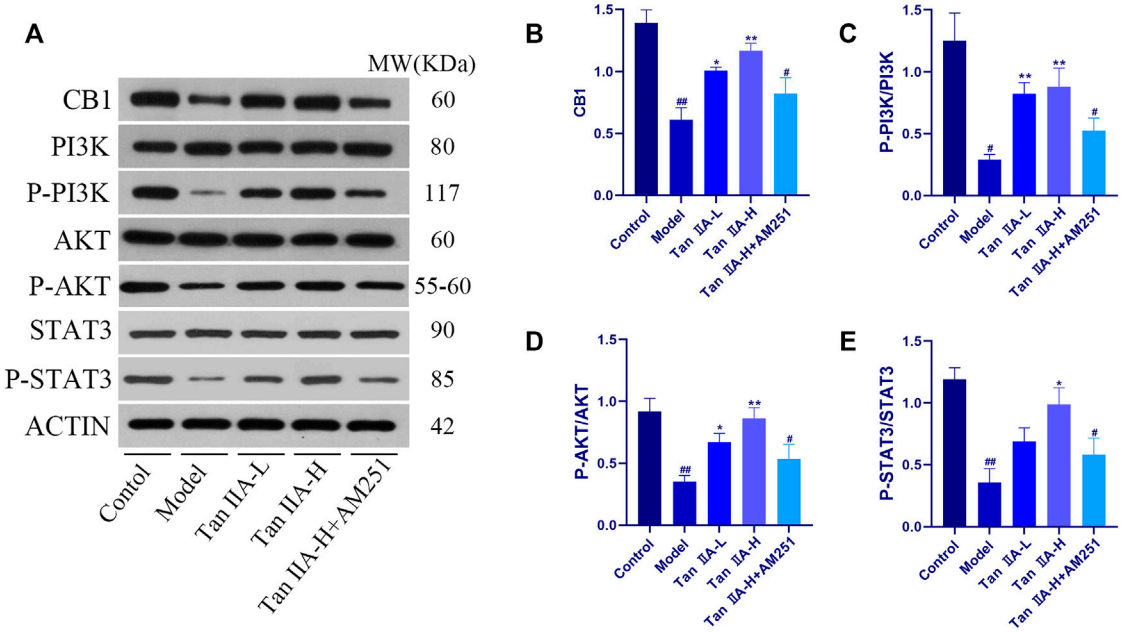

FIGURE 8 | Expressions of CB1, PI3K, AKT and STAT3 were detected using western-blot assay. **(A)** Western-blot stripes. **(B)** CB1/ACTIN: model (##$p < 0.01$) vs. control; Tan IIA-L + AM251 groups (#$p < 0.05$) vs. control; Tan IIA-L (*$p < 0.05$) vs model; Tan IIA-H (**$p < 0.01$) vs model. **(C)** P-PI3K/PI3K:model (#$p < 0.05$) vs. control; Tan IIA-L + AM251 groups (#$p < 0.05$) vs. control; Tan IIA-L (**$p < 0.01$) vs. model; Tan IIA-H (**$p < 0.01$) vs model. **(D)** P-AKT/AKT: model (##$p < 0.01$) vs. control; Tan IIA-L + AM251 groups (#$p < 0.05$) vs. control; Tan IIA-L (*$p < 0.05$) vs model; Tan IIA-H (**$p < 0.01$) vs. model. **(E)** P-STAT3/STAT3:model (##$p < 0.01$) vs. control; Tan IIA-L + AM251 groups (#$p < 0.05$) vs. control; Tan IIA-L (*$p < 0.05$) vs. model.

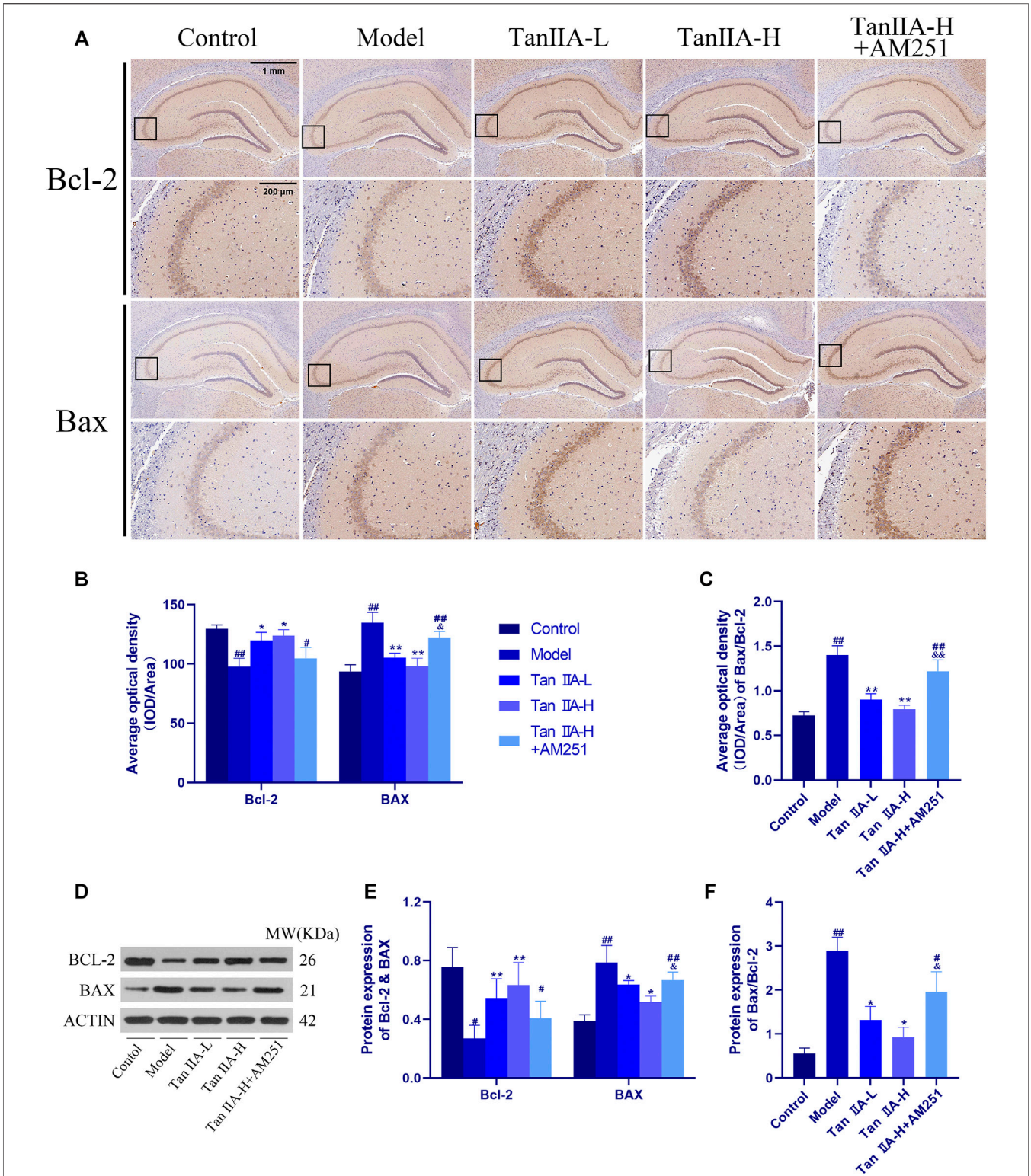

FIGURE 9 | Changes of Bax and Bcl-2 in rat hippocampus. **(A)** Changes of Bax and Bcl-2 in rat hippocampus by immunohistochemistry. **(B)** Average optical density of Bax and Bcl-2. **(C)** Average optical density ratio of Bax/Bcl-2: model (##$p < 0.01$) vs. control; Tan IIA-L + AM251 groups (##$p < 0.01$) vs. control; Tan IIA-L (**$p < 0.01$) vs. model; Tan IIA-H (**$p < 0.01$) vs. model; Tan IIA-L + AM251 groups (&&$p < 0.01$) vs Tan IIA-L groups. **(D)** Western-blot stripes. **(E)** Protein expression: the same trend as immunohistochemistry. **(F)** Protein expression of Bax/Bcl-2: model (##$p < 0.01$) vs. control; Tan IIA-L + AM251 groups (#$p < 0.05$) vs. control; Tan IIA-L (*$p < 0.05$) vs. model; Tan IIA-H (*$p < 0.05$) vs. model; Tan IIA-L + AM251 groups (&$p < 0.05$) vs. Tan IIA-L groups.

Bcl-2 (Guo and Li, 2018). Therefore, we analyzed the expression of Bax and Bcl-2 in the rat hippocampus using immunohistochemical methods. Sleep deprivation increased the Bax/Bcl-2 ratio, and the ratio decreased back after Tan IIA administration, and AM251 blocked the utility of Tan IIA. However, immunohistochemistry does not quantify the protein expression in the hippocampal region well, and can only make a general judgment from a macroscopic point of view. So we also detected the protein expression of Bax and Bcl-2 in the hippocampal region using WB method and the results were consistent with the immunohistochemical results. These results suggest that apoptosis-induced hippocampal neuronal damage may be a factor contributing to memory impairment in sleep deprived rats.

In addition, sleep deprivation can also impair hippocampal function by altering synaptic plasticity at the structural level (Frank and Cantera, 2014; Cirelli and Tononi, 2020). The number of neurons, neuronal dendritic branches and dendritic spine density are all important measures of synaptic plasticity (Lewis, 2016). In this study, we found that the density of dendritic spines of pyramidal neurons in the CA1 region increased significantly after the prophylactic administration of Tan IIA to the model group rats. It indicates that Tan IIA can inhibit the neural damage caused by sleep deprivation at the synaptic level. Therefore, we suggest that apoptosis-related factors Bcl-2 and Bax may be involved in the process of hippocampal lesions caused by acute sleep deprivation in rats, and Tan IIA can effectively inhibit sleep deprivation-induced synaptic loss and neuronal loss and repair hippocampal pathological damage.

Several studies have reported that the endocannabinoid system plays an important role in a variety of brain functions, including the regulation of synaptic plasticity, learning and memory (Castillo et al., 2012). The CNR1 gene encodes the cannabinoid receptor (CB1), a G protein-coupled receptor (GPCR) that is highly expressed in the hippocampus (Herkenham et al., 1991), and is a receptor for endocannabinoids, N-arachidonic ethanolamine (anandide; AEA) and 2-arachidonic glycerol (2-AG), and mediates most of the effects of the active cannabis component phytocannabinoids on the central nervous system (Fletcher-Jones et al., 2020). We used bioinformatics to predict a strong correlation between Tan IIA and CB1 in a population of patients with cognitive dysfunction syndrome, and the results of molecular docking suggest that Tan IIA has a strong binding capacity to CB1. The PI3K/AKT pathway is an intracellular signaling pathway that promotes metabolism, proliferation, cell survival, growth and angiogenesis in response to G protein-coupled receptor signaling, a process mediated by serine or threonine phosphorylation of a range of downstream substrates. Much has been reported about the activation of the PI3K/AKT pathway by signaling from CB1 (Ozaita et al., 2007; Dalton and Howlett, 2012; López-Cardona et al., 2017; Wang et al., 2021). The mechanism of action of Tan IIA in reducing inflammation and oxidative stress and inhibiting apoptosis may also be related to the PI3K/AKT pathway (Zhang et al., 2013; Li et al., 2016; Zhang et al., 2019; Wang et al., 2020b). Our experimental results showed that the expression of P-PI3K and P-AKT were increased after the action of Tan IIA. To confirm that Tan IIA induces neurite growth via CB1, we blocked CB1 using AM251. Although there is no significant difference between the data of the Tan IIA-H and Tan IIA-H + AM251 groups, we can clearly see the difference in the variation in the histograms, which we speculate is due to the insufficient sample size to allow the experimental error to be eliminated and this effect cannot be corrected by statistical principles. It was found that pharmacological blockade of CB1 resulted in reduced activation of PI3K and Akt after Tan IIA treatment, and the blocking effect on Tan IIA efficacy was also demonstrated in animal behavioral experiments and hippocampal pathological sections. STAT3 plays an important role in mediating neurite growth downstream of PI3K/Akt signaling through activation of endogenous cellular CB1 (Wang et al., 2021), (Zhou et al., 2013), which is consistent with our prediction and results. Therefore, we suggest that Tanshinone IIA can exert neuroprotective effects by activating the CNR1/PI3K/AKT signaling pathway.

There are also shortcomings and room for improvement in our research. First, we did not set up a positive drug control group because we did not currently find one that could be put into use as a positive drug based on this mechanism. Although there are many drugs that are effective in relieving short- or long-term insomnia, their mechanisms are well established (e.g., eszopiclone (Wilt et al., 2016; Rösner et al., 2018)—acting on BDZ receptors and enhancing GABA receptor action within the central nervous system), they do not act by affecting the CNR1-PI3K-AKT signaling pathway effects. Second, our experiments do not involve a cellular model because the mechanism of sleep deprivation is complex and the damage caused to the organism is diverse, and the design of a single-factor cellular damage model cannot correspond correctly to our animal model, so we discarded this experimental design. In the future, we hope to explore the pharmacological effects of Tan IIA in neurodegenerative diseases through follow-up experiments; explore the logic and mechanism behind the cannabinoid receptor system as a potential drug for the treatment of neurological diseases.

CONCLUSION

Based on this series of findings, we conclude that Tanshinone IIA may exert neuroprotective effects through activating the CNR1/PI3K/AKT signaling pathway to improve sleep deprivation-induced spatial recognition and learning memory dysfunction in rats; Tanshinone IIA may have an antagonistic effect on apoptosis in the hippocampus in rats. Therefore, Tanshinone IIA may be a prospective candidate for the prevention of sleep deprivation-induced spatial recognition and learning-memory dysfunction.

DATA AVAILABILITY STATEMENT

The datasets presented in this study can be found in online repositories. The names of the repository/repositories and accession number(s) can be found in the article/ **Supplementary Material**.

ETHICS STATEMENT

The animal study was reviewed and approved by the Hubei University of Chinese Medicine Animal Experiment Ethics Committee.

AUTHOR CONTRIBUTIONS

Z-HL designed the study; Z-HL, LC, LD, and CW performed the research; Q-YY and S-BZ collected and analyzed the data; Z-HL wrote the paper.

FUNDING

This study was financially supported by National Natural Science Foundation of China, 2014: Study on the effect and mechanism of sour date palm soup on 5-HTR-based regulation of SCN and VLPO system in elderly insomnia, 2015.1–2018.12, Grant Number: 81473560.

SUPPLEMENTARY MATERIAL

The Supplementary Material for this article can be found online at: https://www.frontiersin.org/articles/10.3389/fphar.2022.823732/full#supplementary-material

REFERENCES

Bates, D., Mächler, M., Bolker, B., and Walker, S. (2015). Fitting Linear Mixed-Effects Models Usinglme4. *J. Stat. Soft.* 67 (1), 1–48. doi:10.18637/jss.v067.i01

Bishir, M., Bhat, A., Essa, M. M., Ekpo, O., Ihunwo, A. O., Veeraraghavan, V. P., et al. (2020). Sleep Deprivation and Neurological Disorders. *Biomed. Res. Int.* 2020, 5764017. doi:10.1155/2020/5764017

Cai, Y., Zhang, W., Chen, Z., Shi, Z., He, C., and Chen, M. (2016). Recent Insights into the Biological Activities and Drug Delivery Systems of Tanshinones. *Int. J. Nanomedicine* 11, 121–130. doi:10.2147/IJN.S84035

Castillo, P. E., Younts, T. J., Chávez, A. E., and Hashimotodani, Y. (2012). Endocannabinoid Signaling and Synaptic Function. *Neuron* 76 (1), 70–81. doi:10.1016/j.neuron.2012.09.020

Chen, J., Bi, Y., Chen, L., Zhang, Q., and Xu, L. (2018). Tanshinone IIA Exerts Neuroprotective Effects on Hippocampus-dependent Cognitive Impairments in Diabetic Rats by Attenuating ER Stress-Induced Apoptosis. *Biomed. Pharmacother.* 104, 530–536. doi:10.1016/j.biopha.2018.05.040

Choshen-Hillel, S., Ishqer, A., Mahameed, F., Reiter, J., Gozal, D., Gileles-Hillel, A., et al. (2021). Acute and Chronic Sleep Deprivation in Residents: Cognition and Stress Biomarkers. *Med. Educ.* 55 (2), 174–184. doi:10.1111/medu.14296

Cirelli, C., and Tononi, G. (2020). Effects of Sleep and Waking on the Synaptic Ultrastructure. *Philos. Trans. R. Soc. Lond. B Biol. Sci.* 375 (1799), 20190235. doi:10.1098/rstb.2019.0235

Dalton, G. D., and Howlett, A. C. (2012). Cannabinoid CB1 Receptors Transactivate Multiple Receptor Tyrosine Kinases and Regulate Serine/threonine Kinases to Activate ERK in Neuronal Cells. *Br. J. Pharmacol.* 165 (8), 2497–2511. doi:10.1111/j.1476-5381.2011.01455.x

Dou, M. Y., Wu, H., Zhu, H. J., Jin, S. Y., Zhang, Y., and He, S. F. (2016). Remifentanil Preconditioning Protects Rat Cardiomyocytes against Hypoxia-Reoxygenation Injury via δ-opioid Receptor Mediated Activation of PI3K/Akt and ERK Pathways. *Eur. J. Pharmacol.* 789, 395–401. doi:10.1016/j.ejphar.2016.08.002

Fletcher-Jones, A., Hildick, K. L., Evans, A. J., Nakamura, Y., Henley, J. M., and Wilkinson, K. A. (2020). Protein Interactors and Trafficking Pathways that Regulate the Cannabinoid Type 1 Receptor (CB1R). *Front. Mol. Neurosci.* 13, 108. doi:10.3389/fnmol.2020.00108

Frank, M. G., and Cantera, R. (2014). Sleep, Clocks, and Synaptic Plasticity. *Trends Neurosci.* 37 (9), 491–501. doi:10.1016/j.tins.2014.06.005

Fu, L., Han, B., Zhou, Y., Ren, J., Cao, W., Patel, G., et al. (2020). The Anticancer Properties of Tanshinones and the Pharmacological Effects of Their Active Ingredients. *Front. Pharmacol.* 11, 193. doi:10.3389/fphar.2020.00193

Ge, Q., Chen, L., Tang, M., Zhang, S., Liu, L., Gao, L., et al. (2018). Analysis of mulberry Leaf Components in the Treatment of Diabetes Using Network Pharmacology. *Eur. J. Pharmacol.* 833, 50–62. doi:10.1016/j.ejphar.2018.05.021

Grayson, B., Leger, M., Piercy, C., Adamson, L., Harte, M., and Neill, J. C. (2015). Assessment of Disease-Related Cognitive Impairments Using the Novel Object Recognition (NOR) Task in Rodents. *Behav. Brain Res.* 285, 176–193. doi:10.1016/j.bbr.2014.10.025

Guo, R., and Li, G. (2018). Tanshinone Modulates the Expression of Bcl-2 and Bax in Cardiomyocytes and Has a Protective Effect in a Rat Model of Myocardial Ischemia-Reperfusion. *Hellenic J. Cardiol.* 59 (6), 323–328. doi:10.1016/j.hjc.2017.11.011

Guo, R., Li, L., Su, J., Li, S., Duncan, S. E., Liu, Z., et al. (2020). Pharmacological Activity and Mechanism of Tanshinone IIA in Related Diseases. *Drug Des. Devel Ther.* 14, 4735–4748. doi:10.2147/DDDT.S266911

He, Y., Ruganzu, J. B., Lin, C., Ding, B., Zheng, Q., Wu, X., et al. (2020). Tanshinone IIA Ameliorates Cognitive Deficits by Inhibiting Endoplasmic Reticulum Stress-Induced Apoptosis in APP/PS1 Transgenic Mice. *Neurochem. Int.* 133, 104610. doi:10.1016/j.neuint.2019.104610

Herkenham, M., Lynn, A. B., Johnson, M. R., Melvin, L. S., de Costa, B. R., and Rice, K. C. (1991). Characterization and Localization of Cannabinoid Receptors in Rat Brain: a Quantitative *In Vitro* Autoradiographic Study. *J. Neurosci.* 11 (2), 563–583. doi:10.1523/jneurosci.11-02-00563.1991

Hillman, D., Mitchell, S., Streatfeild, J., Burns, C., Bruck, D., and Pezzullo, L. (2018). The Economic Cost of Inadequate Sleep. *Sleep* 41 (8), 1. doi:10.1093/sleep/zsy083

Hothorn, T., Bretz, F., and Westfall, P. (2008). Simultaneous Inference in General Parametric Models. *Biom J.* 50 (3), 346–363. doi:10.1002/bimj.200810425

Husain, S., Abdul, Y., and Potter, D. E. (2012). Non-analgesic Effects of Opioids: Neuroprotection in the Retina. *Curr. Pharm. Des.* 18 (37), 6101–6108. doi:10.2174/138161212803582441

Javaheripour, N., Shahdipour, N., Noori, K., Zarei, M., Camilleri, J. A., Laird, A. R., et al. (2019). Functional Brain Alterations in Acute Sleep Deprivation: An Activation Likelihood Estimation Meta-Analysis. *Sleep Med. Rev.* 46, 64–73. doi:10.1016/j.smrv.2019.03.008

Jewett, M. E., Dijk, D. J., Kronauer, R. E., and Dinges, D. F. (1999). Dose-response Relationship between Sleep Duration and Human Psychomotor Vigilance and Subjective Alertness. *Sleep* 22 (2), 171–179. doi:10.1093/sleep/22.2.171

Jia, Q., Zhu, R., Tian, Y., Chen, B., Li, R., Li, L., et al. (2019). Salvia Miltiorrhiza in Diabetes: A Review of its Pharmacology, Phytochemistry, and Safety. *Phytomedicine* 58, 152871. doi:10.1016/j.phymed.2019.152871

Jiang, Z., Gao, W., and Huang, L. (2019). Tanshinones, Critical Pharmacological Components in Salvia Miltiorrhiza. *Front. Pharmacol.* 10, 202. doi:10.3389/fphar.2019.00202

Killgore, W. D. (2010). Effects of Sleep Deprivation on Cognition. *Prog. Brain Res.* 185, 105–129. doi:10.1016/B978-0-444-53702-7.00007-5

Kim, E. Y., Mahmoud, G. S., and Grover, L. M. (2005). REM Sleep Deprivation Inhibits LTP *In Vivo* in Area CA1 of Rat hippocampus. *Neurosci. Lett.* 388 (3), 163–167. doi:10.1016/j.neulet.2005.06.057

Kong, D., Liu, Q., Xu, G., Huang, Z., Luo, N., Huang, Y., et al. (2017). Synergistic Effect of Tanshinone IIA and Mesenchymal Stem Cells on Preventing Learning and Memory Deficits via Anti-apoptosis, Attenuating Tau Phosphorylation and Enhancing the Activity of central Cholinergic System in Vascular Dementia. *Neurosci. Lett.* 637, 175–181. doi:10.1016/j.neulet.2016.11.024

Kong, D., Luo, J., Shi, S., and Huang, Z. (2021). Efficacy of Tanshinone IIA and Mesenchymal Stem Cell Treatment of Learning and Memory Impairment in a Rat Model of Vascular Dementia. *J. Tradit Chin. Med.* 41 (1), 133–139. doi:10.19852/j.cnki.jtcm.2021.01.015

Lai, Z., Zhang, L., Su, J., Cai, D., and Xu, Q. (2016). Sevoflurane Postconditioning Improves Long-Term Learning and Memory of Neonatal Hypoxia-Ischemia

Brain Damage Rats via the PI3K/Akt-mPTP Pathway. *Brain Res.* 1630, 25–37. doi:10.1016/j.brainres.2015.10.050

Leslie, M. (2012). Circadian Rhythms. Sleep Study Suggests Triggers for Diabetes and Obesity. *Science* 336 (6078), 143. doi:10.1126/science.336.6078.143

Lewis, S. (2016). Synaptic Plasticity: Keeping Synapses Quiet. *Nat. Rev. Neurosci.* 17 (8), 465. doi:10.1038/nrn.2016.89

Li, L., Xu, Y., Zhao, M., and Gao, Z. (2020). Neuro-protective Roles of Long Non-coding RNA MALAT1 in Alzheimer's Disease with the Involvement of the microRNA-30b/CNR1 Network and the Following PI3K/AKT Activation. *Exp. Mol. Pathol.* 117, 104545. doi:10.1016/j.yexmp.2020.104545

Li, Q., Shen, L., Wang, Z., Jiang, H. P., and Liu, L. X. (2016). Tanshinone IIA Protects against Myocardial Ischemia Reperfusion Injury by Activating the PI3K/Akt/mTOR Signaling Pathway. *Biomed. Pharmacother.* 84, 106–114. doi:10.1016/j.biopha.2016.09.014

Liao, Y. J., Chen, J. M., Long, J. Y., Zhou, Y. J., Liang, B. Y., and Zhou, Y. (2020). Tanshinone IIA Alleviates CCL2-Induced Leaning Memory and Cognition Impairment in Rats: A Potential Therapeutic Approach for HIV-Associated Neurocognitive Disorder. *Biomed. Res. Int.* 2020, 2702175. doi:10.1155/2020/2702175

Liu, Y., Tong, C., Tang, Y., Cong, P., Liu, Y., Shi, X., et al. (2020). Tanshinone IIA Alleviates Blast-Induced Inflammation, Oxidative Stress and Apoptosis in Mice Partly by Inhibiting the PI3K/Akt/FoxO1 Signaling Pathway. *Free Radic. Biol. Med.* 152, 52–60. doi:10.1016/j.freeradbiomed.2020.02.032

López-Cardona, A. P., Pérez-Cerezales, S., Fernández-González, R., Laguna-Barraza, R., Pericuesta, E., Agirregoitia, N., et al. (2017). CB1 Cannabinoid Receptor Drives Oocyte Maturation and Embryo Development via PI3K/Akt and MAPK Pathways. *FASEB J.* 31 (8), 3372–3382. doi:10.1096/fj.201601382RR

Ma, Y., Liang, L., Zheng, F., Shi, L., Zhong, B., and Xie, W. (2020). Association between Sleep Duration and Cognitive Decline. *JAMA Netw. Open* 3 (9), e2013573. doi:10.1001/jamanetworkopen.2020.13573

McCoy, J. G., and Strecker, R. E. (2011). The Cognitive Cost of Sleep Lost. *Neurobiol. Learn. Mem.* 96 (4), 564–582. doi:10.1016/j.nlm.2011.07.004

Meerlo, P., Mistlberger, R. E., Jacobs, B. L., Heller, H. C., and McGinty, D. (2009). New Neurons in the Adult Brain: the Role of Sleep and Consequences of Sleep Loss. *Sleep Med. Rev.* 13 (3), 187–194. doi:10.1016/j.smrv.2008.07.004

Munagala, R., Aqil, F., Jeyabalan, J., and Gupta, R. C. (2015). Tanshinone IIA Inhibits Viral Oncogene Expression Leading to Apoptosis and Inhibition of Cervical Cancer. *Cancer Lett.* 356 (2 Pt B), 536–546. doi:10.1016/j.canlet.2014.09.037

Nabaee, E., Kesmati, M., Shahriari, A., Khajehpour, L., and Torabi, M. (2018). Cognitive and hippocampus Biochemical Changes Following Sleep Deprivation in the Adult Male Rat. *Biomed. Pharmacother.* 104, 69–76. doi:10.1016/j.biopha.2018.04.197

Ozaita, A., Puighermanal, E., and Maldonado, R. (2007). Regulation of PI3K/Akt/GSK-3 Pathway by Cannabinoids in the Brain. *J. Neurochem.* 102 (4), 1105–1114. doi:10.1111/j.1471-4159.2007.04642.x

Qian, Y. H., Xiao, Q., and Xu, J. (2012). The Protective Effects of Tanshinone IIA on β-amyloid Protein (1-42)-induced Cytotoxicity via Activation of the Bcl-xL Pathway in Neuron. *Brain Res. Bull.* 88 (4), 354–358. doi:10.1016/j.brainresbull.2012.03.007

Rajizadeh, M. A., Esmaeilpour, K., Masoumi-Ardakani, Y., Bejeshk, M. A., Shabani, M., Nakhaee, N., et al. (2018). Voluntary Exercise Impact on Cognitive Impairments in Sleep-Deprived Intact Female Rats. *Physiol. Behav.* 188, 58–66. doi:10.1016/j.physbeh.2017.12.030

Rösner, S., Englbrecht, C., Wehrle, R., Hajak, G., and Soyka, M. (2018). Eszopiclone for Insomnia. *Cochrane Database Syst. Rev.* 10, CD010703. doi:10.1002/14651858.CD010703.pub2

Shen, J. L., Chen, Y. S., Lin, J. Y., Tien, Y. C., Peng, W. H., Kuo, C. H., et al. (2011). Neuron Regeneration and Proliferation Effects of Danshen and Tanshinone IIA. *Evid. Based Complement. Alternat Med.* 2011, 378907. doi:10.1155/2011/378907

Sung, H. J., Choi, S. M., Yoon, Y., and An, K. S. (1999). Tanshinone IIA, an Ingredient of Salvia Miltiorrhiza BUNGE, Induces Apoptosis in Human Leukemia Cell Lines through the Activation of Caspase-3. *Exp. Mol. Med.* 31 (4), 174–178. doi:10.1038/emm.1999.28

Szabó, G. G., Lenkey, N., Holderith, N., Andrási, T., Nusser, Z., and Hájos, N. (2014). Presynaptic Calcium Channel Inhibition Underlies CB_1 Cannabinoid Receptor-Mediated Suppression of GABA Release. *J. Neurosci.* 34 (23), 7958–7963. doi:10.1523/JNEUROSCI.0247-14.2014

Tai, F., Wang, C., Deng, X., Li, R., Guo, Z., Quan, H., et al. (2020). Treadmill Exercise Ameliorates Chronic REM Sleep Deprivation-Induced Anxiety-like Behavior and Cognitive Impairment in C57BL/6J Mice. *Brain Res. Bull.* 164, 198–207. doi:10.1016/j.brainresbull.2020.08.025

Vorhees, C. V., and Williams, M. T. (2006). Morris Water Maze: Procedures for Assessing Spatial and Related Forms of Learning and Memory. *Nat. Protoc.* 1 (2), 848–858. doi:10.1038/nprot.2006.116

Wang, C., Bangdiwala, S. I., Rangarajan, S., Lear, S. A., AlHabib, K. F., Mohan, V., et al. (2019). Association of Estimated Sleep Duration and Naps with Mortality and Cardiovascular Events: a Study of 116 632 People from 21 Countries. *Eur. Heart J.* 40 (20), 1620–1629. doi:10.1093/eurheartj/ehy695

Wang, J., He, X., Chen, W., Zhang, N., Guo, J., Liu, J., et al. (2020). Tanshinone IIA Protects Mice against Atherosclerotic Injury by Activating the TGF-β/PI3K/Akt/eNOS Pathway. *Coron. Artery Dis.* 31 (4), 385–392. doi:10.1097/MCA.0000000000000835

Wang, W., Yang, L., Liu, T., Wang, J., Wen, A., and Ding, Y. (2020). Ellagic Acid Protects Mice against Sleep Deprivation-Induced Memory Impairment and Anxiety by Inhibiting TLR4 and Activating Nrf2. *Aging (Albany NY)* 12 (11), 10457–10472. doi:10.18632/aging.103270

Wang, Z., Zheng, P., Xie, Y., Chen, X., Solowij, N., Green, K., et al. (2021). Cannabidiol Regulates CB1-pSTAT3 Signaling for Neurite Outgrowth, Prolongs Lifespan, and Improves Health Span in *Caenorhabditis elegans* of Aβ Pathology Models. *FASEB J.* 35 (5), e21537. doi:10.1096/fj.202002724R

Whelehan, D. F., Alexander, M., Connelly, T. M., McEvoy, C., and Ridgway, P. F. (2021). Sleepy Surgeons: A Multi-Method Assessment of Sleep Deprivation and Performance in Surgery. *J. Surg. Res.* 268, 145–157. doi:10.1016/j.jss.2021.06.047

Wilt, T. J., MacDonald, R., Brasure, M., Olson, C. M., Carlyle, M., Fuchs, E., et al. (2016). Pharmacologic Treatment of Insomnia Disorder: An Evidence Report for a Clinical Practice Guideline by the American College of Physicians. *Ann. Intern. Med.* 165 (2), 103–112. doi:10.7326/M15-1781

Wu, W. Y., Wang, W. Y., Ma, Y. L., Yan, H., Wang, X. B., Qin, Y. L., et al. (2013). Sodium Tanshinone IIA Silate Inhibits Oxygen-Glucose Deprivation/recovery-Induced Cardiomyocyte Apoptosis via Suppression of the NF-Kb/tnf-α Pathway. *Br. J. Pharmacol.* 169 (5), 1058–1071. doi:10.1111/bph.12185

Wu, X. Q., Chen, J., Yang, L. Q., Jia, T., Wu, Y. X., Ma, W. T., et al. (2013). Impact of 36-hour Sleep Deprivation on Visuo-Motor Coupling Mechanism in Young Soldiers. *Zhongguo Yi Xue Ke Xue Yuan Xue Bao* 35 (4), 439–443. doi:10.3881/j.issn.1000-503X.2013.04.015

Xie, G., Huang, X., Li, H., Wang, P., and Huang, P. (2021). Caffeine-related Effects on Cognitive Performance: Roles of Apoptosis in Rat hippocampus Following Sleep Deprivation. *Biochem. Biophys. Res. Commun.* 534, 632–638. doi:10.1016/j.bbrc.2020.11.029

Xie, J., Liu, J., Liu, H., Liang, S., Lin, M., Gu, Y., et al. (2015). The Antitumor Effect of Tanshinone IIA on Anti-proliferation and Decreasing VEGF/VEGFR2 Expression on the Human Non-small Cell Lung Cancer A549 Cell Line. *Acta Pharm. Sin B* 5 (6), 554–563. doi:10.1016/j.apsb.2015.07.008

Xu, X.-J., Long, J.-B., Jin, K.-Y., Chen, L.-B., Lu, X.-Y., and Fan, X.-H. (2021). Danshen-Chuanxiongqin Injection Attenuates Cerebral Ischemic Stroke by Inhibiting Neuroinflammation via the TLR2/TLR4-MyD88-NF-Kb Pathway in tMCAO Mice. *Chin. J. Nat. Medicines* 19 (10), 772–783. doi:10.1016/S1875-5364(21)60083-3

Zhang, M. Q., Zheng, Y. L., Chen, H., Tu, J. F., Shen, Y., Guo, J. P., et al. (2013). Sodium Tanshinone IIA Sulfonate Protects Rat Myocardium against Ischemia-Reperfusion Injury via Activation of PI3K/Akt/FOXO3A/Bim Pathway. *Acta Pharmacol. Sin* 34 (11), 1386–1396. doi:10.1038/aps.2013.91

Zhang, X., Zhou, Y., and Gu, Y. E. (2019). Tanshinone IIA Induces Apoptosis of Ovarian Cancer Cells *In Vitro* and *In Vivo* through Attenuation of PI3K/AKT/JNK Signaling Pathways. *Oncol. Lett.* 17 (2), 1896–1902. doi:10.3892/ol.2018.9744

Zhao, Y. P., Wang, F., Jiang, W., Liu, J., Liu, B. L., Qi, L. W., et al. (2019). A Mitochondrion-Targeting Tanshinone IIA Derivative Attenuates Myocardial Hypoxia Reoxygenation Injury through a SDH-dependent Antioxidant Mechanism. *J. Drug Target.* 27 (8), 896–902. doi:10.1080/1061186X.2019.1566338

Zhong, S., Ding, W., Sun, L., Lu, Y., Dong, H., Fan, X., et al. (2020). Decoding the Development of the Human hippocampus. *Nature* 577 (7791), 531–536. doi:10.1038/s41586-019-1917-5

Zhou, H., Zhang, Z., Wei, H., Wang, F., Guo, F., Gao, Z., et al. (2013). Activation of STAT3 Is Involved in Neuroprotection by Electroacupuncture Pretreatment via Cannabinoid CB1 Receptors in Rats. *Brain Res.* 1529, 154–164. doi:10.1016/j.brainres.2013.07.006

Zhou, W., Yuan, W. F., Chen, C., Wang, S. M., and Liang, S. W. (2016). Study on Material Base and Action Mechanism of Compound Danshen Dripping Pills for Treatment of Atherosclerosis Based on Modularity Analysis. *J. Ethnopharmacol* 193, 36–44. doi:10.1016/j.jep.2016.07.014

Zhu, J., Liao, S., Zhou, L., and Wan, L. (2017). Tanshinone IIA Attenuates Aβ25-35 -induced Spatial Memory Impairment via Upregulating Receptors for Activated C Kinase1 and Inhibiting Autophagy in hippocampus. *J. Pharm. Pharmacol.* 69 (2), 191–201. doi:10.1111/jphp.12650

Zhu, J., Xu, Y., Ren, G., Hu, X., Wang, C., Yang, Z., et al. (2017). Tanshinone IIA Sodium Sulfonate Regulates Antioxidant System, Inflammation, and Endothelial Dysfunction in Atherosclerosis by Downregulation of CLIC1. *Eur. J. Pharmacol.* 815, 427–436. doi:10.1016/j.ejphar.2017.09.047

Conflict of Interest: The authors declare that the research was conducted in the absence of any commercial or financial relationships that could be construed as a potential conflict of interest.

Publisher's Note: All claims expressed in this article are solely those of the authors and do not necessarily represent those of their affiliated organizations, or those of the publisher, the editors and the reviewers. Any product that may be evaluated in this article, or claim that may be made by its manufacturer, is not guaranteed or endorsed by the publisher.

frontiers in Pharmacology

ORIGINAL RESEARCH
published: 18 March 2022
doi: 10.3389/fphar.2022.864591

Gene Expression Analysis of the Endocannabinoid System in Presymptomatic APP/PS1 Mice

*Laura Vidal-Palencia†, Carla Ramon-Duaso†, Jose Antonio González-Parra and Arnau Busquets-Garcia**

"Cell-Type Mechanisms in Normal and Pathological Behavior" Research Group, IMIM-Hospital del Mar Medical Research Institute, PRBB, Barcelona, Spain

OPEN ACCESS

Edited by:
Paula Morales, Institute of Medical Chemistry (CSIC), Spain

Reviewed by:
Roberto Coccurello, National Research Council (CNR), Italy
Luigi Bellocchio, INSERM U1215 Neurocentre Magendie, France

***Correspondence:**
Arnau Busquets-Garcia
abusquets@imim.es

†These authors have contributed equally to this work and share first authorship

Specialty section:
This article was submitted to Neuropharmacology, a section of the journal Frontiers in Pharmacology

Received: *28 January 2022*
Accepted: *02 March 2022*
Published: *18 March 2022*

Citation:
Vidal-Palencia L, Ramon-Duaso C, González-Parra JA and Busquets-Garcia A (2022) Gene Expression Analysis of the Endocannabinoid System in Presymptomatic APP/PS1 Mice. Front. Pharmacol. 13:864591. doi: 10.3389/fphar.2022.864591

Alzheimer's disease (AD) is the most common type of dementia and neurodegeneration. The actual cause of AD progression is still unknown and no curative treatment is available. Recently, findings in human samples and animal models pointed to the endocannabinoid system (ECS) as a promising therapeutic approach against AD. However, the specific mechanisms by which cannabinoid drugs induce potential beneficial effects are still undefined. For this reason, it is required a full characterization of the ECS at different time points of AD progression considering important factors such as sex or the analysis of different brain regions to improve future cannabinoid-dependent therapies in AD. Thus, the main aim of the present study is to expand our knowledge of the status of the ECS in a presymptomatic period (3 months of age) using the AD mouse model APP/PS1 mice. First, we evaluated different behavioral domains including anxiety, cognitive functions, and social interactions in male and female APP/PS1 mice at 4 months of age. Although a mild working memory impairment was observed in male APP/PS1 mice, in most of the behaviors assessed we found no differences between genotypes. At 3 months of age, we performed a characterization of the ECS in different brain regions of the APP/PS1 mice considering the sex variable. We assessed the expression of the ECS components by quantitative Real-Time Polymerase Chain Reaction in the hippocampus, prefrontal cortex, hypothalamus, olfactory bulb, and cerebellum. Interestingly, gene expression levels of the type-1 and type-2 cannabinoid receptors and the anabolic and catabolic enzymes, differed depending on the brain region and the sex analyzed. For example, CB1R expression levels decreased in both hippocampus and prefrontal cortex of male APP/PS1 mice but increased in female mice. In contrast, CB2R expression was decreased in females, whereas males tended to have higher levels. Overall, our data indicated that the ECS is already altered in APP/PS1 mice at the presymptomatic stage, suggesting that it could be an early event contributing to the pathophysiology of AD or being a potential predictive biomarker.

Keywords: Alzheimer Disease, APP/PS1 mice, brain-region analysis, mouse behaviour, CB1 receptors, sex-dependent

1 INTRODUCTION

Dementia, which is characterized by several behavioral alterations that affect patients' daily life, is one of the greatest global challenges for health in the 21st century (Livingston et al., 2017; Mullane and Williams, 2020). There are many different types of dementia, but Alzheimer's disease (AD) is the most common one (Livingston et al., 2017; Jacobs et al., 2018; Ray and Buggia-Prevot, 2021). AD is a progressive, age-dependent process, characterized by specific molecular hallmarks that accompany the behavioral dysfunctions including cognitive and social alterations (Lane et al., 2018; Avila and Perry, 2020; Coles et al., 2020). The prevalence of AD is increasing as life expectancy is improving, yet the very few treatments available are symptomatic and do not modify disease progression (Livingston et al., 2017; Ray and Buggia-Prevot, 2021).

There are several progressive stages of AD based on the evolution of the behavioral and molecular deficits (Braak and Braak, 1991; Guo et al., 2017; Jack et al., 2018; Jacobs et al., 2018; Dibattista et al., 2020). An interesting period in this progression is the presymptomatic stage, which occurs between the earliest pathogenic event of AD and the appearance of behavioral symptoms such as cognitive deficits. This stage could serve to identify early molecular alterations and novel interventions to delay, detect or counteract AD pathophysiology (Maccarrone et al., 2018; Qin et al., 2020). Indeed, animal models have become a useful tool to characterize possible molecular changes prior to any behavioral alteration (Caselli and Reiman, 2012). Thus, an accurate understanding of AD pathogenesis is required by untangling the possible molecular pathways that lead to behavioral disturbances.

Taking into account the repertoire of possible molecular mechanisms involved in AD, the endocannabinoid system (ECS) has emerged as a potential therapeutic approach against this neurodegenerative disease (Cristino et al., 2020). The ECS is a retrograde neuromodulatory system involved in a plethora of physiological processes such as the regulation of brain homeostasis, neurotransmitter release, and synaptic transmission processes. By doing this, the ECS can modulate some behavioral outputs such as learning and memory, motor coordination, energy balance, and olfactory functions (Castillo et al., 2012; Busquets-Garcia et al., 2015; Cristino et al., 2020). Briefly, this system comprises at least two G protein-coupled receptors (GPCRs), known as type-1 and type-2 cannabinoid receptors (CB1R and CB2R), the lipid-derived signaling molecules anandamide (AEA) and 2-arachidonoylglycerol (2-AG), and the endocannabinoid metabolizing enzymes (Castillo et al., 2012; Busquets-Garcia et al., 2015; Roger, 2015; Cristino et al., 2020).

There are still many unresolved questions aiming at better understanding the association between the ECS and AD. Alterations in the expression and/or activity of the different components of the ECS have been described both in AD animal models and in human patients (Aso and Ferrer, 2014; Berry et al., 2020; Cristino et al., 2020). Interestingly, *in vitro* and *in vivo* pharmacological activation of CB1Rs displayed efficacy in reducing the neurotoxic effects of amyloid-β (Aβ) peptide and in counteracting the cognitive impairment found in AD mouse models (Aso et al., 2012; Haghani et al., 2012). Nevertheless, most of these previous results have focused only on particular brain regions (e.g., hippocampus and/or cortex) (Kalifa et al., 2011; Aso et al., 2012; Haghani et al., 2012; Aso et al., 2016; Aso et al., 2018; Medina-Vera et al., 2020) without providing a full characterization of the ECS in other brain regions, and without taking into account potential sex-dependent differences in most of the studies.

As a thorough characterization of the ECS in AD mouse models is required, the main goal of the present study was to analyze the expression of the main components of the ECS in a presymptomatic stage of AD considering the sex differences and brain region-dependent changes using male and female APP/PS1 mice. This AD mouse model recapitulates major features of amyloid and behavioral pathology of AD in a progressive manner (Aso et al., 2016; Jankowsky and Zheng, 2017; Aso et al., 2018). First, we evaluated behavioral and molecular alterations at early stages, confirming that this is a period with mild behavioral impairments and absence of other neuropathological alterations according to previous literature (Bilkei-Gorzo, 2014; Webster et al., 2014; Jankowsky and Zheng, 2017; Kosel et al., 2020; Peng et al., 2021). Second, we characterized the gene expression of the ECS components in APP/PS1 mice at 3 months of age to identify possible sex- and brain region-dependent molecular dysfunctions at early stages of AD pathology.

2 MATERIALS AND METHODS

2.1 Animals

Male and female APPswe/PS1ΔE9 (APP/PS1) mice on a C57BL/6J background (#034832-JAX, Jackson Laboratory, Bar Harbor, ME, United States) and their wild-type (WT) littermates were used in this project. This double transgenic animal co-express a chimeric mouse/human amyloid precursor protein (Mo/HuAPP695swe), and the human exon-9-deleted variant of PS1 (PS1-dE9) (Bilkei-Gorzo, 2014; Kosel et al., 2020). To generate APP/PS1 and WT littermates, mice were bred in the Barcelona Biomedical Research Park (PRBB) animal facility (Barcelona, Spain) that has full accreditation from the Association for Assessment and Accreditation of Laboratory Animal Care (AAALAC). Animals were grouped-housed and maintained in a temperature (20–24°C) and humidity (40%–70%) controlled condition under a 12 h light/dark cycle and had *ad libitum* access to food and water. Behavioral studies were performed during the dark cycle by trained researchers that were blind to the different experimental conditions. All the procedures are adhered to the guidelines of the European Directive on the protection of animals used for scientific purposes (2010/62/EU) and approved by the Animal Ethics Committee of the PRBB (CEEA-PRBB, ABG-19-0041) and from the Generalitat de Catalunya (10785).

2.1.1 Mouse Genotyping

Mice were identified by ear snips at P21 (weaning), and the tissue collected was used to determine the genotype by PCR

TABLE 1 | Primers used for mouse genotyping.

Primer	Forward primer (5′-3′)	Reverse primer (5′-3′)
APP transgene	AGGACTGACCACTCGACCAG	CGGGGGTCTAGTTCTGCAT
Internal Positive Control	CTAGGCCACAGAATTGAAAGATCT	GTAGGTGGAAATTCTAGCATCATCC

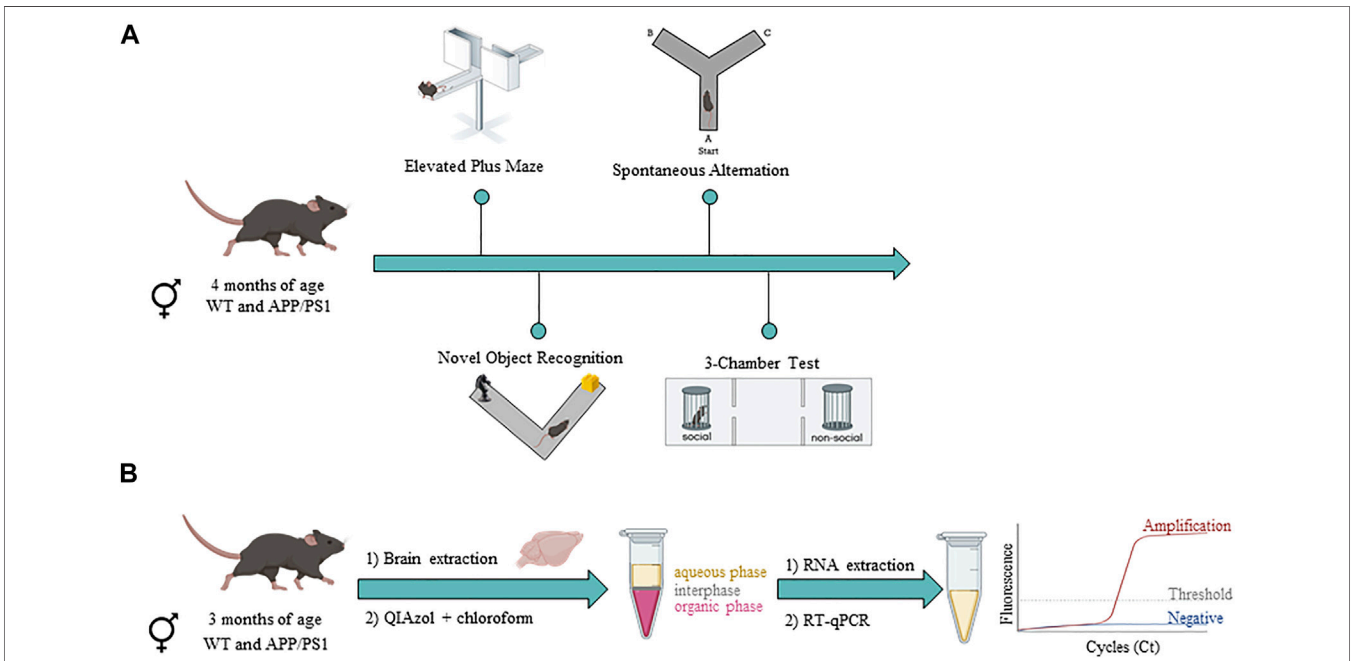

FIGURE 1 | Timeline of experimental procedures in male and female WT and APP/PS1 mouse line. **(A)** Behavioral assessment in WT (male *n* = 9; female *n* = 12) and APP/PS1 (male *n* = 13; female *n* = 11) mice at 4 months of age. **(B)** Gene expression analysis in WT (male *n* = 9–10; female *n* = 9–10) and APP/PS1 (male *n* = 9–10; female *n* = 9–10) mice at 3 months of age. Figure created with BioRender.com.

analysis of isolated genomic DNA (gDNA). Briefly, ear samples were digested with proteinase K (Roche Diagnostics, Mannheim, Germany) and gDNA was isolated and amplified using GoTaq® Master Mix (Promega, Madison, WI, United States). Genotyping primers used to detect the APP transgene were obtained from Jackson Laboratories (see **Table 1** for sequences). Amplification was performed in 40 cycles, each one consisting of 30 s at 94°C, 1 min at 65°C, and 1 min at 72°C. Genotypes were confirmed by running the samples in a 2.5% agarose gel electrophoresis and visualized with a chemiluminescence system (ChemiDoc XRS+, Bio-Rad). When mice were euthanized at the end of the behavioral experiments, genotypes were re-confirmed using a portion of the tail.

2.2 Behavioral Evaluation

To assess potential behavioral phenotypes in male and female APP/PS1 mice compared to their WT littermates, we performed a behavioral battery (**Figure 1A**). Hereby, anxiety-like behavior (Elevated Plus Maze), cognition (Novel Object Recognition test and Spontaneous alternation task), and social behavior (3-chamber test) were assessed at 4 months of age. All experiments were manually analyzed by researchers that were blind to the experimental conditions.

2.2.1 Elevated Plus Maze

Male and female WT and APP/PS1 mice were tested for anxiety-like behavior using the EPM (Walf and Frye, 2007). The EPM consisted of an elevated cross-shaped apparatus with 2 oppositely positioned open arms and 2 enclosed arms delimited by walls 30 cm in height, and a center square (Panlab s.l.u., Barcelona, Spain). The open arms were illuminated by indirect white light at 90 lux while closed arms were set at 15 lux. This behavioral task focuses on the innate response of mice to prefer enclosed and dark spaces and to avoid open and illuminated areas as they perceive it as a possible threatening environment. During the 5-min test, the time spent in open arms were calculated. An entry into an arm was considered when all 4 limbs were positioned within the arm. In general, an anxiety-like state is pointed as an increase in the percentage of time spent in open arms (time open arms*100/300).

2.2.2 Novel Object Recognition Test

Long-term memory was evaluated in male and female WT and APP/PS1 mice using the NOR test in a V-maze apparatus as previously described (Puighermanal et al., 2009; Oliveira da Cruz et al., 2020). This task is based on the fact that animals will explore more time a novel object than a familiar one to satisfy their innate curiosity and exploratory instinct (Webster et al., 2013). The NOR test consisted of three phases of 9 min each separated by 24 h: habituation to an empty maze, familiarization with the presentation of two identical objects, and the test, in which the familiar object is replaced by a novel one. The exploration time of the novel (Tn) and familiar (Tf) objects in the test phase was measured to assess the discrimination index (DI = (Tn − Tf)/(Tn + Tf)) as an outcome of memory recognition. We defined object exploration as when mice oriented themselves towards the object and touch it with the nose.

2.2.3 Y-Maze Spontaneous Alternation Test

Spontaneous alternation activity was calculated as a measure of spatial working memory in male and female WT and APP/PS1 mice. This test was performed in a Y-shaped maze (Panlab s.l.u., Barcelona, Spain) consisting of three arms illuminated at 40 lux and is based on the inherent preference of rodents to explore a new and unvisited arm rather than reexamining a previous investigated one. During the 8 min of the test, the total number of entries and the number of correct alternations were measured as a proxy of spatial working memory. We defined a correct alternation when mice entered into 3 different arms of the maze consecutively and we considered an entry when the 4 paws were within the arm. With these parameters, we calculated the percentage of spontaneous alternation (number of correct alternations/[total number of entries − 2] *100).

2.2.4 Three-Chamber Test

Social behavior can be measured using the three-chamber test. This task was performed in a three-chambered apparatus (Panlab s.l.u., Barcelona, Spain) separated each of the compartments by an open door with an illumination of 70 lux and was divided into two consecutive phases of 10 min each. In the first phase or habituation phase, male and female WT and APP/PS1 mice were allowed to explore the maze with two empty wire cups located at opposite corners of the maze. In the sociability phase, an unfamiliar C57BL/6J mouse (sex- and strain-matched) was placed in one of the wire cups (social cup) while the other remained empty (non-social cup). We measured the interaction time (sniffing) towards the social cup and non-social cup to determine a social index (time sniffing social cup/[time sniffing social cup + time sniffing non-social cup]). An increase in the social index reflects greater sociability.

2.3 Molecular Characterization

2.3.1 Quantitative Real-Time PCR Analysis

To characterize the different components of the ECS, a separate group of male and female WT and APP/PS1 mice were sacrificed by cervical dislocation at 3 months of age and different brain regions were manually dissected and stored at −80°C until use (**Figure 1B**). For each brain region, we applied an extraction method that allowed us to analyze the total RNA fraction. Briefly, brain areas were placed in a Douncer containing 1 ml (for prefrontal cortex, hippocampus, and cerebellum) or 500 µl (for olfactory bulb and hypothalamus) of QIAzol Lysis Reagent. Later, brain homogenates were mixed with 200 µl of chloroform and after centrifugation, we transferred the supernatant (aqueous phase) to a new tube. To isolate total RNA from the aqueous phase, the RNeasy Lipid Tissue Mini Kit (QIAGEN) was used according to the manufacturer's instructions. The quality and concentration of RNA from each sample was determined by a NanoDrop 1000 Spectrophotometer (Thermo Fisher Scientific) and then all were quickly stored at −80°C until use.

For each brain-region sample, complementary DNA (cDNA) was obtained using the High-Capacity cDNA Reverse Transcription Kit (Applied Biosystems, CA, United States) in a 20-µl reaction tube and stored at −20°C until use. Reverse transcriptase reactions were carried out at 25°C for 10 min, 2 h at 37°C, and followed by 5 min at 85°C. All samples were adjusted with autoclaved Milli-Q water to a final cDNA concentration of 30 ng/µl per sample.

We quantified the gene expression levels of *Cnr1* and *Cnr2*, the enzymes related with the endocannabinoid's biosynthesis diacylglycerol lipase-alpha (*Dglα*), diacylglycerol lipase-beta (*Dglβ*), and N-acyl phosphatidylethanolamine phospholipase D (*Napepld*), and the ones related with its hydrolysis which are the monoglyceride lipase (*Mgll*) and fatty acid amide hydrolase (*Faah*). Moreover, we analyzed astroglia and microglia activation (or reactivity) via the measurement of the transcriptional levels of Aldehyde Dehydrogenase 1 L1 (*Aldh1l1* gene) and Signal Transducer and Activator of Transcription 3 (*Stat3* gene) for reactive astrocytes, and Allograft Inflammatory Factor 1 (*Aif1* gene) and chemokine (C-X3-C) Receptor 1 (*Cx3cr1* gene) for microglia reactivity. All samples were tested in triplicate for each qRT-PCR, and β-actin was used as an endogenous housekeeping gene to normalize the transcriptional levels of all target genes analyzed. Primers were designed and verified using the primer-BLAST designing tool (see **Table 2** for sequences).

qRT-PCR was performed in an Optical 384-well plate with a QuantStudio™ 12K Sequence Detection System (Applied Biosystems, CA, United States) consisting of 2 activation stops (50°C for 2 min, then 95°C for 10 min) followed by 45 cycles of melting (95°C for 15 s) and annealing (60 °C for 1 min). The PCR reaction contained PowerUp SYBR Green Master Mix (Applied Biosystems, CA, United States). The comparative cycle threshold (ΔΔCt) method was applied to determine gene expression relative quantification (RQ) and the results were reported as fold change compared with the control group for each sex.

2.4 Statistical Analysis

One-way ANOVA was used to analyze the behavioral assessment at 4 months of age (SPSS Inc., Chicago, IL, United States). For gene expression analysis, data was analyzed considering the genotype differences (male or female APP/PS1 mice compared

TABLE 2 | Primers used for qRT-PCR experiments.

Primers for ECS characterization			
Name	**Gene**	**Forward primer (5′-3′)**	**Reverse primer (5′-3′)**
β-actin	*Actb*	TCCATCATGAAGTGTGACGT	GAGCAATGATCTTGATCTTCAT
Signal transducer and activator of transcription 3 (STAT3)	*Stat3*	ACCCAACAGCCGCCGTAG	CAGACTGGTTGTTTCCATTCAGAT
Aldehyde dehydrogenase 1 family (ALDH1L1)	*Aldh1l1*	GCAGGTACTTCTGGGTTGCT	GGAAGGCACCCAAGGTCAAA
Allograft inflammatory factor 1 (Aif1)	*Aif1*	GGAGACGTTCAGCTACTCTGAC	CATCCACCTCCAATCAGGGC
CX3C chemokine receptor 1 (CX3CR1)	*Cx3cr1*	CGTGAGACTGGGTGAGTGAC	GGACATGGTGAGGTCCTGAG
CB1 receptor (CB1R)	*Cnr1*	GAAGCCTTTCTTCAGCTCGAC	AACAGCACACTGGTGACTCC
CB2 receptor (CB2R)	*Cnr2*	TATGCTGGTTCCCTGCACTG	GAGCGAATCTCTCCACTCCG
Diacylglycerol lipase, alpha (DAGL α)	*Dglα*	AATTTGCGGACTTACAACCTGCGG	TCCCAGACAGGAAAGCCAAGATGT
Diacylglycerol lipase, beta (DAGL β)	*Dglβ*	AGGGATGGATGTGATCCCCA	AACAGTAGCCCGGGGAGTAT
N-acyl phosphatidylethanolamine phospholipase D (NAPE)	*Napepld*	ATGCAGAAATGTGGCTGCGAGAAC	ACCACCTTGGTTCATAAGCTCCGA
Monoglyceride lipase (MAGL)	*Mgll*	TGGCATGGTCCTGATTTCACCTCT	TTCAGCAGCTGTATGCCAAAGCAC
Fatty acid amide hydrolase (FAAH)	*Faah*	TAGCTTGCCAGTATTGACCTGGCT	AGGAAGTAATCGGGAGGTGCCAAA

with its corresponding WT group), and the non-parametric Mann–Whitney test was applied since the data did not follow a normal distribution according to the Shapiro-Wilk test (SPSS Inc., Chicago, IL, United States). In addition, to analyze sex-dependent differences, we calculated the relative difference of fold change in percentage (%) between WT and APP/PS1 mice for males and females and we performed a Mann–Whitney test for statistical analysis. All data are presented as mean ± SEM (Standard Error of the Mean) using the GraphPad Prism 8.0 software (GraphPad Software, La Jolla, CA, United States). Statistical significance was considered at the $p < 0.05$ level.

3 RESULTS

3.1 Behavioral and Molecular Characterization of APP/PS1 Mice at Early Stages

First, we performed a battery of behavioral tests to assess anxiety, cognition and social-related behaviors. In most of the behavioral tasks (i.e., EPM, NOR, or social interaction), no significant differences between genotypes were found (**Figure 2**). In the spontaneous alternation task, one-way ANOVA revealed a significant effect of genotype between groups [$F(1, 19) = 9.8$, $p < 0.005$] in males (**Figure 2E**), but not in females (**Figure 2F**), suggesting that male APP/PS1 mice displayed significant working memory deficits in comparison with their WT littermates. Overall, the lack of behavioral phenotypes in most of the behavioral tasks and the mild cognitive deficit observed in male APP/PS1 indicates that the stage prior to 4 months of age can be considered as a presymptomatic period in APP/PS1 mice, which might be relevant to study potential molecular alterations that could predict or be involved in AD pathophysiology. Then, we decided to study other molecular alterations that have been associated with AD pathology such as astrogliosis or microgliosis. Comparing the hippocampus and prefrontal cortex of male and female WT and APP/PS1 mice at 3 months of age, any significant difference was observed in the ratio between Stat3/Aldh1l1 (*astrogliosis*) or between Aif1/Cx3cr1 (*microgliosis*) gene expression (**Figure 3**). These results suggest a lack of these pathological neuroinflammatory processes associated with AD pathology at early stages in APP/PS1 mice.

3.2 APP/PS1 Mice Present Alterations in the ECS at 3 Months of Age

To characterize the main components of the ECS at a presymptomatic stage, we analyzed the gene expression of different components of the ECS in WT and APP/PS1 mice at 3 months of age.

3.2.1 Cannabinoid Receptors

The statistical analysis of *Cnr1* revealed that male APP/PS1 mice presented lower gene expression levels in both prefrontal cortex ($U = 11.0$, $p < 0.05$) and hippocampus ($U = 10.0$, $p < 0.05$) compared to WT mice. In contrast, higher levels of *Cnr1* were found in the hypothalamus ($U = 11.0$, $p < 0.05$) (**Figure 4A**). In females, APP/PS1 mice showed significantly greater mRNA levels of *Cnr1* in the olfactory bulb ($U = 14.0$, $p < 0.05$), prefrontal cortex ($U = 17.0$, $p < 0.05$), and hypothalamus ($U = 6.0$, $p < 0.05$) than WT mice (**Figure 4B**). Regarding *Cnr2*, male APP/PS1 mice displayed significantly higher levels in cerebellum ($U = 14.0$, $p < 0.05$) compared with WT mice, while no significant differences were found in the rest of the brain-regions analyzed (**Figure 4C**). Female APP/PS1 mice also showed a significant enhancement of *Cnr2* levels in the cerebellum ($U = 17.0$, $p < 0.05$) with respect to WT group, but less expression in the hippocampus ($U = 20.0$, $p < 0.05$) (**Figure 4D**). Additionally, we analyzed the impact of sex on those alterations found in both *Cnr1* and *Cnr2* gene expression levels. Mann-Whitney U test revealed a main effect of sex in the prefrontal cortex ($U = 0.000$, $p < 0.001$) and hippocampus ($U = 0.000$, $p < 0.001$) for *Cnr1* expression (**Figure 5A**), whereas a significant effect of sex was found in the olfactory bulb ($U = 2.0$, $p < 0.001$), hypothalamus ($U = 13.0$, $p < 0.05$) and hippocampus ($U = 4.0$, $p < 0.001$) for *Cnr2* expression (**Figure 5B**). Altogether, these data suggest that the gene expression levels of cannabinoid receptors are already altered in a sex-dependent manner during

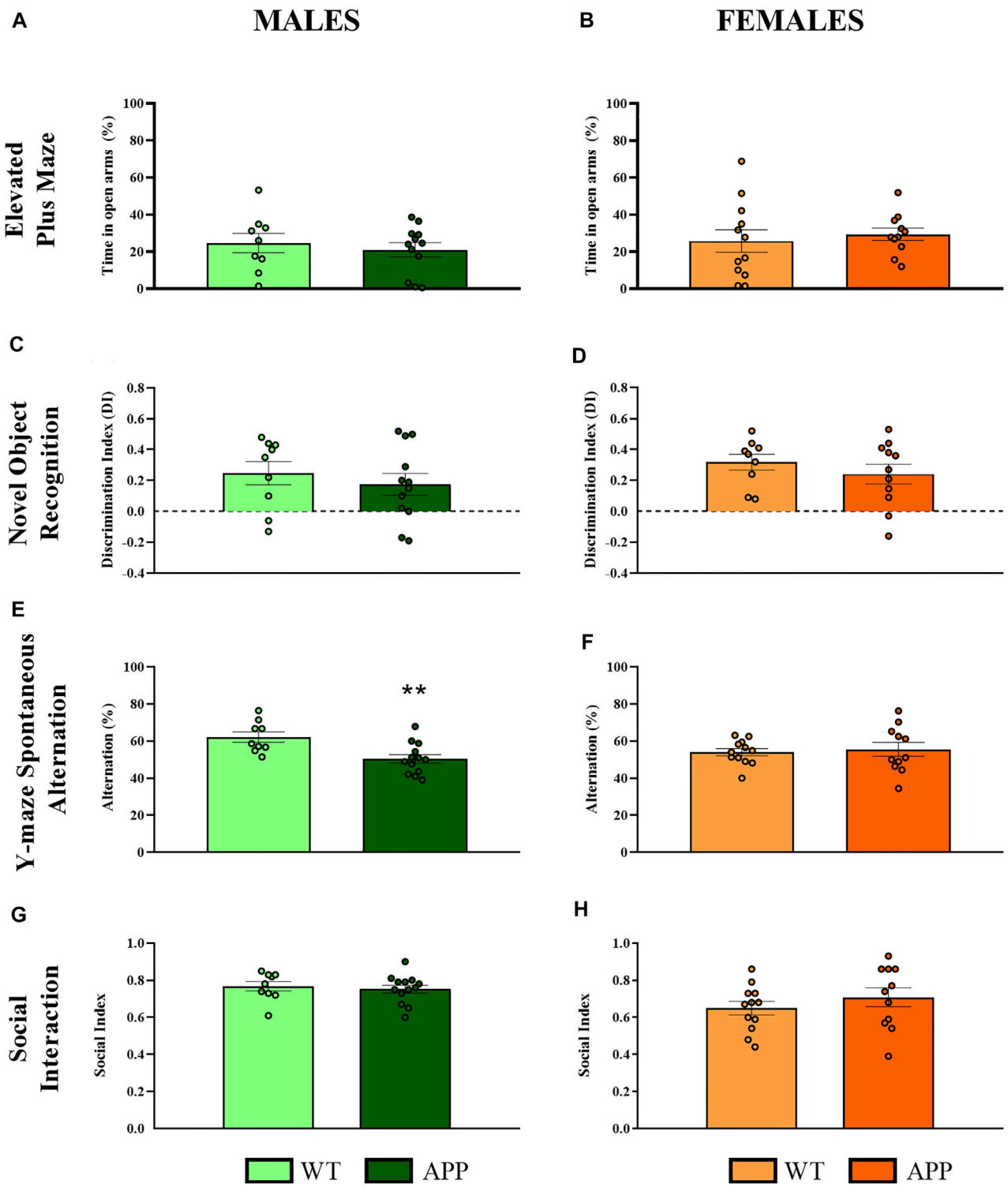

FIGURE 2 | Behavioral evaluation in WT (male *n* = 9; female *n* = 12) and APP/PS1 (male *n* = 13; female *n* = 11) mice at 4 months of age. **(A,B)** Percentage of time spent in open arms to assess anxiety-like behavior in the EPM. **(C,D)** Discrimination index as a long-term memory recognition in the NOR. **(E,F)** Percentage of spontaneous alternation in the Y-maze as a measure of spatial working memory. **(G,H)** Social index as a measure of social interaction using the three-chamber test. Values are the mean ± SEM. $^{**}p < 0.01$ vs. WT group (one-way ANOVA).

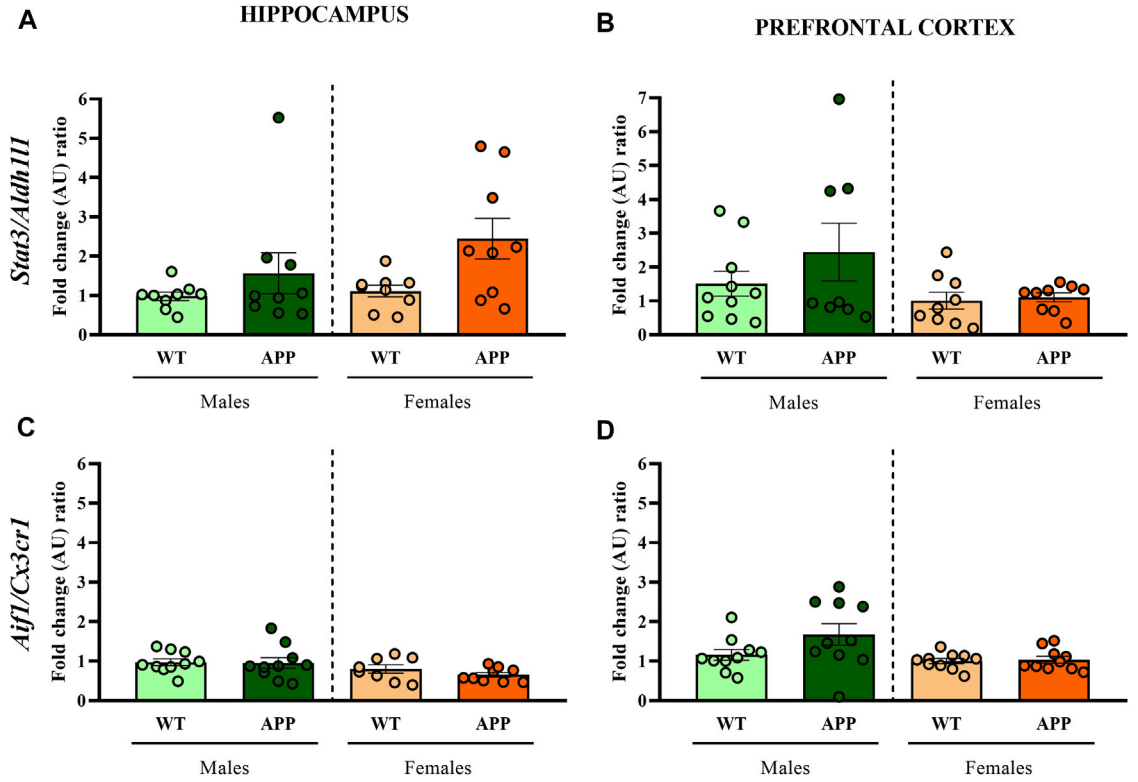

FIGURE 3 | Fold change ratio of *Stat3/Aldh1l1* and *Aif1/Cx3cr1* in WT (male *n* = 10; female *n* = 10) and APP/PS1 (male *n* = 10; female *n* = 10) mice. Fold change ratio of *Stat3/Aldh1l1* (as a proxy for astrogliosis) and *Aif1/Cx3cr1* (as a proxy for microgliosis) in the **(A,C)** hippocampus and **(B,D)** prefrontal cortex respectively, of male and female WT and APP/PS1 mice at 3 months of age. The *X* axis shows the four groups analyzed: male APP/PS1 mice compared with their corresponding WT littermates, and female APP/PS1 mice compared with their control group. The *Y* axis shows the mRNA expression as a fold change ratio. Values are presented as the mean ± SEM; (Mann–Whitney test).

the presymptomatic period of the AD-like disease present in APP/PS1 mice.

3.2.2 2-AG Signaling

In male APP/PS1 mice, *Dglα* expression levels were significantly decreased in both prefrontal cortex (U = 17.0, $p < 0.05$) and cerebellum (U = 11.0, $p < 0.05$) with respect to controls (**Figure 6A**), whereas female APP/PS1 mice only presented this significant reduction in the cerebellum (U = 15.0, $p < 0.05$) (**Figure 6B**). As for *Dglβ*, we did not observe any significant change in male mice (**Figure 6C**), while female APP/PS1 mice presented significantly enhanced expression in the prefrontal cortex (U = 10.0, $p < 0.05$) in comparison with WT mice (**Figure 6D**). The statistical analysis of the *Mgll* expression revealed that male APP/PS1 mice presented significantly higher expression in the hippocampus (U = 16.0, $p < 0.05$) compared to controls (**Figure 6E**). However, female APP/PS1 mice showed a significant reduction in the hippocampus (U = 17.0, $p < 0.05$) and cerebellum (U = 11.0, $p < 0.05$) (**Figure 6F**). These results indicate that the three brain regions where 2-AG signaling could be most affected in APP/PS1 mice at a presymptomatic stage are the prefrontal cortex, hippocampus, and cerebellum.

3.2.3 AEA Signaling

Finally, we analyzed the mRNA levels of *Napepld* and *Faah*, the endocannabinoid metabolizing enzymes of AEA. Concerning *Napepld*, the statistical analysis only detected a significant increase of its expression in the hypothalamus (U = 13.0, $p < 0.05$) of male APP/PS1 mice compared to the WT (**Figure 7A**), with no significant changes in females (**Figure 7B**). On the other hand, we found a significant decrease in the gene expression levels of *Faah* in the prefrontal cortex (U = 16.0, $p < 0.05$) of male APP/PS1 mice compared to the WT (**Figure 7C**). In female APP/PS1 mice, a decrease of *Faah* expression in the prefrontal cortex (U = 15.0, $p < 0.05$) and hippocampus (U = 15.0, $p < 0.05$) was significantly found in relation to its WT littermates (**Figure 7D**). These results point out that the prefrontal cortex, and to a lesser extent the hypothalamus, are the brain regions where most potential differences are found regarding AEA signaling.

4 DISCUSSION

To develop new therapeutic strategies against complex brain diseases such as AD, there is an urgent need to better

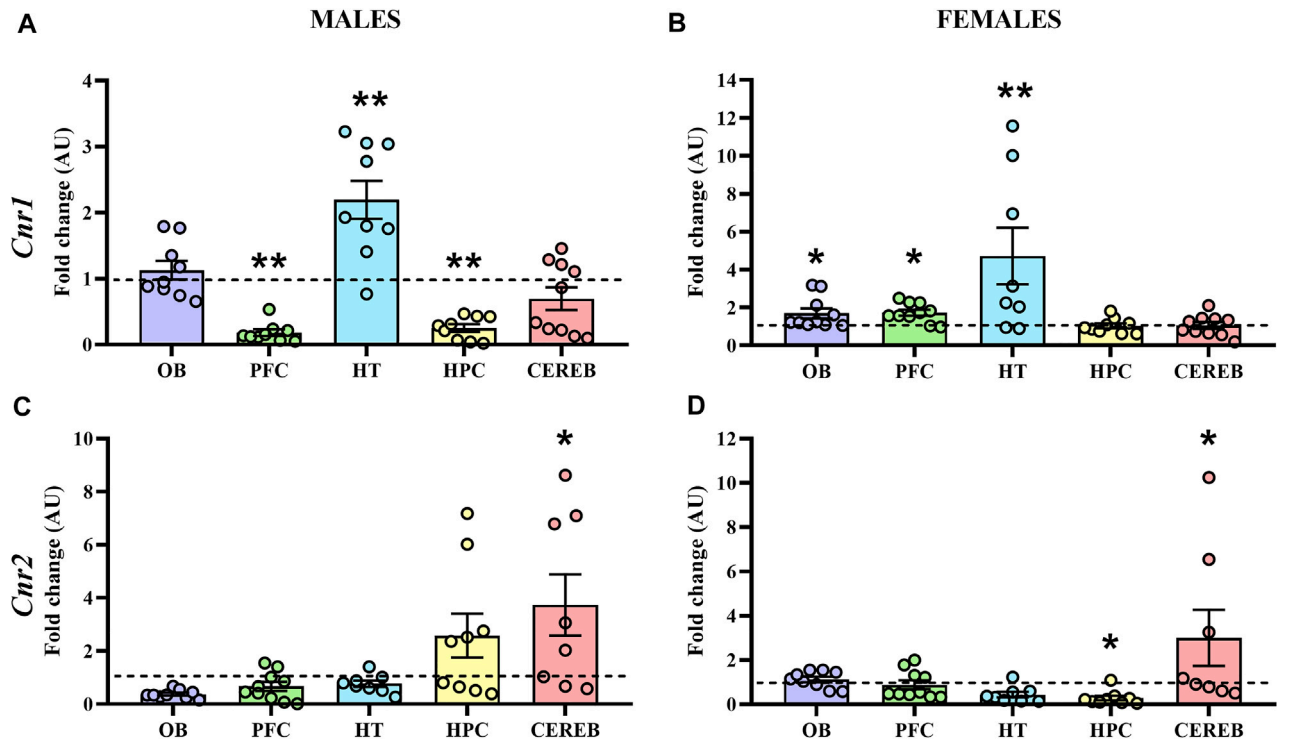

FIGURE 4 | Gene expression of CB1R and CB2R in WT (male *n* = 10; female *n* = 10) and APP/PS1 (male *n* = 10; female *n* = 10) mice at 3 months of age. RT-qPCR assay was performed to analyze the expression of *Cnr1* in **(A)** males and **(B)** females, as well as the expression of *Cnr2* in **(C)** males and **(D)** females. The *X* axis shows the five brain-regions analyzed: olfactory bulb (OB), prefrontal cortex (PFC), hypothalamus (HT), hippocampus (HPC), and cerebellum (CEREB). The *Y* axis shows the mRNA expression as a fold change comparing male and female APP/PS1 mice with its corresponding WT (represented as a dashed line). Values are presented as the mean ± SEM. **p* < 0.05, ***p* < 0.01, vs. WT group (genotype effect); (Mann–Whitney test).

understand their pathophysiology considering potential factors that have been unexplored such as differences between sexes or brain regions. This study, by combining behavioral and gene expression analysis in APP/PS1 mice, aimed to characterize the ECS in male and female WT and APP/PS1 mice during a presymptomatic period (3 months of age) considering the sex variable in the brain regions analyzed. Strikingly, we found interesting differences in the expression levels of several components of the ECS in different brain regions and between sex, which could indicate that the ECS is already altered in APP/PS1 mice at presymptomatic stages becoming an early event contributing to AD pathology or a potential predictive biomarker.

Transgenic AD mouse models are extensively used because they partially mimic the behavioral and molecular dysfunctions found in AD patients. The pathological onset of AD in humans and animal models is generally silent as it takes some time from the first disease-related alteration to the declining of behavioral skills (McKhann et al., 2011). Thus, a better understanding of this presymptomatic period could bring some new therapeutic approaches to slow down disease progression (DeKosky et al., 2008; Holmes et al., 2008; Martin et al., 2008). Indeed, current therapeutic failures might be the result of an intervention that is either too late (i.e., with established symptoms) or that targets processes that are not directly involved in the onset of the disease or progression (Hyman, 2011). However, initiating preventive treatments in presymptomatic periods requires a better comprehension of what distinguishes preclinical AD from normal aging, and which potential alterations are causally associated with the pathophysiology of the disease. Previous studies suggested that the ECS might be a therapeutic target against AD, but it is still unknown whether it is an altered system because of the disease or it is indeed a possible cause of AD pathophysiology. Our gene expression results give some insights on the alterations of the ECS during the presymptomatic period in APP/PS1 mice. These results are quite intriguing as most of them are found in brain areas that are evidently affected in AD such as the hippocampus or prefrontal cortex. Even so, whether changes in mRNA expression have any biological meaning is still a matter of debate (Liu et al., 2016). Therefore, although differences in mRNA(s) of different ECS components can indicate an early alteration of this system in AD, future studies will need to assess protein expression and/or associated metabolites to fully establish the ECS relevance during the AD presymptomatic period. Moreover, it would be also interesting to analyze the specific localization of ECS components in different stages of AD pathology. For instance, it has been already shown

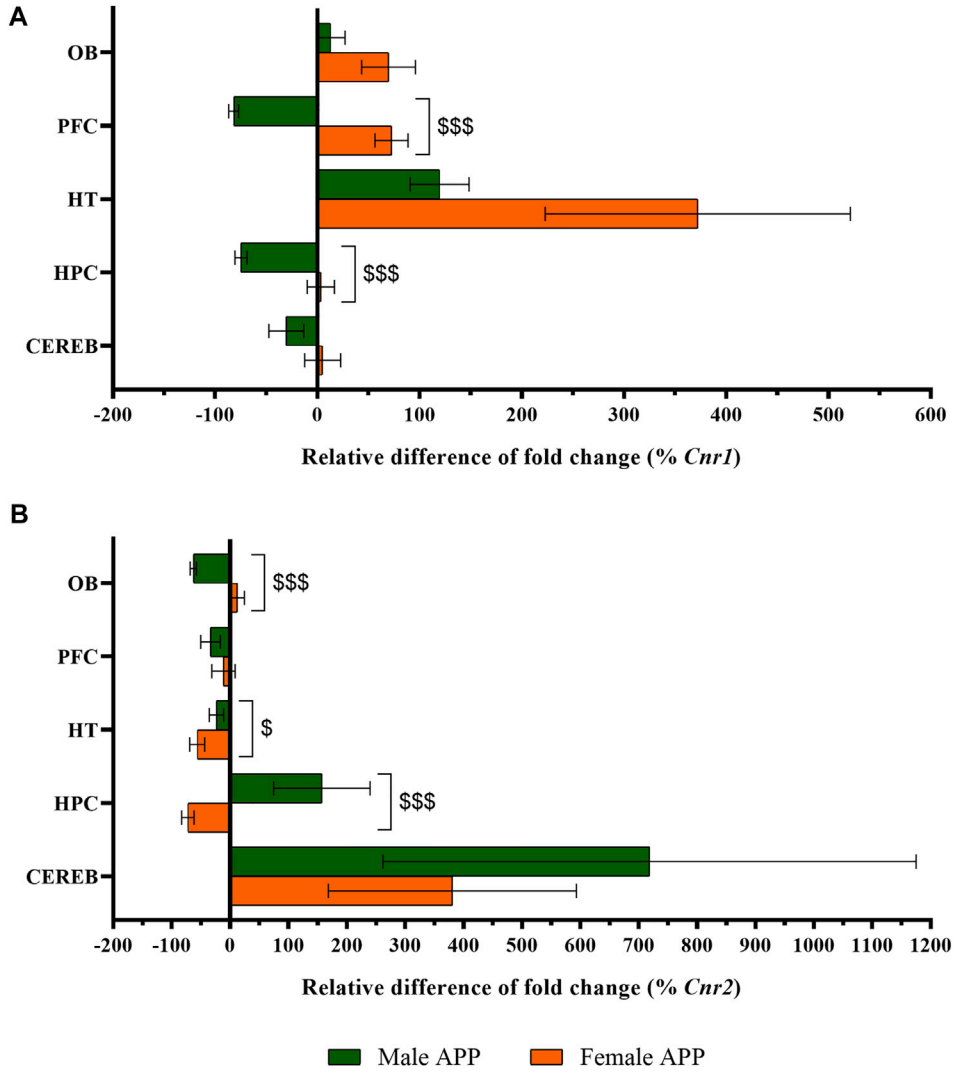

FIGURE 5 | Sex-differences in CB1R and CB2R gene expression between WT and APP/PS1 mice (male $n = 9–10$, female $n = 9–10$). Expression of **(A)** *Cnr1* and **(B)** *Cnr2*. The *X* axis represents the relative difference of the fold change in percentage. The *Y* axis shows the five brain-regions analyzed: olfactory bulb (OB), prefrontal cortex (PFC), hypothalamus (HT), hippocampus (HPC), and cerebellum (CEREB). Values are expressed as mean ± SEM. \$ $p < 0.05$, \$\$\$ $p < 0.001$, vs. female APP mice (sex effect); (Mann–Whitney test).

an altered membrane localization of CB1R in AD pathology, which has an impact on the coupling to its effector proteins and in its inhibitory control (Maccarrone et al., 2018).

A potential sexual dimorphism has been identified in AD (Aso et al., 2012, 2016, 2018; Haghani et al., 2012; Jiao et al., 2016). For example, female mice exhibit higher pathological levels of Aβ40 and Aβ42 peptides and show differences in the nature of their behavioral impairment (Bilkei-Gorzo, 2014; Cheng et al., 2014; Coles et al., 2020). Importantly, analyzing the link between AD and the ECS considering the sex variable is especially interesting as there are sex differences in humans regarding the availability and sensitivity of the ECS (Laurikainen et al., 2019; Wagner, 2016), which could be also present in rodents (Rubino and Parolaro, 2011; Calakos et al., 2017). Therefore, given the relevance of sex in AD, sex-dependent analyses minimize the loss of information that can occur when sex is not included as a variable in previous studies. Notably, our results indicate a sex effect regarding the mRNA levels of cannabinoid receptors that need to be further explored in the future. For example, these sex-dependent differences in CB1R and CB2R gene expression are mostly found in brain regions involved in learning and memory processes, which could be one of the reasons explaining the potential behavioral differences at the later stages between males and females. However, a better characterization of the cognitive skills of APP/PS1 mice at later stages is required in the future to fully link these sex-dependent changes on mRNA expression and the potential behavioral differences.

Our results showed that CB1R mRNA levels are decreased in both hippocampus and prefrontal cortex of APP/PS1 male mice.

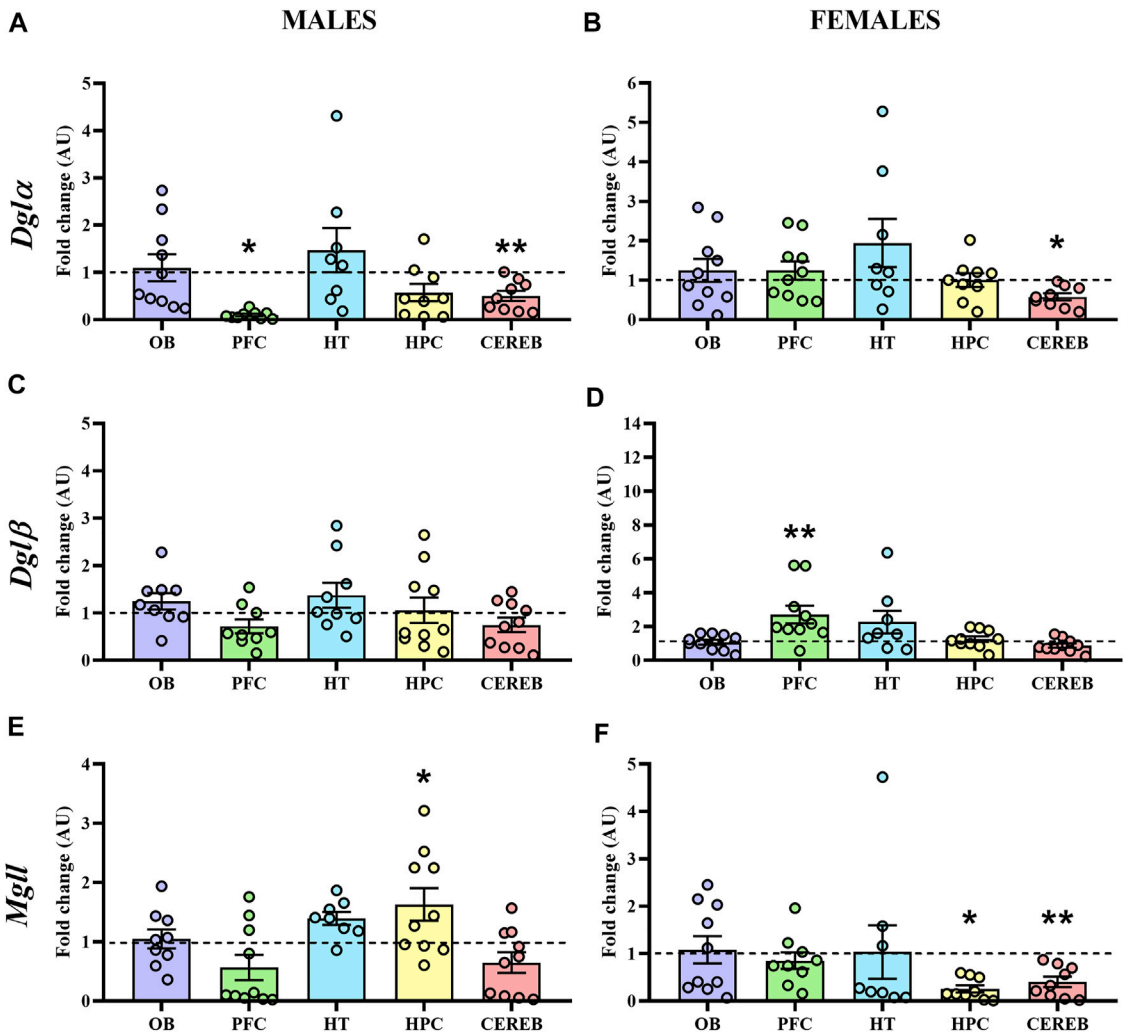

FIGURE 6 | Gene expression of the enzymes involved in the 2-AG signaling in WT (male *n* = 10; female *n* = 10) and APP/PS1 (male *n* = 10; female *n* = 10) mice at 3 months of age. RT-qPCR assay was performed to analyze the expression of *Dglα*, *Dglβ* and *Mgll* in **(A,C,E)** males and **(B,D,F)** females, respectively. The *X* axis shows the five brain-regions analyzed: olfactory bulb (OB), prefrontal cortex (PFC), hypothalamus (HT), hippocampus (HPC), and cerebellum (CEREB). The *Y* axis shows the mRNA expression as a fold change comparing male and female APP/PS1 mice with its corresponding WT (represented as a dashed line). Values are presented as the mean ± SEM. **p* < 0.05, ***p* < 0.01, vs. WT group (genotype effect); (Mann–Whitney test).

Accordingly, alterations in CB1R expression have been reported in both human AD brains (Manuel et al., 2014; Talarico et al., 2018; Berry et al., 2020; Medina-Vera et al., 2020) and AD mouse models (Kalifa et al., 2011; Aso et al., 2012; Bedse et al., 2014a). In contrast, an increase of CB1R immunostaining in the neocortex of APP/PS1 male mice at 3 months (Aso et al., 2012) or unchanged CB1R protein expression in the hippocampus and prefrontal cortex at 2 and 4 months of age in other AD animal models (Bedse et al., 2014b; Maccarrone et al., 2018) have been recently described. Discrepancies between these different studies might be due to the different techniques used, the AD mouse model, the age studied, or the brain region analyzed. In addition, although some studies showed no changes in the expression levels, the specific CB1R localization and signaling could be different between genotypes impacting AD pathology (Maccarrone et al., 2018). Nevertheless, our results indicate sex differences that have not been fully studied in previous studies. In addition, the reduction of CB1R gene expression in cognitive-related brain regions in male APP/PS1 mice at 3 months of age could participate in the cognitive deficits observed in later stages, and the sex differences found could point to distinct alterations in the AD progression of male and female APP/PS1 mice.

CB2R alterations have also been detected in both AD patients' brains (Benito et al., 2003; Solas et al., 2013; Talarico et al., 2018; Berry et al., 2020; Medina-Vera et al., 2020) and AD mouse models (Medina-Vera et al., 2020). The present study revealed a CB2R reduction in the hippocampus of female APP/PS1 mice, while male APP/PS1 mice tended to have higher mRNA levels. Previous studies indicate that CB2R levels are increased specifically in the microglia surrounding Aβ plaques and astrocytes as a result of inflammatory damage (Benito et al., 2003; Ramírez et al., 2005; Solas et al., 2013; Aso et al., 2016;

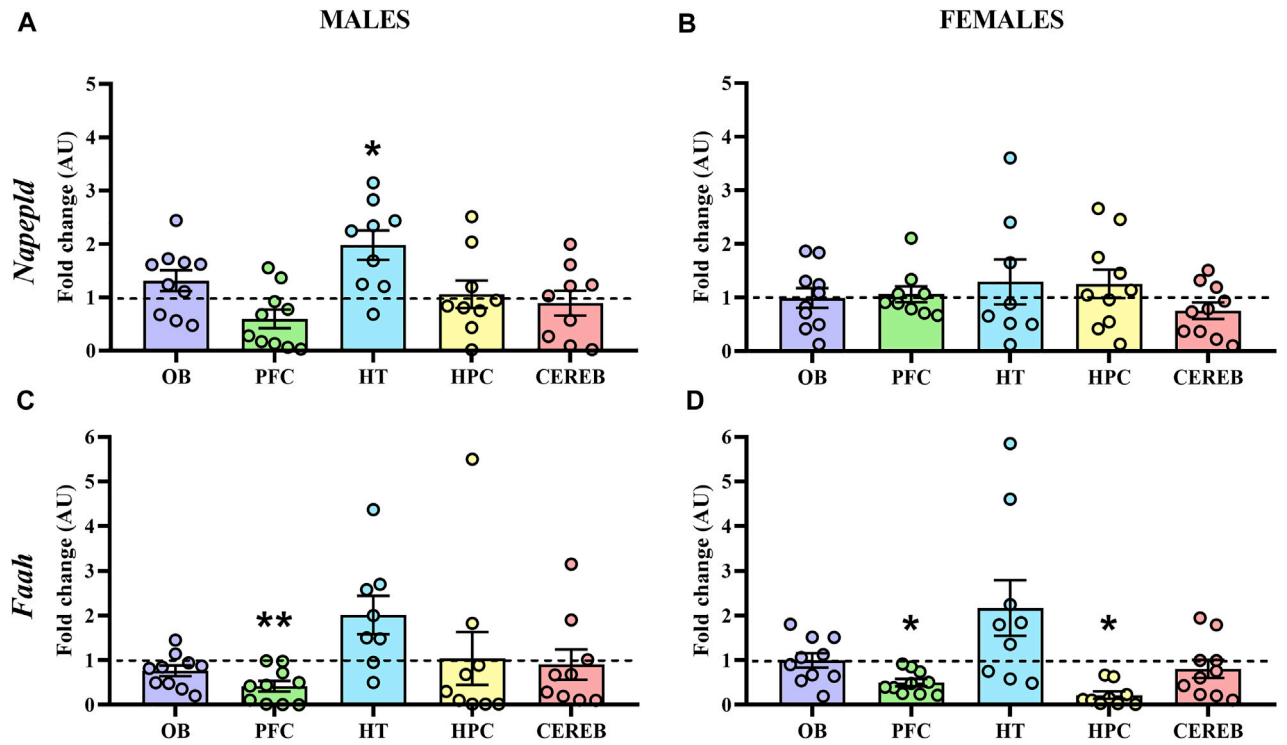

FIGURE 7 | Gene expression of the AEA metabolizing enzymes in WT (male *n* = 10; female *n* = 10) and APP/PS1 (male *n* = 10; female *n* = 10) mice at 3 months of age. RT-qPCR assay was performed to analyze the expression of *Napepld* and *Faah* in **(A,C)** males and **(B,D)** females, respectively. The *X* axis shows the five brain-regions analyzed: olfactory bulb (OB), prefrontal cortex (PFC), hypothalamus (HT), hippocampus (HPC), and cerebellum (CEREB). The *Y* axis shows the mRNA expression as a fold change comparing male and female APP/PS1 mice with its corresponding WT (represented as a dashed line). Values are presented as the mean ± SEM. *$p < 0.05$, **$p < 0.01$, vs. WT group (genotype effect); (Mann–Whitney test).

Medina-Vera et al., 2020), although the distinction between males and females was missing. Considering these facts, an interesting hypothesis to be tested in the future is whether CB2R expression levels could differ between male and female APP/PS1 mice because of a sex-dependent level of neuroinflammation. Our current results show no differences regarding astrogliosis or microgliosis at 3 months of age although the link between CB2R and chronic neuroinflammation has to be further explored both at early and late stages of the disease. In this sense, it has been previously demonstrated that CB2R activation reduces inflammatory processes, facilitates Aβ removal, modulates tau hyperphosphorylation and oxidative stress, and ameliorates cognitive abilities in AD mouse models (Ramírez et al., 2005; Van Der Stelt et al., 2006; Esposito et al., 2007; Fakhfouri et al., 2012; Aso et al., 2013; Wu et al., 2013; Aso et al., 2016; Li et al., 2019). Even though, whether this neuroinflammation could be linked with the differences in cognitive deficits is unknown. Altogether, our results regarding CB1R and CB2R mRNA levels indicate that both cannabinoid receptors could be useful biomarkers or therapeutic targets during the presymptomatic stage of AD.

Alterations of the enzymes involved in the biosynthesis and degradation of endocannabinoids (eCBs) have also been reported in AD patients (Benito et al., 2003; Mulder et al., 2011; Bedse et al., 2014a; Berry et al., 2020) and AD mouse models (Piro et al., 2012; Bedse et al., 2014b; Medina-Vera et al., 2020). In our study, we also analyzed the endocannabinoid anabolic and catabolic enzymes finding the 2-AG signaling altered in the prefrontal cortex and cerebellum, and the AEA signaling altered in the prefrontal cortex and hypothalamus of APP/PS1 mice. These alterations could be linked with alterations in the levels of the eCBs, specifically 2-AG and AEA. Indeed, the possible overproduction of eCBs has already been described in other studies, which could probably reflect an anti-inflammatory response due to neuronal damage (Marsicano et al., 2003; Chen et al., 2012; Medina-Vera et al., 2020). Notably, it has been demonstrated that the inhibition of MAGL or FAAH, which increases the levels of eCBs indirectly, suppresses neuroinflammation and prevents neurodegeneration against harmful insults (Chen et al., 2012; Piro et al., 2012; Ren et al., 2020). Indeed, FAAH deletion in microglial cells decreased inflammatory processes (Tanaka et al., 2019) and specific FAAH inhibitors are able to drive these cells towards an anti-inflammatory phenotype in the context of AD (Grieco et al., 2021). This is relevant as decreased FAAH gene expression levels have been found in the prefrontal cortex and hippocampus of female mice. On the other hand, we speculated that male APP/PS1 at 3 months of age present a 2-AG deficiency in the prefrontal cortex in contrast to female APP/PS1, which likely have higher 2-AG levels in the hippocampus and prefrontal cortex. However, all

these hypotheses should be tested in future projects to better understand the impact of eCBs in AD pathophysiology.

Although the main AD symptoms are associated with cognitive decline, AD is also accompanied by disturbances in energy metabolism (Vercruysse et al., 2018; Zheng et al., 2018), olfactory alterations (Murphy, 2019; Mitrano et al., 2021), and motor coordination deficits (Wagner et al., 2019). Interestingly, the ECS has been involved in all these functions (Busquets-Garcia et al., 2015; Roger, 2015). Thus, we decided to analyze the ECS components in brain regions that have not been extensively studied in the context of AD such as the hypothalamus, the olfactory bulb, and the cerebellum, which are involved in all these functions. Although further research is needed to elucidate the possible link between AD, the ECS, and the metabolic, olfactory, or motor alterations, our results pointed out that alterations of the ECS components in the hypothalamus, olfactory cortex and cerebellum could appear in the early stages of disease progression in the APP/PS1 mice and could contribute to some of the behavioral alterations that are associated with AD (Zheng et al., 2018; Murphy, 2019; Wagner et al., 2019) but have been less studied.

We must acknowledge some open questions arising from our study. Firstly, the presymptomatic stage has been defined as the period without major behavioral alterations and the lack of astrogliosis and microgliosis, which are hallmarks of AD pathology at later stages. Although previous studies show the absence of amyloid plaques at this stage (Garcia-Alloza et al., 2006; Aso et al., 2012), future analysis must extend these evaluations by exploring other neuropathological events such as levels of soluble amyloid peptides or alterations on synaptic loss at these early stages. Secondly, the impact of sex hormones on the sex differences observed was not directly assessed in the present study. The role of sex hormones on neuroscience research in general (Shansky, 2019), or in the cannabinoid field (Fattore and Fratta, 2010) in particular, has been widely discussed. Future experiments must address whether testosterone and/or estrogens are responsible or contribute to mRNA expression levels differences when comparing male and female APP/PS1 mice. In the third place, as discussed above, although clear and interesting findings arise from the present work, future experiments will determine if differences in mRNA levels are accompanied by changes at the protein level and from a functional point of view. In the last place, future experimental designs must aim to causally link these early alterations in the ECS with the later behavioral alterations with especial emphasis on sex-dependent behavioral phenotypes. Although a mild deficit was observed in the spontaneous alternation in male APP/PS1 mice, we considered that we are still in the early stages of AD progression and a behavioral assessment at the later stages is required as all the other behavioral tests show no genotypic differences. Furthermore, with the present results, is difficult to attribute sex-dependent differences in this task as control female mice do not show proper behavior in the Y maze and figuring out the reason is out of the scope of the present project. Although we should consider these aspects in future works, the present study revealed that the main components of the ECS are already altered in APP/PS1 mice at the presymptomatic stage in a sex-dependent manner, suggesting that it could be an early event contributing to AD pathology, or a potential predictive biomarker. Future similar analysis in presymptomatic patients or other mouse models must confirm the early alterations of the ECS in AD. In addition, future experiments can also target the analysis to other interesting receptors or enzymes that have been linked with ECS components forming the so-called "endocannabinoidome."

DATA AVAILABILITY STATEMENT

The original contributions presented in the study are included in the article/Supplementary Material, further inquiries can be directed to the corresponding author.

ETHICS STATEMENT

The animal study was reviewed and approved by the Animal Ethics Committee of the PRBB (CEEA-PRBB, ABG-19-0041) and from the Generalitat de Catalunya (10785).

AUTHOR CONTRIBUTIONS

AB-G conceived the idea of this project. LV-P, JG-P, and CR-D performed behavioral and molecular experiments. LV-P, CR-D, JG-P, and AB-G wrote the manuscript. All co-authors, edited and approved the final version of the manuscript.

FUNDING

This work was supported by a funded project from the Agencia Estatal de Investigación-FEDER (RTI2018-093667-A-100) and the IBRO Return Home Fellowships 2019 received by AB-G. AB-G is a Ramon y Cajal researcher (RYC-2017-21776, funded by MCIN/AEI/10.13039/501100011033 and FSE). LV-P is a FI predoctoral fellow (2021 FI_B 00133) from the Generalitat de Catalunya (AGAUR).

ACKNOWLEDGMENTS

The authors would like to acknowledge the rest of the "Cell-type mechanisms in normal and pathological behavior" Research Group for their support in the experimental procedures and the scientific discussion of the results. In addition, the authors also want to specially thank the "Integrative pharmacology and systems neuroscience" Research Group led by Dr. Rafael de la Torre, the "Applied Metabolomics" Research group led by Dr. Oscar Pozo and Dr. Ester Aso, for the scientific discussion and support related to the project. Finally, we would like to thank the common services from the PRBB that have been fundamental for the present project (PRBB Animal facility and the UPF Genomic Core facility).

REFERENCES

Aso, E., Andrés-Benito, P., Carmona, M., Maldonado, R., and Ferrer, I. (2016). Cannabinoid Receptor 2 Participates in Amyloid-β Processing in a Mouse Model of Alzheimer's Disease but Plays a Minor Role in the Therapeutic Properties of a Cannabis-Based Medicine. *J. Alzheimers Dis.* 51, 489–500. doi:10.3233/JAD-150913

Aso, E., Andrés-Benito, P., and Ferrer, I. (2018). Genetic Deletion of CB1 Cannabinoid Receptors Exacerbates the Alzheimer-like Symptoms in a Transgenic Animal Model. *Biochem. Pharmacol.* 157, 210–216. doi:10.1016/j.bcp.2018.08.007

Aso, E., and Ferrer, I. (2014). Cannabinoids for Treatment of Alzheimer's Disease: Moving toward the Clinic. *Front. Pharmacol.* 5, 37–11. doi:10.3389/fphar.2014.00037

Aso, E., Juvés, S., Maldonado, R., and Ferrer, I. (2013). CB2 Cannabinoid Receptor Agonist Ameliorates Alzheimer-like Phenotype in AβPP/PS1 Mice. *J. Alzheimers Dis.* 35, 847–858. doi:10.3233/JAD-130137

Aso, E., Palomer, E., Juvés, S., Maldonado, R., Muñoz, F. J., and Ferrer, I. (2012). CB1 Agonist ACEA Protects Neurons and Reduces the Cognitive Impairment of AβPP/PS1 Mice. *J. Alzheimers Dis.* 30, 439–459. doi:10.3233/JAD-2012-111862

Avila, J., and Perry, G. (2020). A Multilevel View of the Development of Alzheimer's Disease. *Neuroscience* 457, 283–293. doi:10.1016/j.neuroscience.2020.11.015

Bedse, G., Romano, A., Cianci, S., Lavecchia, A. M., Lorenzo, P., Elphick, M. R., et al. (2014a). Altered Expression of the CB1 Cannabinoid Receptor in the Triple Transgenic Mouse Model of Alzheimer's Disease. *J. Alzheimers Dis.* 40, 701–712. doi:10.3233/JAD-131910

Bedse, G., Romano, A., Lavecchia, A. M., Cassano, T., and Gaetani, S. (2014b). The Role of Endocannabinoid Signaling in the Molecular Mechanisms of Neurodegeneration in Alzheimer's Disease. *J. Alzheimers Dis.* 43, 1115–1136. doi:10.3233/JAD-141635

Benito, C., Núñez, E., Tolón, R. M., Carrier, E. J., Rábano, A., Hillard, C. J., et al. (2003). Cannabinoid CB2 Receptors and Fatty Acid Amide Hydrolase Are Selectively Overexpressed in Neuritic Plaque-Associated Glia in Alzheimer's Disease Brains. *J. Neurosci.* 23, 11136–11141. doi:10.1523/jneurosci.23-35-11136.2003

Berry, A. J., Zubko, O., Reeves, S. J., and Howard, R. J. (2020). Endocannabinoid System Alterations in Alzheimer's Disease: A Systematic Review of Human Studies. *Brain Res.* 1749, 147135. doi:10.1016/j.brainres.2020.147135

Bilkei-Gorzo, A. (2014). Genetic Mouse Models of Brain Ageing and Alzheimer's Disease. *Pharmacol. Ther.* 142, 244–257. doi:10.1016/j.pharmthera.2013.12.009

Braak, H., and Braak, E. (1991). Neuropathological Stageing of Alzheimer-Related Changes. *Acta Neuropathol.* 82, 239–259. doi:10.1007/BF00308809

Busquets-Garcia, A., Desprez, T., Metna-Laurent, M., Bellocchio, L., Marsicano, G., and Soria-Gomez, E. (2015). Dissecting the Cannabinergic Control of Behavior: The where Matters. *BioEssays* 37, 1215–1225. doi:10.1002/bies.201500046

Calakos, K. C., Bhatt, S., Foster, D. W., and Cosgrove, K. P. (2017). Mechanisms Underlying Sex Differences in Cannabis Use. *Curr. Addict. Rep.* 4, 439–453. doi:10.1007/s40429-017-0174-7

Caselli, R. J., and Reiman, E. M. (2012). Characterizing the Preclinical Stages of Alzheimer's Disease and the prospect of Presymptomatic Intervention. *J. Alzheimers Dis.* 33 Suppl 1, S405–S416. doi:10.3233/JAD-2012-129026

Castillo, P. E., Younts, T. J., Chávez, A. E., and Hashimotodani, Y. (2012). Endocannabinoid Signaling and Synaptic Function. *Neuron* 76, 70–81. doi:10.1016/j.neuron.2012.09.020

Chen, R., Zhang, J., Wu, Y., Wang, D., Feng, G., Tang, Y. P., et al. (2012). Monoacylglycerol Lipase Is a Therapeutic Target for Alzheimer's Disease. *Cell Rep* 2, 1329–1339. doi:10.1016/j.celrep.2012.09.030

Cheng, D., Low, J. K., Logge, W., Garner, B., and Karl, T. (2014). Novel Behavioural Characteristics of Female APPSwe/PS1ΔE9 Double Transgenic Mice. *Behav. Brain Res.* 260, 111–118. doi:10.1016/j.bbr.2013.11.046

Coles, M., Watt, G., Kreilaus, F., and Karl, T. (2020). Medium-Dose Chronic Cannabidiol Treatment Reverses Object Recognition Memory Deficits of APPSwe/PS1ΔE9 Transgenic Female Mice. *Front. Pharmacol.* 11, 1–15. doi:10.3389/fphar.2020.587604

Cristino, L., Bisogno, T., and Di Marzo, V. (2020). Cannabinoids and the Expanded Endocannabinoid System in Neurological Disorders. *Nat. Rev. Neurol.* 16, 9–29. doi:10.1038/s41582-019-0284-z

DeKosky, S. T., Williamson, J. D., Fitzpatrick, A. L., Kronmal, R. A., Ives, D. G., Saxton, J. A., et al. (2008). Ginkgo Biloba for Prevention of Dementia: A Randomized Controlled Trial. *JAMA* 300, 2253–2262. doi:10.1001/jama.2008.683

Dibattista, M., Pifferi, S., Menini, A., and Reisert, J. (2020). Alzheimer's Disease: What Can We Learn from the Peripheral Olfactory System? *Front. Neurosci.* 14, 440. doi:10.3389/fnins.2020.00440

Esposito, G., Iuvone, T., Savani, C., Scuderi, C., De Filippis, D., Papa, M., et al. (2007). Opposing Control of Cannabinoid Receptor Stimulation on Amyloid-Beta-Induced Reactive Gliosis: *In Vitro* and *In Vivo* Evidence. *J. Pharmacol. Exp. Ther.* 322, 1144–1152. doi:10.1124/jpet.107.121566

Fakhfouri, G., Ahmadiani, A., Rahimian, R., Grolla, A. A., Moradi, F., and Haeri, A. (2012). WIN55212-2 Attenuates Amyloid-Beta-Induced Neuroinflammation in Rats through Activation of Cannabinoid Receptors and PPAR-γ Pathway. *Neuropharmacology* 63, 653–666. doi:10.1016/j.neuropharm.2012.05.013

Fattore, L., and Fratta, W. (2010). How Important Are Sex Differences in Cannabinoid Action? *Br. J. Pharmacol.* 160, 544–548. doi:10.1111/j.1476-5381.2010.00776.x

Garcia-Alloza, M., Robbins, E. M., Zhang-Nunes, S. X., Purcell, S. M., Betensky, R. A., Raju, S., et al. (2006). Characterization of Amyloid Deposition in the APPswe/PS1dE9 Mouse Model of Alzheimer Disease. *Neurobiol. Dis.* 24, 516–524. doi:10.1016/j.nbd.2006.08.017

Grieco, M., De Caris, M. G., Maggi, E., Armeli, F., Coccurello, R., Bisogno, T., et al. (2021). Fatty Acid Amide Hydrolase (Faah) Inhibition Modulates Amyloid-Beta-Induced Microglia Polarization. *Int. J. Mol. Sci.* 22, 7711. doi:10.3390/ijms22147711

Guo, T., Noble, W., and Hanger, D. P. (2017). Roles of Tau Protein in Health and Disease. *Acta Neuropathol.* 133, 665–704. doi:10.1007/s00401-017-1707-9

Haghani, M., Shabani, M., Javan, M., Motamedi, F., and Janahmadi, M. (2012). CB1 Cannabinoid Receptor Activation Rescues Amyloid β-induced Alterations in Behaviour and Intrinsic Electrophysiological Properties of Rat Hippocampal CA1 Pyramidal Neurones. *Cell. Physiol. Biochem.* 29, 391–406. doi:10.1159/000338494

Holmes, C., Boche, D., Wilkinson, D., Yadegarfar, G., Hopkins, V., Bayer, A., et al. (2008). Long-term Effects of Abeta42 Immunisation in Alzheimer's Disease: Follow-Up of a Randomised, Placebo-Controlled Phase I Trial. *Lancet* 372, 216–223. doi:10.1016/S0140-6736(08)61075-2

Hyman, B. T. (2011). Amyloid-dependent and Amyloid-independent Stages of Alzheimer Disease. *Arch. Neurol.* 68, 1062–1064. doi:10.1001/archneurol.2011.70

Jack, C. R., Bennett, D. A., Blennow, K., Carrillo, M. C., Dunn, B., Haeberlein, S. B., et al. (2018). NIA-AA Research Framework: Toward a Biological Definition of Alzheimer's Disease. *Alzheimers Dement* 14, 535–562. doi:10.1016/j.jalz.2018.02.018

Jacobs, H. I. L., Hopkins, D. A., Mayrhofer, H. C., Bruner, E., Van Leeuwen, F. W., Raaijmakers, W., et al. (2018). The Cerebellum in Alzheimer's Disease: Evaluating its Role in Cognitive Decline. *Brain* 141, 37–47. doi:10.1093/brain/awx194

Jankowsky, J. L., and Zheng, H. (2017). Practical Considerations for Choosing a Mouse Model of Alzheimer's Disease. *Mol. Neurodegener.* 12, 89–22. doi:10.1186/s13024-017-0231-7

Jiao, S. S., Bu, X. L., Liu, Y. H., Liu, C., Wang, Q. H., Shen, L. L., et al. (2016). Sex Dimorphism Profile of Alzheimer's Disease-type Pathologies in an APP/PS1 Mouse Model. *Neurotox. Res.* 29, 256–266. doi:10.1007/s12640-015-9589-x

Kalifa, S., Polston, E. K., Allard, J. S., and Manaye, K. F. (2011). Distribution Patterns of Cannabinoid CB1 Receptors in the hippocampus of APPswe/PS1ΔE9 Double Transgenic Mice. *Brain Res.* 1376, 94–100. doi:10.1016/j.brainres.2010.12.061

Kosel, F., Pelley, J. M. S., and Franklin, T. B. (2020). Behavioural and Psychological Symptoms of Dementia in Mouse Models of Alzheimer's Disease-Related Pathology. *Neurosci. Biobehav. Rev.* 112, 634–647. doi:10.1016/j.neubiorev.2020.02.012

Lane, C. A., Hardy, J., and Schott, J. M. (2018). Alzheimer's Disease. *Eur. J. Neurol.* 25, 59–70. doi:10.1111/ene.13439

Laurikainen, H., Tuominen, L., Tikka, M., Merisaari, H., Armio, R. L., Sormunen, E., et al. (2019). Sex Difference in Brain CB1 Receptor Availability in Man. *Neuroimage* 184, 834–842. doi:10.1016/j.neuroimage.2018.10.013

Li, C., Shi, J., Wang, B., Li, J., and Jia, H. (2019). CB2 Cannabinoid Receptor Agonist Ameliorates Novel Object Recognition but Not Spatial Memory in Transgenic APP/PS1 Mice. *Neurosci. Lett.* 707, 134286. doi:10.1016/j.neulet.2019.134286

Liu, Y., Beyer, A., and Aebersold, R. (2016). On the Dependency of Cellular Protein Levels on mRNA Abundance. *Cell* 165, 535–550. doi:10.1016/j.cell.2016.03.014

Livingston, G., Sommerlad, A., Orgeta, V., Costafreda, S. G., Huntley, J., Ames, D., et al. (2017). Dementia Prevention, Intervention, and Care. *Lancet* 390, 2673–2734. doi:10.1016/S0140-6736(17)31363-6

Maccarrone, M., Totaro, A., Leuti, A., Giacovazzo, G., Scipioni, L., Mango, D., et al. (2018). Early Alteration of Distribution and Activity of Hippocampal Type-1 Cannabinoid Receptor in Alzheimer's Disease-like Mice Overexpressing the Human Mutant Amyloid Precursor Protein. *Pharmacol. Res.* 130, 366–373. doi:10.1016/j.phrs.2018.02.009

Manuel, I., González de San Román, E., Giralt, M. T., Ferrer, I., and Rodríguez-Puertas, R. (2014). Type-1 Cannabinoid Receptor Activity during Alzheimer's Disease Progression. *J. Alzheimers Dis.* 42, 761–766. doi:10.3233/JAD-140492

Marsicano, G., Goodenough, S., Monory, K., Hermann, H., Eder, M., Cannich, A., et al. (2003). CB1 Cannabinoid Receptors and On-Demand Defense against Excitotoxicity. *Science* 302, 84–88. doi:10.1126/science.1088208

Martin, B. K., Martin, B. K., Szekely, C., Brandt, J., Piantadosi, S., Breitner, J. C., et al. (2008). Cognitive Function over Time in the Alzheimer's Disease Anti-inflammatory Prevention Trial (ADAPT): Results of a Randomized, Controlled Trial of Naproxen and Celecoxib. *Arch. Neurol.* 65, 896–905. doi:10.1001/archneur.2008.65.7.nct70006

McKhann, G. M., Knopman, D. S., Chertkow, H., Hyman, B. T., Jack, C. R., Kawas, C. H., et al. (2011). The Diagnosis of Dementia Due to Alzheimer's Disease: Recommendations from the National Institute on Aging-Alzheimer's Association Workgroups on Diagnostic Guidelines for Alzheimer's Disease. *Alzheimers Dement* 7, 263–269. doi:10.1016/j.jalz.2011.03.005

Medina-Vera, D., Rosell-Valle, C., López-Gambero, A. J., Navarro, J. A., Zambrana-Infantes, E. N., Rivera, P., et al. (2020). Imbalance of Endocannabinoid/Lysophosphatidylinositol Receptors Marks the Severity of Alzheimer's Disease in a Preclinical Model: A Therapeutic Opportunity. *Biology* 9, 377–422. doi:10.3390/biology9110377

Mitrano, D. A., Houle, S. E., Pearce, P., Quintanilla, R. M., Lockhart, B. K., Genovese, B. C., et al. (2021). Olfactory Dysfunction in the 3xTg-AD Model of Alzheimer's Disease. *IBRO Neurosci. Rep.* 10, 51–61. doi:10.1016/j.ibneur.2020.12.004

Mulder, J., Zilberter, M., Pasquaré, S. J., Alpár, A., Schulte, G., Ferreira, S. G., et al. (2011). Molecular Reorganization of Endocannabinoid Signalling in Alzheimer's Disease. *Brain* 134, 1041–1060. doi:10.1093/brain/awr046

Mullane, K., and Williams, M. (2020). Alzheimer's Disease beyond Amyloid: Can the Repetitive Failures of Amyloid-Targeted Therapeutics Inform Future Approaches to Dementia Drug Discovery? *Biochem. Pharmacol.* 177, 113945. doi:10.1016/j.bcp.2020.113945

Murphy, C. (2019). Olfactory and Other Sensory Impairments in Alzheimer Disease. *Nat. Rev. Neurol.* 15, 11–24. doi:10.1038/s41582-018-0097-5

Oliveira da Cruz, J. F., Gomis-Gonzalez, M., Maldonado, R., Marsicano, G., Ozaita, A., and Busquets-Garcia, A. (2020). An Alternative Maze to Assess Novel Object Recognition in Mice. *Bio-Protocol* 10, 1–13. doi:10.21769/bioprotoc.3651

Peng, Y. G., Cai, P. J., Hu, J. H., Jiang, J. X., Zhang, J. J., and Liu, K. F. (2021). Altered Corticostriatal Synchronization Associated with Compulsive-like Behavior in APP/PS1 Mice. *Exp. Neurol.* 344, 113805. doi:10.1016/j.expneurol.2021.113805

Piro, J. R., Benjamin, D. I., Duerr, J. M., Pi, Y., Gonzales, C., Wood, K. M., et al. (2012). A Dysregulated Endocannabinoid-Eicosanoid Network Supports Pathogenesis in a Mouse Model of Alzheimer's Disease. *Cel Rep* 1, 617–623. doi:10.1016/j.celrep.2012.05.001

Puighermanal, E., Marsicano, G., Busquets-Garcia, A., Lutz, B., Maldonado, R., and Ozaita, A. (2009). Cannabinoid Modulation of Hippocampal Long-Term Memory Is Mediated by mTOR Signaling. *Nat. Neurosci.* 12, 1152–1158. doi:10.1038/nn.2369

Qin, T., Prins, S., Groeneveld, G. J., Van Westen, G., de Vries, H. E., Wong, Y. C., et al. (2020). Utility of Animal Models to Understand Human Alzheimer's Disease, Using the Mastermind Research Approach to Avoid Unnecessary Further Sacrifices of Animals. *Int. J. Mol. Sci.* 21, 1–27. doi:10.3390/ijms21093158

Ramírez, B. G., Blázquez, C., Gómez del Pulgar, T., Guzmán, M., and De Ceballos, M. L. (2005). Prevention of Alzheimer's Disease Pathology by Cannabinoids: Neuroprotection Mediated by Blockade of Microglial Activation. *J. Neurosci.* 25, 1904–1913. doi:10.1523/JNEUROSCI.4540-04.2005

Ray, W. J., and Buggia-Prevot, V. (2021). Novel Targets for Alzheimer's Disease: A View beyond Amyloid. *Annu. Rev. Med.* 72, 15–28. doi:10.1146/annurev-med-052919-120219

Ren, S. Y., Wang, Z. Z., Zhang, Y., and Chen, N. H. (2020). Potential Application of Endocannabinoid System Agents in Neuropsychiatric and Neurodegenerative Diseases-Focusing on FAAH/MAGL Inhibitors. *Acta Pharmacol. Sin.* 41, 1263–1271. doi:10.1038/s41401-020-0385-7

Roger, G. (2015). Endocannabinoids and Their Pharmacological Actions. *Handb Exp. Pharmacol.* 231, 1–37. doi:10.1007/978-3-319-20825-1

Rubino, T., and Parolaro, D. (2011). Sexually Dimorphic Effects of Cannabinoid Compounds on Emotion and Cognition. *Front. Behav. Neurosci.* 5, 64–65. doi:10.3389/fnbeh.2011.00064

Shansky, R. M. (2019). Are Hormones a "Female Problem" for Animal Research? *Science* 364, 825–826. doi:10.1126/science.aaw7570

Solas, M., Francis, P. T., Franco, R., and Ramirez, M. J. (2013). CB2 Receptor and Amyloid Pathology in Frontal Cortex of Alzheimer's Disease Patients. *Neurobiol. Aging* 34, 805–808. doi:10.1016/j.neurobiolaging.2012.06.005

Talarico, G., Trebbastoni, A., Bruno, G., and de Lena, C. (2018). Modulation of the Cannabinoid System: A New Perspective for the Treatment of the Alzheimer's Disease. *Curr. Neuropharmacol.* 17, 176–183. doi:10.2174/1570159x16666180702144644

Tanaka, M., Yagyu, K., Sackett, S., and Zhang, Y. (2019). Anti-Inflammatory Effects by Pharmacological Inhibition or Knockdown of Fatty Acid Amide Hydrolase in BV2 Microglial Cells. *Cells* 8, 491. doi:10.3390/cells8050491

Van Der Stelt, M., Mazzola, C., Esposito, G., Matias, I., Petrosino, S., De Filippis, D., et al. (2006). Endocannabinoids and Beta-Amyloid-Induced Neurotoxicity *In Vivo*: Effect of Pharmacological Elevation of Endocannabinoid Levels. *Cell. Mol. Life Sci.* 63, 1410–1424. doi:10.1007/s00018-006-6037-3

Vercruysse, P., Vieau, D., Blum, D., Petersén, Å., and Dupuis, L. (2018). Hypothalamic Alterations in Neurodegenerative Diseases and Their Relation to Abnormal Energy Metabolism. *Front. Mol. Neurosci.* 11, 2–16. doi:10.3389/fnmol.2018.00002

Wagner, E. J. (2016). Sex Differences in Cannabinoid-Regulated Biology: A Focus on Energy Homeostasis. *Front. Neuroendocrinol.* 40, 101–109. doi:10.1016/j.yfrne.2016.01.003

Wagner, J. M., Sichler, M. E., Schleicher, E. M., Franke, T. N., Irwin, C., Löw, M. J., et al. (2019). Analysis of Motor Function in the Tg4-42 Mouse Model of Alzheimer's Disease. *Front. Behav. Neurosci.* 13, 107–113. doi:10.3389/fnbeh.2019.00107

Walf, A. A., and Frye, C. A. (2007). The Use of the Elevated Plus Maze as an Assay of Anxiety-Related Behavior in Rodents. *Nat. Protoc.* 2, 322–328. doi:10.1038/nprot.2007.44

Webster, S. J., Bachstetter, A. D., Nelson, P. T., Schmitt, F. A., and Van Eldik, L. J. (2014). Using Mice to Model Alzheimer's Dementia: an Overview of the Clinical Disease and the Preclinical Behavioral Changes in 10 Mouse Models. *Front. Genet.* 5, 88–23. doi:10.3389/fgene.2014.00088

Webster, S. J., Bachstetter, A. D., and Van Eldik, L. J. (2013). Comprehensive Behavioral Characterization of an APP/PS-1 Double Knock-In Mouse Model of Alzheimer's Disease. *Alzheimers Res. Ther.* 5, 28. doi:10.1186/alzrt182

Wu, J., Bie, B., Yang, H., Xu, J. J., Brown, D. L., and Naguib, M. (2013). Activation of the CB2 Receptor System Reverses Amyloid-Induced Memory Deficiency. *Neurobiol. Aging* 34, 791–804. doi:10.1016/j.neurobiolaging.2012.06.011

Zheng, H., Zhou, Q., Du, Y., Li, C., Xu, P., Lin, L., et al. (2018). The Hypothalamus as the Primary Brain Region of Metabolic Abnormalities in APP/PS1 Transgenic Mouse Model of Alzheimer's Disease. *Biochim. Biophys. Acta Mol. Basis Dis.* 1864, 263–273. doi:10.1016/j.bbadis.2017.10.028

Conflict of Interest: The authors declare that the research was conducted in the absence of any commercial or financial relationships that could be construed as a potential conflict of interest.

frontiers in Pharmacology

ORIGINAL RESEARCH
published: 25 March 2022
doi: 10.3389/fphar.2022.861799

Electroacupuncture Reduces Visceral Pain Via Cannabinoid CB2 Receptors in a Mouse Model of Inflammatory Bowel Disease

Hong Zhang[1], Wei He[2], Xue-Fei Hu[1], Yan-Zhen Li[1], Yong-Min Liu[1], Wen-Qiang Ge[1], Ou-Yang Zhanmu[1], Chao Chen[1], Yu-Ye Lan[1], Yang-Shuai Su[2], Xiang-Hong Jing[2], Bing Zhu[2], Hui-Lin Pan[3], Ling-Ling Yu[4] and Man Li[1]**

[1]Department of Neurobiology, School of Basic Medicine, Tongji Medical College, Huazhong University of Science and Technology, Wuhan, China, [2]Research Center of Meridians, Institute of Acupuncture and Moxibustion, China Academy of Chinese Medical Sciences, Beijing, China, [3]Department of Anesthesiology and Perioperative Medicine, The University of Texas MD Anderson Cancer Center, Houston, TX, United States, [4]Institute of Integrated Traditional Chinese and Western Medicine, Tongji Hospital, Tongji Medical College, Huazhong University of Science and Technology, Wuhan, China

OPEN ACCESS

Edited by:
Paula Morales,
Spanish National Research Council (CSIC), Spain

Reviewed by:
ROCÍO GIRÓN,
Rey Juan Carlos University, Spain
Nadine Jagerovic,
Spanish National Research Council (CSIC), Spain

***Correspondence:**
Ling-Ling Yu
527679774@qq.com
Man Li
liman73@mails.tjmu.edu.cn

Specialty section:
This article was submitted to Neuropharmacology, a section of the journal Frontiers in Pharmacology

Received: 25 January 2022
Accepted: 07 March 2022
Published: 25 March 2022

Citation:
Zhang H, He W, Hu X-F, Li Y-Z, Liu Y-M, Ge W-Q, Zhanmu O-Y, Chen C, Lan Y-Y, Su Y-S, Jing X-H, Zhu B, Pan H-L, Yu L-L and Li M (2022) Electroacupuncture Reduces Visceral Pain Via Cannabinoid CB2 Receptors in a Mouse Model of Inflammatory Bowel Disease. Front. Pharmacol. 13:861799. doi: 10.3389/fphar.2022.861799

Inflammatory bowel disease (IBD) results in chronic abdominal pain in patients due to the presence of inflammatory responses in the colon. Electroacupuncture (EA) is effective in alleviating visceral pain and colonic inflammation associated with IBD. Cannabinoid CB2 receptor agonists also reduce colonic inflammation in a mouse model of IBD. However, whether EA reduces visceral pain and colonic inflammation *via* the CB2 receptor remains unknown. Here, we determined the mechanism of the antinociceptive effect of EA in a mouse model of IBD induced by rectal perfusion of 2,4,6-trinitrobenzenesulfonic acid solution (TNBS). EA or sham EA was performed at the bilateral Dachangshu (BL25) point for seven consecutive days. The von Frey and colorectal distension tests were performed to measure mechanical referred pain and visceral pain. Western blotting and immunohistochemistry assays were carried out to determine the expression of IL-1β and iNOS and activation of macrophages in the colon tissues. We found that EA, but not sham EA, attenuated visceral hypersensitivity and promoted activation of CB2 receptors, which in turn inhibited macrophage activation and the expression of IL-1β and iNOS. The effects of EA were blocked by AM630, a specific CB2 receptor antagonist, and by CB2 receptor knockout. Our findings suggest that EA attenuates mechanical allodynia and visceral hypersensitivity associated with IBD by activating CB2 receptors and subsequent inhibition of macrophage activation and expression of IL-1β and iNOS.

Keywords: electroacupunture, inflammatory bowel disease, CB2 receptor, visceral pain, macrophage

PERSPECTIVE

This study presents new evidence about CB2 receptors in the antinociceptive effect of EA in a mouse model of IBD. This work helps the clinicians to understand how EA reduces visceral pain associated with IBD.

INTRODUCTION

Inflammatory bowel disease (IBD) is caused by inflammation in the gastrointestinal tract and is accompanied by chronic abdominal pain, diarrhea, bloody stools, anemia, and weight loss. Crohn's disease and ulcerative colitis represent two forms of IBD and are characterized by uncontrolled activation of the host's intestinal immune cells (Neurath, 2019). The recurrent nature of the inflammatory process in IBD highlights the clinical need for effective anti-inflammatory therapies. However, current therapies have limited efficacy and produce serious side effects. Therefore, there is an urgent need for effective and safety anti-inflammatory treatment options for IBD patients.

EA has been widely used to treat many acute and chronic diseases and is effective for the gastrointestinal system disorders, particularly IBD (Wang et al., 2020). The antinociceptive effect of EA on IBD may involve anti-inflammatory effect *via* the cholinergic reflex (Borovikova et al., 2000) and the hypothalamic-pituitary-adrenal axis (Wei et al., 2019). Other mechanisms may include the opioid system (Kim et al., 2005), the adenosine pathway (Song et al., 2019), and macrophage polarization (Song et al., 2019). It is unclear whether these mechanisms mediate the effect of EA on the inflammatory response in IBD.

The cannabinoid system, which has a long history as a treatment for symptoms associated with gastrointestinal disorders, is involved in the control of tissue homeostasis and important gut functions such as motor and sensory activity, nausea, vomiting, maintenance of epithelial barrier integrity and proper cellular micro-environment (Yuce et al., 2010; Sharkey et al., 2014; Garcia-Arencibia et al., 2019; Scheau et al., 2021). Cannabis or its components act through CB1 and CB2 receptors, which are found throughout the GI system (e.g., liver, pancreas, stomach, small and large intestine) (Naftali et al., 2014). CB2 receptors mainly exist in immune cells, such as plasma cells and macrophages (Wright et al., 2005). In recent years, the role of CB2 receptors in colitis has been increasingly recognized. Administration of the CB2 receptor agonist AM1241 reduces colonic inflammation in a mouse model of TNBS-induced colitis (Storr et al., 2009). This leads to a reasonable speculation that the activation of CB2 receptors may contribute to the amelioration of colitis. Thus, targeting the CB2 receptor may constitute an alternative approach to treat IBD, because this receptor is mainly expressed in immune cells.

In this study, we determined whether EA attenuates mechanical allodynia, visceral hyperalgesia, and intestinal inflammation by activating CB2 receptors in TNBS-treated IBD in mice. Our study suggest that EA reduces pain symptoms in IBD by reducing intestinal inflammation *via* CB2 receptor activation. This new information provides a rationale for using EA to treat visceral pain associated with IBD.

MATERIALS AND METHODS

Animals

Adult male C57 BL/6 mice (8-week-old; 20–25 g, n = 6 mice/group) were purchased from Experimental Animal Center of Tongji Medical College of Huazhong University of Science and Technology. Twenty-four CB2 receptor knockout mice were kindly provided by Dr. Nancy E. Buckley (National Institutes of Health, Bethesda, United States). Animals were individually housed in cages at 22 ± 2°C and a 12 h light/dark cycle and had free access to food and water. All animal procedures were approved by the Institutional Animal Care and Use Committee at Huazhong University of Science and Technology and conformed to the ethical guidelines of the International Association for the Study of Pain (IASP).

IBD Model

The IBD model was induced by slow intra-rectal instillation of TNBS (Sigma-Aldrich, St. Louis, MO, United States) solution (50 µl of 5% w/v TNBS mixed with 50 µl absolute ethanol) into the lumen of the colon in anesthetized mice, as previously reported (Hou et al., 2019). An experimental design timeline is presented in **Figure 1A**.

Nociceptive Behavioral Tests

Animal behavior tests were performed from 9:00 a.m. to 12:00 p.m. Mice were first habituated to the test environment for 30 min. The mechanical thresholds were tested for 3 days before TNBS injection and the average value of the 3-day tests was calculated as the baseline threshold. After TNBS injection, the nociceptive thresholds were tested once a day for seven consecutive days. Then a series of calibrated von Frey filaments (0.02, 0.04, 0.07, 0.16, 0.4, 0.6, 1.0 and 1.4 g, Wood Dale, United States) were applied perpendicularly to the mid-plantar surface of the left hind paw to bend the filament for 6s. The mechanical threshold of mice was measured by using the "up and down" method (Chaplan et al., 1994) and the test of withdrawal threshold was repeated two times in each mouse, and the mean value was calculated. Paw withdrawal or licking feet was considered as a pain-like response.

Visceral hyperalgesia measurements were made on the seventh day after TNBS injection. The colorectal distension (CRD) method was used to observe the abdominal withdrawal reflex scores (AWRs) of mice to assess visceral hyperalgesia. The CRD test was performed in a step-by-step compression mode (20/40/60/80 mmHg). Each pressure value was measured twice, each test lasting 30 s, with an interval of 4 min, AWRs were recorded and averaged. The scoring criteria were the same as the Al-Chaer's method (Bao et al., 2019): no behavioral response to CRD was rated as 0, short pauses in head or body movements during stimulation was rated as 1; abdominal muscle contraction during stimulation was rated as 2; abdominal lifting was rated as 3; and body arch, pelvic cavity or scrotum lifting was rated as 4.

EA Treatment

EA treatment started on day 1 after TNBS injection. Before EA, mice were gently immobilized using homemade clothes (10 × 10 cm) and their limbs were pulled out through holes in the clothes. A pair of stainless steel acupuncture needles (0.25 mm × 13 mm, Beijing Zhongyan Taihe Medical Instruments Co., Ltd., China) were inserted into a depth of 4 mm into bilateral sides of Dachangshu (BL25, the waist of the fourth lumbar vertebra at about 7 mm bilaterally to midline) acupoint (Wang et al., 2015). The handles of these needles were connected to Han's Acupoint Nerve Stimulator (LH202, Huawei Co., Ltd., Beijing, China) with a frequency of 2 Hz and intensity of 1 mA for 30 min, once per day for seven consecutive days. In this study, for sham EA group, real acupuncture needles were shallowly inserted into nonacupoint locations (0.3–0.5 mm), so as to reduce the physiological effect of sham acupuncture group. The animals remained awake and motionless during the treatment and showed no evident signs of distress. The control group and TNBS group were only manipulated with self-made clothes without other treatment.

Drug Administration

The CB2 receptor inhibitor AM630 (Sigma-Aldrich, St. Louis, United States) was dissolved in a vehicle consisting of 1:2:7 ratio of dimethylsulfoxide (DMSO), Tween 80 and normal saline as previously described (Liu et al., 2021). Mice were intraperitoneally administrated with 100 μl of AM630 at 5 mg/kg body weight (Lopes et al., 2020) or vehicle 30 min before EA treatment, every day for 7 days.

Experimental Design

To test the EA's effect, C57BL/6 mice were randomly divided into Control (vehicle of TNBS), TNBS, TNBS plus EA (TNBS + EA) or TNBS plus sham EA (TNBS + sham EA) groups. To determine the role of CB2 receptor in EA in the treatment of IBD-associated visceral hypersensitivity and inflammation, C57BL/6 mice were randomly divided into Control + DMSO (vehicle of AM630, sterilized DMSO), TNBS + DMSO, TNBS + EA + DMSO, TNBS + AM630 + EA groups; CB2 receptor knockout mice were randomly divided into Control (vehicle of TNBS), TNBS, TNBS plus EA (TNBS + EA) or TNBS plus sham EA (TNBS + sham EA) groups.

Western Blotting

Mice were anaesthetized with 3% isoflurane, and their colon tissues were immediately excised. Tissues were initially placed on ice and stored at −80°C, pending protein extraction. The tissues were then lysed by adding 40 mg/ml RIPA lysis buffer (Biosharp, China) and 40 mg/ml phenylmethyl sulfonyl fluoride (Biosharp, China) to the samples for 30 min. The lysate was collected and centrifuged at 12,000 rpm for 15 min at 4°C, and the protein contents were quantified by using the Enhanced BCA Protein Assay Kit (Beyotime Biotechnology, China). The protein (40 mg) was denatured in loading buffer at 95°C for 5 min, separated on a 10%/12% glycine-SDS-PAGE gel (10%: CB2 receptor, iNOS; 12%: IL-1β) (Beyotime Biotechnology, China), and then transferred onto a PVDF membrane (Millipore Immobilon-P, United States). The membranes were blocked with 5% non-fat milk at room temperature for 1 h, followed by primary antibodies at 4°C overnight: anti-CB2 receptor rabbit antibody (diluted 1/500; Abcam), anti-Turblin mouse antibody (diluted 1/2000; Santa Cruz Technology), anti-iNOS rabbit antibody (diluted 1/1000; Abcam), and anti-IL-1β rabbit antibody (diluted 1/1000, Abcam). Then, the membranes were incubated with IgG (diluted 1/20,000, Abcam). The signals were developed using Super Signal West Pico chemiluminescent substrate (Thermo Scientific, United States). The densitometric analysis of the protein band images was performed using ImageJ software (NIH, Bethesda, MD, United States).

Histopathology Assessment

For histological examination, the colonic tissue was dehydrated with 4% paraformaldehyde and then paraffin embedded. Tissue sections (4 μm) were de-paffinized in xylene and stained with hematoxylin and eosin (H&E) to assess intestinal inflammation. H&E staining was scored by a blinded observer using a previously described method (Kim et al., 2012): crypt architecture (normal is 0 point, loss of crypts is 3 point), inflammatory cell infiltration (normal is 0 point, dense inflammatory infiltrate is 3 point), muscle thickening (base of crypt sits on the muscularis mucosae is 0 point, marked muscle thickening present is 3 point), goblet cell depletion (absent is 0 point, present is 3 point) and crypt abscess (absent is 0 point, present is one point).

Immunofluorescence Labeling

Mice were deeply anesthetized by intraperitoneal injection of 6% chloral hydrate. The heart was perfused with 0.9% normal saline (40°C) and then fixed with 4% paraformaldehyde (4°C) for 12 h. Colon tissues were dehydrated in 20% sucrose solution (12 h) and 30% sucrose solution (12 h) prepared with 0.1 M PBS buffer. Transverse section of the colon was cut to 15 μm thick using a cryostat. The sections were pasted on gelatin-coated glass slides and dried overnight. The slides were washed in 0.01 M PBS for four times in PBS for 5 min, and blocked for 1 h with 5% donkey serum and 0.3% triton X100 in PBS and then incubated with the following primary antibodies at 4°C overnight: mouse anti-CD68 (1:200; Abcam, Cambrige, United Kingdom, #ab955) for identification of macrophages, rabbit anti-iNOS (1:200; Abcam, #ab178945) and rabbit anti-CB2 receptor (1:200; Abcam, #ab3561). Subsequently, sections were rinsed four times in PBS for 5 min and incubated with corresponding secondary antibodies at room temperature for 1 h: donkey anti-mouse IgG conjugated with Dylight 488 (1:400) or donkey anti-rabbit IgG conjugated with Dylight 594 (1:400). The slides were washed 4 times with 0.01 M PBST for 5 min each time. Sections were washed three times in PBS and then incubated with Hoechst for the nucleus staining for 5 min. Lastly, sections were washed three times in PBS for 5 min and then cover-slipped. The tissue sections were viewed under a laser confocal microscope (FV500-IX7, Olympus, Japan).

The images were analyzed using ImageJ software (NIH, Bethesda, United States).

Statistical Analysis

The results were presented as the mean ± SEM. Two-way repeated measures ANOVA followed by Bonferroni's *post hoc* test was used to compare the mechanical pain threshold and AWRs in each group. One-way ANOVA and Newman-Keuls *post hoc* test were used in the analysis of biochemical data. SPSS 23.0 was used for the data analysis. p value of less than 0.05 was considered statistically significant.

RESULTS

EA Alleviates Visceral Hyperalgesia, Mechanical Allodynia and Intestinal Pathology Induced by TNBS

We first established a mouse model of TNBS-induced colitis. In the von Frey test, a measure of referred pain, the withdrawal threshold was significantly decreased at the second day after TNBS injection, and this effect lasted at least 7 days ($p < 0.05$, **Figure 1C**). In the CRD test, TNBS-treated mice exhibited a significant decrease in AWRs ($p < 0.05$, **Figure 1D**).

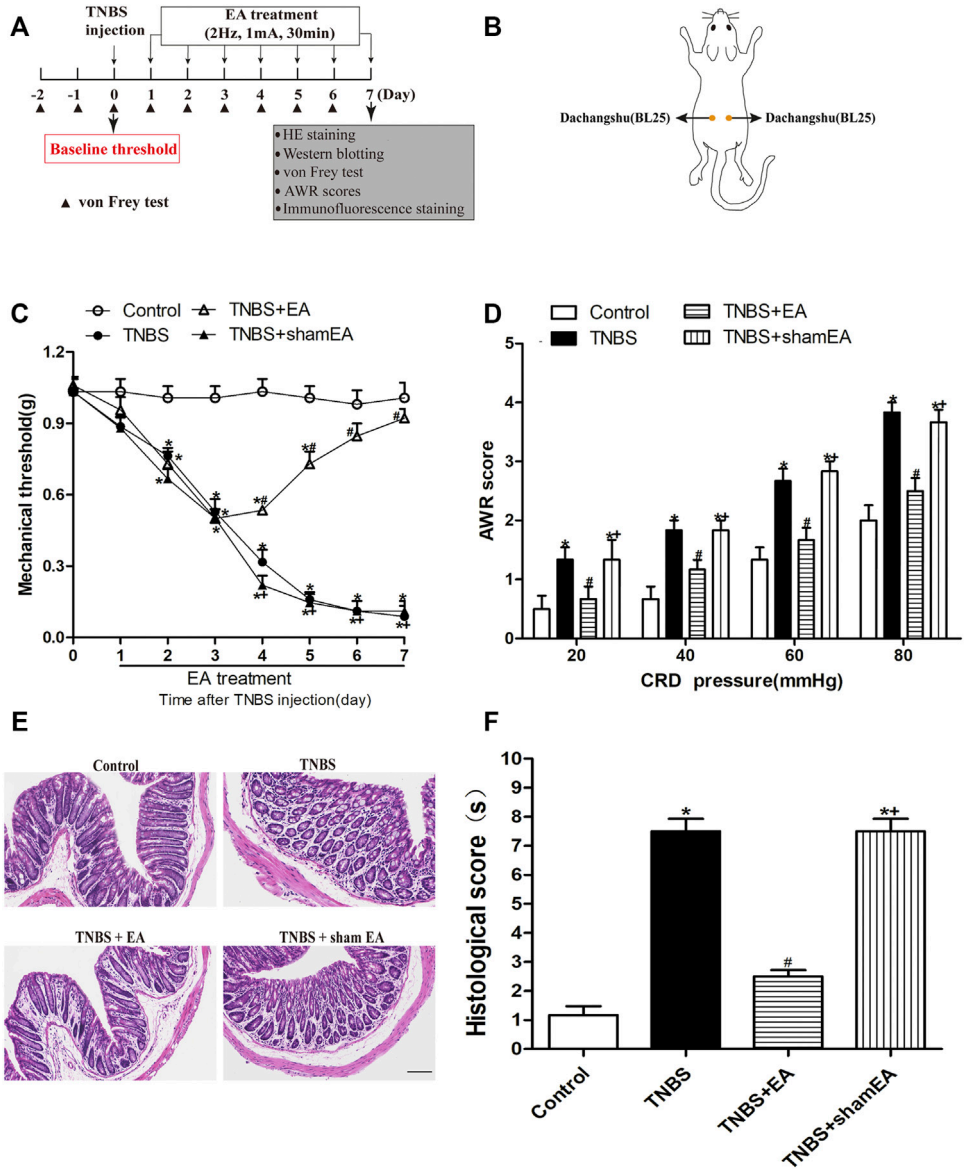

FIGURE 1 | EA attenuates TNBS-induced mechanical allodynia, visceral hyperalgesia and inflammatory in the intestine. **(A)** Experimental flowchart. **(B)** Schematic show the lumbodorsal BL25 acupoint. **(C)** Time course of the effect of BL25 EA on mechanical withdrawal threshold of the hind paws of TNBS-treated mice. **(D)** AWR scores of vehicle-treated and TNBS-treated mice on day 7 after vehicle or TNBS treatment. **(E)** Representative H&E staining of the colon tissue sections. Scale bar, 200 μm. **(F)** Histological score in each group ($n = 6$ per group). *$p < 0.05$ versus with Control group, #$p < 0.05$ versus with TNBS group, +$p < 0.05$ versus with TNBS + EA group.

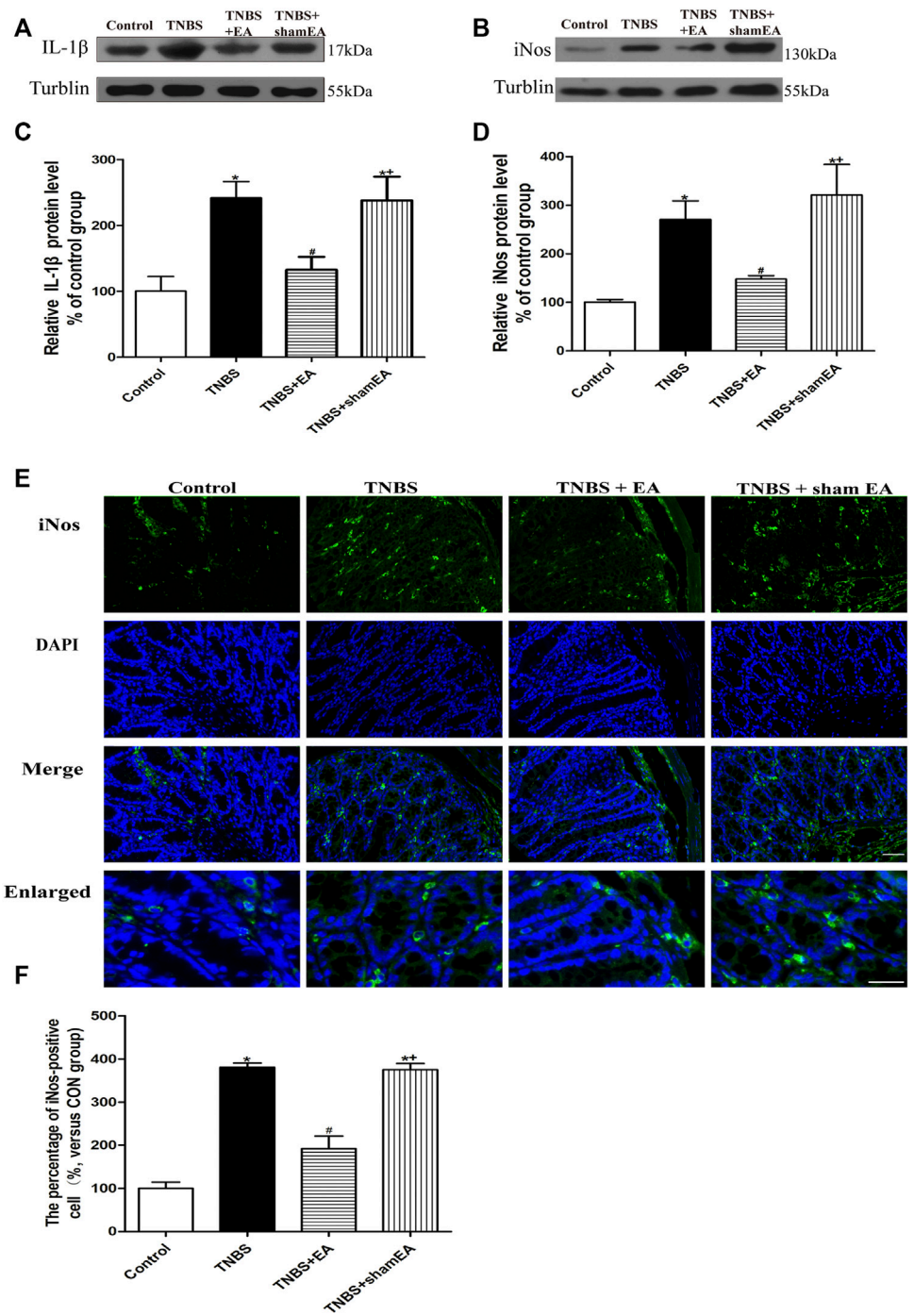

FIGURE 2 | EA inhibits inflammatory responses in TNBS-treated mice. **(A–E)** Representative western blot images show the protein levels of IL-1β **(A)** and iNOS **(B)** in the colon tissues. Summary data show the relative protein level of IL-1β **(C)** and iNOS **(D)** in the colon tissues. **(E)** Representative images of immunofluorescence staining in which cell nuclei were labeled with DAPI (blue) and anti-iNOS antibody (green) in the colon tissues. **(F)** Summary data showing the number of iNOS-positive cells per observation field. Data are expressed as mean ± SEM ($n = 6$ per group). Scale bar, 50 μm *$p < 0.05$ versus with Control group, #$p < 0.05$ versus with TNBS group, +$p < 0.05$ versus with TNBS + EA group.

To examine the role of EA on TNBS-induced nociceptive responses, EA was performed at BL25 acupoints for 30 min on days 1–7 after TNBS injection. EA, but not sham EA, reduced mechanical allodynia measured on days 4–7 and visceral hyperalgesia measured on the seventh day. No significant differences in behavioral responses were observed at any time among C57BL/6 mice treated with Control or Control + EA ($p > 0.05$, **Figures 1C,D**).

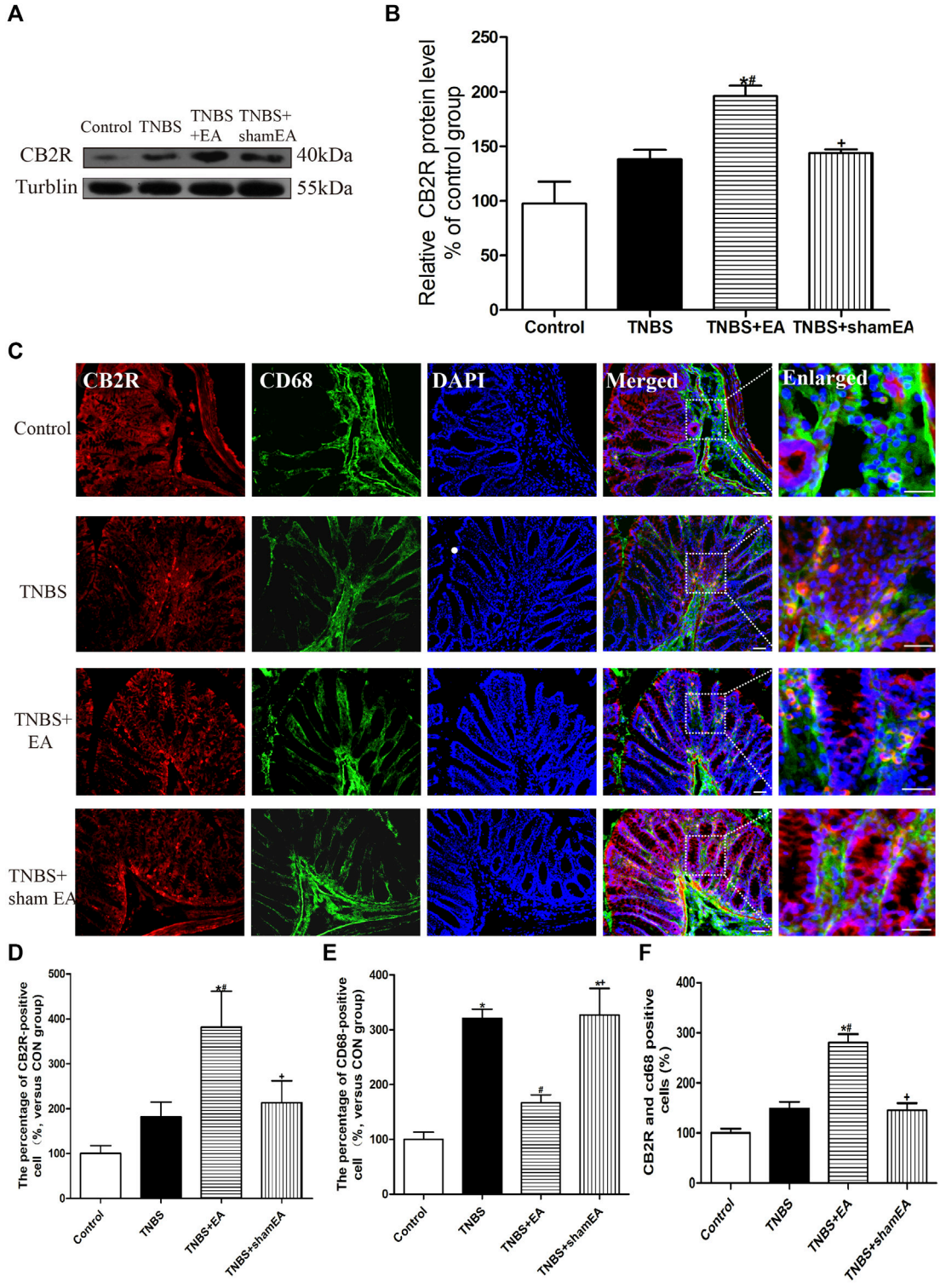

FIGURE 3 | EA increased CB2 receptor activation in macrophages in the colon tissues. **(A)** Representative western blot images show the protein level of CB2 receptors in the colon tissues. **(B)** Summary data show the relative protein level of CB2 receptors in the colon tissues. **(C)** Representative images of immunofluorescence staining using DAPI (blue), anti-CD68 antibody (macrophages) (green) and CB2 receptor antibody (red) in the colon tissues. Summary of the number of CB2 receptor- **(D)** and $CD68^{-}$ **(E)** positive cells per observation field. **(F)** Summary data show the percentage of double-labeled cells in the colon tissues. Data are expressed as mean ± SEM ($n = 6$ per group). Merged, scale bar, 50 μm; Enlarged, scale bar, 50 μm *$p < 0.05$ versus with Control group, #$p < 0.05$ versus with TNBS group, +$p < 0.05$ versus with TNBS + EA group.

As shown in **Figure 1E**, the TNBS group clearly exhibited an acute inflammatory response with mucosal erosion, congestion, crypt reduction, neutrophil cell infiltrates and goblet cells disrupted destruction compared to the Control group. Compared with the TNBS group, EA showed a significant improvement in mucosal inflammatory, but not by sham EA (**Figure 1F**). These results suggest that EA at BL25 is effective in reducing the nociceptive and inflammatory responses in the colon induced by TNBS.

EA Inhibits the Expression of IL-1β and iNOS in Inflamed Colon Tissues of TNBS-Treated Mice

To determine the anti-inflammatory effect of EA, we examined the effect of EA on the expression level of IL-1β and iNOS in the colonic tissue of TNBS-treated mice. TNBS-treated mice significantly increased the protein levels of IL-1β and iNOS in colonic tissues compared with the Control group ($p < 0.05$, **Figures 2A–D**). EA significantly decreased the expression levels of IL-1β and iNOS compared with the TNBS group ($p < 0.05$, **Figures 2A–D**) or the sham EA group. Similarly, in the immunofluorescent assays, TNBS significantly elevated iNOS expression, and EA significantly decreased the iNOS expression ($p < 0.05$, **Figures 2E,F**). These findings indicated that EA attenautes the colonic inflammatory response by inhibiting the expression of pro-inflammatory cytokines such as IL-1β and iNOS.

EA Increases CB2 Receptor Expression and Attenuates Macrophages Activation in Inflamed Colon Tissues of TNBS-Treated Mice

We have shown that the antinociceptive effect of EA on inflammatory pain is mediated by peripheral CB2 receptors and that CB2 receptors activation inhibits NLRP3 inflammasomes in macrophages *in vitro* (Gao et al., 2018). Next, we determined whether EA affects the intestinal CB2 receptor expression induced by TNBS. Compared with the Control group, TNBS significantly reduced the expression level of CB2 receptors in the colonic tissues ($p < 0.05$, **Figures 3A,B**). EA treatment significantly increased the protein level of CB2 receptors in the colonic tissues ($p < 0.05$, **Figures 3A,B**).

Double immunofluorescence labeling showed that CB2 receptors were colocalized with CD68, a macrophages marker. Comparable with the Control group, TNBS treatment increased CD68 labeling and decreased the number of colocalized CD68 and CB2 receptors ($p < 0.05$, **Figures 3C–F**). Comparable with the TNBS group, EA at BL25 inhibited the expression of CD68 and increased the number of colocalized CD68 and CB2 receptors ($p < 0.05$, **Figures 3C–F**). These data suggest that EA reduces macrophages activation and increases CB2 receptor expression in the inflamed colon tissues of TNBS-treated mice.

Blocking CB2 Receptors Antagonizes the Antinociceptive and Anti-Inflammatory Effects of EA

To determine the role of CB2 receptors in EA's antinociceptive and anti-inflammatory in TNBS-treated mice, wild-type (WT) mice received systemic delivery of AM630, a specific CB2 receptor antagonist 30 min before each EA treatment. The antinociceptive effects of EA were blocked by administration of AM630 ($p > 0.05$, **Figures 4B,C**). Compared with the Control + DMSO group, the TNBS + DMSO group and TNBS + AM630 + EA group showed an inflammatory response characterized with mucosal erosion, congestion, reduced or absent crypt and neutrophil infiltration. The TNBS + EA + DMSO group significantly improved the colonic lesions (**Figures 4D,E**).

Treatment with AM630 antagonized the anti-inflammatory effect of EA (**Figure 5**). In the presence of AM630, EA failed to reduce the protein levels of IL-1β and iNOS ($p > 0.05$, **Figures 5A–D**) and the number of fluorescence-positive cells for iNOS and CD68 in the inflamed colon tissues by TNBS ($p > 0.05$, **Figures 5E,F**). These results suggest that the antinociceptive and anti-inflammatory effects of EA are mediated by the CB2 receptors.

The Antinociceptive and Anti-Inflammatory Effects of EA on TNBS-Treated Mice Depend on CB2 Receptors

To validate the role of CB2 receptors in the therapeutic effect of EA on TNBS-induced colitis in mice, we tested the EA's effect in CB2 KO mice treated with TNBS. The visceral hyperalgesia and mechanical allodynia were present in wild-type and CB2 receptor KO mice after TNBS treatment. However, EA failed to reduce visceral hyperalgesia and mechanical allodynia in CB2 KO mice treated with TNBS ($p > 0.05$, **Figures 6A–D**). Also, treatment with EA had no significant effect on the histological inflammation and pathology of colitis in CB2 KO mice treated with TNBS, as evidenced by extensive destruction of tissue architecture, loss of intestinal crypts and goblet cells, marked mucosal erosion and congestion ($p > 0.05$, **Figures 6E,F**).

Similar to WT mice, TNBS significantly increased the protein levels of IL-1β mature fragments and iNOS and the number of iNOS- and CD68-positive cells in the colonic tissues in CB2 receptor KO mice ($p > 0.05$, **Figures 7A–D**). However, EA treatment failed to significantly reduce the elevated protein levels of IL-1β mature fragments and iNOS and the number of iNOS- and CD68-positive cells in the colonic tissues ($p > 0.05$, **Figures 7A–D**). These data suggest that CB2 receptors play a critical role in the antinociceptive and anti-inflammatory effects of EA in the mouse model of IBD.

DISCUSSION

Disorders of the intestinal immune system play a major role in the pathophysiology of IBD. The macrophages residing in the lamina propria maintain intestinal homeostasis under normal physiological conditions, but after inflammation or infection, the resident monocytes in the intestine and their derived pro-inflammatory macrophages enter the myenteric layer and further recruit more pro-inflammatory macrophages, thus further exacerbating IBD by releasing inflammatory factors (Grainger et al., 2017; Bain and

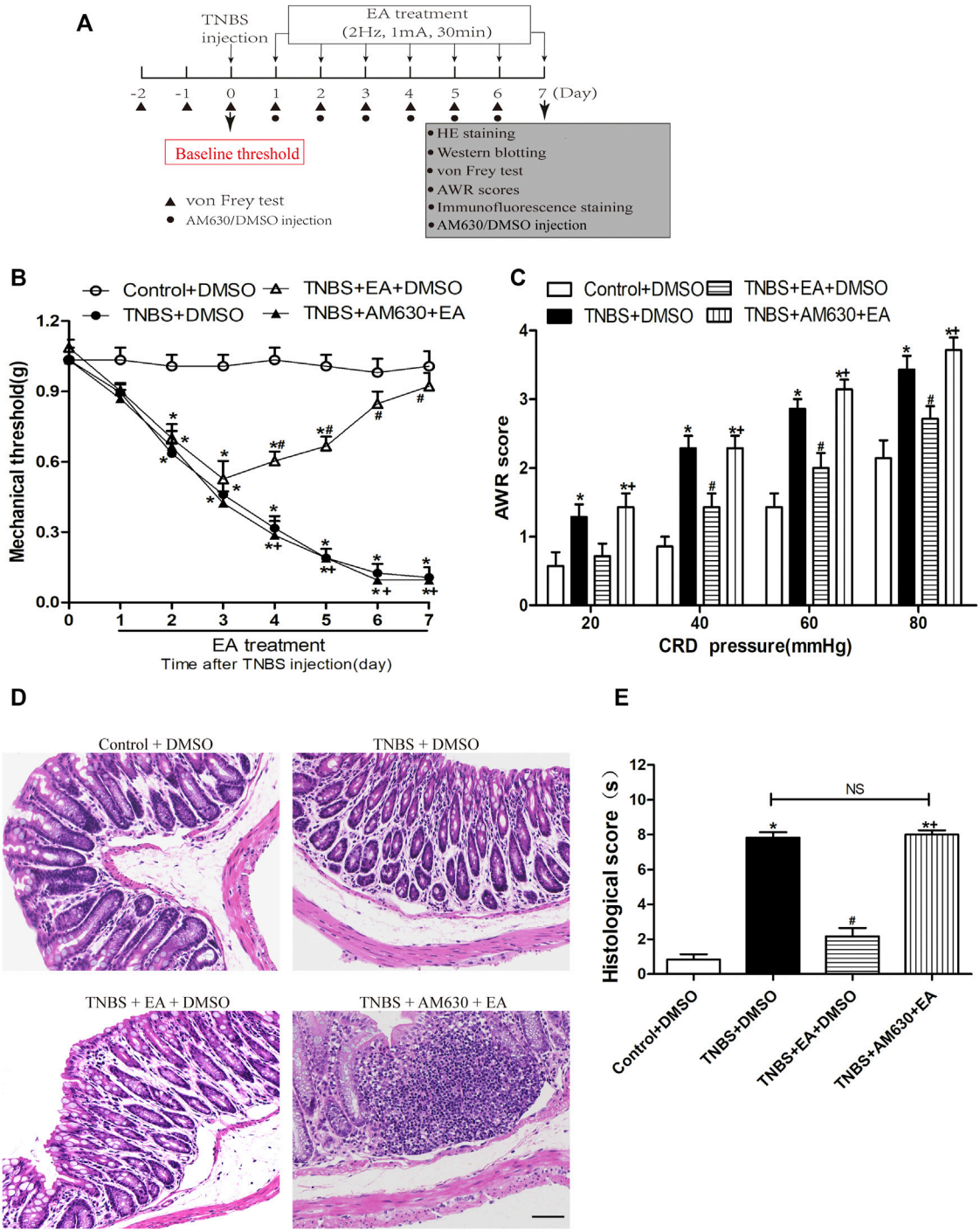

FIGURE 4 | Pharmacological blockade of CB2 receptors reverses the EA's effects on TNBS-induced visceral hypersensitivities and colonic morphology. **(A)** Experimental protocol show treatment schedule of AM630, the specific CB2 receptor antagonist. **(B)** Time course effect of AM630 treatment on the EA's antinociceptive effect on TNBS-treated mice. **(C)** AWR scores of TNBS-treated mice on day 7. **(D)** Representative H&E staining of colon tissue sections. Scale bar, 200 μm. **(E)** Histological score in each group ($n = 6$ per group). *$p < 0.05$ versus with Control + DMSO group, #$p < 0.05$ versus with TNBS + DMSO group, +$p < 0.05$ versus with TNBS + EA + DMSO group. NS: no significance versus TNBS + EA + AM630 group as indicated.

Schridde, 2018). In the present study, we showed that only a small number of macrophages were present in the control group, which is consistent with the finding that in the normal intestine, only a few infiltrating immune cells are present (He et al., 2019). The increased abundance of macrophage expression after TNBS indicates that dysregulated

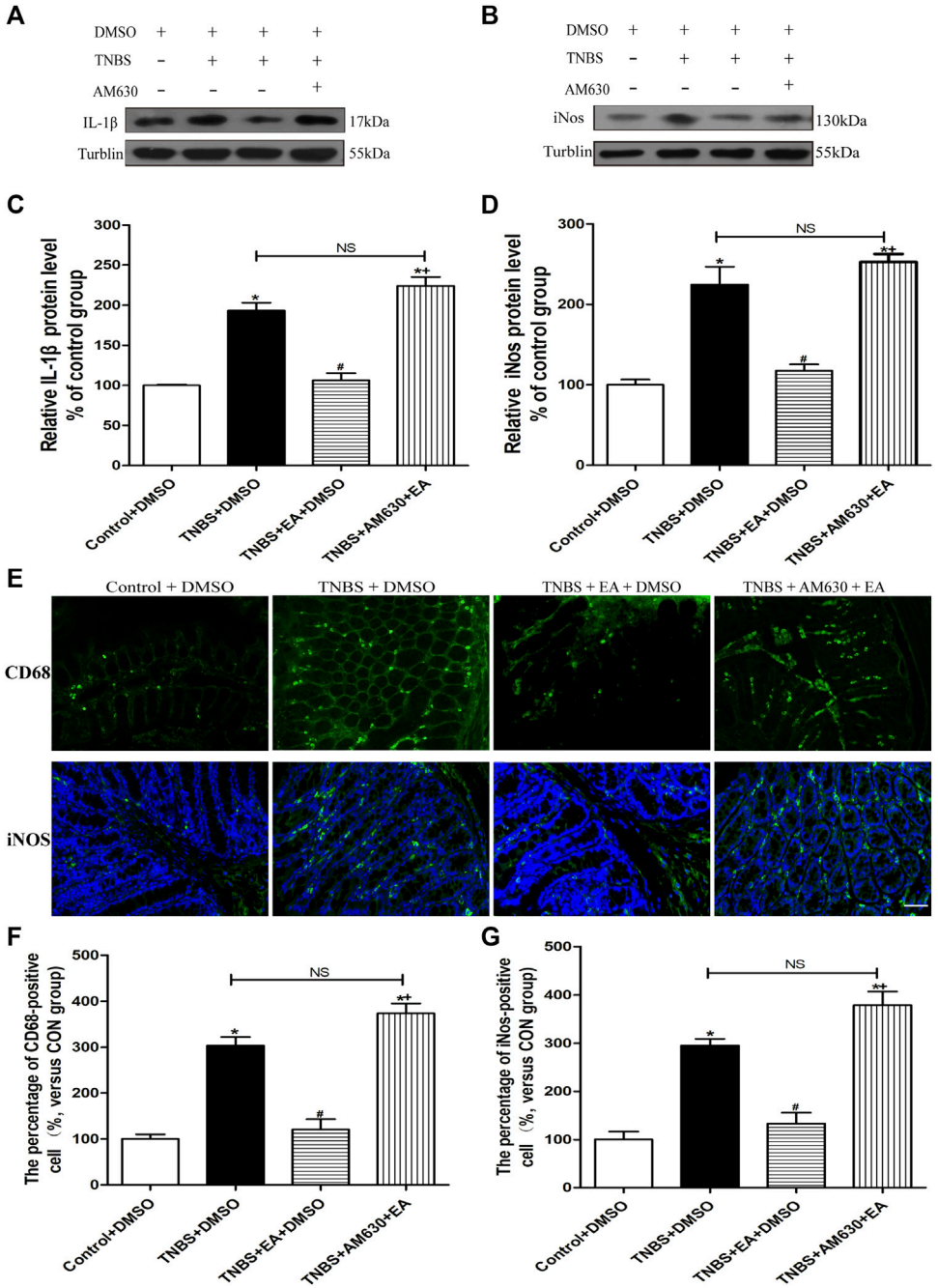

FIGURE 5 | AM630 reverses the EA's anti-inflammatory effects in TNBS-treated mice. Representative western blot images show the protein level of IL-1β **(A)** and iNOS **(B)** in the colon tissues. Summary data show the relative protein levels of IL-1β **(C)** and iNOS **(D)** in the colon tissues. **(E)** Representative images of immunofluorescence staining in which cell membrane were labeled with anti-CD68 and anti-iNOS in the colon tissues. Summary of the number of $CD68^{-}$ **(F)** and iNOS- **(G)** positive cells per observation field. Data are expressed as mean ± SEM ($n = 6$ per group). Scale bar, 50 μm $^{*}p < 0.05$ versus with Control + DMSO group, $\#p < 0.05$ versus with TNBS + DMSO group, $+p < 0.05$ versus with TNBS + EA + DMSO group. NS, no significance versus TNBS + EA + AM630 group as indicated.

immune/inflammatory responses on play a role in IBD. Importantly, we found that EA suppressed the newly recruited macrophages in the muscle layer, inhibited IL-1β and iNOS overexpression, and attenuated TNBS-induced visceral hypersensitivity. In addition, EA further increased the CB2 receptor expression on the macrophages in the colonic tissues. However, the CB2 receptor antagonist or CB2 receptor deletion antagonized the antinociceptive and anti-inflammatory effects of EA, suggesting that the beneficial effects of EA are mediated by CB2 receptors. Therefore, EA at

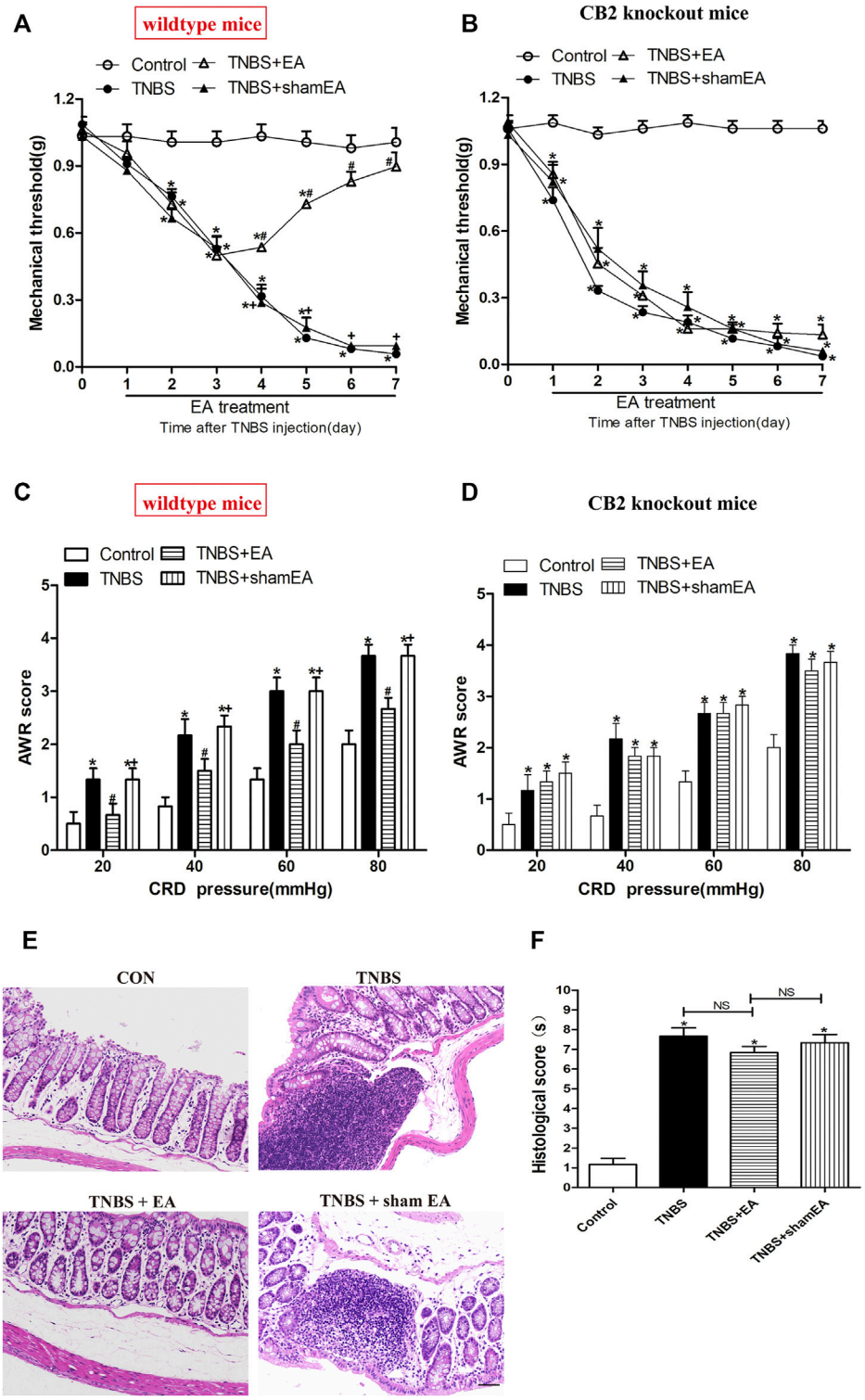

FIGURE 6 | EA attenuates pain hypersensitivity induced by TNBS through CB2 receptors. **(A–D)** Time course of mechanical withdrawal threshold in wild-type **(A)** and CB2 receptor knockout **(B)** mice treated with TNBS. AWR scores in wild-type **(C)** and CB2 receptor knockout **(D)** mice treated with TNBS on day 7. **(E)** Representative H&E staining of the colon tissue sections in CB2 receptor knockout mice. Scale bar, 50 μm. **(F)** Histological score in each group ($n = 6$ per group). *$p <$ 0.05 versus with Control group, #$p < 0.05$ versus with TNBS group, +$p < 0.05$ versus with TNBS + EA group. NS, no significance versus Sham EA group as indicated.

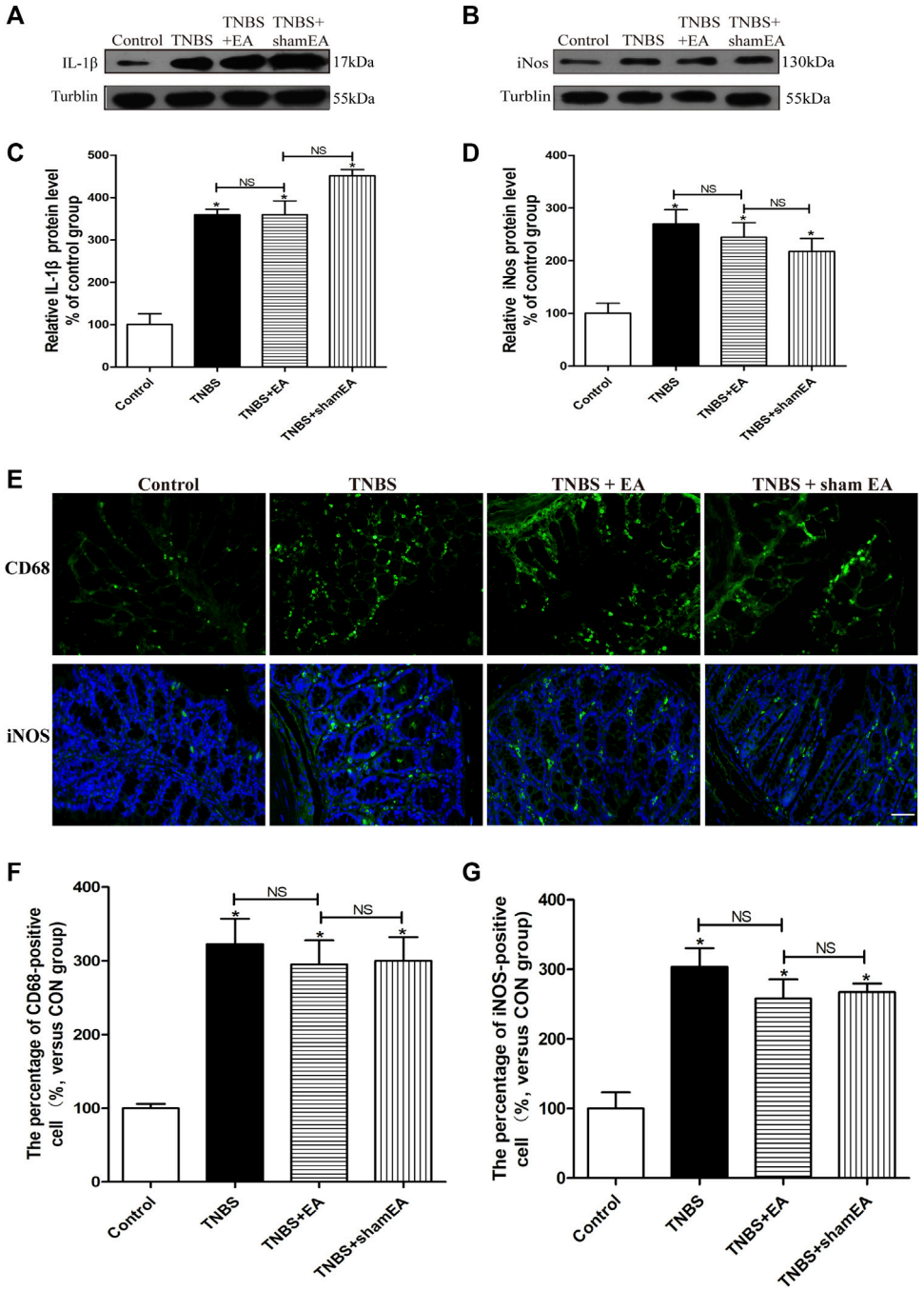

FIGURE 7 | EA's anti-inflammatory effects on TNBS-treated mice is mediated by CB2 receptors. **(A–D)** Representative western blot images show the protein level of IL-1β **(A)** and iNOS **(B)** in the colon tissues. Summary data show the relative protein levels of IL-1β **(C)** and iNOS **(D)** in the colon tissues. **(E)** Representative images of immunofluorescence labeled with anti-CD68 and anti-iNOS antibodies in the colon tissues. Summary data show the number of $CD68^{-}$ **(F)** and iNOS- **(G)** positive cells per observation field. Data are expressed as mean ± SEM (n = 6 per group). Scale bar, 50 μm *p < 0.05 versus with Control group, #p < 0.05 versus with TNBS group, +p < 0.05 versus with TNBS + EA group. NS: no significance versus Sham EA group as indicated.

BL25 points likely reduces TNBS-induced inflammation by activating CB2 receptors. EA may exert anti-inflammatory and antinociceptive effects by inhibiting the accumulation of newly recruited macrophages and reducing the levels of inflammatory cytokines. Collectively, these results suggest that CB2 receptors in the colonic tissues are a major component of the EA-produced anti-inflammatory and antinociceptive actions in the IBD model.

TNBS triggers visceral and somatic hypersensitivity after intracolonic injection (Viana-Cardoso et al., 2015). The onset and maintenance of colonic hypersensitivity may arise from the nociceptive inputs from the colon that sensitize the spinal dorsal horn neurons to cause somatic and visceral hypersensitivity (Zhou et al., 2008). This explanation is supported by the findings that the mechanical pain threshold after TNBS treatment begins to decrease significantly on the third day and reaches a peak on the fifth day. The rat colonic tissues recovered after 7 days of enema administration of 2,4-dinitrobenzene sulfonic acid (Lucarini et al., 2020). Similarly, we found that 7 days after TNBS treatment, histological analysis of the colon showed partial recovery of the mucosa, but a small amount of ulcerated areas were still seen with the loss of lining epithelium and infiltration of wall-permeable immune cells (mainly neutrophils, lymphocytes and macrophages), crypt abscesses, altered goblet cells and edema. Lv et al. reported that EA stimulation reduced the macroscopic pathologic changes and visceral hypersensitive of TNBS-induced colitis in rats (Lv et al., 2019). Similarly, our study also consistently found that EA alleviates visceral hyperalgesia, mechanical allodynia and intestinal pathology induced by TNBS. In a word, EA plays a key role in the recovery of IBD.

Resident macrophages that maintain intestinal homeostasis have a strong phagocytic effect but do not elicit a significant inflammatory response in mouse and human intestines (Bernardo et al., 2018; Bujko et al., 2018). When the homeostasis is disturbed, the composition of the human intestinal macrophage pool will change significantly. In the mucosa of patients with IBD, there is an accumulation of pro-inflammatory macrophages that produce large amounts of IL-1β, IL-6, TNF-α, reactive oxygen intermediates, and nitric oxide, making them different from the macrophages in the healthy intestine (Singh et al., 2016). A similar infiltration of pro-inflammatory monocytes and macrophages is seen in animal models of dextran sulphate sodium (DSS) (Gong et al., 2018; Mei et al., 2019). This infiltration is characterized by the reversal of the ratio of resident macrophages to proinflammatory macrophages, which is due to the accumulation of monocytes and their derived macrophages. Infiltrated macrophages showed typical pro-inflammatory features, including the production of TNF-α, IL-6, IL-1β production, and the expression of iNOS. Similarly, in our TNBS-treated model, intestinal homeostasis was disrupted, as reflected by macrophage activation, increased the expression of IL-1β and iNOS.

Neuron-glia-immune interaction in the DRG, spinal cord and enteric nervous system is now considered to play a key role in the development of visceral hypersensitivity, which is associated with visceral pain accompanying IBD (Qiao and Tiwari, 2020). Inflammatory mediators released by macrophages can directly activate and sensitize colon-innervating afferents, leading to an enhanced response to chemical and mechanical stimuli, known as visceral pain/hypersensitivity (Kwon et al., 2013; Domoto et al., 2021). Thus, inactivation of macrophages may be at least partially underlie the antinociceptive effects of EA. Our results indicated that EA inhibited macrophage activation, along with suppressing the increased expression of IL-1β and iNOS. Thus, EA may regulated immune function and visceral hypersensitive in the gastrointestinal tract by inhibiting macrophage activation.

In the gastrointestinal tract, the activated endogenous cannabinoid system is involved in regulating gut motility, intestinal secretion and epithelial permeability, and immune function through cannabinoid receptors present (Hasenoehrl et al., 2016; Perisetti et al., 2020). The antinociceptive effects of cannabinoid oil used in adolescent and young adult patients with IBD have been clinically demonstrated (Hoffenberg et al., 2019). However, the addictive side effects of cannabis have led to ongoing restrictions on the clinical use of cannabis for IBD. Anandamide (AEA) and 2-arachidonoylglycerol (2-AG) function as retrograde messengers in descending pain regulatory pathways, and they are transported to the peripheral terminals of the CNS and primary afferent neurons to inhibit neurotransmitter release from presynaptic terminals (Gondim et al., 2012; Kano, 2014). In our previous study, in a rat model of CFA-induced inflammatory pain, EA significantly increased the level of AEA in inflammatory skin tissues and produced antinociceptive effects through activation of peripheral CB2 receptors (Chen et al., 2009). Our study showed for the first time that EA exerts antinociceptive effects and inhibits activation of macrophages and suppresses the expression of mature IL-1β and iNOS through activating CB2 receptors in the colonic tissues. The CB2 receptor antagonist AM630 or CB2 receptor knockout blocked the inhibitory effects of EA on macrophages activation in the colon tissues. This is consistent with previous studies showing that activation of CB2 receptors ameliorates DSS-induced colitis by enhancing the inhibition of NLRP3 inflammasome activation in macrophages (Ke et al., 2016).

Therefore, it is reasonable assumption that EA at BL25 appears to reduce TNBS-induced IBD inflammation by increasing endogenous cannabinoids and then increasing CB2 receptors, thereby inhibits activation of macrophages and suppresses inflammatory cytokine levels and visceral hypersensitivity. Thus, CB2 receptor agonists could be used to treat IBD.

Although our findings have great potential for EA in the treatment of IBD patients, there are some limitations to this study. At present, this study is lack of EA for the determination of the content of other components of endocannabinoid system; In addition, other more effective acupoints for IBD should be explored.

CONCLUSION

Our study shows that EA at BL25 is effective in reducing visceral pain in a mouse model of IBD. Our results further suggest that the antinociceptive effect of EA may be attributed to the CB2 receptor-mediated inhibition of macrophage activation and expression of IL-1β and iNOS. Our findings provide new information on the mechanism by which EA activates CB2 receptors to reduce visceral pain associated with IBD.

DATA AVAILABILITY STATEMENT

The original contributions presented in the study are included in the article/**Supplementary Material**, further inquiries can be directed to the corresponding authors.

ETHICS STATEMENT

The animal study was reviewed and approved by Institutional Animal Care and Use Committee at Huazhong University of Science and Technology.

AUTHOR CONTRIBUTIONS

ML and L-LY provided the conception and design of research, drafted and revised the manuscript. HZ, X-FH, and Y-ZL performed the experiments; Y-ML, W-QG, and CC helped to analyze the data and interpreted the results of experiments; O-YZ, Y-YL, and Y-SS prepared the figures; WH and BZ provided some guidance in experimental designing; H-LP and X-HJ provided some help in the experiments; All authors approved the final edited version.

FUNDING

This work was supported by the National Key research and development Program of China (No.2019YFC1709002), the National Natural Science Foundation of China (No.82004491, 82174500, 81973949, 81403475), the Scientific Research project of TCM of Hubei Provincial Health Commission (No. ZY2021M010; ZY2019Z010) and the China Postdoctoral Science (No.2020M682428).

SUPPLEMENTARY MATERIAL

The Supplementary Material for this article can be found online at: https://www.frontiersin.org/articles/10.3389/fphar.2022.861799/full#supplementary-material

REFERENCES

Bain, C. C., and Schridde, A. (2018). Origin, Differentiation, and Function of Intestinal Macrophages. *Front. Immunol.* 9, 2733. doi:10.3389/fimmu.2018.02733

Bao, C. H., Wang, C. Y., Li, G. N., Yan, Y. L., Wang, D., Jin, X. M., et al. (2019). Effect of Mild Moxibustion on Intestinal Microbiota and NLRP6 Inflammasome Signaling in Rats with post-inflammatory Irritable Bowel Syndrome. *World J. Gastroenterol.* 25 (32), 4696–4714. doi:10.3748/wjg.v25.i32.4696

Bernardo, D., Marin, A. C., Fernández-Tomé, S., Montalban-Arques, A., Carrasco, A., Tristán, E., et al. (2018). Human Intestinal Pro-inflammatory CD11chighCCR2+CX3CR1+ Macrophages, but Not Their Tolerogenic CD11c-CCR2-Cx3cr1- Counterparts, Are Expanded in Inflammatory Bowel Disease. *Mucosal Immunol.* 11 (4), 1114–1126. doi:10.1038/s41385-018-0030-7

Borovikova, L. V., Ivanova, S., Zhang, M., Yang, H., Botchkina, G. I., Watkins, L. R., et al. (2000). Vagus Nerve Stimulation Attenuates the Systemic Inflammatory Response to Endotoxin. *Nature* 405 (6785), 458–462. doi:10.1038/35013070

Bujko, A., Atlasy, N., Landsverk, O. J. B., Richter, L., Yaqub, S., Horneland, R., et al. (2018). Transcriptional and Functional Profiling Defines Human Small Intestinal Macrophage Subsets. *J. Exp. Med.* 215 (2), 441–458. doi:10.1084/jem.20170057

Chaplan, S. R., Bach, F. W., Pogrel, J. W., Chung, J. M., and Yaksh, T. L. (1994). Quantitative Assessment of Tactile Allodynia in the Rat Paw. *J. Neurosci. Methods* 53 (1), 55–63. doi:10.1016/0165-0270(94)90144-9

Chen, L., Zhang, J., Li, F., Qiu, Y., Wang, L., Li, Y. H., et al. (2009). Endogenous Anandamide and Cannabinoid Receptor-2 Contribute to Electroacupuncture Analgesia in Rats. *J. Pain* 10 (7), 732–739. doi:10.1016/j.jpain.2008.12.012

Domoto, R., Sekiguchi, F., Tsubota, M., and Kawabata, A. (2021). Macrophage as a Peripheral Pain Regulator. *Cells* 10 (8). doi:10.3390/cells10081881

Gao, F., Xiang, H. C., Li, H. P., Jia, M., Pan, X. L., Pan, H. L., et al. (2018). Electroacupuncture Inhibits NLRP3 Inflammasome Activation through CB2 Receptors in Inflammatory Pain. *Brain Behav. Immun.* 67, 91–100. doi:10.1016/j.bbi.2017.08.004

Garcia-Arencibia, M., Molina-Holgado, E., and Molina-Holgado, F. (2019). Effect of Endocannabinoid Signalling on Cell Fate: Life, Death, Differentiation and Proliferation of Brain Cells. *Br. J. Pharmacol.* 176 (10), 1361–1369. doi:10.1111/bph.14369

Gondim, D. V., Araújo, J. C., Cavalcante, A. L., Havt, A., Quetz, Jda. S., Brito, G. A., et al. (2012). CB1 and CB2 Contribute to Antinociceptive and Anti-inflammatory Effects of Electroacupuncture on Experimental Arthritis of the Rat Temporomandibular Joint. *Can. J. Physiol. Pharmacol.* 90 (11), 1479–1489. doi:10.1139/y2012-130

Gong, Z., Zhao, S., Zhou, J., Yan, J., Wang, L., Du, X., et al. (2018). Curcumin Alleviates DSS-Induced Colitis via Inhibiting NLRP3 Inflammsome Activation and IL-1β Production. *Mol. Immunol.* 104, 11–19. doi:10.1016/j.molimm.2018.09.004

Grainger, J. R., Konkel, J. E., Zangerle-Murray, T., and Shaw, T. N. (2017). Macrophages in Gastrointestinal Homeostasis and Inflammation. *Pflugers Arch.* 469 (3-4), 527–539. doi:10.1007/s00424-017-1958-2

Hasenoehrl, C., Taschler, U., Storr, M., and Schicho, R. (2016). The Gastrointestinal Tract - a central Organ of Cannabinoid Signaling in Health and Disease. *Neurogastroenterol Motil.* 28 (12), 1765–1780. doi:10.1111/nmo.12931

He, J., Song, Y., Li, G., Xiao, P., Liu, Y., Xue, Y., et al. (2019). Fbxw7 Increases CCL2/7 in CX3CR1hi Macrophages to Promote Intestinal Inflammation. *J. Clin. Invest.* 129 (9), 3877–3893. doi:10.1172/JCI123374

Hoffenberg, E. J., Mcwilliams, S., Mikulich-Gilbertson, S., Murphy, B., Hoffenberg, A., and Hopfer, C. J. (2019). Cannabis Oil Use by Adolescents and Young Adults with Inflammatory Bowel Disease. *J. Pediatr. Gastroenterol. Nutr.* 68 (3), 348–352. doi:10.1097/MPG.0000000000002189

Hou, T., Xiang, H., Yu, L., Su, W., Shu, Y., Li, H., et al. (2019). Electroacupuncture Inhibits Visceral Pain via Adenosine Receptors in Mice with Inflammatory Bowel Disease. *Purinergic Signal.* 15 (2), 193–204. doi:10.1007/s11302-019-09655-4

Kano, M. (2014). Control of Synaptic Function by Endocannabinoid-Mediated Retrograde Signaling. *Proc. Jpn. Acad. Ser. B Phys. Biol. Sci.* 90 (7), 235–250. doi:10.2183/pjab.90.235

Ke, P., Shao, B. Z., Xu, Z. Q., Wei, W., Han, B. Z., Chen, X. W., et al. (2016). Activation of Cannabinoid Receptor 2 Ameliorates DSS-Induced Colitis through Inhibiting NLRP3 Inflammasome in Macrophages. *PLoS One* 11 (9), e0155076. doi:10.1371/journal.pone.0155076

Kim, H. Y., Hahm, D. H., Pyun, K. H., Lee, S. K., Lee, H. J., Nam, T. C., et al. (2005). Effects of Acupuncture at GV01 on Experimentally Induced Colitis in Rats: Possible Involvement of the Opioid System. *Jpn. J. Physiol.* 55 (3), 205–210. doi:10.2170/jjphysiol.S647

Kim, J. J., Shajib, M. S., Manocha, M. M., and Khan, W. I. (2012). Investigating Intestinal Inflammation in DSS-Induced Model of IBD. *J. Vis. Exp.*, 3678. doi:10.3791/3678

Kwon, M. J., Kim, J., Shin, H., Jeong, S. R., Kang, Y. M., Choi, J. Y., et al. (2013). Contribution of Macrophages to Enhanced Regenerative Capacity of Dorsal Root Ganglia Sensory Neurons by Conditioning Injury. *J. Neurosci.* 33 (38), 15095–15108. doi:10.1523/JNEUROSCI.0278-13.2013

Liu, Y., Jia, M., Wu, C., Zhang, H., Chen, C., Ge, W., et al. (2021). Transcriptomic Profiling in Mice with CB1 Receptor Deletion in Primary Sensory Neurons Suggests New Analgesic Targets for Neuropathic Pain. *Front. Pharmacol.* 12, 781237. doi:10.3389/fphar.2021.781237

Lopes, J. B., Bastos, J. R., Costa, R. B., Aguiar, D. C., and Moreira, F. A. (2020). The Roles of Cannabinoid CB1 and CB2 Receptors in Cocaine-Induced Behavioral Sensitization and Conditioned Place Preference in Mice. *Psychopharmacology (Berl)* 237 (2), 385–394. doi:10.1007/s00213-019-05370-5

Lucarini, E., Parisio, C., Branca, J. J. V., Segnani, C., Ippolito, C., Pellegrini, C., et al. (2020). Deepening the Mechanisms of Visceral Pain Persistence: An Evaluation of the Gut-Spinal Cord Relationship. *Cells* 9 (8), 1772. doi:10.3390/cells9081772

Lv, P. R., Su, Y. S., He, W., Wang, X. Y., Shi, H., Zhang, X. N., et al. (2019). Electroacupuncture Alleviated Referral Hindpaw Hyperalgesia via Suppressing Spinal Long-Term Potentiation (LTP) in TNBS-Induced Colitis Rats. *Neural Plast.* 2019, 2098083. doi:10.1155/2019/2098083

Mei, Y., Fang, C., Ding, S., Liu, X., Hu, J., Xu, J., et al. (2019). PAP-1 Ameliorates DSS-Induced Colitis with Involvement of NLRP3 Inflammasome Pathway. *Int. Immunopharmacol* 75, 105776. doi:10.1016/j.intimp.2019.105776

Naftali, T., Mechulam, R., Lev, L. B., and Konikoff, F. M. (2014). Cannabis for Inflammatory Bowel Disease. *Dig. Dis.* 32 (4), 468–474. doi:10.1159/000358155

Neurath, M. F. (2019). Targeting Immune Cell Circuits and Trafficking in Inflammatory Bowel Disease. *Nat. Immunol.* 20 (8), 970–979. doi:10.1038/s41590-019-0415-0

Perisetti, A., Rimu, A. H., Khan, S. A., Bansal, P., and Goyal, H. (2020). Role of Cannabis in Inflammatory Bowel Diseases. *Ann. Gastroenterol.* 33 (2), 134–144. doi:10.20524/aog.2020.0452

Qiao, L. Y., and Tiwari, N. (2020). Spinal Neuron-Glia-Immune Interaction in Cross-Organ Sensitization. *Am. J. Physiol. Gastrointest. Liver Physiol.* 319 (6), G748–G760. doi:10.1152/ajpgi.00323.2020

Scheau, C., Caruntu, C., Badarau, I. A., Scheau, A. E., Docea, A. O., Calina, D., et al. (2021). Cannabinoids and Inflammations of the Gut-Lung-Skin Barrier. *J. Pers Med.* 11 (6), 494. doi:10.3390/jpm11060494

Sharkey, K. A., Darmani, N. A., and Parker, L. A. (2014). Regulation of Nausea and Vomiting by Cannabinoids and the Endocannabinoid System. *Eur. J. Pharmacol.* 722, 134–146. doi:10.1016/j.ejphar.2013.09.068

Singh, U. P., Singh, N. P., Murphy, E. A., Price, R. L., Fayad, R., Nagarkatti, M., et al. (2016). Chemokine and Cytokine Levels in Inflammatory Bowel Disease Patients. *Cytokine* 77, 44–49. doi:10.1016/j.cyto.2015.10.008

Song, S., An, J., Li, Y., and Liu, S. (2019). Electroacupuncture at ST-36 Ameliorates DSS-Induced Acute Colitis via Regulating Macrophage Polarization Induced by Suppressing NLRP3/IL-1β and Promoting Nrf2/HO-1. *Mol. Immunol.* 106, 143–152. doi:10.1016/j.molimm.2018.12.023

Storr, M. A., Keenan, C. M., Zhang, H., Patel, K. D., Makriyannis, A., and Sharkey, K. A. (2009). Activation of the Cannabinoid 2 Receptor (CB2) Protects against Experimental Colitis. *Inflamm. Bowel Dis.* 15 (11), 1678–1685. doi:10.1002/ibd.20960

Viana-Cardoso, K. V., Silva, M. T., Peixoto-Junior, A. A., Marinho, L. S., Matias, N. S., Soares, P. M., et al. (2015). Sensory and Inflammatory Colonic Changes Induced by Vincristine in Distinct Rat Models of Colitis. *Auton. Autacoid Pharmacol.* 34 (3-4), 27–34. doi:10.1111/aap.12020

Wang, S. J., Yang, H. Y., Wang, F., and Li, S. T. (2015). Acupoint Specificity on Colorectal Hypersensitivity Alleviated by Acupuncture and the Correlation with the Brain-Gut Axis. *Neurochem. Res.* 40 (6), 1274–1282. doi:10.1007/s11064-015-1587-0

Wang, X., Zhao, N. Q., Sun, Y. X., Bai, X., Si, J. T., Liu, J. P., et al. (2020). Acupuncture for Ulcerative Colitis: a Systematic Review and Meta-Analysis of Randomized Clinical Trials. *BMC Complement. Med. Ther.* 20 (1), 309. doi:10.1186/s12906-020-03101-4

Wei, D., Zhao, N., Xie, L., Huang, B., Zhuang, Z., Tang, Y., et al. (2019). Electroacupuncture and Moxibustion Improved Anxiety Behavior in DSS-Induced Colitis Mice. *Gastroenterol. Res. Pract.* 2019, 2345890. doi:10.1155/2019/2345890

Wright, K., Rooney, N., Feeney, M., Tate, J., Robertson, D., Welham, M., et al. (2005). Differential Expression of Cannabinoid Receptors in the Human colon: Cannabinoids Promote Epithelial Wound Healing. *Gastroenterology* 129 (2), 437–453. doi:10.1016/j.gastro.2005.05.026

Yüce, B., Kemmer, M., Qian, G., Müller, M., Sibaev, A., Li, Y., et al. (2010). Cannabinoid 1 Receptors Modulate Intestinal Sensory and Motor Function in Rat. *Neurogastroenterol Motil.* 22 (6), 672–e205. doi:10.1111/j.1365-2982.2010.01473.x

Zhou, Q., Price, D. D., Caudle, R. M., and Verne, G. N. (2008). Visceral and Somatic Hypersensitivity in a Subset of Rats Following TNBS-Induced Colitis. *Pain* 134 (1-2), 9–15. doi:10.1016/j.pain.2007.03.029

Conflict of Interest: The authors declare that the research was conducted in the absence of any commercial or financial relationships that could be construed as a potential conflict of interest.

Publisher's Note: All claims expressed in this article are solely those of the authors and do not necessarily represent those of their affiliated organizations, or those of the publisher, the editors and the reviewers. Any product that may be evaluated in this article, or claim that may be made by its manufacturer, is not guaranteed or endorsed by the publisher.

frontiers | Frontiers in Pharmacology

REVIEW
published: 01 June 2022
doi: 10.3389/fphar.2022.888222

Cannabinoids as Glial Cell Modulators in Ischemic Stroke: Implications for Neuroprotection

Andrés Vicente-Acosta[1,2], *Maria Ceprian*[3], *Pilar Sobrino*[4], *Maria Ruth Pazos*[5]* and *Frida Loría*[5]*

[1]Centro de Biología Molecular Severo Ochoa (CSIC-UAM), Madrid, Spain, [2]Departamento de Biología Molecular, Universidad Autónoma de Madrid, Madrid, Spain, [3]ERC Team, PGNM, INSERM U1315, CNRS UMR5261, University of Lyon 1, University of Lyon, Lyon, France, [4]Departamento de Neurología, Hospital Universitario Fundación Alcorcón, Alcorcón, Spain, [5]Laboratorio de Apoyo a la Investigación, Hospital Universitario Fundación Alcorcón, Alcorcón, Spain

Stroke is the second leading cause of death worldwide following coronary heart disease. Despite significant efforts to find effective treatments to reduce neurological damage, many patients suffer from sequelae that impair their quality of life. For this reason, the search for new therapeutic options for the treatment of these patients is a priority. Glial cells, including microglia, astrocytes and oligodendrocytes, participate in crucial processes that allow the correct functioning of the neural tissue, being actively involved in the pathophysiological mechanisms of ischemic stroke. Although the exact mechanisms by which glial cells contribute in the pathophysiological context of stroke are not yet completely understood, they have emerged as potentially therapeutic targets to improve brain recovery. The endocannabinoid system has interesting immunomodulatory and protective effects in glial cells, and the pharmacological modulation of this signaling pathway has revealed potential neuroprotective effects in different neurological diseases. Therefore, here we recapitulate current findings on the potential promising contribution of the endocannabinoid system pharmacological manipulation in glial cells for the treatment of ischemic stroke.

Keywords: cannabinoids, neuroinflammation, ischemic stroke, glia, drug target

OPEN ACCESS

Edited by:
Carmen Rodriguez Cueto, Center for Biomedical Research on Neurodegenerative Diseases (CIBERNED), Spain

Reviewed by:
Alline C. Campos, University of São Paulo, Brazil
Robert B. Laprairie, University of Saskatchewan, Canada

***Correspondence:**
Maria Ruth Pazos
ruth.pazos@salud.madrid.org
Frida Loría
frida.loria@salud.madrid.org

Specialty section:
This article was submitted to Neuropharmacology, a section of the journal Frontiers in Pharmacology

Received: *02 March 2022*
Accepted: *10 May 2022*
Published: *01 June 2022*

Citation:
Vicente-Acosta A, Ceprian M, Sobrino P, Pazos MR and Loría F (2022) Cannabinoids as Glial Cell Modulators in Ischemic Stroke: Implications for Neuroprotection. Front. Pharmacol. 13:888222. doi: 10.3389/fphar.2022.888222

INTRODUCTION

Stroke is a rapidly developing neurological pathology that involves the appearance of clinical symptoms due to a global or focal disturbance of brain function, generally with vascular origin (Sacco et al., 2013). It is the second leading cause of death worldwide after coronary and heart disease, constituting 10% of total mortality, the first cause of disability, and the second cause of dementia, causing a significant family, healthcare, and socioeconomic cost (Feigin, 2021). Moreover, data from different studies indicate that stroke prevalence is increasing and will continue to rise, probably due to an increment in life expectancy globally (Feigin, 2021). Stroke is a heterogeneous disease and depending on the nature of the brain injury, two major types can be distinguished, hemorrhagic

Abbreviations: AEA, N-arachidonoylethanolamine or anandamide; BBB, blood-brain barrier; BCP, β-caryophyllene; CBD, cannabidiol; CBDV, cannabidivarin; CBG, cannabigerol; CB, cannabinoid; CB_1R, cannabinoid receptor type 1; CB_2R, cannabinoid receptor type 2; CBF, cerebral blood flow; CNS, central nervous system; DAGL, diacylglycerol-lipase; eCB, endocannabinoid; ECS, endocannabinoid system; GFAP, glial fibrillary acidic protein; HI, hypoxia-ischemia; IL-1β, interleukin-1beta; intraperitoneal, i.p.; intravenous, i.v.; LPS, lipopolysaccharide.

stroke (15% of cases) and ischemic stroke (85% of cases), which in some cases could be transient ischemic attacks (van Asch et al., 2010; Meschia and Brott, 2018). Hemorrhagic stroke is caused by the rupture of a blood vessel in the brain and ischemic stroke, the focus of this review, occurs when a cerebral artery is occluded by a blood clot, causing a cerebral infarction (Pekny et al., 2019). Thrombus formation can have different etiologies, such as atherothrombosis, cardioembolism, small vessel occlusive disease, rare cause (infection, neoplasia, myeloproliferative syndrome, metabolic disorders, coagulation disorders) or even cryptogenic stroke (Díez Tejedor et al., 2001; Meschia and Brott, 2018). As the brain and its proper functioning depend on an adequate supply of oxygen and glucose, its cessation causes neuronal death and glial activation that lead to functional alterations not only in the affected area but also in related brain areas (Pekny et al., 2019).

Due to the high prevalence of ischemic stroke and to a higher opportunity for an effective therapeutic intervention than for hemorrhagic, a great effort has generally been devoted to the study of ischemic stroke. It has been observed that primary prevention, which acts on modifiable or potentially modifiable vascular risk factors, can considerably reduce the incidence of ischemic strokes. Among the modifiable risk factors, the most important are arterial hypertension, tobacco use, diabetes mellitus, hypercholesterolemia, obesity, physical inactivity, and atrial fibrillation (Kuriakose and Xiao, 2020). However, due in part to the estimated global increase in the prevalence of ischemic stroke and the need to find appropriate treatments to reduce sequelae, it is essential to thoroughly study the molecular mechanisms underlying the disease in order to find new treatments that will eventually lead to functional recovery of patients.

Molecular Mechanisms of Ischemic Stroke

After the ischemic event, there is a central zone of irreversibly damaged tissue known as core that receives less than 15% of normal cerebral blood flow (CBF), a surrounding area of damaged tissue that may recover its function known as penumbra, receiving less than 40% of normal CBF, and the peri-infarct region, which receives between 40 and 100% of normal CBF (Meschia and Brott, 2018; Feske, 2021). In the acute phase of cerebral ischemia, precisely due to the reduced CBF, the affected tissue experiences cellular energy depletion, with a dysfunction of the ATP-dependent ionic pumps producing the intracellular accumulation of calcium (Ca^{2+}). This in turn induce the release and accumulation of excitotoxic amino acids like glutamate in the extracellular space (Qureshi et al., 2003; Lai et al., 2014). As a consequence of the intracellular Ca^{2+} increase, Ca^{2+}-dependent enzymes are activated, resulting in mitochondrial dysfunction and cell death, mainly by necrosis (Fernández-Ruiz et al., 2015; Belov Kirdajova et al., 2020; Kuriakose and Xiao, 2020). In this first stage, microglial cells act as early players and their activation leads to the production of pro-inflammatory mediators, such as tumour necrosis factor-alpha (TNF-α), interleukin-1beta (IL-1β), and reactive oxygen species (ROS) (Lambertsen et al., 2005; Clausen et al., 2008; Allen and Bayraktutan, 2009; Chen et al., 2019). These factors recruit other inflammatory cell populations into the ischemic area, mainly circulating monocytes, which interact with astrocytes through the secretion of cytokines and chemokines, possibly contributing to astrocyte activation (Kim and Cho, 2016; Frik et al., 2018; Hersh and Yang, 2018; Rizzo et al., 2019). Once astrocytes are activated, they shift their morphology and function according to the biological context. Indeed, increasing evidence sustains the critical role of these cells in the brain's response to stroke (Pekny et al., 2016), but their harmful or beneficial contribution to the ischemic pathway is currently under intense debate (Liddelow et al., 2017). Astrocytes are also critical for glial scar formation surrounding the infarct zone, which may help limit immune cell infiltration (Liddelow and Barres, 2015, 2017). Moreover, vasogenic edema, characterized by extravasation and extracellular accumulation of fluid into the cerebral parenchyma caused by disruption of the blood-brain barrier (BBB), takes place during the subacute phase (24–72 after the ischemic event) (Chen et al., 2019; Belov Kirdajova et al., 2020). Regarding the role of oligodendrocytes in stroke, available data indicate there is a substantial oligodendrocyte loss due to excitotoxicity and oxidative stress in the ischemic core; however, a significant increase in this cell population takes place within the penumbra (for a review see Jadhav et al., 2022). Finally, the chronic phase can extend for weeks after the initial damage, being probably caused by a delayed apoptotic neuronal death involving several factors like an uncontrolled inflammatory response, the persistent presence of neurotoxic/neuroinhibitory factors, and oxidative stress, among others (Allen and Bayraktutan, 2009; Zhang et al., 2012; Belov Kirdajova et al., 2020).

Current Therapeutic Approaches to Ischemic Stroke

In recent years, several effective treatments have been developed for the treatment of ischemic stroke within the acute phase. Besides, the coordination between the emergency teams, neurologists, and hospital stroke units implementing what is known as "stroke code," allows a faster intervention, which facilitates the patient's admission to the stroke unit and administration of treatments that help reduce mortality and sequelae (Indredavik et al., 1991). Currently, the reperfusion therapies available for the treatment of ischemic stroke in the acute phase are intravenous (i.v.) thrombolysis and mechanical thrombectomy (Kuriakose and Xiao, 2020; Feske, 2021); however, due to the narrow therapeutic time window for effective intervention, less than 5% of patients can benefit from these treatments (Fernández-Ruiz et al., 2015; Choi et al., 2019). There are two types of thrombolytic treatments: i.v. injection of recombinant tissue plasminogen activator and tenecteplase, which are administered within the first 4.5 h after stroke onset. These treatments improve the patient's clinical and functional outcome, evaluated within 3 months (Alonso de Leciñana et al., 2014). Another therapeutic option used when thrombolytic treatment cannot be administered or has not been effective is mechanical thrombectomy. There are several randomized studies that demonstrate the efficacy of this procedure when applied within 6 h of symptom onset (Powers et al., 2018).

With the aim of reducing sequelae and improving the functional evolution of patients, neuroprotective treatments are continuously under investigation (Miller et al., 2011; Kolb et al., 2019). Still, despite having promising results in animal models using neuroprotective drugs, these treatments have failed to improve neurological outcomes after ischemic stroke in clinical trials, probably because neuronal survival is not enough to promote brain recovery (Gleichman and Carmichael, 2014; Choi et al., 2019). For that reason, the study of glial cells as novel therapeutic targets in stroke has gained attention recently, not only because these cells have been demonstrated to be essential for proper brain functioning but also for their neuroprotective potential in different neurological pathologies, including stroke (Gleichman and Carmichael, 2014; Hersh and Yang, 2018; Jha et al., 2019).

The Endocannabinoid System

The endocannabinoid system (ECS) constitutes an intercellular communication system that plays a fundamental role in the regulation of multiple physiological processes such as synaptic transmission, memory processes, nociception, inflammation, appetite, or thermoregulation, among others (Fernández-Ruiz et al., 2015; Cristino, Bisogno and Di Marzo, 2020; Estrada and Contreras, 2020). Consequently, the ECS and the elements that constitute it (receptors, endogenous ligands, and synthesis and breakdown enzymes) play a key role in neurotransmission, in the endocrine and the immune system.

Cannabinoids (CBs) exert their effects mainly via cannabinoid receptor 1 (CB_1R) and cannabinoid receptor 2 (CB_2R) (Matsuda et al., 1990; Munro et al., 1993). CB_1R is widely expressed in the central nervous system (CNS), mostly in neurons but also in glial cells, while CB_2R is characteristic of the immune system, being expressed as well by CNS cells like microglia, astrocytes and oligodendrocytes (Munro et al., 1993; Howlett, 2002; Molina-Holgado et al., 2002; Gulyas et al., 2004; Núñez et al., 2004; Benito et al., 2007; Navarrete and Araque, 2008; Turcotte et al., 2016; Fernández-Trapero et al., 2017). CBs also activate other receptors such as orphan G protein-coupled receptors (GPCRs), peroxisome proliferator-activated receptors (PPARs), or the adenosine A_{2A} receptor ($A_{2A}R$) (Morales and Reggio, 2017; Franco et al., 2019; Iannotti and Vitale, 2021).

The main endogenous ligands or endocannabinoids (eCBs) are 2-arachidonoylglycerol (2-AG) (Mechoulam et al., 1995; Sugiura et al., 1995) and N-arachidonoylethanolamine or anandamide (AEA) (Devane et al., 1992). Both eCBs are synthesized "on demand" from membrane lipid precursors. 2-AG is the most abundant eCB and a full CB_1R/CB_2R agonist (Sugiura et al., 1995; Stella et al., 1997). It is synthesized by the enzyme diacylglycerol-lipase (DAGL) (Tanimura et al., 2010; Shonesy et al., 2015) and metabolized to arachidonic acid and glycerol by monoacylglycerol lipase (MAGL) (Dinh et al., 2002). By contrast, AEA is a partial CB_1R agonist and it does not bind to CB_2R (Silva et al., 2013; Zou and Kumar, 2018). AEA has a complex synthesis mechanism involving the action of the enzyme N-arachidonoyl phosphatidylethanolamine-phospholipase D (NAPE-PLD) (Di Marzo et al., 1994; Blankman and Cravatt, 2013), meanwhile, its degradation is carried out by the enzyme fatty acid amide hydrolase (FAAH), which metabolizes AEA to arachidonic acid and ethanolamide (Zou and Kumar, 2018).

Role of the ECS in Ischemic Stroke

Similar to other neuropathologies, several studies have proved that the ECS is altered in ischemic stroke, as it has been reviewed elsewhere (Hillard, 2008; Fernández-Ruiz et al., 2015; Kolb et al., 2019; Cristino et al., 2020). However, contradictory and conflicting results have been found and to date, the role of the ECS in stroke has not been elucidated.

Endocannabinoid tone alterations have been reported in clinical studies and plasma levels of AEA were significantly elevated in samples from acute stroke patients (Schäbitz et al., 2002; Naccarato et al., 2010). Moreover, higher levels of 2-AG and other ECS-lipid mediators, such as palmitoylethanolamide (PEA), are positively correlated with neurological impairment (Naccarato et al., 2010). Very recently, an increased expression of CB_2R and the microRNA miR-665, a potential CB_2R regulator, were found in circulating monocytes of patients with acute ischemic stroke (Greco et al., 2021). These observations at the peripheral level could be reflecting disturbances at the central level, in line with those observed in postmortem tissues (Caruso et al., 2016), or suggesting its involvement in the modulation of the peripheral immune response in stroke patients (Greco et al., 2021).

The involvement of the ECS in the pathophysiology of stroke is even more evident in animal models (Schäbitz et al., 2002; Muthian et al., 2004; Zarruk et al., 2012; Sun, and Fang, 2013). In the transient middle cerebral artery occlusion (tMCAO) model using $CB_1R^{-/-}$ mice, a greater lesion volume was observed than in wild-type animals due to a decrease in CBF after reperfusion, probably due to a direct effect of CB_1R activation on cerebrovascular smooth muscle cells (Hillard, 2000; Parmentier-Batteur et al., 2002). However, the administration of pharmacological treatments aimed at modulating CB_1R function show controversial results. On the one hand, several works have shown that CB_1R antagonism has neuroprotective effects in animal models of stroke (Muthian et al., 2004; Zhang et al., 2008; Schmidt et al., 2012; Knowles et al., 2016; Reichenbach et al., 2016). For example, the treatment with CB_1R antagonists such as SR141716 (5 mg/kg) increases CBF in the affected brain area, decreases the lesion volume in both the tMCAO and the photothrombotic permanent MCAO (pMCAO) models, and improves the neurological function after stroke (Zhang et al., 2008; Reichenbach et al., 2016). In a rat model of global brain ischemia, the treatment with the CB_1R antagonist AM251 (2 mg/kg) also shows neuroprotective effects on areas of the reward system, reducing neuronal death and improving behavioral test performance (Knowles et al., 2016). On the other hand, CB_1R activation with the selective CB_1R agonist ACEA, both after intracerebral and intraperitoneal (i.p.) administration (10 μM and 1 mg/kg, respectively), has also shown neuroprotective effects in the endothelin-induced MCAO (eMCAO) and pMCAO models, reducing neuronal death and brain injury volume (Schmidt et al., 2012; Caltana et al., 2015). Regarding the role of CB_2R in ischemic stroke, there seems to be a greater consensus, since the majority of studies

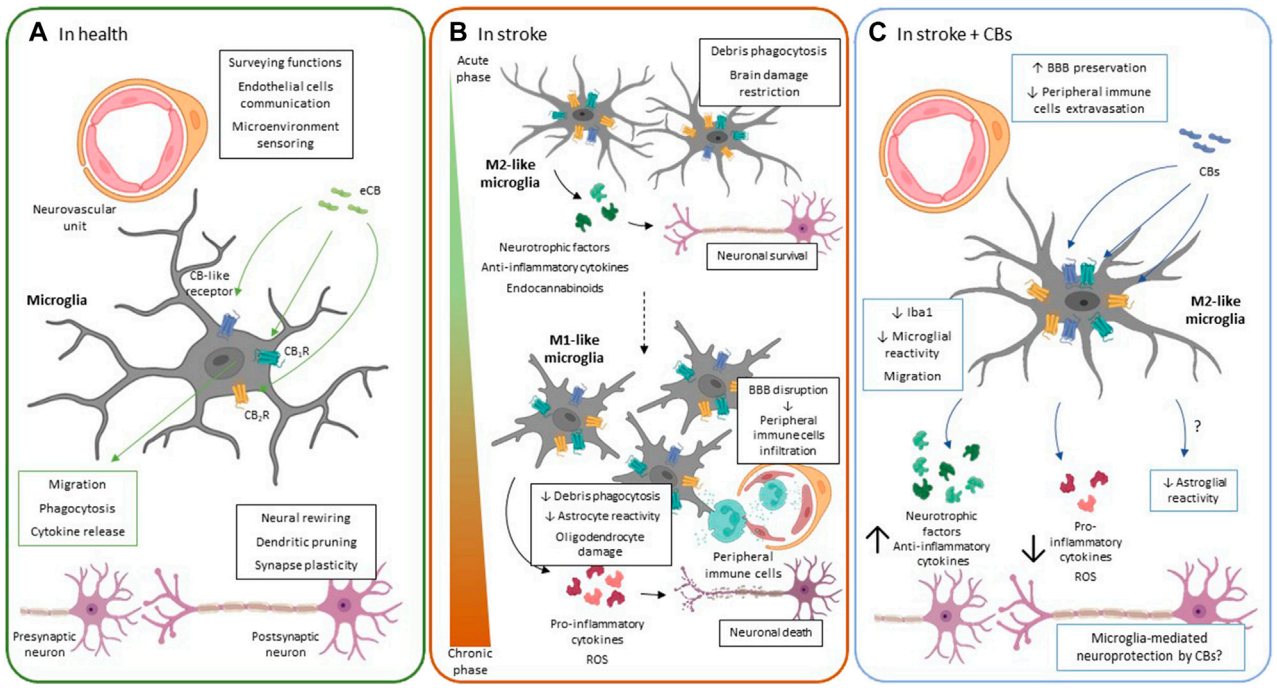

FIGURE 1 | Microglial ECS function. **(A).** In healthy conditions, microglia participate in pivotal functions for proper neuronal functioning such as dendritic pruning, neural rewiring, secretion of trophic factors and synaptic plasticity. The main function of resting microglia is to monitor the brain parenchyma through their widely branched morphology and to quickly detect any type of cellular alteration or damage. Cannabinoid receptor activation regulates the phenotypic polarization of microglia, migration, cytokine production and phagocytic capacity of these cells. **(B).** Microglial response to ischemic stroke follows a spatio-temporal pattern. Initially, in the acute phase, there is a significant increase in the number of M2-like microglial cells in the ischemic area. The M2-like phenotype is considered protective since it acquires phagocytic capacity that allows it to eliminate the dead cells debris. In addition, they release neurotrophic factors and anti-inflammatory cytokines in an attempt to limit neuronal damage. However, during the chronic phase of stroke M1-like cells proliferate and are recruited to the injury area. M1 microglia release pro-inflammatory cytokines and ROS that contribute to exacerbate neuronal death, oligodendrocyte damage and astrocyte activation. The inflammatory response also contributes to BBB rupture and the release of chemoattractant factors from peripheral immune cells. The M1 phenotype is characterized by the acquisition of an amoeboid morphology, without branching and losing its phagocytic capacity thus preventing tissue repair. The expression of CB_1R and CB_2R as well as other ECS-related receptors has been upregulated in different *in vitro* and *in vivo* stroke models. However, its specific role in microglia is still unknown. **(C).** The protective effects observed after treatment with CBs in different stroke models include modulation of microgliosis. Reduction in the number of microglia cells was not only observed, but also induced polarization towards the M2-like phenotype. The M2-like microglia contributes to tissue repair, as it has phagocytic capacity and releases trophic factors. In addition, it releases anti-inflammatory cytokines limiting brain damage and preserving the BBB, thus decreasing peripheral immune cell extravasation. Green arrows and boxes: eCB-mediated effects; blue arrows and boxes: CB-mediated effects. BBB: brain-blood barrier; CB_1R: cannabinoid receptor 1: CB_2R: cannabinoid receptor 2; CBs: cannabinoids; eCBs: endocannabinoids; ROS: reactive oxygen species.

report a neuroprotective effect i.e., a reduction of infarct volume when CB_2R agonists are administered in different animal models (Schomacher et al., 2008; Zhang et al., 2008; Reichenbach et al., 2016; Choi et al., 2018).

Although the role of the ECS in stroke may appear more complex than in other neurological pathologies, CB-based therapies begin to acquire special relevance for patients suffering from ischemic stroke (Kolb et al., 2019; Cristino et al., 2020). One of the main features of CB-based therapies is that they are multi-target molecules able to regulate the three main pathological mechanisms involved in neurodegenerative diseases, especially in ischemic stroke: inflammation, excitotoxicity, and oxidative stress. These effects could be mediated not only by CB_1R and CB_2R but other ECS-related receptors may also be involved, such as PPARγ or G-protein receptor 55 (GPR55) (Fernández-Ruiz et al., 2015; Aymerich et al., 2018). Although considerable progress has been made in the study of the ECS in neurons, there is also extensive evidence supporting the important modulatory role of the glial ECS for the proper function of these cells and their interactions with other cell types. However, the precise role of glial ECS remains a field barely explored but with great potential in stroke and other neurological pathologies (Egaña-Huguet et al., 2021; Jadhav et al., 2022).

MICROGLIA

Microglia, discovered in 1919 by the Spanish physician and histologist Pio del Rio-Hortega, constitute the first line of defense of the CNS (Mecha et al., 2016; Prinz, Jung and Priller, 2019). Microglia are highly dynamic cells included in the phagocytic-mononuclear cell lineage along with peripheral and CNS-associated macrophages (CAMS), monocytes, and dendritic cells (Ginhoux et al., 2010; Goldmann et al., 2016; Mecha et al., 2016; Prinz et al., 2019). However, there is currently an intense debate about its origin, since recent publications

suggest that microglial cells originate in the yolk sac from myeloid progenitors during embryonic development whereas peripheral macrophages develop from hematopoietic stem cells (Prinz, Jung and Priller, 2019). After embryogenesis, microglia maintain a population of 5–20% of total glial cells in the mouse brain and around 0.5%–16.6% in the human brain by a process of self-renewal (Mittelbronn et al., 2001; Ginhoux et al., 2010; Askew et al., 2017). Long considered the macrophages of the brain, microglia have multiple functions in physiological and pathophysiological conditions. Very recently, it has been shown that mouse and human microglia also exhibit regional phenotypic heterogeneity (Böttcher et al., 2019), however, whether this heterogeneity correlates with a regional-specific function or if this is relevant for different pathologies, remains to be investigated.

Under physiological conditions, microglial cells participate in important functions like dendritic pruning, neural rewiring, oligodendrocyte precursor cells (OPCs) differentiation, and synaptic plasticity, among other cellular processes (**Figure 1A**) (Nakajima et al., 2001; Wake et al., 2009; Matcovitch-Natan et al., 2016; Filipello et al., 2018). *In vivo* imaging studies have demonstrated that resting microglia show a small soma with highly dynamic branching morphology, acting as sensors that detect changes in the brain parenchyma. Following an acute injury, microglia are activated, changing their morphology to an amoeboid shape and modifying their branching pattern that rapidly are directed towards the lesion site (Davalos et al., 2005; Nimmerjahn et al., 2005). Changes also occur at the molecular level, including epigenetic, transcriptomic, and proteomic modifications (Mecha et al., 2015; Prinz et al., 2019). Moreover, once activated after a harmful event in the CNS, microglia undergo the process of phenotypic polarization, shifting toward one of two main opposite phenotypes: the classically activated pro-inflammatory state (M1-like) or the alternative anti-inflammatory protective state (M2-like). In addition, similarly to the phenotypic classification of macrophages, within the M2-like phenotype, different microglial subtypes (M2a, M2b, and M2c) have been associated with repairing, immunoregulatory, or deactivating phenotype functions, respectively (Zawadzka et al., 2012; Mecha et al., 2016; Kanazawa et al., 2017). However, because most studies have been performed in cell culture, further *in vivo* studies are needed to establish not only the function of the different subtypes of the microglial M2-like phenotype, but even their existence in the pathophysiological context, as recently reviewed by Tanaka et al. (2020).

The phenotypic polarization of microglial cells to M1 upon stimulation with bacterial-derivative molecules such as lipopolysaccharide (LPS) or even interferon gamma (IFN-γ) has been characterized *in vitro*. Under these conditions, M1 cells release a wide variety of pro-inflammatory cytokines and chemokines like TNF-α, IL-1α, IL-1β, IL-6, or IL-12 (Michelucci et al., 2009; Zawadzka et al., 2012; Malek et al., 2015; Mecha et al., 2015). Polarization to M1 also induces the expression of genes such as iNOS, ROS production, and the activation of the inflammasome complex (Shi et al., 2012; Gong et al., 2018). Stimulation with anti-inflammatory cytokines, i.e. IL-4 or IL-10 promotes a polarization toward the M2-like phenotype (Michelucci et al., 2009; Lively and Schlichter, 2013). Other cytokines and certain chemokines, including IL-3, IL-21, CCL2, and CXCL4, also induce M2 polarization. M2 cells in turn release anti-inflammatory cytokines such as IL-4, IL-10, IL-13, or TFG-β (Michelucci et al., 2009; Mecha et al., 2015).

The role of the different microglial phenotypes has been the subject of intense study in recent years and is becoming increasingly relevant given the dual functions of these cells in pathophysiological processes associated with acute and chronic diseases, including ischemic stroke (Kanazawa et al., 2017; Qin et al., 2019).

Microglial Function in Ischemic Stroke

The contribution of microglia to the neuroinflammatory context of ischemic stroke is controversial, as microglial cells could exert both detrimental and beneficial effects (for review consult Qin et al., 2019). On the one hand, post-ischemic inflammation has been considered a negative factor that worsens patient outcome, since activated microglia carry out striping processes that disrupt synaptic connections resulting in the functional impairment of neuronal circuits after ischemic damage (Wake et al., 2009). But on the other hand, it seems to be a necessary process for the clearance of cellular debris and dead cells through phagocytosis and to trigger repairing processes that promote functional brain recovery (Ma et al., 2017; Qin et al., 2019; Rajan et al., 2019).

Following an ischemic stroke, activated microglial cells change their morphology and rapidly migrate to the focus of injury as they are sensitive to fluctuations in blood flow and respond to BBB rupture and to cell death occurring in the acute phase of stroke (Nimmerjahn et al., 2005; Masuda et al., 2011; Ju et al., 2018). Besides, in response to damage, CNS resident microglia continuously proliferate, contributing with new cells to the resident microglial pool (Li et al., 2013). The extravasation and migration of peripheral immune cells (Iadecola et al., 2020), as well as the mobilization of pericytes close to the injury, also increase the microglial pool site (Özen et al., 2014; Roth et al., 2019). Despite monocyte extravasation in stroke has recently gained a considerable amount of interest, the specific contribution of individual cell types to the progression or repair of ischemic damage is still under intense study (Urra et al., 2009; Rajan et al., 2019). Overall, the microglial response to ischemic stroke is very complex and follows a spatio-temporal pattern. First, studies in animal models of both permanent and transient ischemia, have demonstrated a dramatic increase in microglial cells between 24 h and 7 days post-ischemia (Michalski et al., 2012; Li et al., 2013; Cotrina et al., 2017; Rajan et al., 2019). This peak in cell number in the ischemic core appears later in models of photothrombotic ischemia, being a slightly more moderate response (Li et al., 2013; Cotrina et al., 2017). Furthermore, in a tMCAO model, M2-like microglia is greatly increased in the ischemic zone, probably as an immediate response to neuronal damage that tries to eliminate cellular debris and limiting the extent of tissue damage (**Figure 1B**) (Hu et al., 2012). Soon after microglial activation in the pMCAO model, phagocytic microglial cells enclosing MAP2-positive neurons are observed (Cotrina et al., 2017). However, this context changes during the

chronic phase of stroke in which M1 microglial cells proliferate and are recruited. M1 microglia release pro-inflammatory cytokines and ROS that contribute to exacerbating neuronal death, BBB breakdown, and also have a reduced phagocytic capacity that prevents tissue repair (**Figure 1B**) (Hu et al., 2012; Chen et al., 2019). Phenotypic changes of microglia are also region-specific, with amoeboid-shaped cells being located in the core and penumbra of the lesion and less branched cells in the peri-infarct zone (Li et al., 2013; Cotrina et al., 2017; Rajan et al., 2019).

Activated microglia orchestrate the response to ischemic damage by communicating not only with neurons but also with non-neuronal cells and BBB structural components (Mecha et al., 2016; Huang et al., 2020). In fact, the interaction between activated microglia and astrocytes plays a crucial role in the process of neuroinflammation. The release of cytokines and trophic factors by microglia promotes phenotypic change in astrocytes, thus, M1 microglia releases, among other factors TNF-α, IL-1β or C1q, favoring the neurotoxic reactivity state of astrocytes (Liddelow et al., 2017). This communication is bidirectional, such that astrocytes also influence microglial phenotypic changes in a neuroinflammatory context by secreting a wide range of chemokines (for review, Jha et al., 2019; Liu et al., 2020). Besides, activated microglia also interact with oligodendrocytes, with a vast amount of data suggesting a deleterious effect of M1 microglia and the pro-inflammatory cytokines they release, on oligodendrocyte survival (Moore et al., 2015; Fan et al., 2019). On the other hand, in multiple sclerosis models, an increased differentiation of OPCs and, therefore, activation of remyelination processes favored by M2-like microglia has been described (Miron et al., 2013). This oligodendrocyte-protective effect has also been observed in an animal model of bilateral common carotid artery stenosis, where the treatment with the immunomodulatory drug Fingolimod promotes the polarization of microglia towards the M2-like phenotype leading to increased survival of OPCs and favoring myelin repair processes (Qin et al., 2017). In light of the complex microglial response in stroke and the dual effect of the phenotypes described, the search for new therapeutic options with a modulating effect on cell polarization in stroke has intensified in recent years (Qin et al., 2017; Liu et al., 2019; Lu et al., 2021).

Microglia and the ECS

Under physiological conditions, both in animals and humans, microglia hardly express CB_1R and CB_2R (Benito et al., 2007; López et al., 2018; Egaña-Huguet et al., 2021). However, numerous studies show that the expression pattern of both receptors are altered in microglial cells in neuropathological conditions, e.g., Alzheimer's disease (Benito et al., 2003; López et al., 2018), multiple sclerosis (Benito et al., 2007), Down's syndrome (Núñez et al., 2008), spinocerebellar ataxia (Rodríguez-Cueto et al., 2014), immunodeficiency virus infection (Benito, 2005) or Huntington's disease (Palazuelos et al., 2009).

In general, in an *in vivo* neuroinflammatory context, an increase in CB_2R levels is associated mostly with the presence of microglia around neuropathological hallmarks, e.g., protein aggregates (Benito et al., 2007; Núñez et al., 2008; López et al., 2018). However, *in vitro* studies show the complexity of the microglial response since microglial activation and polarization seem to vary depending on the stimulus used, the manipulation of the cell culture, or even the intrinsic heterogeneity of these cells (Pietr et al., 2009; Mecha et al., 2016; Gosselin et al., 2017). A few years ago, Mecha and others demonstrated changes in the different constituents of the ECS when microglia polarization proceeds *in vitro*. The classical activation of rodent microglia with LPS induces a downregulation not only of CB_1R and CB_2R but also of the eCB synthesis and degradation enzymes (Malek et al., 2015; Mecha et al., 2015). By contrast, alternative activation, which polarizes microglia towards the M2-like phenotype, upregulates the expression of CB_2R and the eCB synthesis enzymes. Consequently, M2 microglia are able to produce and release 2-AG and AEA in greater quantities than in the resting state (Walter et al., 2003; Mecha et al., 2015). However, the use of other stimuli, such as IFNγ, does not seem to influence the expression of CB_2R (Carlisle et al., 2002; Maresz et al., 2005). Finally, activation of CB_2R regulates pivotal functions of microglia, such as their migration capacity (Walter et al., 2003; Guida et al., 2017), phagocytosis (Tolón et al., 2009), and cytokine release (Malek et al., 2015) (**Figure 1A**).

Regarding CB_1R, it has been recently demonstrated that the human microglial cell line N9 expresses this receptor in the resting state. Although no changes in CB_1R expression levels are detected after stimulation with LPS and IFNγ, proximity ligation assays show that CB_1R-CB_2R heterodimers are formed following the inflammatory stimulus (Navarro and Borroto-Escuela, 2018). Another study has shown that despite low CB_1R expression, the treatment with the selective CB_1R antagonist SR141716A (1 μM) induces the polarization of BV-2 microglia towards the M1 phenotype. Moreover, the use of this antagonist prevents the anti-inflammatory effects of the non-selective cannabinoid agonist, WIN55,212-2 (1 μM) (Lou et al., 2018). All these data could suggest the involvement of CB_1R in microglial polarization and function, raising the possibility of its pharmacological manipulation to modulate the inflammatory response in neurological diseases.

Microglia also express other non-CB receptors through which certain CBs can exert their effects. This is the case of PPARs, which seem to play a relevant role in microglial polarization (Ji et al., 2018). In particular, PPARα can be activated *in vitro* by the eCB-like compound PEA, leading to an increase in CB_2R expression and 2-AG production (Guida et al., 2017), and the migration capacity of these cells (Franklin et al., 2003; Guida et al., 2017). The orphan receptor GPR55 is also expressed in microglia and is attracting special attention in different neuroinflammatory pathologies (Marichal-Cancino, 2017; Saliba et al., 2018; Burgaz et al., 2021). This receptor appears to follow a similar expression pattern to CB_2R when microglia are stimulated with LPS. However, differences have been observed between the use of cell lines and primary microglial cultures. These differences are probably due to an intrinsic heterogeneity in the microglia cell lines used, or even to the possibility that in primary cultures, microglia are in a primed state due to the handling necessary for

the development of *in vitro* assays (Pietr et al., 2009; Saliba et al., 2018). GPR55 blockage has anti-inflammatory effects by reducing prostaglandin production by microglia following LPS stimulation (Saliba et al., 2018). Finally, GPR55 activation by 2-AG or the synthetic cannabinoid abnormal-cannabidiol (abn-CBD), promotes BV-2 cell activation and migration (Franklin and Stella, 2003; Walter et al., 2003; Ryberg et al., 2007).

Microglial ECS Pharmacological Modulation in Stroke

Although the molecular mechanisms involved in CB-based neuroprotection are still not known in detail, we do know that microglia and microglial ECS play a relevant role in stroke. Due to the role of CB_2R on microglial migration and polarization and also on extravasation of peripheral immune cells to the CNS, the study of this receptor has received a great interest in stroke (Zhang et al., 2008; Hosoya et al., 2017; Greco et al., 2021). Several reports have shown an increased expression of CB_2R in the ischemic penumbra in tMCAO, eMCAO, and also in both adult and neonatal hypoxia-ischemia (HI) murine models (Ashton et al., 2007; Zhang et al., 2008; Fernández-López et al., 2012; Schmidt et al., 2012). This upregulation occurred in macrophage-like cells that could be resident microglia or infiltrated peripheral monocytes (Ashton et al., 2007; Schmidt et al., 2012). A more recent study, using a model of photothrombotic ischemia combined with positron emission tomography and histological techniques, describes an early increase in CB_2R expression in the peri-infarct area that colocalizes with some microglial cells showing amoeboid morphology. They even detect CB_2R in branched microglia of the contralateral hemisphere that could be in a primed state, highlighting the role of this receptor in the different states of microglial activation (Hosoya et al., 2017). Pharmacological CB_2R activation using selective agonists leads to a reduction in lesion volume and cognitive improvement in different animal models of stroke (Ashton et al., 2007; Zhang et al., 2008; Schmidt et al., 2012; Ronca et al., 2015). In addition, improved regional microcirculation in the affected area, decreased leukocyte rolling and extravasation, and preserved BBB integrity (Zhang et al., 2007, 2008). The involvement of microglial CB_2R in BBB preservation has also been studied in animal models of intracerebral hemorrhage and traumatic brain injury. In these studies, selective CB_2R activation reduces the release of pro-inflammatory cytokines by microglia and upregulates the expression of molecules necessary for the maintenance of tight junctions such as zo-1 or claudin-5, which are essential for BBB integrity (**Figure 1C**) (Amenta et al., 2012; Li et al., 2018). Recently, the protective and neuroinflammatory-modulating potential of β-caryophyllene (BCP), a terpene derived from *Cannabis sativa*, which acts as a CB_2R agonist, has been demonstrated. In a model of photothrombotic ischemia, the treatment with BCP alone or in combination with cannabidiol (CBD), the main non-psychoactive constituent of *Cannabis sativa*, reduced the infarct area in a dose-dependent manner, and modulated both the number and morphology of microglial cells (Yokubaitis et al., 2021).

CB_1R expression is also altered in stroke patients and in animal models (Zhang et al., 2008; Schmidt et al., 2012; Caltana et al., 2015; Caruso et al., 2016). A study performed in postmortem samples from patients revealed increased CB_1R immunohistochemical labeling in the ischemic area. This pattern was associated both with neuronal and non-neuronal cells suggesting a role of CB_1R in the glial neuroinflammatory response following acute ischemic damage (Caruso et al., 2016). However, the use of CB_1R agonists and antagonists in different animal models of stroke have shown controversial results as previously explained. These results could be explained by the diversity of animal models used that may affect differently the receptor's abundance after ischemic injury, to CB_1R desensitization effects depending on the ligand used and the dose, or even by the different roles played by this receptor depending on the cell type where it is expressed. To date, little is known about the specific role of CB_1R in microglia in the context of ischemic stroke. In the tMCAO model, an early and modest increase in CB_1R expression has been described in microglia after ischemic damage in the ipsilateral hemisphere (Schmidt et al., 2012). Moreover, CB_1R activation by 1 mg/kg i.p. administration of ACEA in a pMCAO model, not only reduces lesion volume, but also reduces glial reactivity, by decreasing the number of lectin-positive cells. Notably, it also reduced the number of microglial cells with amoeboid morphology in favor of cells with a more branched morphology, both in the short and long term (Caltana et al., 2015). These data, together with those previously mentioned (Lou et al., 2018; Navarro and Borroto-Escuela, 2018), indicate that the study of this receptor and its function in relation to the phenotypic polarization of microglia should be further explored.

In recent years, CBD has gained special importance in the context of ischemic brain injury (Hayakawa et al., 2010; Fernández-Ruiz et al., 2015; Mori et al., 2017, 2021; Martínez-Orgado et al., 2021; Yokubaitis et al., 2021; Khaksar et al., 2022). CBD is a multitarget molecule with a complex pharmacology. Although it initially showed a low affinity for CB receptors, it has subsequently been shown that it can act as an antagonist of CB_1R and CB_2R at low concentrations (Pertwee, 2008; Navarro and Reyes-Resina, 2018). Noteworthy, CBD also has an affinity for other ECS-related receptors such as GPR55, $5\text{-}HT_{1A}$, TRPA1, TRPV1-4 or PPARγ (Pertwee, 2008; Britch et al., 2021). In the different animal models of stroke used, it has been shown that CBD treatment improves the motor deficits observed after ischemic damage and reduces the area of injury (Hayakawa et al., 2004; Schiavon et al., 2014; Ceprián et al., 2017; Mori et al., 2017). In adult animals, CBD facilitates neuroplasticity after tMCAO by decreasing glial reactivity, reducing both the number of reactive microglia and astrocytes in the hippocampus, and favoring the release of neurotrophic factors, such as brain-derived neurotrophic factor (Schiavon et al., 2014; Mori et al., 2017). Interestingly, neuroprotective effects of CBD have also been observed in a neonatal HI stroke model, both in the short and long term. Besides, there is an improvement in the performance of motor tests despite the fact that no decrease in lesion volume is observed. In the same study, administration of 5 mg/kg of CBD, also decreased glial reactivity, decreasing the number of

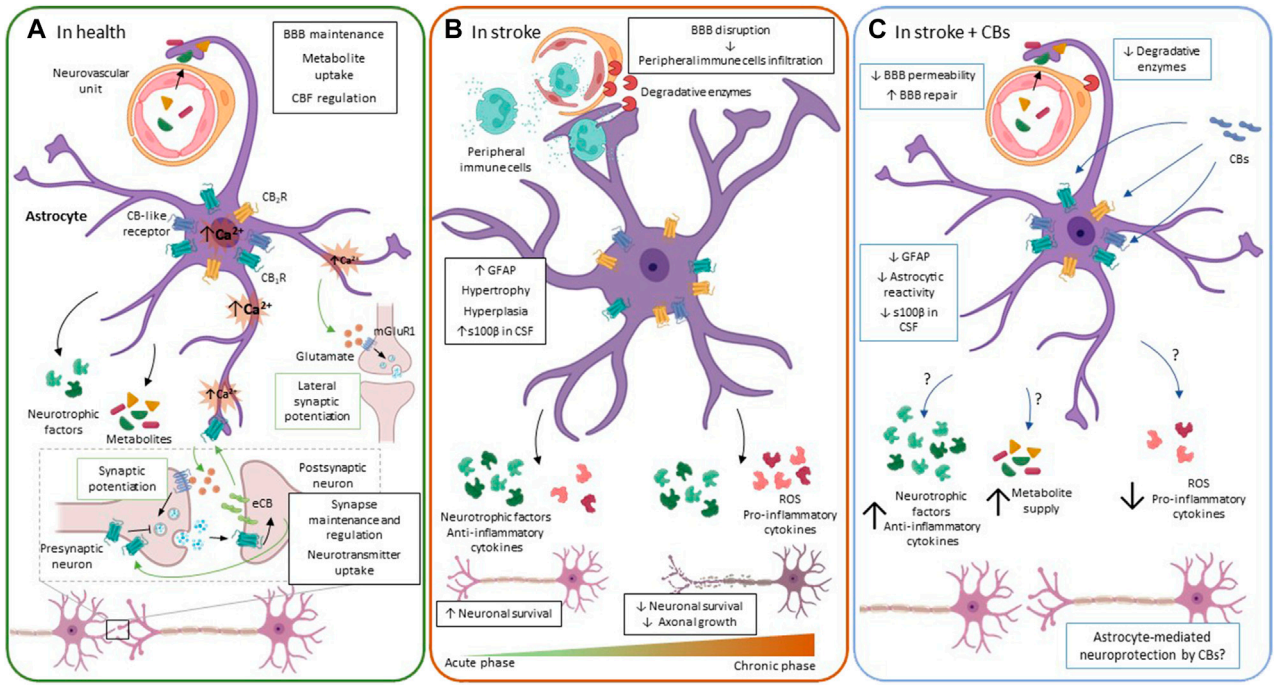

FIGURE 2 | The ECS functioning in astrocytes. **(A).** In physiological conditions, astrocytes regulate processes that are crucial for neuronal functioning, e.g., providing metabolic and trophic support for neurons, controlling CBF, BBB permeability, and regulating synapse maintenance and plasticity, among others. Astrocytes participate in synapse plasticity through the tripartite synapse. When neurotransmitter is released by presynaptic neurons, it increases intracellular Ca^{2+} both in post-synaptic terminals and in astrocytes. In post-synaptic neurons, Ca^{2+} elevation induces eCB release to the extracellular space, inhibiting neurotransmitter release from the presynaptic neuron. In astrocytes, eCB binding to their receptors mobilize Ca^{2+} from internal stores, triggering gliotransmitter release, i.e., glutamate, which in turn promotes mGluR1-mediated neurotransmitter release from the presynaptic neuron, a phenomenon called synaptic potentiation. Besides, as Ca^{2+} spreads intracellularly in the astrocyte, it is able to release glutamate at distal points, stimulating synapsis that are at a certain distance from the synapse that was initially stimulated. This results in the so-called lateral synaptic potentiation. **(B).** During the acute/subacute phase after an ischemic event, astrocytes undergo significant morphological and functional changes like hypertrophy, hyperplasia and increased GFAP levels. To increase neuronal survival, astrocytes release neurotrophic factors and anti-inflammatory cytokines. Nevertheless, they also release pro-inflammatory cytokines that negatively affect neuronal survival. Moreover, at the neurovascular unit, astrocytes upregulate the expression of surface receptors and enzymes that are strongly associated with inflammatory responses that actively contribute to BBB disruption and leukocyte infiltration into the CNS, becoming a source of inflammation if this process becomes chronic. Over time, reactive glial cells rearrange, creating a barrier composed of densely packed cells that separate the ischemic core from the penumbra. **(C)**. Main molecular changes induced in astrocytes by CBs after stroke. CB modulation of astrocyte reactivity includes reduced GFAP immunoreactivity and release of catalytic enzymes, leading to attenuation of BBB disruption. These molecules also increase neuronal survival after ischemia; however, it remains unclear whether the neuroprotection exerted by CBs is mediated by astrocytes. Green arrows and boxes: eCB-mediated effects; blue arrows and boxes: CB-mediated effects. BBB: brain-blood barrier; CB_1R: cannabinoid receptor 1: CB_2R: cannabinoid receptor 2; CBs: cannabinoids; CSF: cerebrospinal fluid; eCB: endocannabinoids; ROS: reactive oxygen species.

microglial cells in the ipsilateral hemisphere (Ceprián et al., 2017). These results are similar to those obtained in neonatal models of HI in piglets and in rodents. In those studies, 1 mg/kg of CBD, shows neuroprotective effects by decreasing neuronal death and anti-inflammatory effects by modulating cytokine release and decreasing the number of reactive astrocytes and microglia after HI injury (**Figure 1C**) (Lafuente et al., 2011, 2016; Pazos et al., 2012, 2013; Mohammed et al., 2017; Barata et al., 2019). CBD appears to modulate microglial polarization by promoting a less amoeboid and more branching phenotype (Mohammed et al., 2017; Barata et al., 2019). Several pieces of evidence demonstrate the multitarget effect of CBD in stroke and/or HI models involving the CB_1R, CB_2R, GPR55, 5-HT_{1A}, and PPARγ receptors (Mishima et al., 2005; Castillo et al., 2010; Pazos et al., 2013; Mori et al., 2021). Since microglia express most of these receptors, this strengthens the idea of the important role played by the ECS in the polarization, cell renewal and migration of microglia particularly in the context of stroke. However, there are still many unknowns about the precise role of the ECS in microglial polarization and function and the molecular mechanisms involved in those processes, which must be addressed to find new CB-based therapies for stroke treatment.

ASTROCYTES

Astrocytes are one of the most numerous cell populations in the CNS, where they exert many crucial homeostatic functions that allow the development and proper function of this system and the brain cells (Sofroniew and Vinters, 2010; Clarke and Barres, 2013; Verkhratsky and Nedergaard, 2018). These functions include the regulation of extracellular concentrations of ions and neurotransmitters, the formation and elimination of synapses, cytokine and neurotrophin secretion, CBF and metabolism

regulation, among others (**Figure 2A**) (Sofroniew, 2020). Classically, astroglial cells have been classified in two different groups according to their location and morphology with protoplasmic astrocytes located mainly in gray matter, and fibrous astrocytes predominantly found in white matter (Miller and Raff, 1984). However, over the last years, increasing evidence has changed this conception and now it is acknowledged that astrocytes are highly heterogeneous, exhibiting important morphological and physiological differences among brain regions and significant differences in gene expression and protein content (Molofsky et al., 2012; Höft et al., 2014; John Lin et al., 2017; Miller, 2018). Thus, astrocyte functions vary depending on the neural populations they are associated with and/or the biological environment surrounding them. Moreover, astrocyte heterogeneity is species-dependent, with higher morphological and possibly functional complexity in the human brain compared to rodents (Kettenmann and Verkhratsky, 2008). In the healthy brain, astroglial cells provide structural support for neurons, actively participating in the regulation of neuronal growth and synapse formation, maturation, maintenance, and pruning (Sofroniew and Vinters, 2010; Clarke and Barres, 2013). They also play an active role in synaptic transmission, by being part of the tri-partite synapse, they support neuronal signaling, neurotransmitter uptake regulation, gliotransmitter and calcium release, modulating in this way synaptic plasticity and learning (Pereira and Furlan, 2010; Sofroniew and Vinters, 2010; Verkhratsky et al., 2012). One important function of astrocytes is their involvement in the maintenance and functionality of the BBB, particularly via astrocyte endfeet, together with endothelial cells and pericytes (Alvarez et al., 2013; Siqueira et al., 2018). Astrocytes are responsible for the selective diffusion of molecules through the BBB, allowing ion diffusion and regulating the entry of small molecules and water to the CNS. At the same time, these cells regulate the supply of oxygen and nutrients to neurons by taking up glucose, lactate, or ketone bodies from the bloodstream and transferring them to neurons as a source of energy, and/or by releasing trophic factors that are essential for neuronal survival (Rouach et al., 2008; Alvarez et al., 2013; Dezonne et al., 2013; Sotelo-Hitschfeld et al., 2015; Benarroch, 2016). In addition, these cells directly regulate BBB function by releasing molecules i.e. sonic hedgehog, nitric oxide, and vascular endothelial growth factor, which are involved in tight junction development, vasodilation, and angiogenesis (Nian et al., 2020).

In homeostatic conditions, astrocytes are in a quiescent or resting state and become reactive in response to different stimuli or insults to the CNS like infections, trauma, neurodegenerative diseases, and stroke (Moulson et al., 2021). Astrocyte reactivity is in the first instance a physiological response that involves phenotypic and molecular changes aimed at restoring homeostasis and neurological function through diverse mechanisms (Sofroniew, 2020). However, in pathological conditions, these cells have biphasic functions, being beneficial or detrimental through cell-autonomous or non-cell-autonomous mechanisms, depending on the biological context. For example, if the initial insult is not resolved and becomes chronic, astrocytes can contribute to exacerbating the damage either by losing/gaining functions (Sofroniew, 2020). Recently, it was demonstrated the existence of at least two different types of reactive astrocytes (Zamanian et al., 2012; Liddelow et al., 2017). Under neuroinflammatory conditions, astrocytes polarize toward an A1-neurotoxic reactivity state, expressing different pro-inflammatory proteins and possibly other toxic molecules that induce synapse loss and neuronal death, whilst A2-neuroprotective reactive astrocytes are induced after an ischemic insult and promote neuronal survival (Liddelow et al., 2017; Guttenplan et al., 2021). Nevertheless, late discoveries on regional and local heterogeneity of astrocytes are shedding light on their complex developmental, morphological, molecular, physiological, and functional diverseness, modifying this dual classification of astrocytes (for a review on this topic see (Pestana et al., 2020). Newer hypotheses sustain the existence of mixed populations (subtypes) of astroglial cells that coexist in the resting state with a continuum in the intensity of reactivity states (Miller, 2018; Khakh and Deneen, 2019; Pestana et al., 2020; Sofroniew, 2020). Thus, the existence of different astrocyte subtypes in the resting state could explain different responses to the same insult, resulting in a variety of reactive states, an idea supported by data from various neurodegenerative disease models (Clarke et al., 2018; Yun et al., 2018; Smith et al., 2020). As the knowledge of astrocyte biology is constantly evolving due to the development and availability of new tools/experimental approaches, like single-cell transcriptomics, which provides valuable data on astrocyte heterogeneity and reactivity (Moulson et al., 2021), we could expect more refined and possibly unified concepts in the forthcoming years, as recently discussed by Escartin et al. (2021).

Astrocyte Function in Ischemic Stroke

Similar to what occurs with other CNS cells, astrocytes undergo significant morphological, molecular, and functional modifications after an ischemic event (**Figure 2B**). These changes are very dynamic and rely not only on astrocytes but also on interactions and intercommunication with other CNS cells, notably neurons, microglia, and oligodendrocytes. In pathological circumstances like stroke, injured neurons and other cells communicate with astrocytes by releasing cytokines and other molecules, triggering astrocyte activation and causing profound changes in the synthesis and expression of other molecules (Sofroniew, 2009; Scarisbrick et al., 2012). After the stroke, there is a massive response of astrocytes, called reactive astrogliosis, but the timeline of astroglial activation is slower than in neurons or in microglia (Revuelta et al., 2019). Reactive astrogliosis is characterized by an increased expression of the glial fibrillary acidic protein (GFAP) and changes in cell morphology like hyperplasia and hypertrophy (Sofroniew, 2009; Scarisbrick et al., 2012; Kozela et al., 2017). Moreover, activated astrocytes release pro-inflammatory cytokines, like IL-1β, IL-6, and TNF-α, modulating the immune response and actively participating in the inflammatory process initiated after an ischemic event (Zamanian et al., 2012). Reactive astrocytes also synthesize and release some anti-inflammatory cytokines and neurotrophic factors that protect neurons, enhance neuronal synapses and plasticity, and improve functional

outcomes after the stroke (Swanson et al., 2004; Li et al., 2008; Cekanaviciute et al., 2014). Noteworthy, astrocyte response after an ischemic event will significantly depend on the astrocyte subtype and possibly on the brain region affected. On the one hand, proliferative reactive astrocytes will increase their number and form limitant borders surrounding the infarcted area, constituting in conjunction with other cells a physical barrier around the necrotic tissue in the brain. These limitant borders allow setting boundaries to the damaged area, releasing molecules that promote neuronal growth and survival, and avoiding the spreading of neuroinflammation (Swanson, Ying and Kauppinen, 2004; Li et al., 2008; Huang et al., 2014; Sofroniew, 2020). However, these densely packed reactive astrocytes are also considered a source of pro-inflammatory molecules, ROS, and neurotoxicity that ultimately inhibit axonal regeneration (Gris et al., 2007). On the other hand, nonproliferative reactive astrocytes acquire diverse reactivity states. In contrast to microglial cells, which are very mobile, these astrocytes do not migrate from the penumbra to the ischemic core, instead, they polarize their processes to be able to exert their phagocytic abilities (Huang et al., 2014), having as well the ability to change their gene expression pattern and functions depending on their particular context. If the acute initial insult is not resolved and becomes chronic, nonproliferative reactive astrocytes can contribute to exacerbating the damage either by losing/gaining functions, as mentioned lines above (Sofroniew, 2020).

Another major event that occurs after stroke is BBB integrity disruption (Fernández-López et al., 2012; Arba et al., 2017), which favors ROS generation, the infiltration of inflammatory cells like leukocytes, and the production of proteolytic enzymes that ultimately exacerbate brain edema and neuroinflammation (**Figure 2B**) (Fernández-López et al., 2012; Arba et al., 2017). The BBB is constituted by endothelial cells, pericytes, and astrocytes. Some evidence indicates that changes in astrocytic proteins involved in BBB maintenance like metalloproteinase-2 and the toll-like receptor 4/metalloproteinase-9 (TLR4/MMP9) signaling pathway are upregulated after stroke, contributing to the disruption of astrocyte-endothelial junctions, consequently altering BBB permeability (Liu et al., 2017; Rosciszewski et al., 2018).

There are apparently contradictory roles of reactive astrocytes after stroke regarding the extent of their putative toxic or protective effects that could be difficult to measure, but several studies using $GFAP^{-/-}$ mice in models of stroke and acute trauma are shedding some light on this matter (Nawashiro et al., 2000; Wilhelmsson et al., 2004; Li et al., 2008). For example, $GFAP^{-/-}$ mice showed an impaired physiological response to ischemia in the pMCAO with transient carotid artery occlusion (CAO) model (Nawashiro et al., 2000), and $GFAP^{-/-}Vimentin^{-/-}$ mice had a higher infarct area and decreased glutamate transport by astrocytes than wild type mice after MCA transection (Li et al., 2008). Besides, $GFAP^{-/-}Vimentin^{-/-}$ mice subjected to an acute entorhinal cortex lesion model showed an attenuated astrocyte reactivity response, evidenced by fewer processes and dysregulation of endothelin B receptors, which allowed synaptic recovery in the hippocampus, changes that were associated with improved post-traumatic regeneration (Wilhelmsson et al., 2004).

Recently, Rakers and co-authors explored in more detail astrocyte reactivity in mice subjected to the tMCAO stroke model and found an upregulation of the canonical markers of reactive astrogliosis, the so-called pan-reactive transcripts, and a prominent increase of A2-reactivity specific transcripts (Rakers et al., 2019). Their observations suggest that these A2-like reactive astrocytes protect neurons and promote neuroregeneration after stroke. Moreover, they also observed significant changes in the expression of genes related to extracellular matrix composition, cell migration, cell-cell adhesion, and glial scar formation, further indicating that A2-astrocytes may help contain and restrict neuroinflammation and support neuronal survival (Rakers et al., 2019). Nevertheless, among the upregulated genes they found were several genes related to neuroinflammation, the complement cascade, apoptosis, and leukocyte transendothelial migration. Thus, they observed the coexistence of genes with potentially neurotoxic and neuroprotective functions in astrocytes from brain homogenates of mice subjected to tMCAO. Whether this phenomenon is due to the presence of astrocytes with a spectrum of different phenotypes that vary from neuroprotective to neurotoxic, or due to the activation of neuroprotective and neurotoxic signaling pathways within individual astrocytes remains to be determined.

Astrocytes and the ECS

The presence of CB_1R, CB_2R, and other CB-like receptors has been demonstrated in astrocytes (Pazos et al., 2005; Sheng et al., 2005; Navarrete and Araque, 2008; Stella, 2010; Yang et al., 2019; Cristino et al., 2020). Besides, these glial cells are able to produce and release the endogenous ligands 2-AG and AEA and also express the intracellular degradation enzymes FAAH and MAGL (Stella et al., 1997; Walter et al., 2002; Vázquez et al., 2015; Grabner et al., 2016). CB_1R activation in astrocytes not only controls their metabolic functions and signaling but also regulates synaptic transmission, through the tripartite synapse (Gorzkiewicz and Szemraj, 2018). When the electrical impulse causes neurotransmitter release from a presynaptic neuron, depolarization of the postsynaptic neuron occurs, leading to eCB release into the synaptic cleft and their binding to receptors located both in neurons and astrocytes (Stempel et al., 2016). While eCB binding to CB_1R inhibits neurotransmitter release in presynaptic neurons, a process known as retrograde signaling (Stempel et al., 2016), it increases intracellular Ca^{2+} levels in neighboring astrocytes (Navarrete and Araque, 2010; Covelo and Araque, 2016). This Ca^{2+} increase stimulates glutamate release from astrocytes, which in turn causes a synaptic potentiation through mGluR1 receptors located in the presynaptic neuron. As the intracellular Ca^{2+} signal extends within astrocytes, it stimulates glutamate release in distal astrocyte regions, modulating in this way the synaptic transmission of many lateral synapses to the original source of eCBs (**Figure 2A**) (Navarrete and Araque, 2010; Covelo and Araque, 2016). In addition, CB_1R activation in astrocytes also contributes to the regulation of CBF and the energy supply to neurons by increasing the glucose oxidation rate and ketogenesis (Shivachar et al., 1996; Bermudez-Silva et al., 2010; Stella, 2010; Jimenez-Blasco et al., 2020). Notably, most perivascular

astrocytes express CB_1R, highlighting their importance for CBF and metabolism (Rodriguez et al., 2001). On the other hand, despite CB_2R expression in astrocytes is limited under physiological conditions, data show a significant upregulation of this receptor and the endocannabinoid tone in general upon different insults. Moreover, it also changes in neuroinflammatory conditions, suggesting an important role of the astroglial ECS in processes associated with brain damage and/or recovery (Shohami et al., 2011; Fernández-Ruiz et al., 2015; Cassano et al., 2017). In this sense, the study of different CBs has attributed them anti-oxidant and anti-inflammatory effects in experimental models of several pathologies (Cristino et al., 2020). In astrocytes, CBs regulate astrocyte activation and astrocyte-mediated neurotoxicity by reducing the release of inflammatory mediators and increasing prosurvival factors (Fernández-Ruiz et al., 2015; Estrada and Contreras, 2020). In different experimental settings, ECS modulation in astrocytes reduces TNF-α and IL-1β levels, which are upregulated following various inflammatory challenges (Grabner et al., 2016; Labra et al., 2018; Rodríguez-Cueto et al., 2018; Jia et al., 2020), suggesting that modulation of these cells with CBs could be contributing to neuroprotection through non-cell-autonomous mechanisms.

Astrocyte ECS Pharmacological Modulation in Stroke

After an ischemic event, astrocytes are more resilient than neurons, being important for the post-acute phase because they preserve their viability and remain metabolically active both at the infarct core and penumbra regions (Thoren et al., 2005; Gürer et al., 2009). Considering the critical functions of these cells in the CNS, astrocytes are gaining notoriety as possible therapeutic targets for different neurological conditions including hypoxia and/or brain ischemia. At the same time, given their potent anti-oxidant and immunomodulatory effects, numerous studies have focused on the neuroprotective effects of CBs, mainly CBD, for stroke therapy (England et al., 2015). However, limited evidence is available concerning the mechanisms by which CBs modulate astrocyte function and astrocyte-mediated effects in the context of ischemic stroke. Here, we summarize the findings regarding the effects of CBs on astrocyte activation in the tMCAO, pMCAO and related models in adult animals, the HI model in neonate animals, and the oxygen and glucose deprivation/re-oxygenation (OGD/R) *in vitro* model of stroke.

In adult animals subjected to transient or permanent ischemia, the most consistent outcome in astroglial cells is increased astrogliosis, i.e., high GFAP immunoreactivity in CNS areas such as the motor cortex, the striatum, the hippocampus, or the spinal cord. Astrocytes with longer and wider projections, and other parameters that suggest a functional impairment of these cells are also observed (**Figure 2B**) (Hayakawa et al., 2008, 2009; Schiavon et al., 2014; Caltana et al., 2015; Kossatz et al., 2016; Ceprián et al., 2017; Jing et al., 2020). The inhibition of stroke-induced reactive gliosis was also observed in the pMCAO mouse model at 7 and 28 days after administering 1 mg/kg of ACEA (Caltana et al., 2015). In that study, CB_1R expression was downregulated in ischemic conditions, which could be contributing to increase inflammation, neuronal degeneration, and astroglial reactivity, suggesting that upregulation of the eCB tone with ACEA could help revert these deleterious effects (Caltana et al., 2015). On the other hand, GFAP staining was significantly elevated in different brain areas of both adult wild type and $CB_2R^{-/-}$ mice after HI (Kossatz et al., 2016), and in rats subjected to HI in the spinal cord (Jing et al., 2020). In the study by Jing et al. (2020), i.p. pretreatment of rats with 1 mg/kg of the CB_2R selective agonist JWH-133 1 h before ischemia not only inhibited astrocyte reactivity, determined by GFAP immunostaining but also reduced perivascular expression of TLR4/MMP9. Notably, TLR4 upregulation in astrocytes has been associated with a pro-inflammatory reactivity phenotype in astrocytes and with BBB disruption in the cortical devascularization brain ischemia model (Rosciszewski et al., 2018). The TLR4/MMP9-mediated reduction of astrocyte reactivity after ECS activation via CB_2R is of special interest for stroke, as it has been suggested elsewhere that attenuation of the inflammatory process could be neuroprotective after tMCAO in rats (Piao et al., 2003). Although it remains to be determined whether the limitation of inflammation in those experimental conditions is mediated by astrocytes. In summary, in addition to having neuroprotective effects, the administration of different CB compounds like CBD, ACEA, and JWH-133 at various doses, duration of administration, and delivery methods prevented the increase in GFAP immunoreactivity, limiting astrocyte activation (Hayakawa et al., 2008, 2009; Schiavon et al., 2014; Caltana et al., 2015; Ceprián et al., 2017). In the majority of the aforementioned studies, the reduction of astroglial activation was observed with the administration of CBs that act through different receptors. For instance, while ACEA and JWH-133 are CB_1R and CB_2R agonists, respectively, it has been demonstrated that CBD preferentially binds to other receptors. Nevertheless, the precise molecular mechanism(s) by which the activation of the ECS is able to limit astrogliosis after stroke is not known yet and remains to be addressed experimentally. Moreover, there is scarce direct evidence showing that the modulation of astrocyte activity with CBs increases neuronal survival after stroke. Even so, a recent study in mice has shown that the increase in the eCB tone through the inhibition of FAAH and MAGL with the compound JZL195 (20 mg/kg, i.p.), induces long-term depression (LTD) at CA3-CA1 synapses in the hippocampus, and confers astrocyte-mediated neuroprotection after stroke (Wang et al., 2019). In that study, JZL195-induced LTD was used as a preconditioning insult to determine its potential neuroprotective effect against subsequent ischemia. Noteworthy, it was observed that preconditioning before tMCAO increased the number of surviving neurons through a mechanism dependent on a sequential activation of astroglial CB_1R, and not neuronal CB_1R, and postsynaptic glutamate receptors (Wang et al., 2019).

Over the years, the neuroprotective effects of CBD have been clearly demonstrated in experimental models of HI in rodents and notably in newborn pigs (Kicman and Toczek, 2020), but only a limited number of studies have characterized/evaluated astroglial reactivity as a neurological outcome. Evidence of GFAP

immunoreactivity reduction after CBD treatment (5 mg/kg) has been reported both in newborn rats after tMCAO (Ceprián et al., 2017), and in newborn mice (1 mg/kg) after HI (Mohammed et al., 2017). In addition to decreasing perilesional gliosis volume in rats, CBD treatment limited astrocyte dysfunction, evidenced by the recovery of the *ex vivo* H^+-MRS myoinositol/creatinine ratio, which had diminished after tMCAO (Ceprián et al., 2017). However, another work found that the number of activated astrocytes and IL-1β expression levels were downregulated in $TRPV1^{-/-}$ neonatal mice following HI, indicating that TRPV1 is modulating astrocyte reactivity. These results might suggest that *in vivo*, the neuroprotective effects of CBD may not involve TRPV1 binding, at least in astrocytes (Yang et al., 2019). On the other hand, in newborn pigs, some data indicate that CBD modulates astrogliosis after HI-induced brain damage. In the short term, i.v. administration of CBD (1 mg/kg) after acute HI promotes an increase in the number of astrocytes in the peri-infarct area (Pazos et al., 2013). However, by using the same animal model but conducting histological analyses 72 h after the induction of HI, CBD treatment (0.1 mg/kg) preserved the number, size, and morphology of GFAP-positive astrocytes in newborn pigs (Lafuente et al., 2011). Apart from analyzing GFAP reactivity by immunohistochemistry, some studies have detected high levels of the protein S100β, a possible biomarker of astrocyte damage, in the cerebrospinal fluid (CSF) of piglets after HI (Lafuente et al., 2011; Garberg et al., 2016, 2017). Noteworthy, in only one of those studies CBD administration decreased S100β levels (Lafuente et al., 2011), but this result might be explained by the lack of neuroprotective effects of i.v. administration of 1 mg/kg and 50 mg/kg of CBD observed in the works by Garber and co-authors (Garberg et al., 2016, 2017). Future research will clarify the ability of CBD to revert or not the increase in S100β levels observed after HI.

The most widely used experimental paradigm to investigate *in vitro* the effects of ischemia is OGD/R. Given the relevance of the BBB and the neurovascular unit in this pathology, the status of the ECS, as well as the effects of CBs have been studied in BBB models. In normoxia, the ECS has a modulatory role in BBB permeability in co-cultures of endothelial cells and astrocytes. In specific, AEA (10 μM) and OEA (10 μM) decrease BBB permeability through CB_2R, TRPV1, CGRP, and PPARα receptors (Hind et al., 2015). Besides, in astrocyte monocultures, CBD diminishes IL-6 and vascular cell adhesion molecule-1 and increases lactate dehydrogenase release (LDH) values when administered at high concentrations (10 μM) (Hind et al., 2016). In these same *in vitro* BBB models, the eCB-like molecules OEA, PEA, and virodhamine (all 10 μM), as well as CBD (100 nM and 10 μM) attenuated the increase in BBB permeability induced by OGD/R (Hind et al., 2015; Hind et al., 2016). In a similar way, it was recently demonstrated that cannabidivarin (CBDV) and cannabigerol (CBG), two phytocannabinoids, are protective against OGD/R in human endothelial cells, astrocytes, and pericytes, the different cells that form the BBB (Stone et al., 2021). In astrocyte monocultures, CBG (10 nM–3 μM) and CBDV (30 nM, 1 and 3 μM) diminished IL-6 levels after OGD/R. And 1 and 3 μM of CBG and 10 nM, 1 and 3 μM of CBDV, reduced OGD/R-induced levels of LDH release, but the mechanisms by which these two compounds provide protection need to be further investigated (Stone et al., 2021). Despite the evidence indicating an active role of the ECS in regulating astrocyte metabolism *in vitro*, there is a generalized lack of evidence regarding the newest findings on the role of astrocytes as neuroprotectors or neurotoxic in this and other *in vitro* models of stroke or in *ex vivo* experiments. Overall, the evidence available so far indicates that the modulation of astrocyte function/reactivity with CBs could be used as a possible therapeutic approach to limit/arrest neurotoxic processes or promote recovery mechanisms in ischemic stroke (**Figure 2C**).

OLIGODENDROCYTES

Oligodendrocytes are the myelinating cells of the CNS. The myelin layers, composed mostly of water and lipids but also proteins, enwrap the axon and form a multilamellar compacted myelin sheath, protecting and isolating the axon (Morell and Quarles, RH, 1999). Myelin electrically isolates axons, allowing the saltatory impulse propagation and speeding the impulse transmission (Nave and Trapp, 2008). Besides this structural function, oligodendrocytes play a key role in the metabolic support of axons by producing lactate that is then transported to axons (**Figure 3A**) (Fünfschilling et al., 2012; Jha and Morrison, 2020). OPCs are widely distributed throughout the adult rat brain and participate in the modulation of the BBB and in angiogenesis (Dawson et al., 2003; Maki et al., 2015; Maki, 2017). Thus, oligodendrocytes are vital for brain circuit activity and neuron support, and their death and later remyelination failure have deleterious consequences in stroke outcome.

Oligodendrocytes in Ischemic Stroke

Although the majority of studies on stroke focus on gray matter damage, the relevance of white matter injury has rapidly grown over the last years. Noteworthy, white matter injury occupies approximately half of the infarct area after a stroke (Ho et al., 2005), and myelinating disturbances resulting from stroke directly correlate with a poorer cognitive and motor outcome (Wang et al., 2016).

Oligodendrocytes are particularly susceptible to stroke due to their sensitivity to excitotoxicity and oxidative stress. In these cells, the expression of AMPA and NMDA receptors is developmentally regulated and correlates with their maturation from OPCs to mature myelinating oligodendrocytes (Káradóttir et al., 2005; Salter and Fern, 2005; Spitzer et al., 2019). The activation of AMPA and NMDA receptors in oligodendrocytes induces the retraction of their processes and causes oligodendrocyte cell death in the OGD model, effects that are prevented by blocking both receptors (Salter and Fern, 2005). Oligodendrocytes are also sensitive to the increase in the excitatory neurotransmitter ATP that takes place in stroke, through the P2X7 receptor (Domercq et al., 2009).

Oligodendrocytes are the brain cells with the highest concentration of iron, which is used to synthesize myelin (Reinert et al., 2019). This makes them extremely sensitive to variations in oxidative stress, as nicely reviewed elsewhere

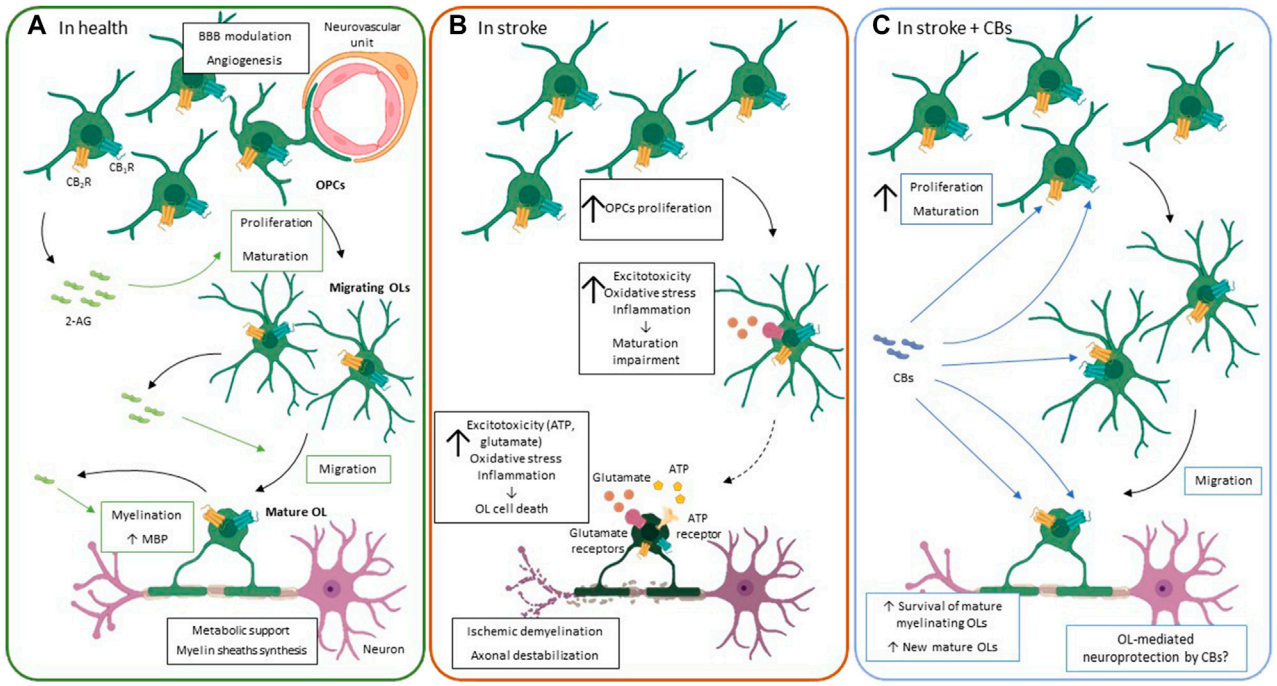

FIGURE 3 | The ECS functioning in oligodendrocytes. **(A).** Under physiological conditions, oligodendrocytes play a key role in the metabolic support of axons, myelin sheath synthesis and BBB regulation, among others. In the CNS, the endocannabinoid system, particularly 2-AG, is involved in oligodendrocyte proliferation, maturation, migration and myelination of oligodendrocytes. 2-AG is produced in an autocrine manner and exerts its effects through its binding to CB_1R and CB_2R. **(B).** An ischemic event induces mature oligodendrocytes cell death due to the high sensitivity of these cells to: 1) glutamate and ATP receptor-induced excitotoxicity, 2) oxidative stress, i.e., high iron content and deficient antioxidant system, and 3) inflammation, through release of cytokines like TNF-α. In an attempt to repair the damage caused by stoke there is a strong oligoproliferative response. However, the maturation of these new oligodendrocytes is impaired, and they do not reach the mature myelinating oligodendrocyte stage, perpetuating myelinating deficits that contribute to motor and sensitive impairment observed after stroke. **(C).** Although the evidence of the oligoprotective potential of CBs after stroke is scarce, they seem to reduce the myelination impairment by 1) reducing oligodendrocyte cell death and 2) promoting oligodendrocyte proliferation and maturation into myelinating oligodendrocyte after the insult. Green arrows and boxes: eCB-mediated effects; blue arrows and boxes: CB-mediated effects. 2-AG: 2-Arachidonoylglycerol; BBB: blood-brain barrier; CB_1R: cannabinoid receptor 1: CB_2R: cannabinoid receptor 2; CBs: cannabinoids; MBP: myelin binding protein; OL: oligodendrocyte; OPC: oligodendrocyte progenitor cell.

(Bresgen and Eckl, 2015). Furthermore, mature oligodendrocytes and, especially OPCs, are characterized by having limited antioxidant defenses (Fragoso et al., 2004; Spaas et al., 2021). This vulnerability is particularly strong in earlier stages of oligodendrocyte maturation, which may affect the stroke-induced oligoreparative response (Fragoso et al., 2004). Confirming this high oligodendrocyte sensitivity to stroke, oligodendrocyte cell death can be identified *in vivo* as early as 30 min after stroke (Pantoni et al., 1996). Meanwhile, alterations in the morphology of oligodendrocytes that survive have been described 24 h after insult (Mages et al., 2019). On the other hand, stroke induces a strong proliferative response of OPCs, which migrate to the affected area and mature into myelinating oligodendrocytes (**Figure 3B**) (Zhang et al., 2011; Bonfanti et al., 2017). This proliferative response seems to be age-dependent (Dingman et al., 2018). However, the proportion of the newly formed oligodendrocytes that reach a mature stage after stroke is surprisingly low (Bonfanti et al., 2017; Dingman et al., 2018). The mechanisms of this developmental impairment are not yet clear, although excitotoxicity, inflammation, and oxidative stress seem to play a key role (**Figure 3B**).

Oligodendrocytes and the ECS

The ECS modulates oligodendrocyte maturation at every step: from the proliferation of OPCs, to their migration and maturation until the final step of myelination (Gomez et al., 2010; Fernández-López et al., 2012; Sanchez-Rodriguez et al., 2018; Tomas-Roig et al., 2020). In these cells, CB receptors are found along white matter tracts, and the first experiments activating CB_1R showed that it promotes myelin basic protein (MBP) expression in the rat subcortical white matter (Herkenham et al., 1991; Arévalo-Martín et al., 2007). Particularly important for oligodendrocyte development is the constitutive production of 2-AG (Gomez et al., 2010, 2015; Sanchez-Rodriguez et al., 2018). The expression of the 2-AG synthesis enzymes, DAGLα and DAGLβ, is higher in OPCs than in mature oligodendrocytes, whereas the degradation enzyme MAGL is upregulated in mature oligodendrocytes The effect of 2-AG in these cells is mediated by CB_1R/CB_2R (**Figure 3A**) (Gomez et al., 2010). The administration of different antagonists of these receptors reduces oligodendrocyte proliferation and migration. It also impairs oligodendrocyte maturation, revealed by a reduced arborization of immature oligodendrocytes, and myelin

production *in vitro*, with lower expression levels of MBP and myelin-associated glycoprotein (Gomez et al., 2011, 2015; Sanchez-Rodriguez et al., 2018). Actually, $CB_1R^{-/-}$ animals are characterized by having less cell proliferation, evidenced by $BrdU^+$ cells, in the subventricular zone (SVZ) and in the dentate gyrus of rats (Jin et al., 2004). Although the molecular pathways associated with these effects are not well characterized, the PI3K/mTOR pathway has been proved to be involved in the proliferative effect of 2-AG in oligodendrocytes, and the ERK/MAPK signaling pathway has been associated with oligodendrocyte maturation (Gomez et al., 2010, 2011).

Interestingly, the pharmacological modulation of the ECS has direct effects on oligodendrocyte maturation and migration, and increased survival of OPCs has been observed in models of white matter injury. The *in vitro* administration of the MAGL inhibitor JZL-184 at 1 mg/kg, which increases 2-AG levels, accelerates oligodendrocyte differentiation, and increases the percentage of migrating cells (Gomez et al., 2010; Sanchez-Rodriguez et al., 2018). Indeed, it has been observed that the direct administration of 2-AG promotes oligodendrocyte migration (Sanchez-Rodriguez et al., 2018). The therapeutic effects of 2-AG have also been described in pathologies like spinal cord injury. For instance, the administration of 5 mg/kg of 2-AG 30 min after a moderate contusive SCI in rats reduced white matter injury and promoted oligodendrocyte survival, even 28 days after injury (Arevalo-Martin, Garcia-Ovejero and Molina-Holgado, 2010). Furthermore, the inhibition of 2-AG degradation with the MAGL inhibitor UCM03025 (5 mg/kg) improved motor impairment and recovered MBP expression in a multiple sclerosis model, with higher $BrdU^+/Olig2^+$ cells, i.e., new OPCs, in the spinal cord of affected mice that were treated with the compound (Feliú et al., 2017).

CB_1R/CB_2R selective agonists or even non-selective agonists, such as WIN55,212-2, also promote OPCs proliferation, oligodendrocyte maturation, with cells showing a more complex morphology, and myelinization, by increasing MBP production (Arévalo-Martín et al., 2007; Gomez et al., 2011, 2015; Tomas-Roig et al., 2020). The daily administration of 0.5 mg/kg of WIN55,212-2 prevented demyelination and promoted remyelination, increasing the number of myelinated axons, in a cuprizone model of demyelination in mice (Tomas-Roig et al., 2016; Tomas-Roig et al., 2020). However, the CB dose should be thoroughly tested, as the daily administration of 1 mg/kg potentiated axonal demyelination, probably due to a downregulation of CB_1R (Tomas-Roig et al., 2016; Tomas-Roig et al., 2020).

CB_2R activation has also been shown to be oligoprotective *in vitro* with the CB_2R agonist BCP. This compound reduced LPS-induced oligodendrocyte death by decreasing oxidative stress and TNF-α (Askari and Shafiee-Nick, 2019). Actually, administration of tetrahydrocannabinol (THC), the main psychoactive compound in *Cannabis sativa*, for 5 days at 3 mg/kg in the cuprizone mouse model, reduced myelin loss and improved motor impairment (Aguado et al., 2021). In this study, electron microscopy analysis showed lower g-ratios in the THC-treated group versus control, indicating that THC effect is on remyelination (Aguado et al., 2021). CBs can also promote oligodendrocyte survival by CB_1R and CB_2R independent mechanisms. For example, 1 μM CBD was able to prevent oligodendrocyte death induced by inflammatory and oxidative stress stimuli through the reduction of endoplasmic reticulum stress in primary cell cultures (Mecha et al., 2012).

In summary, the evidence suggests that, due to its role in promoting oligodendrocyte lineage survival and remyelination, the ECS is a promising therapeutic target for functional recovery after demyelinating pathologies, including stroke.

Oligodendrocyte ECS Pharmacological Modulation in Stroke

Despite the aforementioned data on the possible therapeutic effects of the ECS modulation in oligodendrocytes, very few works have explored either the ECS system itself or the oligoprotective potential of CBs during or after an ischemic event. In agreement with the above-mentioned results, the administration of WIN55,212-2, at the high concentration of 9 mg/kg, increased the proliferation rate of OPCs in the ipsilateral SVZ of adult rats 24 h after pMCAO (Sun and Fang, 2013). Moreover, WIN55,212-2 was also able to increase the number of $NG2^+$-OPCs within the stroke penumbra and reduce the $NG2^+$/caspase-3^+ cells during 14 days post-damage in a pMCAO model, an effect that could be related to the increased expression of CB_1R in that area (Sun and Fang, 2013). Interestingly, this increased proliferation/protection in OPCs seemed to translate into new mature myelinating oligodendrocytes, an effect that was partially mediated by CB_1R (**Figure 3C**). In addition, the amelioration of MBP loss was also prevented via CB_1R activation and that was associated with an increase in the number of myelinated axons and lower g-ratio values (Sun and Fang, 2013; Sun and Fang, 2013). In a rodent model of neonatal HI, 1 mg/kg WIN55,212-2 also promoted oligodendrocyte proliferation in the SVZ up to 14 days after the insult. This increase positively correlated with the presence of new $APC^+/BrdU^+$ mature oligodendrocytes in the injured dorsal striatum observed 28 days after the damage. In addition, an upregulation of CB_2R expression was observed in the SVZ in the short term; however, it is not known whether WIN55,212-2 modulates the expression of this receptor in the SVZ (Fernández-López et al., 2010). This CB-mediated protection of oligodendrocytes and myelin has also been observed with the administration of CBD, a compound with excellent antioxidant and anti-inflammatory properties (Atalay et al., 2019). Notably, the administration of the low dose of 1 mg/kg CBD in a neonatal model of HI was oligoprotective in the ipsilateral cortex and corpus callosum. Similar to what happens in humans, the hypomyelination induced by the insult was directly related to the motor and cognitive impairment outcomes. Interestingly, CBD treatment reduced insult-induced oligodendrocyte impairment and preserved myelin (**Figure 3C**) (Ceprián et al., 2019).

We can conclude from these studies that the modulation of the oligodendroglial ECS is a promising field for the treatment of myelin disturbances associated with stroke and its motor/cognitive sequelae. Although more experimental evidence is

necessary, the results obtained so far in stroke and other pathologies that share key points in pathophysiology, have shown that CBs may help reduce myelin loss, promote oligodendrocyte development and/or recovery, and eventually reduce the behavioral impairment associated with stroke.

CONCLUDING REMARKS

In recent years, significant efforts have been devoted to searching for new therapeutic options aimed at limiting/arresting the post-stroke inflammatory response, including the possibility of modulating glial cells. These cells, mainly microglia and astrocytes, are gaining notoriety as potential therapeutic targets in part because they exert critical functions in the CNS and rapidly respond to the lack of blood supply to the brain, contributing to the subsequent immune response. In this review, we have summarized the role and function of microglia, astrocytes, and oligodendrocytes in homeostatic conditions and their response to harmful challenges like an ischemic event.

The ECS, among other physiological functions, participates in the regulation of the immune system and the inflammatory response in the healthy brain, and substantial evidence suggests a neuroprotective effect after the pharmacological manipulation of this system in stroke. However, the experimental evidence regarding the possible therapeutic effects of manipulating the ECS in glial cells is promising but less abundant. Thus, we have also analyzed the evidence of pharmacologically modulating the ECS on microglia, astrocytes, and oligodendrocytes in the context of ischemic stroke.

As we have reviewed here, glial cells are highly dynamic and complex heterogeneous cells that work synergistically and in a highly coordinated way in the CNS. Their role in the pathophysiology of stroke is extraordinarily complex and depends on the timing after stroke, the affected region, the inherent heterogeneity of glial cells, and the interactions between different cell types. Therefore, we must take into account that similar to what occurs in other pathological conditions, an ischemic event perturbs their functioning both individually and collectively. In this sense, it is fundamental to comprehend and consider that in addition to inducing changes that are region-specific, hypoxia alters neuron-glia intercommunications at all levels. Thus, new approaches targeting glial cells in stroke should also investigate the interplay among all the aforementioned cellular players; microglia-astrocytes-oligodendrocytes-neurons. These future studies should also consider evaluating intercellular interactions at all possible levels, morphological, functional, and even metabolically.

The ECS seems to have a significant role in the modulation of glial cell function, not only on cell reactivity or phenotype polarization but also by promoting cell survival and/or preventing their functional impairment. Notably, all glial cells described in this review express to a greater or lesser degree the different elements that integrate the ECS. Indeed, ischemic stroke induces an imbalance of different elements of the glial ECS that would potentially have an impact on neurons and other glial cells, most probably altering cell-to-cell interactions as well. Recently, microglia-astrocyte crosstalk has gained attention, due to the putative dual effect that these cells have under pathological conditions, being able to incline the balance toward a neuroprotective or a neurodegenerative environment. Thus, it is likely that in addition to having beneficial effects on each cell type individually, the pharmacological manipulation of the ECS would have a positive impact on intercellular interactions that would in turn contribute to inclining the balance toward a neuroprotective microenvironment. However, due to the dual effects reported in astrocytes/microglia in stroke, the precise molecular mechanisms underlying the effects of the ECS modulation in these cells and their interaction with other cells must be thoroughly investigated. Further studies are needed to understand the precise role of the ECS on glial cell function and to consider if CBs could be used as therapeutic agents aimed at protecting glial cells per se or if CB-treated glial cells could be used as a neurorepair strategy for stroke.

Finally, we are now beginning to understand the significance of white matter damage in stroke, the sensitivity of oligodendrocytes to the insult, and the impaired remyelination directly related to stroke's sequelae. In that sense, the ECS and its modulation seem to be a promising target to promote oligodendrocyte survival and remyelination, not only because it directly influences oligodendrocyte maturation and myelination; but also by an indirect influence on astrocytes and microglia, promoting an improvement of the microenvironment that in turn could induce a successful oligodendrocyte remyelinating response.

In summary, due to the profound implication of glial cells in stroke, the pharmacological modulation of the glial ECS could represent a significant advantage to help reduce/limit neuronal damage and stroke-associated sequelae.

AUTHOR CONTRIBUTIONS

Study conception and design: MRP and FL; graphical art: AV-A; analysis and interpretation of literature: AV-A, MC, MP, and FL; draft manuscript preparation: AV-A, MC, PS, MP, and FL. All authors have reviewed and approved the final version of the manuscript.

FUNDING

This work was supported by research grants from Hospital Universitario Fundación Alcorcón (HUFA-15044) to PS and Instituto de Salud Carlos III (PI20/00934, co-funded by Fondo Europeo de Desarollo Regional, FEDER) to FL. AV-A is supported by a contract from Comunidad Autónoma de Madrid (NEUROMETAB-CM, B2017/BMD-3700). The funders had no role in designing or conducting the study.

ACKNOWLEDGMENTS

All schematics were created with Biorender (BioRender.com).

REFERENCES

Aguado, T., Huerga-Gómez, A., Sánchez-de la Torre, A., Resel, E., Chara, J. C., Matute, C., et al. (2021). Δ^9 -Tetrahydrocannabinol Promotes Functional Remyelination in the Mouse Brain. *Br. J. Pharmacol.* 178 (20), 4176–4192. doi:10.1111/bph.15608

Allen, C. L., and Bayraktutan, U. (2009). Oxidative Stress and its Role in the Pathogenesis of Ischaemic Stroke. *Int. J. Stroke* 4 (6), 461–470. doi:10.1111/j.1747-4949.2009.00387.x

Alonso de Leciñana, M., Egido, J. A., and Casado, I. (2014). Guía para el tratamiento del infarto cerebral agudo. *Neurología* 29 (2), 102–122. doi:10.1016/j.nrl.2011.09.012

Alvarez, J. I., Katayama, T., and Prat, A. (2013). Glial Influence on the Blood Brain Barrier. *Glia* 61 (12), 1939–1958. doi:10.1002/glia.22575

Amenta, P. S., Jallo, J. I., Tuma, R. F., and Elliott, M. B. (2012). A Cannabinoid Type 2 Receptor Agonist Attenuates Blood-Brain Barrier Damage and Neurodegeneration in a Murine Model of Traumatic Brain Injury. *J. Neurosci. Res.* 90 (12), 2293–2305. doi:10.1002/jnr.23114

Arba, F., Leigh, R., Inzitari, D., Warach, S. J., Luby, M., and Lees, K. R. (2017). Blood-brain Barrier Leakage Increases with Small Vessel Disease in Acute Ischemic Stroke. *Neurology* 89 (21), 2143–2150. doi:10.1212/WNL.0000000000004677

Arevalo-Martin, A., Garcia-Ovejero, D., and Molina-Holgado, E. (2010). The Endocannabinoid 2-arachidonoylglycerol Reduces Lesion Expansion and White Matter Damage after Spinal Cord Injury. *Neurobiol. Dis.* 38 (2), 304–312. doi:10.1016/j.nbd.2010.02.002

Arévalo-Martín, Á., García-Ovejero, D., Rubio-Araiz, A., Gómez, O., Molina-Holgado, F., and Molina-Holgado, E. (2007). Cannabinoids Modulate Olig2 and Polysialylated Neural Cell Adhesion Molecule Expression in the Subventricular Zone of Post-natal Rats through Cannabinoid Receptor 1 and Cannabinoid Receptor 2. *Eur. J. Neurosci.* 26 (6), 1548–1559. doi:10.1111/j.1460-9568.2007.05782.x

Ashton, J. C., Rahman, R. M., Nair, S. M., Sutherland, B. A., Glass, M., and Appleton, I. (2007). Cerebral Hypoxia-Ischemia and Middle Cerebral Artery Occlusion Induce Expression of the Cannabinoid CB2 Receptor in the Brain. *Neurosci. Lett.* 412 (2), 114–117. doi:10.1016/j.neulet.2006.10.053

Askari, V. R., and Shafiee-Nick, R. (2019). Promising Neuroprotective Effects of β-caryophyllene against LPS-Induced Oligodendrocyte Toxicity: A Mechanistic Study. *Biochem. Pharmacol.* 159, 154–171. doi:10.1016/j.bcp.2018.12.001

Askew, K., Li, K., Olmos-Alonso, A., Garcia-Moreno, F., Liang, Y., Richardson, P., et al. (2017). Coupled Proliferation and Apoptosis Maintain the Rapid Turnover of Microglia in the Adult Brain. *Cell. Rep.* 18 (2), 391–405. doi:10.1016/j.celrep.2016.12.041

Atalay, S., Jarocka-Karpowicz, I., and Skrzydlewska, E. (2019). Antioxidative and Anti-inflammatory Properties of Cannabidiol. *Antioxidants (Basel)* 9 (1), 21. doi:10.3390/antiox9010021

Aymerich, M. S., Aso, E., Abellanas, M. A., Tolon, R. M., Ramos, J. A., Ferrer, I., et al. (2018). Cannabinoid Pharmacology/therapeutics in Chronic Degenerative Disorders Affecting the Central Nervous System. *Biochem. Pharmacol.* 157, 67–84. doi:10.1016/j.bcp.2018.08.016

Barata, L., Arruza, L., Rodríguez, M. J., Aleo, E., Vierge, E., Criado, E., et al. (2019). Neuroprotection by Cannabidiol and Hypothermia in a Piglet Model of Newborn Hypoxic-Ischemic Brain Damage. *Neuropharmacology* 146, 1–11. doi:10.1016/j.neuropharm.2018.11.020

Belov Kirdajova, D., Kriska, J., Tureckova, J., and Anderova, M. (2020). Ischemia-Triggered Glutamate Excitotoxicity from the Perspective of Glial Cells. *Front. Cell. Neurosci.* 14, 51. doi:10.3389/fncel.2020.00051

Benarroch, E. E. (2016). Astrocyte Signaling and Synaptic Homeostasis: I: Membrane Channels, Transporters, and Receptors in Astrocytes. *Neurology* 87 (3), 324–330. doi:10.1212/WNL.0000000000002875

Benito, C., Kim, W. K., Kim, W. K., Chavarría, I., Hillard, C. J., Mackie, K., et al. (2005). A Glial Endogenous Cannabinoid System Is Upregulated in the Brains of Macaques with Simian Immunodeficiency Virus-Induced Encephalitis. *J. Neurosci.* 25 (10), 2530–2536. doi:10.1523/JNEUROSCI.3923-04.2005

Benito, C., Núñez, E., Tolón, R. M., Carrier, E. J., Rábano, A., Hillard, C. J., et al. (2003). Cannabinoid CB2 Receptors and Fatty Acid Amide Hydrolase Are Selectively Overexpressed in Neuritic Plaque-Associated Glia in Alzheimer's Disease Brains. *J. Neurosci.* 23 (35), 11136–11141. doi:10.1523/JNEUROSCI.23-35-11136.2003

Benito, C., Romero, J. P., Tolón, R. M., Clemente, D., Docagne, F., Hillard, C. J., et al. (2007). Cannabinoid CB1 and CB2 Receptors and Fatty Acid Amide Hydrolase Are Specific Markers of Plaque Cell Subtypes in Human Multiple Sclerosis. *J. Neurosci.* 27 (9), 2396–2402. doi:10.1523/JNEUROSCI.4814-06.2007

Bermudez-Silva, F. J., Viveros, M. P., McPartland, J. M., and Rodriguez de Fonseca, F. (2010). The Endocannabinoid System, Eating Behavior and Energy Homeostasis: the End or a New Beginning? *Pharmacol. Biochem. Behav.* 95 (4), 375–382. doi:10.1016/j.pbb.2010.03.012

Blankman, J. L., and Cravatt, B. F. (2013). "Chemical Probes of Endocannabinoid Metabolism,". Editor E. L. Barker, 65, 849–871. doi:10.1124/pr.112.006387*Pharmacol. Rev.*2

Bonfanti, E., Gelosa, P., Fumagalli, M., Dimou, L., Viganò, F., Tremoli, E., et al. (2017). The Role of Oligodendrocyte Precursor Cells Expressing the GPR17 Receptor in Brain Remodeling after Stroke. *Cell. Death Dis.* 8 (6), e2871. doi:10.1038/cddis.2017.256

Böttcher, C., au, fnm., Schlickeiser, S., Sneeboer, M. A. M., Kunkel, D., Knop, A., et al. (2019). Human Microglia Regional Heterogeneity and Phenotypes Determined by Multiplexed Single-Cell Mass Cytometry. *Nat. Neurosci.* 22 (1), 78–90. doi:10.1038/s41593-018-0290-2

Bresgen, N., and Eckl, P. M. (2015). Oxidative Stress and the Homeodynamics of Iron Metabolism. *Biomolecules* 5 (2), 808–847. doi:10.3390/biom5020808

Britch, S. C., Babalonis, S., and Walsh, S. L. (2021). Cannabidiol: Pharmacology and Therapeutic Targets. *Psychopharmacol. Berl.* 238 (1), 9–28. doi:10.1007/s00213-020-05712-8

Burgaz, S., García, C., Gonzalo-Consuegra, C., Gómez-Almería, M., Ruiz-Pino, F., Unciti, J. D., et al. (2021). Preclinical Investigation in Neuroprotective Effects of the GPR55 Ligand VCE-006.1 in Experimental Models of Parkinson's Disease and Amyotrophic Lateral Sclerosis. *Molecules* 26 (24), 7643. doi:10.3390/molecules26247643

Caltana, L., Saez, T. M., Aronne, M. P., and Brusco, A. (2015). Cannabinoid Receptor Type 1 Agonist ACEA Improves Motor Recovery and Protects Neurons in Ischemic Stroke in Mice. *J. Neurochem.* 135 (3), 616–629. doi:10.1111/jnc.13288

Carlisle, S. J., Marciano-Cabral, F., Staab, A., Ludwick, C., and Cabral, G. A. (2002). Differential Expression of the CB2 Cannabinoid Receptor by Rodent Macrophages and Macrophage-like Cells in Relation to Cell Activation. *Int. Immunopharmacol.* 2 (1), 69–82. doi:10.1016/S1567-5769(01)00147-3

Caruso, P., Naccarato, M., Faoro, V., Pracella, D., Borando, M., Dotti, I., et al. (2016). Expression of the Endocannabinoid Receptor 1 in Human Stroke: An Autoptic Study. *J. Stroke Cerebrovasc. Dis.* 25 (9), 2196–2202. doi:10.1016/j.jstrokecerebrovasdis.2016.03.006

Cassano, T., Calcagnini, S., Pace, L., De Marco, F., Romano, A., and Gaetani, S. (2017). Cannabinoid Receptor 2 Signaling in Neurodegenerative Disorders: From Pathogenesis to a Promising Therapeutic Target. *Front. Neurosci.* 11, 30. doi:10.3389/fnins.2017.00030

Castillo, A., Tolón, M. R., Fernández-Ruiz, J., Romero, J., and Martinez-Orgado, J. (2010). The Neuroprotective Effect of Cannabidiol in an *In Vitro* Model of Newborn Hypoxic-Ischemic Brain Damage in Mice Is Mediated by CB(2) and Adenosine Receptors. *Neurobiol. Dis.* 37 (2), 434–440. doi:10.1016/j.nbd.2009.10.023

Cekanaviciute, E., Fathali, N., Doyle, K. P., Williams, A. M., Han, J., and Buckwalter, M. S. (2014). Astrocytic Transforming Growth Factor-Beta Signaling Reduces Subacute Neuroinflammation after Stroke in Mice. *Glia* 62 (8), 1227–1240. doi:10.1002/glia.22675

Ceprián, M., Jiménez-Sánchez, L., Vargas, C., Barata, L., Hind, W., and Martínez-Orgado, J. (2017). Cannabidiol Reduces Brain Damage and Improves Functional Recovery in a Neonatal Rat Model of Arterial Ischemic Stroke. *Neuropharmacology* 116, 151–159. doi:10.1016/j.neuropharm.2016.12.017

Ceprián, M., Vargas, C., García-Toscano, L., Penna, F., Jiménez-Sánchez, L., Achicallende, S., et al. (2019). Cannabidiol Administration Prevents Hypoxia-Ischemia-Induced Hypomyelination in Newborn Rats. *Front. Pharmacol.* 10, 1131. doi:10.3389/fphar.2019.01131

Chen, A. Q., Fang, Z., Chen, X. L., Yang, S., Zhou, Y. F., Mao, L., et al. (2019). Microglia-derived TNF-α Mediates Endothelial Necroptosis Aggravating Blood

Brain-Barrier Disruption after Ischemic Stroke. *Cell. Death Dis.* 10 (7), 487. doi:10.1038/s41419-019-1716-9

Choi, S. H., Arai, A. L., Mou, Y., Kang, B., Yen, C. C., Hallenbeck, J., et al. (2018). Neuroprotective Effects of MAGL (Monoacylglycerol Lipase) Inhibitors in Experimental Ischemic Stroke. *Stroke* 49 (3), 718–726. doi:10.1161/STROKEAHA.117.019664

Choi, S. H., Mou, Y., and Silva, A. C. (2019). Cannabis and Cannabinoid Biology in Stroke. *Stroke* 50 (9), 2640–2645. doi:10.1161/STROKEAHA.118.023587

Clarke, L. E., and Barres, B. A. (2013). Emerging Roles of Astrocytes in Neural Circuit Development. *Nat. Rev. Neurosci.* 14 (5), 311–321. doi:10.1038/nrn3484

Clarke, L. E., Liddelow, S. A., Chakraborty, C., Münch, A. E., Heiman, M., and Barres, B. A. (2018). Normal Aging Induces A1-like Astrocyte Reactivity. *Proc. Natl. Acad. Sci. U. S. A.* 115 (8), E1896–E1905. doi:10.1073/pnas.1800165115

Clausen, B. H., Lambertsen, K. L., Babcock, A. A., Holm, T. H., Dagnaes-Hansen, F., and Finsen, B. (2008). Interleukin-1beta and Tumor Necrosis Factor-Alpha Are Expressed by Different Subsets of Microglia and Macrophages after Ischemic Stroke in Mice. *J. Neuroinflammation* 5 (1), 46. doi:10.1186/1742-2094-5-46

Cotrina, M. L., Lou, N., Tome-Garcia, J., Goldman, J., and Nedergaard, M. (2017). Direct Comparison of Microglial Dynamics and Inflammatory Profile in Photothrombotic and Arterial Occlusion Evoked Stroke. *Neuroscience* 343, 483–494. doi:10.1016/j.neuroscience.2016.12.012

Covelo, A., and Araque, A. (2016). Lateral Regulation of Synaptic Transmission by Astrocytes. *Neuroscience* 323, 62–66. doi:10.1016/j.neuroscience.2015.02.036

Cristino, L., Bisogno, T., and Di Marzo, V. (2020). Cannabinoids and the Expanded Endocannabinoid System in Neurological Disorders. *Nat. Rev. Neurol.* 16 (1), 9–29. doi:10.1038/s41582-019-0284-z

Davalos, D., Grutzendler, J., Yang, G., Kim, J. V., Zuo, Y., Jung, S., et al. (2005). ATP Mediates Rapid Microglial Response to Local Brain Injury *In Vivo*. *Nat. Neurosci.* 8 (6), 752–758. doi:10.1038/nn1472

Dawson, M. R., Polito, A., Levine, J. M., and Reynolds, R. (2003). NG2-expressing Glial Progenitor Cells: an Abundant and Widespread Population of Cycling Cells in the Adult Rat CNS. *Mol. Cell. Neurosci.* 24 (2), 476–488. doi:10.1016/s1044-7431(03)00210-0

Devane, W. A., Hanus, L., Breuer, A., Pertwee, R. G., Stevenson, L. A., Griffin, G., et al. (1992). Isolation and Structure of a Brain Constituent that Binds to the Cannabinoid Receptor. *Science* 258 (5090), 1946–1949. doi:10.1126/science.1470919

Dezonne, R. S., Stipursky, J., Araujo, A. P., Nones, J., Pavão, M. S., Porcionatto, M., et al. (2013). Thyroid Hormone Treated Astrocytes Induce Maturation of Cerebral Cortical Neurons through Modulation of Proteoglycan Levels. *Front. Cell. Neurosci.* 7, 125. doi:10.3389/fncel.2013.00125

Di Marzo, V., Fontana, A., Cadas, H., Schinelli, S., Cimino, G., Schwartz, J. C., et al. (1994). Formation and Inactivation of Endogenous Cannabinoid Anandamide in Central Neurons. *Nature* 372 (6507), 686–691. doi:10.1038/372686a0

Díez Tejedor, E., del Brutto Perrone, O. H., Álvarez Sabín, J., Muñoz Collazos, M., and Abiusi, G. R. P. (2001). Clasificación de las enfermedades cerebrovasculares. Sociedad Iberoamericana de ECV. *RevNeurol* 33 (05), 455. doi:10.33588/rn.3305.2001246

Dingman, A. L., Rodgers, K. M., Dietz, R. M., Hickey, S. P., Frazier, A. P., Clevenger, A. C., et al. (2018). Oligodendrocyte Progenitor Cell Proliferation and Fate after White Matter Stroke in Juvenile and Adult Mice. *Dev. Neurosci.* 40 (5–6), 601–616. doi:10.1159/000496200

Dinh, T. P., Carpenter, D., Leslie, F. M., Freund, T. F., Katona, I., Sensi, S. L., et al. (2002). Brain Monoglyceride Lipase Participating in Endocannabinoid Inactivation. *Proc. Natl. Acad. Sci. U. S. A.* 99 (16), 10819–10824. doi:10.1073/pnas.152334899

Domercq, M., Perez-Samartin, A., Aparicio, D., Alberdi, E., Pampliega, O., and Matute, C. (2009). P2X7 Receptors Mediate Ischemic Damage to Oligodendrocytes. *Glia*. doi:10.1002/glia.20958

Egaña-Huguet, J., Soria-Gómez, E., and Grandes, P. (2021). The Endocannabinoid System in Glial Cells and Their Profitable Interactions to Treat Epilepsy: Evidence from Animal Models. *Ijms* 22 (24), 13231. doi:10.3390/ijms222413231

England, T. J., Hind, W. H., Rasid, N. A., and O'Sullivan, S. E. (2015). Cannabinoids in Experimental Stroke: a Systematic Review and Meta-Analysis. *J. Cereb. Blood Flow. Metab.* 35 (3), 348–358. doi:10.1038/jcbfm.2014.218

Escartin, C., Galea, E., Lakatos, A., O'Callaghan, J. P., Petzold, G. C., Serrano-Pozo, A., et al. (2021). Reactive Astrocyte Nomenclature, Definitions, and Future Directions. *Nat. Neurosci.* 24 (3), 312–325. doi:10.1038/s41593-020-00783-4

Estrada, J. A., and Contreras, I. (2020). Endocannabinoid Receptors in the CNS: Potential Drug Targets for the Prevention and Treatment of Neurologic and Psychiatric Disorders. *Curr. Neuropharmacol.* 18 (8), 769–787. doi:10.2174/1570159X18666200217140255

Fan, H., Tang, H. B., Shan, L. Q., Liu, S. C., Huang, D. G., Chen, X., et al. (2019). Quercetin Prevents Necroptosis of Oligodendrocytes by Inhibiting Macrophages/microglia Polarization to M1 Phenotype after Spinal Cord Injury in Rats. *J. Neuroinflammation* 16 (1), 206. doi:10.1186/s12974-019-1613-2

Feigin, V. L. (2021). Global, Regional, and National Burden of Stroke and its Risk Factors, 1990–2019: a Systematic Analysis for the Global Burden of Disease Study 2019. *Lancet Neurology* 20 (10), 795–820. doi:10.1016/S1474-4422(21)00252-0

Feliú, A., Bonilla del Río, I., Carrillo-Salinas, F. J., Hernández-Torres, G., Mestre, L., Puente, N., et al. (2017). 2-Arachidonoylglycerol Reduces Proteoglycans and Enhances Remyelination in a Progressive Model of Demyelination. *J. Neurosci.* 37 (35), 8385–8398. doi:10.1523/JNEUROSCI.2900-16.2017

Fernández-López, D., Faustino, J., Derugin, N., Wendland, M., Lizasoain, I., Moro, M. A., et al. (2012). Reduced Infarct Size and Accumulation of Microglia in Rats Treated with WIN 55,212-2 after Neonatal Stroke. *Neuroscience* 207, 307–315. doi:10.1016/j.neuroscience.2012.01.008

Fernández-Ruiz, J., Moro, M. A., and Martínez-Orgado, J. (2015). Cannabinoids in Neurodegenerative Disorders and Stroke/Brain Trauma: From Preclinical Models to Clinical Applications. *Neurotherapeutics* 12 (4), 793–806. doi:10.1007/s13311-015-0381-7

Fernández-Trapero, M., Espejo-Porras, F., Rodríguez-Cueto, C., Coates, J. R., Pérez-Díaz, C., de Lago, E., et al. (2017). Up-regulation of CB2 Receptors in Reactive Astrocytes in Canine Degenerative Myelopathy, a Disease Model of Amyotrophic Lateral Sclerosis. *Dis. Models Mech.*, 028373. doi:10.1242/dmm.028373

Ferna´ndez-Lo´pez, D., Pradillo, J. M., Garci´a-Ye´benes, I., Marti´nez-Orgado, J. A., Moro, M. A., and Lizasoain, I. (2010). The Cannabinoid WIN55212-2 Promotes Neural Repair after Neonatal Hypoxia-Ischemia. *Stroke* 41 (12), 2956–2964. doi:10.1161/STROKEAHA.110.599357

Feske, S. K. (2021). Ischemic Stroke. *Am. J. Med.* 134 (12), 1457–1464. doi:10.1016/j.amjmed.2021.07.027

Filipello, F., Morini, R., Corradini, I., Zerbi, V., Canzi, A., Michalski, B., et al. (2018). The Microglial Innate Immune Receptor TREM2 Is Required for Synapse Elimination and Normal Brain Connectivity. *Immunity* 48 (5), 979–e8. doi:10.1016/j.immuni.2018.04.016

Fragoso, G., Martínez-Bermúdez, A. K., Liu, H. N., Khorchid, A., Chemtob, S., Mushynski, W. E., et al. (2004). Developmental Differences in HO-Induced Oligodendrocyte Cell Death: Role of Glutathione, Mitogen-Activated Protein Kinases and Caspase 3. *J. Neurochem.* 90 (2), 392–404. doi:10.1111/j.1471-4159.2004.02488.x

Franco, R., Reyes-Resina, I., Aguinaga, D., Lillo, A., Jiménez, J., Raïch, I., et al. (2019). Potentiation of Cannabinoid Signaling in Microglia by Adenosine A2A Receptor Antagonists. *Glia* 67 (12), 2410–2423. doi:10.1002/glia.23694

Franklin, A., Parmentier-Batteur, S., Walter, L., Greenberg, D. A., and Stella, N. (2003). Palmitoylethanolamide Increases after Focal Cerebral Ischemia and Potentiates Microglial Cell Motility. *J. Neurosci.* 23 (21), 7767–7775. doi:10.1523/jneurosci.23-21-07767.2003

Franklin, A., and Stella, N. (2003). Arachidonylcyclopropylamide Increases Microglial Cell Migration through Cannabinoid CB2 and Abnormal-Cannabidiol-Sensitive Receptors. *Eur. J. Pharmacol.* 474 (2–3), 195–198. doi:10.1016/S0014-2999(03)02074-0

Frik, J., Merl-Pham, J., Plesnila, N., Mattugini, N., Kjell, J., Kraska, J., et al. (2018). Cross-talk between Monocyte Invasion and Astrocyte Proliferation Regulates Scarring in Brain Injury. *EMBO Rep.* 19 (5). doi:10.15252/embr.201745294

Fünfschilling, U., Supplie, L. M., Mahad, D., Boretius, S., Saab, A. S., Edgar, J., et al. (2012). Glycolytic Oligodendrocytes Maintain Myelin and Long-Term Axonal Integrity. *Nature* 485 (7399), 517–521. doi:10.1038/nature11007

Garberg, H. T., Huun, M. U., Escobar, J., Martinez-Orgado, J., Løberg, E. M., Solberg, R., et al. (2016). Short-term Effects of Cannabidiol after Global

Hypoxia-Ischemia in Newborn Piglets. *Pediatr. Res.* 80 (5), 710–718. doi:10.1038/pr.2016.149

Garberg, H. T., Solberg, R., Barlinn, J., Martinez-Orgado, J., Løberg, E. M., and Saugstad, O. D. (2017). High-Dose Cannabidiol Induced Hypotension after Global Hypoxia-Ischemia in Piglets. *Neonatology* 112 (2), 143–149. doi:10.1159/000471786

Ginhoux, F., Greter, M., Leboeuf, M., Nandi, S., See, P., Gokhan, S., et al. (2010). Fate Mapping Analysis Reveals that Adult Microglia Derive from Primitive Macrophages. *Science* 330, 841–845. doi:10.1126/science.1194637

Gleichman, A. J., and Carmichael, S. T. (2014). Astrocytic Therapies for Neuronal Repair in Stroke. *Neurosci. Lett.* 565, 47–52. doi:10.1016/j.neulet.2013.10.055

Goldmann, T., Wieghofer, P., Jordão, M. J., Prutek, F., Hagemeyer, N., Frenzel, K., et al. (2016). Origin, Fate and Dynamics of Macrophages at Central Nervous System Interfaces. *Nat. Immunol.* 17 (7), 797–805. doi:10.1038/ni.3423

Gomez, O., Arevalo-Martin, A., Garcia-Ovejero, D., Ortega-Gutierrez, S., Cisneros, J. A., Almazan, G., et al. (2010). The Constitutive Production of the Endocannabinoid 2-arachidonoylglycerol Participates in Oligodendrocyte Differentiation. *Glia* 58 (16), 1913–1927. doi:10.1002/glia.21061

Gomez, O., Sanchez-Rodriguez, A., Le, M., Sanchez-Caro, C., Molina-Holgado, F., and Molina-Holgado, E. (2011). Cannabinoid Receptor Agonists Modulate Oligodendrocyte Differentiation by Activating PI3K/Akt and the Mammalian Target of Rapamycin (mTOR) Pathways. *Br. J. Pharmacol.* 163 (7), 1520–1532. doi:10.1111/j.1476-5381.2011.01414.x

Gomez, O., Sanchez-Rodriguez, M. A., Ortega-Gutierrez, S., Vazquez-Villa, H., Guaza, C., Molina-Holgado, F., et al. (2015). A Basal Tone of 2-Arachidonoylglycerol Contributes to Early Oligodendrocyte Progenitor Proliferation by Activating Phosphatidylinositol 3-Kinase (PI3K)/AKT and the Mammalian Target of Rapamycin (MTOR) Pathways. *J. Neuroimmune Pharmacol.* 10 (2), 309–317. doi:10.1007/s11481-015-9609-x

Gong, Z., Pan, J., Shen, Q., Li, M., and Peng, Y. (2018). Mitochondrial Dysfunction Induces NLRP3 Inflammasome Activation during Cerebral Ischemia/reperfusion Injury. *J. Neuroinflammation* 15 (1), 242. doi:10.1186/s12974-018-1282-6

Gorzkiewicz, A., and Szemraj, J. (2018). Brain Endocannabinoid Signaling Exhibits Remarkable Complexity. *Brain Res. Bull.* 142, 33–46. doi:10.1016/j.brainresbull.2018.06.012

Gosselin, D., Skola, D., Coufal, N. G., Holtman, I. R., Schlachetzki, J. C. M., Sajti, E., et al. (2017). An Environment-dependent Transcriptional Network Specifies Human Microglia Identity. *Science* 356 (6344), eaal3222. doi:10.1126/science.aal3222

Grabner, G. F., Eichmann, T. O., Wagner, B., Gao, Y., Farzi, A., Taschler, U., et al. (2016). Deletion of Monoglyceride Lipase in Astrocytes Attenuates Lipopolysaccharide-Induced Neuroinflammation. *J. Biol. Chem.* 291 (2), 913–923. doi:10.1074/jbc.M115.683615

Greco, R., Demartini, C., Zanaboni, A., Tumelero, E., Elisa, C., Persico, A., et al. (2021). Characterization of CB2 Receptor Expression in Peripheral Blood Monocytes of Acute Ischemic Stroke Patients. *Transl. Stroke Res.* 12 (4), 550–558. doi:10.1007/s12975-020-00851-8

Gris, P., Tighe, A., Levin, D., Sharma, R., and Brown, A. (2007). Transcriptional Regulation of Scar Gene Expression in Primary Astrocytes. *Glia* 55 (11), 1145–1155. doi:10.1002/glia.20537

Guida, F., Luongo, L., Boccella, S., Giordano, M. E., Romano, R., Bellini, G., et al. (2017). Palmitoylethanolamide Induces Microglia Changes Associated with Increased Migration and Phagocytic Activity: Involvement of the CB2 Receptor. *Sci. Rep.* 7 (1), 375. doi:10.1038/s41598-017-00342-1

Gulyas, A. I., Cravatt, B. F., Bracey, M. H., Dinh, T. P., Piomelli, D., Boscia, F., et al. (2004). Segregation of Two Endocannabinoid-Hydrolyzing Enzymes into Pre- and Postsynaptic Compartments in the Rat hippocampus, Cerebellum and Amygdala. *Eur. J. Neurosci.* 20 (2), 441–458. doi:10.1111/j.1460-9568.2004.03428.x

Gürer, G., Gursoy-Ozdemir, Y., Erdemli, E., Can, A., and Dalkara, T. (2009). Astrocytes are more resistant to focal cerebral ischemia Than neurons and die by a delayed necrosis. *Brain Pathol. (Zurich, Switz.* 19 (4), 630–641. doi:10.1111/j.1750-3639.2008.00226.x

Guttenplan, K. A., Weigel, M. K., Prakash, P., Wijewardhane, P. R., Hasel, P., Rufen-Blanchette, U., et al. (2021). Neurotoxic Reactive Astrocytes Induce Cell Death via Saturated Lipids. *Nature* 599 (7883), 102–107. doi:10.1038/s41586-021-03960-y

Hayakawa, K., Irie, K., Sano, K., Watanabe, T., Higuchi, S., Enoki, M., et al. (2009). Therapeutic Time Window of Cannabidiol Treatment on Delayed Ischemic Damage via High-Mobility Group Box1-Inhibiting Mechanism. *Biol. Pharm. Bull.* 32 (9), 1538–1544. doi:10.1248/bpb.32.1538

Hayakawa, K., Mishima, K., Abe, K., Hasebe, N., Takamatsu, F., Yasuda, H., et al. (2004). Cannabidiol Prevents Infarction via the Non-CB1 Cannabinoid Receptor Mechanism. *NeuroReport* 15 (15), 2381–2385. doi:10.1097/00001756-200410250-00016

Hayakawa, K., Mishima, K., and Fujiwara, M. (2010). Therapeutic Potential of Non-psychotropic Cannabidiol in Ischemic Stroke. *Pharm. (Basel)* 3 (7), 2197–2212. doi:10.3390/ph3072197

Hayakawa, K., Mishima, K., Irie, K., Hazekawa, M., Mishima, S., Fujioka, M., et al. (2008). Cannabidiol Prevents a Post-ischemic Injury Progressively Induced by Cerebral Ischemia via a High-Mobility Group Box1-Inhibiting Mechanism. *Neuropharmacology* 55 (8), 1280–1286. doi:10.1016/j.neuropharm.2008.06.040

Herkenham, M., Lynn, A. B., Johnson, M. R., Melvin, L. S., de Costa, B. R., and Rice, K. C. (1991). Characterization and Localization of Cannabinoid Receptors in Rat Brain: a Quantitative *In Vitro* Autoradiographic Study. *J. Neurosci.* 11 (2), 563–583. doi:10.1523/jneurosci.11-02-00563.1991

Hersh, J., and Yang, S. H. (2018). Glia-immune Interactions Post-ischemic Stroke and Potential Therapies. *Exp. Biol. Med. (Maywood)* 243 (17–18), 1302–1312. doi:10.1177/1535370218818172

Hillard, C. J. (2000). Endocannabinoids and Vascular Function. *J. Pharmacol. Exp. Ther.* 294 (1), 27–32.

Hillard, C. J. (2008). Role of Cannabinoids and Endocannabinoids in Cerebral Ischemia. *Curr. Pharm. Des.* 14 (23), 2347–2361. doi:10.2174/138161208785740054

Hind, W. H., England, T. J., and O'Sullivan, S. E. (2016). Cannabidiol Protects an *In Vitro* Model of the Blood-Brain Barrier from Oxygen-Glucose Deprivation via PPARγ and 5-HT1A Receptors. *Br. J. Pharmacol.* 173 (5), 815–825. doi:10.1111/bph.13368

Hind, W. H., Tufarelli, C., Neophytou, M., Anderson, S. I., England, T. J., and O'Sullivan, S. E. (2015). Endocannabinoids Modulate Human Blood-Brain Barrier Permeability *In Vitro*. *Br. J. Pharmacol.* 172 (12), 3015–3027. doi:10.1111/bph.13106

Ho, P. W., Reutens, D. C., Phan, T. G., Wright, P. M., Markus, R., Indra, I., et al. (2005). Is White Matter Involved in Patients Entered into Typical Trials of Neuroprotection? *Stroke* 36 (12), 2742–2744. doi:10.1161/01.STR.0000189748.52500.a7

Höft, S., Griemsmann, S., Seifert, G., and Steinhäuser, C. (2014). Heterogeneity in Expression of Functional Ionotropic Glutamate and GABA Receptors in Astrocytes across Brain Regions: Insights from the Thalamus. *Phil. Trans. R. Soc. B* 369 (1654), 20130602. doi:10.1098/rstb.2013.0602

Hosoya, T., Fukumoto, D., Kakiuchi, T., Nishiyama, S., Yamamoto, S., Ohba, H., et al. (2017). *In Vivo* TSPO and Cannabinoid Receptor Type 2 Availability Early in Post-stroke Neuroinflammation in Rats: a Positron Emission Tomography Study. *J. Neuroinflammation* 14 (1), 69. doi:10.1186/s12974-017-0851-4

Howlett, A. C., Barth, F., Bonner, T. I., Cabral, G., Casellas, P., Devane, W. A., et al. (2002). International Union of Pharmacology. XXVII. Classification of Cannabinoid Receptors. *Pharmacol. Rev.* 54 (2), 161–202. doi:10.1124/pr.54.2.161

Hu, X., Li, P., Guo, Y., Wang, H., Leak, R. K., Chen, S., et al. (2012). Microglia/Macrophage Polarization Dynamics Reveal Novel Mechanism of Injury Expansion after Focal Cerebral Ischemia. *Stroke* 43 (11), 3063–3070. doi:10.1161/STROKEAHA.112.659656

Huang, L., Wu, Z. B., Zhuge, Q., Zheng, W., Shao, B., Wang, B., et al. (2014). Glial Scar Formation Occurs in the Human Brain after Ischemic Stroke. *Int. J. Med. Sci.* 11 (4), 344–348. doi:10.7150/ijms.8140

Huang, Y., Chen, S., Luo, Y., and Han, Z. (2020). Crosstalk between Inflammation and the BBB in Stroke. *Curr. Neuropharmacol.* 18 (12), 1227–1236. doi:10.2174/1570159X18666200620230321

Iadecola, C., Buckwalter, M. S., and Anrather, J. (2020). Immune Responses to Stroke: Mechanisms, Modulation, and Therapeutic Potential. *J. Clin. Investig.* 130 (6), 2777–2788. doi:10.1172/JCI135530

Iannotti, F. A., and Vitale, R. M. (2021). The Endocannabinoid System and PPARs: Focus on Their Signalling Crosstalk, Action and Transcriptional Regulation. *Cells* 10 (3), 586. doi:10.3390/cells10030586

Indredavik, B., Bakke, F., Solberg, R., Rokseth, R., Haaheim, L. L., and Holme, I. (1991). Benefit of a Stroke Unit: a Randomized Controlled Trial. *Stroke* 22 (8), 1026–1031. doi:10.1161/01.STR.22.8.1026

Jadhav, P., Karande, M., Sarkar, A., Sahu, S., Sarmah, D., Datta, A., et al. (2022). Glial Cells Response in Stroke. *Cell. Mol. Neurobiol.* doi:10.1007/s10571-021-01183-3

Jha, M. K., Jo, M., Kim, J. H., and Suk, K. (2019). Microglia-Astrocyte Crosstalk: An Intimate Molecular Conversation. *Neuroscientist* 25 (3), 227–240. doi:10.1177/1073858418783959

Jha, M. K., and Morrison, B. M. (2020). Lactate Transporters Mediate Glia-Neuron Metabolic Crosstalk in Homeostasis and Disease. *Front. Cell. Neurosci.* 14, 589582. doi:10.3389/fncel.2020.589582

Ji, J., Xue, T. F., Guo, X. D., Yang, J., Guo, R. B., Wang, J., et al. (2018). Antagonizing Peroxisome Proliferator-Activated Receptor γ Facilitates M1-To-M2 Shift of Microglia by Enhancing Autophagy via the LKB1-AMPK Signaling Pathway. *Aging Cell.* 17 (4), e12774. doi:10.1111/acel.12774

Jia, Y., Deng, H., Qin, Q., and Ma, Z. (2020). JWH133 Inhibits MPP+-induced Inflammatory Response and Iron Influx in Astrocytes. *Neurosci. Lett.* 720, 134779. doi:10.1016/j.neulet.2020.134779

Jimenez-Blasco, D., Busquets-Garcia, A., Hebert-Chatelain, E., Serrat, R., Vicente-Gutierrez, C., Ioannidou, C., et al. (2020). Glucose Metabolism Links Astroglial Mitochondria to Cannabinoid Effects. *Nature* 583 (7817), 603–608. doi:10.1038/s41586-020-2470-y

Jin, K., Xie, L., Kim, S. H., Parmentier-Batteur, S., Sun, Y., Mao, X. O., et al. (2004). Defective Adult Neurogenesis in CB1 Cannabinoid Receptor Knockout Mice. *Mol. Pharmacol.* 66 (2), 204–208. doi:10.1124/mol.66.2.204

Jing, N., Fang, B., Li, Z., and Tian, A. (2020). Exogenous Activation of Cannabinoid-2 Receptor Modulates TLR4/MMP9 Expression in a Spinal Cord Ischemia Reperfusion Rat Model. *J. Neuroinflammation* 17 (1), 101. doi:10.1186/s12974-020-01784-7

John Lin, C. C., Yu, K., Hatcher, A., Huang, T. W., Lee, H. K., Carlson, J., et al. (2017). Identification of Diverse Astrocyte Populations and Their Malignant Analogs. *Nat. Neurosci.* 20 (3), 396–405. doi:10.1038/nn.4493

Ju, F., Ran, Y., Zhu, L., Cheng, X., Gao, H., Xi, X., et al. (2018). Increased BBB Permeability Enhances Activation of Microglia and Exacerbates Loss of Dendritic Spines after Transient Global Cerebral Ischemia. *Front. Cell. Neurosci.* 12, 236. doi:10.3389/fncel.2018.00236

Kanazawa, M., Ninomiya, I., Hatakeyama, M., Takahashi, T., and Shimohata, T. (2017). Microglia and Monocytes/Macrophages Polarization Reveal Novel Therapeutic Mechanism against Stroke. *Int. J. Mol. Sci.* 18 (10), 2135. doi:10.3390/ijms18102135

Káradóttir, R., Cavelier, P., Bergersen, L. H., and Attwell, D. (2005). NMDA Receptors Are Expressed in Oligodendrocytes and Activated in Ischaemia. *Nature* 438 (7071), 1162–1166. doi:10.1038/nature04302

Kettenmann, H., and Verkhratsky, A. (2008). Neuroglia: the 150 Years after. *Trends Neurosci.* 31 (12), 653–659. doi:10.1016/j.tins.2008.09.003

Khakh, B. S., and Deneen, B. (2019). The Emerging Nature of Astrocyte Diversity. *Annu. Rev. Neurosci.* 42 (1), 187–207. doi:10.1146/annurev-neuro-070918-050443

Khaksar, S., Bigdeli, M., Samiee, A., and Shirazi-Zand, Z. (2022). Antioxidant and Anti-apoptotic Effects of Cannabidiol in Model of Ischemic Stroke in Rats. *Brain Res. Bull.* 180, 118–130. doi:10.1016/j.brainresbull.2022.01.001

Kicman, A., and Toczek, M. (2020). The Effects of Cannabidiol, a Non-intoxicating Compound of Cannabis, on the Cardiovascular System in Health and Disease. *Int. J. Mol. Sci.* 21 (18), 6740. doi:10.3390/ijms21186740

Kim, E., and Cho, S. (2016). Microglia and Monocyte-Derived Macrophages in Stroke. *Neurotherapeutics* 13 (4), 702–718. doi:10.1007/s13311-016-0463-1

Knowles, M. D., de la Tremblaye, P. B., Azogu, I., and Plamondon, H. (2016). Endocannabinoid CB1 Receptor Activation upon Global Ischemia Adversely Impact Recovery of Reward and Stress Signaling Molecules, Neuronal Survival and Behavioral Impulsivity. *Prog. Neuropsychopharmacol. Biol. Psychiatry* 66, 8–21. doi:10.1016/j.pnpbp.2015.10.010

Kolb, B., Saber, H., Fadel, H., and Rajah, G. (2019). The Endocannabinoid System and Stroke: A Focused Review. *Brain Circ.* 5 (1), 1–7. doi:10.4103/bc.bc_29_18

Kossatz, E., Maldonado, R., and Robledo, P. (2016). CB2 Cannabinoid Receptors Modulate HIF-1α and TIM-3 Expression in a Hypoxia-Ischemia Mouse Model. *Eur. Neuropsychopharmacol.* 26 (12), 1972–1988. doi:10.1016/j.euroneuro.2016.10.003

Kozela, E., Juknat, A., and Vogel, Z. (2017). Modulation of Astrocyte Activity by Cannabidiol, a Nonpsychoactive Cannabinoid. *Int. J. Mol. Sci.* 18 (8), 1669. doi:10.3390/ijms18081669

Kuriakose, D., and Xiao, Z. (2020). Pathophysiology and Treatment of Stroke: Present Status and Future Perspectives. *Int. J. Mol. Sci.* 21 (20), 7609. doi:10.3390/ijms21207609

Labra, V. C., Santibáñez, C. A., Gajardo-Gómez, R., Díaz, E. F., Gómez, G. I., and Orellana, J. A. (2018). The Neuroglial Dialog between Cannabinoids and Hemichannels. *Front. Mol. Neurosci.* 11, 79. doi:10.3389/fnmol.2018.00079

Lafuente, H., Alvarez, F. J., Pazos, M. R., Alvarez, A., Rey-Santano, M. C., Mielgo, V., et al. (2011). Cannabidiol Reduces Brain Damage and Improves Functional Recovery after Acute Hypoxia-Ischemia in Newborn Pigs. *Pediatr. Res.* 70 (3), 272–277. doi:10.1203/PDR.0b013e3182276b11

Lafuente, H., Pazos, M. R., Alvarez, A., Mohammed, N., Santos, M., Arizti, M., et al. (2016). Effects of Cannabidiol and Hypothermia on Short-Term Brain Damage in New-Born Piglets after Acute Hypoxia-Ischemia. *Front. Neurosci.* 10, 323. doi:10.3389/fnins.2016.00323

Lai, T. W., Zhang, S., and Wang, Y. T. (2014). Excitotoxicity and Stroke: Identifying Novel Targets for Neuroprotection. *Prog. Neurobiol.* 115, 157–188. doi:10.1016/j.pneurobio.2013.11.006

Lambertsen, K. L., Meldgaard, M., Ladeby, R., and Finsen, B. (2005). A Quantitative Study of Microglial-Macrophage Synthesis of Tumor Necrosis Factor during Acute and Late Focal Cerebral Ischemia in Mice. *J. Cereb. Blood Flow. Metab.* 25 (1), 119–135. doi:10.1038/sj.jcbfm.9600014

Li, L., Lundkvist, A., Andersson, D., Wilhelmsson, U., Nagai, N., Pardo, A. C., et al. (2008). Protective Role of Reactive Astrocytes in Brain Ischemia. *J. Cereb. Blood Flow. Metab.* 28 (3), 468–481. doi:10.1038/sj.jcbfm.9600546

Li, L., Yun, D., Zhang, Y., Tao, Y., Tan, Q., Qiao, F., et al. (2018). A Cannabinoid Receptor 2 Agonist Reduces Blood-Brain Barrier Damage via Induction of MKP-1 after Intracerebral Hemorrhage in Rats. *Brain Res.* 1697, 113–123. doi:10.1016/j.brainres.2018.06.006

Li, T., Pang, S., Yu, Y., Wu, X., Guo, J., and Zhang, S. (2013). Proliferation of Parenchymal Microglia Is the Main Source of Microgliosis after Ischaemic Stroke. *Brain* 136 (12), 3578–3588. doi:10.1093/brain/awt287

Liddelow, S., and Barres, B. (2015). SnapShot: Astrocytes in Health and Disease. *Cell.* 162 (5), 1170–e1. doi:10.1016/j.cell.2015.08.029

Liddelow, S. A., and Barres, B. A. (2017). Reactive Astrocytes: Production, Function, and Therapeutic Potential. *Immunity* 46 (6), 957–967. doi:10.1016/j.immuni.2017.06.006

Liddelow, S. A., Guttenplan, K. A., Clarke, L. E., Bennett, F. C., Bohlen, C. J., Schirmer, L., et al. (2017). Neurotoxic Reactive Astrocytes Are Induced by Activated Microglia. *Nature* 541 (7638), 481–487. doi:10.1038/nature21029

Liu, L. R., Liu, J. C., Bao, J. S., Bai, Q. Q., and Wang, G. Q. (2020). Interaction of Microglia and Astrocytes in the Neurovascular Unit. *Front. Immunol.* 11, 1024. doi:10.3389/fimmu.2020.01024

Liu, X., Su, P., Meng, S., Aschner, M., Cao, Y., Luo, W., et al. (2017). Role of Matrix Metalloproteinase-2/9 (MMP2/9) in Lead-Induced Changes in an *In Vitro* Blood-Brain Barrier Model. *Int. J. Biol. Sci.* 13 (11), 1351–1360. doi:10.7150/ijbs.20670

Liu, Z. J., Ran, Y. Y., Qie, S. Y., Gong, W. J., Gao, F. H., Ding, Z. T., et al. (2019). Melatonin Protects against Ischemic Stroke by Modulating Microglia/macrophage Polarization toward Anti-inflammatory Phenotype through STAT3 Pathway. *CNS Neurosci. Ther.* 25 (12), 1353–1362. doi:10.1111/cns.13261

Lively, S., and Schlichter, L. C. (2013). The Microglial Activation State Regulates Migration and Roles of Matrix-Dissolving Enzymes for Invasion. *J. Neuroinflammation* 10 (1), 75. doi:10.1186/1742-2094-10-75

López, A., Aparicio, N., Pazos, M. R., Grande, M. T., Barreda-Manso, M. A., Benito-Cuesta, I., et al. (2018). Cannabinoid CB2 Receptors in the Mouse Brain: Relevance for Alzheimer's Disease. *J. Neuroinflammation* 15 (1), 158. doi:10.1186/s12974-018-1174-9

Lou, Z. Y., Cheng, J., Wang, X. R., Zhao, Y. F., Gan, J., Zhou, G. Y., et al. (2018). The Inhibition of CB1 Receptor Accelerates the Onset and Development of EAE Possibly by Regulating Microglia/macrophages Polarization. *J. Neuroimmunol.* 317, 37–44. doi:10.1016/j.jneuroim.2018.02.001

Lu, Y., Zhou, M., Li, Y., Li, Y., Hua, Y., and Fan, Y. (2021). Minocycline Promotes Functional Recovery in Ischemic Stroke by Modulating Microglia Polarization

through STAT1/STAT6 Pathways. *Biochem. Pharmacol.* 186, 114464. doi:10.1016/j.bcp.2021.114464

Ma, Y., Wang, J., Wang, Y., and Yang, G. Y. (2017). The Biphasic Function of Microglia in Ischemic Stroke. *Prog. Neurobiol.* 157, 247–272. doi:10.1016/j.pneurobio.2016.01.005

Mages, B., Aleithe, S., Blietz, A., Krueger, M., Härtig, W., and Michalski, D. (2019). Simultaneous Alterations of Oligodendrocyte-specific CNP, Astrocyte-specific AQP4 and Neuronal NF-L Demarcate Ischemic Tissue after Experimental Stroke in Mice. *Neurosci. Lett.* 711, 134405. doi:10.1016/j.neulet.2019.134405

Maki, T., Maeda, M., Uemura, M., Lo, E. K., Terasaki, Y., Liang, A. C., et al. (2015). Potential Interactions between Pericytes and Oligodendrocyte Precursor Cells in Perivascular Regions of Cerebral White Matter. *Neurosci. Lett.* 597, 164–169. doi:10.1016/j.neulet.2015.04.047

Maki, T. (2017). Novel Roles of Oligodendrocyte Precursor Cells in the Developing and Damaged Brain. *Clin. Exp. Neuroimmunol.* 8 (1), 33–42. doi:10.1111/cen3.12358

Malek, N., Popiolek-Barczyk, K., Mika, J., Przewlocka, B., and Starowicz, K. (20152015). Anandamide, Acting viaCB2Receptors, Alleviates LPS-Induced Neuroinflammation in Rat Primary Microglial Cultures. *Neural Plast.* 2015, 1–10. doi:10.1155/2015/130639

Maresz, K., Carrier, E. J., Ponomarev, E. D., Hillard, C. J., and Dittel, B. N. (2005). Modulation of the Cannabinoid CB2 Receptor in Microglial Cells in Response to Inflammatory Stimuli. *J. Neurochem.* 95 (2), 437–445. doi:10.1111/j.1471-4159.2005.03380.x

Marichal-Cancino, B. A., Fajardo-Valdez, A., Ruiz-Contreras, A. E., Mendez-Díaz, M., and Prospero-García, O. (2017). Advances in the Physiology of GPR55 in the Central Nervous System. *Curr. Neuropharmacol.* 15 (5), 771–778. doi:10.2174/1570159X14666160729155441

Martínez-Orgado, J., Villa, M., and del Pozo, A. (2021). Cannabidiol for the Treatment of Neonatal Hypoxic-Ischemic Brain Injury. *Front. Pharmacol.* 11, 584533. doi:10.3389/fphar.2020.584533

Masuda, T., Croom, D., Hida, H., and Kirov, S. A. (2011). Capillary Blood Flow Around Microglial Somata Determines Dynamics of Microglial Processes in Ischemic Conditions. *Glia* 59 (11), 1744–1753. doi:10.1002/glia.21220

Matcovitch-Natan, O., Winter, D. R., Giladi, A., Vargas Aguilar, S., Spinrad, A., Sarrazin, S., et al. (2016). Microglia Development Follows a Stepwise Program to Regulate Brain Homeostasis. *Science* 353 (6301), aad8670. doi:10.1126/science.aad8670

Matsuda, L. A., Lolait, S. J., Brownstein, M. J., Young, A. C., and Bonner, T. I. (1990). Structure of a Cannabinoid Receptor and Functional Expression of the Cloned cDNA. *Nature* 346 (6284), 561–564. doi:10.1038/346561a0

Mecha, M., Carrillo-Salinas, F. J., Feliú, A., Mestre, L., and Guaza, C. (2016). Microglia Activation States and Cannabinoid System: Therapeutic Implications. *Pharmacol. Ther.* 166, 40–55. doi:10.1016/j.pharmthera.2016.06.011

Mecha, M., Feliú, A., Carrillo-Salinas, F. J., Rueda-Zubiaurre, A., Ortega-Gutiérrez, S., de Sola, R. G., et al. (2015). Endocannabinoids Drive the Acquisition of an Alternative Phenotype in Microglia. *Brain Behav. Immun.* 49, 233–245. doi:10.1016/j.bbi.2015.06.002

Mecha, M., Torrao, A. S., Mestre, L., Carrillo-Salinas, F. J., Mechoulam, R., and Guaza, C. (2012). Cannabidiol Protects Oligodendrocyte Progenitor Cells from Inflammation-Induced Apoptosis by Attenuating Endoplasmic Reticulum Stress. *Cell. Death Dis.* 3 (6), e331. doi:10.1038/cddis.2012.71

Mechoulam, R., Ben-Shabat, S., Hanus, L., Ligumsky, M., Kaminski, N. E., Schatz, A. R., et al. (1995). Identification of an Endogenous 2-monoglyceride, Present in Canine Gut, that Binds to Cannabinoid Receptors. *Biochem. Pharmacol.* 50 (1), 83–90. doi:10.1016/0006-2952(95)00109-D

Meschia, J. F., and Brott, T. (2018). Ischaemic Stroke. *Eur. J. Neurol.* 25 (1), 35–40. doi:10.1111/ene.13409

Michalski, D., Heindl, M., Kacza, J., Laignel, F., Küppers-Tiedt, L., Schneider, D., et al. (2012). Spatio-temporal Course of Macrophage-like Cell Accumulation after Experimental Embolic Stroke Depending on Treatment with Tissue Plasminogen Activator and its Combination with Hyperbaric Oxygenation. *Eur. J. Histochem* 56, e14. doi:10.4081/ejh.2012.14

Michelucci, A., Heurtaux, T., Grandbarbe, L., Morga, E., and Heuschling, P. (2009). Characterization of the Microglial Phenotype under Specific Pro-inflammatory and Anti-inflammatory Conditions: Effects of Oligomeric and Fibrillar Amyloid-Beta. *J. Neuroimmunol.* 210 (1–2), 3–12. doi:10.1016/j.jneuroim.2009.02.003

Miller, D. J., Simpson, J. R., and Silver, B. (2011). Safety of Thrombolysis in Acute Ischemic Stroke: A Review of Complications, Risk Factors, and Newer Technologies. *Neurohospitalist* 1 (3), 138–147. doi:10.1177/1941875211408731

Miller, R. H., and Raff, M. C. (1984). Fibrous and Protoplasmic Astrocytes Are Biochemically and Developmentally Distinct. *J. Neurosci.* 4 (2), 585–592. doi:10.1523/JNEUROSCI.04-02-00585.1984

Miller, S. J. (2018). Astrocyte Heterogeneity in the Adult Central Nervous System. *Front. Cell. Neurosci.* 12, 401. doi:10.3389/fncel.2018.00401

Miron, V. E., Boyd, A., Zhao, J. W., Yuen, T. J., Ruckh, J. M., Shadrach, J. L., et al. (2013). M2 Microglia and Macrophages Drive Oligodendrocyte Differentiation during CNS Remyelination. *Nat. Neurosci.* 16 (9), 1211–1218. doi:10.1038/nn.3469

Mishima, K., Hayakawa, K., Abe, K., Ikeda, T., Egashira, N., Iwasaki, K., et al. (2005). Cannabidiol Prevents Cerebral Infarction via a Serotonergic 5-Hydroxytryptamine 1A Receptor-dependent Mechanism. *Stroke* 36 (5), 1071–1076. doi:10.1161/01.STR.0000163083.59201.34

Mittelbronn, M., Dietz, K., Schluesener, H. J., and Meyermann, R. (2001). Local Distribution of Microglia in the Normal Adult Human Central Nervous System Differs by up to One Order of Magnitude. *Acta Neuropathol.* 101 (3), 249–255. doi:10.1007/s004010000284

Mohammed, N., Ceprian, M., Jimenez, L., Pazos, M. R., and Martínez-Orgado, J. (2017). Neuroprotective Effects of Cannabidiol in Hypoxic Ischemic Insult. The Therapeutic Window in Newborn Mice. *CNS Neurol. Disord. Drug Targets* 16 (1), 102–108. doi:10.2174/1871527315666160927110305

Molina-Holgado, F., Molina-Holgado, E., Guaza, C., and Rothwell, N. J. (2002). Role of CB1 and CB2 Receptors in the Inhibitory Effects of Cannabinoids on Lipopolysaccharide-Induced Nitric Oxide Release in Astrocyte Cultures. *J. Neurosci. Res.* 67 (6), 829–836. doi:10.1002/jnr.10165

Molofsky, A. V., Krencik, R., Krenick, R., Ullian, E. M., Ullian, E., Tsai, H. H., et al. (2012). Astrocytes and Disease: a Neurodevelopmental Perspective. *Genes. Dev.* 26 (9), 891–907. doi:10.1101/gad.188326.112

Moore, C. S., Cui, Q. L., Warsi, N. M., Durafourt, B. A., Zorko, N., Owen, D. R., et al. (2015). Direct and Indirect Effects of Immune and Central Nervous System-Resident Cells on Human Oligodendrocyte Progenitor Cell Differentiation. *J. Immunol.* 194 (2), 761–772. doi:10.4049/jimmunol.1401156

Morales, P., and Reggio, P. H. (2017). An Update on Non-CB1, Non-CB2 Cannabinoid Related G-Protein-Coupled Receptors. *Cannabis Cannabinoid Res.* 2 (1), 265–273. doi:10.1089/can.2017.0036

Morell, P., and Quarles, R. H. (1999). "Characteristic Composition of Myelin," in *Basic Neurochemistry: Molecular, Cellular and Medical Aspects*. G. J. Siegel, B. W. Agranoff, and R. W. Albers. 6th Edition (Philadelphia: Lippincott-Raven).

Mori, M. A., Meyer, E., da Silva, F. F., Milani, H., Guimarães, F. S., and Oliveira, R. M. W. (2021). Differential Contribution of CB1, CB2, 5-HT1A, and PPAR-γ Receptors to Cannabidiol Effects on Ischemia-Induced Emotional and Cognitive Impairments. *Eur. J. Neurosci.* 53 (6), 1738–1751. doi:10.1111/ejn.15134

Mori, M. A., Meyer, E., Soares, L. M., Milani, H., Guimarães, F. S., and de Oliveira, R. M. W. (2017). Cannabidiol Reduces Neuroinflammation and Promotes Neuroplasticity and Functional Recovery after Brain Ischemia. *Prog. Neuropsychopharmacol. Biol. Psychiatry* 75, 94–105. doi:10.1016/j.pnpbp.2016.11.005

Moulson, A. J., Squair, J. W., Franklin, R. J. M., Tetzlaff, W., and Assinck, P. (2021). Diversity of Reactive Astrogliosis in CNS Pathology: Heterogeneity or Plasticity? *Front. Cell. Neurosci.* 15, 703810. doi:10.3389/fncel.2021.703810

Munro, S., Thomas, K. L., and Abu-Shaar, M. (1993). Molecular Characterization of a Peripheral Receptor for Cannabinoids. *Nature* 365 (6441), 61–65. doi:10.1038/365061a0

Muthian, S., Rademacher, D. J., Roelke, C. T., Gross, G. J., and Hillard, C. J. (2004). Anandamide Content Is Increased and CB1 Cannabinoid Receptor Blockade Is Protective during Transient, Focal Cerebral Ischemia. *Neuroscience* 129 (3), 743–750. doi:10.1016/j.neuroscience.2004.08.044

Naccarato, M., Pizzuti, D., Petrosino, S., Simonetto, M., Ferigo, L., Grandi, F. C., et al. (2010). Possible Anandamide and Palmitoylethanolamide Involvement in Human Stroke. *Lipids Health Dis.* 9 (1), 47. doi:10.1186/1476-511X-9-47

Nakajima, K., Honda, S., Tohyama, Y., Imai, Y., Kohsaka, S., and Kurihara, T. (2001). Neurotrophin Secretion from Cultured Microglia. *J. Neurosci. Res.* 65 (4), 322–331. doi:10.1002/jnr.1157

Navarrete, M., and Araque, A. (2008). Endocannabinoids Mediate Neuron-Astrocyte Communication. *Neuron* 57 (6), 883–893. doi:10.1016/j.neuron.2008.01.029

Navarrete, M., and Araque, A. (2010). Endocannabinoids Potentiate Synaptic Transmission through Stimulation of Astrocytes. *Neuron* 68 (1), 113–126. doi:10.1016/j.neuron.2010.08.043

Navarro, G., Borroto-Escuela, D., Angelats, E., Etayo, Í., Reyes-Resina, I., Pulido-Salgado, M., et al. (2018). Receptor-heteromer Mediated Regulation of Endocannabinoid Signaling in Activated Microglia. Role of CB1 and CB2 Receptors and Relevance for Alzheimer's Disease and Levodopa-Induced Dyskinesia. *Brain Behav. Immun.* 67, 139–151. doi:10.1016/j.bbi.2017.08.015

Navarro, G., Reyes-Resina, I., Rivas-Santisteban, R., Sánchez de Medina, V., Morales, P., Casano, S., et al. (2018). Cannabidiol Skews Biased Agonism at Cannabinoid CB1 and CB2 Receptors with Smaller Effect in CB1-CB2 Heteroreceptor Complexes. *Biochem. Pharmacol.* 157, 148–158. doi:10.1016/j.bcp.2018.08.046

Nave, K. A., and Trapp, B. D. (2008). Axon-glial Signaling and the Glial Support of Axon Function. *Annu. Rev. Neurosci.* 31, 535–561. doi:10.1146/annurev.neuro.30.051606.094309

Nawashiro, H., Brenner, M., Fukui, S., Shima, K., and Hallenbeck, J. M. (2000). High Susceptibility to Cerebral Ischemia in GFAP-Null Mice. *J. Cereb. Blood Flow. Metab.* 20 (7), 1040–1044. doi:10.1097/00004647-200007000-00003

Nian, K., Harding, I. C., Herman, I. M., and Ebong, E. E. (2020). Blood-Brain Barrier Damage in Ischemic Stroke and its Regulation by Endothelial Mechanotransduction. *Front. Physiol.* 11, 605398. doi:10.3389/fphys.2020.605398

Nimmerjahn, A., Kirchhoff, F., and Helmchen, F. (2005). Resting Microglial Cells Are Highly Dynamic Surveillants of Brain Parenchyma *In Vivo*. *Science* 308 (5726), 1314–1318. doi:10.1126/science.1110647

Núñez, E., Benito, C., Pazos, M. R., Barbachano, A., Fajardo, O., González, S., et al. (2004). Cannabinoid CB2receptors Are Expressed by Perivascular Microglial Cells in the Human Brain: An Immunohistochemical Study. *Synapse* 53 (4), 208–213. doi:10.1002/syn.20050

Núñez, E., Benito, C., Tolón, R. M., Hillard, C. J., Griffin, W. S. T., and Romero, J. (2008). Glial Expression of Cannabinoid CB2 Receptors and Fatty Acid Amide Hydrolase Are Beta Amyloid-Linked Events in Down's Syndrome. *Neuroscience* 151 (1), 104–110. doi:10.1016/j.neuroscience.2007.10.029

Özen, I., Deierborg, T., Miharada, K., Padel, T., Englund, E., Genové, G., et al. (2014). Brain Pericytes Acquire a Microglial Phenotype after Stroke. *Acta Neuropathol.* 128 (3), 381–396. doi:10.1007/s00401-014-1295-x

Palazuelos, J., Aguado, T., Pazos, M. R., Julien, B., Carrasco, C., Resel, E., et al. (2009). Microglial CB2 Cannabinoid Receptors Are Neuroprotective in Huntington's Disease Excitotoxicity. *Brain* 132 (11), 3152–3164. doi:10.1093/brain/awp239

Pantoni, L., Garcia, J. H., and Gutierrez, J. A. (1996). Cerebral White Matter Is Highly Vulnerable to Ischemia. *Stroke* 27 (9), 1641–1647. doi:10.1161/01.str.27.9.1641

Parmentier-Batteur, S., Jin, K., Mao, X. O., Xie, L., and Greenberg, D. A. (2002). Increased Severity of Stroke in CB1 Cannabinoid Receptor Knock-Out Mice. *J. Neurosci.* 22 (22), 9771–9775. doi:10.1523/JNEUROSCI.22-22-09771.2002

Pazos, M. R., Cinquina, V., Gómez, A., Layunta, R., Santos, M., Fernández-Ruiz, J., et al. (2012). Cannabidiol Administration after Hypoxia-Ischemia to Newborn Rats Reduces Long-Term Brain Injury and Restores Neurobehavioral Function. *Neuropharmacology* 63 (5), 776–783. doi:10.1016/j.neuropharm.2012.05.034

Pazos, M. R., Mohammed, N., Lafuente, H., Santos, M., Martínez-Pinilla, E., Moreno, E., et al. (2013). Mechanisms of Cannabidiol Neuroprotection in Hypoxic-Ischemic Newborn Pigs: Role of 5HT(1A) and CB2 Receptors. *Neuropharmacology* 71, 282–291. doi:10.1016/j.neuropharm.2013.03.027

Pazos, M. R., Núñez, E., Benito, C., Tolón, R. M., and Romero, J. (2005). Functional Neuroanatomy of the Endocannabinoid System. *Pharmacol. Biochem. Behav.* 81 (2), 239–247. doi:10.1016/j.pbb.2005.01.030

Pekny, M., Pekna, M., Messing, A., Steinhäuser, C., Lee, J. M., Parpura, V., et al. (2016). Astrocytes: a Central Element in Neurological Diseases. *Acta Neuropathol.* 131 (3), 323–345. doi:10.1007/s00401-015-1513-1

Pekny, M., Wilhelmsson, U., Tatlisumak, T., and Pekna, M. (2019). Astrocyte Activation and Reactive Gliosis-A New Target in Stroke? *Neurosci. Lett.* 689, 45–55. doi:10.1016/j.neulet.2018.07.021

Pereira, A., and Furlan, F. A. (2010). Astrocytes and Human Cognition: Modeling Information Integration and Modulation of Neuronal Activity. *Prog. Neurobiol.* 92 (3), 405–420. doi:10.1016/j.pneurobio.2010.07.001

Pertwee, R. G. (2008). The Diverse CB1and CB2receptor Pharmacology of Three Plant Cannabinoids: Δ9-tetrahydrocannabinol, Cannabidiol and Δ9-tetrahydrocannabivarin. *Br. J. Pharmacol.* 153 (2), 199–215. doi:10.1038/sj.bjp.0707442

Pestana, F., Edwards-Faret, G., Belgard, T. G., Martirosyan, A., and Holt, M. G. (2020). No Longer Underappreciated: The Emerging Concept of Astrocyte Heterogeneity in Neuroscience. *Brain Sci.* 10 (3), E168. doi:10.3390/brainsci10030168

Piao, C. S., Kim, J. B., Han, P. L., and Lee, J. K. (2003). Administration of the P38 MAPK Inhibitor SB203580 Affords Brain Protection with a Wide Therapeutic Window against Focal Ischemic Insult. *J. Neurosci. Res.* 73 (4), 537–544. doi:10.1002/jnr.10671

Pietr, M., Kozela, E., Levy, R., Rimmerman, N., Lin, Y. H., Stella, N., et al. (2009). Differential Changes in GPR55 during Microglial Cell Activation. *FEBS Lett.* 583 (12), 2071–2076. doi:10.1016/j.febslet.2009.05.028

Powers, W. J., Rabinstein, A. A., Ackerson, T., Adeoye, O. M., Bambakidis, N. C., Becker, K., et al. (2018). 2018 Guidelines for the Early Management of Patients with Acute Ischemic Stroke: A Guideline for Healthcare Professionals from the American Heart Association/American Stroke Association. *Stroke* 49 (3), e46. doi:10.1161/STR.0000000000000158

Prinz, M., Jung, S., and Priller, J. (2019). Microglia Biology: One Century of Evolving Concepts. *Cell.* 179 (2), 292–311. doi:10.1016/j.cell.2019.08.053

Qin, C., Fan, W. H., Liu, Q., Shang, K., Murugan, M., Wu, L. J., et al. (2017). Fingolimod Protects against Ischemic White Matter Damage by Modulating Microglia toward M2 Polarization via STAT3 Pathway. *Stroke* 48 (12), 3336–3346. doi:10.1161/STROKEAHA.117.018505

Qin, C., Zhou, L. Q., Ma, X. T., Hu, Z. W., Yang, S., Chen, M., et al. (2019). Dual Functions of Microglia in Ischemic Stroke. *Neurosci. Bull.* 35 (5), 921–933. doi:10.1007/s12264-019-00388-3

Qureshi, A. I., Ali, Z., Suri, M. F., Shuaib, A., Baker, G., Todd, K., et al. (2003). Extracellular Glutamate and Other Amino Acids in Experimental Intracerebral Hemorrhage: An *In Vivo* Microdialysis Study. *Crit. Care Med.* 31 (5), 1482–1489. doi:10.1097/01.CCM.0000063047.63862.99

Rajan, W. D., Wojtas, B., Gielniewski, B., Gieryng, A., Zawadzka, M., and Kaminska, B. (2019). Dissecting Functional Phenotypes of Microglia and Macrophages in the Rat Brain after Transient Cerebral Ischemia. *Glia* 67 (2), 232–245. doi:10.1002/glia.23536

Rakers, C., Schleif, M., Blank, N., Matušková, H., Ulas, T., Händler, K., et al. (2019). Stroke Target Identification Guided by Astrocyte Transcriptome Analysis. *Glia* 67 (4), 619–633. doi:10.1002/glia.23544

Reichenbach, Z. W., Li, H., Ward, S. J., and Tuma, R. F. (2016). The CB1 Antagonist, SR141716A, Is Protective in Permanent Photothrombotic Cerebral Ischemia. *Neurosci. Lett.* 630, 9–15. doi:10.1016/j.neulet.2016.07.041

Reinert, A., Morawski, M., Seeger, J., Arendt, T., and Reinert, T. (2019). Iron Concentrations in Neurons and Glial Cells with Estimates on Ferritin Concentrations. *BMC Neurosci.* 20 (1), 25. doi:10.1186/s12868-019-0507-7

Revuelta, M., Elicegui, A., Moreno-Cugnon, L., Bührer, C., Matheu, A., and Schmitz, T. (2019). Ischemic Stroke in Neonatal and Adult Astrocytes. *Mech. Ageing Dev.* 183, 111147. doi:10.1016/j.mad.2019.111147

Rizzo, M. D., Crawford, R. B., Bach, A., Sermet, S., Amalfitano, A., and Kaminski, N. E. (2019). Imiquimod and Interferon-Alpha Augment Monocyte-Mediated Astrocyte Secretion of MCP-1, IL-6 and IP-10 in a Human Co-culture System. *J. Neuroimmunol.* 333, 576969. doi:10.1016/j.jneuroim.2019.576969

Rodriguez, J. J., Mackie, K., and Pickel, V. M. (2001). Ultrastructural Localization of the CB1 Cannabinoid Receptor in Mu-Opioid Receptor Patches of the Rat Caudate Putamen Nucleus. *J. Neurosci.* 21 (3), 823–833. doi:10.1523/JNEUROSCI.21-03-00823.2001

Rodríguez-Cueto, C., Benito, C., Fernández-Ruiz, J., Romero, J., Hernández-Gálvez, M., and Gómez-Ruiz, M. (2014). Changes in CB1and CB2receptors in the Post-mortem Cerebellum of Humans Affected by Spinocerebellar Ataxias. *Br. J. Pharmacol.* 171 (6), 1472–1489. doi:10.1111/bph.12283

Rodríguez-Cueto, C., Santos-García, I., García-Toscano, L., Espejo-Porras, F., Bellido, M., Fernández-Ruiz, J., et al. (2018). Neuroprotective Effects of the Cannabigerol Quinone Derivative VCE-003.2 in SOD1G93A Transgenic Mice, an Experimental Model of Amyotrophic Lateral Sclerosis. *Biochem. Pharmacol.* 157, 217–226. doi:10.1016/j.bcp.2018.07.049

Ronca, R. D., Myers, A. M., Ganea, D., Tuma, R. F., Walker, E. A., and Ward, S. J. (2015). A Selective Cannabinoid CB2 Agonist Attenuates Damage and Improves Memory Retention Following Stroke in Mice. *Life Sci.* 138, 72–77. doi:10.1016/j.lfs.2015.05.005

Rosciszewski, G., Cadena, V., Murta, V., Lukin, J., Villarreal, A., Roger, T., et al. (2018). Toll-Like Receptor 4 (TLR4) and Triggering Receptor Expressed on Myeloid Cells-2 (TREM-2) Activation Balance Astrocyte Polarization into a Proinflammatory Phenotype. *Mol. Neurobiol.* 55 (5), 3875–3888. doi:10.1007/s12035-017-0618-z

Roth, M., Gaceb, A., Enström, A., Padel, T., Genové, G., Özen, I., et al. (2019). Regulator of G-Protein Signaling 5 Regulates the Shift from Perivascular to Parenchymal Pericytes in the Chronic Phase after Stroke. *FASEB J.* 33 (8), 8990–8998. doi:10.1096/fj.201900153R

Rouach, N., Koulakoff, A., Abudara, V., Willecke, K., and Giaume, C. (2008). Astroglial Metabolic Networks Sustain Hippocampal Synaptic Transmission. *Science* 322 (5907), 1551–1555. doi:10.1126/science.1164022

Ryberg, E., Larsson, N., Sjögren, S., Hjorth, S., Hermansson, N. O., Leonova, J., et al. (2007). The Orphan Receptor GPR55 Is a Novel Cannabinoid Receptor. *Br. J. Pharmacol.* 152 (7), 1092–1101. doi:10.1038/sj.bjp.0707460

Sacco, R. L., Kasner, S. E., Broderick, J. P., Caplan, L. R., Connors, J. J., Culebras, A., et al. (2013). An Updated Definition of Stroke for the 21st Century: A Statement for Healthcare Professionals from the American Heart Association/American Stroke Association. *Stroke* 44 (7), 2064–2089. doi:10.1161/STR.0b013e318296aeca

Saliba, S. W., Jauch, H., Gargouri, B., Keil, A., Hurrle, T., Volz, N., et al. (2018). Anti-neuroinflammatory Effects of GPR55 Antagonists in LPS-Activated Primary Microglial Cells. *J. Neuroinflammation* 15 (1), 322. doi:10.1186/s12974-018-1362-7

Salter, M. G., and Fern, R. (2005). NMDA Receptors Are Expressed in Developing Oligodendrocyte Processes and Mediate Injury. *Nature* 438 (7071), 1167–1171. doi:10.1038/nature04301

Sanchez-Rodriguez, M. A., Gomez, O., Esteban, P. F., Garcia-Ovejero, D., and Molina-Holgado, E. (2018). The Endocannabinoid 2-arachidonoylglycerol Regulates Oligodendrocyte Progenitor Cell Migration. *Biochem. Pharmacol.* 157, 180–188. doi:10.1016/j.bcp.2018.09.006

Scarisbrick, I. A., Radulovic, M., Burda, J. E., Larson, N., Blaber, S. I., Giannini, C., et al. (2012). Kallikrein 6 Is a Novel Molecular Trigger of Reactive Astrogliosis. *Biol. Chem.* 393 (5), 355–367. doi:10.1515/hsz-2011-0241

Schäbitz, W.-R., Giuffrida, A., Berger, C., Aschoff, A., Schwaninger, M., Schwab, S., et al. (2002). Release of Fatty Acid Amides in a Patient with Hemispheric Stroke. *Stroke* 33 (8), 2112–2114. doi:10.1161/01.STR.0000023491.63693.18

Schiavon, A. P., Soares, L. M., Bonato, J. M., Milani, H., Guimarães, F. S., and Weffort de Oliveira, R. M. (2014). Protective Effects of Cannabidiol against Hippocampal Cell Death and Cognitive Impairment Induced by Bilateral Common Carotid Artery Occlusion in Mice. *Neurotox. Res.* 26 (4), 307–316. doi:10.1007/s12640-014-9457-0

Schmidt, W., Schäfer, F., Striggow, V., Fröhlich, K., and Striggow, F. (2012). Cannabinoid Receptor Subtypes 1 and 2 Mediate Long-Lasting Neuroprotection and Improve Motor Behavior Deficits after Transient Focal Cerebral Ischemia. *Neuroscience* 227, 313–326. doi:10.1016/j.neuroscience.2012.09.080

Schomacher, M., Müller, H. D., Sommer, C., Schwab, S., and Schäbitz, W. R. (2008). Endocannabinoids Mediate Neuroprotection after Transient Focal Cerebral Ischemia. *Brain Res.* 1240, 213–220. doi:10.1016/j.brainres.2008.09.019

Sheng, W. S., Hu, S., Min, X., Cabral, G. A., Lokensgard, J. R., and Peterson, P. K. (2005). Synthetic Cannabinoid WIN55,212-2 Inhibits Generation of Inflammatory Mediators by IL-1beta-stimulated Human Astrocytes. *Glia* 49 (2), 211–219. doi:10.1002/glia.20108

Shi, F., Yang, L., Kouadir, M., Yang, Y., Wang, J., Zhou, X., et al. (2012). The NALP3 Inflammasome Is Involved in Neurotoxic Prion Peptide-Induced Microglial Activation. *J. Neuroinflammation* 9 (1), 73. doi:10.1186/1742-2094-9-73

Shivachar, A. C., Martin, B. R., and Ellis, E. F. (1996). Anandamide- and Delta9-Tetrahydrocannabinol-Evoked Arachidonic Acid Mobilization and Blockade by SR141716A [N-(Piperidin-1-yl)-5-(4-chlorophenyl)-1-(2,4-dichlorophenyl)-4 -Methyl-1h-Pyrazole-3-Carboximide Hydrochloride]. *Biochem. PharmacolBiochemical Pharmacol.* 51 (5), 669–676. doi:10.1016/s0006-2952(95)02248-1

Shohami, E., Cohen-Yeshurun, A., Magid, L., Algali, M., and Mechoulam, R. (2011). Endocannabinoids and Traumatic Brain Injury. *Br. J. Pharmacol.* 163 (7), 1402–1410. doi:10.1111/j.1476-5381.2011.01343.x

Shonesy, B. C., Winder, D. G., Patel, S., and Colbran, R. J. (2015). The Initiation of Synaptic 2-AG Mobilization Requires Both an Increased Supply of Diacylglycerol Precursor and Increased Postsynaptic Calcium. *Neuropharmacology* 91, 57–62. doi:10.1016/j.neuropharm.2014.11.026

Silva, G. B., Atchison, D. K., Juncos, L. I., and García, N. H. (2013). Anandamide Inhibits Transport-Related Oxygen Consumption in the Loop of Henle by Activating CB1 Receptors. *Am. J. Physiol. Ren. Physiol.* 304 (4), F376–F381. doi:10.1152/ajprenal.00239.2012

Siqueira, M., Francis, D., Gisbert, D., Gomes, F. C. A., and Stipursky, J. (2018). Radial Glia Cells Control Angiogenesis in the Developing Cerebral Cortex through TGF-B1 Signaling. *Mol. Neurobiol.* 55 (5), 3660–3675. doi:10.1007/s12035-017-0557-8

Smith, H. L., Freeman, O. J., Butcher, A. J., Holmqvist, S., Humoud, I., Schätzl, T., et al. (2020). Astrocyte Unfolded Protein Response Induces a Specific Reactivity State that Causes Non-cell-autonomous Neuronal Degeneration. *Neuron* 105 (5), 855–e5. doi:10.1016/j.neuron.2019.12.014

Sofroniew, M. V. (2020). Astrocyte Reactivity: Subtypes, States, and Functions in CNS Innate Immunity. *Trends Immunol.* 41 (9), 758–770. doi:10.1016/j.it.2020.07.004

Sofroniew, M. V. (2009). Molecular Dissection of Reactive Astrogliosis and Glial Scar Formation. *Trends Neurosci.* 32 (12), 638–647. doi:10.1016/j.tins.2009.08.002

Sofroniew, M. V., and Vinters, H. V. (2010). Astrocytes: Biology and Pathology. *Acta Neuropathol.* 119 (1), 7–35. doi:10.1007/s00401-009-0619-8

Sotelo-Hitschfeld, T., Niemeyer, M. I., Mächler, P., Ruminot, I., Lerchundi, R., Wyss, M. T., et al. (2015). Channel-mediated Lactate Release by K^+-stimulated Astrocytes. *J. Neurosci.* 35 (10), 4168–4178. doi:10.1523/JNEUROSCI.5036-14.2015

Spaas, J., van Veggel, L., Schepers, M., Tiane, A., van Horssen, J., Wilson, D. M., et al. (2021). Oxidative Stress and Impaired Oligodendrocyte Precursor Cell Differentiation in Neurological Disorders. *Cell. Mol. Life Sci.* 78 (10), 4615–4637. doi:10.1007/s00018-021-03802-0

Spitzer, S. O., Sitnikov, S., Kamen, Y., Evans, K. A., Kronenberg-Versteeg, D., Dietmann, S., et al. (2019). Oligodendrocyte Progenitor Cells Become Regionally Diverse and Heterogeneous with Age. *Neuron* 101 (3), 459–e5. doi:10.1016/j.neuron.2018.12.020

Stella, N. (2010). Cannabinoid and Cannabinoid-like Receptors in Microglia, Astrocytes, and Astrocytomas. *Glia* 58 (9), 1017–1030. doi:10.1002/glia.20983

Stella, N., Schweitzer, P., and Piomelli, D. (1997). A Second Endogenous Cannabinoid that Modulates Long-Term Potentiation. *Nature* 388 (6644), 773–778. doi:10.1038/42015

Stempel, A. V., Stumpf, A., Zhang, H. Y., Özdoğan, T., Pannasch, U., Theis, A. K., et al. (2016). Cannabinoid Type 2 Receptors Mediate a Cell Type-specific Plasticity in the Hippocampus. *Neuron* 90 (4), 795–809. doi:10.1016/j.neuron.2016.03.034

Stone, N. L., England, T. J., and O'Sullivan, S. E. (2021). Protective Effects of Cannabidivarin and Cannabigerol on Cells of the Blood-Brain Barrier under Ischemic Conditions. *Cannabis Cannabinoid Res.* 6 (4), 315–326. doi:10.1089/can.2020.0159

Sugiura, T., Kondo, S., Sukagawa, A., Nakane, S., Shinoda, A., Itoh, K., et al. (1995). 2-Arachidonoylglycerol: a Possible Endogenous Cannabinoid Receptor Ligand in Brain. *Biochem. Biophys. Res. Commun.* 215 (1), 89–97. doi:10.1006/bbrc.1995.2437

Sun, J., Fang, Y., Chen, T., Guo, J., Yan, J., Song, S., et al. (2013). WIN55, 212-2 Promotes Differentiation of Oligodendrocyte Precursor Cells and Improve Remyelination through Regulation of the Phosphorylation Level of the ERK 1/2 via Cannabinoid Receptor 1 after Stroke-Induced Demyelination. *Brain Res.* 1491, 225–235. doi:10.1016/j.brainres.2012.11.006

Sun, J., Fang, Y. Q., Ren, H., Chen, T., Guo, J. J., Yan, J., et al. (2013). WIN55,212-2 Protects Oligodendrocyte Precursor Cells in Stroke Penumbra Following Permanent Focal Cerebral Ischemia in Rats. *Acta Pharmacol. Sin.* 34 (1), 119–128. doi:10.1038/aps.2012.141

Swanson, R. A., Ying, W., and Kauppinen, T. M. (2004). Astrocyte Influences on Ischemic Neuronal Death. *Curr. Mol. Med.* 4 (2), 193–205. doi:10.2174/1566524043479185

Tanaka, M., Sackett, S., and Zhang, Y. (2020). Endocannabinoid Modulation of Microglial Phenotypes in Neuropathology. *Front. Neurol.* 11, 87. doi:10.3389/fneur.2020.00087

Tanimura, A., Yamazaki, M., Hashimotodani, Y., Uchigashima, M., Kawata, S., Abe, M., et al. (2010). The Endocannabinoid 2-arachidonoylglycerol Produced by Diacylglycerol Lipase Alpha Mediates Retrograde Suppression of Synaptic Transmission. *Neuron* 65 (3), 320–327. doi:10.1016/j.neuron.2010.01.021

Thoren, A. E., Helps, S. C., Nilsson, M., and Sims, N. R. (2005). Astrocytic Function Assessed from 1-14c-Acetate Metabolism after Temporary Focal Cerebral Ischemia in Rats. *J. Cereb. Blood Flow. Metab.* 25 (4), 440–450. doi:10.1038/sj.jcbfm.9600035

Tolón, R. M., Núñez, E., Pazos, M. R., Benito, C., Castillo, A. I., Martínez-Orgado, J. A., et al. (2009). The Activation of Cannabinoid CB2 Receptors Stimulates *In Situ* and *In Vitro* Beta-Amyloid Removal by Human Macrophages. *Brain Res.* 1283, 148–154. doi:10.1016/j.brainres.2009.05.098

Tomas-Roig, J., Wirths, O., Salinas-Riester, G., and Havemann-Reinecke, U. (2016). The Cannabinoid CB1/CB2 Agonist WIN55212.2 Promotes Oligodendrocyte Differentiation *In Vitro* and Neuroprotection during the Cuprizone-Induced Central Nervous System Demyelination. *CNS Neurosci. Ther.* 22 (5), 387–395. doi:10.1111/cns.12506

Tomas-Roig, J., Agbemenyah, H. Y., Celarain, N., Quintana, E., Ramió-Torrentà, L., and Havemann-Reinecke, U. (2020). Dose-dependent Effect of Cannabinoid WIN-55,212-2 on Myelin Repair Following a Demyelinating Insult. *Sci. Rep.* 10 (1), 590. doi:10.1038/s41598-019-57290-1

Turcotte, C., Blanchet, M. R., Laviolette, M., and Flamand, N. (2016). The CB2 Receptor and its Role as a Regulator of Inflammation. *Cell. Mol. Life Sci.* 73 (23), 4449–4470. doi:10.1007/s00018-016-2300-4

Urra, X., Villamor, N., Amaro, S., Gómez-Choco, M., Obach, V., Oleaga, L., et al. (2009). Monocyte Subtypes Predict Clinical Course and Prognosis in Human Stroke. *J. Cereb. Blood Flow. Metab.* 29 (5), 994–1002. doi:10.1038/jcbfm.2009.25

van Asch, C. J., Luitse, M. J., Rinkel, G. J., van der Tweel, I., Algra, A., and Klijn, C. J. (2010). Incidence, Case Fatality, and Functional Outcome of Intracerebral Haemorrhage over Time, According to Age, Sex, and Ethnic Origin: a Systematic Review and Meta-Analysis. *Lancet Neurol.* 9 (2), 167–176. doi:10.1016/S1474-4422(09)70340-0

Vázquez, C., Tolón, R. M., Pazos, M. R., Moreno, M., Koester, E. C., Cravatt, B. F., et al. (2015). Endocannabinoids Regulate the Activity of Astrocytic Hemichannels and the Microglial Response against an Injury: *In Vivo* Studies. *Neurobiol. Dis.* 79, 41–50. doi:10.1016/j.nbd.2015.04.005

Verkhratsky, A., and Nedergaard, M. (2018). Physiology of Astroglia. *Physiol. Rev.* 98 (1), 239–389. doi:10.1152/physrev.00042.2016

Verkhratsky, A., Sofroniew, M. V., Messing, A., deLanerolle, N. C., Rempe, D., Rodríguez, J. J., et al. (2012). Neurological Diseases as Primary Gliopathies: a Reassessment of Neurocentrism. *ASN Neuro* 4 (3), 4. doi:10.1042/AN20120010

Wake, H., Moorhouse, A. J., Jinno, S., Kohsaka, S., and Nabekura, J. (2009). Resting Microglia Directly Monitor the Functional State of Synapses *In Vivo* and Determine the Fate of Ischemic Terminals. *J. Neurosci.* 29 (13), 3974–3980. doi:10.1523/JNEUROSCI.4363-08.2009

Walter, L., Franklin, A., Witting, A., Moller, T., and Stella, N. (2002). Astrocytes in Culture Produce Anandamide and Other Acylethanolamides. *J. Biol. Chem.* 277 (23), 20869–20876. doi:10.1074/jbc.M110813200

Walter, L., Franklin, A., Witting, A., Wade, C., Xie, Y., Kunos, G., et al. (2003). Nonpsychotropic Cannabinoid Receptors Regulate Microglial Cell Migration. *J. Neurosci.* 23 (4), 1398–1405. doi:10.1523/JNEUROSCI.23-04-01398.2003

Wang, F., Han, J., Higashimori, H., Wang, J., Liu, J., Tong, L., et al. (2019). Long-term Depression Induced by Endogenous Cannabinoids Produces Neuroprotection via Astroglial CB1R after Stroke in Rodents. *J. Cereb. Blood Flow. Metab.* 39 (6), 1122–1137. doi:10.1177/0271678X18755661

Wang, Y., Liu, G., Hong, D., Chen, F., Ji, X., and Cao, G. (2016). White Matter Injury in Ischemic Stroke. *Prog. Neurobiol.* 141, 45–60. doi:10.1016/j.pneurobio.2016.04.005

Wilhelmsson, U., Li, L., Pekna, M., Berthold, C. H., Blom, S., Eliasson, C., et al. (2004). Absence of Glial Fibrillary Acidic Protein and Vimentin Prevents Hypertrophy of Astrocytic Processes and Improves Post-traumatic Regeneration. *J. Neurosci.* 24 (21), 5016–5021. doi:10.1523/JNEUROSCI.0820-04.2004

Yang, X. L., Wang, X., Shao, L., Jiang, G. T., Min, J. W., Mei, X. Y., et al. (2019). TRPV1 Mediates Astrocyte Activation and Interleukin-1β Release Induced by Hypoxic Ischemia (HI). *J. Neuroinflammation* 16 (1), 114. doi:10.1186/s12974-019-1487-3

Yokubaitis, C. G., Jessani, H. N., Li, H., Amodea, A. K., and Ward, S. J. (2021). Effects of Cannabidiol and Beta-Caryophyllene Alone or in Combination in a Mouse Model of Permanent Ischemia. *Int. J. Mol. Sci.* 22 (6), 2866. doi:10.3390/ijms22062866

Yun, S. P., Kam, T. I., Panicker, N., Kim, S., Oh, Y., Park, J. S., et al. (2018). Block of A1 Astrocyte Conversion by Microglia Is Neuroprotective in Models of Parkinson's Disease. *Nat. Med.* 24 (7), 931–938. doi:10.1038/s41591-018-0051-5

Zamanian, J. L., Xu, L., Foo, L. C., Nouri, N., Zhou, L., Giffard, R. G., et al. (2012). Genomic Analysis of Reactive Astrogliosis. *J. Neurosci.* 32 (18), 6391–6410. doi:10.1523/JNEUROSCI.6221-11.2012

Zarruk, J. G., Fernández-López, D., García-Yébenes, I., García-Gutiérrez, M. S., Vivancos, J., Nombela, F., et al. (2012). Cannabinoid Type 2 Receptor Activation Downregulates Stroke-Induced Classic and Alternative Brain Macrophage/Microglial Activation Concomitant to Neuroprotection. *Stroke* 43 (1), 211–219. doi:10.1161/STROKEAHA.111.631044

Zawadzka, M., Dabrowski, M., Gozdz, A., Szadujkis, B., Sliwa, M., Lipko, M., et al. (2012). Early Steps of Microglial Activation Are Directly Affected by Neuroprotectant FK506 in Both *In Vitro* Inflammation and in Rat Model of Stroke. *J. Mol. Med. Berl.* 90 (12), 1459–1471. doi:10.1007/s00109-012-0925-9

Zhang, J., Zhang, Y., Xing, S., Liang, Z., and Zeng, J. (2012). Secondary Neurodegeneration in Remote Regions after Focal Cerebral Infarction: a New Target for Stroke Management? *Stroke* 43 (6), 1700–1705. doi:10.1161/STROKEAHA.111.632448

Zhang, M., Martin, B. R., Adler, M. W., Razdan, R. K., Ganea, D., and Tuma, R. F. (2008). Modulation of the Balance between Cannabinoid CB(1) and CB(2) Receptor Activation during Cerebral Ischemic/reperfusion Injury. *Neuroscience* 152 (3), 753–760. doi:10.1016/j.neuroscience.2008.01.022

Zhang, M., Martin, B. R., Adler, M. W., Razdan, R. K., Jallo, J. I., and Tuma, R. F. (2007). Cannabinoid CB(2) Receptor Activation Decreases Cerebral Infarction in a Mouse Focal Ischemia/reperfusion Model. *J. Cereb. Blood Flow. Metab.* 27 (7), 1387–1396. doi:10.1038/sj.jcbfm.9600447

Zhang, R. L., Chopp, M., Roberts, C., Jia, L., Wei, M., Lu, M., et al. (2011). Ascl1 Lineage Cells Contribute to Ischemia-Induced Neurogenesis and Oligodendrogenesis. *J. Cereb. Blood Flow. Metab.* 31 (2), 614–625. doi:10.1038/jcbfm.2010.134

Zou, S., and Kumar, U. (2018). Cannabinoid Receptors and the Endocannabinoid System: Signaling and Function in the Central Nervous System. *Int. J. Mol. Sci.* 19 (3), 833. doi:10.3390/ijms19030833

Conflict of Interest: The authors declare that the research was conducted in the absence of any commercial or financial relationships that could be construed as a potential conflict of interest.

frontiers | Frontiers in Pharmacology

ORIGINAL RESEARCH
published: 08 July 2022
doi: 10.3389/fphar.2022.919553

Electroacupuncture Reduces Anxiety Associated With Inflammatory Bowel Disease By Acting on Cannabinoid CB1 Receptors in the Ventral Hippocampus in Mice

Xue-Fei Hu[1], Hong Zhang[1], Ling-Ling Yu[2], Wen-Qiang Ge[1], Ou-Yang Zhan-mu[1], Yan-Zhen Li[1], Chao Chen[1], Teng-Fei Hou[1], Hong-Chun Xiang[1], Yuan-Heng Li[1], Yang-Shuai Su[3], Xiang-Hong Jing[3], Jie Cao[4], Hui-Lin Pan[5], Wei He[3] and Man Li[1]**

[1]Department of Neurobiology, School of Basic Medicine, Tongji Medical College of Huazhong University of Science and Technology, Wuhan, China, [2]Institute of Integrated Traditional Chinese and Western Medicine, Tongji Hospital, Tongji Medical College, Huazhong University of Science and Technology, Wuhan, China, [3]Institute of Acupuncture and Moxibustion, China Academy of Chinese Medical Sciences (CACMS), Beijing, China, [4]Department of Neurology, Tongji Hospital, Tongji Medical College, Huazhong University of Science and Technology, Wuhan, China, [5]Department of Anesthesiology and Perioperative Medicine, The University of Texas MD Anderson Cancer Center, Houston, TX, United States

The therapeutic effects of electroacupuncture (EA) on the comorbidity of visceral pain and anxiety in patients with inflammatory bowel disease (IBD) is well known. It has been known that the ventral hippocampus (vHPC) and the cannabinoid type 1 receptors (CB1R) are involved in regulating anxiety and pain. Therefore, in this study, we determined whether EA reduces visceral pain and IBD-induced anxiety *via* CB1R in the vHPC. We found that EA alleviated visceral hyperalgesia and anxiety in TNBS-treated IBD mice. EA reversed overexpression of CB1R in IBD mice and decreased the percentage of CB1R-expressed GABAergic neurons in the vHPC. Ablating CB1R of GABAergic neurons in the vHPC alleviated anxiety in TNBS-treated mice and mimicked the anxiolytic effect of EA. While ablating CB1R in glutamatergic neurons in the vHPC induced severe anxiety in wild type mice and inhibited the anxiolytic effect of EA. However, ablating CB1R in either GABAergic or glutamatergic neurons in the vHPC did not alter visceral pain. In conclusion, we found CB1R in both GABAergic neurons and glutamatergic neurons are involved in the inhibitory effect of EA on anxiety but not visceral pain in IBD mice. EA may exert anxiolytic effect *via* downregulating CB1R in GABAergic neurons and activating CB1R in glutamatergic neurons in the vHPC, thus reducing the release of glutamate and inhibiting the anxiety circuit related to vHPC. Thus, our study provides new information about the cellular and molecular mechanisms of the therapeutic effect of EA on anxiety induced by IBD.

Keywords: acupuncture, visceral pain, anxiety, CB1 receptors, ventral hippocampus

OPEN ACCESS

Edited by:
Carmen Rodriguez Cueto, Center for Biomedical Research on Neurodegenerative Diseases (CIBERNED), Spain

Reviewed by:
Hector Romo-Parra, Anahuac University of North Mexico, Mexico
Roberta Imperatore, University of Sannio, Italy
Haijun Zhao, Shandong University of Traditional Chinese Medicine, China

****Correspondence:***
Wei He
hazel7811@hotmail.com
Man Li
liman73@mails.tjmu.edu.cn

Specialty section:
This article was submitted to Neuropharmacology, a section of the journal Frontiers in Pharmacology

Received: *13 April 2022*
Accepted: *23 May 2022*
Published: *08 July 2022*

Citation:
Hu X-F, Zhang H, Yu L-L, Ge W-Q, Zhan-mu O-Y, Li Y-Z, Chen C, Hou T-F, Xiang H-C, Li Y-H, Su Y-S, Jing X-H, Cao J, Pan H-L, He W and Li M (2022) Electroacupuncture Reduces Anxiety Associated With Inflammatory Bowel Disease By Acting on Cannabinoid CB1 Receptors in the Ventral Hippocampus in Mice. Front. Pharmacol. 13:919553. doi: 10.3389/fphar.2022.919553

1 INTRODUCTION

Inflammatory bowel disease (IBD), including Crohn's disease and ulcerative colitis, is a prevalent clinical problem worldwide (Mittermaier et al., 2004; Molodecky et al., 2012; Neuendorf et al., 2016). In addition to gastrointestinal symptoms, patients with IBD also experience emotion disorders, such as anxiety and depression (Ng et al., 2017), which in turn exaggerate gastrointestinal symptoms (Ananthakrishnan, 2015). Several reports have shown that the comorbidity of visceral pain and anxiety in IBD mice resulted from the bidirectional communication between the gut microbiota and the brain (Moloney et al., 2016; Banfi et al., 2021). Electroacupuncture (EA) is an effective treatment for gastrointestinal diseases, pain symptoms and mood disorders through electrical stimulation of needles inserted into specific acupoints (Wu et al., 1999; Errington-Evans, 2012; Lv et al., 2019; Smith et al., 2019; Song et al., 2019; Wang et al., 2019). However, the underlying mechanism of the therapeutic effects of EA on IBD remains largely unknown.

Several pieces of evidence indicate that the ventral hippocampus (vHPC) plays a key role in modulating anxiety-like behaviors (Allsop et al., 2014; Bannerman et al., 2014; Shah et al., 2021) and pain process (Fasick et al., 2015; Vasic and Schmidt, 2017; Liu et al., 2018). Pathological anxiety and chronic stress lead to structural degeneration and impaired function of the hippocampus (Mah et al., 2016; Price and Duman, 2020). In addition, the hippocampus plays an important role in the development and maintenance of pain disorder (Fasick et al., 2015; Vasic and Schmidt, 2017). It needs to be determined whether EA attenuates IBD induced visceral pain and anxiety *via* the vHPC.

Cannabinoid type 1 receptors (CB1R) are highly expressed in the brain areas (Evans and Van'T, 1975; Tsou et al., 1998; Fletcher-Jones et al., 2020) and are related to the control of anxiety response (Haller et al., 2004; Rey et al., 2012) and pain process (Padilla-Coreano et al., 2016; Wang et al., 2020), such as vHPC in particular. CB1R are mainly located at presynaptic terminals and inhibit the release of several classic neurotransmitters, including glutamate and GABA (Egertova et al., 1998; Lisboa et al., 2015). CB1R are preferentially expressed in GABAergic neurons (Hill et al., 2013), but less expressed in glutamatergic neurons (Katona and Freund, 2012). Moreover, CB1R in glutamatergic and GABAergic neurons in the cortex have an opposing role in controlling anxiety-like behaviors (Lafenetre et al., 2009; Haring et al., 2011; Ruehle et al., 2013). However, little is known about the role of CB1R in glutamatergic and GABAergic neurons in the vHPC in visceral pain and anxiety in IBD. It is also unclear whether EA attenuates these symptoms via CB1R expressed in the vHPC.

Based on these pieces of evidence, the present study investigated whether EA alleviate visceral pain and anxiety in 2,4,6-trinitrobenzene sulfonic acid (TNBS)-induced IBD mice. Then, we observed the distribution of CB1R in glutamatergic or GABAergic neurons in the vHPC before and after TNBS and EA treatment. We determined whether genetically ablating CB1R expressed in glutamatergic or GABAergic neurons in the vHPC altered the effects of EA on visceral pain and anxiety in IBD mice. Our findings provide new evidence that CB1R expressed in the vHPC might be involved in the effects of EA on IBD induced anxiety, but not on IBD induced visceral pain.

2 MATERIALS AND METHOD

2.1 Animals

Adult male C57BL/6 mice (8 weeks old; 20—25 g) were raised in home-cages in the environment of 23°C ± 2°C and a 12 h light/dark cycle. The mice had free access to food and water. All CB1R-flox mice (mCnr1flox/flox) and their wild-type littermate (WT) mice (male, aged 8 weeks, and 18–21 g) were bought from the Cyagen biosciences laboratory (Nanjing, China). All animal procedures were approved by the Institutional Animal Care and Use Committee at Huazhong University of Science and Technology and conformed to the ethical guidelines of the International Association for the Study of Pain and Anxiety.

2.2 Viruses Constructs and Surgery

The Cre/loxP system (Kos, 2004) was used to delete CB1R in GABAergic and glutamatergic neurons. The recombinant adeno-associated viruses (rAAV)-mDIX-cre-WPRE-pA viruses were used to delete CB1R in GABAergic neurons. The rAAV-CaMKII-cre-WPRE-pA viruses were used to delete CB1R in glutamatergic neurons. All viruses used in this research were purchased from the Brain VTA scientific and technical corporation (Wuhan, China).

Before microinjection, the mice received an intraperitoneal injection (i.p.) of 100 mg/kg of tribromoethanol for anesthesia and were fixed in the stereotaxic apparatus (RWD Instruments, China). An incision with a length of 1.5 cm was made along the midline of the skull and the periosteum on the surface of the skull was removed. Then, a small hole was grinded by ironic rotor. Viruses injection was performed based on the coordinate of vHPC (2.95 mm backward from the bregma, 2.75 mm lateral from the midline, and 3.75 mm ventral to the skull) (Allsop et al., 2014). Designed viruses vectors (200 nl) were injected into vHPC at a rate of 50 nl per 60 s. Data were excluded from analysis if the viruses infection exceeded area of the vHPC.

2.3 IBD Model

IBD was induced in mice as described previously (Silva et al., 2019). Mice were anesthetized with tribromoethanol. A PVC-Fr4 catheter (Φ 2.7 mm, YN Medical Instrument, Yangzhou, China) lubricated by corn oil was inserted into the anus to the colon at a distance of 4 cm, and the other end of PVC-Fr4 catheter was attached with a 1 ml syringe. The TNBS intra-rectal (IR) solution included 50 µl of 5% w/v TNBS solution (Sigma-Aldrich, St. Louis, MO, United States) and 50 µl

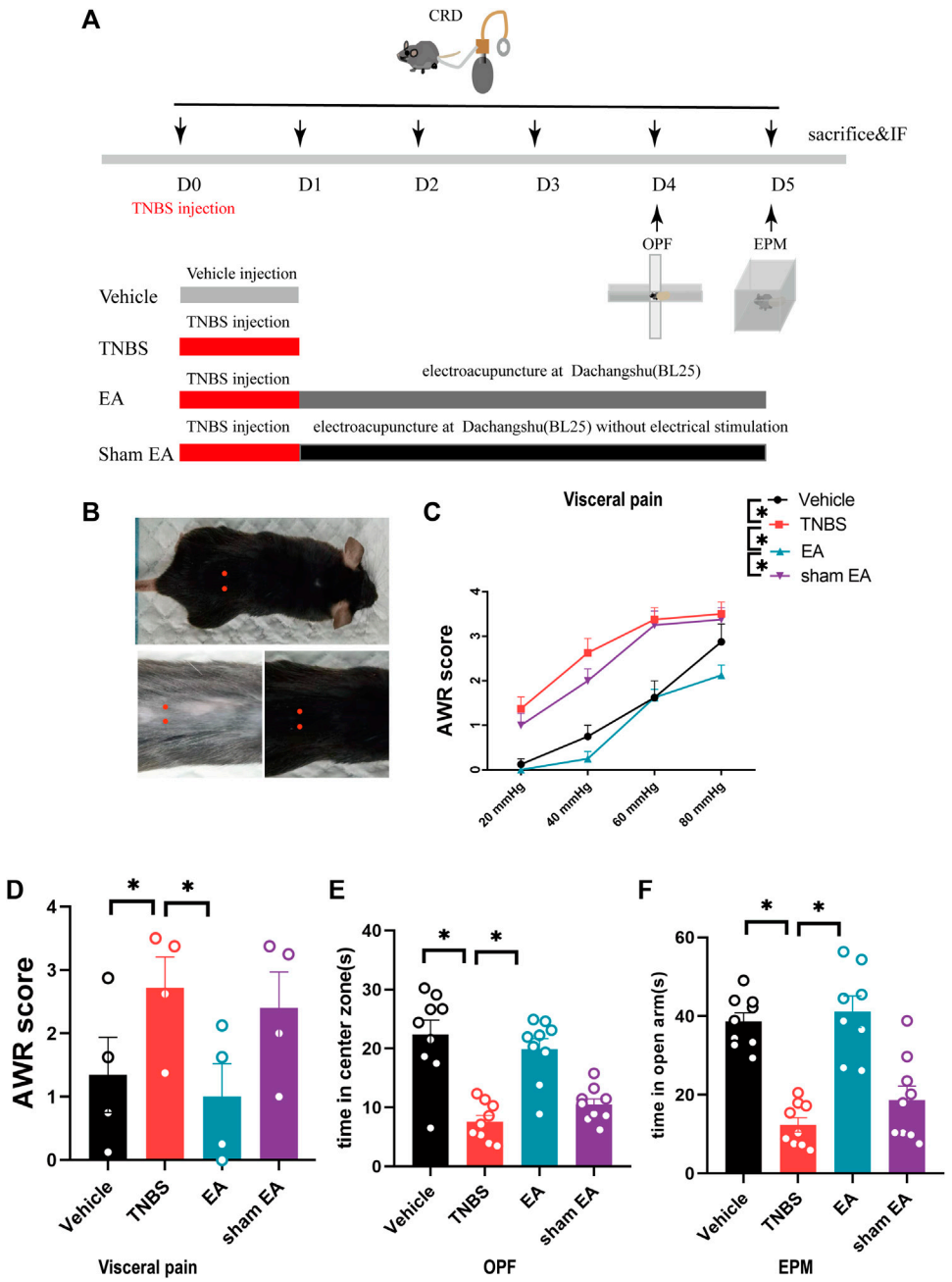

FIGURE 1 | EA relieved the visceral hyperalgesia and anxiety-like behaviors of IBD mice. **(A)** Experimental flowchart. **(B)** Schematic diagram of Dachangshu points (BL25) on the skin surface. **(C,D)** Visceral hyperalgesia was evaluated by CRD. **(E)** Anxiety-related behaviors were recorded as time in center zone in the OPF. **(F)** Anxiety-related behaviors were recorded as time in open arms in the EPM. The data are expressed as mean ± SEM ($n = 9$ mice). *represents $p < 0.05$ between marked groups.

absolute ethanol, which was injected into the colon of anesthetized mice. Mice of the vehicle control group received an injection solution comprised of 50 µl distilled water and 50 µl absolute ethanol. After injection, mice were kept in an upside-down position for 5 min to prevent solution leakage. The mice were placed on a heating pad until recovery from anesthesia.

2.4 EA Treatment

EA treatment was applied to bilateral "Dachangshu" (BL25) acupoints 1 day after TNBS injection. The BL25 acupoints were located at both side of the waist and 7 mm lateral to the fourth lumbar spinous. After mice were restrained by specialized fabric equipment, acupuncture needles were inserted into acupoints with a depth of 2.5 mm. Then,

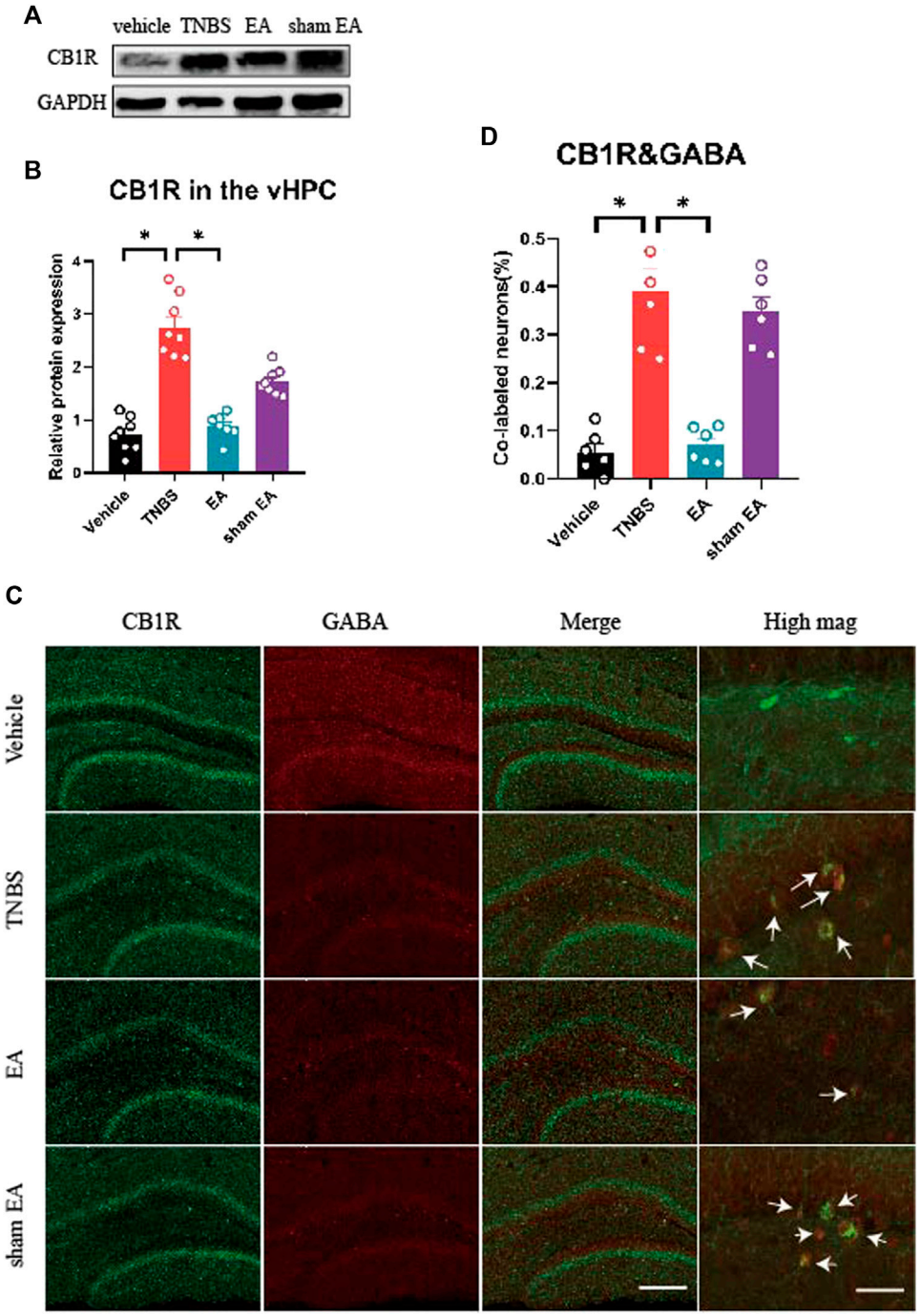

FIGURE 2 | EA reversed over-expression of CB1R and decreased the percentage of CB1R-expressed GABAergic neurons in the vHPC of IBD mice. **(A)** Representative immunoblots of CB1R and GAPDH protein expression in the vHPC. **(B)** Densitometric analysis of CB1R protein normalized to the loading control. **(C)** Immunofluorescence images showed CB1R (green) co-expressed with GABA (red) in the vHPC. **(D)** Percentage of CB1R-expressed neurons co-labeled with GABA, which is (CB1R and GABA co-labeled neurons /total GABA neurons) *100%. Scale bar for merge images, 100 μm. Scale bar for high magnification images (high mag), 20 μm. The data are expressed as mean ± SEM (n = 9 mice). *represents $p < 0.05$ between marked groups.

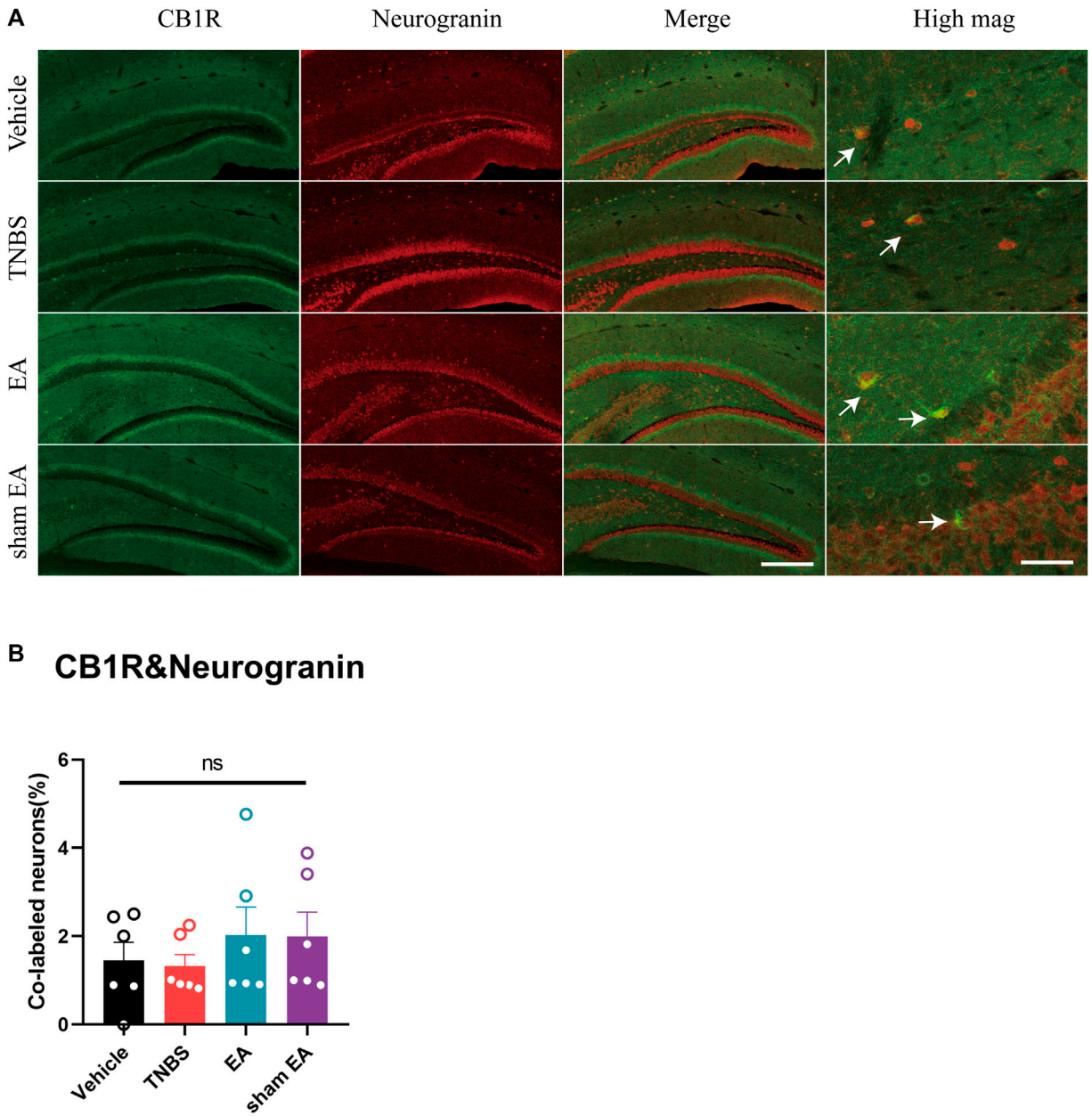

FIGURE 3 | TNBS and EA had no effect on the percentage of CB1R-expressed glutamatergic neurons in the vHPC of IBD mice. **(A)** Immunofluorescence images showed CB1R (green) co-expressed with neurogranin (a marker of glutamatergic neurons, red) in the vHPC. **(B)** Percentage of CB1R-expressed neurons co-labeled with neurogranin, which is (CB1R and neurogranin co-labeled neurons /total neurogranin neurons) *100%. Scale bar for merge images, 100 μm. Scale bar for high magnification images (high mag), 20 μm. Ns represents $p > 0.05$ between marked groups.

acupuncture needles were connected to an EA stimulator (Huatuo brand, Suzhou, China) and electrical stimulation pulses (1 mA, 2 Hz, intermittent wave) were applied for 30 min.

As for sham EA, acupuncture needles only adhered to the specific points, neither penetrated the skin nor received electrical stimulation pulses. Half an hour after EA treatment, the related behavior tests were performed.

2.5 Behavioral Tests

2.5.1 Measurement of Visceral Hyperalgesia

Measurements were made continuous 5 days after TNBS injection. The colorectal distension (CRD) method was used to obtain the abdominal withdrawal reflex (AWR) score of mice to evaluate the degree of visceral hyperalgesia. The mice were placed in a plexiglass compartment (20 cm × 20 cm × 10 cm) for 5 min. The PVC-Fr4 catheter was inserted into the latex balloon (length

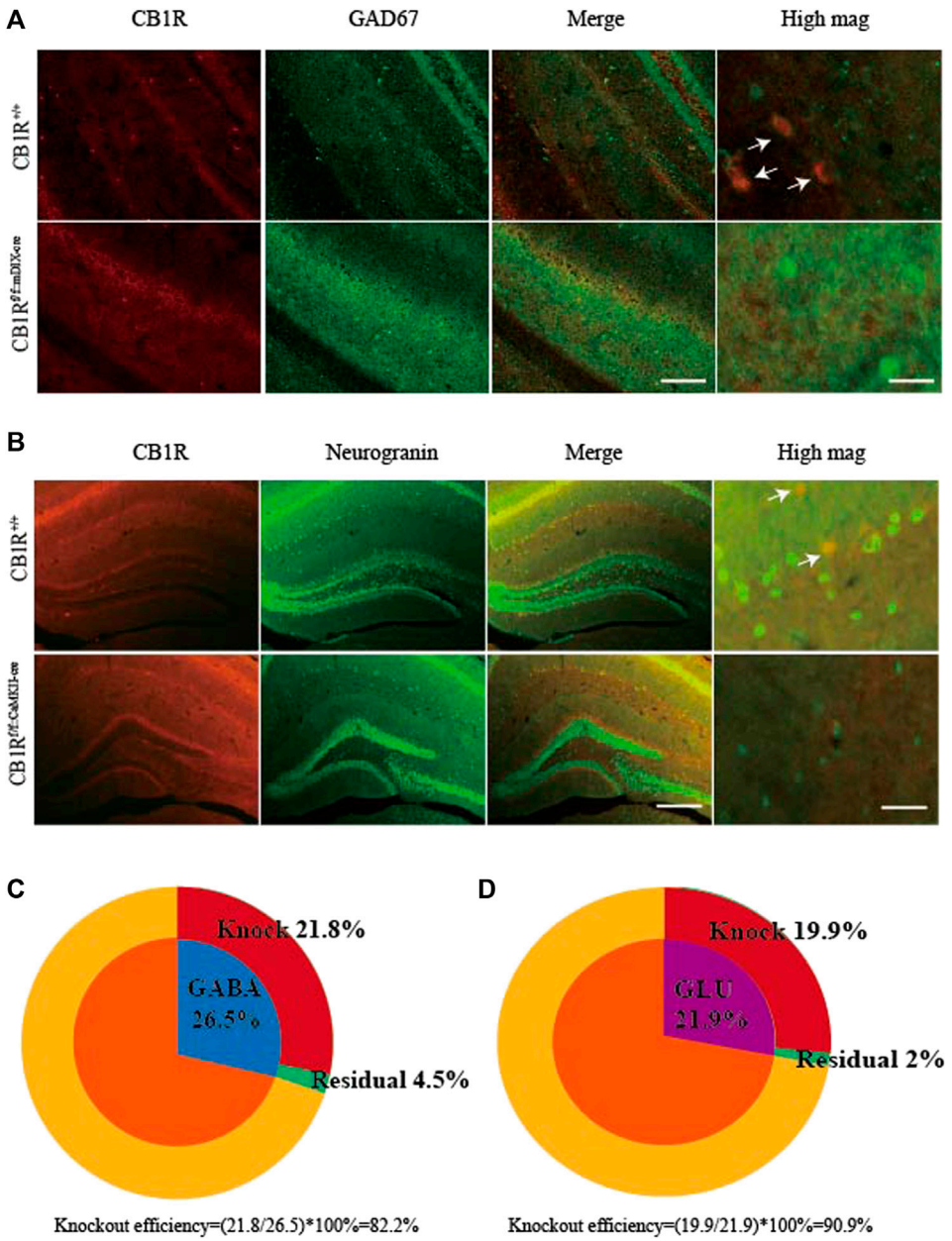

FIGURE 4 | Specific knockout of the CB1R in GABAergic and glutamatergic neurons in the vHPC. **(A)** After rAAV-mDlX-cre-WPRE-pA viruses were injected into bilateral vHPC of CB1R-flox mice, immunofluorescence images showed CB1R (red) co-expressed with GAD67 (labeled GABAergic neurons, green) in the vHPC. Scale bar for merge images, 200 μm. Scale bar for high magnification images (high mag), 40 μm. **(B)** After rAAV-CaMKII-cre-WPRE-pA viruses were injected into bilateral vHPC of CB1R-flox mice, immunofluorescence images showed CB1R (red) co-expressed with neurogranin (a marker of glutamatergic neurons, green) in the vHPC. Scale bar for merge images, 100 μm. Scale bar for high magnification images (high mag), 20 μm. **(C)** Summary data show the percentage of GABAergic neurons whose CB1 receptors were knocked out (red). **(D)** Summary data show the percentage of glutamatergic neurons whose CB1 receptors were knocked out (red). Data are expressed as the means ± SEM (n = 3 mice in each group).

4–5 cm), and the end of the balloon was firmly tied to the test catheter. The catheter is connected with one end of the disposable medical three-way tubing, one end of the three-way tubing was connected to a sphygmomanometer. The other end is connected with 20 ml disposable syringe, and 20 ml of 20°C water was injected into the syringe. The balloon was inserted into the rectum until the catheter reached the colon (2 cm from the end of the balloon). The balloon catheter was fixed to the bottom of the tail to prevent it from sliding out.

The CRD test was performed in a step-by-step compression mode (20/40/60/80 mmHg). Each pressure value was measured twice. Each test lasted 30s with an interval of 4 min. The AWR

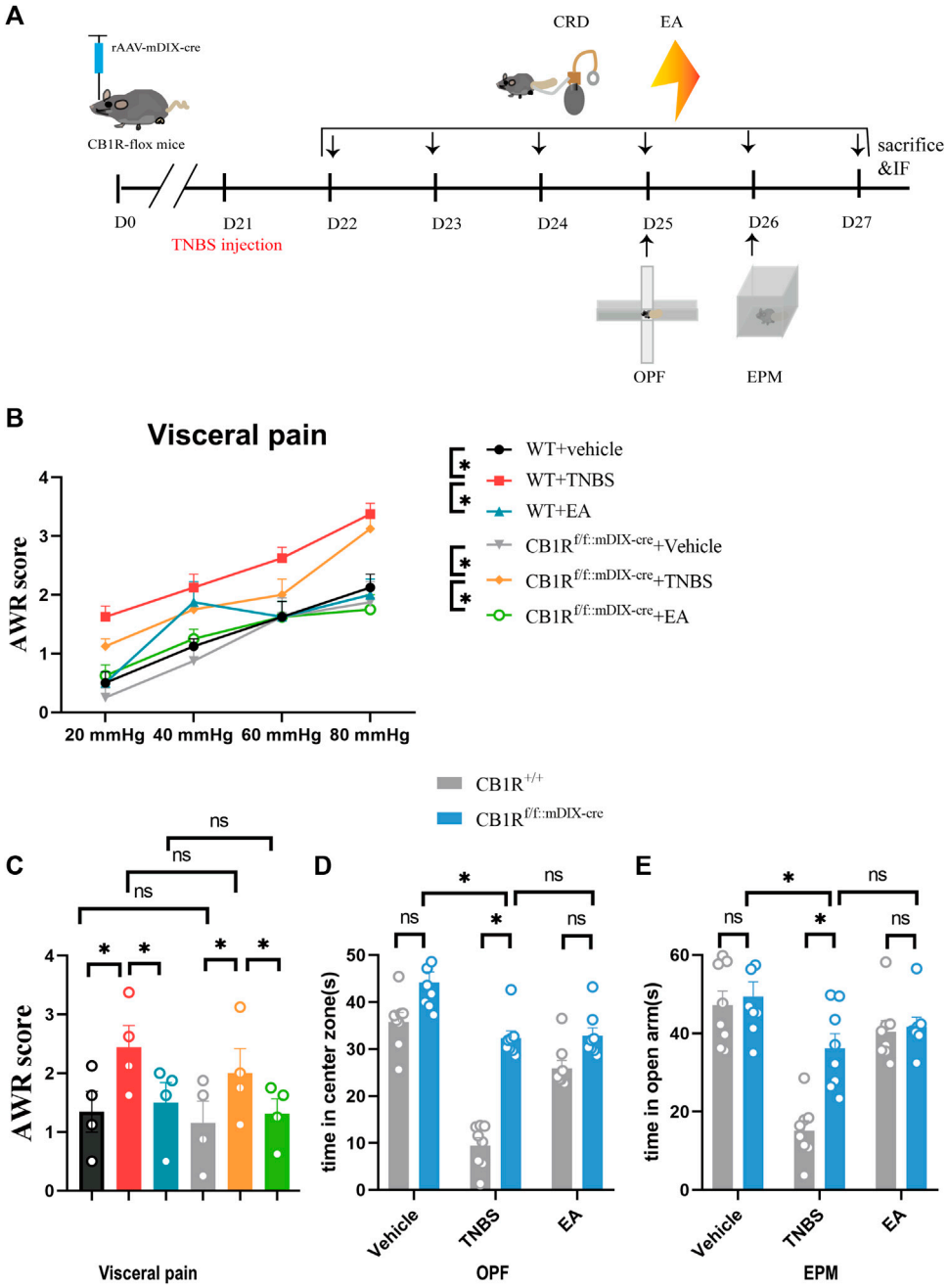

FIGURE 5 | Specific knock out of the CB1R in GABAergic neurons in the vHPC mimicked the anxiolytic but not analgesic effect of EA on IBD mice. **(A)** Experimental flowchart. **(B,C)** Visceral hyperalgesia was evaluated by CRD. **(D)** Anxiety-related behaviors were recorded as time in center zone in the OPF. **(E)** Anxiety-related behaviors were recorded as time in open arms in the EPM. The data are expressed as mean ± SEM (n = 8 mice). * represents $p < 0.05$ between marked groups, ns represents $p > 0.05$ between marked groups.

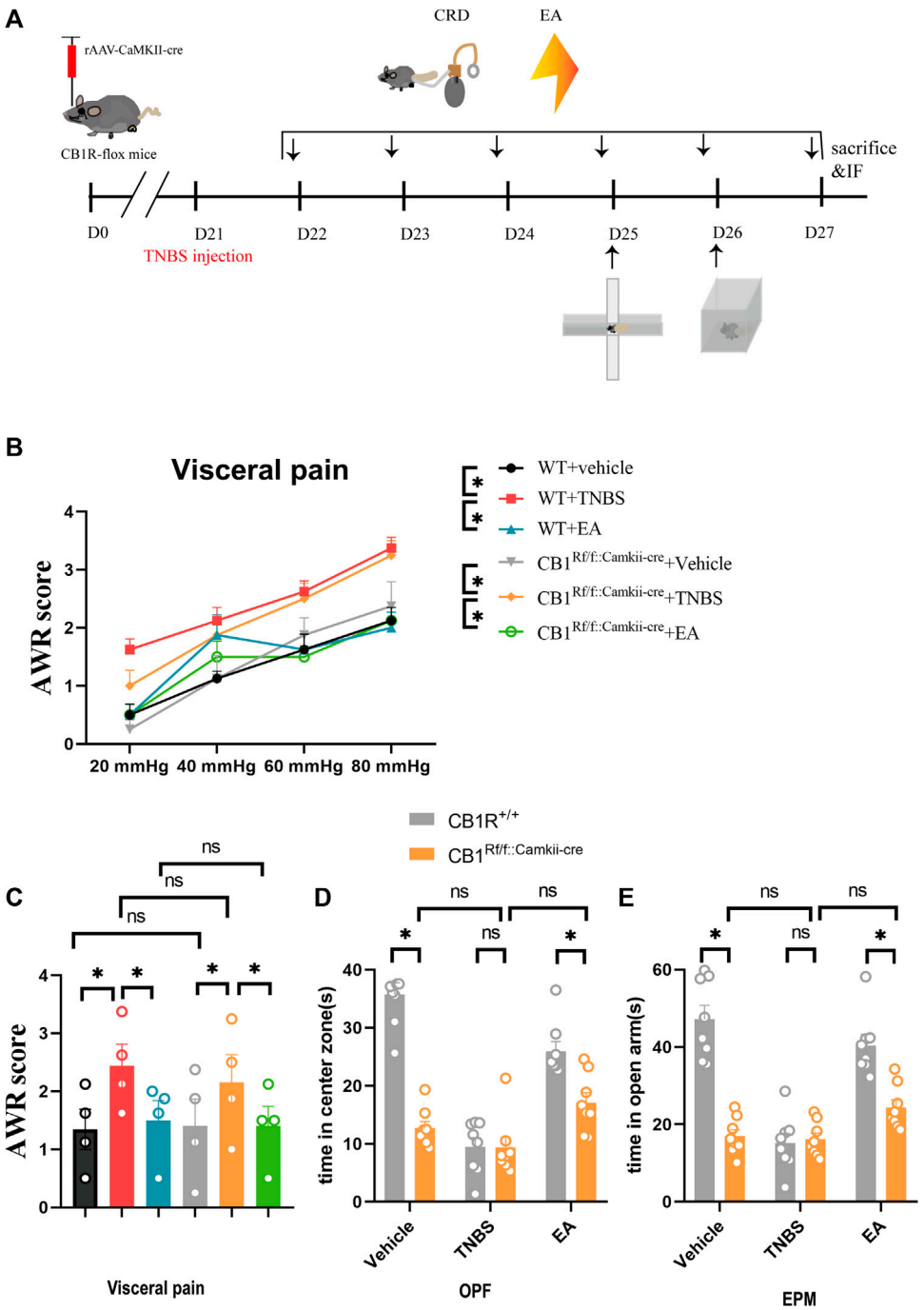

FIGURE 6 | Specific knock out of the CB1R in glutamatergic neurons in the vHPC reversed the anxiolytic but not analgesic effect of EA on IBD mice. **(A)** Experimental flowchart. **(B,C)** Visceral hyperalgesia was evaluated by CRD. **(D)** Anxiety-related behaviors were recorded as time in center zone in the OPF. **(E)** Anxiety-related behaviors were recorded as time in open arms in the EPM. The data are expressed as mean ± SEM (n = 8 mice). *represents $p < 0.05$ between marked groups, ns represents $p > 0.05$ between marked groups.

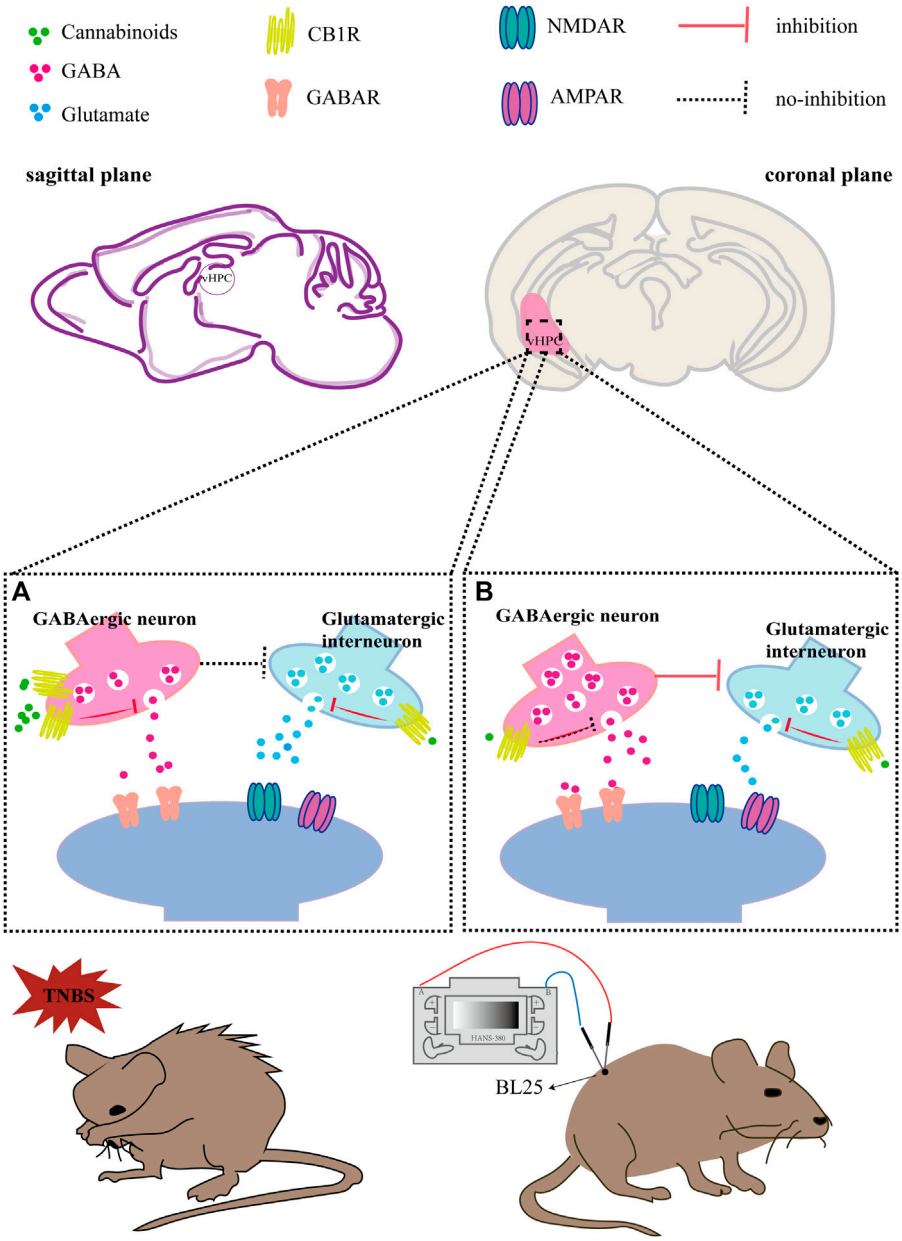

FIGURE 7 | Hypothesis diagram of EA inhibiting IBD induced anxiety *via* CB1R in the vHPC. **(A)** In TNBS-induced IBD mice, CB1R was over-expressed in GABAergic neurons in the vHPC, which was activated by endocannabinoid and the release amount of GABA was reduced. As a result, the release amount of glutamate is increased because of decreased inhibition of GABA. The increased release of glutamate in the vHPC may excite anxiety-related neuronal circuits starting from vHPC, thus inducing anxiety-related behaviors in IBD mice. **(B)** In TNBS-induced IBD mice with EA treatment, EA downregulated CB1R in GABAergic neurons in the vHPC, which disinhibit the release of GABA. In turn, excessive GABA inhibited the release of glutamate. Meanwhile, CB1R in glutamatergic neurons can also be activated by EA induced endocannabinoid, which can also decrease the release amount of glutamate. To sum up, EA may exert anxiolytic effect *via* downregulating CB1R in GABAergic neurons and activating CB1R in glutamatergic neurons in the vHPC, thus reducing the release of glutamate and inhibiting the anxiety-related neuronal circuits.

score was calculated based on Al-Chaer's method (Al-Chaer et al., 2000): no behavioral response to CRD was rated as 0 point, short pauses in head or body movements during stimulation was rated as 1 point; abdominal muscle contraction during stimulation was rated as 2 point; abdominal lifting was rated as 3 point; body arch, pelvic cavity or scrotum lifting was rated as 4 point.

2.5.2 Open Field Test

OFT was used to evaluate anxiety-related behaviors of mice (Choleris et al., 2001). Mice were placed in the center of a polystyrene enclosure (50 cm × 50 cm × 50 cm) and recorded by videotape instrument for 5 min. The center area was defined as the centric 25 cm × 25 cm area. The open field was cleaned with

75% ethanol between each trial and the track was analyzed using LabState software (Xinruan information technology co., LTD, Shanghai, China). Time spent in the center area was recorded.

2.5.3 Elevated Plus-Maze

Anxiety-related behaviors were also tested on an EPM apparatus, which was comprised of 100 cm open arms and 100 cm close arms (Campos et al., 2013). Free-moving mice were recorded by videotape instrument for 5 min. The elevated plus-maze was cleaned with 75% ethanol between each trial and the track was analyzed using ANY-maze software (Xinruan information technology co., LTD, Shanghai, China). Time spent in the open arm was recorded.

2.6 Immunofluorescence Labeling

Mice were deeply anesthetized with tribromoethanol and were transcardially perfused with 100 ml of 37°C normal saline followed by 50 ml of 4% paraformaldehyde in 0.1 M phosphate buffer (PBS, pH 7.4) at 4°C for fixation. The brain tissues were quickly separated and post-fixed for 6–8 h in the same fixative solution and dehydrated in 20% sucrose in 0.1 M PBS for 24 h and 30% sucrose in 0.1 M PBS for 24 h at 4 C. The brain were removed immediately and post-fixed in PFA. The optimal cutting temperature compound (OCT) embedded blocks were sectioned to 30 μm thickness.

Sections from each group were rinsed in 0.01M PBS and blocked for 2 h with blocking solution (5% donkey serum and 0.2% Tween 20 in 0.01 M PBS) at room temperature. The sections were incubated with the following antibodies: rabbit anti-CB1R (1:500, Santa Cruz, United States), mouse anti-neurogranin (1: 1000, Abcam, United States), guinea pig anti-GABA (1:1000, Abcam, United States) and mouse anti-GAD 67 (1:500, Abcam, United States). Subsequently, the free-floating sections were washed with 0.01M PBS 3 times and incubated with following secondary antibodies for 2 h: donkey anti-rabbit IgG conjugated with Dylight 594 (1:500, Abcam, United States), donkey anti-rabbit IgG conjugated with Dylight 488 (1:500, Abcam, United States), donkey anti-mouse IgG conjugated with Dylight 594 (1:500, Abcam, United States), goat anti-mouse IgG conjugated with Dylight 488 (1:500, Abcam, United States), and goat anti-guinea pig IgG conjugated with Dylight 594 (1:500, Abcam, United States). The sections were washed 3 times in 0.01M PBS and then cover-slipped. Olympus BX51 fluorescence microscope was used to view the sections, and images were captured using Qimaging Camera and QCapture software. Images were analyzed using the NIH Image J software (Bethesda, MD, United States). The layouts of the images were based on Photoshop CS5 (ADOBE Company, United States).

2.7 Western Blotting

Mice were deeply anesthetized with tribromoethanol and were transcardially perfused with 100 ml of 37°C normal saline. The brain tissues (vHPC regions) were immediately removed and stored at -80°C. The tissues were lysed by adding 40 mg/ml RIPA lysis buffer (Biosharp, China) and 40 mg/ml phenylmethyl sulfonyl fluoride (Biosharp, China) to the samples for 30 min. The lysed tissues were centrifuged at 12,000 rpm for 15 min at 4°C and supernatant liquids were collected. The protein contents were quantified by using the Enhanced BCA Protein Assay Kit (Beyotime Biotechnology, China).

The protein (40 mg) was denatured in loading buffer at 95°C for 5 min, separated on a 10%/12% glycine-SDS-PAGE gel (Beyotime Biotechnology, China), and then transferred onto a PVDF membrane (Millipore Immobilon-P, United States). The membranes were blocked with 5% BSA (Beyotime Biotechnology, China) at room temperature for 1 h, followed by incubation with primary antibodies at 4°C overnight: rabbit anti-CB1R antibody (1:500, Santa Cruz, United States) and rabbit anti-GAPDH antibody (1:1000, Thermo Scientific, United States). The membranes were washed in 0.01M Tris-HCI buffer salt solution and 0.2% Tween 20 (TBST) 6 times and incubated with following secondary antibodies for 2h: goat anti-rabbit IgG (1:5000, Abcam, United States). The signals were recorded using Super Signal West Pico chemiluminescent substrate (Thermo Scientific, United States). The densitometric analysis of the protein band images was performed using the NIH Image J software (Bethesda, MD, United States).

2.8 Statistical Analysis

The analysis for behavioral tests was performed by experimenters who were blinded to the treatment. All data were presented as mean ± standard errors of means (s.e.m.), unless otherwise specified. Each data set was firstly tested for normal distribution and those fitted Gaussian distribution were used for parametric analysis. Student *t*-test (paired or unpaired) was used for comparison between two groups and one-way analysis of variance was used to analyze the difference among more than two groups, followed by Tukey post-hoc comparison. When two independent variables were considered, two-way ANOVA was used. For those data that did not fit the Gaussian distribution, Wilcoxon matched-pairs rank test was used for paired comparison and Kolmogorov-Smirnov test was employed to compare between two independent samples. A statistical significance was defined as $p < 0.05$. All statistical analysis and data plotting were performed by GraphPad Prism ver8.0 (GraphPad Inc, United States).

3 RESULTS

3.1 EA Alleviated Visceral Hyperalgesia and Anxiety in TNBS-Treated IBD Mice

Five days after TNBS injection, the AWR score of CRD in TNBS group was significantly increased compared with vehicle control mice (**Figures 1A–D**, $p < 0.05$), suggesting the presence of visceral hyperalgesia. Treatment with EA dramatically lowered the increased AWR score in TNBS-treated mice (**Figures 1A–D**, $p < 0.05$). These results support the analgesic effect of EA on visceral hyperalgesia in TNBS-treated IBD mice.

In addition, compared with the vehicle control group, TNBS-treated IBD mice spent much less time in the center zone of OPF and the open arms of EPM. However, EA-treated mice spent more time in the center zone of OPF and the open arms of EPM than TNBS-treated mice (**Figures 1E,F**,

$p < 0.05$). These results suggest that EA can reduce anxiety behaviors of TNBS-treated IBD mice. Of note, sham EA had no effects on pain and anxiety behaviors in TNBS-treated IBD mice.

3.2 EA Reversed Over-Expression of CB1R in GABAergic Neurons But Not Glutamatergic Neurons in the vHPC of IBD Mice

The CB1R is associated with chronic pain and associated emotion disorders, such as anxiety (Davis, 2014; Patel et al., 2017; Yin et al., 2019). However, it is not clear whether CB1R in the vHPC play a role in the inhibitory effects of EA on anxiety and visceral hyperalgesia. To explore this question, we compared the expression of CB1R in the vHPC of TNBS-treated mice and vehicle control mice. Our results showed that the protein level of CB1R in the vHPC of the TNBS group was higher than that of the vehicle control group. EA reduced the protein level of CB1R in TNBS-treated IBD mice (**Figures 2A,B**, $p < 0.05$). These data suggest that EA reversed CB1R upregulation. However, EA have no effect on the protein level of CB1R in the amygdala (**Supplementary Figures S1A,B**).

To dissect the roles of CB1R in GABAergic or glutamatergic neurons in the vHPC, we investigated the co-localization of CB1R and GABA or neurogranin (a marker of glutamatergic neurons) (Xiang et al., 2020). Our results showed that the percentage of CB1R-expressed GABAergic neurons in the vHPC of TNBS-treated group was significantly higher than that of vehicle control group. Compared with TNBS-treated IBD mice, EA significantly reduced the percentage of CB1R and GABA co-labeled neurons (**Figures 2C,D**, $p < 0.05$). However, there were no difference in the percentage of CB1R-expressed glutamatergic neurons in the vHPC among four groups (**Figures 3A,B**).

3.3 Ablating CB1R in GABAergic Neurons in the vHPC Alleviated Anxiety in TNBS-Treated Mice and Mimicked the Anxiolytic Effect of EA

Based on the above findings, we further determined whether EA may reduce visceral pain and anxiety associated with IBD by acting on CB1R in GABAergic neurons in the vHPC. The rAAV-mDlX-CRE-WPRE-pA viruses were bilaterally injected into the vHPC of CB1R-flox mice to ablate CB1R in GABAergic neurons in the vHPC (**Figure 5A**). Four weeks after viruses injection, the percentage of CB1R and GAD67 co-labeled neurons in the vHPC was decreased in the CB1R-flox mice compared with wild type mice (**Figure 4A**) and the knockout efficiency was 82.2% (**Figure 4C**). Ablating CB1R in GABAergic neurons in the vHPC had no effect on the AWR score and can't reverse the effect of EA on visceral hyperalgesia (**Figures 5A–C**).

In the OPF and EPM test, CB1R deletion in GABAergic neurons in the vHPC increased the time of mice staying in the center zone and open arms in the TNBS group, compared with TNBS-treated wild type mice (**Figures 5D,E**, $p < 0.05$). However, there was no difference in the time of mice stayed in center zone and open arms between the TNBS group and the EA group after ablating CB1R in GABAergic neurons in the vHPC (**Figures 5D,E**). It is possible that the anxiolytic effect of ablating CB1R in GABAergic neurons in the TNBS group had reached a peak and could not be further increased by EA. Thus, inhibiting the expression of CB1R in GABAergic neurons in the vHPC likely mediates the anxiolytic effect of EA.

3.4 CB1R in Glutamatergic Neurons in the vHPC Participated in the Anxiolytic Effect of EA

In order to determine the role of CB1R in glutamatergic neurons in the analgesic and anxiolytic effects of EA, the rAAV-CaMKII-CRE-WPRE-pA viruses were bilaterally injected into the vHPC of CB1R-flox mice to ablate CB1R in glutamatergic neurons in the vHPC (**Figure 6A**). The percentage of CB1R and neurogranin (a marker of glutamatergic neurons) co-labeled neurons was decreased in CB1Rf/f:CaMKII-cre mice compared with wild type mice (**Figure 4B**) and the knockout efficiency was 90.9% (**Figure 4D**). Ablating CB1R in glutamatergic neurons in the vHPC did not affect AWR score and can't reverse the effect of EA on visceral hyperalgesia (**Figures 6A–C**).

In the OPF and EPM tests, the time of mice stayed in the center zone and open arms was decreased in the vehicle control group but not TNBS group in CB1Rf/f:CaMKII-cre mice, compared with the corresponding groups in wild type mice (**Figures 6D,E**, $p < 0.05$). Moreover, after CB1R deletion in glutamatergic neurons in the vHPC, there was no difference between the vehicle control group and the TNBS group (**Figures 6D,E**). It is possible that vehicle control mice with CB1R deletion in glutamatergic neurons showed a high level of anxiety, which could not be further increased by TNBS treatment. The time of mice stayed in center zone and open arms in the EA group was not significantly different with the TNBS group of CB1Rf/f:CaMKII-cre mice, but was significantly lower than the EA group of wild type mice (**Figures 6D,E**, $p < 0.05$). These data suggested that EA attenuates anxiety *via* activation of CB1R in glutamatergic neurons in the vHPC.

4 DISCUSSION

Patients with IBD have several chronic visceral disorders, including abdominal pain, rectal bleeding, and diarrhea (Gracie et al., 2018). In addition, these patients often have mood disorders, such as anxiety or depression (Walker et al., 2008; Neuendorf et al., 2016; Gracie et al., 2018). Our study found that TNBS-treated IBD mice displayed visceral hyperalgesia and anxiety-like behaviors. Several reports showed that EA relieved mechanical allodynia and visceral hyperalgesia associated with IBD (Ji et al., 2013; Lv et al., 2019; Wang et al., 2019). In addition, EA had an anxiolytic effect (Errington-Evans, 2012; Yue et al., 2018). Our present

study showed that EA is effective in reducing visceral hyperalgesia and anxiety in a mouse model of IBD.

The hippocampus is not only a key region for memory and learning but also is closely involved in chronic pain and anxiety (Jones and Gebhart, 1986; Covey et al., 2000; Li et al., 2017; Parfitt et al., 2017). Direct manipulation of the hippocampus alters nociceptive behaviors (Lathe, 2001; Reckziegel et al., 2021). Moreover, hippocampus, especially vHPC has been viewed a target to treat anxiety (Li et al., 2017; Parfitt et al., 2017). The CB1R play a role in the regulation of mood disorder and chronic pain processes (Jones and Gebhart, 1986; Davis, 2014; Seltzman et al., 2016; Yin et al., 2019). In this study, EA reduced the protein level of CB1R in the vHPC of TNBS-treated IBD mice. We wonder whether CB1R in the vHPC may be involved in analgesic or anxiolytic effect of EA.

Peripherally restricted CB1R agonists may hold promise as a viable treatment for visceral pain (Di Sabatino et al., 2011). Also, CB1R in the hippocampus may be targeted for treating anxiety disorders (Jiang et al., 2005; Lisboa et al., 2015). In the hippocampus, the CB1R is present on both GABAergic and glutamatergic axon terminals (Marsicano and Lutz, 1999). Deletion of CB1R in GABAergic neurons decreases hippocampal long-term potential (LTP). In contrast, ablating CB1R in glutamatergic neurons seems to enhance hippocampal LTP (Monory et al., 2015). In order to distinguish the different effects of CB1R of excitatory and inhibitory neurons on EA, we observed the distribution of CB1R and the influence of conditional deletion of CB1R in analgesic and anxiolytic effects of EA. We found that EA reversed the upregulation of CB1R in GABAergic neurons but not glutamatergic neurons in the vHPC.

In addition, our study showed that ablating CB1R of GABAergic neurons in the vHPC alleviated anxiety in TNBS-treated IBD mice and also mimicked the anxiolytic effect of EA. Previous study found that stimulating CB1R in GABAergic neurons in the vHPC can lead to an anxiogenic response *via* a decreasing GABAergic transmission (Roohbakhsh et al., 2009). We hypothesized that in TNBS-induced IBD mice, CB1R was over-expressed in GABAergic neurons in the vHPC, which was activated by endocannabinoid and reduced the release amount of GABA. Since glutamatergic neurons in the brain are usually regulated by inhibitory GABAergic neurons, the release amount of glutamate is increased because of decreased inhibition of GABA (Katona and Freund, 2008). The increased release of glutamate in the vHPC may excite anxiogenic neuronal circuits starting from vHPC, to basolateral amygdala (BLA) (Allsop et al., 2014) or the medial prefrontal cortex (mPFC) (Adhikari, 2014), thus inducing anxiety-related behaviors in IBD mice (**Figure 7A**). Interestingly, EA may exert anxiolytic effect by downregulating CB1R in GABAergic neurons in the vHPC, which in turn increased release of GABA and subsequently inhibited the release of glutamate, thus alleviating anxiety-like behaviors (**Figure 7B**).

In contrast, ablating CB1R in glutamatergic neurons in the vHPC only induced severe anxiety in vehicle control mice, but did not deteriorate anxiogenic response of TNBS-treated IBD mice. Since the CB1R in glutamatergic terminals may reduce the release amount of glutamate (Marsicano and Lutz, 1999), the reason of anxiety in vehicle control mice may be that the absence of CB1R in glutamatergic neurons in the vHPC induces excessive glutamate release, thus exciting the neuronal circuits for anxiety. Since the level of anxiety in vehicle control mice has reached a peak, it would not further increase after TNBS injection (**Figure 7A**). Moreover, CB1R deletion in glutamatergic neurons also inhibited the anxiolytic effect of EA. It suggested that EA may exert anxiolytic effect *via* activation of CB1R in glutamatergic neurons in the vHPC, thus reducing the release of glutamate and inhibiting the activation of neuronal circuits of anxiety (**Figure 7B**).

To our surprise, ablating CB1R in either GABAergic or glutamatergic neurons in the vHPC did not alter visceral hyperalgesia. It suggested that CB1R in the vHPC may not contribute to visceral pain. In our previous study, we found that EA can increase the level of endocannabinoid 2-arachidonoylglycerol in the midbrain in chronic pain, which can bidirectionally regulate GABAergic and glutamatergic neurons *via* the CB1R in the vlPAG to produce analgesic effects (Yuan et al., 2018; Zhu et al., 2019). In our study, CB1R in other brain region, such as vlPAG, may be responsible for the analgesic effect of EA in IBD induced visceral pain.

In conclusion, our findings reveal that CB1R expressed on GABAergic and glutamatergic neurons are involved in the inhibitory effect of EA on anxiety in IBD mice. EA may exert anxiolytic effect *via* downregulating CB1R in GABAergic neurons and activating CB1R in glutamatergic neurons in the vHPC, thus reducing the release of glutamate and inhibiting the anxiogenic neuronal circuits related to vHPC. Thus, our study provides new information about the cellular and molecular mechanisms of the therapeutic effect of EA on anxiety induced by IBD.

DATA AVAILABILITY STATEMENT

The original contributions presented in the study are included in the article/**Supplementary Materials**, further inquiries can be directed to the corresponding authors.

ETHICS STATEMENT

The animal study was approved by Institutional Animal Care and Use Committee of Tongji Medical college of Huazhong University of Science and Technology.

AUTHOR CONTRIBUTIONS

ML and WH designed all experiments. X-FH performed the experiments and analyzed data. HZ drafted the manuscript and analyzed data. W-QG, O-YZ-M, Y-ZL, and CC assisted in molecular and behavioral assays and data analysis. The manuscript was revised by L-LY, T-FH, H-CX, Y-HL, Y-SS,

X-HJ, JC and H-LP. All experiments were supervised by ML and WH. All authors approved the final edited version.

FUNDING

This work was supported by the Key Program of the National Natural Science Foundation of China (No.82130122), the National Key R&D Program of China (2019YFC1709002), the National Natural Science Foundation of China (No.82004491, 82174500), Hubei knowledge innovation project (2019CFC921) and TCM Scientific research project of Hubei Province Health Commission (ZY2021M045).

SUPPLEMENTARY MATERIAL

The Supplementary Material for this article can be found online at: https://www.frontiersin.org/articles/10.3389/fphar.2022.919553/full#supplementary-material

REFERENCES

Adhikari, A. (2014). Distributed Circuits Underlying Anxiety. *Front. Behav. Neurosci.* 8, 112. doi:10.3389/fnbeh.2014.00112

Al-Chaer, E. D., Kawasaki, M., and Pasricha, P. J. (2000). A New Model of Chronic Visceral Hypersensitivity in Adult Rats Induced by Colon Irritation during Postnatal Development. *Gastroenterology* 119 (5), 1276–1285. doi:10.1053/gast.2000.19576

Allsop, S. A., Vander Weele, C. M., Wichmann, R., and Tye, K. M. (2014). Optogenetic Insights on the Relationship between Anxiety-Related Behaviors and Social Deficits. *Front. Behav. Neurosci.* 8, 241. doi:10.3389/fnbeh.2014.00241

Ananthakrishnan, A. N. (2015). Epidemiology and Risk Factors for IBD. *Nat. Rev. Gastroenterol. Hepatol.* 12 (4), 205–217. doi:10.1038/nrgastro.2015.34

Banfi, D., Moro, E., Bosi, A., Bistoletti, M., Cerantola, S., Crema, F., et al. (2021). Impact of Microbial Metabolites on Microbiota-Gut-Brain Axis in Inflammatory Bowel Disease. *Int. J. Mol. Sci.* 22 (4), 1623. doi:10.3390/ijms22041623

Bannerman, D. M., Sprengel, R., Sanderson, D. J., Mchugh, S. B., Rawlins, J. N., Monyer, H., et al. (2014). Hippocampal Synaptic Plasticity, Spatial Memory and Anxiety. *Nat. Rev. Neurosci.* 15 (3), 181–192. doi:10.1038/nrn3677

Campos, A. C., Fogaça, M. V., Aguiar, D. C., and Guimarães, F. S. (2013). Animal Models of Anxiety Disorders and Stress. *Braz J. Psychiatry* 35 (Suppl. 2), S101–S111. doi:10.1590/1516-4446-2013-1139

Choleris, E., Thomas, A. W., Kavaliers, M., and Prato, F. S. (2001). A Detailed Ethological Analysis of the Mouse Open Field Test: Effects of Diazepam, Chlordiazepoxide and an Extremely Low Frequency Pulsed Magnetic Field. *Neurosci. Biobehav Rev.* 25 (3), 235–260. doi:10.1016/s0149-7634(01)00011-2

Covey, W. C., Ignatowski, T. A., Knight, P. R., and Spengler, R. N. (2000). Brain-derived TNFalpha: Involvement in Neuroplastic Changes Implicated in the Conscious Perception of Persistent Pain. *Brain Res.* 859 (1), 113–122. doi:10.1016/s0006-8993(00)01965-x

Davis, M. P. (2014). Cannabinoids in Pain Management: CB1, CB2 and Non-Classic Receptor Ligands. *Expert Opin. Investig. Drugs* 23 (8), 1123–1140. doi:10.1517/13543784.2014.918603

Di Sabatino, A., Battista, N., Biancheri, P., Rapino, C., Rovedatti, L., Astarita, G., et al. (2011). The Endogenous Cannabinoid System in the Gut of Patients with Inflammatory Bowel Disease. *Mucosal Immunol.* 4 (5), 574–583. doi:10.1038/mi.2011.18

Egertová, M., Giang, D. K., Cravatt, B. F., and Elphick, M. R. (1998). A New Perspective on Cannabinoid Signalling: Complementary Localization of Fatty Acid Amide Hydrolase and the CB1 Receptor in Rat Brain. *Proc. Biol. Sci.* 265 (1410), 2081–2085. doi:10.1098/rspb.1998.0543

Errington-Evans, N. (2012). Acupuncture for Anxiety. *CNS Neurosci. Ther.* 18 (4), 277–284. doi:10.1111/j.1755-5949.2011.00254.x

Evans, L. S., and Van'T, H. J. (1975). Dose Rate, Mitotic Cycle Duration, and Sensitivity of Cell Transitions from G1 Leads to S and G2 Leads to M to Protracted Gamma Radiation in Root Meristems. *Radiat. Res.* 64 (2), 331–343. doi:10.2307/3574269

Fasick, V., Spengler, R. N., Samankan, S., Nader, N. D., and Ignatowski, T. A. (2015). The hippocampus and TNF: Common Links between Chronic Pain and Depression. *Neurosci. Biobehav Rev.* 53, 139–159. doi:10.1016/j.neubiorev.2015.03.014

Fletcher-Jones, A., Hildick, K. L., Evans, A. J., Nakamura, Y., Henley, J. M., and Wilkinson, K. A. (2020). Protein Interactors and Trafficking Pathways that Regulate the Cannabinoid Type 1 Receptor (CB1R). *Front. Mol. Neurosci.* 13, 108. doi:10.3389/fnmol.2020.00108

Gracie, D. J., Guthrie, E. A., Hamlin, P. J., and Ford, A. C. (2018). Bi-Directionality of Brain-Gut Interactions in Patients with Inflammatory Bowel Disease. *Gastroenterology* 154 (6), 1635–1646. e3. doi:10.1053/j.gastro.2018.01.027

Haller, J., Varga, B., Ledent, C., Barna, I., and Freund, T. F. (2004). Context-Dependent Effects of CB1 Cannabinoid Gene Disruption on Anxiety-Like and Social Behaviour in Mice. *Eur. J. Neurosci.* 19 (7), 1906–1912. doi:10.1111/j.1460-9568.2004.03293.x

Häring, M., Kaiser, N., Monory, K., and Lutz, B. (2011). Circuit Specific Functions of Cannabinoid CB1 Receptor in the Balance of Investigatory Drive and Exploration. *PLoS One* 6 (11), e26617. doi:10.1371/journal.pone.0026617

Hill, M. N., Kumar, S. A., Filipski, S. B., Iverson, M., Stuhr, K. L., Keith, J. M., et al. (2013). Disruption of Fatty Acid Amide Hydrolase Activity Prevents the Effects of Chronic Stress on Anxiety and Amygdalar Microstructure. *Mol. Psychiatry* 18 (10), 1125–1135. doi:10.1038/mp.2012.90

Ji, J., Lu, Y., Liu, H., Feng, H., Zhang, F., Wu, L., et al. (2013). Acupuncture and Moxibustion for Inflammatory Bowel Diseases: A Systematic Review and Meta-Analysis of Randomized Controlled Trials. *Evid. Based Complement. Altern. Med.* 2013, 158352. doi:10.1155/2013/158352

Jiang, W., Zhang, Y., Xiao, L., Van Cleemput, J., Ji, S. P., Bai, G., et al. (2005). Cannabinoids Promote Embryonic and Adult Hippocampus Neurogenesis and Produce Anxiolytic- and Antidepressant-Like Effects. *J. Clin. Invest.* 115 (11), 3104–3116. doi:10.1172/JCI25509

Jones, S. L., and Gebhart, G. F. (1986). Quantitative Characterization of Ceruleospinal Inhibition of Nociceptive Transmission in the Rat. *J. Neurophysiol.* 56 (5), 1397–1410. doi:10.1152/jn.1986.56.5.1397

Katona, I., and Freund, T. F. (2008). Endocannabinoid Signaling as a Synaptic Circuit Breaker in Neurological Disease. *Nat. Med.* 14 (9), 923–930. doi:10.1038/nm.f.1869

Katona, I., and Freund, T. F. (2012). Multiple Functions of Endocannabinoid Signaling in the Brain. *Annu. Rev. Neurosci.* 35, 529–558. doi:10.1146/annurev-neuro-062111-150420

Kos, C. H. (2004). Cre/loxP System for Generating Tissue-Specific Knockout Mouse Models. *Nutr. Rev.* 62 (6 Pt 1), 243–246. doi:10.1301/nr2004.jun243-246

Lafenêtre, P., Chaouloff, F., and Marsicano, G. (2009). Bidirectional Regulation of Novelty-Induced Behavioral Inhibition by the Endocannabinoid System. *Neuropharmacology* 57 (7-8), 715–721. doi:10.1016/j.neuropharm.2009.07.014

Lathe, R. (2001). Hormones and the Hippocampus. *J. Endocrinol.* 169 (2), 205–231. doi:10.1677/joe.0.1690205

Li, M., Li, C., Yu, H., Cai, X., Shen, X., Sun, X., et al. (2017). Lentivirus-Mediated Interleukin-1β (IL-1β) Knock-Down in the Hippocampus Alleviates Lipopolysaccharide (LPS)-Induced Memory Deficits and Anxiety- and Depression-Like Behaviors in Mice. *J. Neuroinflammation* 14 (1), 190. doi:10.1186/s12974-017-0964-9

Lisboa, S. F., Borges, A. A., Nejo, P., Fassini, A., Guimarães, F. S., and Resstel, L. B. (2015). Cannabinoid CB1 Receptors in the Dorsal hippocampus and Prelimbic Medial Prefrontal Cortex Modulate Anxiety-Like Behavior in Rats: Additional Evidence. *Prog. Neuropsychopharmacol. Biol. Psychiatry* 59, 76–83. doi:10.1016/j.pnpbp.2015.01.005

Liu, H. Y., Chou, K. H., and Chen, W. T. (2018). Migraine and the Hippocampus. *Curr. Pain Headache Rep.* 22 (2), 13. doi:10.1007/s11916-018-0668-6

Lv, P. R., Su, Y. S., He, W., Wang, X. Y., Shi, H., Zhang, X. N., et al. (2019). Electroacupuncture Alleviated Referral Hindpaw Hyperalgesia via Suppressing Spinal Long-Term Potentiation (LTP) in TNBS-Induced Colitis Rats. *Neural Plast.* 2019, 2098083. doi:10.1155/2019/2098083

Mah, L., Szabuniewicz, C., and Fiocco, A. J. (2016). Can Anxiety Damage the Brain? *Curr. Opin. Psychiatry* 29 (1), 56–63. doi:10.1097/YCO.0000000000000223

Marsicano, G., and Lutz, B. (1999). Expression of the Cannabinoid Receptor CB1 in Distinct Neuronal Subpopulations in the Adult Mouse Forebrain. *Eur. J. Neurosci.* 11 (12), 4213–4225. doi:10.1046/j.1460-9568.1999.00847.x

Mittermaier, C., Dejaco, C., Waldhoer, T., Oefferlbauer-Ernst, A., Miehsler, W., Beier, M., et al. (2004). Impact of Depressive Mood on Relapse in Patients with Inflammatory Bowel Disease: A Prospective 18-Month Follow-Up Study. *Psychosom. Med.* 66 (1), 79–84. doi:10.1097/01.psy.0000106907.24881.f2

Molodecky, N. A., Soon, I. S., Rabi, D. M., Ghali, W. A., Ferris, M., Chernoff, G., et al. (2012). Increasing Incidence and Prevalence of the Inflammatory Bowel Diseases with Time, Based on Systematic Review. *Gastroenterology* 142 (1), 46–54. doi:10.1053/j.gastro.2011.10.001

Moloney, R. D., Johnson, A. C., O'Mahony, S. M., Dinan, T. G., Greenwood-Van Meerveld, B., and Cryan, J. F. (2016). Stress and the Microbiota-Gut-Brain Axis in Visceral Pain: Relevance to Irritable Bowel Syndrome. *CNS Neurosci. Ther.* 22 (2), 102–117. doi:10.1111/cns.12490

Monory, K., Polack, M., Remus, A., Lutz, B., and Korte, M. (2015). Cannabinoid CB1 Receptor Calibrates Excitatory Synaptic Balance in the Mouse Hippocampus. *J. Neurosci.* 35 (9), 3842–3850. doi:10.1523/JNEUROSCI.3167-14.2015

Neuendorf, R., Harding, A., Stello, N., Hanes, D., and Wahbeh, H. (2016). Depression and Anxiety in Patients with Inflammatory Bowel Disease: A Systematic Review. *J. Psychosom. Res.* 87, 70–80. doi:10.1016/j.jpsychores.2016.06.001

Ng, S. C., Shi, H. Y., Hamidi, N., Underwood, F. E., Tang, W., Benchimol, E. I., et al. (2017). Worldwide Incidence and Prevalence of Inflammatory Bowel Disease in the 21st Century: A Systematic Review of Population-Based Studies. *Lancet* 390 (10114), 2769–2778. doi:10.1016/S0140-6736(17)32448-0

Padilla-Coreano, N., Bolkan, S. S., Pierce, G. M., Blackman, D. R., Hardin, W. D., Garcia-Garcia, A. L., et al. (2016). Direct Ventral Hippocampal-Prefrontal Input is Required for Anxiety-Related Neural Activity and Behavior. *Neuron* 89 (4), 857–866. doi:10.1016/j.neuron.2016.01.011

Parfitt, G. M., Nguyen, R., Bang, J. Y., Aqrabawi, A. J., Tran, M. M., Seo, D. K., et al. (2017). Bidirectional Control of Anxiety-Related Behaviors in Mice: Role of Inputs Arising from the Ventral Hippocampus to the Lateral Septum and Medial Prefrontal Cortex. *Neuropsychopharmacology* 42 (8), 1715–1728. doi:10.1038/npp.2017.56

Patel, S., Hill, M. N., Cheer, J. F., Wotjak, C. T., and Holmes, A. (2017). The Endocannabinoid System as a Target for Novel Anxiolytic Drugs. *Neurosci. Biobehav Rev.* 76 (Pt A), 56–66. doi:10.1016/j.neubiorev.2016.12.033

Price, R. B., and Duman, R. (2020). Neuroplasticity in Cognitive and Psychological Mechanisms of Depression: An Integrative Model. *Mol. Psychiatry* 25 (3), 530–543. doi:10.1038/s41380-019-0615-x

Reckziegel, D., Abdullah, T., Wu, B., Wu, B., Huang, L., Schnitzer, T. J., et al. (2021). Hippocampus Shape Deformation: A Potential Diagnostic Biomarker for Chronic Back Pain in Women. *Pain* 162 (5), 1457–1467. doi:10.1097/j.pain.0000000000002143

Rey, A. A., Purrio, M., Viveros, M. P., and Lutz, B. (2012). Biphasic Effects of Cannabinoids in Anxiety Responses: CB1 and GABA(B) Receptors in the Balance of GABAergic and Glutamatergic Neurotransmission. *Neuropsychopharmacology* 37 (12), 2624–2634. doi:10.1038/npp.2012.123

Roohbakhsh, A., Keshavarz, S., Hasanein, P., Rezvani, M. E., and Moghaddam, A. H. (2009). Role of Endocannabinoid System in the Ventral Hippocampus of Rats in the Modulation of Anxiety-Like Behaviours. *Basic Clin. Pharmacol. Toxicol.* 105 (5), 333–338. doi:10.1111/j.1742-7843.2009.00449.x

Ruehle, S., Remmers, F., Romo-Parra, H., Massa, F., Wickert, M., Wörtge, S., et al. (2013). Cannabinoid CB1 Receptor in Dorsal Telencephalic Glutamatergic Neurons: Distinctive Sufficiency for Hippocampus-Dependent and Amygdala-Dependent Synaptic and Behavioral Functions. *J. Neurosci.* 33 (25), 10264–10277. doi:10.1523/JNEUROSCI.4171-12.2013

Seltzman, H. H., Shiner, C., Hirt, E. E., Gilliam, A. F., Thomas, B. F., Maitra, R., et al. (2016). Peripherally Selective Cannabinoid 1 Receptor (CB1R) Agonists for the Treatment of Neuropathic Pain. *J. Med. Chem.* 59 (16), 7525–7543. doi:10.1021/acs.jmedchem.6b00516

Shah, H. E., Bhawnani, N., Ethirajulu, A., Alkasabera, A., Onyali, C. B., Anim-Koranteng, C., et al. (2021). Iron Deficiency-Induced Changes in the Hippocampus, Corpus Striatum, and Monoamines Levels that Lead to Anxiety, Depression, Sleep Disorders, and Psychotic Disorders. *Cureus* 13 (9), e18138. doi:10.7759/cureus.18138

Silva, I., Pinto, R., and Mateus, V. (2019). Preclinical Study *In Vivo* for New Pharmacological Approaches in Inflammatory Bowel Disease: A Systematic Review of Chronic Model of TNBS-Induced Colitis. *J. Clin. Med.* 8 (10), 1574. doi:10.3390/jcm8101574

Smith, C. A., de Lacey, S., Chapman, M., Ratcliffe, J., Norman, R. J., Johnson, N. P., et al. (2019). The Effects of Acupuncture on the Secondary Outcomes of Anxiety and Quality of Life for Women Undergoing IVF: A Randomized Controlled Trial. *Acta Obstet. Gynecol. Scand.* 98 (4), 460–469. doi:10.1111/aogs.13528

Song, G., Fiocchi, C., and Achkar, J. P. (2019). Acupuncture in Inflammatory Bowel Disease. *Inflamm. Bowel Dis.* 25 (7), 1129–1139. doi:10.1093/ibd/izy371

Tsou, K., Brown, S., Sañudo-Peña, M. C., Mackie, K., and Walker, J. M. (1998). Immunohistochemical Distribution of Cannabinoid CB1 Receptors in the Rat Central Nervous System. *Neuroscience* 83 (2), 393–411. doi:10.1016/s0306-4522(97)00436-3

Vasic, V., and Schmidt, M. H. H. (2017). Resilience and Vulnerability to Pain and Inflammation in the Hippocampus. *Int. J. Mol. Sci.* 18 (4), 739. doi:10.3390/ijms18040739

Walker, J. R., Ediger, J. P., Graff, L. A., Greenfeld, J. M., Clara, I., Lix, L., et al. (2008). The Manitoba IBD Cohort Study: A Population-Based Study of the Prevalence of Lifetime and 12-Month Anxiety and Mood Disorders. *Am. J. Gastroenterol.* 103 (8), 1989–1997. doi:10.1111/j.1572-0241.2008.01980.x

Wang, H., Dong, P., He, C., Feng, X. Y., Huang, Y., Yang, W. W., et al. (2020). Incerta-Thalamic Circuit Controls Nocifensive Behavior via Cannabinoid Type 1 Receptors. *Neuron* 107 (3), 538–551. e7. doi:10.1016/j.neuron.2020.04.027

Wang, Y. L., Su, Y. S., He, W., and Jing, X. H. (2019). Electroacupuncture Relieved Visceral and Referred Hindpaw Hypersensitivity in Colitis Rats by Inhibiting Tyrosine Hydroxylase Expression in the Sixth Lumbar Dorsal Root Ganglia. *Neuropeptides* 77, 101957. doi:10.1016/j.npep.2019.101957

Wu, H. G., Zhou, L. B., Pan, Y. Y., Huang, C., Chen, H. P., Shi, Z., et al. (1999). Study of the Mechanisms of Acupuncture and Moxibustion Treatment for Ulcerative Colitis Rats in View of the Gene Expression of Cytokines. *World J. Gastroenterol.* 5 (6), 515–517. doi:10.3748/wjg.v5.i6.515

Xiang, Y., Xin, J., Le, W., and Yang, Y. (2020). Neurogranin: A Potential Biomarker of Neurological and Mental Diseases. *Front. Aging Neurosci.* 12, 584743. doi:10.3389/fnagi.2020.584743

Yin, A. Q., Wang, F., and Zhang, X. (2019). Integrating Endocannabinoid Signaling in the Regulation of Anxiety and Depression. *Acta Pharmacol. Sin.* 40 (3), 336–341. doi:10.1038/s41401-018-0051-5

Yuan, X. C., Zhu, B., Jing, X. H., Xiong, L. Z., Wu, C. H., Gao, F., et al. (2018). Electroacupuncture Potentiates Cannabinoid Receptor-Mediated Descending Inhibitory Control in a Mouse Model of Knee Osteoarthritis. *Front. Mol. Neurosci.* 11, 112. doi:10.3389/fnmol.2018.00112

Yue, N., Li, B., Yang, L., Han, Q. Q., Huang, H. J., Wang, Y. L., et al. (2018). Electro-Acupuncture Alleviates Chronic Unpredictable Stress-Induced Depressive- and Anxiety-Like Behavior and Hippocampal Neuroinflammation in Rat Model of Depression. *Front. Mol. Neurosci.* 11, 149. doi:10.3389/fnmol.2018.00149

Zhu, H., Xiang, H. C., Li, H. P., Lin, L. X., Hu, X. F., Zhang, H., et al. (2019). Inhibition of GABAergic Neurons and Excitation of Glutamatergic Neurons in the Ventrolateral Periaqueductal Gray Participate in Electroacupuncture

Analgesia Mediated by Cannabinoid Receptor. *Front. Neurosci.* 13, 484. doi:10.3389/fnins.2019.00484

Conflict of Interest: The authors declare that the research was conducted in the absence of any commercial or financial relationships that could be construed as a potential conflict of interest.

Publisher's Note: All claims expressed in this article are solely those of the authors and do not necessarily represent those of their affiliated organizations, or those of the publisher, the editors and the reviewers. Any product that may be evaluated in this article, or claim that may be made by its manufacturer, is not guaranteed or endorsed by the publisher.

frontiers | Frontiers in Pharmacology

TYPE Original Research
PUBLISHED 26 August 2022
DOI 10.3389/fphar.2022.956030

OPEN ACCESS

EDITED BY
Paula Morales,
Institute of Medical Chemistry (CSIC), Spain

REVIEWED BY
Eduardo Muñoz,
University of Cordoba, Spain
Bruno Miguel Fonseca,
University of Porto, Portugal

*CORRESPONDENCE
Robert B. Laprairie,
robert.laprairie@usask.ca

SPECIALTY SECTION
This article was submitted to Neuropharmacology, a section of the journal Frontiers in Pharmacology

RECEIVED 29 May 2022
ACCEPTED 15 July 2022
PUBLISHED 26 August 2022

CITATION
Zagzoog A, Cabecinha A, Abramovici H and Laprairie RB (2022), Modulation of type 1 cannabinoid receptor activity by cannabinoid by-products from Cannabis sativa and non-cannabis phytomolecules. *Front. Pharmacol.* 13:956030. doi: 10.3389/fphar.2022.956030

Modulation of type 1 cannabinoid receptor activity by cannabinoid by-products from *Cannabis sativa* and non-cannabis phytomolecules

Ayat Zagzoog[1], Ashley Cabecinha[2], Hanan Abramovici[2] and Robert B. Laprairie[1,3]*

[1]College of Pharmacy and Nutrition, University of Saskatchewan, Saskatoon, SK, Canada, [2]Office of Cannabis Science and Surveillance, Controlled Substances and Cannabis Branch, Health Canada, Ottawa, ON, Canada, [3]Department of Pharmacology, College of Medicine, Dalhousie University, Halifax, NS, Canada

Cannabis sativa contains more than 120 cannabinoids and 400 terpene compounds (i.e., phytomolecules) present in varying amounts. *Cannabis* is increasingly available for legal medicinal and non-medicinal use globally, and with increased access comes the need for a more comprehensive understanding of the pharmacology of phytomolecules. The main transducer of the intoxicating effects of *Cannabis* is the type 1 cannabinoid receptor (CB1R). Δ^9-tetrahydrocannabinolic acid (Δ^9-THCa) is often the most abundant cannabinoid present in many cultivars of *Cannabis*. Decarboxylation converts Δ^9-THCa to Δ^9-THC, which is a CB1R partial agonist. Understanding the complex interplay of phytomolecules—often referred to as "the entourage effect"—has become a recent and major line of inquiry in cannabinoid research. Additionally, this interest is extending to other non-*Cannabis* phytomolecules, as the diversity of available *Cannabis* products grows. Here, we chose to focus on whether 10 phytomolecules (Δ^8-THC, $\Delta^{6a,10a}$-THC, 11-OH-Δ^9-THC, cannabinol, curcumin, epigallocatechin gallate, olivetol, palmitoylethanolamide, piperine, and quercetin) alter CB1R-dependent signaling with or without a co-treatment of Δ^9-THC. Phytomolecules were screened for their binding to CB1R, inhibition of forskolin-stimulated cAMP accumulation, and βarrestin2 recruitment in Chinese hamster ovary cells stably expressing human CB1R. Select compounds were assessed further for cataleptic, hypothermic, and anti-nociceptive effects on male mice. Our data revealed partial agonist activity for the cannabinoids tested, as well as modulation of Δ^9-THC-dependent binding and signaling properties of phytomolecules *in vitro* and *in vivo*. These data represent a first step in understanding the complex pharmacology of *Cannabis*- and non-*Cannabis*-derived phytomolecules at CB1R and determining whether these interactions may affect the physiological outcomes, adverse effects, and abuse liabilities associated with the use of these compounds.

KEYWORDS

cannabinoid, phytomolecule, terpene, type 1 cannabinoid receptor, molecular pharmacology, cAMP, βarrestin

Introduction

In 2018, Canada became the first G7 country to legalize *Cannabis sativa* for non-medical purposes. Despite decades of research and significant legislative and policy advances, our scientific understanding of *Cannabis* and cannabinoid pharmacology remains quite limited. Gaining a more comprehensive understanding of cannabinoid pharmacology to better shed further light on the beneficial and harmful effects of cannabis is critically important. There are many biologically active compounds in cannabis. "Phytocannabinoids" are generally 21-carbon bicyclic compounds, some of which are known to act at the cannabinoid receptors. Terpenes, on the other hand, are a large and structurally diverse group of hydrocarbon molecules present in nearly all plants that produce characteristic odors. Here, we will refer to these groups collectively as "phytomolecules." The two best known phytocannabinoids are Δ^9-tetrahydrocannabinol (Δ^9-THC) and cannabidiol (CBD). All vertebrates studied to date also naturally produce endogenous cannabinoids anandamide (AEA) and 2-arachidonoylglycerol (2-AG). These cannabinoids act to modulate the brain and body's cannabinoid receptors: CB1R and CB2R, which act to limit neurotransmitter release throughout the brain and inflammatory processes, respectively (Pertwee, 2008). Beyond Δ^9-THC and CBD, more than 500 phytomolecules have been identified in extracts from the *Cannabis* plant (Figure 1) (Howlett and Abood, 2017). The pharmacodynamic and pharmacokinetic properties of these compounds alone and in unique combinations present in plant chemotypes remain largely unknown (Pertwee, 2008; Howlett and Abood, 2017).

In Canada, Δ^9-THC and CBD content in legal *Cannabis* products is monitored and must be labeled on *Cannabis* products for retail sale because these constituents are recognized as being pharmacologically active drug compounds, and in the case of Δ^9-THC, are known to produce intoxication and other effects. However, it is possible that minor constituents of *Cannabis* products may also be psychoactive and/or intoxicating, and it

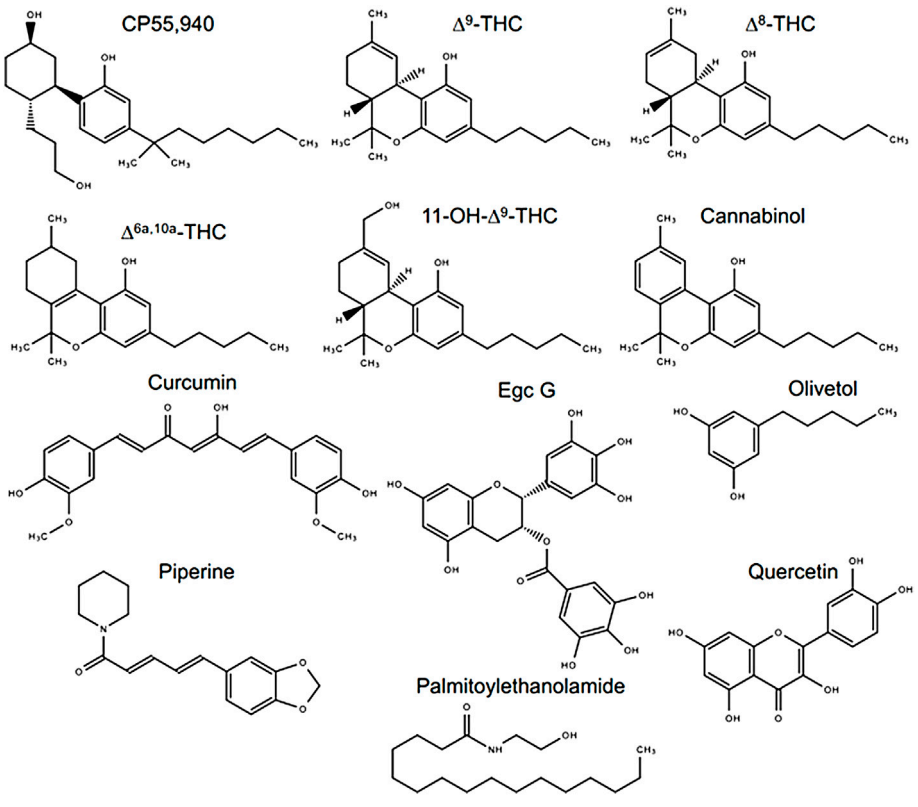

FIGURE 1
Compounds assessed in this study. Chemical structures were drawn in Microsoft PowerPoint by the authors. Egc G, epigallocatechin gallate.

is important to explore that aspect further to better understand the risks of cannabis use. The cannabis product market is also rapidly evolving. Products such as cannabis extracts, cannabis topicals, and edible cannabis often contain ingredients in addition to cannabis. As the variety of cannabis products increases, so does the landscape of ingredients that are being or could be combined with cannabis. It is unknown whether some of the ingredients used in cannabis products, or components thereof, activate or modulate cannabinoid receptor activity. While the majority of ingredients are likely to be benign, it is important to understand those that may impact cannabinoid receptor activity and impact the risk profile of such products. Furthermore, phytomolecules may activate or modulate cannabinoid receptor activity via inhibitory, agonist, partial agonist, or allosteric mechanisms. This novel pharmacology would increase our knowledge about what types of substances change cannabinoid receptor activity—and how—which we can then correlate to their chemical structures. Knowledge of the structure–activity relationship between a substance's structure and its function at a receptor can lead to the creation of a "novel drug scaffold;" that is, a bare minimum chemical structure required to produce some known biological effect. Therefore, the research undertaken here could yield novel drug scaffolds based on phytomolecules for new—previously unknown—therapies.

The potential unique pharmacological effects arising through unique combinations of *Cannabis* phytomolecules are referred to as "the entourage effect" (Russo 2011). Several *in vitro* studies have shown that some terpenes present in *Cannabis*—α- and β-pinene, β-caryophyllene, β-myrcene, linalool, α-humulene, and limonene—do not have direct modulatory effects on CB1R, CB2R, transient receptor potential ankyrin 1 (TRPA1), or transient receptor potential vanilloid 1 (TRPV1) (Santiago et al., 2019; Finlay et al., 2020; Heblinski et al., 2020). Our group recently demonstrated that select, isolated, minor cannabinoids display weak partial agonist activity on CB1R and CB2R (Zagzoog et al., 2020). Also, there is mounting evidence from rodent studies that *Cannabis* products produce different pharmacology from isolated Δ^9-THC or CBD (Devsi et al., 2020; LaVigne et al., 2021; Roebuck et al., 2022). In addition, our group and several others have shown that cannabinoids may behave as allosteric ligands in cell culture models, modulating the signaling of GPCRs via indirect means (Laprairie et al., 2015; Martinez-Pinilla et al., 2017; Tham et al., 2018; Navarro et al., 2021). Consequently, cannabinoids are phytomolecules likely capable of affecting cellular signaling through a myriad of mechanisms. It is important to continue assessing combinations of phytomolecules to determine how these mixtures may alter the pharmacodynamics and pharmacokinetics of *Cannabis* products.

CB1R is activated by a wide spectrum of structurally diverse molecules (Howlett and Abood, 2017). CB1R modulates intracellular signaling through $G\alpha_{i/o}$-dependent inhibition of cAMP, inhibition of Ca^{2+} currents and inwardly rectifying K^+ channels, and recruitment of βarrestins. Therefore, in order to understand the potential effects that phytomolecules may have on CB1R, it is important to assess several endpoints, such as ligand binding, G-protein-dependent signaling, and βarrestin recruitment.

The purpose of this study was to assess 10 select phytomolecules (Δ^8-THC, $\Delta^{6a,10a}$-THC, 11-OH-Δ^9-THC, cannabinol [CBN], curcumin, epigallocatechin gallate [Egc G], olivetol, palmitoylethanolamide [PEA], piperine, and quercetin) in combination with Δ^9-THC to determine how these compounds modulate ligand binding and signaling *via* CB1R *in vitro*, and catalepsy, body temperature, and nociception *in vivo*. These data represent an initial step in determining whether phytomolecules could alter the pharmacological effects of cannabinoids and cannabis.

Materials and methods

Compounds

Compounds were purchased from Sigma-Aldrich (Oakville, ON), with the exceptions of Δ^9-THC, which was purchased from Toronto Research Chemicals (Toronto, ON) and SR141716A, which was purchased from Cayman Chemicals (Ann Arbor, MI). [^{3}H]CP55,940 (174.6 Ci/mmol) was obtained from PerkinElmer (Guelph, ON). All reagents were obtained from Sigma-Aldrich unless specifically noted. Compounds were dissolved in DMSO (final concentration of 0.1% in assay media for all assays) and added directly to the media at the concentrations and times indicated. For all experiments, 0.1% DMSO was used as the vehicle control.

Cell culture

Chinese hamster ovary (CHO)-K1 cells stably expressing human cannabinoid CB1R (hCB1R) were maintained at 37°C and 5% CO_2 in F-12 DMEM containing 1 mM L-glutamine, 10% FBS, and 1% penicillin–streptomycin as well as hygromycin B (300 μg/ml) and G418 (600 μg/ml) (Bolognini et al., 2012). For membrane preparation, cells were removed from flasks by scraping, centrifuged, and then frozen as a pellet at −80°C until required. Before use in a radioligand binding assay, cells were defrosted, diluted in Tris buffer (50 mM Tris–HCl and 50 mM Tris–base), and homogenized with a 1 ml hand-held homogenizer (Bolognini et al., 2012). HitHunter (cAMP) and PathHunter (βarrestin2) CHO-K1 cells stably expressing hCB1R from DiscoveRx® (Eurofins, Fremont, CA) were maintained at 37°C and 5% CO_2 in F-12 DMEM containing 10% FBS and 1% penicillin–streptomycin with 800 μg/ml geneticin

(HitHunter) or 800 μg/ml G418 and 300 μg/ml hygromycin B (PathHunter).

CHO cell membrane preparation and radioligand displacement assay

As described in previous work from our group, CHO-K1 hCB1R cells were disrupted by cavitation in a pressure cell and membranes were sedimented by ultracentrifugation (Zagzoog et al., 2020). The pellet was resuspended in TME buffer (50 mM Tris–HCl, 5 mM $MgCl_2$, and 1 mM EDTA, pH 7.4), and membrane proteins were quantified with a Pierce BCA Protein Assay Kit (Thermo Scientific, Rockford, United States).

Radioligand binding assays were carried out as described previously (Zagzoog et al., 2020). Briefly, binding was initiated by mixing CHO-K1 hCB1R cell membranes (25 μg protein per well) with 1 nM [^{3}H]CP55,940 in Tris binding buffer (50 mM Tris–HCl, 50 mM Tris–base, and 0.1% BSA, pH 7.4; total assay volume 2 ml), followed immediately by the addition of the compounds or vehicle (0.1% DMSO). All assays were performed at 37°C for 120 min before termination by the addition of ice-cold Tris-binding buffer, followed by vacuum filtration using a 24-well sampling manifold (Brandel Cell Harvester; Brandel Inc., Gaithersburg, MD, United States). Each reaction well was washed six times with a 1.2 ml aliquot of Tris-binding buffer. The filters were air-dried and then placed in 5 ml of scintillation fluid overnight (Ultima Gold XR, PerkinElmer). Radioactivity was quantified by liquid scintillation spectrometry. Specific binding was calculated as the difference between the binding that occurred in the presence and absence of 1 μM unlabeled CP55,940.

HitHunter cAMP assay

Inhibition of forskolin (FSK)-stimulated cAMP was determined using the DiscoveRx HitHunter assay in CHO-K1 hCB1R cells as described previously (Zagzoog et al., 2020). A total of 20,000 CHO-K1 hCB1R cells/well were grown in low-volume 96-well plates and incubated overnight in Opti-MEM containing 1% FBS at 37°C and 5% CO_2. Opti-MEM was removed and replaced with cell assay buffer (DiscoveRx), and the cells were simultaneously treated at 37°C with 10 μM FSK and compounds for 90 min. cAMP antibody solution and cAMP working detection solutions were added according to the manufacturer's directions (DiscoveRx), and cells were incubated for 60 min at room temperature. cAMP solution A was added (DiscoveRx), and cells were incubated for an additional 60 min at room temperature before chemiluminescence was measured on a Cytation5 plate reader (top read, gain 200, integration time 10,000 ms).

PathHunter βarrestin2 assay

βarrestin2 recruitment was measured as described previously (Zagzoog et al., 2020). A total of 20,000 CHO-K1 hCB1R cells/well were grown in low-volume 96-well plates and incubated overnight in Opti-MEM containing 1% FBS at 37°C and 5% CO_2. Cells were simultaneously treated at 37°C with compounds for 90 min. A detection solution was added to the cells according to the manufacturer's directions (DiscoveRx), and the cells were incubated for 60 min at room temperature. Chemiluminescence was measured on a Cytation5 plate reader (top read, gain 200, integration time 10,000 ms).

In vivo analyses

Male C57BL/6 mice between 8 and 12 weeks of age were used for these studies. Animals were group housed at the Laboratory Animal Services Unit (LASU) at the University of Saskatchewan (3 animals/cage) with a standard 12:12 light-dark cycle, *ad libitum* access to food and water, and environmental enrichment. Compounds were prepared in the vehicle [ethanol and cremophor in saline (1:1:8)] and administered intraperitoneally (i.p.). Catalepsy was assessed in the bar holding assay 5 min after compound administration with animals placed so that their forepaws clasped a 0.7-cm ring clamp 4.5 cm above the surface of the testing space (Garai et al., 2020). The length of time the ring was held was recorded up to 60 s (i.e., percent maximum possible effect [MPE] 60 s) with the trial ending if the mouse turned its head or body or made three consecutive escape attempts. Body temperature was measured 15 min after compound administration by using a rectal thermometer. Anti-nociceptive effects were measured in warm water (52 ± 2°C) using the tail-flick test 20 min after compound administration to a maximum of 20 s (i.e., percent maximum possible effect [MPE] 20 s). Compounds were administered at the doses indicated. Experimenters were blinded to treatment for all behavioral assessments and analyses. Animals were purchased, rather than bred, to reduce animal numbers. In all cases, experiments were performed with the approval of the University Animal Care Committee (UACC) at the University of Saskatchewan and in keeping with the guidelines of the Canadian Council on Animal Care (CCAC).

Statistical analyses

[^{3}H]CP55,940 binding data are represented as % change from maximal [^{3}H]CP55,940 bound (i.e., 100%). Change in [^{3}H]CP55,940 binding is represented as a downward deflection of the curve, and efficacy data are, therefore, represented as E_{min} (Table 1). HitHunter cAMP and PathHunter βarrestin2 data are shown as % of maximal CP55,940 response (i.e., 100%). Change in these assays is represented as an upward deflection of the curve, and efficacy data are, therefore, represented as E_{max} (Table 1). Concentration–response

TABLE 1 Activity of compounds at hCB1R.

Compound	[^{3}H]CP55,940		cAMP inhibition		βarrestin2 recruitment	
	K_i (nM)	E_{min} (%)	EC_{50} (nM)	E_{max} (%)	EC_{50} (nM)	E_{max} (%)
CP55,940	13 (5.6—33)	1.0 ± 4.7	1.0 (0.13—3.9)	100 ± 6.2	910 (700—1,200)	100 ± 3.3
Δ^9-THC	35 (17—71)	0.0 ± 3.5	5.2 (0.52—11)	70 ± 7.7*	600 (200—840)	47 ± 7.8*
Δ^8-THC	360 (120—1,000)*#	30 ± 5.0*#	440 (76—620)*#	56 ± 9.6*#	>10,000	21 ± 1.8*#
CBN	140 (47—670)*	71 ± 3.1*#	49 (14 – 160)*#	64 ± 4.6*#	>10,000	6.9 ± 0.96*#
$\Delta^{6a,10a}$-THC	1,000 (470 – 2,000)*#	1.7 ± 6.5	600 (260—1,300)*#	100 ± 11#	>10,000	54 ± 4.9*
11-OH-Δ^9-THC	0.37 (0.10—1.3)*#	70 ± 1.7*#	11 (2.0—49)	28 ± 3.9*#	>10,000	47 ± 9.4*
Curcumin	>10,000	100 ± 2.0*#	>10,000	6.2 ± 0.76*#	>10,000	8.9 ± 2.2*#
Egc G	>10,000	95 ± 3.4*#	>10,000	5.6 ± 0.52*#	>10,000	7.2 ± 0.85*#
Olivetol	17 (3.3—90)	57 ± 5.5*#	>10,000	5.6 ± 1.6*#	>10,000	8.3 ± 2.1*#
PEA	>10,000	46 ± 5.3*#	730 (210—1,600)*#	26 ± 1.8*#	2,100 (920—3,100)	5.6 ± 3.3*#
Piperine	>10,000	37 ± 2.8*#	>10,000	5.5 ± 0.63*#	>10,000	7.9 ± 0.97*#
Quercetin	350 (44—860)*	78 ± 8.1*#	>10,000	4.6 ± 0.80*#	>10,000	7.0 ± 1.2*#
Δ^8-THC + Δ^9-THC	2.6 (0.46—6.5)*#	7.0 ± 3.1	2.1 (0.58—12)	54 ± 1.6*#	>10,000	8.7 ± 3.0*#
CBN + Δ^9-THC	170 (17—260)	20 ± 5.4	>10,000	60 ± 7.1*	>10,000	3.0 ± 0.21*#
$\Delta^{6a,10a}$-THC + Δ^9-THC	8.8 (0.29—14)#	1.5 ± 4.1	7.7 (0.89—19)	100 ± 4.4#	>10,000	56 ± 2.7*
11-OH-Δ^9-THC + Δ^9-THC	1.2 (0.23—7.4)#	5.1 ± 3.1	11 (2.0—29)	23 ± 4.4*#	>10,000	44 ± 5.4*
Curcumin + Δ^9-THC	>10,000	24 ± 6.8	3.1 (0.62—16)	2.4 ± 5.0*#	>10,000	1.8 ± 0.27*#
Egc G + Δ^9-THC	7.9 (1.4—7.1)#	3.0 ± 3.9	4.0 (0.88—18)	13 ± 4.1*#	>10,000	2.5 ± 0.28*#
Olivetol + Δ^9-THC	4.6 (0.83—29)	1.1 ± 2.7	>10,000	61 ± 7.7*	>10,000	1.4 ± 0.31*#
PEA + Δ^9-THC	>10,000	1.7 ± 2.1	57 (10—280)	103 ± 4.8#	>10,000	14 ± 2.2*#
Piperine + Δ^9-THC	>10,000	12 ± 7.2	>10,000	48 ± 7.6*#	>10,000	1.7 ± 0.28*#
Quercetin + Δ^9-THC	350 (68—590)	3.2 ± 8.1	19 (5.3—95)	0.59 ± 4.3*#	>10,000	1.2 ± 0.44*#

Compound activity was quantified for [3H]CP55,940 binding, inhibition of forskolin-stimulated cAMP, or βarrestin2 recruitment in CHO cells stably expressing hCB1R and treated with phytomolecules. Data were fit to a variable slope (four parameters) non-linear regression in GraphPad (v. 9.0). $n \geq 6$ independent experiments were performed in triplicate. E_{max} and E_{min} refer to the top and bottom of the concentration–response curves, respectively. Data are expressed as nM with 95% CI or %CP55,940 response, mean ± SEM. *p < 0.05 compared to CP55,940; #p < 0.05 compared to Δ^9-THC within assay and measurement as determined via non-overlapping 95% CI or one-way ANOVA followed by Tukey's *post hoc* test.

curves (CRCs) were fit using non-linear regression with variable slopes (four parameters) and used to calculate EC_{50}, E_{min}, and E_{max} (GraphPad, Prism, v. 9.0). Statistical analyses were conducted by one-way analysis of variance (ANOVA) using GraphPad. *Post hoc* analyses were performed using Tukey's tests. Homogeneity of variance was confirmed using Bartlett's test. All results are reported as the mean ± the standard error of the mean (SEM) or 95% confidence interval (CI), as indicated. *In vivo* data were analyzed via one-way ANOVA followed by Tukey's *post hoc* test. GraphPad Prism 9.0 was used to analyze *in vivo* data, and $p < 0.05$ was considered to be statistically significant.

Results

Radioligand binding

When tested alone, the cannabinoids (Δ^8-THC, $\Delta^{6a,10a}$-THC, 11-OH-Δ^9-THC, and CBN) reduced [^{3}H]CP55,940 binding to hCB1R to some extent (Figure 2A). However, only $\Delta^{6a,10a}$-THC was able to fully compete [^{3}H]CP55,940 from hCB1R (Figure 2A). The observed affinity (K_i) for Δ^8-THC, $\Delta^{6a,10a}$-THC, and 11-OH-Δ^9-THC was less than that of CP55,940 or Δ^9-THC (Table 1). The affinity of CBN for hCB1R was less than that of CP55,940 but not different from Δ^9-THC (Table 1). Δ^8-THC, CBN, $\Delta^{6a,10a}$-THC, and 11-OH-Δ^9-THC displayed greater E_{min} values than either CP55,940 or Δ^9-THC, indicating that they did not completely displace [^{3}H]CP55,940 from hCB1R and suggesting an incomplete overlap of binding sites between these compounds and [^{3}H]CP55,940 (Table 1). These cannabinoids were further assessed in the presence of 100 nM Δ^9-THC to determine whether these cannabinoids altered the binding of Δ^9-THC to hCB1R (Figure 2B). Each of these cannabinoids augmented the displacement of [^{3}H]CP55,940 from hCB1R by 100 nM Δ^9-THC relative to 100 nM Δ^9-THC alone (~20%; Figure 2B). Δ^8-THC and $\Delta^{6a,10a}$-THC displayed lower K_i values when co-administered with 100 nM Δ^9-THC for hCB1R relative to being administered alone, suggesting some form of cooperativity between these compounds. No change in K_i was observed for 11-OH-Δ^9-

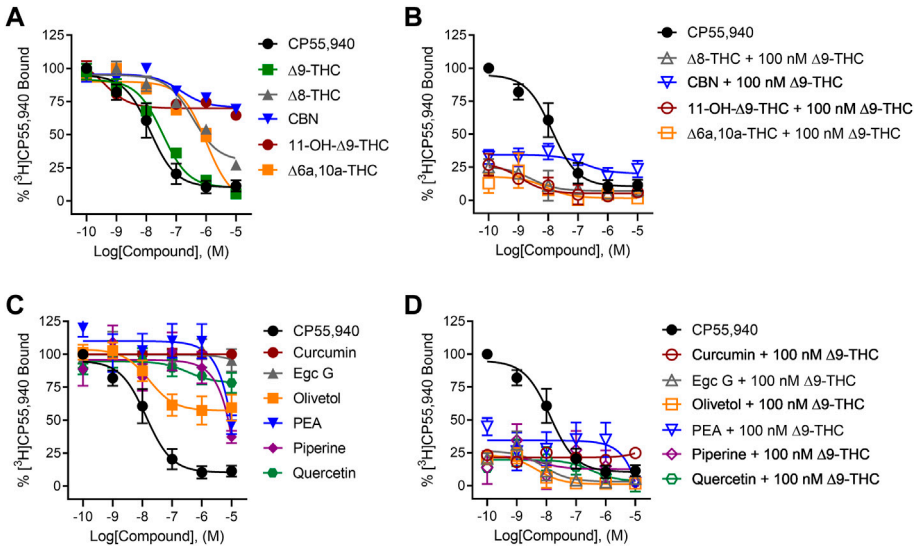

FIGURE 2
[^{3}H]CP55,940 displacement from hCB1R CHO cell membranes. Compound activity was quantified for [^{3}H]CP55,940 binding in CHO cells stably expressing hCB1R and treated with 0.1 nM—10 μM **(A)** cannabinoids; **(B)** cannabinoids + 100 nM Δ^9-THC; **(C)** phytomolecules; and **(D)** phytomolecules + 100 nM Δ^9-THC. Data were fit to a variable slope (four parameters) non-linear regression in GraphPad (v. 9). n ≥ 6 independent experiments were performed in duplicate. Data are expressed as mean ± SEM. K_i and E_{min} are reported in Table 1.

THC + 100 nM Δ^9-THC or CBN + 100 nM Δ^9-THC compared to these compounds alone, suggesting that 11-OH-Δ^9-THC and CBN were primarily responsible for [^{3}H]CP55,940 displacement in the presence of 100 nM Δ^9-THC (Figure 2B; Table 1). These data indicate that select cannabinoids were able to displace [^{3}H]CP55,940 from hCB1R either alone or in concert with Δ^9-THC. For Δ^8-THC and $\Delta^{6a,10a}$-THC, these ligands may have engaged hCB1R cooperatively to displace [^{3}H]CP55,940, but this is not a reflection of functional signaling outcomes at hCB1R.

In contrast to cannabinoids, when the other phytomolecules were tested alone, only olivetol produced a clear reduction in [^{3}H]CP55,940 binding to hCB1R with an estimated K_i that was not different from CP55,940 or Δ^9-THC but did not completely displace [^{3}H]CP55,940 from hCB1R, suggesting that the displacement was not competitive (Figure 2C). Other phytomolecules tested produced some minimal degree of [^{3}H]CP55,940 displacement at the highest concentrations tested (i.e., 1 and 10 μM) (Figure 2C; Table 1). These phytomolecules were further assessed in the presence of 100 nM Δ^9-THC to determine whether they altered the binding of Δ^9-THC to hCB1R (Figure 2D). Curcumin, olivetol, PEA, piperine, and quercetin did not significantly alter [^{3}H]CP55,940 displacement from hCB1R in the presence of 100 nM Δ^9-THC (Table 1). Egc G augmented the displacement of [^{3}H]CP55,940 from hCB1R by Δ^9-THC as indicated by the decrease in observed K_i relative to Δ^9-THC alone (Table 1).

Inhibition of forskolin-stimulated cAMP

All tested cannabinoids increased hCB1R-mediated inhibition of cAMP accumulation (Figure 3A). All cannabinoids tested were partial agonists of cAMP inhibition except for $\Delta^{6a,10a}$-THC, which was a full agonist with low potency (Figure 3A). Δ^8-THC, CBN, and $\Delta^{6a,10a}$-THC were approximately 440x, 49x, and 600x less potent, respectively, than C55,940, whereas the Δ^9-THC metabolite, 11-OH-Δ^9-THC, was not statistically different in its potency compared to CP55,940 and Δ^9-THC (Table 1). Similarly, Δ^8-THC, CBN, and 11-OH-Δ^9-THC displayed lower efficacy than CP55,940 and Δ^9-THC, consistent with previous observations that all of these compounds are hCB1R partial agonists (Table 1) (Ross et al., 1999; ElSohly et al., 2017). In the presence of 100 nM Δ^9-THC, neither Δ^8-THC nor CBN produced a significant change in cAMP inhibition relative to 100 nM Δ^9-THC (Figure 3B), likely due to their weak hCB1R affinity as observed in [^{3}H]CP55,940 competition binding experiments. Also, 11-OH-Δ^9-THC inhibited the activity of 100 nM Δ^9-THC in a concentration-dependent manner and to the level of 11-OH-Δ^9-THC agonism consistent with this ligand's competition for hCB1R binding and activation (Figure 3B). $\Delta^{6a,10a}$-THC elevated cAMP inhibition above the activity of 100 nM Δ^9-THC in a concentration-dependent manner and to the level of $\Delta^{6a,10a}$-THC agonism consistent with that ligand's higher efficacy at hCB1R, but with greater potency than $\Delta^{6a,10a}$-THC alone (Figure 3B; Table 1). This observation with $\Delta^{6a,10a}$-THC may suggest that the

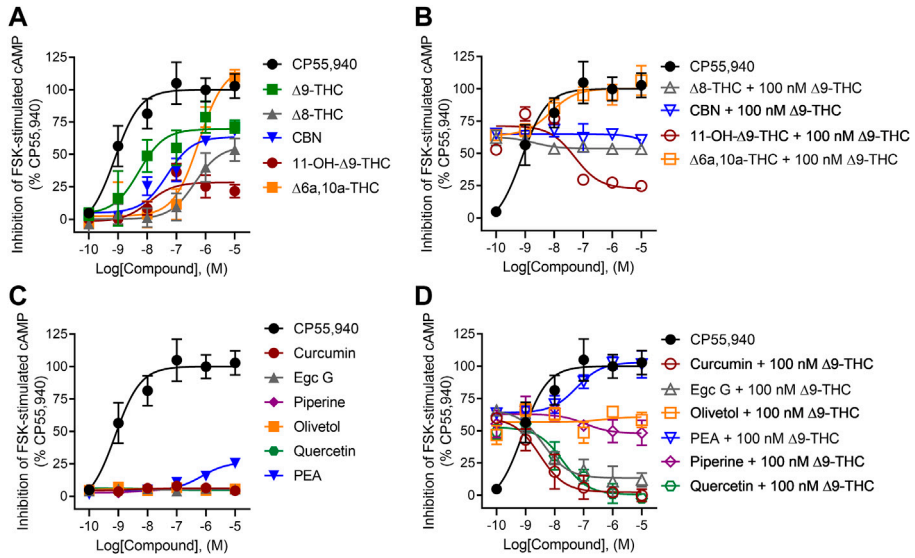

FIGURE 3
hCB1R-dependent inhibition of forskolin-stimulated cAMP accumulation. Compound activity was quantified for inhibition of 10 μM forskolin-stimulated cAMP accumulation in CHO cells stably expressing hCB1R and treated with 0.1 nM—10 μM **(A)** cannabinoids; **(B)** cannabinoids + 100 nM Δ^9-THC; **(C)** phytomolecules; and **(D)** phytomolecules + 100 nM Δ^9-THC for 90 min according to the standard operating procedures of the HitHunter assay. Data were fit to a variable slope (four parameters) non-linear regression in GraphPad (v. 9). n ≥ 6 independent experiments were performed in triplicate. Data are expressed as mean ± SEM. EC_{50} and E_{max} are reported in Table 1.

compound is able to engage hCB1R cooperatively with Δ^9-THC to facilitate G-protein-dependent signaling, consistent with the observations made with [^{3}H]CP55,940. Whether this *in vitro* observation has a direct outcome *in vivo* is not clear from these data.

Among the other phytomolecules tested, only PEA produced weak partial agonist inhibition of cAMP accumulation, having potency and efficacy significantly lower than either CP55,940 or Δ^9-THC (Figure 3C; Table 1). Olivetol and piperine did not change the cAMP inhibitory effects of 100 nM Δ^9-THC, confirming that although these compounds produced some displacement of [^{3}H]CP55,940, they are not agonists of hCB1R (Figure 3D; Table 1). Curcumin, Egc G, and quercetin inhibited the activity of 100 nM Δ^9-THC in a concentration-dependent manner inconsistent with these ligands' weak hCB1R affinity in [^{3}H]CP55,940 binding experiments (Figure 3D; Table 1). Therefore, curcumin, Egc G, and quercetin likely inhibited Δ^9-THC-dependent cAMP inhibition via an indirect mechanism such as altering membrane dynamics, G-protein coupling, or adenylate cyclase activity (Jonsson et al., 2001; Balasubramanyam et al., 2004; Ho et al., 2008; Choi et al., 2009). If such *in vitro* observations manifested *in vivo*, then curcumin, Egc G, and quercetin could limit the effects of Δ^9-THC, such as intoxication. Lastly, PEA augmented the activity of 100 nM Δ^9-THC in a concentration-dependent manner inconsistent with PEA's weak hCB1R affinity in [^{3}H]CP55,940 binding experiments (Figure 3D; Table 1). PEA has been described as a partial hCB1R agonist and bears structural similarity to the endogenous cannabinoid anandamide (AEA) (Jonsson et al., 2001; Ho et al., 2008). Therefore, PEA's activity may be consistent with allosteric agonism of hCB1R (Laprairie et al., 2019; Garai et al., 2020, 2021).

βarrestin2 recruitment

All tested cannabinoids were weak partial agonists of βarrestin2 recruitment, although only Δ^9-THC produced quantifiable potency within the concentration range used (Figure 4A; Table 1). The maximum efficacy observed for Δ^8-THC and CBN was lower than that of CP55,940 and Δ^9-THC (Figure 4A; Table 1). Given the minimal activity observed in the βarrestin2 recruitment assay, it is not surprising that the cannabinoids did not drastically alter βarrestin2 recruitment in the presence of 100 nM Δ^9-THC (Figure 4B). At the highest concentration tested, 10 μM 11-OH-Δ^9-THC and $\Delta^{6a,10a}$-THC elevated βarrestin2 recruitment above the activity of 100 nM Δ^9-THC in a concentration-dependent manner and to the level of their agonism consistent with those ligands' efficacy at hCB1R (Figure 4B).

None of the phytomolecules tested promoted βarrestin2 recruitment when tested alone (Figure 4C). Only one of the phytomolecules tested—PEA—altered the recruitment of βarrestin2 by 100 nM Δ^9-THC (Figure 4D;

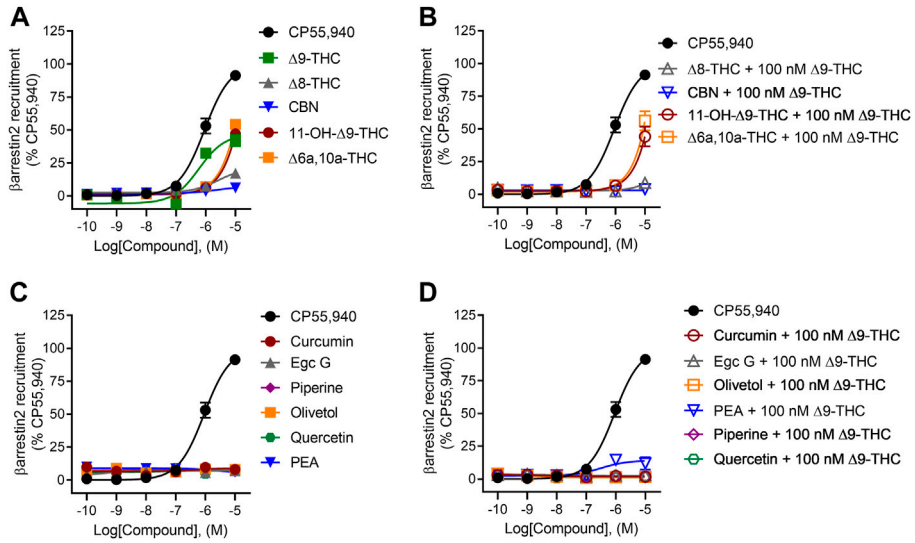

FIGURE 4
hCB1R-dependent recruitment of βarrestin2. Compound activity was quantified for βarrestin2 recruitment in CHO cells stably expressing hCB1R and treated with 0.1 nM—10 μM **(A)** cannabinoids; **(B)** cannabinoids + 100 nM Δ^9-THC; **(C)** phytomolecules; and **(D)** phytomolecules + 100 nM Δ^9-THC for 90 min according to the standard operating procedures of the PathHunter assay. Data were fit to a variable slope (four parameters) non-linear regression in GraphPad (v. 9). n ≥ 6 independent experiments were performed in triplicate. Data are expressed as mean ± SEM. EC_{50} and E_{max} are reported in Table 1.

Table 1). Similar to its activity in the cAMP inhibition assay, PEA slightly increased βarrestin2 recruitment in the presence of 100 nM Δ^9-THC, consistent with the notion that PEA may be an allosteric agonist of hCB1R (Figure 4D; Table 1).

Confirming hCB1R dependence of PEA-mediated cAMP inhibition

In general, we observed partial agonism by the tested cannabinoids and an absence of hCB1R-dependent activity by the other phytomolecules tested. One exception to this generalization was PEA. PEA augmented hCB1R-dependent cAMP inhibition and βarrestin2 recruitment with Δ^9-THC but displayed little to no affinity for the orthosteric site of hCB1R as observed by radioligand binding experiments. The ability of PEA to activate hCB1R was tested in the cAMP inhibition assay in the absence or presence of SR141716A as an hCB1R antagonist/inverse agonist (Figure 5). Co-treatment of hCB1R CHO cells with 1 μM PEA and 1 μM SR141716A—or a combination of 1 μM PEA, 1 μM Δ^9-THC, and 1 μM SR141716A—completely prevented PEA-dependent cAMP inhibition (Figure 5). Previous reports have shown that allosteric or indirect agonism of hCB1R is blocked by SR141716A even when those allosteric ligands are not displaced in radioligand binding experiments (Garai et al., 2020, Garai et al., 2021). Therefore, the collective evidence supports PEA indirectly augmenting the activity of hCB1R *in vitro*.

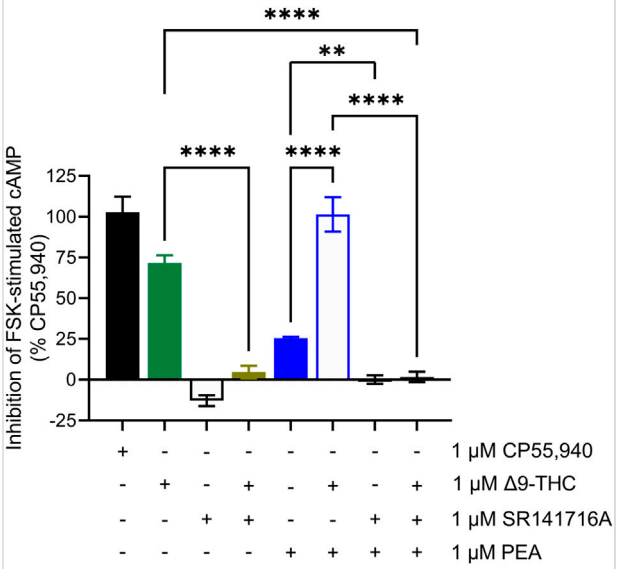

FIGURE 5
hCB1R-dependent inhibition of forskolin-stimulated cAMP accumulation. Compound activity was quantified for inhibition of 10 μM forskolin-stimulated cAMP accumulation in CHO cells stably expressing hCB1R and treated with compounds as indicated for 90 min according to the standard operating procedures of the HitHunter assay. Data were analyzed in GraphPad (v. 9). *n* = 6 independent experiments were performed in triplicate. Data are expressed as mean ± SEM. $^{**}p < 0.01$, $^{****}p < 0.0001$ as determined by one-way ANOVA followed by Tukey's *post hoc* test for multiple comparisons.

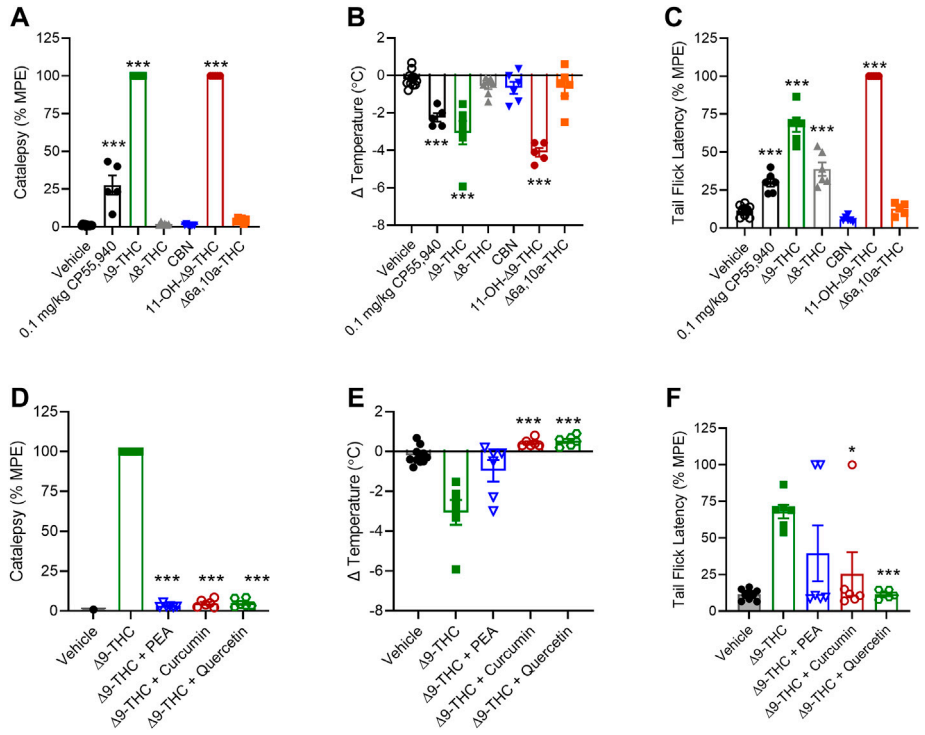

FIGURE 6
In vivo effects of cannabinoids and select phytomolecules in male C57BL/6 mice. Male mice were treated with 10 mg/kg cannabinoids **(A–C)** or 10 mg/kg Δ^9-THC + 10 mg/kg select phytomolecules i. p. **(D–F)** and assessed for catalepsy 5 min post-injection **(A,D)**, body temperature 15 min post-injection **(B,E)**, and nociception in the tail-flick assay 20 min post-injection **(C,F)**. Data for catalepsy are represented as % MPE during a maximum 60 s trial. Data for the tail-flick assay are represented as % MPE during a maximum 20 s trial. All data were analyzed in GraphPad (v. 9). n = 5–10 animals per treatment group. Data are expressed as mean ± SEM. *$p < 0.05$, **$p < 0.01$, and ****$p < 0.001$ as determined by one-way ANOVA followed by Tukey's *post hoc* test for multiple comparisons.

In vivo evaluation

Given our *in vitro* observations, we wanted to determine whether minor cannabinoids and combinations of Δ^9-THC with select phytomolecules affected catalepsy, body temperature, and nociception in mice, which are three physiological parameters well known to be affected by Δ^9-THC. Specifically, we chose to examine whether 10 mg/kg PEA, curcumin, or quercetin altered physiological responses to 10 mg/kg Δ^9-THC because these phytomolecules had augmented (PEA) or inhibited (curcumin and quercetin) Δ^9-THC-dependent inhibition of cAMP to the greatest extent. A dose of 10 mg/kg was chosen because it has been used previously to demonstrate Δ^9-THC-dependent intoxicating effects in rodent models by ourselves and others; and Δ^9-THC plasma levels similar to intoxicating levels were observed after acute cannabis use in humans (Craft and Leitl, 2008; Wakley et al., 2014; Grim et al., 2017; Nguyen et al., 2018; Moore et al., 2021).

Among the cannabinoids tested, Δ^8-THC, CBN, and $\Delta^{6a,10a}$-THC did not produce catalepsy or reduce body temperature in male mice (Figures 6A,B). Δ^8-THC produced an anti-nociceptive effect that was not different from Δ^9-THC, but CBN and $\Delta^{6a,10a}$-THC did not produce such effect (Figure 6C). Also, 11-OH-Δ^9-THC produced equal catalepsy and greater hypothermia and anti-nociceptive responses relative to Δ^9-THC (Figures 6A–C).

When 10 mg/kg PEA, curcumin, or quercetin was tested in combination with 10 mg/kg Δ^9-THC, each of these phytomolecules was capable of blocking Δ^9-THC's effects on catalepsy and body temperature (Figures 6D,E). Curcumin and quercetin also blocked Δ^9-THC's effect in the nociception test, but PEA did not block the effect (Figure 6F). In the case of PEA, the mechanism underlying the observation is unclear because *in vitro* PEA had augmented Δ^9-THC's effects. PEA may have multiple intracellular targets including peroxisome proliferator-activated receptor α (PPARα), GPR55, and GPR119 (Lo Verme et al., 2005; Godlewski et al., 2009). Our results and earlier studies also indicate PEA is unlikely to be a CB1R ligand (O'Sullivan and Kendall, 2010). Therefore, the observed *in vivo* effects of PEA here may be due to PEA acting on other ligand targets not present in our *in vitro* model.

Discussion

In general, we observed that all cannabinoids tested—Δ^9-THC, Δ^8-THC, $\Delta^{6a,10a}$-THC, 11-OH-Δ^9-THC, and CBN—behaved as CB1R partial agonists in the cAMP inhibition assay and were able to partially displace [^{3}H]CP55,940 from CB1R in the competition binding assay. Together, these data support the hypothesis that the cannabinoids tested here are all weak and/or partial agonists of CB1R. These data are in agreement with previously published findings on Δ^8-THC, CBN, and 11-OH-Δ^9-THC (Ross et al., 1999; Pertwee, 2008), and this study represents the first report of activity for $\Delta^{6a,10a}$-THC. The incomplete competition of Δ^8-THC, CBN, and 11-OH-Δ^9-THC with [^{3}H]CP55,940 suggests that the occupied binding site of these ligands differs slightly from that of CP55,940. It is possible that only a subset of amino acids in the CB1R ligand-binding site is engaged by these cannabinoids compared to CP55,940, as shown for CBD, Org27569, rimonabant, and anandamide (Iliff et al., 2011; Baillie et al., 2013; Laprairie et al., 2015; Hua et al., 2017). Future experiments utilizing site-directed mutagenesis are needed to assess this question directly.

After the most abundant phytocannabinoid Δ^9-THC, Δ^8-THC, $\Delta^{6a,10a}$-THC, and CBN are the phytocannabinoids that are most commonly found as less abundant THC-like isoforms in *Cannabis* products (Pertwee, 2008; ElSohly and Gul, 2014; Howlett and Abood, 2017). Previous work has shown that Δ^8-THC behaves as a weak partial agonist of CB1R in GTP binding experiments, consistent with our observations (Ross et al., 1999; Pertwee, 2008). Comparatively, little is known about $\Delta^{6a,10a}$-THC; however, its structural similarities to Δ^9-THC suggest that it is likely to have some cannabinoid receptor modulatory activity (Howlett and Abood, 2017). CBN is both a minor phytocannabinoid and an oxidation product of Δ^9-THC found to accumulate in *Cannabis* products during storage (Felder et al., 1995; Showalter et al., 1996; Howlett and Abood, 2017). Our data suggesting that CBN is a weak partial CB1R agonist are in agreement with previous findings for CBN for both relative potency and efficacy in CHO and AtT-20 cells expressing human CB1R and *ex vivo* tissue studies (Felder et al., 1995; Showalter et al., 1996). The Δ^9-THC metabolite 11-OH-Δ^9-THC has previously been shown to produce CB1R-dependent effects in the rodent tetrad model; our data support earlier work showing CB1R activity for this ligand (Huestis, 2005). The potency and efficacy of 11-OH-Δ^9-THC approximate data observed in earlier works (Felder et al., 1995; Showalter et al., 1996; Huestis, 2005). The weak partial agonist effects displayed by these ligands suggest that they may in fact be functionally antagonistic in the presence of higher agonist concentrations and *in vivo*. This functional antagonism has been previously demonstrated for Δ^9-THC itself (Laprairie et al., 2015; Grim et al., 2017). Future work assessing the potential antagonist activity of these compounds in the presence of a full agonist such as CP55,940 will be able to better classify the mechanisms of action for these compounds beyond what has been performed here.

Comparing our *in vitro* data with our *in vivo* observations suggests that although cannabinoids may be capable of activating CB1R-dependent pathways *in vitro*, these observations may not translate to *in vivo* effects. Of note, however, 11-OH-Δ^9-THC displayed the greatest estimated binding affinity to CB1R, greatest potency in the cAMP inhibition assay among minor phytocannabinoids, and similar efficacy to Δ^9-THC in the βarrestin2 recruitment assay and proved to have the greatest *in vivo* activity. Additional work is required to determine other pharmacological targets of the minor cannabinoids *in vivo* beyond CB1R.

Among the non-cannabinoid phytomolecules tested here, we observed generally weak, minimal, and partial displacement of [^{3}H]CP55,940 in competition binding assays. One notable exception to this was olivetol, which produced a concentration-dependent reduction in [^{3}H]CP55,940 binding. It is unclear whether this loss of [^{3}H]CP55,940 binding was a consequence of direct competition or indirect changes in membrane integrity and lipid dynamics that may occur with these highly lipophilic ligands (Howlett and Abood, 2017). Of note, olivetol did not significantly impact CB1R-dependent signal transduction in other assays. Additional data are required to assess the specific mechanism of competition occurring for olivetol in these experiments. PEA only reduced [^{3}H]CP55,940 binding at concentrations exceeding 1 μM but augmented CB1R- and Δ^9-THC-dependent inhibition of cAMP and βarrestin2 recruitment at approximately 1 μM. These observations for PEA are consistent with a partial agonist or positive allosteric modulator (Jonsson et al., 2001; Ho et al., 2008). PEA is structurally similar to both endogenous cannabinoids anandamide and 2-arachidonoylglycerol, and given this structural similarity, it would not be surprising if the compound activated CB1R. Additional experiments are required to assess whether these effects are allosteric in nature, as indirectly assessed by others (Jonsson et al., 2001; Ho et al., 2008). Finally, the three polyphenolic terpenoid compounds—quercetin, Egc G, and curcumin—all displayed minimal competition with [^{3}H]CP55,940 at CB1R but surprisingly produced a concentration-dependent and potent antagonistic inhibition of CB1R- and Δ^9-THC-mediated inhibition of cAMP. Given these data, we propose that the polyphenolic terpenes tested here indirectly inhibit signaling downstream of CB1R. Quercetin, Egc G, and curcumin have all been shown to have widespread and non-specific antioxidant, lipid raft, and transcription factor modulatory effects that could interfere with GPCR-dependent signaling and

trafficking (Balasubramanyam et al., 2004; Choi et al., 2009). When exploring a subset of these phytomolecules *in vivo*, curcumin's and quercetin's effects are congruent with *in vitro* observations where both phytomolecules inhibited Δ^9-THC-dependent catalepsy, hypothermia, and anti-nociception.

The limitation of this work is that it is an assessment of the pharmacology for a subset of *Cannabis*- and non-*Cannabis*-derived phytomolecules at a single cannabinoid receptor, CB1R. Importantly, this study also focused only on male mice. Planned future studies will incorporate female mice as we and others have observed cannabinoid-dependent sex differences *in vivo* (Craft and Leitl, 2008; Wakley et al., 2014; Kim et al., 2022). Although caution should be exercised when extrapolating *in vitro* cell culture data into the whole animal *in vivo* systems, three observations from our dataset warrant further consideration with regard to effecting cannabis pharmacology. First, the majority of compounds tested—exceptions being curcumin and Egc G—partially or fully competed with [^{3}H]CP55,940 for receptor binding. Therefore, it is possible that these phytomolecules could reduce Δ^9-THC binding at CB1R and thus diminish its medicinal and intoxicating effects if given at least at equimolar concentrations. In particular, Δ^8-THC, $\Delta^{6a,10a}$-THC, and olivetol, with their more potent and near complete competition of CP55,940, could limit Δ^9-THC's binding to CB1R. Second, the cannabinoids tested all yielded CB1R-dependent inhibition of cAMP with less potency and efficacy than Δ^9-THC, with the exception of $\Delta^{6a,10a}$-THC which displayed greater efficacy. When administered alone, we observed that 11-OH-Δ^9-THC was able to reproduce or exceed the effects of Δ^9-THC *in vivo*. If, however, both Δ^9-THC and the cannabinoids tested were present together, it is unlikely that their actions would be additive or synergistic as these effects appear to be CB1R-dependent. In contrast, two compounds—curcumin and quercetin—were able to diminish the intoxicating effects of Δ^9-THC via indirect inhibition of CB1R-dependent signaling. Third, two cannabinoids—$\Delta^{6a,10a}$-THC and 11-OH-Δ^9-THC—produced βarrestin2 recruitment similar to that of Δ^9-THC. At other GPCRs, such as the μ-opioid and serotonin 2A receptors, βarrestin2 recruitment is associated with the intoxicating and impairing effects of receptor activation (Bohn et al., 1999; Schmid et al., 2017; Wacker et al., 2017). Given 11-OH-Δ^9-THC's *in vivo* activity observed here, it is possible that this compound specifically could yield intoxicating effects akin to Δ^9-THC via βarrestin2 (Felder et al., 1995; Showalter et al., 1996; Huestis, 2005), whereas the other compounds tested here would not yield βarrestin2-dependent intoxicating effects.

Although changes in [^{3}H]CP55,940 binding were observed for several cannabinoids and phytomolecules, it is not presently clear whether changes in signaling or protein recruitment were the result of direct, orthosteric activity as opposed to allosteric modulation, or modulation of a separate target whose signaling converges on the same output measure (e.g., membrane fluidity and adenylate cyclase, etc.). In the past, our group and others have explored cannabinoid allostery (Laprairie et al., 2015; Martinez-Pinilla et al., 2017; Tham et al., 2018; Navarro et al., 2021), but this was not the focus of the present study. Δ^9-THC and other cannabinoids affect signaling via many other proteins, including the type 2 cannabinoid receptor (CB2R), the orphan GPCR GPR55, 5HT1A receptor, μ-opioid receptor, peroxisome proliferator-activated receptors (PPARs), and the transient receptor potential vanilloid 1 Ca^{2+} channel (TRPV1), among others (Howlett and Abood, 2017). Therefore, in order to understand the poly-pharmacology of cannabinoids and terpenes in whole organisms, other receptor targets and pharmacokinetic outcomes must be considered.

In conclusion, there exists a great wealth and array of phytomolecules present in cannabis whose pharmacology as single chemicals is still being determined, let alone as a milieu of more than five hundred compounds. Our studies are the first steps toward characterizing the complex mixture of compounds present in cannabis as well as their effects and interactions. It is our goal and the goal of many researchers exploring the potential of an entourage effect (Santiago et al., 2019; Devsi et al., 2020; Finlay et al., 2020; Heblinski et al., 2020; LaVigne et al., 2021) and to determine if and how cannabinoids and terpenes may influence one another's pharmacology. As interest continues to accrue with respect to the use of cannabis for medical and non-medical purposes, the aim of this work was to understand how cannabis and non-cannabis phytomolecules work alone and in combination with one another so they can be used safely.

Data availability statement

The original contributions presented in the study are included in the article/Supplementary Material; further inquiries can be directed to the corresponding author.

Ethics statement

The animal study was reviewed and approved by the University of Saskatchewan's University Animal Care Committee (UACC).

Author contributions

AZ designed, conducted, analyzed cell culture and *in vivo* experimental data, and contributed to the writing and editing of the manuscript. AC and HA contributed to the writing and

editing of the manuscript and assisted with the design of experiments. RL wrote and edited the manuscript.

Funding

This project was funded by a Health Canada Research Contract as well as a CIHR Partnership Grant with GlaxoSmithKline to RBL (#387577).

Acknowledgments

The authors wish to acknowledge Gabriel Picard (Office of Cannabis Science and Surveillance, CSCB, Health Canada) for valuable technical suggestions with respect to the selection of some compounds tested.

Conflict of interest

The authors declare that the research was conducted in the absence of any commercial or financial relationships that could be construed as a potential conflict of interest.

Publisher's note

References

Baillie, G. L., Horswill, J. G., Anavi-Goffer, S., Reggio, P. H., Bolognini, D., Abood, M. E., et al. (2013). CB_1 receptor allosteric modulators display both agonist and signaling pathway specificity. *Mol. Pharmacol.* 83, 322–338. doi:10.1124/mol.112.080879

Balasubramanyam, K., Varier, R. A., Altaf, M., Swaminathan, V., Siddappa, N. B., Ranga, U., et al. (2004). Curcumin, a novel p300/CREB-binding protein-specific inhibitor of acetyltransferase, represses the acetylation of histone/nonhistone proteins and histone acetyltransferase-dependent chromatin transcription. *J. Biol. Chem.* 279, 51163–51171. doi:10.1074/jbc.M409024200

Bohn, L. M., Lefkowitz, R. J., Gainetdinov, R. R., Peppel, K., Caron, M. G., Lin, F. T., et al. (1999). Enhanced morphine analgesia in mice lacking beta-arrestin 2. *Science* 286, 2495–2498. doi:10.1126/science.286.5449.2495

Bolognini, D., Cascio, M. G., Parolaro, D., and Pertwee, R. G. (2012). AM630 behaves as a protean ligand at the human cannabinoid CB2 receptor. *Br. J. Pharmacol.* 165, 2561–2574. doi:10.1111/j.1476-5381.2011.01503.x

Choi, M. R., Medici, C., Gironacci, M. M., Correa, A. H., and Fernandez, B. E. (2009). Angiotensin II regulation of renal dopamine uptake and Na(+),K(+)-ATPase activity. *Nephron. Physiol.* 111, 53–58. doi:10.1159/000209211

Craft, R. M., and Leitl, M. D. (2008). Gonadal hormone modulation of the behavioral effects of Delta9-tetrahydrocannabinol in male and female rats. *Eur. J. Pharmacol.* 578, 37–42. doi:10.1016/j.ejphar.2007.09.004

Devsi, A., Kiyota, B., Ouellette, T., Hegle, A. P., Rivera-Acevedo, R. E., Wong, J., et al. (2020). A pharmacological characterization of Cannabis sativa chemovar extracts. *J. Cannabis Res.* 2, 17. doi:10.1186/s42238-020-00026-0

ElSohly, M. A., and Gul, W. (2014). LC-MS-MS analysis of dietary supplements for N-ethyl-α-ethyl-phenethylamine (ETH), N, N-diethylphenethylamine and phenethylamine. *J. Anal. Toxicol.* 38, 63–72. doi:10.1093/jat/bkt097

ElSohly, M. A., Radwan, M. M., Gul, W., Chandra, S., and Galal, A. (2017). Phytochemistry of cannabis sativa L. *Prog. Chem. Org. Nat. Prod.* 103, 1–36. doi:10.1007/978-3-319-45541-9_1

Felder, C. C., Joyce, K. E., Briley, E. M., Mansouri, J., Mackie, K., Blond, O., et al. (1995). Comparison of the pharmacology and signal transduction of the human cannabinoid CB1 and CB2 receptors. *Mol. Pharmacol.* 48, 443–450.

Finlay, D. B., Sircombe, K. J., Nimick, M., Jones, C., and Glass, M. (2020). Terpenoids from Cannabis do not mediate an entourage effect by acting at cannabinoid receptors. *Front. Pharmacol.* 11, 359. doi:10.3389/fphar.2020.00359

Garai, S., Kulkarni, P. M., Schaffer, P. C., Leo, L. M., Brandt, A. L., Zagzoog, A., et al. (2020). Application of fluorine- and nitrogen-walk approaches: defining the structural and functional diversity of 2-phenylindole class of cannabinoid 1 receptor positive allosteric modulators. *J. Med. Chem.* 63, 542–568. doi:10.1021/acs.jmedchem.9b01142

Garai, S., Leo, L. M., Szczesniak, A. M., Hurst, D. P., Schaffer, P. C., Zagzoog, A., et al. (2021). Discovery of a biased allosteric modulator for cannabinoid 1 receptor: preclinical anti-glaucoma efficacy. *J. Med. Chem.* 64, 8104–8126. doi:10.1021/acs.jmedchem.1c00040

Godlewski, G., Offertaler, L., Wagner, J. A., and Kunos, G. (2009). Receptors for acelethanolamides-GPR55 and GPR119. *Prostagl. other lipid Mediat.* 89, 105–111. doi:10.1016/j.prostaglandins.2009.07.001

Grim, T. W., Morales, A. J., Thomas, B. F., Wiley, J. L., Endres, G. W., Negus, S. S., et al. (2017). Apparent CB1 receptor rimonabant affinity estimates: combination with THC and synthetic cannabinoids in the mouse *in vivo* triad model. *J. Pharmacol. Exp. Ther.* 362, 210–218. doi:10.1124/jpet.117.240192

Heblinski, M., Santiago, M., Fletcher, C., Stuart, J., Connor, M., McGregor, I. S., et al. (2020). Terpenoids commonly found in *Cannabis sativa* do not modulate the actions of phytocannabinoids or endocannabinoids on TRPA1 and TRPV1 channels. *Cannabis Cannabinoid Res.* 5, 305–317. doi:10.1089/can.2019.0099

Ho, W. S., Barrett, D. A., and Randall, M. D. (2008). 'Entourage' effects of N-palmitoylethanolamide and N-oleoylethanolamide on vasorelaxation to anandamide occur through TRPV1 receptors. *Br. J. Pharmacol.* 155, 837–846. doi:10.1038/bjp.2008.324

Howlett, A. C., and Abood, M. E. (2017). CB1 and CB2 receptor pharmacology. *Adv. Pharmacol.* 80, 169–206. doi:10.1016/bs.apha.2017.03.007

Hua, T., Vemuri, K., Nikas, S. P., Laprairie, R. B., Wu, Y., Qu, L., et al. (2017). Crystal structures of agonist-bound human cannabinoid receptor CB1. *Nature* 547, 468–471. doi:10.1038/nature23272

Huestis, M. A. (2005). Pharmacokinetics and metabolism of the plant cannabinoids, d9-tetrahydrocannibinol, cannabidiol and cannabinol. *Handb. Exp. Pharmacol.* 168, 657–690. doi:10.1007/3-540-26573-2_23

Iliff, H. A., Lynch, D. A., Kotsikorou, E., and Reggio, P. H. (2011). Parameterization of Org27569: an allosteric modulator of the cannabinoid CB1 G protein-coupled receptor. *J. Comput. Chem.* 32, 2119–2126. doi:10.1002/jcc.21794

Jonsson, K. O., Vandevoorde, S. V., Lambert, D. M., Tiger, G., and Fowler, C. J. (2001). Effects of homologues and analogues of palmitoylethanolamide upon the inactivation of the endocannabinoid anandamide. *Br. J. Pharmacol.* 133, 1263–1275. doi:10.1038/sj.bjp.0704199

Kim, H. J. J., Zagzoog, A., Black, T., Baccetto, S. L., Ezeaka, U. C., Laprairie, R. B., et al. (2022). Impact of the mouse estrus cycle on cannabinoid receptor agonist-induced molecular and behavioral outcomes. *Pharmacol. Res. Perspect.* 10, e00950. doi:10.1002/prp2.950

Laprairie, R. B., Bagher, A. M., Kelly, M. E. M., and Denovan-Wright, E. M. (2015). Cannabidiol is a negative allosteric modulator of the cannabinoid CB1 receptor. *Br. J. Pharmacol.* 172, 4790–4805. doi:10.1111/bph.13250

Laprairie, R. B., Mohamed, K. A., Zagzoog, A., Kelly, M. E. M., Stevenson, L. A., Pertwee, R., et al. (2019). Indomethacin enhances type 1 cannabinoid receptor signaling. *Front. Mol. Neurosci.* 12, 257. doi:10.3389/fnmol.2019.00257

LaVigne, J. E., Hecksel, R., Keresztes, A., and Streicher, J. M. (2021). Cannabis sativa terpenes are cannabimimetic and selectively enhance cannabinoid activity. *Sci. Rep.* 11, 8232. doi:10.1038/s41598-021-87740-8

Lo Verme, J., Fu, J., Astarita, G., La Rana, G., Russo, R., Calignano, A., et al. (2005). The nuclear receptor peroxisome proliferator-activated receptor-alpha mediates the anti-inflammatory actions of palmitoylethanolamide. *Mol. Pharmacol.* 67, 15–19. doi:10.1124/mol.104.006353

Martinez-Pinilla, E., Varani, K., Reyes-Resina, I., Angelats, E., Vincenzi, F., Ferreiro-Vera, C., et al. (2017). Binding and signaling studies disclose a potential allosteric site for cananbidiol in cannabinoid CB2 receptors. *Front. Pharmacol.* 8, 744. doi:10.3389/fphar.2017.00744

Moore, C. F., Davis, C. M., Harvey, E. L., Taffe, M. A., and Weerts, E. M. (2021). Appetitive, antinociceptive, and hypothermic effects of vaped and injected Δ-9-tetrahydrocannabinol (THC) in rats: exposure and dose-effect comparisons by strain and sex. *Pharmacol. Biochem. Behav.* 202, 173116. doi:10.1016/j.pbb.2021.173116

Navarro, G., Gonzalez, A., Sanchez-Morales, A., Casajuana-Martin, N., Gomez-Ventura, M., Cordomi, A., et al. (2021). Design of negative and positive allosteric modulators of the cannabinoid CB2 receptor derived from the natural product cannabidiol. *J. Med. Chem.* 64, 9354–9364. doi:10.1021/acs.jmedchem.1c00561

Nguyen, J. D., Grant, Y., Kerr, T. M., Gutierrez, A., Cole, M., Taffe, M. A., et al. (2018). Tolerance to hypothermic and antinoceptive effects of Δ9-tetrahydrocannabinol (THC) vapor inhalation in rats. *Pharmacol. Biochem. Behav.* 172, 33–38. doi:10.1016/j.pbb.2018.07.007

O'Sullivan, S. E., and Kendall, D. A. (2010). Cannabinoid activation of peroxisome proliferator-activated receptors: potential for modulation of inflammatory disease. *Immunobiology* 215, 611–616. doi:10.1016/j.imbio.2009.09.007

Pertwee, R. G. (2008). Ligands that target cannabinoid receptors in the brain: from THC to anandamide and beyond. *Addict. Biol.* 13, 147–159. doi:10.1111/j.1369-1600.2008.00108.x

Roebuck, A. J., Greba, Q., Onofrychuk, T. J., McElroy, D. L., Sandini, T. M., Zagzoog, A., et al. (2022). Dissociable changes in spike and wave discharges following exposure to injected cannabinoids and smoke cannabis in Genetic Absence Epilepsy Rats from Strasbourg. *Eur. J. Neurosci.* 55, 1063–1078. doi:10.1111/ejn.15096

Ross, R. A., Gibson, T. M., Stevenson, L. A., Saha, B., Crocker, P., Razdan, R. K., et al. (1999). Structural determinants of the partial agonist-inverse agonist properties of 6'-azidohex-2'-yne-delta8-tetrahydrocannabinol at cannabinoid receptors. *Br. J. Pharmacol.* 128, 735–743. doi:10.1038/sj.bjp.0702836

Russo, E. B. (2011). Taming THC: potential cannabis synergy and phytocannabinoid-terpenoid entourage effects. *Br. J. Pharmacol.* 163, 1344–1364. doi:10.1111/j.1476-5381.2011.01238.x

Santiago, M., Sachdev, S., Arnold, J. C., McGregor, I. S., and Connor, M. (2019). Absence of entourage: terpenoids commonly found in cannabis sativa do not modulate the functional activity of d9-THC at human CB1 and CB2 receptors. *Cannabis Cannabinoid Res.* 4, 165–176. doi:10.1089/can.2019.0016

Schmid, C. L., Kennedy, N. M., Ross, N. C., Lovell, K. M., Yue, Z., Morgenweck, J., et al. (2017). Bias factor and therapeutic window correlate to predict safer opioid analgesics. *Cell* 171, 1165–1175. doi:10.1016/j.cell.2017.10.035

Showalter, V. M., Compton, D. R., Martin, B. R., and Abood, M. E. (1996). Evaluation of binding in a transfected cell line expressing a peripheral cannabinoid receptor (CB2): identification of cannabinoid receptor subtype selective ligands. *J. Pharmacol. Exp. Ther.* 278, 989–999.

Tham, M., Yilmaz, O., Alaverdashvili, M., Kelly, M. E. M., Denovan-Wright, E. M., Laprairie, R. B., et al. (2018). Allosteric and orthosteric pharmacology of cannabidiol and cannabidiol-dimethylheptyl at the type 1 and type 2 cannabinoid receptors. *Br. J. Pharmacol.* 176, 1455–1469. doi:10.1111/bph.14440

Wacker, D., Wang, S., McCorvy, J. D., Betz, R. M., Venkatakrishnan, A. J., Levit, A., et al. (2017). Crystal structure of an LSD-bound human serotonin receptor. *Cell* 168, 377–389. doi:10.1016/j.cell.2016.12.033

Wakley, A. A., Wiley, J. L., and Craft, R. M. (2014). Sex differences in antinociceptive tolerance to delta-9-tetrahydrocannabinol in the rat. *Drug Alcohol Depend.* 143, 22–28. doi:10.1016/j.drugalcdep.2014.07.029

Zagzoog, A., Mohamed, K. A., Kim, H. J. J., Kim, E. D., Frank, C. S., Black, T., et al. (2020). *In vitro* and *in vivo* pharmacological activity of minor cannabinoids isolated from Cannabis sativa. *Sci. Rep.* 10, 20405. doi:10.1038/s41598-020-77175-y

frontiers | Frontiers in Pharmacology

TYPE Original Research
PUBLISHED 06 September 2022
DOI 10.3389/fphar.2022.972828

OPEN ACCESS

EDITED BY
Concepcion Garcia,
Complutense University of Madrid, Spain

REVIEWED BY
Eliseo A. Eugenin,
University of Texas Medical Branch at Galveston, United States
Di Wen,
Hebei Medical University, China
Noelia Granado,
Cajal Institute (CSIC), Spain

*CORRESPONDENCE
Shijun Hong,
hongshijun@kmmu.edu.cn
Lihua Li,
lilihua1229@126.com

†These authors have contributed equally to this work and share first authorship

SPECIALTY SECTION
This article was submitted to Neuropharmacology, a section of the journal Frontiers in Pharmacology

RECEIVED 19 June 2022
ACCEPTED 15 August 2022
PUBLISHED 06 September 2022

CITATION
Shen B, Zhang R, Yang G, Peng Y, Nie Q, Yu H, Dong W, Chen B, Song C, Tian Y, Qin L, Shu J, Hong S and Li L (2022), Cannabidiol prevents methamphetamine-induced neurotoxicity by modulating dopamine receptor D1-mediated calcium-dependent phosphorylation of methyl-CpG-binding protein 2. *Front. Pharmacol.* 13:972828. doi: 10.3389/fphar.2022.972828

Cannabidiol prevents methamphetamine-induced neurotoxicity by modulating dopamine receptor D1-mediated calcium-dependent phosphorylation of methyl-CpG-binding protein 2

Baoyu Shen†, Ruilin Zhang†, Genmeng Yang†, Yanxia Peng, Qianyun Nie, Hao Yu, Wenjuan Dong, Bingzheng Chen, Chunhui Song, Yan Tian, Lixiang Qin, Junjie Shu, Shijun Hong* and Lihua Li*

Key Laboratory of Drug Addiction Medicine of National Health Commission (NHC), School of Forensic Medicine, Kunming Medical University, Kunming, China

In the past decade, methamphetamine (METH) abuse has sharply increased in the United States, East Asia, and Southeast Asia. METH abuse not only leads to serious drug dependence, but also produces irreversible neurotoxicity. Currently, there are no approved pharmacotherapies for the treatment of METH use disorders. Cannabidiol (CBD), a major non-psychoactive (and non-addictive) cannabinoid from the cannabis plant, shows neuroprotective, antioxidative, and anti-inflammatory properties under METH exposure. At present, however, the mechanisms underlying these properties remain unclear, which continues to hinder research on its therapeutic potential. In the current study, computational simulations showed that CBD and METH may directly bind to the dopamine receptor D1 (DRD1) via two overlapping binding sites. Moreover, CBD may compete with METH for the PHE-313 binding site. We also found that METH robustly induced apoptosis with activation of the caspase-8/caspase-3 cascade *in-vitro* and *in-vivo*, while CBD pretreatment prevented these changes. Furthermore, METH increased the expression of DRD1, phosphorylation of Methyl-CpG-binding protein 2 (MeCP2) at serine 421 (Ser421), and level of intracellular Ca^{2+} *in-vitro* and *in-vivo*, but these effects were blocked by CBD pretreatment. The DRD1 antagonist SCH23390 significantly prevented METH-induced apoptosis, MeCP2 phosphorylation, and Ca^{2+} overload *in-vitro*. In contrast, the DRD1 agonist SKF81297 markedly increased apoptosis, MeCP2 phosphorylation, and Ca^{2+} overload, which were blocked by CBD pretreatment *in-vitro*. These results indicate that CBD prevents METH-induced neurotoxicity by modulating DRD1-mediated phosphorylation of MeCP2 and Ca^{2+} signaling. This study suggests that CBD pretreatment may resist the effects of METH on DRD1 by competitive binding.

KEYWORDS

methamphetamine, cannabidiol, dopamine receptor D1, methyl-CpG-binding protein 2, calcium

Introduction

Methamphetamine (METH) use has markedly increased in North America, East Asia, and Southeast Asia in recent years (UNODC, 2021). Of concern, the continuous use of METH can trigger serious neurotoxicity (Kim et al., 2020; Jayanthi et al., 2021), ultimately leading to neurological impairment, tissue damage, and neuropsychological disturbance (Cadet and Krasnova, 2009; Lappin et al., 2018; Shukla and Vincent, 2020). Evidence suggests that METH-induced neurotoxicity involves many mechanisms (Jayanthi et al., 2021), including dopamine (DA) release, oxidative stress, mitochondrial stress, endoplasmic reticulum (ER) stress, microglial and astrocyte activation, ubiquitin/proteasome system (UPS) dysfunction, immediate early gene (IEG) modification, and autophagy. However, the specific mechanisms underlying METH-induced neurotoxicity remain poorly understood.

As a methyl DNA-binding transcriptional regulator, methyl-CpG-binding protein 2 (MeCP2) participates in transcription repression (Jones et al., 1998; Nan et al., 1998) and activation (Chahrour et al., 2008), RNA splicing regulation (Young et al., 2005), and transcriptional noise suppression (Skene et al., 2010). MeCP2 is also a critical regulator of neurodevelopment and adult brain function (Gulmez Karaca et al., 2019), and dysfunction in MeCP2 can cause Rett syndrome and other neuropsychiatric disorders (Amir et al., 1999; Chin and Goh, 2019). Furthermore, MeCP2-mediated neurotoxicity may also contribute to neuropsychiatric disorders (Russell et al., 2007; Dastidar et al., 2012; Montgomery et al., 2018) and participate in METH-induced behavioral disorders in rodents (Lewis et al., 2016; Wu et al., 2016; Fan et al., 2020). However, the role of MeCP2-mediated neurotoxicity in METH use disorders remains poorly understood. Phosphorylation has been suggested as a potential mechanism by which MeCP2 modulates gene expression (Chao and Zoghbi, 2009; Damen and Heumann, 2013). The phosphorylation of MeCP2 (pMeCP2) at serine 80 (Ser80) increases MeCP2 binding to target gene promoters and restricts transcription, while phosphorylation of MeCP2 at serine 421 (Ser421) increases MeCP2 dissociation from promoters and transcription activation (Chen et al., 2003; Chao and Zoghbi, 2009). Phosphorylation of MeCP2 at Ser421 is mediated by a calcium-dependent mechanism (Chen et al., 2003; Buchthal et al., 2012). Phosphorylation of MeCP2 at Ser421 contributes to neural and behavioral responses to psychostimulants in mice, whereas phosphorylation of MeCP2 in the nucleus accumbens (NAc) is mediated by D1-like DA receptors, including DA receptors D1 (DRD1) and D5 (DRD5) (Deng et al., 2010). There is growing evidence that both calcium signaling and DRD1 are involved in METH-induced neurotoxicity (Ares-Santos et al., 2012; Ares-Santos et al., 2013; Friend and Keefe, 2013; Andres et al., 2015; Sun et al., 2015; Nguyen et al., 2018), and activation of DRD1 can significantly induce neuronal damage (Park et al., 2019). Therefore, DRD1-mediated phosphorylation of MeCP2 may be a critical mechanism in METH-induced neurotoxicity.

Cannabidiol (CBD) is a primary non-psychoactive cannabinoid in the cannabis plant and exhibits considerable therapeutic potential in the treatment of neuropsychiatric disorders, including epilepsy, Parkinson's disease (PD), Alzheimer's disease (AD), depression, anxiety, psychosis, and drug dependence (Elsaid et al., 2019; Premoli et al., 2019; Vitale et al., 2021). Recent research has indicated that CBD exerts neuroprotective effects on METH-induced neurotoxicity in rats (Razavi et al., 2021). Furthermore, some evidence has suggested that CBD modulates several receptors in METH exposure, such as D1-like DA receptors (Nouri et al., 2021; Shen et al., 2022), D2-like DA receptors (Hassanlou et al., 2021), Sigma-1 receptors (Yang et al., 2020), and Toll-like type-4 receptors (TLR4) (Majdi et al., 2019). We previously showed that CBD may modulate DRD1 to attenuate METH-induced DA release (Shen et al., 2022). However, the underlying mechanism related to the neuroprotective effects of CBD on METH-induced neurotoxicity remains elusive. In the current study, we hypothesized that METH induces neurotoxicity *via* DRD1-mediated phosphorylation of MeCP2 at Ser421 with calcium influx, and CBD treatment prevents METH-induced neurotoxicity *via* modulation of DRD1.

Materials and methods

Molecular docking

Molecular docking was performed using AutoDock v4.2.6 in accordance with previous research (Bian et al., 2019; Zhang et al., 2021). Structural information on rat DRD1 was obtained from the AlphaFold Protein Structure Database (https://alphafold.ebi.ac.uk/), and structural information on METH and CBD was obtained from PubChem (https://pubchem.ncbi.nlm.nih.gov/). First, preparation of DRD1 was performed using AutoDockTools v1.5.6, including the addition of hydrogens and calculation of atomic charges with the Kollman all-atom approach (Bian et al., 2019). The atomic charges of CBD and METH were calculated using the Gasteiger-Hückel approach with AutoDockTools v1.5.6 (Bian et al., 2019). A three-dimensional (3D) search grid with 40 × 44 × 40 points was created using the AutoGrid algorithm, and the maximum number of poses per ligand was set to 200.

Next, all postures for CBD and METH were docked using AutoDock v4.2.6. The docking parameters were set to default, as per previous research (Zhang et al., 2021). The docking scores of all postures were extracted using AutoDockTools v1.5.6. The affinity score was greater than −5 kcal/mol, indicating a reliable docking process. The best docking posture was then selected. Finally, binding site analysis was performed using Discovery Studio Visualizer v4.5 and visualized using PyMol v2.5.2.

Drugs

For the *in-vitro* experiments, methamphetamine hydrochloride (National Institutes for Food and Drug Control, #171212–200603, Beijing, China) was dissolved in phosphate-buffered saline (PBS; pH 7.2; Biological Industries, #02-024-1ACS, Beit HaEmek, Israel). SCH23390 hydrochloride (Bio-Techne, #0925, Minneapolis, MN, United States) or SKF81297 hydrobromide (Bio-Techne, #1447, Minneapolis, MN, United States) was dissolved in PBS with gentle warming. In addition, CBD (Pulis Biological Technology Co. Ltd., #PD0155, Chengdu, China) was dissolved in dimethyl sulfoxide (DMSO) (MP Biomedicals, #196055, CA, United States). The final concentration of DMSO in the culture medium was not more than 0.1%. For the *in-vivo* experiments, methamphetamine hydrochloride was dissolved in saline and CBD was mixed with 5% DMSO and 5% Tween-80 (Solarbio Life Sciences, #T8360, Beijing, China) in saline with gentle warming. Preparation of CBD was based on research from other laboratories (Hampson et al., 1998; Ryan et al., 2009; Hay et al., 2018; Luján et al., 2018) and our previous studies (Yang et al., 2020; Shen et al., 2022).

Primary culture of neurons

Neurons for primary culture were isolated from the brain of early postnatal Sprague-Dawley rats following previous research, with slight modification (Chen et al., 2016; Li et al., 2019; Ding et al., 2020). Briefly, mesaticephalic and cortical tissues were gathered from brains of early postnatal rats and digested with trypsin solution (Gibco, #25200–072, Grand Island, NE, United States of America). Tissue mixtures were filtered with a 70-μm cell strainer (Biosharp Life Sciences, #BS-70-XBS, Hefei, China) and centrifuged at 3,000 × *rpm* for 5 min at 4°C. The sediments were resuspended in high glucose culture medium (Biological Industries, #06-1055-57-1ACS, Beit HaEmek, Israel) with 10% fetal bovine serum (Biological Industries, #04-001-1ACS, Beit HaEmek, Israel) and 2% penicillin/streptomycin (Gibco, #15140-122, Grand Island, NE, United States). After 24-h *in-vitro* culture, the medium was replaced with neurobasal medium (STEMCELL Technologies, #05790, Canada) containing 10% fetal bovine serum, 2% B-27 (Gibco, #17504-044, Grand Island, NE, United States), 1% glutamine (Gibco, #35050-061, Grand Island, NE, United States), and 2% penicillin/streptomycin, which was replaced every 3 days. We identified the purity of primary neurons before all experiments in our previous work (Shen et al., 2022). Therefore, the results of neuronal purity are reported in our earlier manuscript (Shen et al., 2022). For the cell viability test, neurons were treated with 50, 100, 200, 400, 800, or 1,000 μM METH for 24 h, and subsequently treated with 400 μM METH for 3, 6, 12, 24, or 48 h. In addition, 0.1, 1, or 10 μM CBD was used as a pretreatment for 1 h before the addition of METH. For the DRD1 experiment, 10 μM SCH23390 (DRD1 antagonist) was used as a pretreatment for 1 h before the addition of METH, and 10 μM SKF81297 (DRD1 agonist) was used for 1 h after the addition of CBD. The concentrations were based on research from other laboratories, with slight modification (Sun et al., 2015; Chakraborty et al., 2016; Chen et al., 2016; Uno et al., 2017; Branca et al., 2019).

Cell counting kit-8 assay

Neurons were seeded at a density of 5×10^3 cells/well in a 96-well plate. After the neurons were incubated with drugs following the above procedures, cell viability was detected using Cell counting kit-8 (CCK-8) reagent (Dalian Meilun Biotechnology Co. Ltd., #MA0218, Dalian, China). Absorbance was obtained on a microplate reader at 450 nm. Cell viability was calculated according to the formula provided by the kit.

Western blotting

Neurons and brain tissue from rats were suspended in RIPA lysis buffer (Beyotime, #P0013B, Shanghai, China) containing protease inhibitors (Beyotime, #ST506-2, 1:100, Shanghai, China) and phosphatase inhibitor cocktail A (Beyotime, #P1082, 1:50, Shanghai, China). After the neurons and tissue samples were homogenized using a sonicator, the homogenate was lysed for 30 min on ice. The lysates were then centrifuged at 12,000 × *g* for 15 min at 4°C, and the supernatant was subjected to BCA protein assay (Beyotime, #P0012, Shanghai, China) to determine protein concentration. Total protein (25 μg) was separated by 12% sodium dodecyl sulfate-polyacrylamide gel electrophoresis (SDS-PAGE) (Beyotime, #P0012AC, Shanghai, China) and transferred onto polyvinylidene fluoride (PVDF) membranes (Sigma-Aldrich, IPVH00010, St. Louis, MO, United States). The membranes were blocked with 5% dry skimmed milk in Tris-buffered saline and incubated overnight at 4°C in blocking solution containing primary antibodies against DRD1 (Bio-Techne, #NB110-60017, 1:800, Minneapolis, MN, United States), pMeCP2 (phospho Ser421) (Abcam, #ab254050, 1:1,000, Cambridge, United Kingdom), caspase-8 (Abcam,

#ab25901, 1:1,000, Cambridge, United Kingdom), cleaved caspase-8 (Proteintech, #66093-1-Ig, 1:2,000, IL, United States), caspase-3 (Cell Signaling Technology, #9662, 1:1,000, MA, United States), cleaved caspase-3 (Cell Signaling Technology, #9664, 1:1,000, MA, United States), and β-actin (Proteintech, #66009–1, 1:5,000, IL, United States). After rinsing three times with Tris-buffered saline containing Tween-20 (TBST) (Solarbio Life Sciences, #T8220, Beijing, China), the membranes were incubated with rabbit horseradish peroxidase (HRP) (Cell Signaling Technology, #7074S, 1:5,000, MA, United States) or mouse HRP secondary antibodies (Cell Signaling Technology, #7076S, 1:5,000, MA, United States), followed by rinsing three times with TBST. Immunoreactive proteins were detected using a chemiluminescence reaction (Biosharp Life Sciences, #BL520A, Hefei, China). Images were obtained using an immunoblotting detection system (Bio-Rad Laboratories, Hercules, CA, United States) and analyzed with ImageJ software.

Immunofluorescence staining

After incubation with drugs, the neurons were fixed in 4% paraformaldehyde (Biosharp Life Sciences, #BL539A, Hefei, China) for 30 min and rinsed three times with PBS. For immunolabeling, the neurons were first penetrated with 0.2% Triton X-100 (Solarbio Life Sciences, #T8200, Beijing, China) for 30 min, then blocked with 10% goat serum (Solarbio Life Sciences, #SL038, Beijing, China) for 2 h at room temperature. The neurons were then incubated with PBS containing antibodies against DRD1 (Bio-Techne, #NB110-60017, 1:200, Minneapolis, MN, United States), pMeCP2 (phospho Ser421) (Abcam, #ab254050, 1:200, Cambridge, United Kingdom), cleaved caspase-8 (Proteintech, #66093-1-Ig, 1:200, IL, United States), or cleaved caspase-3 (Cell Signaling Technology, #9664, 1:200, MA, United States) overnight at 4°C. Correspondingly, species-specific fluorescent-conjugated secondary antibodies were applied to detect immunoreactive proteins. The nucleus was labeled with DAPI (Cell Signaling Technology, #8961S, MA, United States). Images were obtained using a fluorescent microscope (Olympus Corporation, #BX53, Tokyo, Japan) and analyzed with ImageJ.

Intracellular Ca^{2+} detection

Intracellular Ca^{2+} was detected as per previous study (Sun et al., 2015). For the *in-vitro* experiments, drug-treated neurons were rinsed three times with Hanks' balanced salt solution (HBSS, Sigma-Aldrich, #H6648, St. Louis, MO, United States) and incubated with HBSS containing 10 μM Fluo-3-AM solution (Sigma-Aldrich, #39294, St. Louis, MO, United States) for 60 min at 37°C. For the *in-vivo* experiments for Ca^{2+} detection, tissue sections were first penetrated with HBSS containing 0.2% Triton X-100 and 0.1% sodium citrate (Solarbio Life Sciences, #C1032, Beijing, China) for 30 min, then incubated with HBSS containing 10 μM Fluo-3-AM solution for 60 min at 37°C. After incubation with Fluo-3-AM solution, the neurons and tissue sections were rinsed three times with HBSS. Observations were performed with a fluorescent microscope at a detection wavelength of 488 nm. Obtained images were analyzed with ImageJ.

Terminal deoxynucleotidyl transferase dUTP nick-end labeling staining

Apoptosis was detected using a Terminal Deoxynucleotidyl Transferase dUTP Nick-end Labeling (TUNEL) assay kit (Sigma-Aldrich, #11684817 910 or #12156792910, St. Louis, MO, United States) according to the manufacturer's protocols. For the *in-vitro* experiments, neurons were fixed in 4% paraformaldehyde for 30 min and rinsed with PBS. For the *in-vivo* experiments, tissue sections were rinsed three times with PBS. After incubation with 3% H_2O_2 for 10 min at room temperature, the neurons and tissue sections were rinsed with PBS, then penetrated with PBS containing 0.2% Triton X-100 and 0.1% sodium citrate for 2 min on ice. For TUNEL staining, the samples were incubated with TUNEL reaction mixture for 60 min at 37°C. After the samples were rinsed three times with PBS, DAPI was used to localize nuclei. A fluorescent microscope was used to obtain images with the detection wavelength at 488 nm or 580 nm. DAPI- and TUNEL-positive cells were counted using ImageJ (n = 5). TUNEL-positive cell ratio = TUNEL-positive cells/DAPI-positive cells.

Animals

Adult male Sprague-Dawley rats (8–9 weeks old, n = 40) were purchased from the Laboratory Animal Center, Kunming Medical University. The rats were housed in a humidity- (50% ± 10%) and temperature-controlled (22°C ± 1°C) room on a 12-h reverse light/dark cycle. Food and water were available *ad libitum*. All animal procedures were conducted according to the National Institutes of Health (NIH) Guide for the Care and Use of Laboratory Animals and were approved by the Animal Care and Use Committee of Kunming Medical University (permit number: kmmu2020403). The rats were randomly distributed into four groups: i.e., Saline (n = 10), CBD 40 mg/kg (n = 10), METH 15 mg/kg (n = 10), and CBD 40 mg/kg + METH 15 mg/kg (n = 10) groups.

Animal treatments

After 1 week of habituation, the rats received intraperitoneal injections of METH (eight injections,

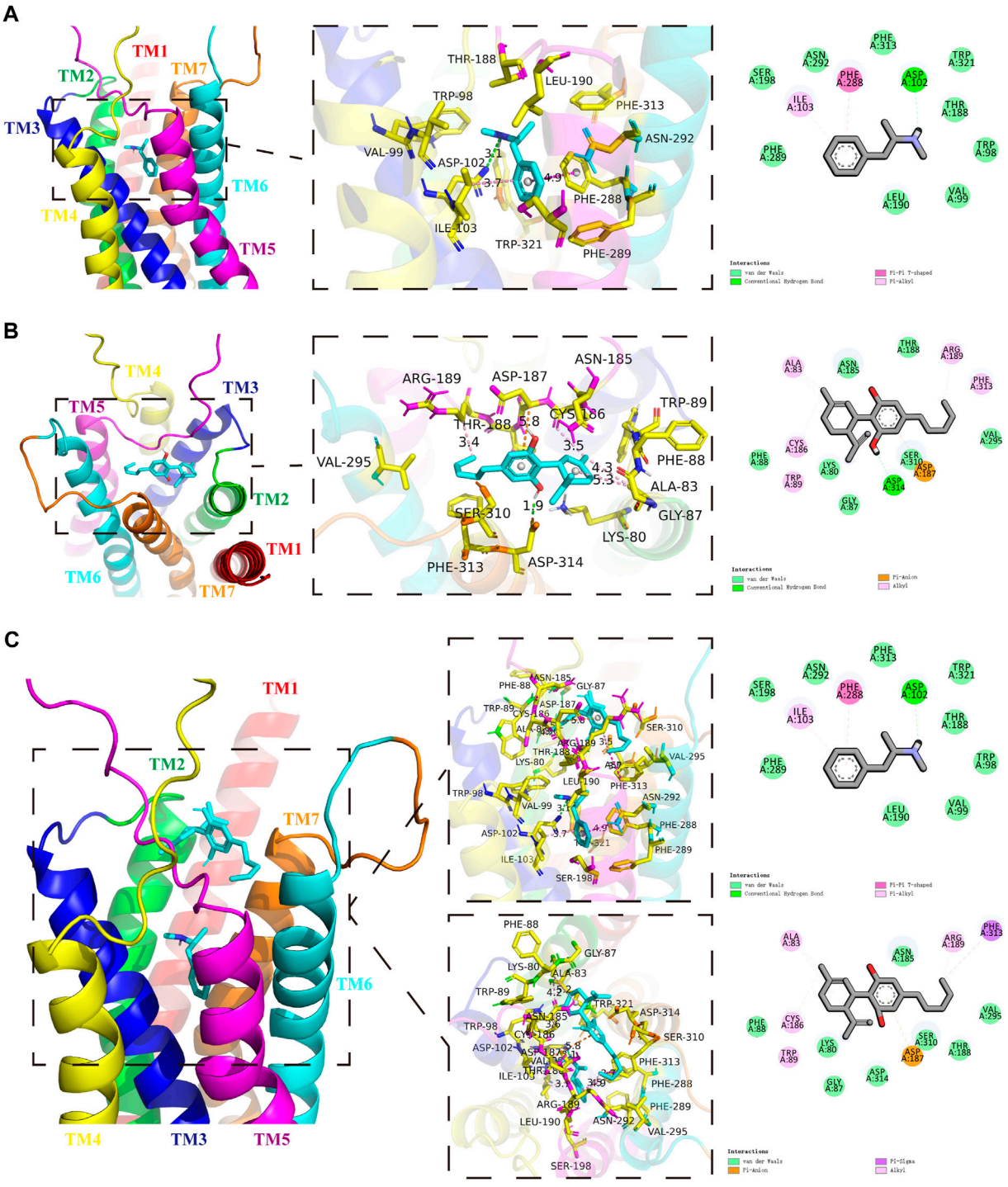

FIGURE 1
Protein-drug binding simulations. Seven transmembrane domains of DRD1 are shown as multicolor bands. METH or CBD are marked in cyan, while key DRD1 residues are marked in yellow. **(A)** Docking pose, binding sites, and interactions between DRD1 model and METH. **(B)** Docking pose, binding sites, and interactions between DRD1 model and CBD. **(C)** Docking pose, binding sites, and interactions among CBD, METH, and DRD1 model.

15 mg/kg/injection, 12-h intervals). Injections were performed at 08:00 and 20:00 for 4 days. This exposure paradigm was selected based on previous studies (Qiao et al., 2014; Huang et al., 2015; Xie et al., 2018; Xu et al., 2018; Huang et al., 2019; Chen et al., 2020). CBD was injected intraperitoneally at a dose of 40 mg/kg 1 h before METH

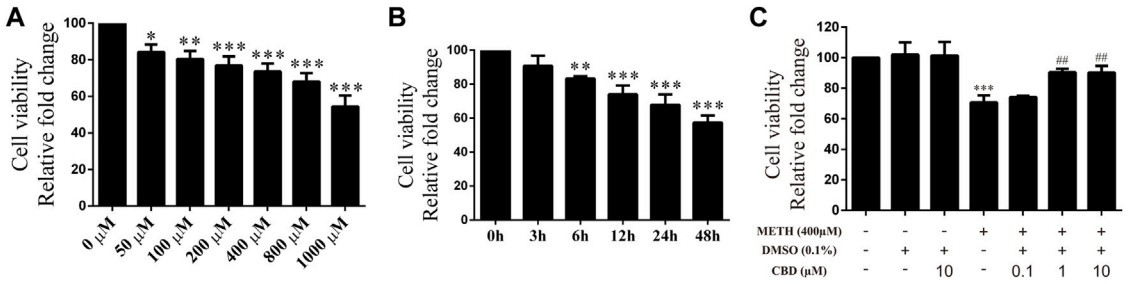

FIGURE 2
Cell viability of neurons incubated with different drugs. **(A)** Cell viability of neurons incubated with METH for 24 h at different concentrations (50, 100, 200, 400, 800, and 1,000 μM). **(B)** Cell viability of neurons incubated with 400 μM METH at different time points (3, 6, 12, 24, and 48 h). **(C)** Cell viability of neurons incubated with CBD (0.1, 1, and 10 μM) and/or METH (400 μM). $*p < 0.05$, $**p < 0.01$, or $***p < 0.001$ compared with control group, $^{\#\#}p < 0.01$ compared with METH group; Tukey HSD *post-hoc* comparison after significant ANOVA.

administration, following our previous studies (Yang et al., 2020; Shen et al., 2022). During treatment, body weights were recorded every day. In addition, METH-stereotyped behavior was observed as described previously (Sams-Dodd, 1998; Roberts et al., 2010; Qiao et al., 2014). Briefly, an observer blind to the experiment visually assessed several classified behaviors, including: (0) No repetitive head movements; 1) Weak repetitive side-to-side head movements; 2) Strong repetitive side-to-side head movements; and 3) Stationary stereotyped behavior with strong side-to-side or circular head movements. Rats were anesthetized 24 h after the last injection, and perfused transcardially with saline. After perfusion with saline, the brains of rats were removed, and the prefrontal cortex (PFC) and hippocampus (Hip) were dissected bilaterally on ice and stored at −80°C for detection of proteins. For tissue sections, the rats were perfused transcardially with 4% paraformaldehyde and brains were preserved in 4% paraformaldehyde at 4°C. After 2 weeks of fixation, the brains were sunk in increasing concentrations of sucrose (10%, 20%, and 30%). Brains were sectioned (15 μm) along the coronal plane incorporating the PFC and Hip on a freezing microtome (Leica Biosystems, #CM 1860, Nussloch, Germany) kept at −20°C.

Statistical analyses

All data were analyzed using SPSS v26.0 and presented as mean ± standard deviation (SD). One-way analysis of variance (ANOVA) was used to analyze data from parts A and B of the CCK-8 assay, with factors defined as METH treatments (corresponding to "METH dose" and "treatment time" levels). Three-way repeated-measures ANOVA was used to analyze data from the behavioral experiment, with factors defined as CBD treatment, METH treatment, and Time. Two-way ANOVA (no repeated measures) was used to analyze data from other *in-vitro* and *in-vivo* experiments. For the first part of the *in-vitro* experiments and other *in-vivo* experiments, factors were defined as CBD and METH treatments. For the second part of the *in-vitro* experiments, factors were defined as SCH23390 and METH treatments. For the third part of the *in-vitro* experiments, factors were defined as CBD and SKF81297 treatments. ANOVA was followed by Tukey HSD *post-hoc* tests. Before ANOVA, normality and homogeneity of equal variance were confirmed. The level of significance was set to 0.05.

Results

Methamphetamine and cannabidiol bind with DA receptors D1

We first screened the METH-binding pocket in the DRD1 model from 7 reliable binding pockets. We chose the METH-binding pocket with the highest affinity (−5.8 kcal/mol). Specially, 12 amino acid residues of DRD1 formed the boundary of the pocket, including PHE-289, SER-198, ILE-103, ASN-292, PHE-288, PHE-313, ASP-102, TRP-321, THR-188, TRP-98, VAL-99, and LEU-190 (Figure 1A). Among these amino acids, one hydrogen bond was observed between residue ASP-102 from transmembrane (TM) 3 and METH at 3.1 Å. In addition, residue PHE-288 from TM6 and METH formed a Pi-Pi T-shaped non-covalent interaction at 4.9 Å, while residue ILE-103 from TM3 and METH formed a Pi-Alkyl non-covalent interaction at 3.7 Å (Figure 1A). We also performed docking simulation with the DRD1 model and CBD. In total, 15 reliable CBD-binding pockets were found, with the highest affinity of −7.3 kcal/mol. The best CBD-binding pocket in the DRD1 model consisted of 14 amino acid residues, including ALA-83, ASN-185, ARG-189, PHE-313, VAL-295,

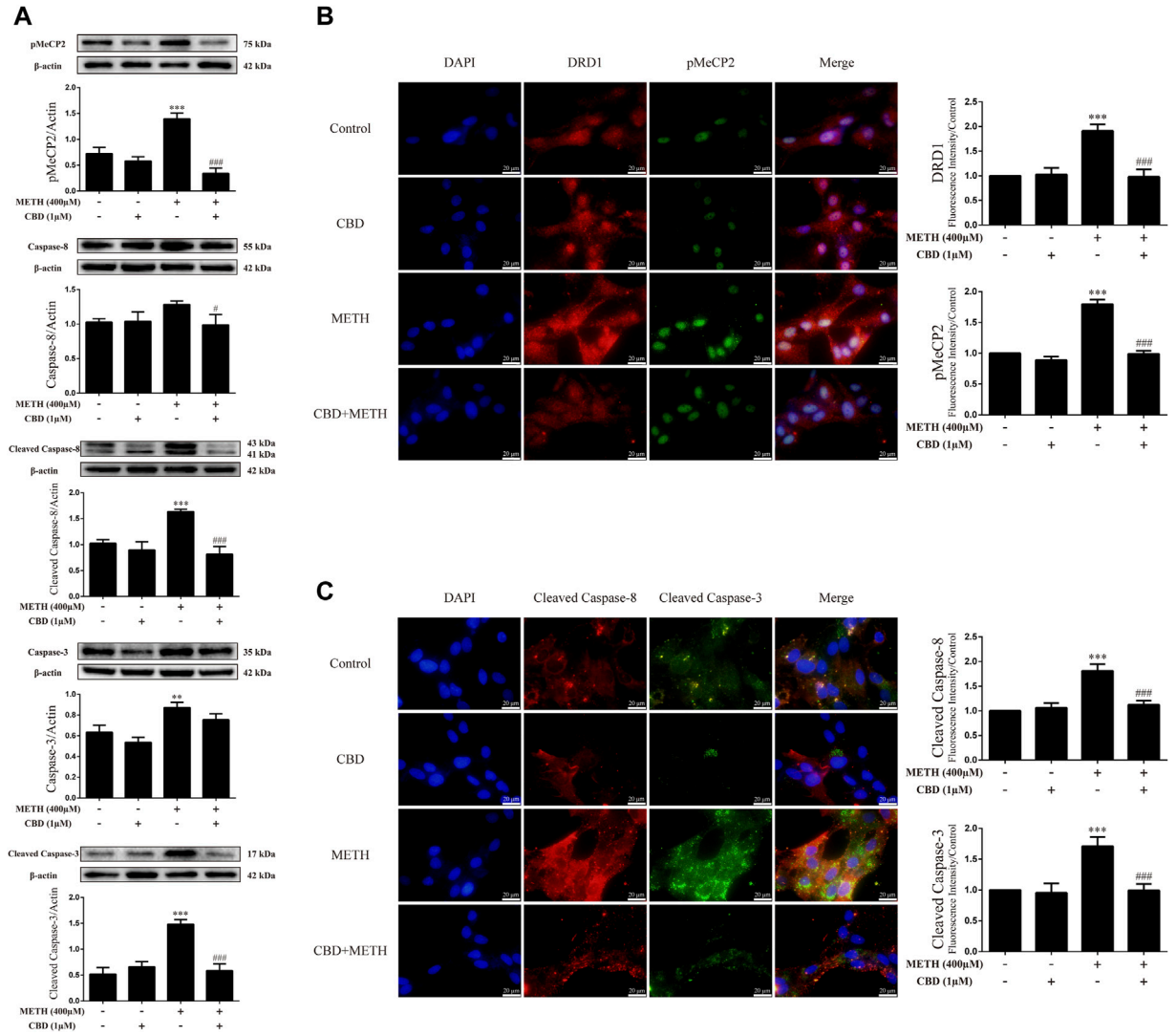

FIGURE 3
Protein levels and colocalization in neurons incubated with CBD and/or METH. **(A)** Levels of pMeCP2 and apoptosis-related proteins. **(B)** DRD1 and pMeCP2 levels and their colocalization. **(C)** Cleaved caspase-8 and cleaved caspase-3 levels and their colocalization. $^{**}p < 0.01$ or $^{***}p < 0.001$ compared with control group, $^{\#}p < 0.05$ or $^{\#\#\#}p < 0.001$ compared with METH group; Tukey HSD *post-hoc* comparison after significant ANOVA.

THR-188, SER-310, ASP-187, ASP-314, GLY-87, LYS-80, TRP-89, CYS-186, and PHE-88 (Figure 1B). A hydrogen bond was observed between residue ASP-314 from TM7 and CBD at 1.9 Å, while residue ASP-187 from TM5 and CBD formed a Pi-Anion non-covalent interaction at 5.8 Å. In addition, several Alkyl-Alkyl interactions were found between CBD and TRP-89, CYS-186, ALA-83, ARG-189, and PHE-313. To determine whether CBD competes with METH for binding sites, we docked METH and CBD with DRD1 based on the above pockets simultaneously. Results showed that CBD was bound to DRD1 near the METH-binding pocket (Figure 1C). Interestingly, for CBD and DRD1 interactions, the hydrogen bond between residue ASP-314 and CBD (Figure 1B) was converted to van der Waals force (Figure 1C), while the Alkyl-Alkyl interaction between residue PHE-313 (Figure 1B) was transformed into a Pi-Sigma covalent bond (Figure 1C). However, no differences were observed in the interactions between METH and DRD1 compared with METH docking alone (Figure 1C). Overlaps between CBD-binding sites and METH-binding sites were found, e.g., PHE-313 and THR-188 (Figure 1C). The bond strength between CBD and DRD1 was stronger than that of METH in PHE-313, but not that of METH in THR-188 (Figure 1C). This is likely because the covalent Pi-Sigma bond is stronger than van der Waals force for drug loading (Li and Yang, 2015).

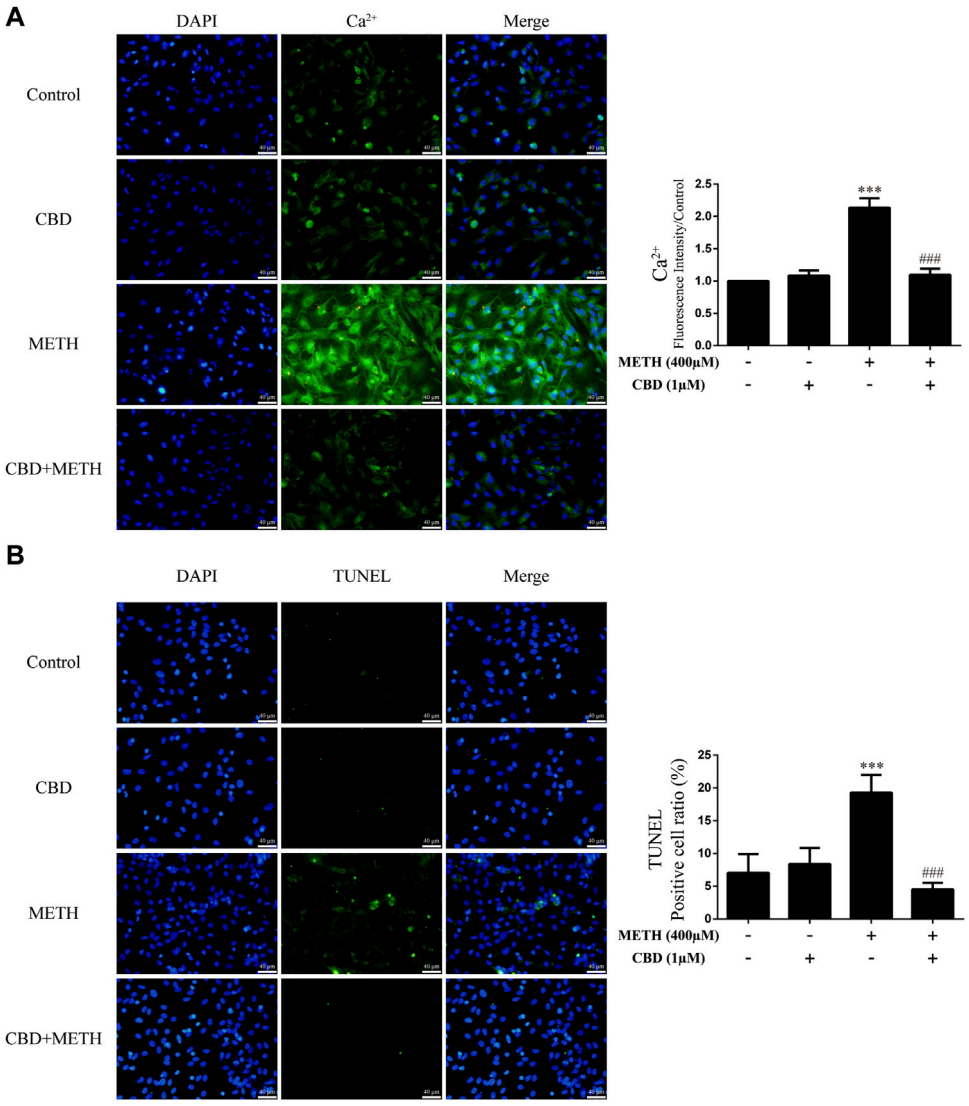

FIGURE 4
Intracellular Ca^{2+} and apoptosis levels in neurons incubated with CBD and/or METH. **(A)** Apoptosis level in neurons. **(B)** Intracellular Ca^{2+} level in neurons. $^{***}p < 0.001$ compared with control group, $^{\#\#\#}p < 0.001$ compared with METH group; Tukey HSD *post-hoc* comparison after significant ANOVA.

Cannabidiol prevented methamphetamine-induced decrease in cell viability

Cultured neurons were treated with various concentrations of METH (50, 100, 200, 400, 800, 1,000 μM) for 24 h, with cell viability then detected using the CCK-8 assay. Cell viability decreased gradually with the increase in METH concentration [Figure 2A; $F(6, 14) = 30.603$, $p < 0.05$, $p < 0.01$, $p < 0.001$]. Based on morphological changes in neurons and other previous studies (Sun et al., 2015; Chen et al., 2016), the 400 μM concentration of METH was chosen for subsequent experiments. The neurons were exposed to 400 μM METH for different times (3, 6, 12, 24, 48 h). As indicated in Figure 2B, cell viability showed a significant and time-dependent decrease [Figure 2B; $F(5, 12) = 36.953$, $p < 0.01$, $p < 0.001$]. These results suggest that METH induces neuronal death in a dose-dependent and time-dependent manner. As cellular damage was easy to detect, we also selected the 400 μM concentration of METH to incubate neurons for 24 h. Before METH exposure, the neurons were incubated with CBD (0.1, 1, and 10 μM) or vehicle (0.1% DMSO) for 1 h. Results showed that cell viability diminished significantly after 400 μM METH exposure [Figure 2C; $F(6, 14) =$

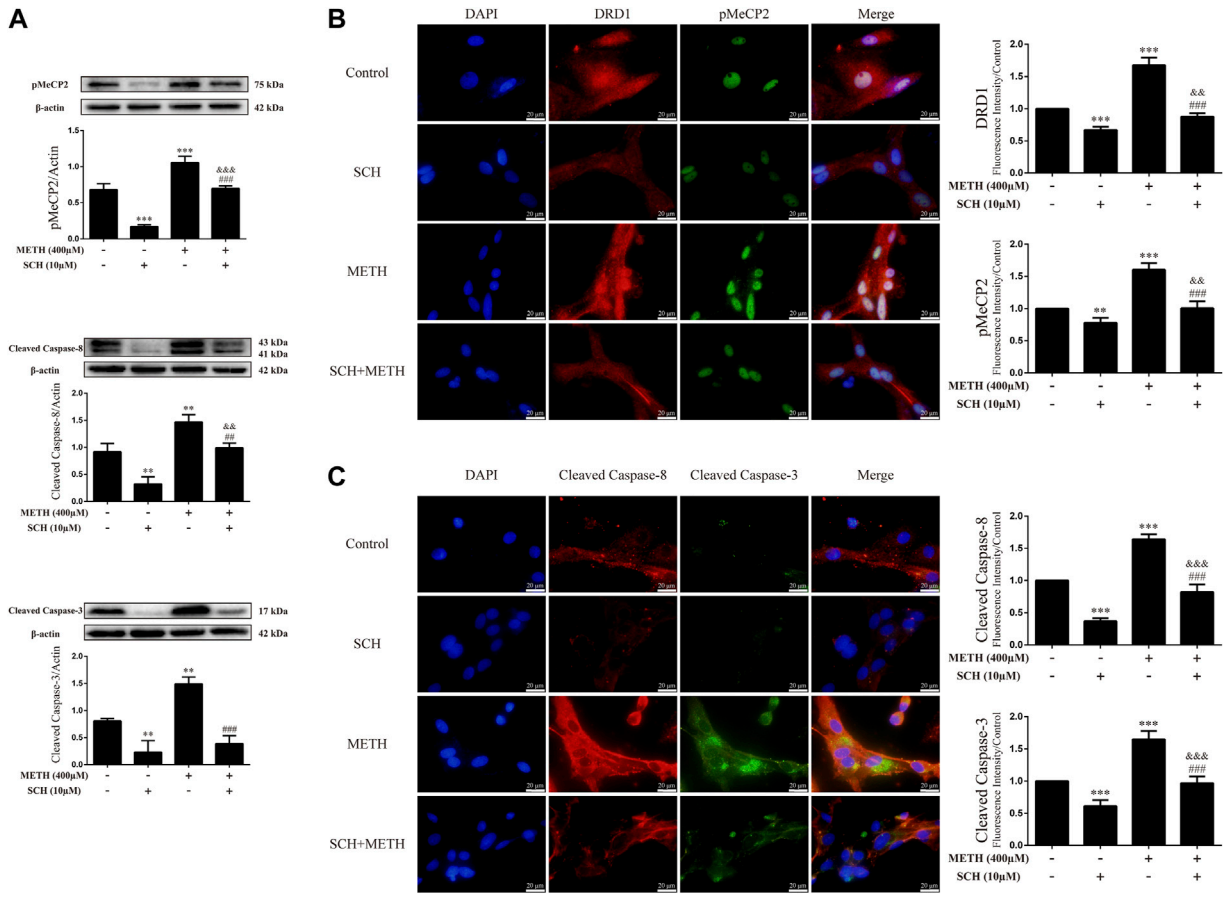

FIGURE 5
Protein levels and colocalization in neurons incubated with SCH23390 and/or METH. **(A)** Levels of pMeCP2 and apoptosis-related proteins. **(B)** DRD1 and pMeCP2 levels and their colocalization. **(C)** Cleaved caspase-8 and cleaved caspase-3 levels and their colocalization. $^{**}p < 0.01$ or $^{***}p < 0.001$ compared with control group, $^{\#\#}p < 0.01$ or $^{\#\#\#}p < 0.001$ compared with METH group, $^{\&\&}p < 0.01$ or $^{\&\&\&}p < 0.001$ compared with SCH23390 group; Tukey HSD *post-hoc* comparison after significant ANOVA.

18.449, $p < 0.001$], increased markedly with CBD pretreatment (≥1 μm) [Figure 2C; F (6, 14) = 18.449, $p < 0.01$], and showed no change under CBD or vehicle alone [Figure 2C; F (6, 14) = 18.449, $p = 1.000$, $p = 0.999$]. Therefore, CBD appears to show a neuroprotective effect on METH exposure. Based on our findings and previous research (Branca et al., 2019), the 1 μM concentration of CBD was chosen to perform subsequent experiments.

Cannabidiol blocked expression of DA receptors D1, phosphorylation of MeCP2, and apoptosis-related proteins induced by methamphetamine exposure *in-vitro*

We next explored the mechanisms underlying the neuroprotective effects of CBD. To corroborate the cell viability findings, we detected the expression levels of apoptosis-related proteins (caspase-8, cleaved caspase-8, caspase-3, and cleaved caspase-3) in primary neurons. We found that METH significantly induced the expression levels of cleaved caspase-8 [Figure 3A; F (3, 8) = 30.841, $p < 0.001$], caspase-3 [Figure 3A; F (3, 8) = 20.211, $p < 0.01$], and cleaved caspase-3 [Figure 3A; F (3, 8) = 48.091, $p < 0.001$] *in-vitro*, but had no significant effect on caspase-8. However, CBD pretreatment prevented the high levels of cleaved caspase-8 [Figure 3A; F (3, 8) = 30.841, $p < 0.001$] and cleaved caspase-3 [Figure 3A; F (3, 8) = 48.091, $p < 0.001$] induced by METH. These findings were further verified by immunofluorescence staining [Figure 3C; F (3, 16) = 85.584, $p < 0.001$; F (3, 16) = 47.347, $p < 0.001$]. METH administration also significantly induced phosphorylation of MeCP2 at Ser421 [Figure 3A; F (3, 8) = 55.573, $p < 0.001$], which was prevented by CBD pretreatment [Figure 3A; F (3, 8) = 55.573, $p < 0.001$]. In addition, DRD1 and pMeCP2 were also expressed in the primary neurons (Figure 3B). Significant increases in DRD1 [Figure 3B; F (3, 16) = 71.533, $p <$

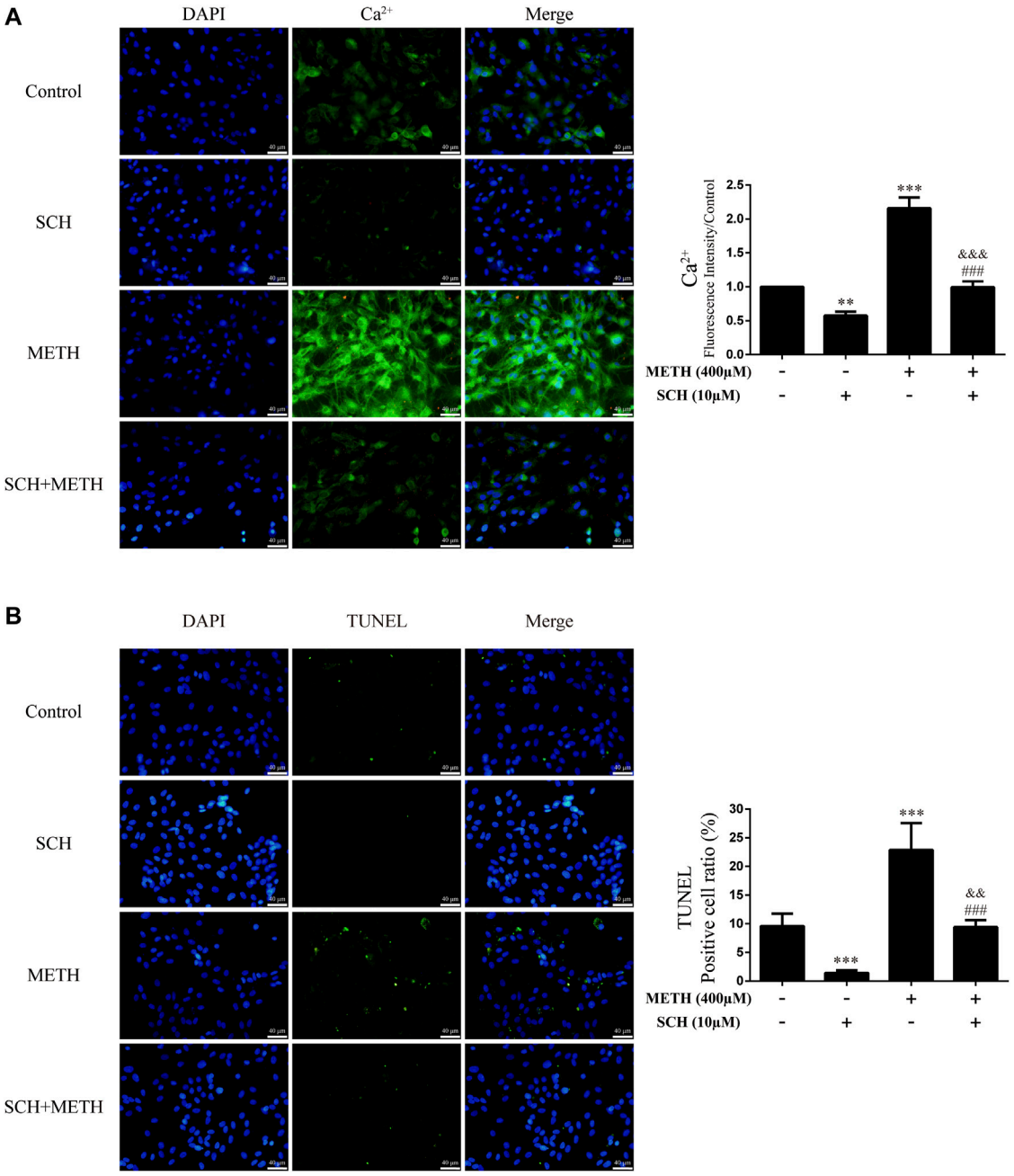

FIGURE 6
Intracellular Ca^{2+} and apoptosis levels in neurons incubated with SCH23390 and/or METH. **(A)** Apoptosis level in neurons. **(B)** Intracellular Ca^{2+} level in neurons. $^{**}p < 0.01$ or $^{***}p < 0.001$ compared with control group, $^{\#\#\#}p < 0.001$ compared with METH group, $^{\&\&}p < 0.01$ or $^{\&\&\&}p < 0.001$ compared with SCH23390 group; Tukey HSD *post-hoc* comparison after significant ANOVA.

0.001] and pMeCP2 [Figure 3B; F (3, 16) = 320.272, $p < 0.001$] were observed after METH administration, but were prevented by CBD pretreatment [DRD1; Figure 3B; F (3, 16) = 71.533, $p < 0.001$; pMeCP2; Figure 3B; F (3, 16) = 320.272, $p < 0.001$]. These results suggest that the neuroprotective effects of CBD may involve DRD1 levels and MeCP2 phosphorylation at Ser421 in neurons.

Cannabidiol prevented Ca^{2+} overload and apoptosis induced by methamphetamine in neurons

As the phosphorylation of MeCP2 at Ser421 is calcium-dependent (Chen et al., 2003; Buchthal et al., 2012), we further investigated the level of intracellular Ca^{2+} in neurons. Results showed

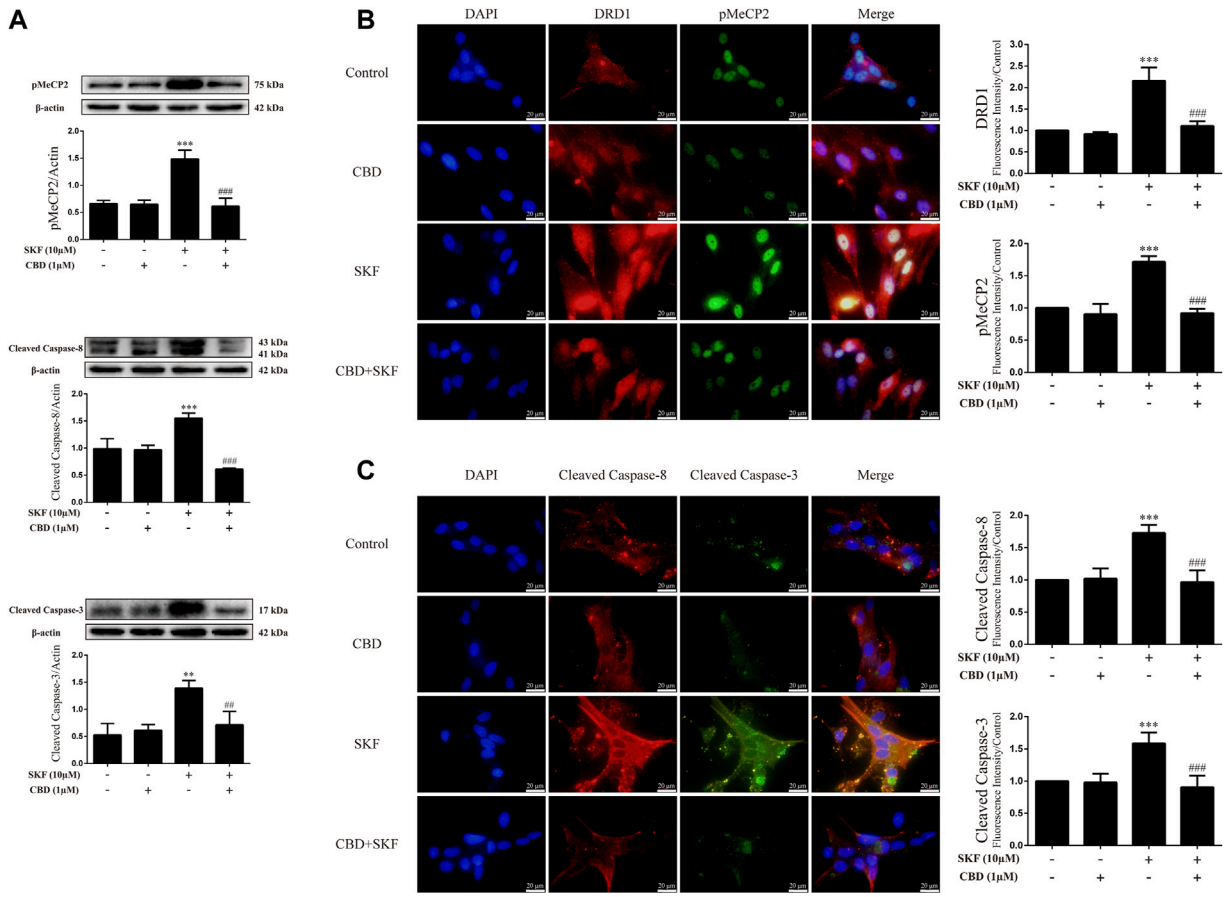

FIGURE 7
Protein levels and colocalization in neurons incubated with CBD and/or SKF81297. **(A)** Levels of pMeCP2 and apoptosis-related proteins. **(B)** DRD1 and pMeCP2 levels and their colocalization. **(C)** Cleaved caspase-8 and cleaved caspase-3 levels and their colocalization. $^{**}p < 0.01$ or $^{***}p < 0.001$ compared with control group, $^{\#\#}p < 0.01$ or $^{\#\#\#}p < 0.001$ compared with METH group; Tukey HSD *post-hoc* comparison after significant ANOVA.

that METH significantly increased intracellular Ca^{2+} in the neurons [Figure 4A; F (3, 16) = 159.367, $p < 0.001$], whereas CBD pretreatment prevented the high level of Ca^{2+} [Figure 4A; F (3, 16) = 159.367, $p < 0.001$]. We applied TUNEL staining to detect neuronal apoptosis. Results showed a significant increase in the level of apoptosis after METH administration [Figure 4B; F (3, 16) = 37.384, $p < 0.001$], but a significant decrease in apoptosis with CBD pretreatment [Figure 4B; F (3, 16) = 37.384, $p < 0.001$]. Thus, intracellular Ca^{2+} may play an important role in the neuroprotective effects of CBD.

Inhibition of DA receptors D1 activity prevented phosphorylation of MeCP2 and apoptosis-related protein expression induced by methamphetamine *in-vitro*

To clarify whether DRD1 signaling mediates apoptosis induced by METH, we applied the DRD1 antagonist SCH23390 to inhibit DRD1 activity in the neurons. Results showed that SCH23390 not only prevented METH-induced expression of cleaved caspase-8 [Figure 5A; F (3, 8) = 37.934, $p < 0.01$] and cleaved caspase-3 [Figure 5A; F (3, 8) = 44.214, $p < 0.01$, $p < 0.001$], but also blocked the phosphorylation of MeCP2 [Figure 5A; F (3, 12) = 127.199, $p < 0.001$] induced by METH. In addition, the phosphorylation of MeCP2 [Figure 5A; F (3, 12) = 127.199, $p < 0.001$] and levels of cleaved caspase-8 [Figure 5A; F (3, 8) = 37.934, $p < 0.01$] and cleaved caspase-3 [Figure 5A; F (3, 8) = 44.214, $p < 0.01$] were lower than that in the control when SCH23390 was administered alone. Immunofluorescence staining showed the preventive effects of SCH23390 on DRD1 expression [Figure 5B; F (3, 16) = 194.609, $p < 0.001$]. The pMeCP2 [Figure 5B; F (3, 16) = 89.432, $p < 0.01$, $p < 0.001$], cleaved caspase-8 [Figure 5C; F (3, 16) = 255.105, $p < 0.001$], and cleaved caspase-3 [Figure 5C; F (3, 16) = 103.056, $p < 0.001$] results were confirmed by immunofluorescence staining. Thus, METH appears to

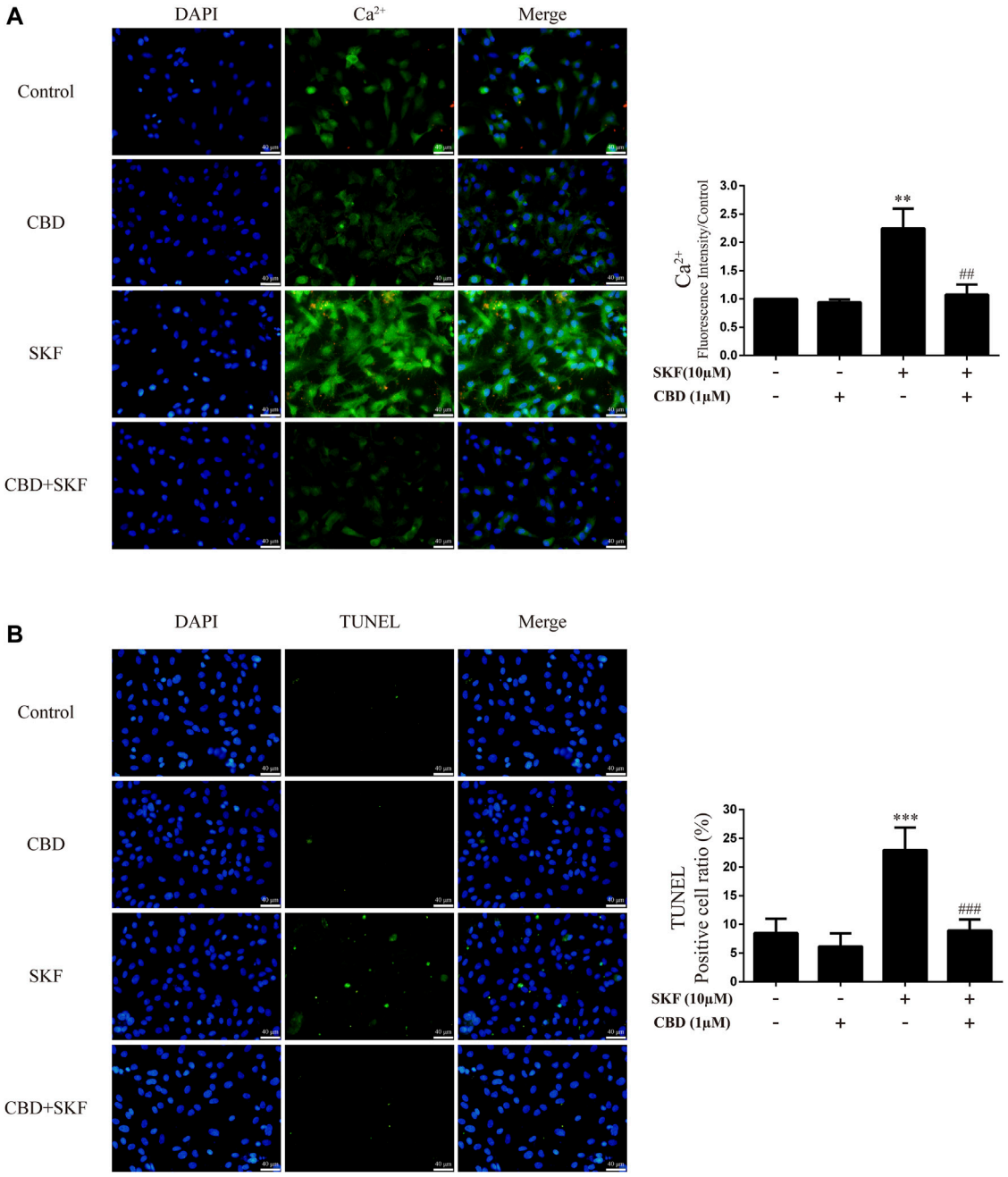

FIGURE 8
Intracellular Ca^{2+} and apoptosis levels in neurons incubated with CBD and/or SKF81297. **(A)** Apoptosis level in neurons. **(B)** Intracellular Ca^{2+} level in neurons. $^{**}p < 0.01$ or $^{***}p < 0.001$ compared with control group, $^{\#\#}p < 0.01$ or $^{\#\#\#}p < 0.001$ compared with METH group; Tukey HSD *post-hoc* comparison after significant ANOVA.

induce neuronal apoptosis *via* DRD1-mediated phosphorylation of MeCP2. However, DRD1 antagonist SCH23390 did not completely block the METH induction of DRD1 expression [Figure 5B; F (3, 16) = 194.609, $p < 0.01$], pMeCP2 expression [Figure 5A; F (3, 12) = 127.199, $p < 0.001$; Figure 5B; F (3, 16) = 89.432, $p < 0.01$], cleaved caspase-8 expression [Figure 5A; F (3, 8) = 37.934, $p < 0.01$; Figure 5C; F (3, 16) = 255.105, $p < 0.001$], or cleaved caspase-3 expression [Figure 5C; F (3, 16) = 103.056, $p < 0.001$]. Therefore, other pathways may also be involved in METH-induced caspase cascade.

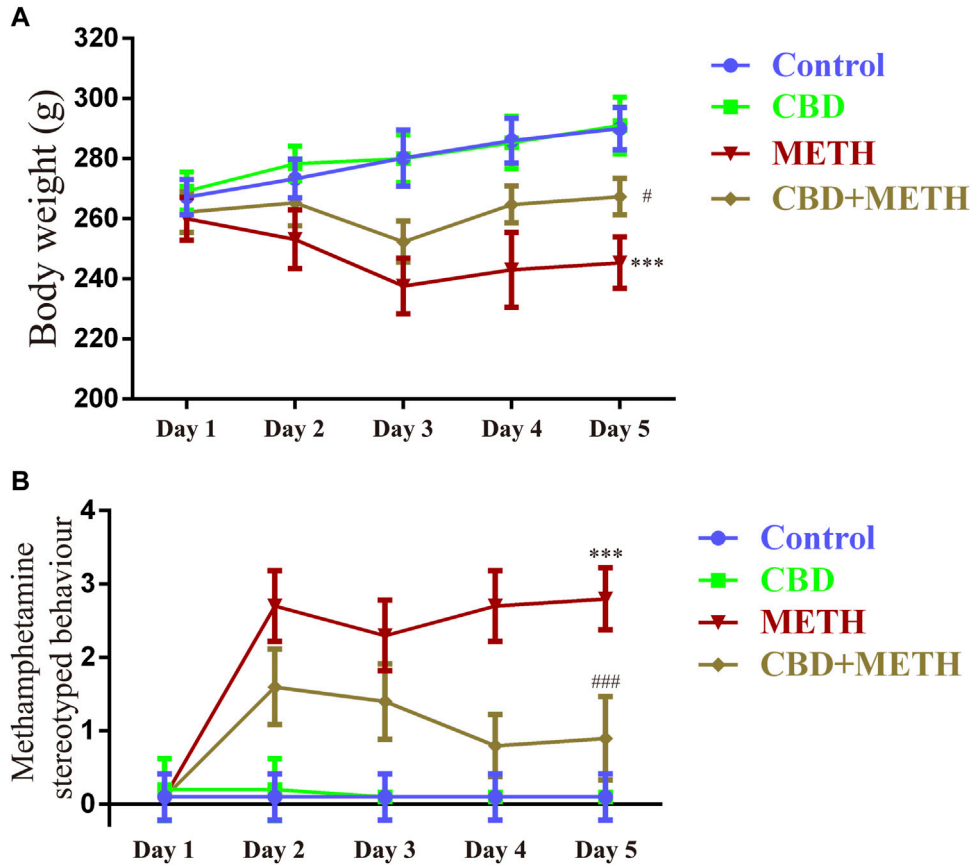

FIGURE 9
Changes in body weight and stereotyped behavior in rats repeatedly exposed to CBD and/or METH. **(A)** Changes in body weight in rats. **(B)** Changes in stereotyped behavior in rats. ***$p < 0.001$ compared with control group, $^{\#}p < 0.05$ or $^{\#\#\#}p < 0.001$ compared with METH group; Tukey HSD *post-hoc* comparison after significant ANOVA.

Repression of DA receptors D1 activity prevented Ca^{2+} overload and apoptosis induced by methamphetamine in neurons

We next investigated intracellular Ca^{2+} and apoptosis levels in neurons when DRD1 activity was inhibited. We found that inhibition of DRD1 activity prevented METH-induced Ca^{2+} overload [Figure 6A; F (3, 16) = 256.570, $p < 0.001$] and inhibited METH-induced apoptosis [Figure 6B; F (3, 16) = 56.240, $p < 0.001$]. Furthermore, the neuronal levels of Ca^{2+} [Figure 6A; F (3, 16) = 256.570, $p < 0.01$] and apoptosis [Figure 6B; F (3, 16) = 56.240, $p < 0.001$] were also reduced compared with the control when administered SCH23390 alone. These results suggest that METH induces neuronal apoptosis *via* DRD1-mediated Ca^{2+} influx. Similarly, the levels of intracellular Ca^{2+} [Figure 6A; F (3, 16) = 256.570, $p < 0.001$] and apoptosis [Figure 6B; F (3, 16) = 56.240, $p < 0.01$] in the SCH23390 + METH group were higher than those in the SCH23390 group. Therefore, other pathways may also contribute to METH-induced Ca^{2+} influx and apoptosis.

Cannabidiol prevented phosphorylation of MeCP2 and apoptosis-related protein expression induced by DA receptors D1 activation *in-vitro*

To determine whether the neuroprotective effects of CBD work by inhibition of DRD1 signaling, we used the DRD1 agonist SKF81297 to activate DRD1. Results showed that DRD1 activation increased the expression levels of cleaved caspase-8 [Figure 7A; F (3, 12) = 48.763, $p < 0.001$] and cleaved caspase-3 [Figure 7A; F (3, 8) = 13.524, $p < 0.01$] and induced the phosphorylation of MeCP2 [Figure 7A; F (3, 8) = 37.637, $p < 0.001$]. As expected, CBD pretreatment prevented the high SKF81297-induced expression of pMeCP2 [Figure 7A; F (3, 8) = 37.637, $p < 0.001$], cleaved caspase-8 [Figure 7A; F (3, 12) = 48.763, $p < 0.001$],

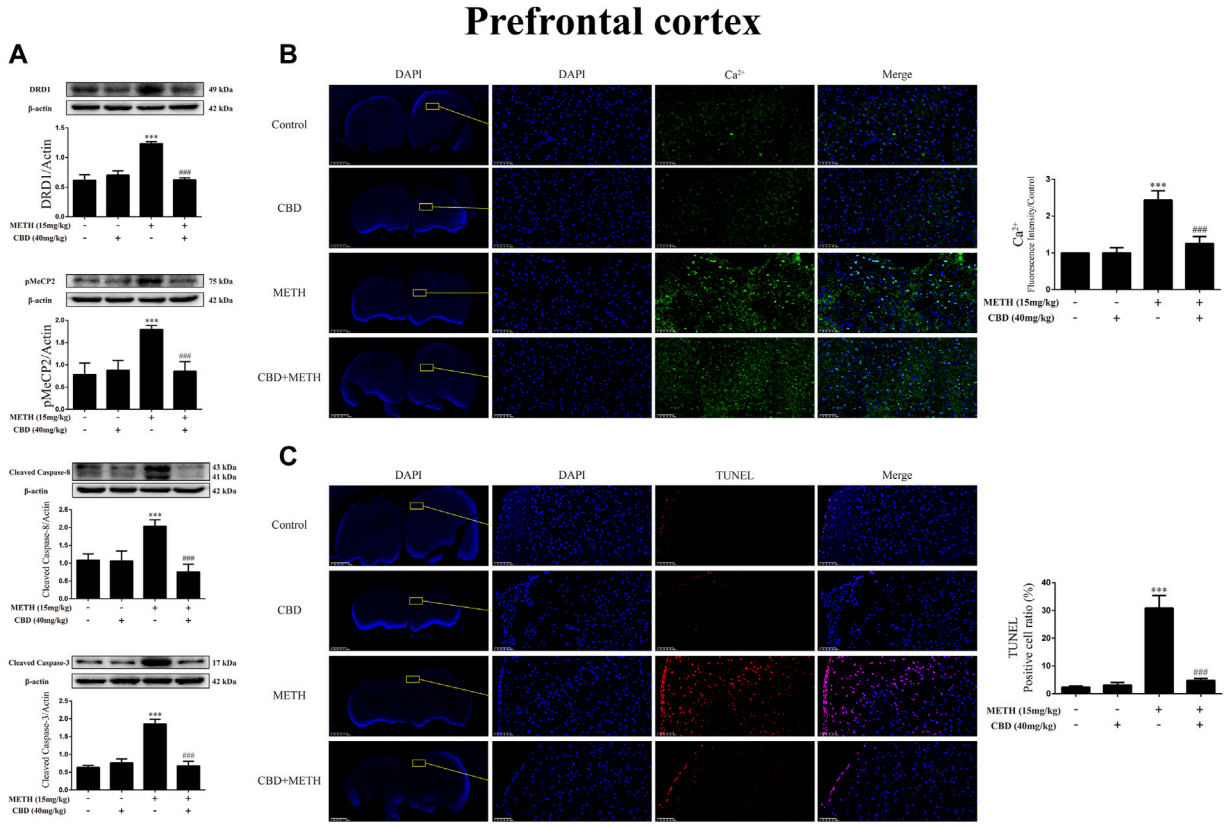

FIGURE 10
Protein, intracellular Ca^{2+}, and apoptosis levels in prefrontal cortex of rats repeatedly exposed to CBD and/or METH. **(A)** Levels of DRD1, pMeCP2, and apoptosis-related proteins in prefrontal cortex. **(B)** Intracellular Ca^{2+} level in prefrontal cortex. **(C)** Apoptosis level in prefrontal cortex. ***$p < 0.001$ compared with control group, $^{###}p < 0.001$ compared with METH group; Tukey HSD *post-hoc* comparison after significant ANOVA.

and cleaved caspase-3 [Figure 6A; F (3, 8) = 13.524, $p < 0.01$]. Immunofluorescence staining also showed that SKF81297 robustly stimulated DRD1 [Figure 7B; F (3, 16) = 60.311, $p < 0.001$], which was blocked by CBD pretreatment [Figure 7B; F (3, 16) = 60.311, $p < 0.001$]. MeCP2 phosphorylation also increased significantly [Figure 7B; F (3, 16) = 80.637, $p < 0.001$], but was prevented by CBD pretreatment [Figure 7B; F (3, 16) = 80.637, $p < 0.001$]. Cleaved caspase-8 [Figure 7C; F (3, 16) = 36.566, $p < 0.001$] and cleaved caspase-3 [Figure 7C; F (3, 16) = 24.377, $p < 0.001$] showed the same immunofluorescence staining results. Therefore, CBD appears to prevent neuronal apoptosis *via* DRD1-mediated phosphorylation of MeCP2.

Cannabidiol blocked Ca^{2+} overload and apoptosis induced by DA receptors D1 activation in neurons

We further investigated the effects of DRD1 activation on intracellular Ca^{2+} and apoptosis in neurons. Results showed that DRD1 activation significantly induced neuronal Ca^{2+} influx [Figure 8A; F (3, 16) = 50.118, $p < 0.01$] and apoptosis [Figure 8B; F (3, 16) = 38.310, $p < 0.001$], but both were blocked by CBD pretreatment [Ca^{2+}; Figure 8A; F (3, 16) = 50.118, $p < 0.01$]; apoptosis; [Figure 8B; F (3, 16) = 38.310, $p < 0.001$]. These results suggest that the neuroprotective effects of CBD work by preventing DRD1-mediated Ca^{2+} influx.

Cannabidiol prevented growth inhibition and stereotyped behavior induced by methamphetamine in rats

To corroborate the findings that CBD resists neurotoxicity induced by METH *in-vitro*, we constructed a rat model using METH. We first investigated the effects of drug exposure on body weight in rats. Compared with the control group, repeated METH exposure inhibited normal weight gain in rats [Figure 9A; F (1, 16) = 25 383.728, $p < 0.001$], while multiple CBD pretreatments prevented the inhibition induced by METH [Figure 9A; F (1, 16) = 25 383.728, $p < 0.05$], although there was no significant effect when treated with CBD alone [Figure 9A; F (1, 16) = 25 383.728, p =

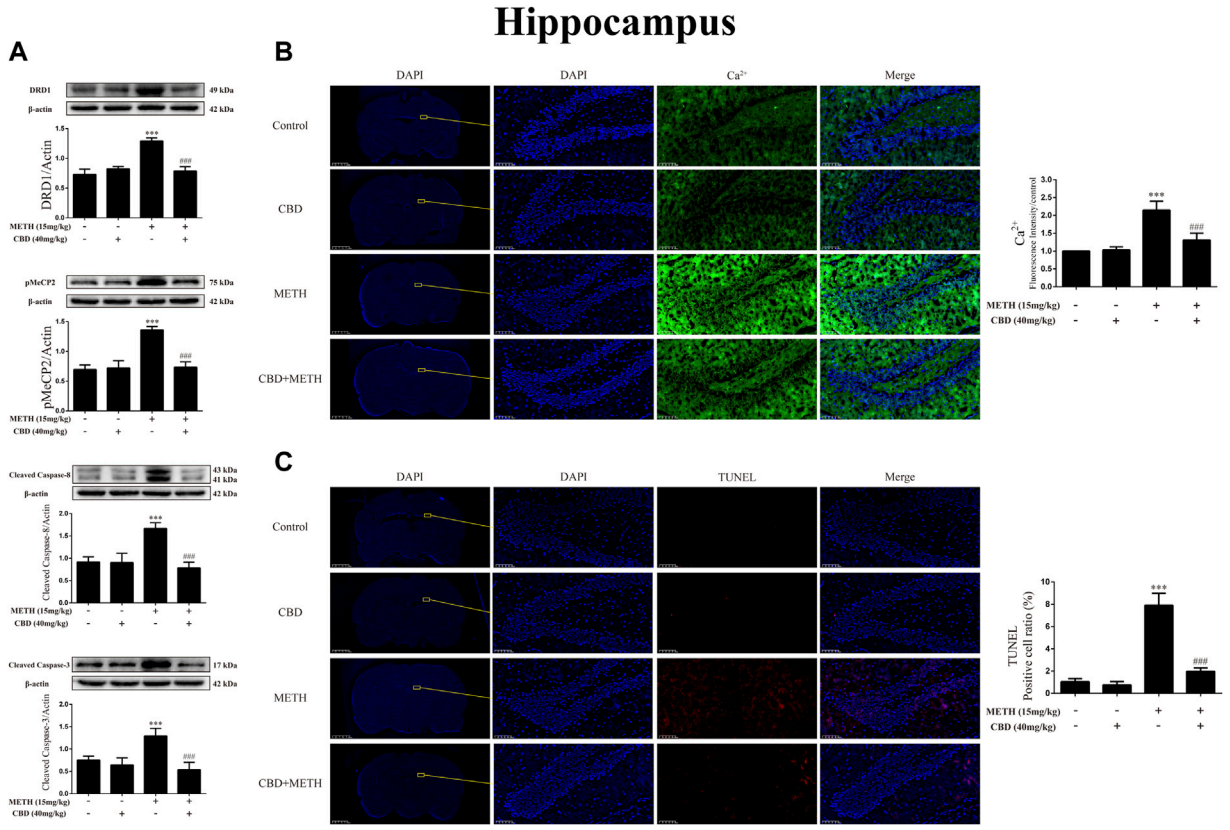

FIGURE 11
Protein, intracellular Ca^{2+}, and apoptosis levels in hippocampus of rats repeatedly exposed to CBD and/or METH. **(A)** Levels of DRD1, pMeCP2, and apoptosis-related proteins in hippocampus. **(B)** Intracellular Ca^{2+} level in hippocampus. **(C)** Apoptosis level in hippocampus. ***$p < 0.001$ compared with control group, ###$p < 0.001$ compared with METH group; Tukey HSD *post-hoc* comparison after significant ANOVA.

0.990]. We further investigated METH-induced stereotyped behavior during drug administration. Results showed that repeated METH exposure robustly induced stereotyped behavior in rats [Figure 9B; F (1, 36) = 279.914, $p < 0.001$] compared with the control group. However, CBD pretreatment blocked this METH-induced stereotyped behavior [Figure 9B; F (1, 36) = 279.914, $p < 0.001$], although CBD treatment alone had no effect [Figure 9B; F (1, 36) = 279.914, $p = 0.992$]. These results indicate that CBD exerts a global interventional effect on METH use disorders, including individual growth and behavioral changes.

Cannabidiol prevented DA receptors D1 expression, phosphorylation of MeCP2, Ca^{2+} overload, and apoptosis induced by methamphetamine in prefrontal cortex of rats

Repeated METH exposure affects cell proliferation and induces apoptosis in the PFC (Kim and Mandyam, 2014). Thus, to further explore the neuroprotective effects of CBD, we investigated protein expression, intracellular Ca^{2+}, and apoptosis levels in the PFC of rats. Results showed that repeated METH exposure markedly increased the expression levels of DRD1 [Figure 10A; F (3, 20) = 127.723, $p < 0.001$], pMeCP2 [Figure 10A; F (3, 12) = 21.619, $p < 0.001$], cleaved caspase-8 [Figure 10A; F (3, 16) = 32.630, $p < 0.001$], and cleaved caspase-3 [Figure 10A; F (3, 20) = 173.065, $p < 0.001$] in the PFC, whereas CBD pretreatment blocked the high expression levels of DRD1 [Figure 10A; F (3, 20) = 127.723, $p < 0.001$], pMeCP2 [Figure 10A; F (3, 12) = 21.619, $p < 0.001$], cleaved caspase-8 [Figure 10A; F (3, 16) = 32.630, $p < 0.001$], and cleaved caspase-3 [Figure 10A; F (3, 20) = 173.065, $p < 0.001$]. Repeated METH exposure also increased intracellular Ca^{2+} [Figure 10B; F (3, 16) = 78.759, $p < 0.001$] and apoptosis [Figure 10C; F (3, 16) = 173.738, $p < 0.001$] in the PFC. CBD pretreatment prevented Ca^{2+} overload [Figure 10B; F (3, 16) = 78.759, $p < 0.001$] and apoptosis [Figure 10C; F (3, 16) = 173.738, $p < 0.001$] induced by METH, but had no effect when administered alone. Thus, CBD shows neuroprotective effects in the PFC of rats.

Cannabidiol blocked DA receptors D1 expression, phosphorylation of MeCP2, Ca^{2+} overload, and apoptosis induced by methamphetamine in hip of rats

As CBD promotes neurogenesis in the Hip of rats under chronic METH exposure (Razavi et al., 2021) and modulates the psychoactive properties of METH *via* DA receptors in the Hip of rats (Hassanlou et al., 2021; Nouri et al., 2021), we repeated the above experiments in the Hip. Results showed that METH exposure induced DRD1 [Figure 11A; F (3, 16) = 74.578, $p < 0.001$], pMeCP2 [Figure 11A; F (3, 16) = 63.564, $p < 0.001$], cleaved caspase-8 [Figure 11A; F (3, 20) = 44.202, $p < 0.001$], and cleaved caspase-3 expression [Figure 11A; F (3, 16) = 25.338, $p < 0.001$] in the Hip, whereas CBD pretreatment blocked the high expression of DRD1 [Figure 11A; F (3, 16) = 74.578, $p < 0.001$], pMeCP2 [Figure 11A; F (3, 16) = 63.564, $p < 0.001$], cleaved caspase-8 [Figure 11A; F (3, 20) = 44.202, $p < 0.001$], and cleaved caspase-3 [Figure 11A; F (3, 16) = 25.338, $p < 0.001$]. Similarly, METH exposure also induced Ca^{2+} influx [Figure 11B; F (3, 20) = 62.846, $p < 0.001$] and apoptosis [Figure 11C; F (3, 16) = 161.004, $p < 0.001$], whereas CBD pretreatment prevented their high levels [Ca^{2+}; Figure 11B; F (3, 20) = 62.846, $p < 0.001$; apoptosis; Figure 11C; F (3, 16) = 161.004, $p < 0.001$] in the Hip.

Discussion

In the molecular docking simulations, we found that METH and CBD bound to residues of DRD1 with two overlapping binding sites. Moreover, CBD and METH competitively interacted for one of the sites. In the biological experiments, we found that METH significantly induced neurotoxicity with DRD1 activation, high MeCP2 phosphorylation at Ser421, and Ca^{2+} overload *in-vitro* and *in-vivo*. However, CBD pretreatment effectively prevented METH-induced neurotoxicity by inhibiting DRD1, pMeCP2, and Ca^{2+} influx *in-vitro* and *in-vivo*. In addition, the DRD1 antagonist SCH23390 significantly prevented METH-induced neurotoxicity, as well as pMeCP2 expression and Ca^{2+} overload *in-vitro*. In contrast, the DRD1 agonist SKF81297 strongly induced neurotoxicity, MeCP2 phosphorylation, and Ca^{2+} overload *in-vitro*, which were also blocked by CBD pretreatment.

METH is an amphetamine-type stimulant that primarily induces extracellular and cytoplasmic DA release by acting on DA transporters and vesicle monoamine transporter-2 (VMAT-2) (Kim et al., 2020). Abundant DA in the extracellular matrix and cytoplasm can produce DA quinones, superoxide anions, and hydrogen oxygen species *via* auto-oxidation, resulting in considerable oxidative damage (LaVoie and Hastings, 1999; Marshall and O'Dell, 2012). Thus, METH-induced DA release is closely related to the process of neurotoxicity (Kim et al., 2020). METH also induces the FasL-Fas death pathway and caspase-3 cleavage in rat neurons, which are mediated by DRD1 (Jayanthi et al., 2005). Here, we found that METH may bind directly with DRD1. Notably, METH exposure significantly induced apoptosis with activation of the caspase-8/caspase-3 cascade *in-vitro* and *in-vivo*, while the DRD1 antagonist SCH23390 markedly prevented the METH-induced caspase-8/caspase-3 cascade and neuronal apoptosis *in-vitro*. In contrast, the DRD1 agonist SKF81297 induced apoptosis *via* activation of the caspase-8/caspase-3 cascade *in-vitro*. These results indicate that DRD1 signaling plays a key role in METH-induced neurotoxicity, as reported in various studies (Ares-Santos et al., 2012; Ares-Santos et al., 2013; Friend and Keefe, 2013; Nguyen et al., 2018). However, some evidence suggests that other molecular pathways may also contribute to cell death under METH-induced neurotoxicity, including oxidative stress, mitochondrial stress, ER stress, UPS dysfunction, transcription factor changes, and autophagy (Jayanthi et al., 2021). Here, the DRD1 antagonist SCH23390 did not completely block the effects of METH on Ca^{2+} influx, MeCP2 phosphorylation, caspase cascade, or neuronal apoptosis. Interestingly, DA induces the expression of DRD1 at low concentration (Sidhu et al., 1999) and functional activity of DRD1 also determines DA release (Shen et al., 2022). This positive feedback mechanism may partially explain why the DRD1 antagonist SCH23390 and DRD1 agonist SKF81297 affected DRD1 expression in our study.

On the other hand, growing evidence indicates that MeCP2 contributes to METH-induced behavioral disorders in rodents (Lewis et al., 2016; Wu et al., 2016; Fan et al., 2020). We observed serious stereotyped behavior in rats under repeated METH exposure, consistent with previous research (Roberts et al., 2010; Qiao et al., 2014). Notably, METH strongly induced stereotyped behavior in rats, with high phosphorylation of MeCP2 at Ser421 in the PFC and Hip. The DRD1 antagonist SCH23390 significantly blocked METH-induced phosphorylation of MeCP2 at Ser421 in the primary neurons of rats. In contrast, the DRD1 agonist SKF81297 strongly induced MeCP2 phosphorylation at Ser421 *in-vitro*. These results suggest that the phosphorylation of MeCP2 at Ser421 is mediated by DRD1, consistent with previous research (Deng et al., 2010). As the phosphorylation of MeCP2 at Ser421 is calcium-dependent (Chen et al., 2003; Buchthal et al., 2012), we further investigated the level of intracellular Ca^{2+}, and found that METH exposure strongly increased Ca^{2+} influx *in-vitro* and *in-vivo*. However, DRD1 inhibition significantly reduced the high level of intracellular Ca^{2+} caused by METH, while DRD1 activation markedly increased intracellular Ca^{2+} in the neurons. These results imply that DRD1-mediated phosphorylation of MeCP2 at Ser421 involves calcium signaling. Several studies suggest that changes in IEGs may also contribute to METH-induced neurotoxicity (Deng et al., 1999; Jayanthi et al., 2005;

Jayanthi et al., 2021). Interestingly, research has shown that phosphorylation of MeCP2 at Ser421 mediates the transcriptional activation of IEGs in psychostimulant-injected mice (Deng et al., 2010). Thus, these findings reveal the potential mechanism underlying METH-induced neurotoxicity involving DRD1-mediated calcium-dependent phosphorylation of MeCP2.

CBD exhibits excellent therapeutic potential in neuropsychiatric disorders such as epilepsy, PD, AD, depression, anxiety, psychosis, and drug dependence (Elsaid et al., 2019; Premoli et al., 2019; Vitale et al., 2021). Under METH exposure, CBD shows neuroprotective (Razavi et al., 2021), antioxidative, and anti-inflammatory properties (Majdi et al., 2019; Karimi-Haghighi et al., 2020). In addition, CBD can restore the adaptation to threshold doses caused by repeated METH exposure (Khanegheini et al., 2021). Our results showed that CBD pretreatment prevented METH-induced caspase-8/caspase-3 cascade and apoptosis *in-vitro* and *in-vivo*. During abstinence periods, CBD has been shown to promote neurogenesis in the Hip dentate gyrus in rats under chronic METH exposure (Razavi et al., 2021). In the current study, we found that CBD pretreatment markedly prevented the increase in caspase-8/caspase-3 cascade and apoptosis in the Hip of rats induced by repeated METH exposure. Given our results and those of the abovementioned studies, CBD shows substantial neuroprotective effects on METH-induced neurotoxicity. However, one major obstacle regarding CBD research is our relatively poor understanding of the mechanisms underlying its therapeutic potential. As CBD has a low-binding affinity toward traditional cannabinoid receptors (CB1-R and CB2-R) (Izzo et al., 2009; Bian et al., 2019; Vitale et al., 2021), determination of the main active target(s) of CBD is essential. Evidence indicates that CBD modulates DA receptors (Hassanlou et al., 2021; Nouri et al., 2021), Sigma-1 receptors (Yang et al., 2020), and TLR4 (Majdi et al., 2019). Here, we found that CBD may directly bind with DRD1 and compete with METH for the PHE-313 binding site. These two partially overlapping binding pockets likely affected ligand and receptor binding. This may explain why the type of interactions between CBD and DRD1 residues were variable when CBD and METH docked with the DRD1 model. Previous molecular docking evidence suggests that CBD is a potential binding ligand for DRD3 (Bian et al., 2019). Therefore, CBD may exert broader effects on DA receptors. In addition, our biological experiments showed that CBD also exhibited significant preventive effects on SKF81297-induced Ca^{2+} influx, MeCP2 Ser421 phosphorylation, caspase-8/caspase-3 cascade, and apoptosis. These results suggest that the preventive effects of CBD on neurotoxicity may be mediated by DRD1.

However, METH-induced neurotoxicity not only involves direct damage to neurons, but also the participation of neuroinflammation (Shaerzadeh et al., 2018; Kim et al., 2020). Previous studies have shown that METH induces neuroinflammation *via* TLR4-or Sigma-1 receptor-related pathways (Kim et al., 2020). In addition, research suggests that METH-stimulative neuroinflammation may involve the participation of D1-like DA receptors (Wang et al., 2019), which are highly expressed in the microglia (Huck et al., 2015). Thus, the contribution of DRD1 to METH-induced neurotoxicity may not be limited to neurons. Furthermore, the phosphorylation of MeCP2 at Ser421 is also observed in microglia after psychostimulant exposure (Cotto et al., 2018). Therefore, the regulatory effects of DRD1-mediated phosphorylation of MeCP2 on METH-induced neurotoxicity may not be limited to neurons but could exert more global effects on multiple types of cells, providing a clear direction for future research.

In conclusion, our results suggest that METH induces neurotoxicity *via* DRD1-mediated calcium-dependent phosphorylation of MeCP2 at Ser421. Moreover, CBD significantly prevents METH-induced neurotoxicity *via* modulation of DRD1. Future research should focus on the contribution of neuroinflammation to neurotoxicity and explore the anti-inflammatory effects of CBD under METH exposure.

Data availability statement

The original contributions presented in the study are included in the article/supplementary material, further inquiries can be directed to the corresponding authors.

Ethics statement

The animal study was reviewed and approved by the Animal Care and Use Committee of Kunming Medical University.

Author contributions

BS: investigation; methodology; data curation; formal analysis; writing—original draft. RZ: conceptualization; methodology; resources. GY: investigation; methodology. YP, QN, HY, WD, BC, CS, YT, LQ, and JS: investigation. SH: conceptualization; funding acquisition; project administration; supervision; writing—review and editing. LL: conceptualization; funding acquisition; supervision.

Funding

This work was supported by the National Natural Science Foundation of China (No. 81760337 and No. 81860332); Program Innovative Research Team in Science and Technology in Yunnan Province (No. 2017HC007); Research Project of NHC Key Laboratory of Drug Addiction Medicine, Kunming Medical University (No. 2020DAMARC-002); and Scientific Research Foundation of Education Department of Yunnan Province (No. 2019Y0343).

Acknowledgments

BS would like to thank LL and SH for their guidance. The authors would like to thank Dr. Hongfei Gao for providing help in the protein-drug binding simulations.

Conflict of interest

The authors declare that the research was conducted in the absence of any commercial or financial relationships that could be construed as a potential conflict of interest.

Publisher's note

All claims expressed in this article are solely those of the authors and do not necessarily represent those of their affiliated organizations, or those of the publisher, the editors and the reviewers. Any product that may be evaluated in this article, or claim that may be made by its manufacturer, is not guaranteed or endorsed by the publisher.

References

Amir, R. E., Van den Veyver, I. B., Wan, M., Tran, C. Q., Francke, U., and Zoghbi, H. Y. (1999). Rett syndrome is caused by mutations in X-linked MECP2, encoding methyl-CpG-binding protein 2. *Nat. Genet.* 23 (2), 185–188. doi:10.1038/13810

Andres, M. A., Cooke, I. M., Bellinger, F. P., Berry, M. J., Zaporteza, M. M., Rueli, R. H., et al. (2015). Methamphetamine acutely inhibits voltage-gated calcium channels but chronically up-regulates L-type channels. *J. Neurochem.* 134 (1), 56–65. doi:10.1111/jnc.13104

Ares-Santos, S., Granado, N., and Moratalla, R. (2013). The role of dopamine receptors in the neurotoxicity of methamphetamine. *J. Intern. Med.* 273 (5), 437–453. doi:10.1111/joim.12049

Ares-Santos, S., Granado, N., Oliva, I., O'Shea, E., Martin, E. D., Colado, M. I., et al. (2012). Dopamine D(1) receptor deletion strongly reduces neurotoxic effects of methamphetamine. *Neurobiol. Dis.* 45 (2), 810–820. doi:10.1016/j.nbd.2011.11.005

Bian, Y. M., He, X. B., Jing, Y. K., Wang, L. R., Wang, J. M., and Xie, X. Q. (2019). Computational systems pharmacology analysis of cannabidiol: A combination of chemogenomics-knowledgebase network analysis and integrated *in silico* modeling and simulation. *Acta Pharmacol. Sin.* 40 (3), 374–386. doi:10.1038/s41401-018-0071-1

Branca, J. J. V., Morucci, G., Becatti, M., Carrino, D., Ghelardini, C., Gulisano, M., et al. (2019). Cannabidiol protects dopaminergic neuronal cells from cadmium. *Int. J. Environ. Res. Public Health* 16 (22), 4420. doi:10.3390/ijerph16224420

Buchthal, B., Lau, D., Weiss, U., Weislogel, J. M., and Bading, H. (2012). Nuclear calcium signaling controls methyl-CpG-binding protein 2 (MeCP2) phosphorylation on serine 421 following synaptic activity. *J. Biol. Chem.* 287 (37), 30967–30974. doi:10.1074/jbc.M112.382507

Cadet, J. L., and Krasnova, I. N. (2009). Molecular bases of methamphetamine-induced neurodegeneration. *Int. Rev. Neurobiol.* 88, 101–119. doi:10.1016/s0074-7742(09)88005-7

Chahrour, M., Jung, S. Y., Shaw, C., Zhou, X., Wong, S. T., Qin, J., et al. (2008). MeCP2, a key contributor to neurological disease, activates and represses transcription. *Science* 320 (5880), 1224–1229. doi:10.1126/science.1153252

Chakraborty, S., Rebecchi, M., Kaczocha, M., and Puopolo, M. (2016). Dopamine modulation of transient receptor potential vanilloid type 1 (TRPV1) receptor in dorsal root ganglia neurons. *J. Physiol.* 594 (6), 1627–1642. doi:10.1113/jp271198

Chao, H. T., and Zoghbi, H. Y. (2009). The yin and yang of MeCP2 phosphorylation. *Proc. Natl. Acad. Sci. U. S. A.* 106 (12), 4577–4578. doi:10.1073/pnas.0901518106

Chen, W. G., Chang, Q., Lin, Y., Meissner, A., West, A. E., Griffith, E. C., et al. (2003). Derepression of BDNF transcription involves calcium-dependent phosphorylation of MeCP2. *Science* 302 (5646), 885–889. doi:10.1126/science.1086446

Chen, X., Qiu, F., Zhao, X., Lu, J., Tan, X., Xu, J., et al. (2020). Astrocyte-derived lipocalin-2 is involved in mitochondrion-related neuronal apoptosis induced by methamphetamine. *ACS Chem. Neurosci.* 11 (8), 1102–1116. doi:10.1021/acschemneuro.9b00559

Chen, X., Xing, J., Jiang, L., Qian, W., Wang, Y., Sun, H., et al. (2016). Involvement of calcium/calmodulin-dependent protein kinase II in methamphetamine-induced neural damage. *J. Appl. Toxicol.* 36 (11), 1460–1467. doi:10.1002/jat.3301

Chin, E. W. M., and Goh, E. L. K. (2019). MeCP2 dysfunction in Rett syndrome and neuropsychiatric disorders. *Methods Mol. Biol.* 2011, 573–591. doi:10.1007/978-1-4939-9554-7_33

Cotto, B., Li, H., Tuma, R. F., Ward, S. J., and Langford, D. (2018). Cocaine-mediated activation of microglia and microglial MeCP2 and BDNF production. *Neurobiol. Dis.* 117, 28–41. doi:10.1016/j.nbd.2018.05.017

Damen, D., and Heumann, R. (2013). MeCP2 phosphorylation in the brain: From transcription to behavior. *Biol. Chem.* 394 (12), 1595–1605. doi:10.1515/hsz-2013-0193

Dastidar, S. G., Bardai, F. H., Ma, C., Price, V., Rawat, V., Verma, P., et al. (2012). Isoform-specific toxicity of Mecp2 in postmitotic neurons: Suppression of neurotoxicity by FoxG1. *J. Neurosci.* 32 (8), 2846–2855. doi:10.1523/jneurosci.5841-11.2012

Deng, J. V., Rodriguiz, R. M., Hutchinson, A. N., Kim, I. H., Wetsel, W. C., and West, A. E. (2010). MeCP2 in the nucleus accumbens contributes to neural and behavioral responses to psychostimulants. *Nat. Neurosci.* 13 (9), 1128–1136. doi:10.1038/nn.2614

Deng, X., Ladenheim, B., Tsao, L. I., and Cadet, J. L. (1999). Null mutation of c-fos causes exacerbation of methamphetamine-induced neurotoxicity. *J. Neurosci.* 19 (22), 10107–10115. doi:10.1523/jneurosci.19-22-10107.1999

Ding, J., Lian, Y., Meng, Y., He, Y., Fan, H., Li, C., et al. (2020). The effect of α-synuclein and Tau in methamphetamine induced neurotoxicity *in vivo* and *in vitro*. *Toxicol. Lett.* 319, 213–224. doi:10.1016/j.toxlet.2019.11.028

Elsaid, S., Kloiber, S., and Le Foll, B. (2019). Effects of cannabidiol (CBD) in neuropsychiatric disorders: A review of pre-clinical and clinical findings. *Prog. Mol. Biol. Transl. Sci.* 167, 25–75. doi:10.1016/bs.pmbts.2019.06.005

Fan, X. Y., Yang, J. Y., Dong, Y. X., Hou, Y., Liu, S., and Wu, C. F. (2020). Oxytocin inhibits methamphetamine-associated learning and memory alterations by regulating DNA methylation at the Synaptophysin promoter. *Addict. Biol.* 25 (1), e12697. doi:10.1111/adb.12697

Friend, D. M., and Keefe, K. A. (2013). A role for D1 dopamine receptors in striatal methamphetamine-induced neurotoxicity. *Neurosci. Lett.* 555, 243–247. doi:10.1016/j.neulet.2013.08.039

Gulmez Karaca, K., Brito, D. V. C., and Oliveira, A. M. M. (2019). MeCP2: A critical regulator of chromatin in neurodevelopment and adult brain function. *Int. J. Mol. Sci.* 20 (18), 4577. doi:10.3390/ijms20184577

Hampson, A. J., Grimaldi, M., Axelrod, J., and Wink, D. (1998). Cannabidiol and (-)Delta9-tetrahydrocannabinol are neuroprotective antioxidants. *Proc. Natl. Acad. Sci. U. S. A.* 95 (14), 8268–8273. doi:10.1073/pnas.95.14.8268

Hassanlou, A. A., Jamali, S., RayatSanati, K., Mousavi, Z., and Haghparast, A. (2021). Cannabidiol modulates the METH-induced conditioned place preference through D2-like dopamine receptors in the hippocampal CA1 region. *Brain Res. Bull.* 172, 43–51. doi:10.1016/j.brainresbull.2021.04.007

Hay, G. L., Baracz, S. J., Everett, N. A., Roberts, J., Costa, P. A., Arnold, J. C., et al. (2018). Cannabidiol treatment reduces the motivation to self-administer methamphetamine and methamphetamine-primed relapse in rats. *J. Psychopharmacol.* 32 (12), 1369–1378. doi:10.1177/0269881118799954

Huang, E., Huang, H., Guan, T., Liu, C., Qu, D., Xu, Y., et al. (2019). Involvement of C/EBPβ-related signaling pathway in methamphetamine-induced neuronal autophagy and apoptosis. *Toxicol. Lett.* 312, 11–21. doi:10.1016/j.toxlet.2019.05.003

Huang, W., Xie, W. B., Qiao, D., Qiu, P., Huang, E., Li, B., et al. (2015). Caspase-11 plays an essential role in methamphetamine-induced dopaminergic neuron apoptosis. *Toxicol. Sci.* 145 (1), 68–79. doi:10.1093/toxsci/kfv014

Huck, J. H., Freyer, D., Böttcher, C., Mladinov, M., Muselmann-Genschow, C., Thielke, M., et al. (2015). De novo expression of dopamine D2 receptors on microglia after stroke. *J. Cereb. Blood Flow. Metab.* 35 (11), 1804–1811. doi:10.1038/jcbfm.2015.128

Izzo, A. A., Borrelli, F., Capasso, R., Di Marzo, V., and Mechoulam, R. (2009). Non-psychotropic plant cannabinoids: New therapeutic opportunities from an ancient herb. *Trends Pharmacol. Sci.* 30 (10), 515–527. doi:10.1016/j.tips.2009.07.006

Jayanthi, S., Daiwile, A. P., and Cadet, J. L. (2021). Neurotoxicity of methamphetamine: Main effects and mechanisms. *Exp. Neurol.* 344, 113795. doi:10.1016/j.expneurol.2021.113795

Jayanthi, S., Deng, X., Ladenheim, B., McCoy, M. T., Cluster, A., Cai, N. S., et al. (2005). Calcineurin/NFAT-induced up-regulation of the Fas ligand/Fas death pathway is involved in methamphetamine-induced neuronal apoptosis. *Proc. Natl. Acad. Sci. U. S. A.* 102 (3), 868–873. doi:10.1073/pnas.0404990102

Jones, P. L., Veenstra, G. J., Wade, P. A., Vermaak, D., Kass, S. U., Landsberger, N., et al. (1998). Methylated DNA and MeCP2 recruit histone deacetylase to repress transcription. *Nat. Genet.* 19 (2), 187–191. doi:10.1038/561

Karimi-Haghighi, S., Dargahi, L., and Haghparast, A. (2020). Cannabidiol modulates the expression of neuroinflammatory factors in stress- and drug-induced reinstatement of methamphetamine in extinguished rats. *Addict. Biol.* 25 (2), e12740. doi:10.1111/adb.12740

Khanegheini, A., Khani, M., Zarrabian, S., Yousefzadeh-Chabok, S., Taleghani, B. K., and Haghparast, A. (2021). Cannabidiol enhanced the development of sensitization to the expression of methamphetamine-induced conditioned place preference in male rats. *J. Psychiatr. Res.* 137, 260–265. doi:10.1016/j.jpsychires.2021.02.045

Kim, A., and Mandyam, C. D. (2014). Methamphetamine affects cell proliferation in the medial prefrontal cortex: A new niche for toxicity. *Pharmacol. Biochem. Behav.* 126, 90–96. doi:10.1016/j.pbb.2014.09.012

Kim, B., Yun, J., and Park, B. (2020). Methamphetamine-induced neuronal damage: Neurotoxicity and neuroinflammation. *Biomol. Ther.* 28 (5), 381–388. doi:10.4062/biomolther.2020.044

Lappin, J. M., Darke, S., and Farrell, M. (2018). Methamphetamine use and future risk for Parkinson's disease: Evidence and clinical implications. *Drug Alcohol Depend.* 187, 134–140. doi:10.1016/j.drugalcdep.2018.02.032

LaVoie, M. J., and Hastings, T. G. (1999). Dopamine quinone formation and protein modification associated with the striatal neurotoxicity of methamphetamine: Evidence against a role for extracellular dopamine. *J. Neurosci.* 19 (4), 1484–1491. doi:10.1523/jneurosci.19-04-01484.1999

Lewis, C. R., Bastle, R. M., Manning, T. B., Himes, S. M., Fennig, P., Conrad, P. R., et al. (2016). Interactions between early Life stress, nucleus accumbens MeCP2 expression, and methamphetamine self-administration in male rats. *Neuropsychopharmacology* 41 (12), 2851–2861. doi:10.1038/npp.2016.96

Li, J., Shi, Q., Wang, Q., Tan, X., Pang, K., Liu, X., et al. (2019). Profiling circular RNA in methamphetamine-treated primary cortical neurons identified novel circRNAs related to methamphetamine addiction. *Neurosci. Lett.* 701, 146–153. doi:10.1016/j.neulet.2019.02.032

Li, Y., and Yang, L. (2015). Driving forces for drug loading in drug carriers. *J. Microencapsul.* 32 (3), 255–272. doi:10.3109/02652048.2015.1010459

Luján, M., Castro-Zavala, A., Alegre-Zurano, L., and Valverde, O. (2018). Repeated Cannabidiol treatment reduces cocaine intake and modulates neural proliferation and CB1R expression in the mouse hippocampus. *Neuropharmacology* 143, 163–175. doi:10.1016/j.neuropharm.2018.09.043

Majdi, F., Taheri, F., Salehi, P., Motaghinejad, M., and Safari, S. (2019). Cannabinoids Δ(9)-tetrahydrocannabinol and cannabidiol may be effective against methamphetamine induced mitochondrial dysfunction and inflammation by modulation of Toll-like type-4(Toll-like 4) receptors and NF-κB signaling. *Med. Hypotheses* 133, 109371. doi:10.1016/j.mehy.2019.109371

Marshall, J. F., and O'Dell, S. J. (2012). Methamphetamine influences on brain and behavior: Unsafe at any speed? *Trends Neurosci.* 35 (9), 536–545. doi:10.1016/j.tins.2012.05.006

Montgomery, K. R., Louis Sam Titus, A. S. C., Wang, L., and D'Mello, S. R. (2018). Elevated MeCP2 in mice causes neurodegeneration involving tau dysregulation and excitotoxicity: Implications for the understanding and treatment of MeCP2 triplication syndrome. *Mol. Neurobiol.* 55 (12), 9057–9074. doi:10.1007/s12035-018-1046-4

Nan, X., Ng, H. H., Johnson, C. A., Laherty, C. D., Turner, B. M., Eisenman, R. N., et al. (1998). Transcriptional repression by the methyl-CpG-binding protein MeCP2 involves a histone deacetylase complex. *Nature* 393 (6683), 386–389. doi:10.1038/30764

Nguyen, P. T., Shin, E. J., Dang, D. K., Tran, H. Q., Jang, C. G., Jeong, J. H., et al. (2018). Role of dopamine D1 receptor in 3-fluoromethamphetamine-induced neurotoxicity in mice. *Neurochem. Int.* 113, 69–84. doi:10.1016/j.neuint.2017.11.017

Nouri, K., Anooshe, M., Karimi-Haghighi, S., Mousavi, Z., and Haghparast, A. (2021). Involvement of hippocampal D1-like dopamine receptors in the inhibitory effect of cannabidiol on acquisition and expression of methamphetamine-induced conditioned place preference. *Neurochem. Res.* 46 (8), 2008–2018. doi:10.1007/s11064-021-03350-w

Park, H. J., Zhao, T. T., Park, K. H., and Lee, M. K. (2019). Repeated treatments with the D(1) dopamine receptor agonist SKF-38393 modulate cell viability via sustained ERK-Bad-Bax activation in dopaminergic neuronal cells. *Behav. Brain Res.* 367, 166–175. doi:10.1016/j.bbr.2019.03.035

Premoli, M., Aria, F., Bonini, S. A., Maccarinelli, G., Gianoncelli, A., Pina, S. D., et al. (2019). Cannabidiol: Recent advances and new insights for neuropsychiatric disorders treatment. *Life Sci.* 224, 120–127. doi:10.1016/j.lfs.2019.03.053

Qiao, D., Xu, J., Le, C., Huang, E., Liu, C., Qiu, P., et al. (2014). Insulin-like growth factor binding protein 5 (IGFBP5) mediates methamphetamine-induced dopaminergic neuron apoptosis. *Toxicol. Lett.* 230 (3), 444–453. doi:10.1016/j.toxlet.2014.08.010

Razavi, Y., Keyhanfar, F., Haghparast, A., Shabani, R., and Mehdizadeh, M. (2021). Cannabidiol promotes neurogenesis in the dentate gyrus during an abstinence period in rats following chronic exposure to methamphetamine. *Metab. Brain Dis.* 36 (6), 1381–1390. doi:10.1007/s11011-021-00774-9

Roberts, A. J., Maung, R., Sejbuk, N. E., Ake, C., and Kaul, M. (2010). Alteration of Methamphetamine-induced stereotypic behaviour in transgenic mice expressing HIV-1 envelope protein gp120. *J. Neurosci. Methods* 186 (2), 222–225. doi:10.1016/j.jneumeth.2009.11.007

Russell, J. C., Blue, M. E., Johnston, M. V., Naidu, S., and Hossain, M. A. (2007). Enhanced cell death in MeCP2 null cerebellar granule neurons exposed to excitotoxicity and hypoxia. *Neuroscience* 150 (3), 563–574. doi:10.1016/j.neuroscience.2007.09.076

Ryan, D., Drysdale, A. J., Lafourcade, C., Pertwee, R. G., and Platt, B. (2009). Cannabidiol targets mitochondria to regulate intracellular Ca2+ levels. *J. Neurosci.* 29 (7), 2053–2063. doi:10.1523/jneurosci.4212-08.2009

Sams-Dodd, F. (1998). Effects of continuous D-amphetamine and phencyclidine administration on social behaviour, stereotyped behaviour, and locomotor activity in rats. *Neuropsychopharmacology* 19 (1), 18–25. doi:10.1016/s0893-133x(97)00200-5

Shaerzadeh, F., Streit, W. J., Heysieattalab, S., and Khoshbouei, H. (2018). Methamphetamine neurotoxicity, microglia, and neuroinflammation. *J. Neuroinflammation* 15 (1), 341. doi:10.1186/s12974-018-1385-0

Shen, B., Zhang, D., Zeng, X., Guan, L., Yang, G., Liu, L., et al. (2022). Cannabidiol inhibits methamphetamine-induced dopamine release via modulation of the DRD1-MeCP2-BDNF-TrkB signaling pathway. *Psychopharmacol. Berl.* 239, 1521–1537. doi:10.1007/s00213-021-06051-y

Shukla, M., and Vincent, B. (2020). The multi-faceted impact of methamphetamine on Alzheimer's disease: From a triggering role to a possible therapeutic use. *Ageing Res. Rev.* 60, 101062. doi:10.1016/j.arr.2020.101062

Sidhu, A., Olde, B., Humblot, N., Kimura, K., and Gardner, N. (1999). Regulation of human D1 dopamine receptor function and gene expression in SK-N-MC neuroblastoma cells. *Neuroscience* 91 (2), 537–547. doi:10.1016/s0306-4522(98)00555-7

Skene, P. J., Illingworth, R. S., Webb, S., Kerr, A. R., James, K. D., Turner, D. J., et al. (2010). Neuronal MeCP2 is expressed at near histone-octamer levels and globally alters the chromatin state. *Mol. Cell* 37 (4), 457–468. doi:10.1016/j.molcel.2010.01.030

Sun, D., Yue, Q., Guo, W., Li, T., Zhang, J., Li, G., et al. (2015). Neuroprotection of resveratrol against neurotoxicity induced by methamphetamine in mouse mesencephalic dopaminergic neurons. *Biofactors* 41 (4), 252–260. doi:10.1002/biof.1221

Uno, K., Miyazaki, T., Sodeyama, K., Miyamoto, Y., and Nitta, A. (2017). Methamphetamine induces Shati/Nat8L expression in the mouse nucleus accumbens via CREB- and dopamine D1 receptor-dependent mechanism. *PLoS One* 12 (3), e0174196. doi:10.1371/journal.pone.0174196

UNODC (2021). World drug report 2021. (United Nations publication, Sales No. E.21.XI.8). Available online: www.unodc.org/unodc/en/data-and-analysis/wdr2021.html (Accessed April 18, 2022).

Vitale, R. M., Iannotti, F. A., and Amodeo, P. (2021). The (Poly)Pharmacology of cannabidiol in neurological and neuropsychiatric disorders: Molecular mechanisms and targets. *Int. J. Mol. Sci.* 22 (9), 4876. doi:10.3390/ijms22094876

Wang, B., Chen, T., Xue, L., Wang, J., Jia, Y., Li, G., et al. (2019). Methamphetamine exacerbates neuroinflammatory response to lipopolysaccharide by activating dopamine D1-like receptors. *Int. Immunopharmacol.* 73, 1–9. doi:10.1016/j.intimp.2019.04.053

Wu, J., Zhu, D., Zhang, J., Li, G., Liu, Z., and Sun, J. (2016). Melatonin treatment during the incubation of sensitization attenuates methamphetamine-induced locomotor sensitization and MeCP2 expression. *Prog. Neuropsychopharmacol. Biol. Psychiatry* 65, 145–152. doi:10.1016/j.pnpbp.2015.09.008

Xie, X. L., He, J. T., Wang, Z. T., Xiao, H. Q., Zhou, W. T., Du, S. H., et al. (2018). Lactulose attenuates METH-induced neurotoxicity by alleviating the impaired autophagy, stabilizing the perturbed antioxidant system and suppressing apoptosis in rat striatum. *Toxicol. Lett.* 289, 107–113. doi:10.1016/j.toxlet.2018.03.015

Xu, X., Huang, E., Luo, B., Cai, D., Zhao, X., Luo, Q., et al. (2018). Methamphetamine exposure triggers apoptosis and autophagy in neuronal cells by activating the C/EBPβ-related signaling pathway. *FASEB J.* 32, 6737–6759. doi:10.1096/fj.201701460RRR

Yang, G., Liu, L., Zhang, R., Li, J., Leung, C. K., Huang, J., et al. (2020). Cannabidiol attenuates methamphetamine-induced conditioned place preference via the Sigma1R/AKT/GSK-3β/CREB signaling pathway in rats. *Toxicol. Res.* 9 (3), 202–211. doi:10.1093/toxres/tfaa021

Young, J. I., Hong, E. P., Castle, J. C., Crespo-Barreto, J., Bowman, A. B., Rose, M. F., et al. (2005). Regulation of RNA splicing by the methylation-dependent transcriptional repressor methyl-CpG binding protein 2. *Proc. Natl. Acad. Sci. U. S. A.* 102 (49), 17551–17558. doi:10.1073/pnas.0507856102

Zhang, Y., Ye, F., Zhang, T., Lv, S., Zhou, L., Du, D., et al. (2021). Structural basis of ketamine action on human NMDA receptors. *Nature* 596 (7871), 301–305. doi:10.1038/s41586-021-03769-9

frontiers | Frontiers in Pharmacology

TYPE Original Research
PUBLISHED 25 October 2022
DOI 10.3389/fphar.2022.919605

OPEN ACCESS

EDITED BY
Carmen Rodriguez Cueto,
Center for Biomedical Research on Neurodegenerative Diseases (CIBERNED), Spain

REVIEWED BY
Elena Cichero,
University of Genoa, Italy
David B Finlay,
University of Otago, New Zealand

*CORRESPONDENCE
Ganesh A. Thakur,
g.thakur@northeastern.edu
Robert B. Laprairie,
robert.laprairie@usask.ca

SPECIALTY SECTION
This article was submitted to Neuropharmacology, a section of the journal Frontiers in Pharmacology

RECEIVED 13 April 2022
ACCEPTED 07 October 2022
PUBLISHED 25 October 2022

CITATION
Brandt AL, Garai S, Zagzoog A, Hurst DP, Stevenson LA, Pertwee RG, Imler GH, Reggio PH, Thakur GA and Laprairie RB (2022), Pharmacological evaluation of enantiomerically separated positive allosteric modulators of cannabinoid 1 receptor, GAT591 and GAT593. *Front. Pharmacol.* 13:919605. doi: 10.3389/fphar.2022.919605

Pharmacological evaluation of enantiomerically separated positive allosteric modulators of cannabinoid 1 receptor, GAT591 and GAT593

Asher L. Brandt[1], Sumanta Garai[2], Ayat Zagzoog[1], Dow P. Hurst[3], Lesley A. Stevenson[4], Roger G. Pertwee[4], Gregory H. Imler[5], Patricia H. Reggio[3], Ganesh A. Thakur[2]* and Robert B. Laprairie[1,6]*

[1]College of Pharmacy and Nutrition, University of Saskatchewan, Saskatoon, SK, Canada, [2]Department of Pharmaceutical Sciences, Bouvé College of Health Sciences, Boston, MA, United States, [3]Center for Drug Discovery, University of North Carolina Greensboro, Greensboro, NC, United States, [4]School of Medicine, Medical Sciences and Nutrition, Institute of Medical Sciences, University of Aberdeen, Aberdeen, Scotland, United Kingdom, [5]Centre for Biomolecular Science and Engineering, Naval Research Laboratory, Washington, DC, United States, [6]Department of Pharmacology, Faculty of Medicine, Dalhousie University, Halifax, NS, Canada

Positive allosteric modulation of the type 1 cannabinoid receptor (CB1R) has substantial potential to treat both neurological and immune disorders. To date, a few studies have evaluated the structure-activity relationship (SAR) for CB1R positive allosteric modulators (PAMs). In this study, we separated the enantiomers of the previously characterized two potent CB1R ago-PAMs GAT591 and GAT593 to determine their biochemical activity at CB1R. Separating the enantiomers showed that the *R*-enantiomers (GAT1665 and GAT1667) displayed mixed allosteric agonist-PAM activity at CB1R while the *S*-enantiomers (GAT1664 and GAT1666) showed moderate activity. Furthermore, we observed that the *R* and *S*-enantiomers had distinct binding sites on CB1R, which led to their distinct behavior both *in vitro* and *in vivo*. The *R*-enantiomers (GAT1665 and GAT1667) produced ago-PAM effects *in vitro*, and PAM effects in the *in vivo* behavioral triad, indicating that the *in vivo* activity of these ligands may occur *via* PAM rather than agonist-based mechanisms. Overall, this study provides mechanistic insight into enantiospecific interaction of 2-phenylindole class of CB1R allosteric modulators, which have shown therapeutic potential in the treatment of pain, epilepsy, glaucoma, and Huntington's disease.

KEYWORDS

type 1 cannabinoid receptor (CB1R), positive allosteric modulator, allosteric agonist, molecular pharmacology, *In silico* modeling, molecular mechanics-generalized born surface area (MMGBSA)

1 Introduction

The endogenous cannabinoid system (ECS) is composed of endogenous ligands (e.g. anandamide [AEA] and 2-arachidonoylglycerol [2-AG]), anabolic and catabolic enzymes, and receptors (the predominant receptors being the type 1 and 2 cannabinoid receptors [CB1R, CB2R]) (Di Marzo, 2018; Estrada and Contereras, 2020). The ECS is ubiquitous in the human body (Patel et al., 2021). Both CB1R and CB2R are class A G protein-coupled receptors (GPCRs) (Lutz, 2020). CB1R is most-abundant in the brain and central nervous system (CNS) whereas CB2R is most-abundant in cells of the immune system (Iannotti et al., 2016; Hryhorowicz et al., 2019). The primary role of CB1R is to regulate mood, diet, sleep and pain sensation whereas CB2R regulates immune responses (Iannotti et al., 2016). Both receptors are activated by the endogenous ligands AEA and 2-AG (Carrera et al., 2020). Due to the ubiquitous nature of CB1R and CB2R, the ECS is considered a potential target for a wide array of diseases, but CB1R in particular is considered a target for the treatment of pain and neurological disorders such as Parkinson's disease, Huntington's disease, and epilepsy (Perez-Olives et al., 2021).

The intoxicating effects of *Cannabis* represent a major limitation to its use as medicine. The intoxicating effects of *Cannabis* are thought to be due to Δ^9-tetrahydrocannabinol (THC) binding to the orthosteric site of CB1R (Slivicki et al., 2020). It has previously been hypothesized that the intoxicating properties of CB1R activation could be avoided if a drug bound to the allosteric site of the receptor promoted endogenous ligand activation without direct activation of CB1R because the endogenous cannabinoids AEA and 2-AG are not known to produce intoxicating effects, tolerance, or dependence (Slivicki et al., 2020). Allosteric modulators may be positive allosteric modulators (PAMs), negative allosteric modulators (NAMs), or silent allosteric modulators (Leo and Abood, 2021). A PAM enhances the effect of the primary ligand, a NAM reduces the effect of the primary ligand, and a silent allosteric ligand does not affect the pharmacology of the orthosteric ligand (Mielnik et al., 2021). The first described CB1R allosteric modulator was the indole carboxamide Org27569, which later drove the development of indole sulfonamides as potent CB1R NAMs (Greig et al., 2016; Dopart et al., 2018).

In a previous paper, we reported on the pharmacology of racemic CB1R allosteric modulators GAT591 and GAT593 (Figure 1), wherein we observed these ligands have both allosteric-agonist and positive allosteric modulator (ago-PAM) properties (Garai et al., 2020). We found that GAT591 and GAT593 act at allosteric sites due to their ability to enhance the binding of [^{3}H]CP55,940 at CB1R and at the same time modulate the receptor in absence of an orthostreric ligand (Garai et al., 2020). Biased agonism describes the ability of a ligand to preferentially activate one signalling pathway compared to another; for example G protein-*versus* βarrestin-mediated signaling (Leo and Abood, 2021; Patel et al., 2021). Our previous work has shown that the racemic mixtures GAT591 and GAT593 displayed bias towards $G\alpha_{i/o}$ signaling as compared to βarrestin (Garai et al., 2020), which earlier work indicated was correlated with improved cell viability (Laprairie et al., 2016, 2019). Additional studies from our group support the idea that G protein bias of PAMs is correlated with improved outcomes in rodent models of Huntington's disease, pain, and absence epilepsy (Laprairie et al., 2019; Slivicki et al., 2020; Roebuck et al., 2021); whereas βarrestin bias may be correlated with reduced cell viability and increases pathology in animal models of absence epilepsy and Huntington's disease (Laprairie et al., 2016; Roebuck et al., 2020). One of the challenges in developing ligands for GPCRs is biased agonism (Leo and Abood, 2021; Patel et al., 2021). To further understand molecular mechanism(s) of action and probe for potential enantio specific interaction, we separated the enantiomers, determined their absolute stereochemistry and did biochemical characterization using cAMP and βarrestin2 assays to determine their allosteric-agonist and PAM activity. Previously we observed the distinct pharmacology between the enantiomers of (±)-GAT211, where (*R*)-GAT228 was an allosteric-agonist and the opposite enantiomer, (*S*)-GAT229, showed PAM activity at CB1R within the assays and cell line used (Laprairie et al., 2017). In this study we observed that the enantiomers of GAT591 and GAT593 display unique *in vitro* and *in vivo* effects that are likely to be associated with their unique modes of binding to CB1R.

2 Experimental section

2.1 *In vitro* evaluation

2.1.1 Compounds used

CP55,940 and THC were purchased from Cayman (Ann Arbor, MI) and Sigma-Aldrich (Mississauga, ON), respectively. All other tested compounds were obtained from Dr. Ganesh Thakur, Northeastern University. All compounds were initially dissolved in dimethylsulfoxide (DMSO) and diluted in a 10% DMSO solution in phosphate-buffered saline (PBS). Compounds were added directly to cell culture at the time and concentrations indicated at a final concentration of 0.1% DMSO.

2.1.2 Cell culture

HitHunter (cAMP) and PathHunter (βarrestin2) Chinese hamster ovary (CHO)-K1 cells stably-expressing human CB1R (hCB1R) from DiscoveRx (Eurofins, Freemont, CA) were maintained at 37°C, 5% CO_2 in DMEM/F-12 containing 10% fetal bovine serum (FBS) and 5 U × 10^4 U penicillin/streptomycin (ThermoFisher, Mississauga, ON). In addition, 800 μg/ml geneticin was used for CHO-K1 hCB1R HitHunter cAMP cells and 800 μg/ml geneticin and 300 μg/ml hygromycin B was used for CHO-K1 hCB1R PathHunter βarrestin2 cells.

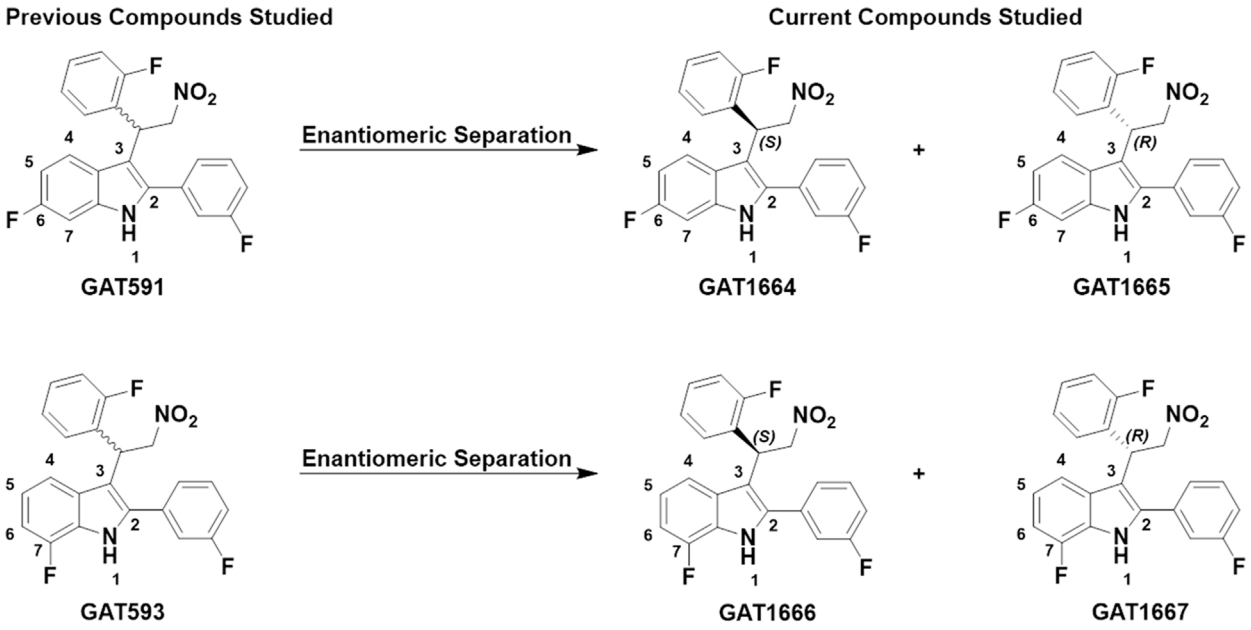

FIGURE 1
GAT591 previously studied was separated out into its respective enantiomers (GAT1664 and GAT1665) and GAT593 was separated out into its respective enantiomers (GAT1666 and GAT1667). The difference between GAT1664 and GAT1665 vs. GAT1666 and GAT1667 is the position of the fluorine in the indole ring.

2.1.3 HitHunter cAMP assay

cAMP inhibition was performed in the presence of 10 μM forskolin (FSK) using the DiscoveRx HitHunter assay in hCB1R CHO-K1 cells. Cells (16,000 cells/well in 96 well plates) were incubated overnight in Opti-MEM (Invitrogen) containing 1% FBS at 37°C and 5% CO_2. Opti-MEM media was removed and replaced with cell assay buffer (DiscoveRx) and then cells were simultaneously treated with 10 μM FSK and experimental compounds (0.10 nM–10 μM) for 90 min cAMP antibody solution and working detection solutions were added according to the manufacturer's protocol (DiscoveRx), and cells were incubated for 60 min at room temperature. cAMP solution A was added according to the manufacturer's protocol (DiscoveRx) and cells were incubated for an additional 60 min at room temperature before chemiluminescence was measured on a Cytation5 plate reader (top read, gain 200, integration time 10 s). Data are presented as percent maximal CP55,940-dependent inhibition of cAMP accumulation.

2.1.4 PathHunter βarrestin2 assay

βarrestin2 recruitment was determined using the hCB1R CHO-K1 cell PathHunter assay (DiscoveRx). Cells (16,000 cells/well in 96 well plates) were incubated overnight in Opti-MEM (Invitrogen) containing 1% FBS at 37°C and 5% CO_2. Cells were then simultaneously treated with experimental compounds (0.10 nM–10 μM) for 90 min. Detection solution was added to cells according to the manufacturer's protocol (DiscoveRx), and cells were incubated for 60 min at room temperature. Chemiluminescence was measured on a Cytation5 plate reader (top read, gain 200, integration time 10 s). Data are presented as percent maximal CP55,940-dependent stimulation.

2.1.5 [^{3}H]CP55,940 radioligand displacement assay

Previous work from our group has shown that CB1R PAMs enhance orthosteric agonist binding (e.g. CP55,940) (Laprairie et al., 2017; Garai et al., 2020). Radioligand binding assays were carried out with 1 nM [^{3}H]CP55,940 in Tris buffer (75 mM Tris-HCl, 12.5 mM $MgCl_2$, 1 mM ethylenediaminetetraacetic acid (EDTA), 1% bovine serum albumin (BSA), pH 7.4) with a total assay volume of 200 μl. The assay began with the addition of transfected hCB1R CHO-K1 cell membranes (25 μg protein per well). The assays were left to equilibrate at room temperature for 2 h before vacuum filtration using a Millipore Sigma 12-well sampling manifold and filter paper that had been soaked in wash buffer. Each reaction well was washed 3 times with a 2 ml aliquot of Tris-binding buffer. The filters were removed then submerged in 5 ml of scintillation fluid (Ultima Gold F, PerkinElmer, Buckinghamshire, United Kingdom). Radioactivity was quantified by liquid scintillation spectrometry. Specific binding was defined as the difference between binding that occurred in

the presence and in the absence of 1 μM unlabeled CP55,940. Data are presented as percent [^{3}H]CP55,940 bound.

2.1.6 [^{35}S]GTPγS assay

This assay was conducted as described in previous reports (Garai et al., 2020). To summarize, the assay was completed in the presence of [35S]GTPγS (0.1 nM), GDP (30 μM), GTPγS (30 μM) using membranes derived from CHO-K1 cells (1 mg/ml) overexpressing hCB1R. Assay buffer consisted of 50 mM Tris, 10 mM MgCl2, 100 mM NaCl, 0.2 mM EDTA and 1 mM dithiothreitol (DTT) at pH 7.4. Membranes were incubated at 30°C for 90 min in a total volume of 500 ml. Reactions were ended by the addition of ice-cold wash buffer (50 mM Tris and 1 mg/ml BSA, pH 7.4) followed by rapid filtration under vacuum through pre-soaked Whatman GF/B glass-fibre filters in a 24-well sampling manifold (Brandel Cell Harvester; Brandel Inc., Gaithersburg, MD, United States). Reaction wells were washed six times with a 1.2 ml aliquots of Tris-binding buffer. Filters were subsequently oven-dried for 60 min and placed in 3 ml of scintillation fluid (Ultima Gold XR, PerkinElmer). Bound radioactivity was determined by liquid scintillation counting. Basal [35S]GTPγS binding was determined in the presence of 20 mM GDP without any compounds present. Non-specific binding was determined in the presence of 10 mM GTPγS.

2.2 *In vivo* evaluation

2.2.1 Triad assessment in mice

Male C57BL/6 mice (Charles River, Senneville, QC) between 4 and 7 months of age were used for these studies. Animals were group housed at the Laboratory Animal Services Unit (LASU) at the University of Saskatchewan (3-5 animals/cage) with a standard 12:12 light-dark cycle, *ad libitum* access to food and water, and environmental enrichment. Compounds administered intraperitoneally (i.p.) were prepared in vehicle [ethanol and cremophor in saline (1:1:8)]. Catalepsy was assessed in the bar holding assay 5 min after drug administration. Mice were placed so that their forepaws clasped a 0.7 cm ring clamp positioned 4.5 cm above the surface of the testing space (Zagzoog et al., 2021). The length of time the ring was held was recorded in seconds. The trial ended if the mouse turned its head or body or made 3 consecutive escape attempts to a maximum of 60 s. Body temperature was measured by rectal thermometer 15 min after drug administration. Anti-nociceptive effects were measured in the warm water (52 ± 2°C) tail-flick test 20 min after drug administration. Response in this case was defined by the removal of the tail from the warm water, with a maximal response time of 20 s. Catalepsy and tail flick data are presented as percent maximum possible effect (MPE). Compounds were administered at the doses indicated. Experimenters were blinded to treatment for all behavioral assessments and analyses. Animals were purchased, rather than bred, to reduce animal numbers. In all cases, experiments were performed with the approval of the University Animal Care Committee (UACC) at the University of Saskatchewan and are in keeping with the guidelines of the Canadian Council on Animal Care (CCAC) and the ARRIVE guidelines (Kilkenny et al., 2010).

2.3 *In silico* evaluation

2.3.1 Ligand Preparation

A conformational analysis was performed on GAT1664, GAT1665, GAT1666, and GAT1667 using Spartan'18 V1.4.5 (Spartan, 2018). A conformational search of each compound was run at ground state with molecular mechanics force fields (MMFF) (Spartan, 2018). Semi empirical calculations utilizing the PM3 Hamiltonian were carried out to calculate the equilibrium geometry of each conformer. After duplicates were eliminated, HF/6-31G* was applied to the remaining rotamers to obtain the global minimum energy conformation (Spartan, 2018).

2.3.2 CB1R model

The CB1R model has been described in detail in Hurst et al. (2019), but in brief: The CB1R model used in this study was based on the CB1R activated state crystal structure (PDB-ID: 5XRA) (Hua et al., 2017) and the cryo-EM CB1/Gi bound structure (PDB-ID: 6N4B) (Krishna Kumar et al., 2019). Structures were prepared with the Protein Preparation protocol (Suite 2019-1, Schrödinger, Inc.), mutations in the 5XRA structure were returned to wild-type, and both models were inspected for close contacts and crystal packing effects. Modification of the 5XRA structure to create the CB1R model involved calculating low free energy conformations for TMH2/7 to accommodate mutation data for S7.39, F2.61, F2.64 (Kapur et al., 2007; Shim et al., 2011). In addition, because of loop compression in the 5XRA structure, the IC1 loop from the 6N4B Gi bound structure was used in the model. TMH4 in the 5XRA CB1R* structure has tight crystal contacts on its IC end with TMH1 of another bundle because of antiparallel packing. For this reason, the conformation of TMH4 in the 6N4B Gi bound structure was used in the model. Modeller was used to remodel the EC3 loop (D6.58 to T7.33) and allow K (373) to interact with D2.63, consistent with mutation results (Fiser and Sali, 2003; Marcu et al., 2013). Modeller was also used to extend and model the N-terminus to S (88) with inclusion of the C (98) to C (107) disulfide bridge (Fay and Farrens, 2013, 2015). The receptor/ligand complex was energy minimized in Prime (Suite 2019-1, Schrödinger, Inc.). The Prime implicit membrane functionality was employed. Hydrophilic residues facing the binding crevice and within the low dielectric region of the implicit membrane were excluded from the low dielectric *via* exclusion spheres placed on each residue. The Generalized Born/Surface Area (GB/SA) continuum

solvation model for water was used with the dielectric set to 80 outside of the implicit membrane region and 2 within. A truncated Newton conjugate gradient minimization was performed using the OPLS3e force field for one iteration up to a maximum of 1,000 steps and with a 0.1 kcal/mol gradient endpoint. Constraints of 1 kcal/mol were placed on the C-alpha atoms of residues R3.50, Y5.58, L6.33, and Y7.53 to prevent the intracellular opening present in the R* structures from closing during the minimization.

2.3.3 Binding Site Identification

To identify potential binding site(s) for GAT1664, GAT1665, GAT1666 and GAT1667 at CB1R, we used the Forced-Biased Metropolis Monte Carlo simulated annealing program (MMC) as the first step (Guarnieri and Mezei, 1996; Clark et al., 2006). The MMC method has been used successfully to identify water binding sites in proteins and on DNA to identify potent and novel p38 kinase inhibitors; to identify thermolysin and T4 and lysosome biding sites; and, to identify the binding site of the negative allosteric modulator, pregnenolone (Morales et al., 2016; Zhang et al., 2020). In MMC, the molecule of interest is first divided into smaller fragments. A series of grand canonical ensembles of a molecular fragment interacting with the protein in a large simulation box are created. The Chemical potential of the system is then annealed at descending chemical potential levels, with each new level starting from the last ensemble generated from the previous one. At each step, fragment ligand poses are sampled throughout the box and over the entire protein. Fragments are treated as rigid solvents that are inserted and deleted millions of times until the lowest energy configuration is found at the explored annealing level. As the chemical potential is annealed, the number of fragments in the box decreases because the method eliminates any fragment that has a poorer free energy of interaction than the annealing level. The output of the calculation is an ensemble of ligand poses at each chemical potential level in the annealing schedule. The method is repeated for each molecular fragment. Data analysis is performed using the GENS tool in the MMC program available from the Mihaly Mezei Laboratory (Mezei, 2011).

Of particular interest in MMC calculations are fragments that persist at particular sites on the protein throughout the annealing schedule, since these fragments clearly have high affinity for those sites. Receptor regions at which all molecular fragments of a studied ligand collect are identified from MMC output. This set of sites is then refined to include only those sites at which the order of the fragments reflects the structure of the entire molecule.

GAT1664 and GAT1665 were broken into fragments that included a 6-fluoro-indole ring, a 2-fluoro-phenyl ring and a 3-fluoro-phenyl ring. GAT1666 and GAT1667 were broken into fragments that included 7-fluoro-indole ring, 2-fluoro-phenyl ring and 3-fluoro-phenyl ring. All fragments were prepared with partial charges using the Amber 2002 force field, a point-charge force field for molecular mechanics simulations of proteins based on condensed-phase quantum MMC (Wang et al., 2018). Six MMC runs were performed in which our CB1R receptor model was immersed in a box filled with copies of one of these fragments. Analysis of the MMC runs for GAT1664 and GAT1666 revealed that while each fragment bound to multiple positions on the CB1R receptor, there was only one region in which all fragments clustered. This was at the extracellular end of TMH2/3, just beneath the EC1 loop. Y2.59, a polar residue that faces lipid was found to attract the nitro group fragment, while D2.63 consistently was found interacting with the fluorinated indole fragments.

Docking: Once the two sites were confirmed, the structures of GAT1664-GAT1667 were docked in the intracellular TMH1/2/4 site with H2.41, F4.46, and W4.50 used as direct interaction sites. GAT1664 and GAT1666 were docked in the TM2/3/EC1 site with Y2.59 and D2.63 as direct interaction sites. In addition, after extensive previously published molecular dynamics calculations on unfluorinated versions of the GAT compounds (GAT1600-3), R (148) was modeled to interact directly with the carbonyl oxygens of the last turn of TMH1 and not the nitro group within the compounds (Garai et al., 2021). The receptor/ligand complexes were energy minimized in Prime (Suite 2019-1, Schrödinger, Inc.). The Prime implicit membrane functionality was employed. Hydrophilic residues facing the binding crevice and within the low dielectric region of the implicit membrane were excluded from the low dielectric *via* exclusion spheres placed on each residue. The Generalized Born/Surface Area (GB/SA) continuum solvation model for water was used with the dielectric set to 80 outside of the implicit membrane region and 2 within. A truncated Newton conjugate gradient minimization was performed using the OPLS3e force field for 1 iteration, up to a maximum of 1,000 steps and with a 0.1 kcal/mol gradient endpoint. Constraints of 1 kcal/mol placed on the c-alpha atoms of residues R3.50, Y5.58, L6.33, and Y7.53 were set to prevent the intracellular opening from closing during the minimization. The resulting docks were refined with the Induced Fit protocol (Suite 2019-1, Schrödinger, Inc.). The Glide box size was set to 12 Å3 centered on the ligand and the SP docking algorithm employed. Residues within 5 Å of the docked ligand were included in the Prime refinement stage, except in the case of the TM2/3 PAM site where S2.60 and K3.28 were excluded based on mutation data (Song and Bonner, 1996; Kapur et al., 2007). The implicit membrane previously used during the initial Prime minimization was employed here as well.

2.3.4 MMGBSA analysis

Each of the GAT1664-GAT1667 ligand-receptor complexes were evaluated *via* MMGBSA. This was the scoring function used to evaluate each complex and not Glide scores. This method is used to estimate the relative binding affinities for a list of ligands

(reported in kcal/mol). As the MMGBSA binding energies are approximate free energies of binding, a more negative value indicated stronger binding. For this computation, the VSGB solvation model was employed while the chosen force field OPLS4 was used.

2.4 Statistical analysis

Data related to EC_{50} and E_{max} in Figures 3, 4 were obtained with nonlinear regression models (3-parameter model, GraphPad Prism 9.0, San Diego, CA). Results were calculated as percent response relative to the reference agonist CP55,940 (Figure 3), percent [^{3}H]CP55,940 bound (Figure 4A), or percent stimulation above baseline (Figures 4B,C). The 3-parameter model was used for [^{3}H]CP55,940 binding assays (Figure 4A) because standard radioligand competition models that fit for K_d do not appropriately account for allosteric interactions. Significance was determined by one- or two-way ANOVA followed by Tukey's or Bonferroni's post-hoc test as indicated. $p < 0.05$ was considered significant and p values were only employed where ANOVA was used. Data related to Figure 5 was analyzed in GraphPad Prism 9.0 was used to analyze *in vivo* data and $p < 0.05$ was considered to be statistically significant. Data are expressed as mean ± SEM. Group sizes for all experiments are described in figure legends.

3 Results and discussion

Our *in vitro* study explored CB1R-dependent modulation of cAMP inhibition and βarrestin2 recruitment in CHO-K1 cells stably-expressing hCB1R with or without CP55,940. Inhibition of cAMP accumulation is $G\alpha_{i/o}$-protein mediated whereas recruitment of βarrestin2 is G-protein independent (Hryhorowicz et al., 2019). In a previous paper, GAT591 and GAT593 displayed mixed agonist and PAM (i.e. ago-PAM) activity (Garai et al., 2020). The compounds GAT591 and GAT593 contain a 50:50 racemic mixture of both *R* and *S* enantiomers. In this paper each enantiomer was investigated to determine their allosteric agonist and PAM activity, as we previously observed these properties to be enantiomerically distinct in the compounds GAT211, GAT228, and GAT229 within those experimental conditions (Laprairie et al., 2017). Separating GAT591 and GAT593 into their respective enantiomers gave GAT1664, GAT1665, GAT1666 and GAT1667 (Figure 1).

3.1 Synthesis, chiral separation and absolute stereochemistry determination

We synthesized GAT591 and GAT593 on a multigram scale using our previously published method (Garai et al., 2020). Both enantiomers of each compound were separated in high optical purity (>99%) using superfluid chiral high performance liquid chromatography (HPLC). The absolute stereochemistry of (+)-GAT1664 and (+)-GAT1666 was determined by single-crystal X-ray diffraction technique (for details see supporting formation) and was found to be "*S*" for both of these enantiomers (Figure 2). Based on this study, we can predict the absolute stereochemistry of each opposite enantiomers, (-)-GAT1665 and (-)-GAT1667 as "*R*" (Figures 1, 2).

3.2 *In vitro* evaluation

Previously, the racemic compounds GAT591 and GAT593 were characterized for their PAM activity in the

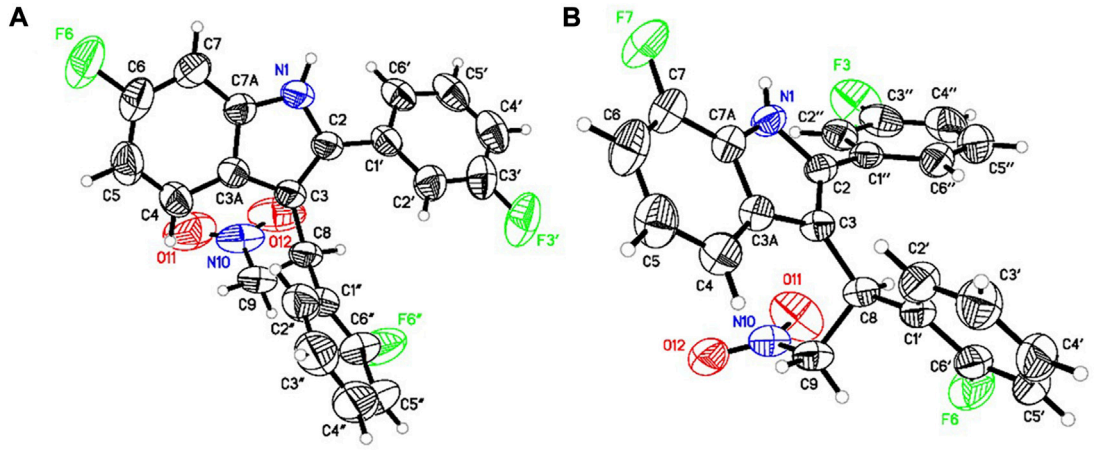

FIGURE 2
ORTEP diagram of (+)-GAT1664 [**(A)**, CCDC no. 2086717] and (+)-GAT1666 [**(B)**, CCDC no. 2086718].

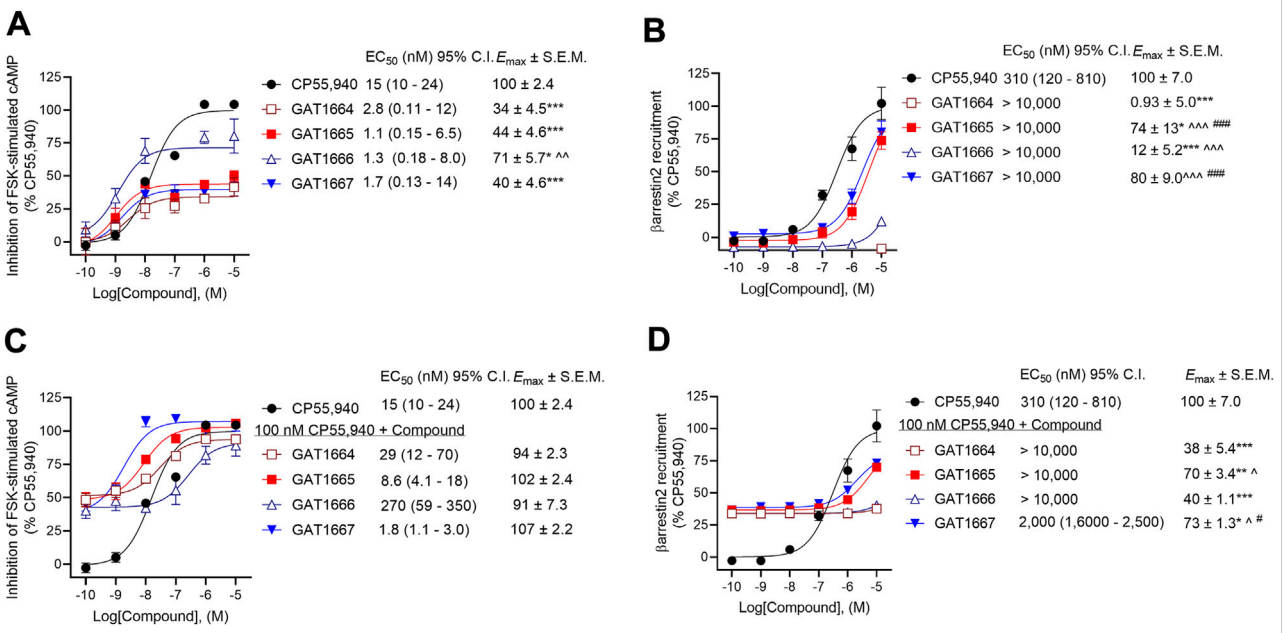

FIGURE 3
Assessment of GAT1664, GAT1665. GAT1666, and GAT1667 signaling. hCB1R CHO-K1 were treated with 0.10 nM–10 μM GAT compounds ±100 nM CP55,940. **(A)** cAMP inhibition of GAT compounds as agonists, **(B)** βarrestin2 recruitment of GAT compounds as agonists, **(C)** cAMP inhibition of GAT compounds as PAMs in the presence of 100 nM CP55,940, and **(D)** βarrestin2 recruitment of GAT compounds as PAMs in the presence of 100 nM CP55,940. cAMP inhibition and βarrestin2 recruitment data are expressed as % CP55,940 max. Data were fit to a nonlinear regression (3-parameter model, GraphPad v. 9.0) to determine EC_{50} and E_{max}. Data are mean ± SEM (E_{max}) or 95% CI (EC_{50}); n = 4 independent experiments performed in triplicate, except for CP55,940 where n = 12 independent experiments performed in triplicate as this compound was included in all assays as a reference compound. *$p < 0.05$, **$p < 0.01$, ***$p < 0.001$ compared to CP55,940; ^$p < 0.05$, ^$p < 0.01$, ^$p < 0.001$ compared to GAT1664, $^{\#}p < 0.05$, $^{\#\#\#}p < 0.001$ compared to GAT1666 as determined by one-way ANOVA followed by Tukey's post-hoc test.

presence of 100 nM CP55,940 (Garai et al., 2020). Here, CP55,940 displayed EC_{50} values of 15 nM and 310 nM in the cAMP inhibition and βarrestin2 recruitment assays respectively (Figure 3). Therefore, 100 nM CP55,940 was used in PAM assays in the current study for consistency between studies and as an intermediate concentration.

All enantiomers displayed G protein-mediated agonist activity at hCB1R as shown by their ability to inhibit cAMP production in the absence of an orthosteric agonist (Figure 3A). The ability of these compounds to augment orthosteric agonist signaling was tested in the presence of 100 nM CP55,940 because we have used this concentration of CP55,940 in previous studies (Garai et al., 2020) and because 100 nM CP55,940 produce an ~65% response relative to the maximum response observed prior to fitting the data to a nonlinear regression (Figure 3). All 4 compounds increased CP55,940's activity above that observed at the 100 nM level, consistent with either positive allosteric modulation or additive non-competitive agonism (i.e. ago-PAMs) of hCB1R in the presence of the orthosteric agonist CP55,940 in the cAMP assay (Figure 3C). As an agonist, GAT1666 displayed greater efficacy than GAT1664, and GAT1667 displayed the greatest efficacy at inhibiting cAMP as a PAM, although this was not statistically different from other compounds tested. All enantiomers displayed low nanomolar potency as agonists (Figure 3A). Although not statistically significant differences, both *R*-enantiomers (GAT1665 and GAT1667) displayed greater PAM potency and efficacy than the *S*-enantiomers (GAT1664 and GAT1666), (Figure 3C). Initial studies with the parent compound scaffold, GAT211, found that PAM activity was associated with GAT229 whereas allosteric agonist activity was associated with GAT228 (Laprairie et al., 2017). Importantly, repeated testing of GAT229 and its structural analogs over the years has shown assay-specific variability and that these enantiomers can display some allosteric agonist activity (Garai et al., 2020), including in the present study. Pure PAM activity has been observed for GAT229 in the autaptic hippocampal neuron *ex vivo* model systems (Mitjavila et al., 2018). These observations are in keeping with our earlier findings with the parent racemic ligands because PAM activity is predominantly attributable to GAT229, which shares the same spatial orientation as GAT1665 and GAT1667, and agonist activity is predominantly attributable to GAT228, which shares the same spatial orientation as GAT1664 and GAT1666 (Laprairie et al., 2017).

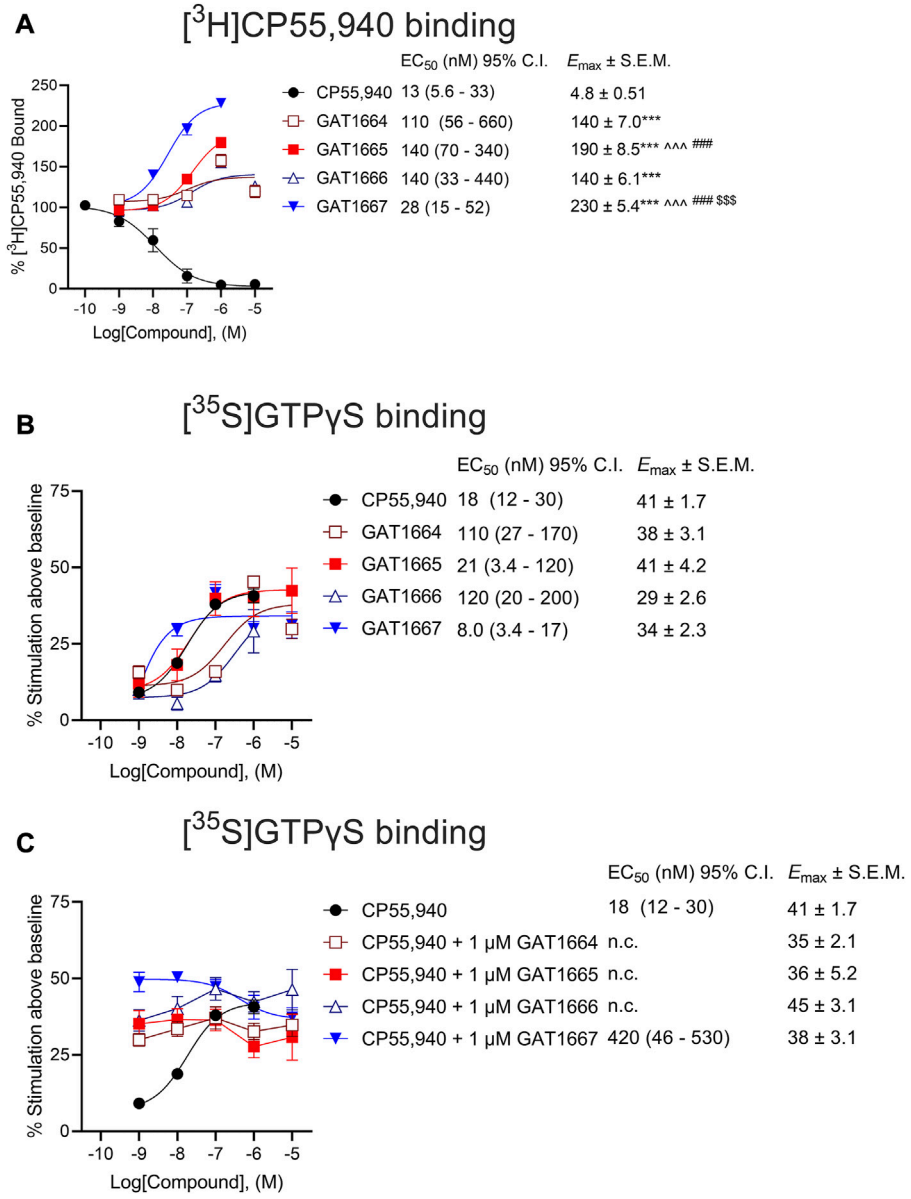

FIGURE 4
(A) Radioligand binding of 1 nM [^{3}H]CP55,940 and **(B,C)** G protein binding of [^{35}S]GTPγS to membranes from hCB1R CHO-K1 cells. hCB1R CHO-K1 cells were treated with 0.10 nM–10 μM compounds in the presence 1 nM [^{3}H]CP55,940 **(A)** or 1 nM [^{35}S]GTPγS **(B)**. Data are expressed as % radioligand bound **(A)** or % stimulation above baseline (i.e. vehicle) levels **(B,C)**. Data were fit to a nonlinear regression (3-parameter model, GraphPad v. 9.0) to determine EC_{50}, and E_{max}. Data are mean ± SEM (E_{max}) or 95% CI (EC_{50}); $n = 6$ independent experiments performed in triplicate, except for CP55,940 where $n = 12$ independent experiments performed in triplicate as this compound was included in all assays as a reference compound. ***$p < 0.001$ compared to CP55,940, ^$p < 0.001$ compared to GAT1664, $^{\$\$\$}p < 0.01$ compared to GAT1665, $^{\#\#\#}p < 0.01$ compared to GAT1666, as determined by one-way ANOVA followed by Tukey's post-hoc test.

For consistency with cAMP inhibition experiments and previous studies (Garai et al., 2020), compounds were tested for their ability to augment CP55,940-dependent βarrestin2 recruitment with 100 nM CP55,940. Both GAT1665 and GAT1667 recruited βarrestin2 as low-potency agonists and PAMs at hCB1R (Figures 3B,D). GAT1664 did not recruit βarrestin2 to hCB1R while GAT1666 displayed a weak ability to do so as an agonist (Figures 3B,D). This suggests that as agonists, GAT1665 and GAT1667 (the *R*-enantiomers) recruit βarrestin2.

The operational model described by Kenakin et al. (2012) cannot be used to describe bias for non-competitive interactions

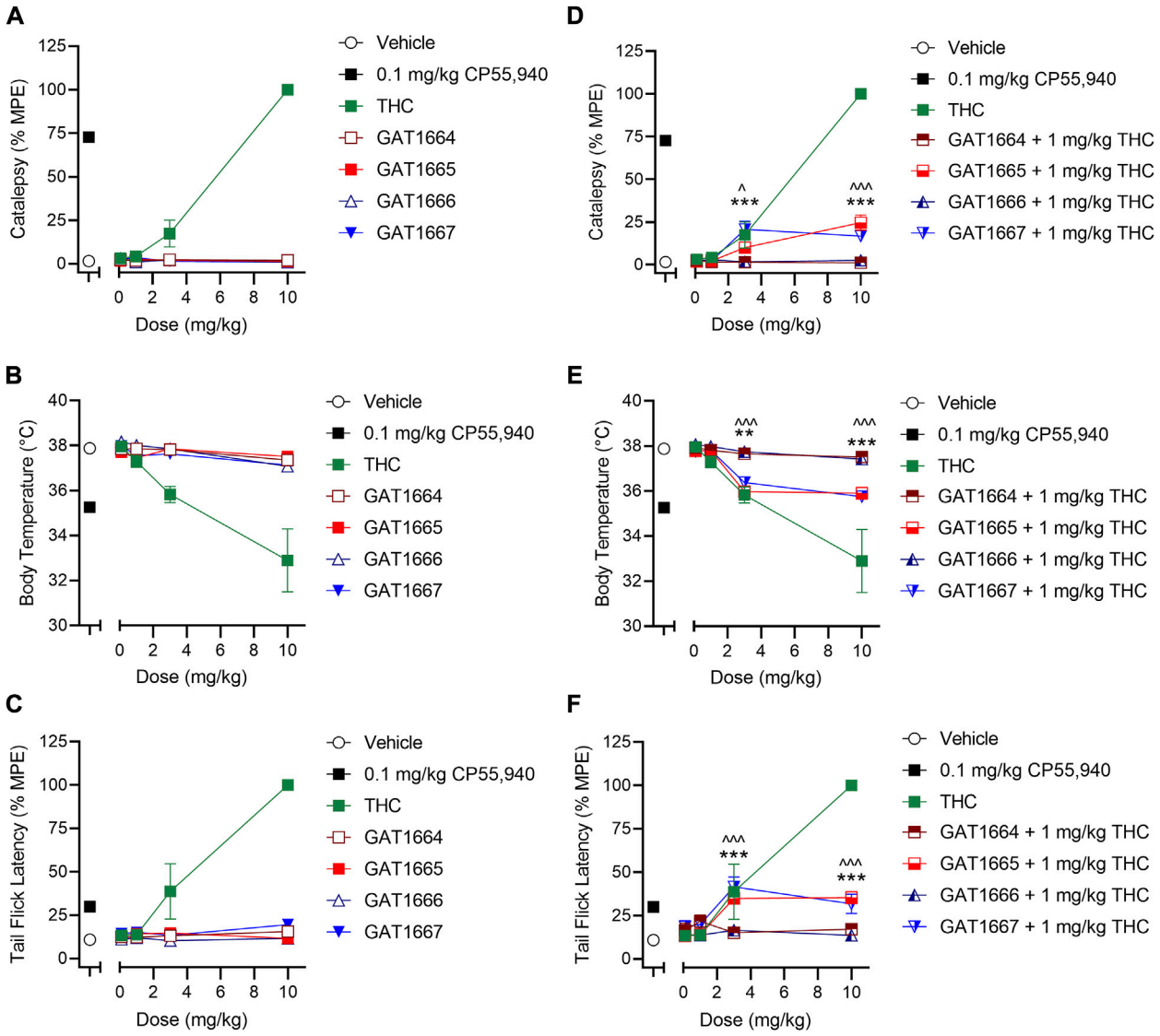

FIGURE 5
In vivo effects of GAT1664, GAT1665, GAT1666 and GAT1667 in male C57BL/6 mice. C57BL/6 mice were administered compounds either alone or co-administered with 1 mg/kg THC to assess catalepsy, hypothermia and nociception. Doses used were 0.1–10 mg/kg compound or volume-matched vehicle control (1:1:18 ethanol/cremaphor/saline) and assessment of catalepsy (%MPE 60 s) **(A,D)**, body temperature **(B,E)**, and nociception in the tail flick assay (%MPE, 20 s) **(C,F)** were performed; n = 5–10/group; data are mean ± SEM. ^$p < 0.05$, ^^^$p < 0.001$ for GAT1665 compared to 1 mg/kg THC; **$p < 0.01$, ***$p < 0.001$ for GAT1667 compared to 1 mg/kg THC as determined by two-way ANOVA followed by Bonferroni's *post-hoc* test.

accurately. Therefore, bias (ΔΔlogR) cannot be directly estimated between cAMP inhibition and βarrestin2 recruitment. Examining the potency and efficacy of compounds directly, however, we observed that as an agonist, GAT1664 displayed no activity βarrestin2 recruitment and this compound appears to heavily favour G protein-dependent inhibition of cAMP (Figure 3). GAT1666 displayed greater potency in the cAMP inhibition assay (Figure 3). GAT1665's potency and efficacy generally favored cAMP inhibition (Figure 3). GAT1667 did appear to favour inhibition of cAMP as an agonist (Figure 3). As PAMs, GAT1664 and GAT1666 displayed no activity in the βarrestin2 recruitment assay (Figure 3). GAT1665 and GAT1667 favoured cAMP inhibition relative to βarrestin2 recruitment (Figure 3F). The parent compound GAT229 shares the same spatial orientation as GAT1665 and GAT1667 and also displayed greater potency in cAMP inhibition assays when tested as a PAM (Laprairie et al., 2017). Therefore, these data confirm previous observations that this scaffold's

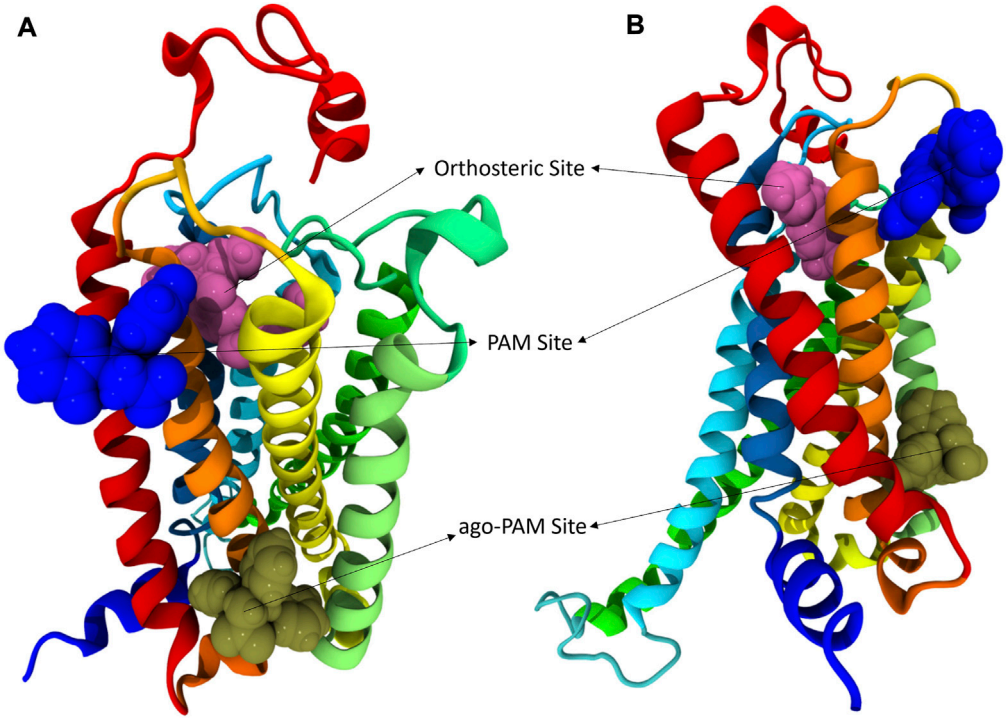

FIGURE 6
hCB1R with three different binding sites shown. In these views of hCB1R the orthosteric site is shown in magenta, an identified PAM site in blue, and another identified putative ago-PAM site in tan. Transmembrane helices are: I red, II orange, III yellow, IV light green, V green, VI cyan, and VII blue. **(A)** is a visualization of CB1R looking down on the extracellular surface. **(B)** is a visualization of CB1R looking across at the transmembrane domains.

TABLE 1 The conformational cost of GAT compounds is displayed as well as the relative affinity represented by binding energy.

Compound	Conformational cost (kcal/mol)	ΔG (kcal/mol)
GAT1664	2.35	−69.68
GAT1665	3.27	−60.77
GAT1666	2.48	−71.99
GAT1667	3.60	−64.55

spatial orientation promotes G protein PAM activity and extends earlier reports to demonstrate increased potency and efficacy of fluorine-substituted ligands as compared to parent compounds (Laprairie et al., 2017).

Next, we sought to assess the ability of these compounds to modulate orthosteric agonist binding to hCB1R. All enantiomers studied augmented [^{3}H]CP55,940 binding, consistent with their proposed PAM activity, with the *R*-enantiomers GAT1665 and to a greater extent GAT1667 increasing [^{3}H]CP55,940 binding (Figure 4A). GAT1667 displayed the greatest potency among the enantiomers tested (EC_{50} = 28 [15–52] nM). Enantiomers were also tested for their ability to promote G protein coupling in the GTPγS assay (Figures 4B,C). All of the enantiomers tested increased G protein coupling alone (i.e. in the absence of the orthosteric agonist CP55,940) with the *R*-enantiomers GAT1665 and GAT1667 being more potent than the *S*-enantiomers and GAT1667 in particular displaying the greatest potency (EC_{50} = 8.0 [3.4–17] nM) (Figure 4B). When 1 μM of each enantiomer was tested in the presence of CP55,940, each enantiomer increased G protein coupling which may be the result of allosteric non-competitive agonism or PAM activity (Figure 4C). Therefore, all enantiomers tested were able to stimulate G protein coupling alone or in the presence of CP55,940, which is consistent with their activity as ago-PAMs. Among the enantiomers tested, GAT1667 consistently displayed the greatest potency and efficacy.

3.3 *In vivo* evaluation

All enantiomers were evaluated in male C57BL/6 mice using a triad of outcomes consisting of catalepsy, body temperature, and nociception. Previous studies have shown that the racemic GAT591 and GAT593 did not produce catalepsy or hypothermia at 0.1, 1, 3, or 10 mg/kg (i.p.) compared to vehicle (Garai et al., 2020). Both GAT591 and GAT593 however did produce a dose-

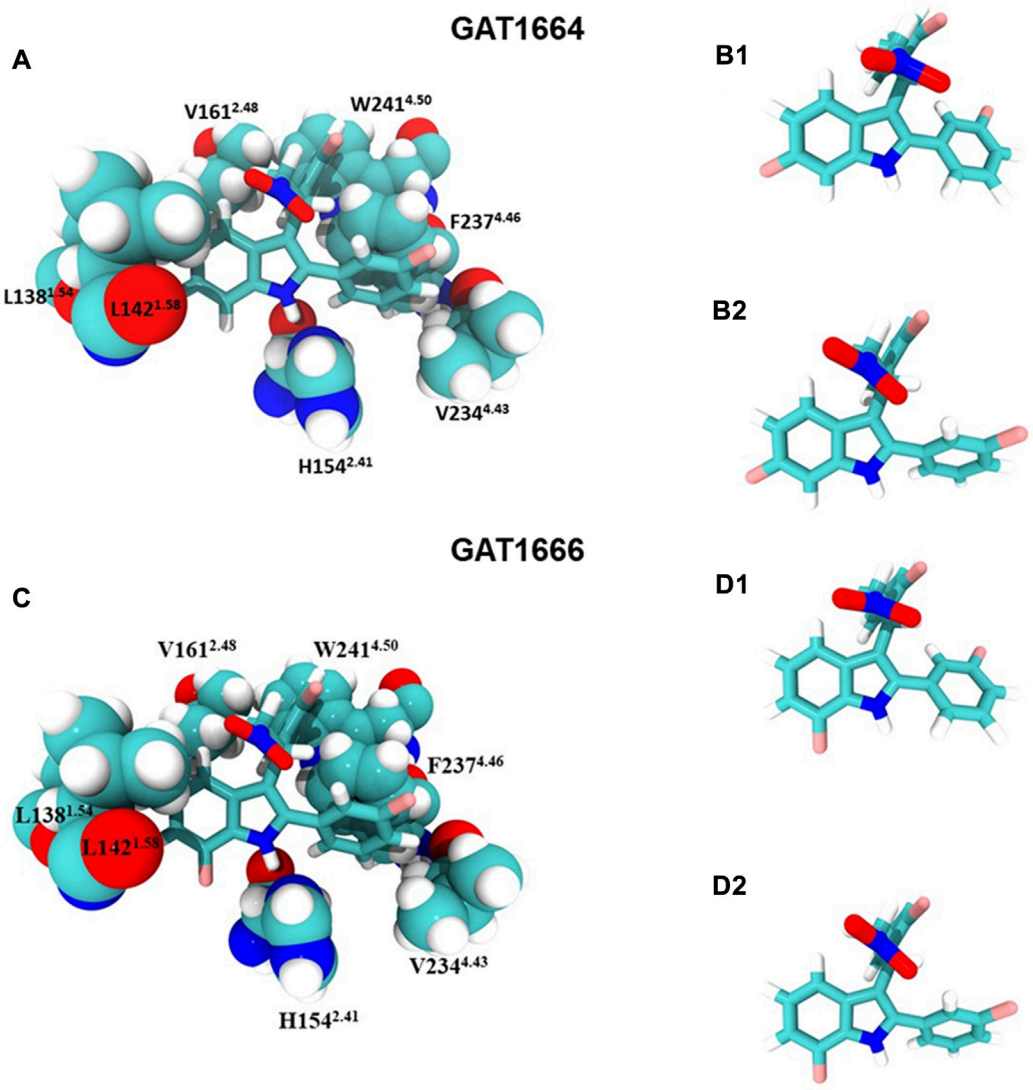

FIGURE 7
GAT1664 and GAT1666 bind to a putative allosteric agonist site. **(A)** GAT1664 main interactions and the amino acid residues of the binding pocket displayed in tan in Figure 6. The conformation of GAT1664 before it binds to hCB1R **(B1)** and then the conformation of GAT1664.after it binds to hCB1R **(B2)**. **(C)** GAT1666 main interactions and the amino acid residues of the binding pocket displayed in tan in Figure 6. The conformation of GAT1666 before it binds to hCB1R **(D1)** and then the conformation of GAT1664 after it binds to hCB1R **(D2)**.

dependent anti-nociceptive effect in the tail flick assay that was significant relative to vehicle at 3 and 10 mg/kg (Garai et al., 2020). In this study we evaluated all separated optically pure enantiomers in a triad assay. When tested alone, GAT1664, GAT1665, GAT1666 and GAT1667 did not produce catalepsy, hypothermia, or anti-nociceptive effects at 0.1, 1, 3, or 10 mg/kg i.p. compared to vehicle (Figures 5A–C). We also tested these enantiomers as PAMs by co-administering a sub-threshold dose of 1 mg/kg THC with each GAT compound. THC was selected as a common CB1R partial agonist that could produce a moderate *in vivo* response to be modulated by our compounds of interest. It was found that GAT1665 and GAT1667 displayed significant cataleptic, hypothermic, and anti-nociceptive effects at 3 and 10 mg/kg i.p. compared to vehicle (Figures 5D–F). Therefore, GAT1664, GAT1665, GAT1666, and GAT1667 did not affect animal responses to catalepsy, body temperature, or nociception in the warm water tail flick assay in normal, otherwise healthy adult mice as agonists; but GAT1665 and GAT1667 were able to augment THC's effects *in vivo* when administered once. For comparison, the racemic parent compounds, GAT591 and GAT593, do evoke anti-nociceptive responses *in vivo* when administered alone (Laprairie et al., 2017; Garai et al., 2020).

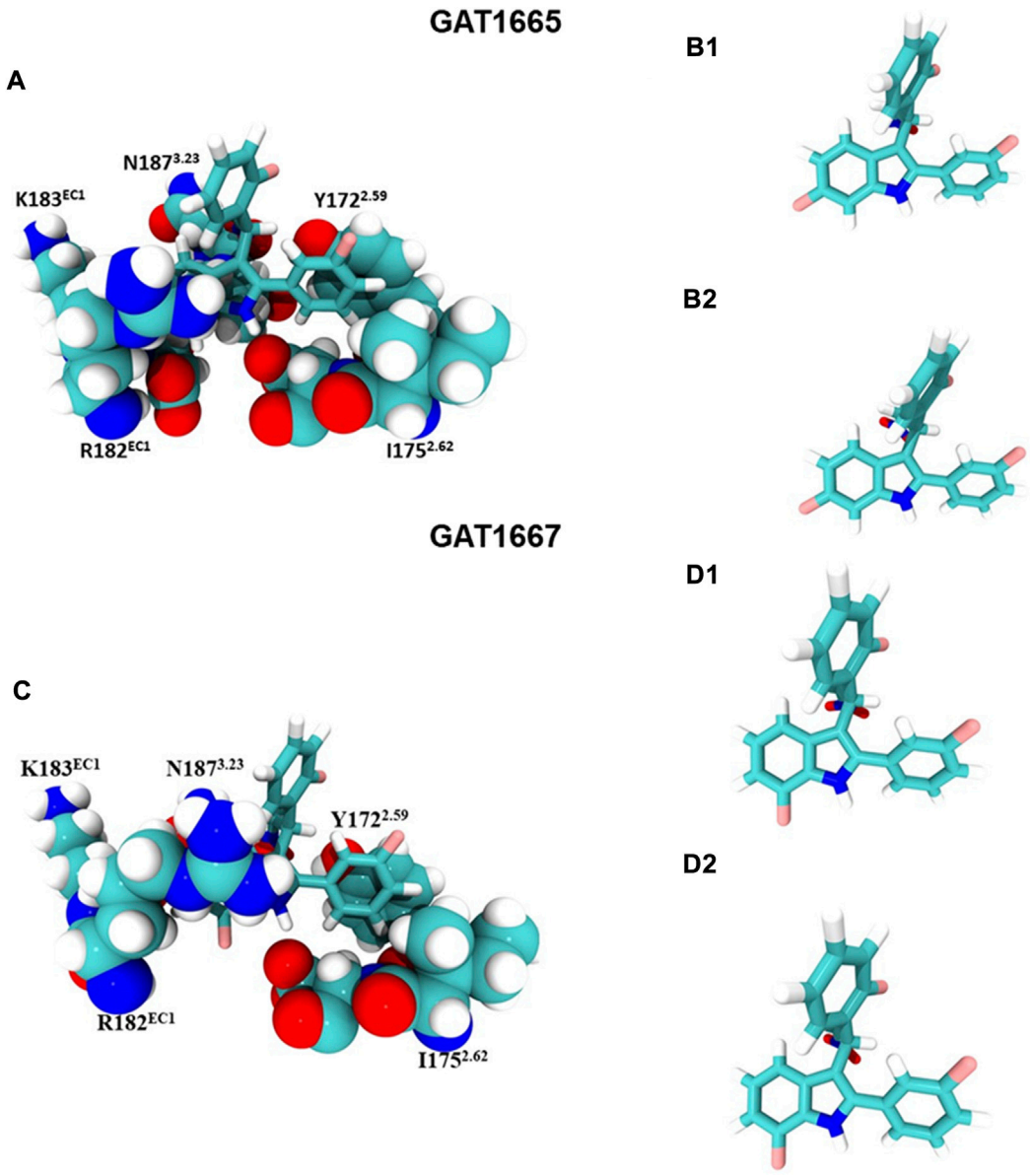

FIGURE 8
GAT1665 and GAT1667 bind to a putative PAM site. (**A**) GAT1665 main interactions and the amino acid residues of the binding pocket displayed in pink in Figure 6. The conformation of GAT1665 before it binds to hCB1R **(B1)** and then the conformation of GAT1665 after it binds to hCB1R **(B2)**. **(C)** GAT1667 main interactions and the amino acid residues of the binding pocket displayed in pink in Figure 6. The conformation of GAT1667 before it binds to hCB1R **(D1)** and then the conformation of GAT1667 after it binds to hCB1R **(D2)**.

3.4 *In silico* studies

Compounds were docked to a modelled structure of hCB1R to determine their putative binding sites within the receptor. GAT1664 and GAT1666 displayed the greatest modelled affinity to an allosteric site on hCB1R proximal to the intracellular face of the receptor in tan (Figures 6A,B). An H-bond exists between the indole hydrogen in white and the nitrogen atom in blue (H–N distance 1.96 Å) on H154$^{2.41}$ (Figure 6A). One of the fluorobenzyl groups on GAT has a face-to-face π-π interaction with F237$^{4.46}$ (4.03Å) while the other fluorobenzyl has a T-shaped π-π interaction with each ring on W241$^{4.50}$ (4.96 Å to the 6—membered ring; 5.09 Å to the 5—membered ring) (Figure 6A). Upon binding to hCB1R the conformation of the *ortho*-fluorobenzyl substituent on GAT1664 rotates 90°. The conformational cost for this rotation is 2.35 kcal/mol (Table 1). GAT1666 has the same binding pose, thus the binding energy was measured to look at

the relative affinity. GAT1666 is more stable than GAT1664 by 2.31 kcal/mol (ΔG GAT1666—ΔG GAT1664) which suggests that it has a higher affinity to the allosteric site of hCB1R shown in tan (Figure 6). This can be attributed to changing the fluorine on the sixth position of the indole (GAT1664) to the seventh position on the indole (GAT1666). The binding of a compound to this site may allow it to act as an agonist by promoting the X1 = *g* + → trans conformation of residue F4.46, facilitating breaking of the R3.50/D6.30 ionic lock which has been shown to activate CB1R (Figures 6, 7) (Hurst et al., 2019).

GAT1665 and GAT1667 displayed the greatest modelled affinity to a distinct allosteric site on hCB1R relative to GAT1664 and GAT1666 (Figures 6, 8). The NO_2 group on GAT1665 has a H-bond between 1 of the oxygens shown in red and a hydrogen atom on $Y172^{2.59}$ (O–H distance 2.17 Å) (Figure 8). Another H-bond exists between the indole hydrogen in white and an oxygen atom in red on $D176^{2.63}$ (H–O distance 2.29 Å) (Figure 8). A cation-π interaction exists between $R182^{EC1}$ and each ring on the indole on GAT1665 (six–membered ring centroid on indole to NH_2^+ on $R182^{EC1}$ distance 3.59 Å; five–membered ring centroid on indole to NH_2^+ on $R182^{EC1}$ distance 3.66 Å) (Figure 8). One of the fluorobenzyl groups on GAT has a face-to-face π-π interaction with $Y172^{2.59}$ (4.05 Å) (Figure 8). Upon binding to hCB1R the conformation of the NO_2 rotates in order to H-bond with $Y172^{2.59}$ (Table 1). The conformational cost for this rotation is 3.27 kcal/mol. If we compare the binding energy of GAT1665 and GAT1667 it is apparent that GAT1667 is more stable than GAT1665 bound to the PAM site by 4.78 kcal/mol (ΔG GAT1667—ΔG GAT1665). This can be attributed to changing the fluorine on the sixth position of the indole (GAT1665) to the seventh position on the indole (GAT1667). The previously characterized compound GAT229 also binds to this site and lacks intrinsic activity thus both these compounds alone cannot induce the active state of hCB1R and thus are PAMs. The *R*-enantiomers (GAT1665 and GAT1667) undergo a smaller conformational cost than the *S*-enantiomers (GAT1664 and GAT1666) upon binding to their respective sites on hCB1R (Table 1). The *R*-enantiomers (GAT1665 and GAT1667) bind to the ago-PAM site (ΔG = −60.77 and −64.55 kcal/mol) significantly weaker than the *S*-enantiomers (GAT1664 and GAT1666) bind to the PAM site (−69.68 and −71.99 kcal/mol). Of note, binding of enantiomers to either site was not absolute but was more energetically favourable for the *S*-enantiomers to bind near the intracellular surface and the *R*-enantiomers to bind near the first extracellular loop.

4 Conclusion

In summary, the purified enantiomers of GAT591 and GAT593 displayed unique pharmacology. The purified enantiomers GAT1664, GAT1665, GAT1666, and GAT1667 bound to hCB1R in the low nM range and were shown to enhance binding of [^{3}H]CP55,940 at hCB1R. Enhancing the binding of an orthosteric ligand is a characteristic of a PAM and these observations are consistent with all compounds operating in part *via* positive allostery and/or non-competitive allosteric agonism (Alaverdashvili and Laprairie, 2018; Kenakin and Strachan, 2018). Future explorations of these compounds will utilize full concentration-response curves of these compounds with and without CP55,940 or an endogenous orthosteric agonist (e.g. 2-AG). Such more in-depth experiments will allow for the use an operational model of allosterism that quantifies co-operativity effects on potency, efficacy, and bias as our group has done previously for both PAMs and NAMs (Laprairie et al., 2016; Laprairie et al., 2017); and determine whether the tested compounds display probe-dependence.

In addition to this, we demonstrated that these enantiomers activate hCB1R-dependent inhibition of cAMP and βarrestin2 recruitment. All of the GAT compounds tested here inhibited cAMP accumulation as allosteric agonists and PAMs (i.e. ago-PAMs), with GAT1665 and GAT1667 displaying the greatest potency and efficacy as CB1R PAMs in the presence of 100 nM CP55,940. In the βarrestin2 assay, GAT1665 and GAT1667 (*R*-enantiomers) acted as ago-PAM's while GAT1664 and GAT1666 (*S*-enantiomers) showed little to no activity as either an agonist or PAM. In the G protein coupling assay, the *R*-enantiomers GAT1665 and GAT1667 also showed higher potency and efficacy than *S*-enantiomers as agonists and PAMs. As for the *in vivo* studies, no compounds tested produced catalepsy, hypothermia at or antinociceptive effects at 0.1, 1, 3 or 10 mg/kg i.p. compared to vehicle when tested alone, but GAT1665 and GAT1667 did potentiate the effects of THC as ago-PAMs. These data are congruent with previous observations that CB1R ago-PAMs are inactive or minimally active *in vivo* in wild-type, otherwise healthy animals under non-pathological and acute conditions (Alaverdashvili and Laprairie, 2018). In planned future studies, these ago-PAMs will be further assessed in rodent models of absence epilepsy and pain to determine whether they are able to augment the endogenous cannabinoid signaling as we observed previously with related allosteric ligands (Slivicki et al., 2020; Roebuck et al., 2021). In addition, the magnitude of observed *in vivo* effects may have been effected by pharmacokinetics of our compounds; planned future studies will assess and optimize the pharmacokinetics of CB1R allosteric ligands. Our *in silico* data support *in vitro* binding and signaling data that indicate these compounds interact with an allosteric site on CB1R that is distinct from the primary orthosteric agonist binding site (Price et al., 2005; Vigolo et al., 2015; Hua et al., 2017; Krishna Kumar et al., 2019). GAT1664 and GAT1666 preferentially bind to a putative allosteric agonist site of hCB1R near the intracellular face of the receptor between transmembrane helices I and IV; while GAT1665 and GAT1667 preferentially bind to a putative PAM site of CB1R on the extracellular receptor surface. Enantiomers may display low affinity to multiple allosteric sites, accounting for the allosteric agonist activity of GAT1665 and GAT1667 (Price et al., 2005; Kapur et al., 2007; Hurst et al., 2019). However, future dynamic modeling and crystallization studies will be required to

fully understand how the putative allosteric sites contribute to partial agonism and positive allosteric modulation, as the current models represent static interactions. Collectively, these data support retained, potent, G protein-selective, ago-PAM activity at hCB1R for the GAT211 ligand scaffold and demonstrate enhanced potency and efficacy of these ligands relative to the parent compound (Laprairie et al., 2017; Garai et al., 2020). Moreover, recent data from the racemic mixtures of these enantiomers indicates fluorine addition improves both metabolic stability and blood brain barrier penetrance; with GAT593—and therefore GAT1667—being superior to GAT591 (Garai et al., 2020). Therefore, studies are now underway to assess the *in vivo* efficacy of GAT1667 in the contexts of absence epilepsy and pain during both acute and chronic treatment paradigms.

4.1 Permission to reuse and copyright

Data availability statement

The original contributions presented in the study are included in the article/Supplementary Material, further inquiries can be directed to the corresponding authors.

Ethics statement

The animal study was reviewed and approved by University Animal Care Committee Animal Research Ethics Board, University of Saskatchewan.

Author contributions

AL designed and executed *in vitro* and *in silico* experiments, analyzed the data, wrote and edited the manuscript. SG conducted chemical synthesis and experiments, analyzed chemical data, wrote and edited the manuscript. AZ designed and executed *in vivo* experiments, analyzed the data, and edited the manuscript. DH and PR assisted in the design and analysis for *in silico* experiments, analyzed the data, wrote and edited the manuscript. LS and RP contributed to the radioligand and G protein coupling *in vitro* data and edited the manuscript. GI assisted with chemical crystallization and edited the manuscript. GT and RL equally aided in the design of the experiments, data analysis, writing and editing of the manuscript.

Funding

This work was supported by a GlaxoSmithKline (GSK)-Canadian Institutes of Health Research (CIHR) partnership grant (201704) and a CIHR Project Grant (201909) held by RL and a National Institutes of Health (NIH) R01 to GAT (EY024727). AZ is supported by a graduate scholarship from the College of Pharmacy and Nutrition, University of Saskatchewan. *In silico* modeling studies were supported by the NIH to PR (DA003934). The x-ray crystallographic work was supported by NIDA through Interagency Agreement #Y1-DA1101 with the Naval Research Laboratory (NRL).

Conflict of interest

The authors declare that the research was conducted in the absence of any commercial or financial relationships that could be construed as a potential conflict of interest.

Publisher's note

Supplementary material

The Supplementary Material for this article can be found online at: https://www.frontiersin.org/articles/10.3389/fphar.2022.919605/full#supplementary-material

References

Alaverdashvili, M., and Laprairie, R. B. (2018). The future of type 1 cannabinoid receptor allosteric ligands. *Drug Metab. Rev.* 50, 14–25. doi:10.1080/03602532.2018.1428341

Black, J. W., Leff, P., Shankley, N. P., and Wood, J. (2010). An operational model of pharmacological agonism : The effect of E/[A] curve shape on agonist

dissociation constant estimation. *Br. J. Pharmacol.* 160, S54–S64. doi:10.1111/j.1476-5381.2010.00855.x

Carrera, J., Tomberlin, J., Kurtz, J., Karakaya, E., Bostanciklioglu, M., and Albayram, O. (2020). Endocannabinoid signaling for GABAergic-microglia (mis)communication in the brain aging. *Front. Neurosci.* 14, 606808. doi:10.3389/fnins.2020.606808

Clark, M., Guarnieri, F., Shkurko, I., and Wiseman, J. (2006). Grand canonical Monte Carlo simulation of ligand-protein binding. *J. Chem. Inf. Model.* 46, 231–242. doi:10.1021/ci050268f

Di Marzo, V. (2018). New approaches and challenges to targeting the endocannabinoid system. *Nat. Rev. Drug Discov.* 17, 623–639. doi:10.1038/nrd.2018.115

Dopart, R., Lu, D., Lichtman, A. H., and Kendall, D. A. (2018). Allosteric modulators of cannabinoid receptor 1: Developing compounds for improved specificity. *Drug Metab. Rev.* 50, 3–13. doi:10.1080/03602532.2018.1428342

Estrada, J. A., and Contereras, I. (2020). Endocannabinoid receptors in the CNS: Potential drug targets for the prevention and treatment of neurologic and psychiatric disorders. *Curr. Neuropharmacol.* 18, 769–787. doi:10.2174/1570159X18666200217140255

Fay, J. F., and Farrens, D. L. (2015). Structural dynamics and energetics underlying allosteric inactivation of the cannabinoid receptor CB1. *Proc. Natl. Acad. Sci. U. S. A.* 112, 8469–8474. doi:10.1073/pnas.1500895112

Fay, J. F., and Farrens, D. L. (2013). The membrane proximal region of the cannabinoid receptor CB1 N-terminus can allosterically modulate ligand affinity. *Biochemistry* 52, 8286–8294. doi:10.1021/bi400842k

Fiser, A., and Sali, A. (2003). ModLoop: Automated modeling of loops in protein structures. *Bioinformatics* 19, 2500–2501. doi:10.1093/bioinformatics/btg362

Garai, S., Kulkarni, P. M., Schaffer, P. C., Leo, L. M., Brandt, A. L., Zagzoog, A., et al. (2020). Application of fluorine- and nitrogen-walk approaches: Defining the structural and functional diversity of 2-phenylindole class of cannabinoid 1 receptor positive allosteric modulators. *J. Med. Chem.* 63, 542–568. doi:10.1021/acs.jmedchem.9b01142

Garai, S., Leo, L. M., Szczesniak, A. M., Hurst, D. P., Schaffer, P. C., Zagzoog, A., et al. (2021). Discovery of a biased allosteric modulator for cannabinoid 1 receptor: Preclinical anti-glaucoma efficacy. *J. Med. Chem.* 64, 8104–8126. doi:10.1021/acs.jmedchem.1c00040

Greig, I. R., Baillie, G. L., Abdelrahman, M., Trembleau, L., and Ross, R. A. (2016). Development of indole sulfonamides as cannabinoid receptor negative allosteric modulators. *Bioorg. Med. Chem. Lett.* 26, 4403–4407. doi:10.1016/j.bmcl.2016.08.018

Guarnieri, F., and Mezei, M. (1996). Simulated annealing of chemical potential: A general procedure for locating bound waters. Application to the study of the differential hydration propensities of the major and minor grooves of DNA. *J. Am. Chem. Soc.* 118, 8493–8494. doi:10.1021/ja961482a

Hryhorowicz, S., Kaczmarek-Rys, M., Andrzejewska, A., Staszak, K., Hryhorowicz, M., Korcz, A., et al. (2019). Allosteric modulation of cannabinoid receptor 1-current challenges and future opportunities. *Int. J. Mol. Sci.* 20, 5874. doi:10.3390/ijms20235874

Hua, T., Vemuri, K., Nikas, S. P., Laprairie, R. B., Wu, Y., Qu, L., et al. (2017). Crystal structures of agonist-bound human cannabinoid receptor CB1. *Nature* 547, 468–471. doi:10.1038/nature23272

Hurst, D. P., Garai, S., Kulkarni, P. M., Schaffer, P. C., Reggio, P. H., and Thakur, G. A. (2019). Identification of Cb1 receptor allosteric sites using force-biased mmc simulated annealing and validation by structure-activity relationship studies. *ACS Med. Chem. Lett.* 10, 1216–1221. doi:10.1021/acsmedchemlett.9b00256

Iannotti, F. A., Di Marzo, V., and Petrosino, S. (2016). Endocannabinoids and endocannabinoid-related mediators: Targets, metabolism and role in neurological disorders. *Prog. Lipid Res.* 62, 107–128. doi:10.1016/j.plipres.2016.02.002

Kapur, A., Hurst, D. P., Fleischer, D., Whitnell, R., Thakur, G. A., Makriyannis, A., et al. (2007). Mutation studies of Ser7.39 and Ser2.60 in the human CB1 cannabinoid receptor: Evidence for a serine-induced bend in CB1 transmembrane helix 7. *Mol. Pharmacol.* 71, 1512–1524. doi:10.1124/mol.107.034645

Kenakin, T., and Strachan, R. T. (2018). PAM-antagonists: A better way to block pathological receptor signaling? *Trends Pharmacol. Sci.* 39, 748–765. doi:10.1016/j.tips.2018.05.001

Kenakin, T., Watson, C., Muniz-Medina, V., Christopoulos, A., and Novick, S. A. (2012). A simple method for quantifying functional selectivity and agonist bias. *ACS Chem. Neurosci.* 3, 193–203. doi:10.1021/cn200111m

Kilkenny, C., Browne, W. J., Cuthill, I. C., Emerson, M., and Altman, D. G. (2010). Improving bioscience research reporting: The arrive guidelines for reporting animal research. *PLoS Biol.* 8, 10004122–e1000510. doi:10.1371/journal.pbio.1000412

Krishna Kumar, K., Shalev-Benami, M., Robertson, M. J., Hu, H., Banister, S. D., Hollingsworth, S. A., et al. (2019). Structure of a signaling cannabinoid receptor 1-G protein complex. *Cell* 176, 448–458. doi:10.1016/j.cell.2018.11.040

Laprairie, R. B., Bagher, A. M., Kelly, M. E., and Denovan-Wright, E. M. (2016). Biased type 1 cannabinoid receptor signaling influences neuronal viability in a cell culture model of Huntington disease. *Mol. Pharmacol.* 89, 364–375. doi:10.1124/mol.115.101980

Laprairie, R. B., Bagher, A. M., Rourke, J. L., Zrein, A., Cairns, E. A., Kelly, M. E. M., et al. (2019). Positive allosteric modulation of the type 1 cannabinoid receptor reduces the signs and symptoms of Huntington's disease in the R6/2 mouse model. *Neuropharmacology* 151, 1–12. doi:10.1016/j.neuropharm.2019.03.033

Laprairie, R. B., Kulkarni, P. M., Deschamps, J. R., Kelly, M. E. M., Janero, D. R., Cascio, M. G., et al. (2017). Enantiospecific allosteric modulation of cannabinoid 1 receptor. *ACS Chem. Neurosci.* 8, 1188–1203. doi:10.1021/acschemneuro.6b00310

Leo, L. M., and Abood, M. E. (2021). CB1 cannabinoid receptor signaling and biased signaling. *Molecules* 26, 5413. doi:10.3390/molecules26175413

Lutz, B. (2020). Neurobiology of cannabinoid receptor signaling. *Dialogues Clin. Neurosci.* 22, 207–222. doi:10.31887/DCNS.2020.22.3/blutz

Marcu, J., Shore, D. M., Kapur, A., Trznadel, M., Makriyannis, A., Reggio, P. H., et al. (2013). Novel insights into CB1 cannabinoid receptor signaling: A key interaction identified between the extracellular-3 loop and transmembrane helix 2. *J. Pharmacol. Exp. Ther.* 345, 189–197. doi:10.1124/jpet.112.201046

Mezei, M. (2011). Mmc: A Monte Carlo and analysis program. *Biophys. J.* 100, 157a. doi:10.1016/j.bpj.2010.12.1075

Mielnik, C. A., Lam, V. M., and Ross, R. A. (2021). CB1 allosteric modulators and their therapeutic potential in CNS disorders. *Prog. Neuropsychopharmacol. Biol. Psychiatry* 106, 110163. doi:10.1016/j.pnpbp.2020.110163

Mitjavila, J., Yin, D., Kulkarni, P. M., Zanato, C., Thakur, G. A., Ross, R., et al. (2018). Enantiomer-specific positive allosteric modulation of CB1 signaling in autaptic hippocampal neurons. *Pharmacol. Res.* 129, 475–481. doi:10.1016/j.phrs.2017.11.019

Morales, P., Goya, P., Jagerovic, N., and Hernandez-Folgado, L. (2016). Allosteric modulators of the CB1 cannabinoid receptor: A structural update review. *Cannabis Cannabinoid Res.* 1, 22–30. doi:10.1089/can.2015.0005

Patel, M., Finlay, D. B., and Glass, M. (2021). Biased agonism at the cannabinoid receptors - evidence from synthetic cannabinoid receptor agonists. *Cell. Signal.* 78, 109865. doi:10.1016/j.cellsig.2020.109865

Perez-Olives, C., Rivas-Santisteban, R., Lillo, J., Navarro, G., and Franco, R. (2021). Recent advances in the potential of cannabinoids for neuroprotection in Alzheimer's, Parkinson's, and Huntington's diseases. *Adv. Exp. Med. Biol.* 1264, 81–92. doi:10.1007/978-3-030-57369-0_6

Price, M. R., Baillie, G. L., Thomas, A., Stevenson, L. A., Easson, M., Goodwin, R., et al. (2005). Allosteric modulation of the cannabinoid CB1 receptor. *Mol. Pharmacol.* 68, 1484–1495. doi:10.1124/mol.105.016162

Roebuck, A. J., Greba, Q., Onofrychuk, T. J., McElroy, D. L., Sandini, T. M., Zagzoog, A., et al. (2020). Dissociable changes in spike and wave discharges following exposure to injected cannabinoids and smoked Cannabis in genetic absence epilepsy rats from strasbourg. *Eur. J. Neurosci.* 55, 1063–1078. doi:10.1111/ejn.15096

Roebuck, A. J., Greba, Q., Smolyakova, A. M., Alaverdashvili, M., Marks, W. N., Garai, S., et al. (2021). Positive allosteric modulation of type 1 cannabinoid receptors reduces spike-and-wave discharges in genetic absence epilepsy rats from strasbourg. *Neuropharmacology* 190, 108553. doi:10.1016/j.neuropharm.2021.108553

Shim, J. Y., Bertalovitz, A. C., and Kendall, D. A. (2011). Identification of essential cannabinoid-binding domains: Structural insights into early dynamic events in receptor activation. *J. Biol. Chem.* 286, 33422–33435. doi:10.1074/jbc.M111.261651

Slivicki, R. A., Iyer, V., Mali, S. S., Garai, S., Thakur, G. A., Crystal, J. D., et al. (2020). Positive allosteric modulation of CB(1) cannabinoid receptor signaling enhances morphine antinociception and attenuates morphine tolerance without enhancing morphine-induced dependence or reward. *Front. Mol. Neurosci.* 13, 54. doi:10.3389/fnmol.2020.00054

Song, Z. H., and Bonner, T. I. (1996). A lysine residue of the cannabinoid receptor is critical for receptor recognition by several agonists but not WIN55212-2. *Mol. Pharmacol.* 49, 891–896.

Spartan (2018). *Spartan'18 parallel suite*. Irvine, CA: Wavefunction.

Vigolo, A., Ossato, A., Trapella, C., Vincenzi, F., Rimondo, C., Seri, C., et al. (2015). Novel halogenated derivates of JWH-018: Behavioral and binding studies in mice. *Neuropharmacology* 95, 68–82. doi:10.1016/j.neuropharm.2015.02.008

Wang, X., Li, Y., Gao, Y., Yang, Z., Lu, C., and Zhu, T. (2018). A quantum mechanical computational method for modeling electrostatic and solvation effects of protein. *Sci. Rep.* 8, 5475–5510. doi:10.1038/s41598-018-23783-8

Zagzoog, A., Brandt, A. L., Black, T., Kim, E. D., Burkart, R., Patel, M., et al. (2021). Assessment of select synthetic cannabinoid receptor agonist bias and selectivity between the type 1 and type 2 cannabinoid receptor. *Sci. Rep.* 11, 10611. doi:10.1038/s41598-021-90167-w

Zhang, J., Chen, Q., and Liu, B. (2020). iDRBP_MMC: Identifying DNA-binding proteins and RNA-binding proteins based on multi-label learning model and motif-based convolutional neural network. *J. Mol. Biol.* 432, 5860–5875. doi:10.1016/j.jmb.2020.09.008

frontiers | Frontiers in Pharmacology

TYPE Original Research
PUBLISHED 04 November 2022
DOI 10.3389/fphar.2022.969883

OPEN ACCESS

EDITED BY
María Gómez-Cañas,
Complutense University of Madrid,
Spain

REVIEWED BY
Gabriele Murineddu,
University of Sassari, Italy
Mengchen Yin,
Shanghai University of Traditional
Chinese Medicine, China
Jahan Marcu,
University of the Sciences, United States

*CORRESPONDENCE
Xiaofeng Zeng,
zxf2004033@163.com
Bofeng Zhu,
zhubofeng7372@126.com

SPECIALTY SECTION
This article was submitted to
Neuropharmacology,
a section of the journal
Frontiers in Pharmacology

RECEIVED 15 June 2022
ACCEPTED 17 October 2022
PUBLISHED 04 November 2022

CITATION
Liu L, Liu J, Zhao M, Cai M, Lei F, Zeng X and Zhu B (2022), A bibliometrics and visualization analysis of cannabidiol research from 2004 to 2021.
Front. Pharmacol. 13:969883.
doi: 10.3389/fphar.2022.969883

A bibliometrics and visualization analysis of cannabidiol research from 2004 to 2021

Liu Liu[1], Jianxing Liu[2], Ming Zhao[1], Meiming Cai[1], Fanzhang Lei[1], Xiaofeng Zeng[2]* and Bofeng Zhu[1]*

[1]Guangzhou Key Laboratory of Forensic Multi-Omics for Precision Identification, School of Forensic Medicine, Southern Medical University, Guangzhou, China, [2]School of Forensic Medicine, Kunming Medical University, Kunming, China

Cannabidiol, a non-psychoactive component extracted from the plant cannabis sativa, has gained growing focus in recent years since its extensive pharmacology effects have been founded. The purpose of this study intends to reveal the hot spots and frontiers of cannabidiol research using bibliometrics and data visualization methods. A total of 3,555 publications with 106,793 citations from 2004 to 2021 related to cannabidiol were retrieved in the Web of Science database, and the co-authorships, research categories, keyword burst, and reference citations in the cannabidiol field were analyzed and visualized by VOSviewer and Citespace software. Great importance has been attached to the pharmacology or pharmacy values of cannabidiol, especially in the treatment of neuropsychiatric disorders, such as epilepsy, anxiety, and schizophrenia. The mechanisms or targets of the cannabidiol have attracted the extreme interest of the researchers, a variety of receptors including cannabinoids type 1, cannabinoids type 2, 5-hydroxytriptamine1A, and G protein-coupled receptor 55 were involved in the pharmacology effects of cannabidiol. Moreover, the latest developed topic has focused on the positive effects of cannabidiol on substance use disorders. In conclusion, this study reveals the development and transformation of knowledge structures and research hotspots in the cannabidiol field from a bibliometrics perspective, exploring the possible directions of future research.

KEYWORDS

cannabidiol, bibliometrics analysis, data visualization, research hotspots, co-citation analysis, burst detection

Introduction

Cannabidiol (CBD), one of the major components of cannabis sativa without psychological dependence (Devinsky et al., 2014), has presented great pharmacology values in neuropsychiatric disorders due to its anti-inflammation and anti-oxidation effects (Campos et al., 2016; Melas et al., 2021; Scarante et al., 2021). A recent double-blind study revealed that cannabidiol decreased the convulsive-seizure frequency in the Dravet syndrome (a complex childhood epilepsy disorder) (Devinsky et al., 2017). In June 2018, the US Food and Drug Administration (FDA) approved the first

CBD-based drug, Epidiolex (GW Pharmaceuticals, England) for the treatment of seizures associated with Dravet syndrome and Lennox-Gastaut syndrome (VanDolah et al., 2019). CBD alleviated Alzheimer's disease (AD)-related neuron damage by regulating inflammation and oxidative stress (Vallée et al., 2017). Preclinical and clinical trials proved the therapeutic effects of CBD on Parkinson's disease (PD)-related non-motor symptoms (Crippa et al., 2019). CBD could also be used as a candidate drug for the treatment of pain (Xiong et al., 2012; De Gregorio et al., 2019). In addition, the pharmacology values of CBD in substance abuse (Lee et al., 2017), anti-tumor (Sultan, 2018), and multiple sclerosis (Mecha et al., 2013) have been investigated in recent years. Another deeply researched topic is the molecular mechanism of CBD in these disorders, which may be related to the endocannabinoid system (ECS), serotonin system, transient receptor potential vanilloid (TRPV) channels, G protein-coupled receptor 55 (GPR55), peroxisome proliferator-activated receptor-gamma (PPARγ), and so on (Campos et al., 2012). Although great research progress has been made in CBD research, the hot spots and frontiers still need to be illustrated to provide useful information for future research directions.

Bibliometrics is a discipline that explores the distribution structure, quantitative relationship, and variation trend of literature using mathematics and statistics methods (Yin et al., 2021). Bibliometrics and data visualization could provide an overview of research categories or themes, co-authorships, keywords frequencies, and most cited articles or journals, which contribute significantly to revealing the hot spots and frontiers in one specific area (Song et al., 2021; Chu et al., 2022).

In this study, we performed the bibliometrics analysis based on the published literature related to CBD research from 2004 to 2021 in the Web of Science (WOS) database, and several networks of categories, keywords, co-authorships, and co-cited references were visualized by VOSviewer and Citespace software. This study aims to better understand the dynamic changes of current CBD research and explore the possible directions for future research.

Materials and methods

Data searching

The literature published in the WOS core collection Science Citation Index Expanded (SCI-E) database from 2004 to 2021 was collected on 15 March 2022. Searching strategies used in this study were as follows: the topic was set as "cannabidiol", the literature types were "article" and "review", and the language was "English" only. Therefore, a dataset consisting of 3,555 publications was exported for subsequent analysis.

Bibliometrics analysis and data visualization

The annual number of publications and citations, and the top 15 most productive countries were visualized in Microsoft Excel version 2019 based on the report of WOS. A world map was generated using Bibliometrix *R* package version 3.2.1 to reveal the geographical distribution of publications. A pie chart was drawn based on WOS categories using Excel. The bibliometrics analysis and data visualization in this study were performed by Citespace version 5.8.R3 and VOSviewer version 1.6.18 software. Citespace could simplify the search for significant papers in a specific area so that one can search for visually salient features, including categories, co-cited references, cluster information, and brust detection (Chen, 2004; Chen, 2006). VOSviewer was used here to perform the networks of co-authorship and keyword co-occurrence.

Results

General analysis

A total of 3555 publications including 2,719 articles (76.48%) and 836 reviews (23.52%) from 2004 to 2021 were retrieved in the WOS SCI-E database, with a sum of 106,793 citations, each of the publications was cited on average 30.04. Figure 1 showed the variation of publications and citations with the years. The annual number of publications increased year by year, except for 2005, 2008 and 2014, and the annual growth of publications exceeded 100 for the first time in 2019. The number of citations per year has grown rapidly from 2019 to 2021. We also retrieve the publications related to CBD that were published in English before 2004 (data not shown). A total of five articles were published with a sum of 74 citations, the first of which was published in 1988 with 11 citations. One of the 5 was divided into pharmacology and pharmacy by WOS, and the rest belongs to chemistry fields.

During this period, a total of 94 countries have published literature related to CBD research. Figure 2A displayed the geographical distribution of publications, and the top 15 most productive countries with their number of publications and citations were shown in Figure 2B. The United States contributed the highest to this topic, publishing 1,144 papers and being cited 36,570 times. The second most productive country was Italy, with 460 publications and 17,887 citations. England published 394 papers with 23,402 citations, an average citations of 59.40 per paper. Notably, Scotland showed the highest average number of citations, each of the literature was cited on average 93.22.

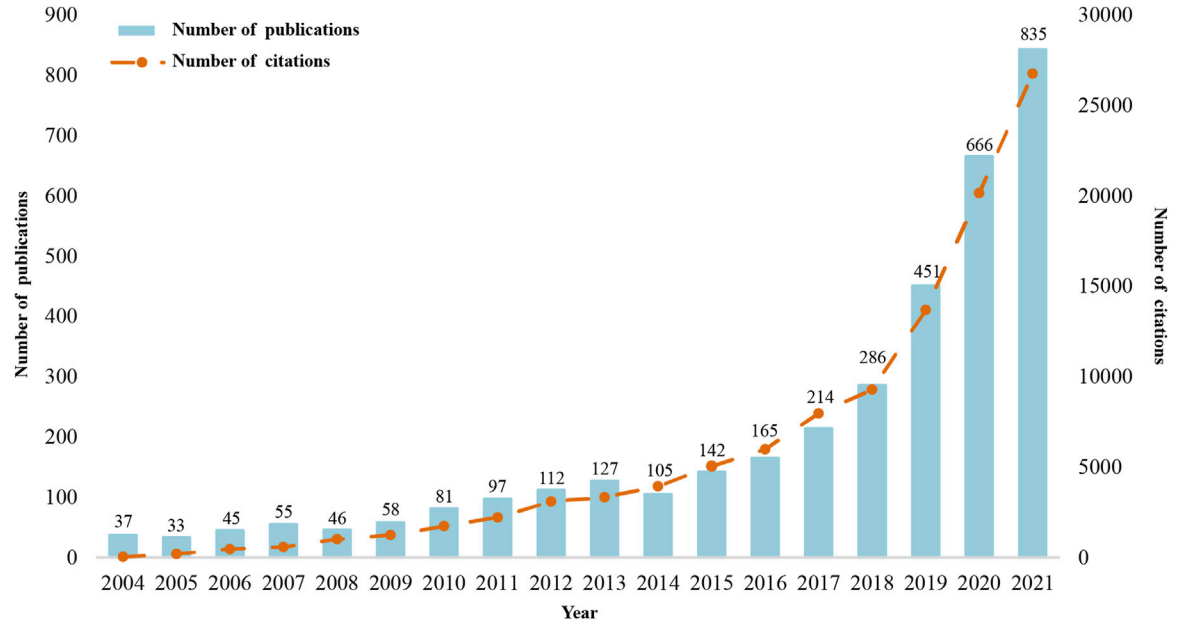

FIGURE 1
Annual number of publications and citations.

Category analysis

The category of publications is an important indicator to reveal the hot spots and applications of CBD research. Figure 3A presented the top 10 most published categories in WOS SCI-E database. There are a total of 1271 publications divided into Pharmacology/Pharmacy, which account for 31.70% of the top 10 most published categories. Neurosciences is the second largest published category, with 651 publications (16.24%), followed by Clinical Neurology with 492 publications (12.17%), Psychiatry with 437 publications (10.90%), and Biochemistry Molecular Biology with 316 publications (7.88%). Subsequently, we performed the co-occurrence network of categories based on the dataset of WOS using Citespace software. 248 nodes and 1190 links were included in the network, and Figure 3B showed the top 10 most published categories. Each of the nodes represents a specific category, and the node size was used here to reflect the frequency of category occurrence. Betweenness centrality provides a method to quantify the importance of the node's position in a network (Chen, 2006), and the nodes with purple trims indicate the high betweenness centrality. Figure 3B revealed that Pharmacology & Pharmacy was the highest co-occurrence category in the network, and its centrality was 0.14. Moreover, Chemistry presented the maximum centrality (0.26), suggesting that Chemistry is a pivotal point or tipping point in the network.

Co-authorship analysis

To investigate the co-authorship between different countries, institutions, and authors, we performed the collaboration network based on the WOS dataset using VOSviewer software. There are a total of 94 countries, 3,569 institutions, and 14,040 authors who have contributed to this topic. As shown in Figure 4, each node represents a different country/institution/author, the node size represents the number of documents, the thickness of connecting lines represents the strength of inter collaboration, and each color represents a cluster. Figure 4A presented the inter collaboration between different countries. Some of the 94 countries in the network were not connected, and the largest set consisted of 86 countries. The United States was the most productive and cooperative country, with 573 link strengths. The second most cooperative country was England, with a sum of 412 link strengths, and the third-highest number of documents. Italy, Spain, Canada, Germany, and Brazil also showed high productivity and cooperative strength in the network.

Figure 4B displayed the inter collaboration between different institutions. We picked out the top 100 most productive institutions to generate the partnership network, but two institutions were excluded due to a lack of cooperation with other institutions. The University of Sao Paulo was the most productive and cited institution, with the highest cooperative link strength. The University of Sao Paulo was the first and the largest modern comprehensive university in Brazil. It is also the most important scientific research center in Brazil. Table 1 submitted detailed information on the top 10 most cooperative institutions.

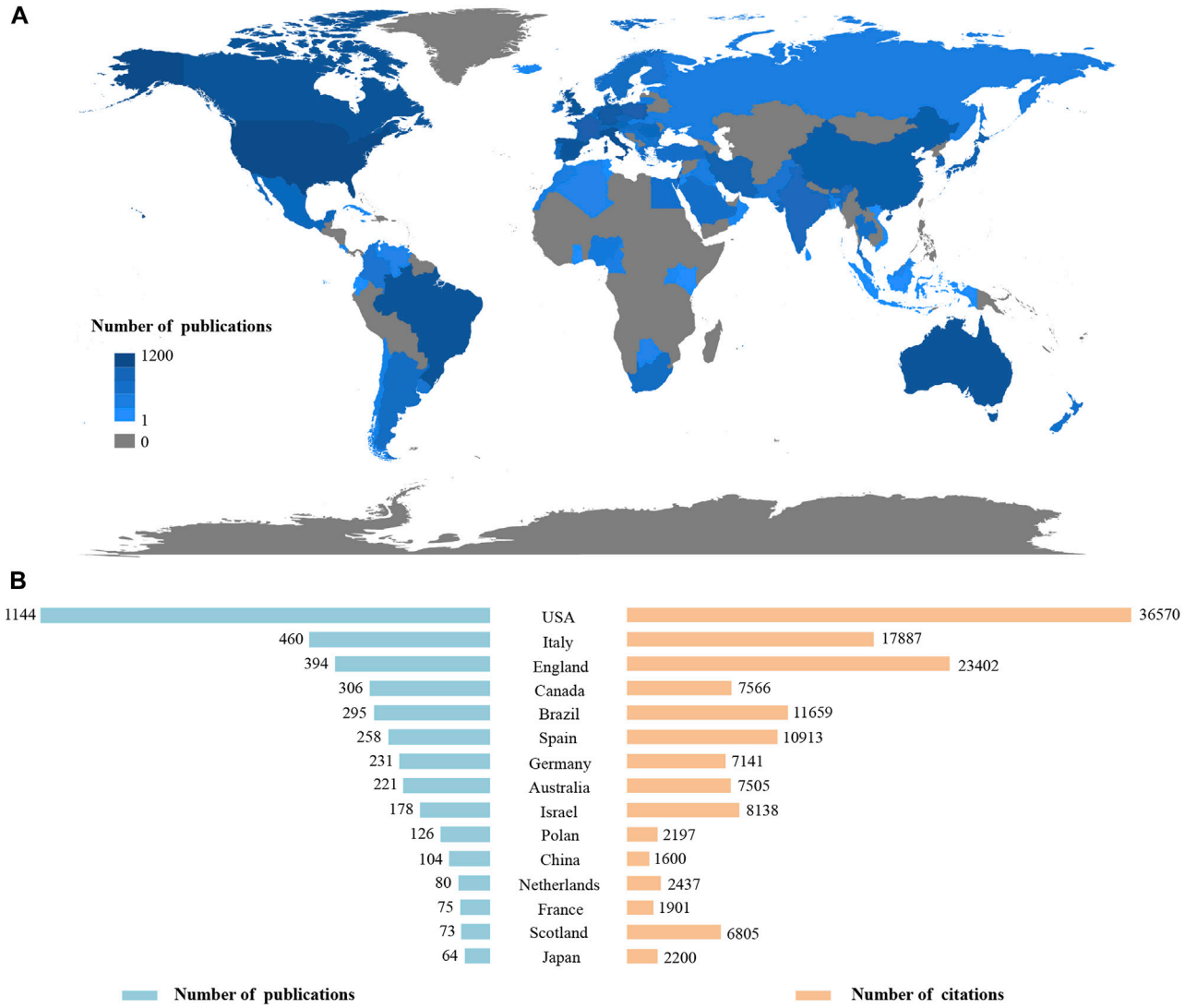

FIGURE 2
(A) Geographical distribution of publications. **(B)** The top 15 most productive countries in the publications and citations.

Nine of the top 10 most cooperative institutions were from different research universities and only one was owned by a pharmaceutical company, indicating that the current study on CBD was still dominated by basic research. GW Res Ltd. established a world-leading position in the development of plant-derived cannabinoid therapeutics, which has developed the first FDA-approved CBD-based drug, Epidiolex for the treatment of Dravet syndrome and Lennox-Gastaut syndrome.

Figure 4C showed the inter collaboration between different authors. 106 authors met the threshold of 10 or more published articles, while only 86 authors were founded to connect with the other authors in the network. The most productive author was Guimaraes FS with a total of 51 documents, 2,406 citations, and 65 link strengths. However, the most cited author was Di Marzo V with a sum of 4,419 citations, 47 documents, and 53 link strengths. The most cooperative author was Huestis MA with a total of 98 link strengths, 45 documents, and 1,684 citations.

Funding agency contribution

The source of funding reflects, to a certain extent, the different levels of the country's support for the field at different stages and the enthusiasm of the research community. Table 2 presented the top 10 most productive funding agencies for CBD research. United States Department of Health and Human Services was listed in the first, providing funds for 426 documents, which accounts for 11.98% of all the publications. The followed funding agencies were the National Institutes of Health (NIH)-USA and the European Commission

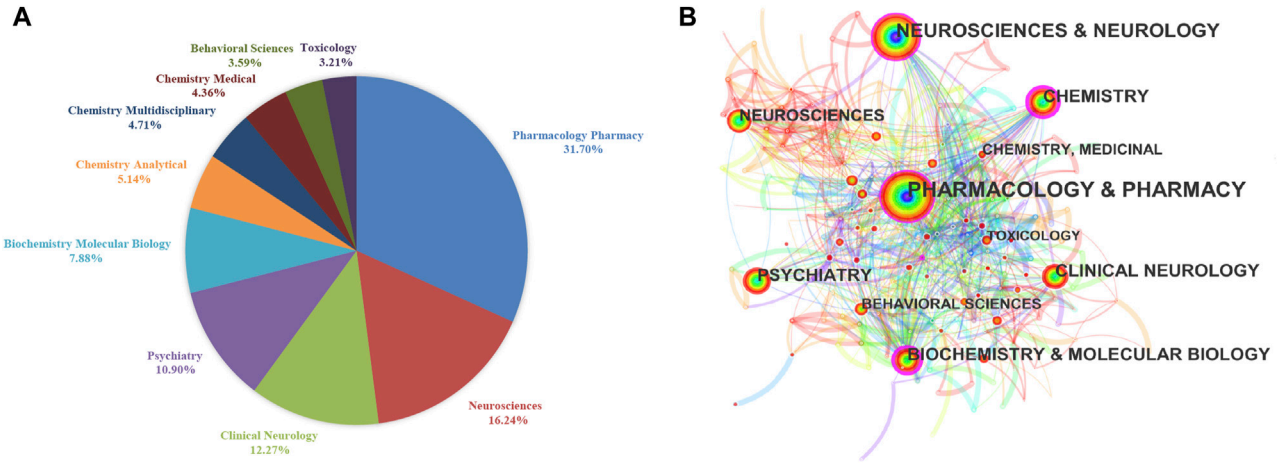

FIGURE 3
(A) The top 10 most published categories. **(B)** The network of the top 10 most published categories.

with 422 and 360 documents, accounting for 11.87% and 10.13% of all the publications, respectively. Three of the top 10 most productive funding agencies were from the United States and sponsored a total of 1,071 publications, which accounts for 30.12% of all the publications. Additionally, the residual top 10 most productive funding agencies including three Brazil agencies, two England agencies, and one Canada agency, accounting for 12.19%, 4.81%, and 1.97% of all the publications, respectively.

Journal contribution

A total of 3,555 publications were published in 999 different journals. Table 3 listed the top 10 most-cited journals in the CBD area. The most cited journal was the *British Journal of Pharmacology* with cited times of 9,906, and a sum of 95 papers were published. *Epilepsia* was listed second with 2,212 citations and 42 papers, followed by *Neuropsychopharmacology* with 2,093 citations and 21 papers. Four of the 10 listed journals were from England, other four journals were from the United States, and the rest were from Germany and Switzerlands. The top three journals with the highest impact factor (IF) were the *British Journal of Pharmacology* (8.739), *Neuropsychopharmacology* (7.885), and *Epilepsia* (5.866). In addition, the H-index and ISSN of the journal were also listed in Table 3.

Keywords co-occurrence and burst detection

The keyword plays an important role to highlight and emphasize the focus and core content of the whole article. The keyword co-occurrence network enables an overview of the core content of published articles, as well as reveals the connections between the content. There are a total of 11,116 keywords included in the 3555 publications, and 282 keywords meeting the frequency threshold of more than 20. Figure 5A displayed the co-occurrence network consisting of 282 keywords using the Vosviewer software. Each node represents a keyword, the node size indicates the frequency of the keyword, and each color reveals a cluster in the network. The top 15 keywords with the highest occurrence frequencies and strongest connection were cannabidiol (1,960, 11,444), cannabinoids (949, 5,747), cannabis (535, 3,336), endocannabinoid system (405, 2,750), delta (9)-tetrahydrocannabinol (394, 2,770), CBD (363, 2,393), marijuana (348, 2,236), THC (326, 2,275), delta-9-tetrahydrocannabinol (303, 2,204), and double-blind (282, 2,024), cannabinoid (248, 1,565), epilepsy (240, 1,565), expression (233, 1,376), *in-vitro* (214, 1,385), seizures (213, 1,316). 282 keywords in the network were divided into five clusters, and the detailed information was summarized as follows: 1) Mechanism was represented by red: cannabinoid receptor, CB1, CB2, inflammation, antioxidant, protein, and apoptosis; 2) Disease was represented by blue: schizophrenia, anxiety, psychosis, behavior, rat, prefrontal cortex, and cognitive impairment; 3) Treatment of epilepsy was represented by purple: epilepsy, Dravet syndrome, therapy, seizures, antiepileptic drugs, and children; 4) Clinical trial was represented by yellow: double-blind, neuropathic pain, efficacy, medical cannabis, safety, risk, and tolerability; 5) Synthesis and metabolism were represented by green: bioavailability, blood, plasma, chromatography, metabolism, pharmacokinetics, synthetic cannabinoids, extraction, identification, and quantification.

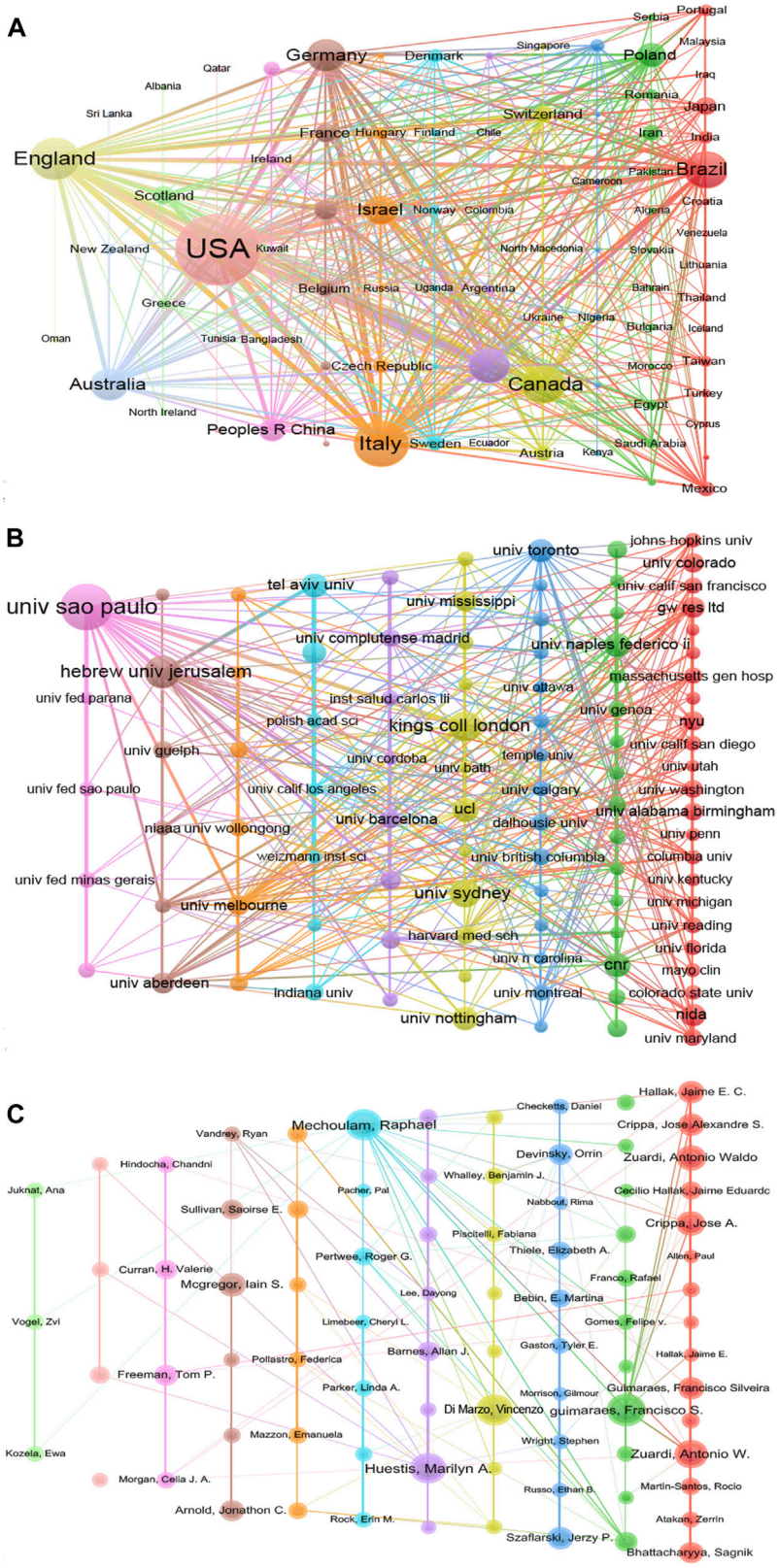

FIGURE 4
Co-authorships analyses. **(A)** Co-authorships between different countries. **(B)** Co-authorships between different institutions. **(C)** Co-authorships between different authors.

TABLE 1 The top 10 most collaborative institutions.

Institution	Documents	Citations	Country	Total collaborative strength
University of Sao Paulo	208	10,140	Brazil	134
King's College London	90	5126	England	108
Hebrew University of Jerusalem	105	6412	Israel	88
GW Research Limited	42	2266	England	67
University of Toronto	52	1259	Canada	65
University of Melbourne	39	2718	Australia	63
University College London	54	2934	England	57
New York University	37	3946	United States	55
University of Naples Federico II	54	3540	Italy	54
Tel Aviv University	56	1818	Israel	46

TABLE 2 The top 10 most productive funding agencies in the cannabidiol field.

Organization	Documents	Country	Percentages (%)
United States Department of Health & Human Services	426	United States	11.98
National Institutes of Health (NIH) - United States	422	United States	11.87
European Commission	360	European Commission	10.13
NIH National Institute on Drug Abuse (NIDA)	223	United States	6.27
Conselho Nacional de Desenvolvimento Cientifico E Tecnologico (CNPQ)	199	Brazil	5.60
Fundacao de Amparo a Pesquisa do Estado de Sao Paulo (FAPESP)	130	Brazil	3.66
Coordenacao de Aperfeicoamento de Pessoal de Nivel Superior (CAPES)	104	Brazil	2.93
United Kingdom Research and Innovation (UKRI)	92	England	2.59
Medical Research Council United Kingdom (MRC)	79	England	2.22
Natural Sciences and Engineering Research Council of Canada (NSERC)	70	Canada	1.97

TABLE 3 The top 10 most-cited journals in the cannabidiol field.

Jorunal	Country	If (2020)	Documents	Citations	H-index	ISSN
British Journal of Pharmacology	England	8.739	95	9906	211	0007–1188
Epilepsia	United States	5.866	42	2212	191	0013–9580
Neuropsychopharmacology	England	7.855	21	2093	219	0893–133X
Psychopharmacology	Germany	4.53	43	1959	196	0033–3158
Journal of Pharmacology and Experimental Therapeutics	United States	4.03	25	1952	225	0022–3565
Journal of Psychopharmacology	England	4.153	34	1834	114	0269–8811
Epilepsy and Behavior	United States	2.937	67	1797	104	1525–5050
Cannabis and Cannabinoid Research	United States	5.8	96	1601	17	2578–5125
Frontiers in Pharmacology	Switzerland	5.811	78	1581	81	1663–9812
Neuropharmacology	England	5.251	45	1572	167	0028–3908

Brust detection served to recognize the emergent terms and sharp increases of interest (Chen, 2006), which significantly contributed to revealing the frontiers in one specific field. We performed the keyword burst detection based on the dataset of WOS using Citespace software, and the top 10 keywords with the strongest bursts were displayed in Figure 5B. Anandamide was the top 1 strongest burst keyword that emerged in 2004 and ended in 2015, revealing that anandamide was extensively

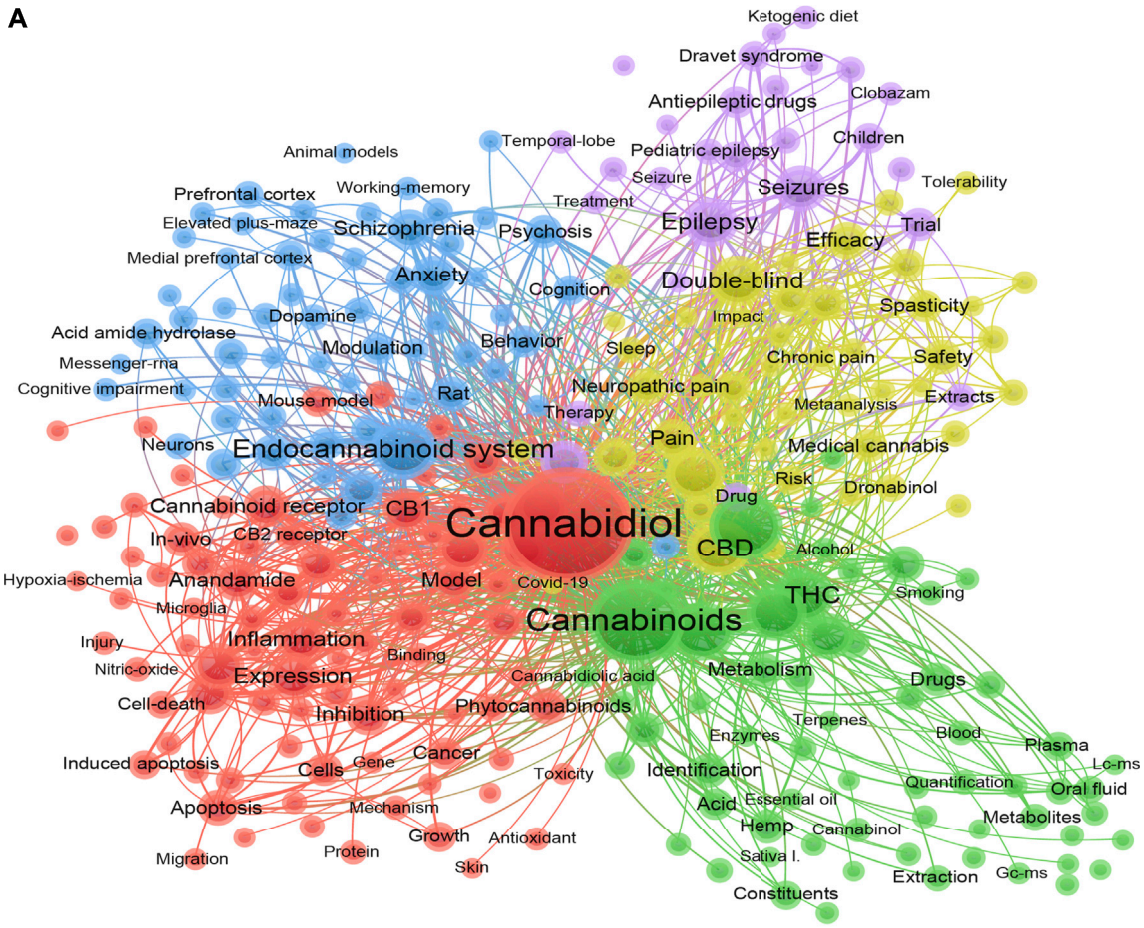

FIGURE 5
Keywords analyses. **(A)** The network of the keywords co-occurrence and clustering. **(B)** The top 10 keywords with the strongest bursts.

TABLE 4 The top 10 most cited articles from 2004 to 2021.

Title	Authors	Journal	Citations	IF (2020)	H-index
The orphan receptor GPR55 is a novel cannabinoid receptor	Ryberg, E, et al.	British Journal of Pharmacology	984	8.739	211
The diverse CB1 and CB2 receptor pharmacology of three plant cannabinoids: Delta (9)-tetrahydrocannabinol, cannabidiol and Delta (9)-tetrahydrocannabivarin	Pertwee, RG.	British Journal of Pharmacology	955	8.739	211
Taming THC: potential cannabis synergy and phytocannabinoid-terpenoid entourage effects	Russo, Ethan B, et al.	British Journal of Pharmacology	664	8.739	211
Trial of Cannabidiol for Drug-Resistant Seizures in the Dravet Syndrome	Devinsky, O, et al.	New England Journal of Medicine	628	91.253	1030
Cannabidiol enhances anandamide signaling and alleviates psychotic symptoms of schizophrenia	Leweke, FM, et al.	Translational Psychiatry	547	6.222	82
The Endocannabinoid System and the Brain	Mechoulam, R, et al.	Annual Review of Psychology	528	24.137	243
Non-psychotropic plant cannabinoids: new therapeutic opportunities from an ancient herb	Izzo, AA, et al.	Trends in Pharmacological Sciences	491	14.819	218
Cannabidiol: Pharmacology and potential therapeutic role in epilepsy and other neuropsychiatric disorders	Devinsky, O, et al.	Epilepsia	459	5.866	191
Changes in Cannabis Potency Over the Last 2 Decades (1995–2014): Analysis of Current Data in the United States	ElSohly, MA, et al.	Biological Psychiatry	450	13.382	319
Cannabidiol in patients with treatment-resistant epilepsy: an open-label interventional trial	Devinsky, O, et al.	Lancet Neurology	444	44.182	291

studied and discussed during this period. The seizure was the most recent keyword with high burst strength that appeared in 2018. The bursts of the keyword cannabinoid receptor, constituent, *in vivo*, mice, and 5-ht1a receptor sustained at least 10 years.

Reference co-citation analysis and timeline map

Reference citation and co-citation frequencies could clearly illustrate the intellectual concerns in a field. In general, an article with a high co-citation frequency suggests it has a high citation frequency. Table 4 listed the top 10 most cited articles from 2004 to 2021 in the CBD field. The most cited reference was published by Ryberg et al. (2007), which revealed that the orphan receptor GPR55 was a novel cannabinoid receptor. A review published by Pertwee (2008) summarized the diverse CB1 and CB2 receptor pharmacology of three plant cannabinoids, indicating that CBD displayed high potency as a CB2 receptor antagonist. The reference published by Russo (2011) reviewed the pharmacology effects of CBD in anti-oxidant, anti-anxiety, anti-depressant, anti-convulsant, and so on, and the possible mechanisms were also discussed. Devinsky et al. (2017) conducted a double-blind trial of cannabidiol for drug-resistant seizures in 120 individuals, revealing that CBD exhibited greater effects in decreasing the convulsive-seizure frequency than placebo. This research was published in the *New England Journal of Medicine* with the highest H-index (1030) in the top 10 most cited articles. Moreover, Leweke et al. (2012) demonstrated that CBD alleviated the psychotic symptoms of schizophrenia by enhancing anandamide signaling. Mechoulam and Parker (2013) summarized the actions of the endocannabinoid system on anxiety, depression, neurogenesis, reward, cognition, learning, and memory. Notably, three of the top 10 most cited articles attached concerns to the pharmacology effects of CBD on seizures, and these articles were published by the team of Devinsky et al. (2014), Devinsky et al. (2016), Devinsky et al. (2017), another three articles focus on the mechanisms and molecular targets of CBD pharmacology effects (Ryberg et al., 2007; Pertwee, 2008; Mechoulam and Parker, 2013).

Next, we performed the co-citation network of reference based on the WOS dataset using the Citespace software. 1,248 nodes and 6,077 links were founded in Figure 6A, and the top 10 most co-cited articles were highlighted in the network. The top 2 most co-cited articles were published by Devinsky et al. (2016), Devinsky et al. (2017), with 354 and 288 co-citations, respectively. The former article assessed the safety, tolerability and efficacy of CBD in patients already receiving stable doses of antiepileptic drugs, indicating that CBD might decrease the frequency of seizure frequency with sufficient safety in children and young adults with highly treatment-resistant epilepsy (Devinsky et al., 2016). The latter focused on drug-resistant epilepsy in Dravet syndrome and evaluated the efficacy and safety of CBD in it, suggesting that cannabidiol reduced the

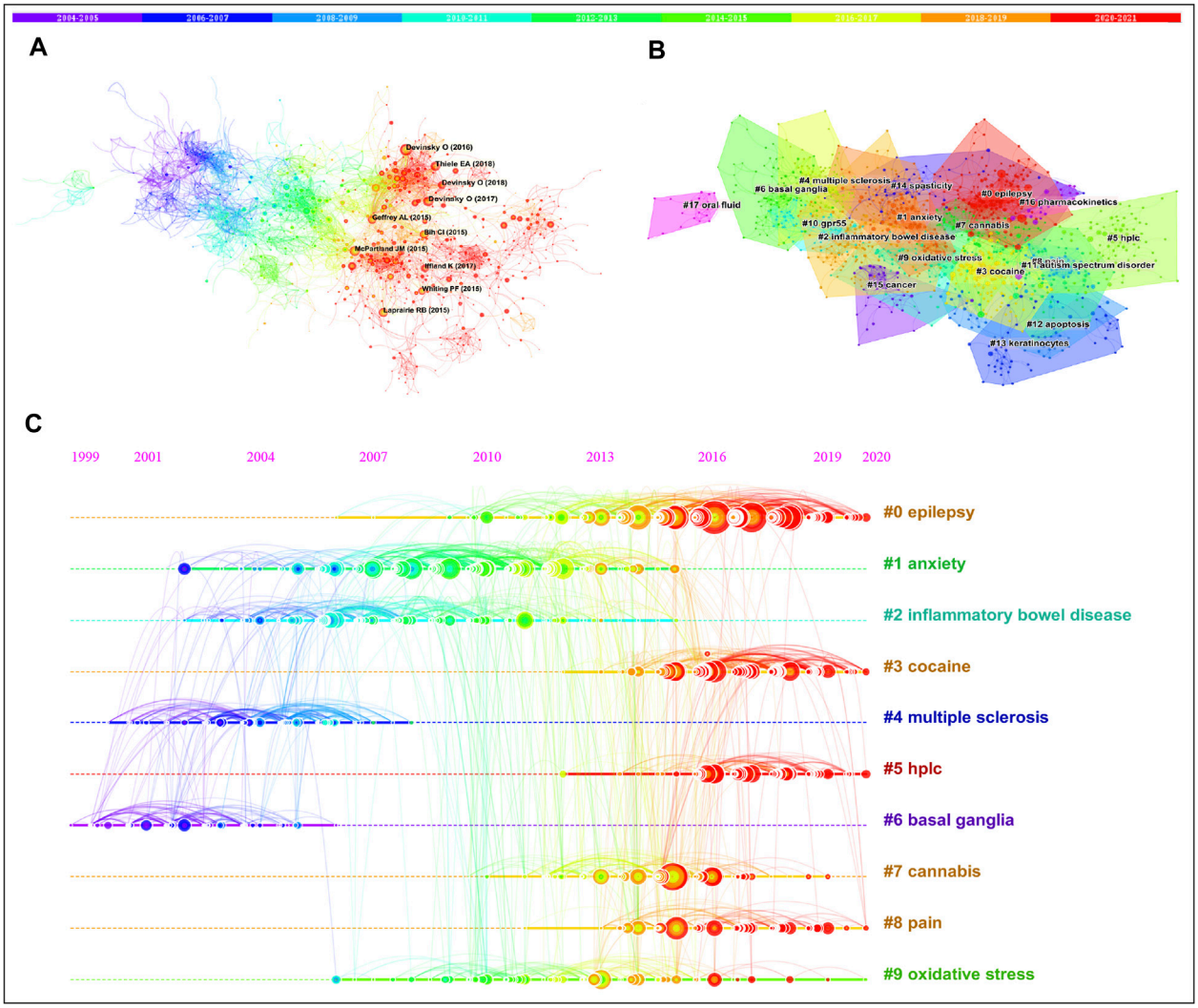

FIGURE 6
Reference co-citation analyses. **(A)** The network of the co-cited articles. **(B)** Cluster analysis of the co-cited articles. **(C)** A timeline view of the top 10 clusters.

frequency of convulsive seizures in children and young adults with Dravet syndrome but was associated with adverse events including somnolence and elevation of liver enzyme levels (Devinsky et al., 2017). The followed most co-cited articles were published by Thiele et al. (2018) with 238 co-citations, and Devinsky et al. (2018) with 222 co-citations, both of them explored the effects of CBD on seizures in the Lennox–Gastaut syndrome through the clinical trial. Laprairie et al. (2015) illustrated that Cannabidiol is a non-competitive negative allosteric modulator of CB1 receptors. Besides, the side effects, toxicity, and drug-drug interaction of CBD therapies were also discussed based on clinical data and animal studies (Geffrey et al., 2015; Whiting et al., 2015; Iffland and Grotenhermen, 2017). In summary, the clinical trials of CBD on seizures have absorbed great interest from researchers, and investigated the mechanism of the CBD effect helps to better elucidate the pharmacology value of CBD. In addition, there are serious concerns about the issues of safety and side effects of CBD, more trials still need to be conducted for solving these problems.

Clusters of co-cited articles provided a method to detect the transition of research frontiers in an area (Chen, 2006). Figure 6B displayed the clusters of co-cited articles using Citespace software. The modularity Q and silhouette values of the clusters were 0.791 and 0.9081, respectively, which indicated the structure of the clusters was significant and all of the clusters were convincing. All of the co-cited articles were assigned to 18 different clusters, and the clusters of the same color represent co-citations made within the same time slice. The first cluster of

TABLE 5 The detailed information of 10 clusters in Figure 5C.

Cluster ID	Size	Silhouette	Mean (year)	Top terms
0	155	0.937	2016	Epilepsy
1	146	0.844	2009	Anxiety
2	124	0.867	2008	Inflammatory bowel disease
3	116	0.889	2017	Cocaine
4	90	0.899	2004	Multiple sclerosis
5	84	0.96	2017	Hplc
6	76	0.889	2002	Basal ganglia
7	71	0.879	2014	Cannabis
8	70	0.943	2016	Pain
9	68	0.876	2012	Oxidative stress

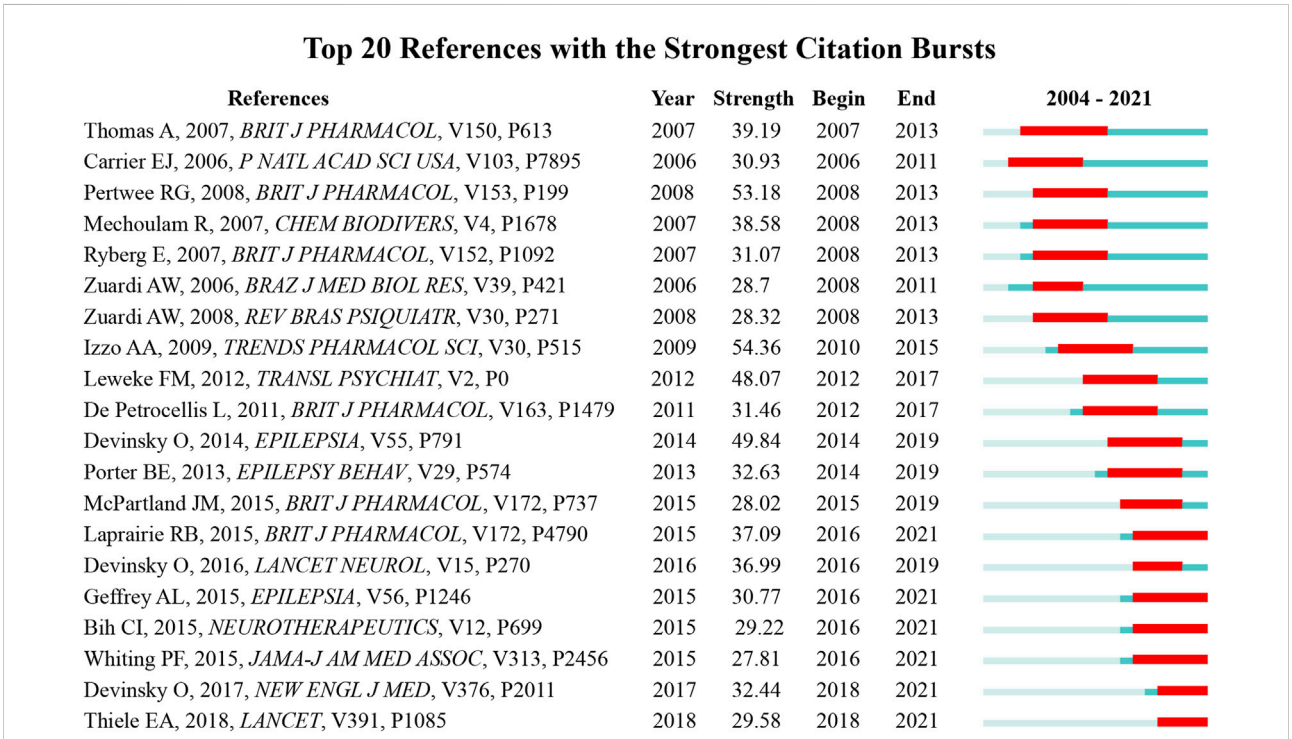

FIGURE 7
The top 20 references with the strongest citation bursts.

co-cited articles was epilepsy, and the followed were anxiety, inflammatory bowel disease, cocaine, multiple sclerosis, HPLC, basal ganglia, cannabis, and oxidative stress. Figure 6C provided a timeline view of the top 10 clusters, and detailed information about these clusters was listed in Table 5. The early studies focused on the pharmacology effects of CBD on multiple sclerosis (2004), inflammatory bowel disease (2008), and anxiety (2009), as well as the regulatory effect of CBD on the endocannabinoid system and the serotonin system in the basal ganglia (2002). In 2012, the anti-oxidative effects of CBD attracted the attention of researchers. In 2014, researchers were interested in exploring the values of cannabis. Notably, the effects of CBD in the treatment of epilepsy have been enthusiastically investigated in 2016, and great progress has also been made in drug development. The most recent themes in the CBD area were cocaine and HPLC. CBD could be used as a potential therapeutic drug for the treatment of cocaine use disorders (Mahmud et al., 2017; Luján et al., 2020).

Burst detection of co-cited reference

Figure 7 presented the top 20 references with the strongest citation bursts. The article with the highest burst strengths was entitled "Non-psychotropic plant cannabinoids: new therapeutic opportunities from an ancient herb" (Izzo et al., 2009), which reviewed the therapeutic applications of CBD in inflammation, diabetes, cancer, affective and neurodegenerative diseases. The article with the earliest citation bursts has begun in 2006 and was entitled "Inhibition of an equilibrative nucleoside transporter by cannabidiol: A mechanism of cannabinoid immunosuppression" (Carrier et al., 2006), which demonstrated that CBD could decrease inflammation by enhancing adenosine signaling. The latest burst articles were "Trial of cannabidiol for drug-resistant seizures in the Dravet syndrome" (Devinsky et al., 2017) and "Cannabidiol in patients with seizures associated with Lennox-Gastaut syndrome (GWPCARE4): a randomised, double-blind, placebo-controlled phase 3 trial" (Thiele et al., 2018), both of them were focused on the clinical trials of CBD in the seizures related Dravet syndrome or Lennox-Gastaut syndrome. According to Figure 7, the themes of the top 20 burst references consisted of the molecular mechanism investigation (7), clinical trial on epilepsy (6), pharmacology effects (6), and treatment of schizophrenia (1).

Discussion

Our present study attempts to reveal the hot spots and research trends in the CBD field, a dataset including 3555 publications from 2004 to 2021 was analyzed using a bibliometrics method. Based on the searching reports of the WOS database, we firstly evaluated the publication and citation trends over the years and the contributions of different counties/funding agencies. The research categories, the collaboration relationships, keywords bursts, and co-cited references were detected by bibliometrics tools.

The number of published articles related to CBD has increased over time except for 2005, 2008, and 2014, and significant growth could be observed from 2019 to 2021. Moreover, the number of citations showed growth continually, especially from 2019 to 2021, indicating increased focus in the field among researchers in recent years. In 2017 and 2018, great concerns were attached to the clinical trials of CBD in epilepsy. With the FDA approval of the first CBD-based drug for the treatment of seizures associated symptoms in 2018, the therapeutic values of CBD in neuropsychiatric disorders have been increasingly recognized by researchers.

Among the 94 countries that have participated in CBD research, the United States was the world leader with 1,114 articles and a total of 36,570 citations, which could be explained by two possible reasons. Firstly, the financial policies of the funding agencies in the field. The United States Department of Health and Human Services, National Institutes of Health (NIH)-USA, and NIH National Institute on Drug Abuse (NIDA) have provided funds for a total of 1,071 publications, which accounts for 30.12% of all the publications. Secondly, the collaboration strength with other countries. The United States was the most cooperative country with other countries, and a total of 573 link strengths could be detected. Still, there is only one United States institution on the list of the top 10 most cooperative institutions. One possible reason is that there are many institutions working in this area in the United States, but they do not have outstanding advantages. Another possible reason has to do with United States funding policies. Fund management departments need to allocate funds to more institutions, but this argument needs more evidence to back it up. England contributed second in citations in the field, with 394 articles cited 23,402 times, which was related to the predominant research institutions, such as King's College London, GW Research Limited, and University College London. Notably, GW Pharmaceuticals has sponsored several impactful clinical trials, which have contributed significantly to the drug development of seizure treatment (Devinsky et al., 2016, 2017; Thiele et al., 2018). On the other hand, England had the second strongest collaboration with other countries, and 412 link strengths were included in the network. In addition, Italy, Canada, and Brazil have also been pivotal in the advancement of the field, due to the high outputs and citations of their articles, and extensive partnership with other countries. In Brazil, the University of Sao Paulo was the most productive institute with 208 documents published, accounting for 70.5% of all the documents. The University of Sao Paulo was also the most collaborative institute with other countries in the CBD field. Furthermore, Brazil accounted for three of the top 10 most productive funding agencies, which indirectly reflected that the Brazil government attaches great importance to CBD research.

Co-authorships analysis revealed the most productive, most cited, and extensive cooperative authors in the CBD field. The top three most productive authors were Guimaraes FS, Mechoulam R, and Di Marzo V, they were from three different institutions, the University of Sao Paulo (Brazil), Hebrew University of the Jerusalem (Israel), and Laval University (Canada). The top three authors with the highest citations were Di Marzo V, Mechoulam R, and Devinsky O (New York University, United States). While the top three authors who had the most corporations with others were completely different from the top three most productive or cited authors. Huestis MA was the most cooperative author with others in the field and was from Jefferson University (United States), the followed authors were Zuardi AW (University of Sao Paulo, Brazil), and Crippa JA (University of Sao Paulo, Brazil).

The category analysis of 3555 publications suggested that Pharmacology/Pharmacy, and Neuroscience/Neurology were the hot researched subjects in the CBD field, and Chemistry plays a

key role in the evolution of research subjects. The cluster analysis of keywords divided 282 keywords with a frequency greater than 20 times into five clusters, which could be concluded as the following five themes: 1) Mechanism; 2) Disease; 3) Treatment of epilepsy; 4) Clinical trial; 5) Synthesis and metabolism. Keywords bursts detection indicated that seizure was one of the research hot spots in the field. Over the past decade, the pharmacology effects of CBD on neuropsychiatric disorders have been widely explored. It is worth noting that great achievements were made in the treatment of seizures, a CBD-based drug, Epidiolex, was approved by the FDA in 2018. However, with the Epidiolex used in the clinical trials, a series of side effects, including somnolence, decreased appetite, diarrhea, rash, sleep disorder, infections, and so on have raised concerns of researchers (Taylor et al., 2018; Pauli et al., 2020). To better elucidate the long-term efficacy, safety, and tolerability of CBD in the treatment of epilepsy, large-scale or in-depth clinical trials and analyses are necessary. In Parkinson's disease, clinical trials indicated that CBD could alleviate the rapid eye movement sleep behaviour disorder (Chagas et al., 2014a), anxiety symptoms (de Faria et al., 2020), and improve the life quality of PD patients (Chagas et al., 2014b). In schizophrenia, CBD showed beneficial effects for anti-psychotic symptoms and improved cognitive performance in patients through anandamide-independent and dopamine-independent mechanisms (McGuire et al., 2018; Leweke et al., 2021). In conclusion, the promising research and application prospects of CBD in neuropsychiatric disorders have been confirmed, and its neuroprotective effect may be an important direction for future drug development of CBD. For the treatment of multiple sclerosis-related symptoms, such as spasticity and pain, a drug combined delta (9)-tetrahydrocannabinol (THC) and CBD, Sativex has been investigated by researchers (Wade et al., 2004; Rog et al., 2005). In 2020, Sativex (GW Pharmaceuticals, England) has been approved by more than 25 countries in the world.

As revealed in the reference co-citation analysis and burst detection, researchers attached great importance to pharmacology effects of CBD in the alleviation of seizures related symptoms. The reference with the highest co-citations illustrated the clinical trials of CBD on epilepsy, and six of the top 20 burst references focused on epilepsy. Notably, the molecular mechanisms, targets, or signaling pathways of the CBD effects were also the hot spots in the field. ECS is involved in modulating the developments and functions of the brain and thus plays an important role in depression, anxiety, cognitive, memory, and rewarding effects (Mechoulam and Parker, 2013; Micale et al., 2013). CB1 and CB2 are the two major receptors of the ESC, but there are still divergences regarding the regulatory role of CBD on these receptors. One view supported that CBD has a low affinity or even no activity for CB1 and CB2 receptors (Ryberg et al., 2007; McPartland et al., 2015). In contrast, another perspective pointed out that CBD was a high-efficiency antagonist of CB1 and CB2 receptor agonists (Thomas et al., 2007; Laprairie et al., 2015). 5-HT1A receptor was one of the top 10 bursts keywords, which has been thoroughly studied in the CBD field. CBD presented effects on antiepileptic, antianxiety, and antidepressant disorders by activating the 5-HT1A receptor (Campos and Guimarães, 2008; Zanelati et al., 2010; Devinsky et al., 2014). GPR55 is a high affinity receptor of the cannabinoids family, and CBD can be activated as a selective antagonist of GPR55 to prevent inflammation-associated impairments (Li et al., 2013; Chiurchiù et al., 2015). In addition, PPARγ has also displayed significant value in the anti-inflammatory and antioxidative effects of CBD (Vallée et al., 2017; Sonego, 2018). TRPV channels are the potential targets for CBD activity, especially TRPV2 medicated Ca2+ dynamics (Nabissi et al., 2013; Hassan et al., 2014). The modulatory effects of CBD on TRPV channels may be involved in anti-neuroinflammation (Hassan et al., 2014), anticancer (Santoni et al., 2020), and antinociception (Maione et al., 2011). The above researches indicates that the anti-inflammation effect of CBD may be one of the core pharmacological mechanisms of CBD. In fact, by targeting inflammation, CBD decreased the AD-related and PD-related neuron damage (Vallée et al., 2017, 2021), preventing multiple sclerosis-associated inflammatory impairments (Mecha et al., 2013) and alcohol-induced liver injury (Wang et al., 2017), and inhibiting methamphetamine-induced reinstatement in rats (Karimi-Haghighi et al., 2020). Additionally, the anti-inflammation effect of CBD was mediated by several signaling pathways, including GPR55, PPARγ, and TRPV channels. Do these signaling pathways exhibit time-specificity and spatial-specificity under the same conditions? Whether these signaling pathways interact with each other or are co-regulated by a specific signaling molecule? These are worthy of deeper consideration and exploration in the future.

The timeline view of the co-cited references revealed the effect of CBD on cocaine use disorders is a newly developed theme in recent years. Studies have reported that CBD effectively attenuated the cocaine-induced rewarding effects, drug-seeking behaviors (Luján et al., 2020; Ledesma et al., 2021), and seizures (Gobira, 2015) in the preclinical trials. A double-blind trial indicated that CBD reduced cue-induced craving and anxiety in heroin use disorders (Hurd et al., 2019). Moreover, the great value of CBD in the treatment of methamphetamine (Karimi-Haghighi and Haghparast, 2018), morphine (Rodríguez-Muñoz et al., 2018), and alcohol (Turna et al., 2019) use disorders have also been proved. In short, these studies provided new perspectives and approaches in treating substance use disorders, however, more researches and efforts are still needed before using CBD as a therapeutic drug.

Conclusion

Our present study performed a bibliometrics analysis in the CBD field based on the literature published from 2004 to 2021 with the expectation to reveal the research hot spots and frontiers. The pharmacology and pharmacy of CBD have always been enthusiastically investigated by researchers, particularly in neuropsychiatric disorders, such as epilepsy, schizophrenia, anxiety, etc. CBD meditated the CB1, CB2, 5-HT1A, GPR55, PPARγ receptors, and TRPV channels may be explained its extensive pharmacology effects. In recent years, the values of CBD in the treatment of substance use disorders have attracted researchers' interest.

Data availability statement

The original contributions presented in the study are included in the article/Supplementary Materials, further inquiries can be directed to the corresponding authors.

Author contributions

LL contributed to data analysis and original manuscript writing; JL collected the data; MZ provided software; MC and FL were responsible for data analysis and validation; XZ and BZ supervised data analysis and revised the manuscript. All authors reviewed the manuscript.

Funding

This work was supported by the National Nature Science Foundation of China (81930055, 82160325), the Yunnan Applied Basic Research Projects Joint Special Project (202201AY070001-020).

Conflict of interest

The authors declare that the research was conducted in the absence of any commercial or financial relationships that could be construed as a potential conflict of interest.

Publisher's note

All claims expressed in this article are solely those of the authors and do not necessarily represent those of their affiliated organizations, or those of the publisher, the editors and the reviewers. Any product that may be evaluated in this article, or claim that may be made by its manufacturer, is not guaranteed or endorsed by the publisher.

References

Campos, A. C., Fogaça, M. V., Sonego, A. B., and Guimarães, F. S. (2016). Cannabidiol, neuroprotection and neuropsychiatric disorders. *Pharmacol. Res.* 112, 119–127. doi:10.1016/j.phrs.2016.01.033

Campos, A. C., and Guimarães, F. S. (2008). Involvement of 5HT1A receptors in the anxiolytic-like effects of cannabidiol injected into the dorsolateral periaqueductal gray of rats. *Psychopharmacology* 199, 223–230. doi:10.1007/s00213-008-1168-x

Campos, A. C., Moreira, F. A., Gomes, F. V., Del Bel, E. A., and Guimarães, F. S. (2012). Multiple mechanisms involved in the large-spectrum therapeutic potential of cannabidiol in psychiatric disorders. *Philos. Trans. R. Soc. Lond. B Biol. Sci.* 367, 3364–3378. doi:10.1098/rstb.2011.0389

Carrier, E. J., Auchampach, J. A., and Hillard, C. J. (2006). Inhibition of an equilibrative nucleoside transporter by cannabidiol: A mechanism of cannabinoid immunosuppression. *Proc. Natl. Acad. Sci. U. S. A.* 103, 7895–7900. doi:10.1073/pnas.0511232103

Chagas, M. H. N., Eckeli, A. L., Zuardi, A. W., Pena-Pereira, M. A., Sobreira-Neto, M. A., Sobreira, E. T., et al. (2014a). Cannabidiol can improve complex sleep-related behaviours associated with rapid eye movement sleep behaviour disorder in Parkinson's disease patients: A case series. *J. Clin. Pharm. Ther.* 39, 564–566. doi:10.1111/jcpt.12179

Chagas, M. H. N., Zuardi, A. W., Tumas, V., Pena-Pereira, M. A., Sobreira, E. T., Bergamaschi, M. M., et al. (2014b). Effects of cannabidiol in the treatment of patients with Parkinson's disease: An exploratory double-blind trial. *J. Psychopharmacol.* 28, 1088–1098. doi:10.1177/0269881114550355

Chen, C., Liang, S. Y., Shih, Y. P., Lee, Y. M., and Chang, L. (2006). CiteSpace II: Detecting and visualizing emerging trends and transient patterns in scientific literature. *J. Clin. Microbiol.* 57, 359–365. doi:10.1128/JCM.44.2.359-365.2006

Chen, C. (2004). Searching for intellectual turning points: Progressive knowledge domain visualization. *Proc. Natl. Acad. Sci. U. S. A.* 101, 5303–5310. doi:10.1073/pnas.0307513100

Chiurchiù, V., Lanuti, M., De Bardi, M., Battistini, L., and Maccarrone, M. (2015). The differential characterization of GPR55 receptor in human peripheral blood reveals a distinctive expression in monocytes and NK cells and a proinflammatory role in these innate cells. *Int. Immunol.* 27, 153–160. doi:10.1093/intimm/dxu097

Chu, P. L., Wang, T., Zheng, J., Xu, C. Q., Yan, Y. J., Ma, Q. S., et al. (2022). Global and current research trends of unilateral biportal endoscopy/biportal endoscopic spinal surgery in the treatment of lumbar degenerative diseases: A bibliometric and visualization study. *Orthop. Surg.* 14, 635–643. doi:10.1111/os.13216

Crippa, J. A. S., Hallak, J. E. C., Zuardi, A. W., Guimarães, F. S., Tumas, V., and dos Santos, R. G. (2019). Is cannabidiol the ideal drug to treat non-motor Parkinson's disease symptoms? *Eur. Arch. Psychiatry Clin. Neurosci.* 269, 121–133. doi:10.1007/s00406-019-00982-6

de Faria, S. M., de Morais Fabrício, D., Tumas, V., Castro, P. C., Ponti, M. A., Hallak, J. E., et al. (2020). Effects of acute cannabidiol administration on anxiety and tremors induced by a Simulated Public Speaking Test in patients with Parkinson's disease. *J. Psychopharmacol.* 34, 189–196. doi:10.1177/0269881119895536

De Gregorio, D., McLaughlin, R. J., Posa, L., Ochoa-Sanchez, R., Enns, J., Lopez-Canul, M., et al. (2019). Cannabidiol modulates serotonergic transmission and reverses both allodynia and anxiety-like behavior in a model of neuropathic pain. *Pain* 160, 136–150. doi:10.1097/j.pain.0000000000001386

Devinsky, O., Cilio, M. R., Cross, H., Fernandez-Ruiz, J., French, J., Hill, C., et al. (2014). Cannabidiol: Pharmacology and potential therapeutic role in epilepsy and other neuropsychiatric disorders. *Epilepsia* 55, 791–802. doi:10.1111/epi.12631

Devinsky, O., Cross, J. H., Laux, L., Marsh, E., Miller, I., Nabbout, R., et al. (2017). Trial of cannabidiol for drug-resistant seizures in the Dravet syndrome. *N. Engl. J. Med.* 376, 2011–2020. doi:10.1056/NEJMoa1611618

Devinsky, O., Marsh, E., Friedman, D., Thiele, E., Laux, L., Sullivan, J., et al. (2016). Cannabidiol in patients with treatment-resistant epilepsy: An open-label interventional trial. *Lancet. Neurol.* 15, 270–278. doi:10.1016/S1474-4422(15)00379-8

Devinsky, O., Patel, A. D., Cross, J. H., Villanueva, V., Wirrell, E. C., Privitera, M., et al. (2018). Effect of cannabidiol on drop seizures in the lennox–gastaut syndrome. *N. Engl. J. Med.* 378, 1888–1897. doi:10.1056/NEJMoa1714631

Geffrey, A. L., Pollack, S. F., Bruno, P. L., and Thiele, E. A. (2015). Drug–drug interaction between clobazam and cannabidiol in children with refractory epilepsy. *Epilepsia* 56, 1246–1251. doi:10.1111/epi.13060

Gobira, P. H., Vilela, L. R., Goncalves, B. D. C., Santos, R. P. M., de Oliveira, A. C., Vieira, L. B., et al. (2015). Cannabidiol, a Cannabis sativa constituent, inhibits cocaine-induced seizures in mice: Possible role of the mTOR pathway and reduction in glutamate release. *Neurotoxicology* 50, 116–121. doi:10.1016/j.neuro.2015.08.007

Hassan, S., Eldeeb, K., Millns, P. J., Bennett, A. J., Alexander, S. P. H., and Kendall, D. A. (2014). Cannabidiol enhances microglial phagocytosis via transient receptor potential (TRP) channel activation. *Br. J. Pharmacol.* 171, 2426–2439. doi:10.1111/bph.12615

Hurd, Y. L., Spriggs, S., Alishayev, J., Winkel, G., Gurgov, K., Kudrich, C., et al. (2019). Cannabidiol for the reduction of cue-induced craving and anxiety in drug-abstinent individuals with heroin use disorder: A double-blind randomized placebo-controlled trial. *Am. J. Psychiatry* 176, 911–922. doi:10.1176/appi.ajp.2019.18101191

Iffland, K., and Grotenhermen, F. (2017). An update on safety and side effects of cannabidiol: A review of clinical data and relevant animal studies. *Cannabis Cannabinoid Res.* 2, 139–154. doi:10.1089/can.2016.0034

Izzo, A. A., Borrelli, F., Capasso, R., Di Marzo, V., and Mechoulam, R. (2009). Non-psychotropic plant cannabinoids: New therapeutic opportunities from an ancient herb. *Trends Pharmacol. Sci.* 30, 515–527. doi:10.1016/j.tips.2009.07.006

Karimi-Haghighi, S., Dargahi, L., and Haghparast, A. (2020). Cannabidiol modulates the expression of neuroinflammatory factors in stress- and drug-induced reinstatement of methamphetamine in extinguished rats. *Addict. Biol.* 25, e12740. doi:10.1111/adb.12740

Karimi-Haghighi, S., and Haghparast, A. (2018). Cannabidiol inhibits priming-induced reinstatement of methamphetamine in REM sleep deprived rats. *Prog. Neuropsychopharmacol. Biol. Psychiatry* 82, 307–313. doi:10.1016/j.pnpbp.2017.08.022

Laprairie, R. B., Bagher, A. M., Kelly, M. E. M., and Denovan-Wright, E. M. (2015). Cannabidiol is a negative allosteric modulator of the cannabinoid CB1 receptor. *Br. J. Pharmacol.* 172, 4790–4805. doi:10.1111/bph.13250

Ledesma, J. C., Manzanedo, C., and Aguilar, M. A. (2021). Cannabidiol prevents several of the behavioral alterations related to cocaine addiction in mice. *Prog. Neuropsychopharmacol. Biol. Psychiatry* 111, 110390. doi:10.1016/j.pnpbp.2021.110390

Lee, J. L. C., Bertoglio, L. J., Guimarães, F. S., and Stevenson, C. W. (2017). Cannabidiol regulation of emotion and emotional memory processing: Relevance for treating anxiety-related and substance abuse disorders. *Br. J. Pharmacol.* 174, 3242–3256. doi:10.1111/bph.13724

Leweke, F. M., Piomelli, D., Pahlisch, F., Muhl, D., Gerth, C. W., Hoyer, C., et al. (2012). Cannabidiol enhances anandamide signaling and alleviates psychotic symptoms of schizophrenia. *Transl. Psychiatry* 2, e94. doi:10.1038/tp.2012.15

Leweke, F. M., Rohleder, C., Gerth, C. W., Hellmich, M., Pukrop, R., and Koethe, D. (2021). Cannabidiol and amisulpride improve cognition in acute schizophrenia in an explorative, double-blind, active-controlled, randomized clinical trial. *Front. Pharmacol.* 12, 614811. doi:10.3389/fphar.2021.614811

Li, K., Feng, J., Li, Y., Yuece, B., Lin, X., Yu, L., et al. (2013). Anti-inflammatory role of cannabidiol and O-1602 in cerulein-induced acute pancreatitis in mice. *Pancreas* 42, 123–129. doi:10.1097/MPA.0b013e318259f6f0

Luján, M. Á., Cantacorps, L., and Valverde, O. (2020). The pharmacological reduction of hippocampal neurogenesis attenuates the protective effects of cannabidiol on cocaine voluntary intake. *Addict. Biol.* 25, e12778. doi:10.1111/adb.12778

Mahmud, A., Gallant, S., Sedki, F., D'Cunha, T., and Shalev, U. (2017). Effects of an acute cannabidiol treatment on cocaine self-administration and cue-induced cocaine seeking in male rats. *J. Psychopharmacol.* 31, 96–104. doi:10.1177/0269881116667706

Maione, S., Piscitelli, F., Gatta, L., Vita, D., De Petrocellis, L., Palazzo, E., et al. (2011). Non-psychoactive cannabinoids modulate the descending pathway of antinociception in anaesthetized rats through several mechanisms of action. *Br. J. Pharmacol.* 162, 584–596. doi:10.1111/j.1476-5381.2010.01063.x

McGuire, P., Robson, P., Cubala, W. J., Vasile, D., Morrison, P. D., Barron, R., et al. (2018). Cannabidiol (CBD) as an adjunctive therapy in schizophrenia: A multicenter randomized controlled trial. *Am. J. Psychiatry* 175, 225–231. doi:10.1176/appi.ajp.2017.17030325

McPartland, J. M., Duncan, M., Di Marzo, V., and Pertwee, R. G. (2015). Are cannabidiol and d9-tetrahydrocannabivarin negative modulators of the endocannabinoid system? A systematic review. *Br. J. Pharmacol.* 172, 737–753. doi:10.1111/bph.12944

Mecha, M., Feliú, A., Iñigo, P. M., Mestre, L., Carrillo-Salinas, F. J., Guaza, C., et al. (2013). Cannabidiol provides long-lasting protection against the deleterious effects of inflammation in a viral model of multiple sclerosis: A role for A2A receptors. *Neurobiol. Dis.* 59, 141–150. doi:10.1016/j.nbd.2013.06.016

Mechoulam, R., and Parker, L. A. (2013). The endocannabinoid system and the brain. *Annu. Rev. Psychol.* 64, 21–47. doi:10.1146/annurev-psych-113011-143739

Melas, P. A., Scherma, M., Fratta, W., Cifani, C., and Fadda, P. (2021). Cannabidiol as a potential treatment for anxiety and mood disorders: Molecular targets and epigenetic insights from preclinical research. *Int. J. Mol. Sci.* 22, 1863. doi:10.3390/ijms22041863

Micale, V., Di Marzo, V., Sulcova, A., Wotjak, C. T., and Drago, F. (2013). Endocannabinoid system and mood disorders: Priming a target for new therapies. *Pharmacol. Ther.* 138, 18–37. doi:10.1016/j.pharmthera.2012.12.002

Nabissi, M., Morelli, M. B., Santoni, M., and Santoni, G. (2013). Triggering of the TRPV2 channel by cannabidiol sensitizes glioblastoma cells to cytotoxic chemotherapeutic agents. *Carcinogenesis* 34, 48–57. doi:10.1093/carcin/bgs328

Pauli, C. S., Conroy, M., Vanden Heuvel, B. D., and Park, S.-H. (2020). Cannabidiol drugs clinical trial outcomes and adverse effects. *Front. Pharmacol.* 11, 63. doi:10.3389/fphar.2020.00063

Pertwee, R. G. (2008). The diverse CB1 and CB2 receptor pharmacology of three plant cannabinoids: delta9-tetrahydrocannabinol, cannabidiol and delta9-tetrahydrocannabivarin. *Br. J. Pharmacol.* 153, 199–215. doi:10.1038/sj.bjp.0707442

Rodríguez-Muñoz, M., Onetti, Y., Cortés-Montero, E., Garzón, J., and Sánchez-Blázquez, P. (2018). Cannabidiol enhances morphine antinociception, diminishes NMDA-mediated seizures and reduces stroke damage via the sigma 1 receptor. *Mol. Brain* 11, 51. doi:10.1186/s13041-018-0395-2

Rog, D. J., Nurmikko, T. J., Friede, T., and Young, C. A. (2005). Randomized, controlled trial of cannabis-based medicine in central pain in multiple sclerosis. *Neurology* 65, 812–819. doi:10.1212/01.wnl.0000176753.45410.8b

Russo, E. B. (2011). Taming THC: Potential cannabis synergy and phytocannabinoid-terpenoid entourage effects. *Br. J. Pharmacol.* 163, 1344–1364. doi:10.1111/j.1476-5381.2011.01238.x

Ryberg, E., Larsson, N., Sjögren, S., Hjorth, S., Hermansson, N.-O., Leonova, J., et al. (2007). The orphan receptor GPR55 is a novel cannabinoid receptor. *Br. J. Pharmacol.* 152, 1092–1101. doi:10.1038/sj.bjp.0707460

Santoni, G., Amantini, C., Maggi, F., Marinelli, O., Santoni, M., Nabissi, M., et al. (2020). The TRPV2 cation channels: From urothelial cancer invasiveness to glioblastoma multiforme interactome signature. *Lab. Investig.* 100, 186–198. doi:10.1038/s41374-019-0333-7

Scarante, F. F., Ribeiro, M. A., Almeida-Santos, A. F., Guimarães, F. S., and Campos, A. C. (2021). Glial cells and their contribution to the mechanisms of action of cannabidiol in neuropsychiatric disorders. *Front. Pharmacol.* 11, 618065. doi:10.3389/fphar.2020.618065

Sonego, A. B., Prado, D. S., Vale, G. T., Sepulveda-Diaz, J. E., Cunha, T. M., Tirapelli, C. R., et al. (2018). Cannabidiol prevents haloperidol-induced vacuos chewing movements and inflammatory changes in mice via PPARγ receptors. *Brain Behav. Immun.* 74, 241–251. doi:10.1016/j.bbi.2018.09.014

Song, Y., Ma, P., Gao, Y., Xiao, P., Xu, L., and Liu, H. (2021). A bibliometrics analysis of metformin development from 1980 to 2019. *Front. Pharmacol.* 12, 645810. doi:10.3389/fphar.2021.645810

Sultan, A. S., Marie, M. A., and Sheweita, S. A. (2018). Novel mechanism of cannabidiol-induced apoptosis in breast cancer cell lines. *Breast* 41, 34–41. doi:10.1016/j.breast.2018.06.009

Taylor, L., Gidal, B., Blakey, G., Tayo, B., and Morrison, G. (2018). A phase I, randomized, double-blind, placebo-controlled, single ascending dose, multiple dose, and Food effect trial of the safety, tolerability and pharmacokinetics of highly purified cannabidiol in healthy subjects. *CNS Drugs* 32, 1053–1067. doi:10.1007/s40263-018-0578-5

Thiele, E. A., Marsh, E. D., French, J. A., Mazurkiewicz-Beldzinska, M., Benbadis, S. R., Joshi, C., et al. (2018). Cannabidiol in patients with seizures associated with lennox-gastaut syndrome (GWPCARE4): A randomised, double-blind, placebo-controlled phase 3 trial. *Lancet* 391, 1085–1096. doi:10.1016/S0140-6736(18)30136-3

Thomas, A., Baillie, G. L., Phillips, A. M., Razdan, R. K., Ross, R. A., and Pertwee, R. G. (2007). Cannabidiol displays unexpectedly high potency as an antagonist of CB1 and CB2 receptor agonists *in vitro*. *Br. J. Pharmacol.* 150, 613–623. doi:10.1038/sj.bjp.0707133

Turna, J., Syan, S. K., Frey, B. N., Rush, B., Costello, M. J., Weiss, M., et al. (2019). Cannabidiol as a novel candidate alcohol use disorder pharmacotherapy: A systematic review. *Alcohol. Clin. Exp. Res.* 43, 550–563. doi:10.1111/acer.13964

Vallée, A., Lecarpentier, Y., Guillevin, R., and Vallée, J.-N. (2017). Effects of cannabidiol interactions with Wnt/β-catenin pathway and PPARγ on oxidative stress and neuroinflammation in Alzheimer's disease. *Acta Biochim. Biophys. Sin.* 49, 853–866. doi:10.1093/abbs/gmx073

Vallée, A., Vallée, J.-N., and Lecarpentier, Y. (2021). Potential role of cannabidiol in Parkinson's disease by targeting the WNT/β-catenin pathway, oxidative stress and inflammation. *Aging (Albany NY)* 13, 10796–10813. doi:10.18632/aging.202951

VanDolah, H. J., Bauer, B. A., and Mauck, K. F. (2019). Clinicians' guide to cannabidiol and hemp oils. *Mayo Clin. Proc.* 94, 1840–1851. doi:10.1016/j.mayocp.2019.01.003

Wade, D. T., Makela, P., Robson, P., House, H., and Bateman, C. (2004). Do cannabis-based medicinal extracts have general or specific effects on symptoms in multiple sclerosis? A double-blind, randomized, placebo-controlled study on 160 patients. *Mult. Scler.* 10, 434–441. doi:10.1191/1352458504ms1082oa

Wang, Y., Mukhopadhyay, P., Cao, Z., Wang, H., Feng, D., Haskó, G., et al. (2017). Cannabidiol attenuates alcohol-induced liver steatosis, metabolic dysregulation, inflammation and neutrophil-mediated injury. *Sci. Rep.* 7, 12064. doi:10.1038/s41598-017-10924-8

Whiting, P. F., Wolff, R. F., Deshpande, S., Di Nisio, M., Duffy, S., Hernandez, A. V., et al. (2015). Cannabinoids for medical use: A systematic review and meta-analysis. *JAMA* 313, 2456–2473. doi:10.1001/jama.2015.6358

Xiong, W., Cui, T., Cheng, K., Yang, F., Chen, S.-R., Willenbring, D., et al. (2012). Cannabinoids suppress inflammatory and neuropathic pain by targeting α3 glycine receptors. *J. Exp. Med.* 209, 1121–1134. doi:10.1084/jem.20120242

Yin, M., Xu, C., Ma, J., Ye, J., and Mo, W. (2021). A bibliometric analysis and visualization of current research trends in the treatment of cervical spondylotic myelopathy. *Glob. Spine J.* 11, 988–998. doi:10.1177/2192568220948832

Zanelati, T., Biojone, C., Moreira, F., Guimarães, F., and Joca, S. (2010). Antidepressant-like effects of cannabidiol in mice: Possible involvement of 5-ht1a receptors. *Br. J. Pharmacol.* 159, 122–128. doi:10.1111/j.1476-5381.2009.00521.x

Frontiers in Pharmacology

Explores the interactions between chemicals and living beings The most cited journal in its field, which advances access to pharmacological discoveries to prevent and treat human disease.

Discover the latest Research Topics

See more →

Frontiers

Avenue du Tribunal-Fédéral 34
1005 Lausanne, Switzerland
frontiersin.org

Contact us

+41 (0)21 510 17 00
frontiersin.org/about/contact